USAID FROM THE AMERICAN PEOPLE | SOUTHERN AFRICA

RESILIM : Resilience in the Limpopo River Basin Program

Conceptual Model, Hydraulic Properties, and Model Dataset Support Progress Report for the Development of Subsurface Mapping for the Transboundary Ramotswa Aquifer, that is part of the Limpopo River Basin, using Airborne Geophysics

JANUARY, 2017

Submitted by:

XRI BLUE

For the Resilience in the Limpopo Basin: the Potential Role of the Transboundary Ramotswa Aquifer

Implemented by:

IWMI International Water Management Institute

CGIAR Research Program on Water, Land and Ecosystems

In partnership with:

igrac International Groundwater Resources Assessment Centre

University of Botswana

Republic of Botswana

University of the Free State / UFS UV

University of Pretoria

University of the Witwatersrand, Johannesburg

This report was made possible by the support of the American people through the United States Agency for International Development (USAID). Its contents are the sole responsibility of XRI operating as a subcontractor to Chemonics International, and do not necessarily reflect the views of USAID or the United States Government.

October 28, 2016

EXTENT OF AQUIFER, CONCEPTUAL HYDROLOGICAL MODEL, HYDRAULIC PROPERTIES, MODEL GRID, AND PROPOSED HYDROGEOLOGICAL DATA PARAMETERS PROGRESS REPORT FOR THE DEVELOPMENT OF SUBSURFACE MAPPING FOR THE TRANS-BOUNDARY RAMOTSWA AQUIFER THAT IS PART OF THE LIMPOPO RIVER BASIN, USING AIRBORNE GEOPHYSICS

Prepared for:
Chemonics International Inc.
1717 H Street, N. W.
Washington, D.C. 20006

Submitted by:
XRI Holdings, LLC
1130 Business Center Dr.
Lake Mary, FL 32746
(407) 416-7806

Contents

1. Introduction

On 25, November 2015, XRI Holdings, LLC ("XRI") entered in to a subcontract agreement ("Sub-Contract") with Chemonics International Inc. ("Chemonics") to provide technical assistance to the Resilience of the Limpopo River Basin (RESILIM) program in the areas of hydrogeological research and training services for the RAMOTSWA project (the "Project"). XRI is to provide research and development of a subsurface model of the trans-boundary Ramotswa aquifer (the "Project Area") that is part of the Limpopo River Basin utilizing airborne electromagnetics ("AEM"). The intent of this research is to contribute to the study of aquifer material properties within the Project Area subsurface which have been previously unidentified by other methodological approaches.

This document serves as an Extent of Aquifer, Conceptual Hydrological Model, Hydraulic Properties, Model Grid, and Proposed Hydrogeological Data Parameters Progress Report ("Report") of XRI's interpretations of the Project Area fulfilling deliverable 5 of the Sub-Contract. This Report contains information on the preliminary conceptual hydrological model, hydraulic properties, and model dataset, including the technical justifications for each. The preliminary conceptual hydrological model, hydraulic properties, and model datasets will be discussed with RESILIM, International Water Management Institute ("IWMI"), and project partners following the submittal of this report.

Appendix A, Figure 1 shows the locations of inverted AEM data within the Ramotswa Project Area. The Ramotswa Project Area has been divided into three (3) areas: Northern (Appendix A, Figure 2), Central (Appendix A, Figure 3), and Southern (Appendix A, Figure 4) to display the associated names of the inverted AEM flight lines. Upon delivery of this report, a .kmz file of the inverted flight line locations will be delivered, to be viewed in Google Earth™ software. When an inverted flight line is selected the name of that flight line will be displayed in an attribute box.

2. Revised Surface Geology of the Project Area

During XRI's field visit to the Botswana Department of Geological Survey ("DGS") in February 2016, the Botswana DGS provided XRI with Geographic Information Systems ("GIS") surface geology shapefiles for the entire country of Botswana (1:1,000,000 scale) and the Lobatse, Botswana area (1:250,000 scale). These GIS shapefiles were merged with downloaded South African (from the Council for Geoscience, South Africa) surface geology shapefiles (1:1,000,000 scale) to create a new shapefile of the surface geology of the Project Area. Referencing existing documents (Eriksson, et al., 1995) and (Pollack, et al., 2009), a simplified surface geology map of the Project Area was then created (Appendix A, Figure 5). This simplified surface geology map is an improvement of the merged surface geology map of the Project Area that existed in January 2016 (Appendix A, Figure 6), and was included in XRI's background hydrogeologic report.

The simplified surface geology map includes seventeen (17) unique formations that use both South African and Botswana naming conventions for the geologic units (Appendix A, Figure 7). Appendix A, Figure 8 provides the name of the simplified geologic units, other geologic formations included in that unit, general lithologic description, and an expected resistivity signature. The simplified surface geology map does include some discrepancies in mapped formations, specifically near the Botswana-South Africa international border. However, this simplified surface geology map provides an improved visualization

and representation of the surface geology for the Ramotswa Project Area. The simplified surface geology map created by XRI is not meant to serve as a final surface geology map of the Ramotswa Project Area, rather a guide that was used to aid in geologic interpretations.

3. Interpretation of Geologic Formations within the Ramotswa Project Area

Information gathered from peer reviewed geologic papers for geologic formation characteristics (including but not limited to thickness, composition, mapped locations of the surface expressions of the geologic formations), general knowledge of expected electrical resistivity ranges of various lithologies, topographic features, and XRI's extensive experience of interpreting subsurface geology based on AEM data were used to interpret the geologic formations within the Ramotswa Project Area from the AEM data. The mapped surface geology locations were used as a guide for interpreting the AEM signature of the various geologic formations. For example, the resistivity signature observed in the subsurface of areas mapped as Silverton Formation ("Silverton") at the surface (Appendix A, Figure 9), indicated that the resistivity signature of the Silverton was very conductive (less than 10 ohm-meters) throughout the project area.

In areas where the mapped surface geology differed from the interpreted AEM signature of a geologic formation, surface expressions were examined in Google Earth™ to determine if there was a noticeable change in the surface material or topography. For example, the Black Reef Quartzite ("Black Reef"), Timeball Hill Formation ("Timeball Hill"), and Ditlojana Quartzite are comprised of materials that do not easily erode, and are usually visible as topographic highs in the Ramotswa Project Area. Therefore, the extents of the topographic features observed in Google Earth™ were used to inform geologic interpretations. Appendix A, Figure 10**,** details the general lithology, interpreted resistivity signature, justification for the geologic interpretation, any surface expression or topographic feature associated with the geologic formation, and a representative example for each of the 17 simplified geologic formations interpreted within the Ramotswa Project Area.

4. Extent of Aquifer

That Ramotswa Dolomite ("Dolomite") is the main water bearing unit in the Ramotswa Project Area. Interpreting the contacts between the Dolomite and the geologic formations that are in contact with the Dolomite, is critical to delineating the extent of the aquifer. Within the Ramotswa Project Area, there are other geologic units (including the Lephala Formation) that are also water bearing, however the primary task given to XRI was to delineate the extent of the Dolomite. Therefore, interpretations of the extents of other aquifers within the Ramotswa Project Area are not included within this report. The Black Reef is stratigraphically below the Dolomite, and in contact with the Dolomite throughout the project area. The Black Reef is in contact with the northern edge of the Dolomite in the Northern portion, the western edge of the Dolomite in the Central portion and the southern edge of the Dolomite in the Southern portion. The contact between the Black Reef and the Dolomite is interpreted as the base of the aquifer. With some exceptions the Black Reef has been mapped throughout the Ramotswa Project Area (Appendix A, Figure 11). The Black Reef is a quartzite, which is electrically resistive, having interpreted resistivities as high as approximately 900 ohm-meters (Ω-m) throughout the Project Area.

There is an unconformity between the Black Reef and the Dolomite, with the base of the Dolomite including a transgressive black shale (Catuneanu & Eriksson, 1999). This shale has been observed in

boreholes within the Ramotswa Project Area (Obbes, 2001). Shales typically have a conductive electrical signature, and within the Ramotswa Project Area the transgressive black shale that indicates the contact between the Dolomite and Black Reef has an approximate resistivity range of 1-3 Ω-m. This shale is interpreted to be a subsurface indicator of the base of the Dolomite. Additionally, throughout the Ramotswa Project Area, the Black Reef had a corresponding topographic high (hill) visible on the surface, with a marked decrease in elevation near the contact of the Black Reef and Dolomite. There is a dike close to the location of the borehole described in the Obbes report. The presence of the dike caused significant interference in the resistivity signature in the area near the borehole, additionally the borehole is located off the flight lines, resulting in the lithology data not being able to be sufficiently used to correlate the borehole data to subsurface resistivity signatures. The change in surface expression in the Black Reef also aided in interpreting the contact between the Black Reef and the Dolomite (Appendix A, Figure 12).

The geologic unit in contact with and stratigraphically above the Dolomite varies throughout the project area. In the Northern portion of the Ramotswa Project Area, the Duitschland Formation ("Duitschland), a shale, is the primary geologic unit above the Dolomite (Appendix A, Figure 13). Therefore, by interpreting the base of the Duitschland, the top of the Dolomite is also interpreted in the Northern portion of the Ramotswa Project Area. Shales are typically very conductive, and the Duitschland has an interpreted approximate resistivity of > 5 Ω-m, which will contrast with the electrically resistive Dolomite (Appendix A, Figure 14).

In the Central portion of the Ramotswa Project Area, the Waterberg Supergroup ("Waterberg") is the main geologic unit that is in contact with, and stratigraphically above the Dolomite (Appendix A, Figure 15). The Waterberg is a geologic mix of conglomerates, sandstone, shales, and siltstones. While the resistivity signature of the Waterberg is mostly resistive (interpreted to be as high as approximately 800 Ω-m**),** the geologic heterogeneity of the supergroup results in varying and changing appearances in the resistivity signature within the Waterberg, which does not appear layered, like other geologic formations in the area (Magaliesberg Formation). It is interpreted that there is an unconformity contact between the Dolomite and Waterberg, where the geologic materials between the two formations have eroded. Areas of outcropped Waterberg in the Ramotswa Project Area have been interpreted with resistivities as high as 1200 Ω-m, and in some cases the outcropped Waterberg forms a distinct topographic high, like Otse Hill, in Botswana. The basis of the interpretation of the top of the Dolomite in the Central Portion of the Ramotswa project area, is a combination of the variations in resistivity signatures between the consistently resistive Dolomite and the varyingly resistive Waterberg, as well as the interpretation that in the Central portion of the Ramotswa Project Area, the Dolomite is thin and steeply dipping (Stettler, 2016) (Appendix A, Figure 16).

In the South-Central portion of Ramotswa Project Area the top of the Dolomite is bounded by several faults (Appendix A, Figure 17). Because of this, abrupt changes or offset in the AEM data are interpreted as the contact between the Dolomite and the other geologic formations (Appendix A, Figure 18). Due to the faults, the Dolomite is in contact with a variety of geologic formations that are stratigraphically above the Dolomite. The geologic formations include: the Ditlojana Volcanics, the Ditlojana Quartzite, Silverton, the Magaliesberg Formation ("Magaliesberg"), and the Woodlands Formation ("Woodlands"). The Ditlojana Volcanics (moderate), Silverton (very conductive), and the Woodlands (mixed) have interpreted resistivity signatures that differ from the Dolomite, and the observed changes in resistivity are the basis for the interpreted contact between the Dolomite and these three formations. In the case of the Ditlojana Quartzite (resistive) and the Magaliesberg (resistive), the resistivity signatures are similar to the Dolomite. However, both the Ditlojana Quartzite and the Magaliesberg both form distinct topographic highs in the project area, which aided in the interpretation of the contact between the Dolomite and these two formations.

In the Southern portion of the Ramotswa Project Area, the Penge Formation ("Penge") and the Rooihoogte Formation ("Rooihoogte") are the main geologic units that are stratigraphically above, and in

contact with the Dolomite (Appendix A, Figure 19). The Penge has an interpreted approximate resistivity of greater than 5 Ω-m, and is composed of shale and banded iron formation ("BIF"). In areas where the Penge has eroded, the Rooihoogte is in direct contact with the Dolomite. The Rooihoogte has an interpreted mixed resistivity range of approximately 5 - 500 Ω-m, due to the fact that it is comprised of a lower conglomerate (typically resistive) member, and an upper shale (typically conductive) member (Eriksson, et al., 1995). The variations in resistivity between the lower and upper members of the Rooihoogte occur in a layered manner, generally placing the more resistive, lower conglomerate member in contact with the Dolomite. The contrasts in resistivity signatures between the resistive Dolomite, conductive Penge (Appendix A, Figure 20), or mixed Rooihoogte (Appendix A, Figure 21) are the basis for the interpretation of the top of the Dolomite in the Southern portion of the Ramotswa Project Area. Additionally, in the Southern portion of the Ramotswa Project Area, the Rooihoogte corresponds to a moderate topographic high, which is used to further refine interpretations of the contact between the Rooihoogte and Dolomite.

The extent of the Ramotswa Dolomite (and by association the Ramotswa Aquifer) is based on the interpretations of the geologic contacts between the Dolomite and surrounding geologic formations (Appendix A, Figure 22 - Figure 24). The base of the aquifer is interpreted by locating a thin conductive layer (shale) between the Black Reef and the Dolomite that indicates the shale is present between the two formations. The top of the Dolomite is interpreted by locating changes in electrical resistivity signatures that are interpreted as the contact between the Dolomite and the Duitschland (Northern portion of the Ramotswa Project Area), the Penge (Southern portion of the Ramotswa Project Area), the Rooihoogte (Southern portion of the Ramotswa Project Area), and the Waterberg (Central portion of the Ramotswa Project Area). The interpretations of the contacts between the geologic formations are also based on changes in surface expressions, such as a distinct topographic high (Rooihoogte) transitioning to an area with no distinct surface expression (Dolomite). There are unique locations where the top of the Ramotswa Dolomite has been interpreted, but a bottom of the Ramotswa Dolomite has not been interpreted, XRI was unable to interpret the bottom of the Ramotswa Dolomite with confidence due to the limitations of the AEM system, geology, and physics (XRIBlue, 2016).

5. Conceptual Hydrological Model

The conceptual hydrologic model of the Ramotswa Project Area is based on the geologic interpretations of the extent of the Dolomite (aquifer material), as well as the other sixteen (16) geologic formations interpreted within the Ramotswa Project Area. The quality of the inversion results, and corresponding conceptual hydrologic model, can be evaluated by the data residuals. A data residual is calculated for each inverted AEM sounding by comparing the measured data with the calculated response from the model after inversion (SkyTEM, 2015). A residual value of 1 or less is desirable, however models producing higher residual values are still useful in the geologic interpretation of the area as a whole. Data residuals greater than 1 may be due to an inconsistency between the 1D model assumed in the inversion and the 2D/3D character of the real world. In areas of the model where the data residuals are greater than 1, XRI has high confidence in the geologic interpretations. Appendix B, includes the data residuals and interpreted geology profiles for the Ramotswa Project Area. Appendix A, Figure 25 shows that there are differences in the previously mapped surface geology versus the interpreted geology from AEM data.

An .xyz file detailing the extents of the geologic formations interpreted and associated data residuals for each interpreted AEM sounding is also included with the delivery of this report. In addition to the extent of the aquifer, structural features like dikes, fractures, faults, and collapse features present in an aquifer are useful in mapping preferential flow or no-flow boundaries in the subsurface. XRI obtained shapefiles of mapped faults and dikes in and around the Ramotswa Project Area from Botswana DGS and Council for Geoscience ("CGS") South Africa (Appendix A, Figure 26).

5.1 Dikes

Airborne magnetic data was collected as a supplemental dataset to the AEM data (Appendix A, Figure 27). Typically, intrusive dikes will be revealed in magnetic data as linear magnetic anomalies. Several linear magnetic anomalies were delineated, within the Ramotswa Project Area (Appendix A, Figure 28). Intrusive dikes can serve as either a preferential flow path for groundwater, or as an aquitard that acts as a no flow boundary. Additionally, anomalies within the AEM data were interpreted to be possible dikes throughout the Ramotswa Project Area. The resistivity signature for a possible dike is disrupted AEM data with a high residual value and no apparent surface infrastructure to create EM coupling (Appendix A, Figure 29**)**. The high residual value was the common feature, and through further discussion with Dr. Edgar Stettler on July 1, 2016, it was agreed that it is appropriate to interpret dikes in these areas (Appendix A, Figure 30). Upon delivery of this report, a .kmz file of the locations of linear magnetic anomalies and dikes interpreted from the AEM data will be included, to be viewed in Google Earth™ software.

Most of the dikes interpreted in the AEM data, are close to or in similar locations as the linear magnetic anomalies, substantiating the interpretation of these AEM anomalies as dikes. A few AEM anomalies interpreted as dikes are not in close proximity to the linear magnetic anomalies, some are located on a broad high in the magnetic data and are likely attributed to a more centralized, less linear, igneous intrusive body, and others may be attributed to faulting or other unknown complexities in the geology.

Groundwater flow implications of dikes in the Ramotswa Project Area are complex. Research on intrusive dikes in the Transvaal Basin indicate that in the subsurface they are nearly impermeable and will act as a barriers to groundwater flow (Meyer, 2014). However, near the surface the dike can be weathered, allowing groundwater to flow across (Meyer, 2014). Additionally, some of the interpreted dikes appear to be offset by faulting, which may alter the expected groundwater flow regime near the dike in the faulted area. Based on the locations of the interpreted dikes (primarily from the airborne magnetic dataset), the Dolomite can be divided into unique compartments, where groundwater flow would be restricted to (Appendix A, Figure 31). The extent of each compartment has been delineated in areas where a dike has been interpreted to continuously exist through the Dolomite, resulting in thirteen (13) unique compartments where groundwater flow may be restricted. Upon delivery of this report, a .kmz file of the locations of the dolomite compartments interpreted from the airborne magnetics data will be included, to be viewed in Google Earth™ software.

5.2 Collapse Features

Multiple collapse features are interpreted within the Ramotswa Project Area based on the AEM data (Appendix A, Figure 32). The collapse features are interpreted in areas where normally linear conductive features observed in a Dolomite formation exhibit an abrupt change in the slope (Appendix A, Figure 33). Many of these collapse features occur near an interpreted geologic contact, fault or dike, where a change in groundwater flow patterns are expected and could lead to increased porosity through dissolution of geologic materials. The collapse features are possibly due to karstification in the subsurface, which is common in the Ramotswa Project Area, and should be areas for further groundwater investigation. Upon delivery of this report, a .kmz file of the locations of the interpreted collapse features will be included, to be viewed in Google Earth™ software.

5.3 Faults

Faults can serve as preferential flow paths for groundwater. Faults were also interpreted from the AEM data, (Appendix A, Figure 34). These faults are in addition to the surface faults provided by Botswana DGS and CGS South Africa. In the AEM profiles, faults were interpreted as areas where there was a

noticeable offset or an abrupt change in the in the resistivity signature. In some instances, the interpreted faults are present in the subsurface, and did not appear to extend to the surface (Appendix A, Figure 35). Other interpreted AEM faults did extend to the surface (Appendix A, Figure 36). Upon delivery of this report, a .kmz file of the locations of the interpreted faults from the AEM data will be included, to be viewed in Google Earth™ software.

5.4 Formations Within Dolomite

The Ramotswa Dolomite consists of five unique geologic formations (from stratigraphic bottom to top): Oaktree, Monte Christo, Lyttleton, Eccles, and Frisco Formations (Appendix A, Figure 37). The five formations have varying chert content; the Monte Christo and Eccles are chert rich, and the Oaktree, Lyttleton, and Frisco are chert poor. Within the Dolomite formations, chert content is interpreted as the primary influence on aquifer quality, as the Monte Christo and Eccles are the primary water bearing formations (Janse van Rensburg, 2002). In the Northern portion of the Ramotswa Project Area (where the dolomite is the thickest), thin (10 – 30 meter) layers are present within the Dolomite with noticeably lower electrical resistivity (1 – 50 Ω-m). These thin conductive layers are interpreted to be the contact between the various formations within the Dolomite (Appendix A, Figure 38). The interpretations of the contact between the different Dolomite formations were also aided by the existing mapped surface extents. In areas where the Dolomite is the thickest, XRI was are able to interpret the extents of the Oaktree through Eccles Formations. In areas where the Dolomite is thin such as the Central portion of the Ramotswa Project Area, no specific dolomite formations were interpreted in the subsurface. In the Southern portion of the Ramotswa Project Area, the thickness of the Dolomite decreases from the North to the South. The decrease in thickness resulted in the interpretation of only the Frisco-Eccles contact (Appendix A, Figure 39).

6. Distributed Hydraulic Properties (porosity, hydraulic conductivity)

6.1 Porosity

Archie's Law (Archie, 1941) relates electrical resistivity, porosity, and soil saturation stating:

$\rho_e = a * \Phi^{-m} * S^{-n} * \rho_w$, where ρ_e is the effective resistivity (bulk resistivity of the sample), Φ is the porosity, **S** is the soil saturation or the volume fraction of pores with water, ρ_w is the apparent resistivity of the pore fluid, **a** is the tortuosity factor, **m** is the cementation exponent, and **n** is the saturation exponent.

Archie's relationship was originally derived for oil reservoir characteristics using samples that were primarily sands saturated in brine (Archie, 1941), therefore, the Archie's relationship may not directly apply to the carbonate rocks that comprise the Dolomite. Additionally, it has been shown that Archie's Law has limited applications for conductive materials (Worthington, 1993). As a result, for the Ramotswa Project Area, a simplified version of the Archie's equation was used for calculating the porosity of carbonates, where $\Phi^{-m} = \rho_e / \rho_w$ (Lucia, 1983). Lucia asserts the range of "m" values for carbonates is 1.8 - 3.0. Due to the lack of porosity data available of the Dolomite, and the heterogeneity of the Dolomite in the Ramotswa Project Area, it was determined that a median value of 2.4 would be used for m. Furthermore, the Kansas Geological Survey has previously recommended an "m" value of 2.3 for carbonates (Doveton, 1999).

Electrical fluid conductivity within boreholes in the Ramotswa Project Area were provided by the Department of Water and Sanitation ("DWS"), South Africa (Altchenko, 2016) and were used to estimate the resistivity of the pore fluid in the Dolomite. The list of boreholes was edited to include only boreholes with electrical resistivity data in the Dolomite based on the interpreted geologic model. The electrical conductivity of the pore fluids was converted to electrical resistivity, revealing an average resistivity of 17.9 Ω-m throughout the Ramotswa Project Area (Appendix A, Figure 40). The Ramotswa Project Area was divided into four (4) regions for fluid resistivity gridding. The boundary between region one and two is a magnetic anomaly that appeared to be a boundary between different fluid resistivity ranges, and therefore a possibly no-flow boundary. The other regions were selected based on the distribution of the borehole information (Appendix A, Figure 41). The fluid resistivities in each region was gridded using minimum curvature and a 200 meter cell size, providing estimated fluid resistivity values throughout each region (Appendix A, Figure 42).

The electrical resistivity data of the Dolomite (from the AEM data), electrical resistivity of the pore fluid, and an "m" value of 2.4, were applied to the Lucia simplification of Archie's Law to estimate porosity for the Dolomite throughout the Ramotswa Project Area (Appendix A, Figure 43 – Figure 45). It was interpreted that due to limitations of Archie's Law for conductive materials (Worthington, 1993), and the likely presence of shales (conductive material) between the Dolomite Formations, a resistivity threshold needed to be applied for the porosity estimates. After applying multiple resistivity thresholds and examining the resultant porosity estimates, it was interpreted that 40 Ω-m was an appropriate threshold. AEM resistivities lower than 40 Ω-m were excluded from porosity calculations due to these limitations. Appendix C includes the final porosity estimates along the flight lines where the Dolomite has been interpreted within the Ramotswa Project Area. Additionally, a .xyz file is included with this report that contains all porosity estimates for the Dolomite.

Within the Ramotswa Project Area, there are anomalous porosity estimates that are greater than 50%. The anomalous porosity estimates may be in areas where significant karstification has occurred, or an area of increased clay content where Archie's law may not apply. The transitions between the different dolomite formations appear to have higher clay content, leading to a decrease in resistivity, but they are also host to interpreted collapse features. It is possible that transitions between the different dolomite formations may have unrealistic porosity estimates. Porosity estimates that are beneath the DOI values are invalid as they are beyond the resolution of the AEM system.

If additional borehole data is collected in the future within the Ramotswa Project Area, specifically resistivity of the pore fluid in the Dolomite, the porosity estimates can be recalculated. The new pore fluid resistivity data would need to be incorporated into the existing pore fluid resistivity dataset. The pore fluid resistivity grid would be recreated for the 4 pore resistivity regions. Then the porosity estimates could be recalculated using the Lucia equation.

6.2 Hydraulic Conductivity

Transmissivity values determined for wells in the Ramotswa Well Field, from both constant rate and step pumping tests (Carlsson, 2006), were extrapolated over field and used in conjunction with the AEM resistivity data to calculate the distribution of estimated hydraulic conductivity for the Dolomite Aquifer. The distribution of hydraulic conductivity in the Dolomite Aquifer has been geoelectrically estimated by applying a generalized log-log linear electrical-hydraulic correlation function, the slope of which is dependent on the geologic and geochemical environment (Purvance & Andricevic, 2000). For a porous medium in which the majority of subsurface electrical conduction is attributed to pore fluid ionization, as is expected with the Dolomite Aquifer, Purvance suggests that the electrical and hydraulic ("eh") correlation function will have a negative slope. An electrically conductive geologic matrix, with an

abundance of smaller grain sized material and increased pore surface area, is shown to have a positive "eh" correlation.

Lithology information was obtained for production well numbers 4358, 4422 and 4423 from the Botswana DGS (Kealeboga, 2016), and other monitoring wells for which there is no corresponding pump test data. Lithology information was obtained for well 4358 and nearby monitoring well 4972. Both wells were drilled to depths greater than 100 meters ("m"), but did not penetrate the Dolomite Aquifer according to the lithology logs. Production wells 4373 and 4340 are also not representative of the Dolomite Aquifer, and were excluded from the calculations of the distribution of estimated hydraulic conductivity.

The electrical resistivity values from the AEM survey, were gridded in 3 dimensions using an ordinary, point estimation, kriging algorithm with a cell size of 250 m in the horizontal directions (X and Y), a 10 m cell size in the vertical direction (Z), an isotropic search radius of 1,000 m, 5 search expansions, and 2 gridding passes, allowing for a minimum of 1 data point to produce a non-null grid node. This extrapolated the AEM derived resistivity model to a sufficient distance from the flight lines to obtain a mean bulk conductivity value for the Dolomite Aquifer at the analyzed wells over the saturated portion of the aquifer. A series of best fit linear functions were used to determine the possible constants and coefficients for the lol-log linear relationship between the natural logarithm of hydraulic conductivity and natural logarithm of electrical conductivity for the analyzed wells.

Distributed hydraulic conductivity estimates were calculated for all AEM resistivity models within the interpreted Dolomite Aquifer and the statistical distribution for various log-log, linear function constants and coefficients. The locations, elevations, provided transmissivity values, well depths, resting water level at the time of pump testing, saturated thickness of the aquifer, calculated hydraulic conductivity, extrapolated bulk resistivity & conductivity values, and distance from the nearest AEM flight line for all boreholes used in the hydraulic conductivity distribution estimations and as well as the graphical and statistical analysis of various well data subsets are presented in Appendix A, Figure 46. Applying the derived relationship from production wells 4336, 4337, Z4400, and 4349 to all AEM derived electrical resistivity values of the subsurface interpreted to be within the Dolomite Aquifer yields the delivered distribution of estimated hydraulic conductivity for the Dolomite throughout the Ramotswa Project Area (Appendix A, Figure 47 - Figure 49, and Appendix D). Additionally, a .xyz file is included with this report that contains all hydraulic conductivity estimates for the Dolomite in Appendix D. The .xyz file uses the WGS84 UTM Zone 35 South coordinate system with an X, Y, and Z unit of meters.

It has been acknowledged that the Notwane River served as a positive boundary during the pumping tests which occurred in spring (Carlsson, 2006), but other groundwater flow direction analysis (Staudt, 2003) suggests that the river acts as a gaining stream and thus negative boundary, throughout the dry seasons. Temporally varying boundary conditions coupled with the complexities introduced by transition of the Dolomite Aquifer at outcrop to a subsurface formation, and the widely recognized karstification and subsequent implications of aquifer anisotropy lead to the estimated hydraulic conductivity distribution of the Dolomite Aquifer over the Ramotswa Project Area to be an example of the application of the distribution of the AEM data set when augmented with sufficient complimentary data sets. The data required to develop substantial correlations between geoelectrical and hydraulic properties is lacking. It is the professional recommendation of XRI Blue that the estimated hydraulic properties presented are used only as a guide. These estimates will need to be refined and recalculated as more data becomes available.

To recalculate and refine the hydraulic conductivity estimates, additional pump or slug tests of wells in the Dolomite would need to be carried out. If pump tests of two nearby wells with recorded screened intervals within the same formation within Dolomite (i.e. both screened in the Eccles Formation) are performed, the hydraulic conductivity of the Dolomite can be estimated for that particular area. Due to

the heterogeneity of the Dolomite throughout the Ramotswa Project Area, it is recommended that multiple pump tests be carried out at various locations and at various screened intervals within the Dolomite formations to re-estimate a more accurate distribution of hydraulic conductivity throughout the Ramotswa Project Area.

7. Proposed Hydrogeological Data Parameters for the Digitized Model

Within the digitized model, the following hydrogeological parameters have been interpreted or estimated. The tops and bottoms of the 17 simplified geologic formations were interpreted within the Ramotswa Project Area based on the AEM data, surface geology maps, limited borehole lithology near the city of Ramotswa, surface expressions, and XRI's experience of interpreting geologic boundaries from geophysical data. The interpretation of the extent of the Dolomite is critical, as it is the primary water bearing unit in the Ramotswa Project Area. In addition to interpreting the tops and bottoms of the various geologic formations, geologic contacts between the unique formations within the Dolomite are interpreted where possible. Geologic structures are interpreted from the AEM data, including faults, dikes, and collapse features. Faults generally serve as either preferential flow paths, but can also act as no flow boundaries for groundwater. The dikes could be impermeable in the subsurface, and act as no flow boundaries for groundwater. The interpreted collapse features may be area(s) where substantial groundwater could collect.

Using a modified version of Archie's Law, porosity estimates were made for the extent of the Dolomite within the Ramotswa Project Area where resistivities were greater than 40 Ω-m. The calculation of porosity estimates was made possible by calculating and gridding the resistivity of the pore fluid in the Dolomite based on borehole data provided by CSG South Africa.

8. Model Grid for a 3D Hydrological Model

Based on the geophysical interpretations of the extent of the different geologic formations, dikes, faults, and collapse features, a hydrological model has been produced and is included as an attachment to this report. The hydrological model uses the WGS84 UTM Zone 35 South coordinate system with an X, Y, and Z units of meters. Due to the complexity of the interpreted geology throughout the Ramotswa Project Area, gridding of the spatially coarse interpreted formation tops and bottoms is not advisable. Additionally, the added structural variations like faults, dikes, and collapse features increase the geologic complexity of the Ramotswa Project Area, resulting in geologic structure inconsistencies when attempting to grid the spatially coarse interpreted formation tops and bottoms (Appendix A, Figure 50).

Gridding of sparse subsurface geologic information is best accomplished where formations are sequentially layered, with minimal subsurface offsetting or change in structural dip. In situations where geologic complexity exists such that a "layer-cake" earth model is not an accurate description of the geologic structure, extreme discretion should be used with the application of any automated gridding algorithms to ensure adherence to the known geologic structure. Application of a variety of gridding algorithms to all interpreted geologic formation contacts across the entire project area yielded the conclusion that most gridding algorithms better adhered to the known geologic structure in areas with denser AEM data coverage. The geologic formation grids provided for the two smaller areas (Appendix A, Figure 50) have been extensively edited, to more accurately represent the complex geologic structure of the Ramotswa Project area. The two smaller areas were selected based on the lack of geologic complexity (i.e. presence of faults, dikes, or collapse features) and density of AEM data coverage within the areas. The lack of geologic complexity and spatially dense data coverage in these unique areas resulted in more geologically realistic grids of the formation tops and bottoms using automated gridding algorithms. The interpreted geologic formation boundaries were initially calculated using the Oasis

Montaj minimum curvature gridding algorithm, with a 100 m cell size. The grids were calculated with a starting coarseness of 16 times the grid cell size, reducing in size with iteration until 99% of the gridded data passed a 1% data tolerance threshold, with a maximum number of 100 iterations. The grids were extended to seven grid cells beyond the convex hull of the gridded data set. The formation grids were trimmed to the two smaller areas prior to any manual editing.

Manual editing of the geologic formation grids included removal of points from the initial grids where basic geologic structure was not accurately modeled. This was done based on formation outcrops, fault structures, formation thicknesses, and dip angles. The manually edited grids were then re-gridded through the removed sections using an Encom PA algorithm that progressively extrapolates the remaining grid data from the outer rim of all holes in the grid towards the center of the hole. Upon completion of manual editing and re-gridding interpolation, a single pass of a three by three ("3x3") average smoothing filter was selectively applied to certain areas of the formations grids. All formation grids have been trimmed to a bottom depth that was determined by applying (within the Encom PA software) a total of four passes of a nine by nine ("9x9"), Gaussian Smoothing Kernel with a standard deviation of one, to the lower depth of investigation grid calculated in Oasis Montaj using the above mentioned minimum curvature gridding algorithm, with a 100 m cell size. In addition to the grids provided within the two smaller areas, a representative schematic of the extent of the Dolomite was created (Appendix A, Figure 51). The representative schematic is not to scale, and is not an accurate description of the geologic structure the Dolomite throughout the Ramotswa Project Area. Caution should be used in presenting this schematic in future work, however it can serve as a useful tool to display an approximation of the extent of the Dolomite.

9. Conclusions and Recommendations

The geology of the Ramotswa Project Area is very complex, with structural features including faults, dikes, and collapse features. The geology and structural features have been successfully interpreted from the AEM data. Due to the geologic complexity of the Ramotswa Project Area, attempts to grid the spatially coarse interpreted geologic formation tops and bottoms across the Ramotswa Project Area, results in geologically invalid representations. Within smaller sections of the Ramotswa Project Area, the interpreted tops and bottoms of the present geologic formations have been gridded. It is interpreted that within these unique areas, the grids are geologically valid, and can be used as an input into a groundwater model. The interpretations detailed in the report have been made based on XRI's extensive experience of interpreting subsurface geology and hydrogeology from AEM data. The interpretations made by XRI are in line with current standards of the geophysical industry, and in-house quality control. Data residuals for the AEM inversions are provided in the .xyz file of geologic interpretations and should be used as a guide for a certainty of the conceptual model.

Due to the limitations of Archie's Law for conductive materials, and areas of lower resistivity within the Dolomite, porosity estimates were not calculated for materials with resistivities less than 40 Ω-m. There are porosity estimates that are greater than 50%, which are interpreted to be anomalous porosity estimates that may further be the results of the higher conductivity limits of Archie's equation, or possibly increased karstification. If additional fluid porosity borehole data in the dolomite were to be collected in the Ramotswa Project Area, it could be used to further refine the porosity estimates and potentially reduce anomalous porosity estimates.

The hydraulic conductivity of the Dolomite was estimated using pump test data collected in the Ramotswa Well Field in 2005, and the porosity estimates detailed in this report. The extrapolation of the relationship between porosity and hydraulic conductivity in the Ramotswa Well Field throughout the entire Ramotswa Project Area, may result in anomalous and unrealistic estimates of the hydraulic conductivity. The hydraulic conductivity estimates throughout the Ramotswa Project Area could be

improved if additional hydraulic data were collected through pump tests between two neighboring wells with recorded screened intervals within the same formation. Due to the heterogeneity of the Dolomite throughout the Ramotswa Project Area, it is recommended that multiple pump tests be carried out at numerous locations.

Due to the limited availability and poor spatial distribution of hydraulic properties data collected in the Ramotswa Project Area prior to AEM data acquisition, the porosity and hydraulic conductivity estimates that have been calculated may be unrealistic. Additionally, the heterogeneity of the Ramotswa Dolomite, as well as Archie's Law limitations when applied to carbonate rocks can further contribute to skepticism when analyzing the estimated hydraulic properties. XRI recommends that further ground data must be collected for the Ramotswa Dolomite with the Ramotswa Project Area, specifically pore fluid resistivity and pump testing, to refine the porosity and hydraulic conductivity estimate distributions. As additional ground data related to hydraulic properties is collected and incorporated to the existing AEM data, the hydraulic property distributions can be recalculated to yield more realistic porosity and hydraulic conductivity estimates.

References

Altchenko, Y., 2016. *Digital well data in an ESRI shapefile format received electronically,* s.l.: Botswana Department of Water Affairs.

Archie, G. E., 1941. The Electrical Resistivity Log as an Aid in Determining Some Reservoir Characteristics.. *Petroleum Technology 1,* pp. 55-62.

Carlsson, L., 2006. *Ramotswa: Test Pumping of Production Boreholes Well Field Pump Testing,* Gabarone: Unpublished Report, digital copy provided by Dr. P. Kenebatho, University of Botswana.

Catuneanu, O. & Eriksson, P. G., 1999. The sequence stratigraphic concept and the Precambrian rock record: an example from the 2.7-2.1 Ga Transvaal Supergroup, Kaapvaal craton. *Precambrian Research,* Issue 97, pp. 215-251.

Doveton, J. H., 1999. *Basics of Oil & Gas Log Analysis,* s.l.: Kansas Geological Survey.

Eriksson, P. G. et al., 1995. Architectural elements from Lower Proterozoic braid-delta and high-energy tidal flat deposits in the Magaliesberg Formation, Transvaal Supergroup. *South Africa Sediment Geology,* Issue 97, pp. 99-117.

Janse van Rensburg, H., 2002. *Determination of Aquifer Abstraction Potential of the Uitvalgrond Dolomitic Area Near Zeerust, Project Report,* Pretoria, South Africa: AquiSim Consulting (Pty) Ltd,.

Kealeboga, D., 2016. *Ramotswa Boreholes,* Lobatse: Unpublished Document, Department of Geological Survey, Botswana.

Lucia, F. J., 1983. Petrophysical Parameters Estimated from Visual Descritpions of Carbonate Rocks: A Field Classification of Carbonate Pore Space. *Society of Petroleum Engineers of AIME,* Volume SPE-10073, pp. 629-637.

Meyer, R., 2014. *Hydrogeology of groundwater region 10: The Karst Belt,* s.l.: Report to the Water Research Commission.

Obbes, A. M., 2001. *Report on Kanfontein Borehole BHW 289,* s.l.: Council for Geosciences, South Africa.

Pollack, G. D., J, K. E. & A, B., 2009. U-Th-Pb-REE systematics of organic-rich shales from the ca. 215 Ga Sengoma Argillite Formation, Botswana: Evidence for oxidative continental weathering during the Great Oxidation Event. *Chemical Geology,* Issue 260, pp. 172-185.

Purvance, D. & Andricevic, R., 2000. On the Electrical-Hydraulic Conductivity Correlation in Aquifers. *Water Resources Research,* 36(10), pp. 2905-2913.

SkyTEM, 2015. *SkyTEM Survey: British Columbia, Canada, Data Report,* Aarhus: SkyTEM.

Staudt, M., 2003. *Environmental Hydrogeology of Ramotswa; South East District, Republic of Botswana,* Lobatse: Department of Geological Survey, Botswana, Environmental Geology Division.

Stettler, D. E., 2016. *Ramotswa Geologic Interpretation Discussion* [Interview] (1 July 2016).

Worthington, P. F., 1993. The uses and abuses of the Archie equations, 1: The formation factor-porosity relationship. *Journal of Applied Geophysics,* Issue 30, pp. 215-228.

XRIBlue, 2016. *Geophysical QA/QC Corrected, and Final Inverted AEM Data Report for the Development of Subsurface Mapping for the Transboundary Ramotswa Aquifer that is part of the Limpopo River Basin, using Airborne Geophysics,* Midland: XRIBlue.

Appendix A: Figures

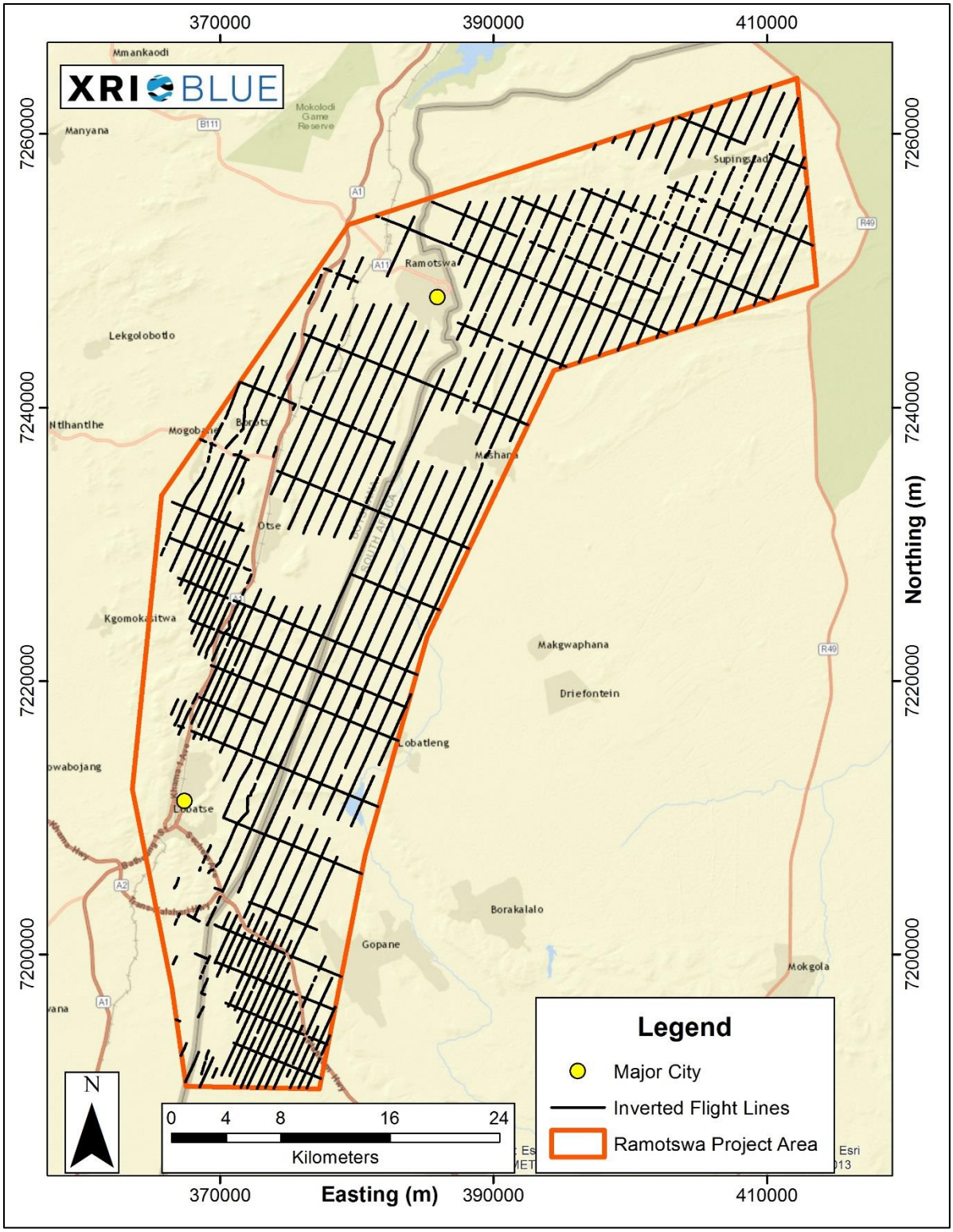

Figure 1: Inverted flight lines within the Ramotswa Project Area.

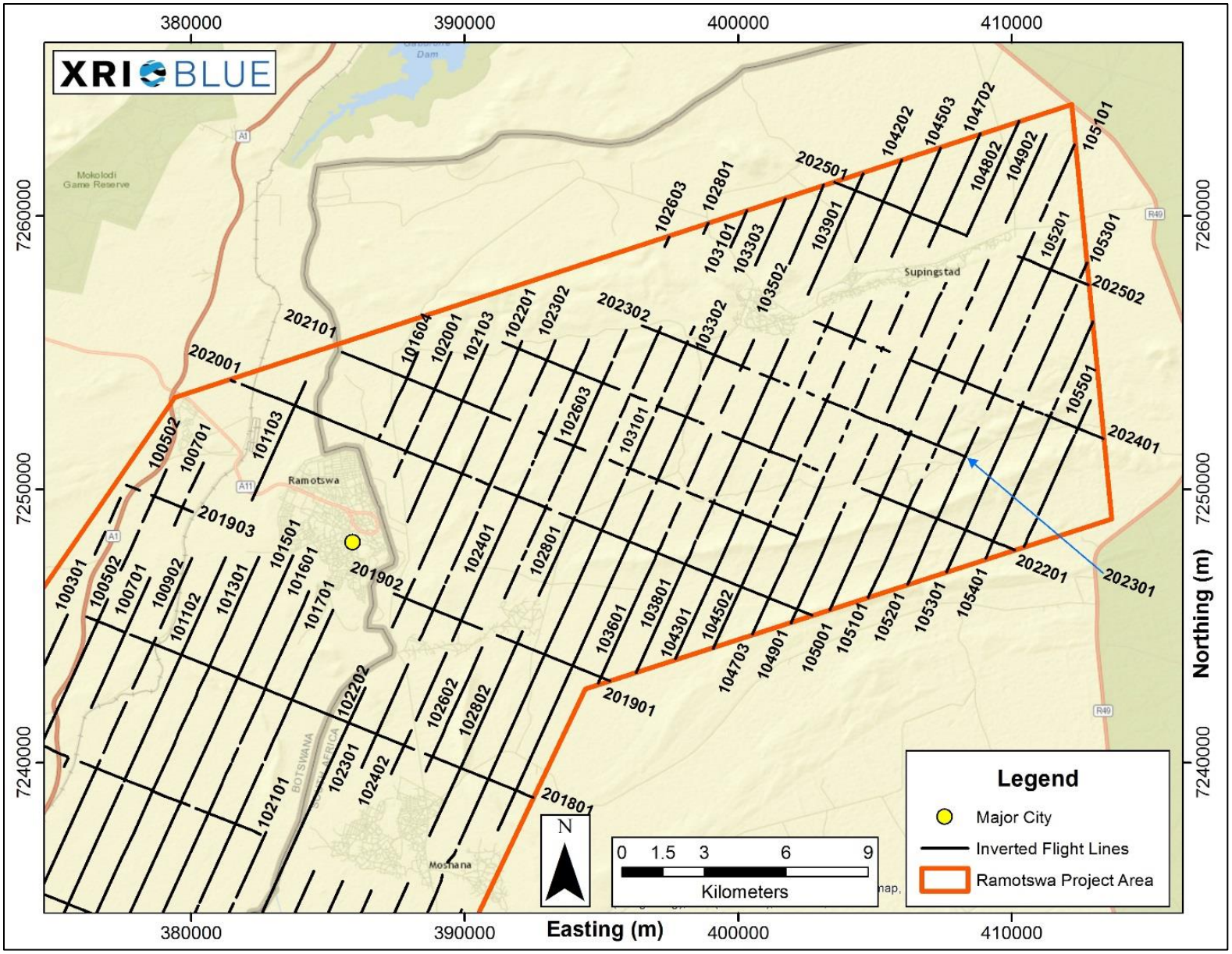

Figure 2: Labeled inverted flight lines in the Northern portion of the Ramotswa Project Area.

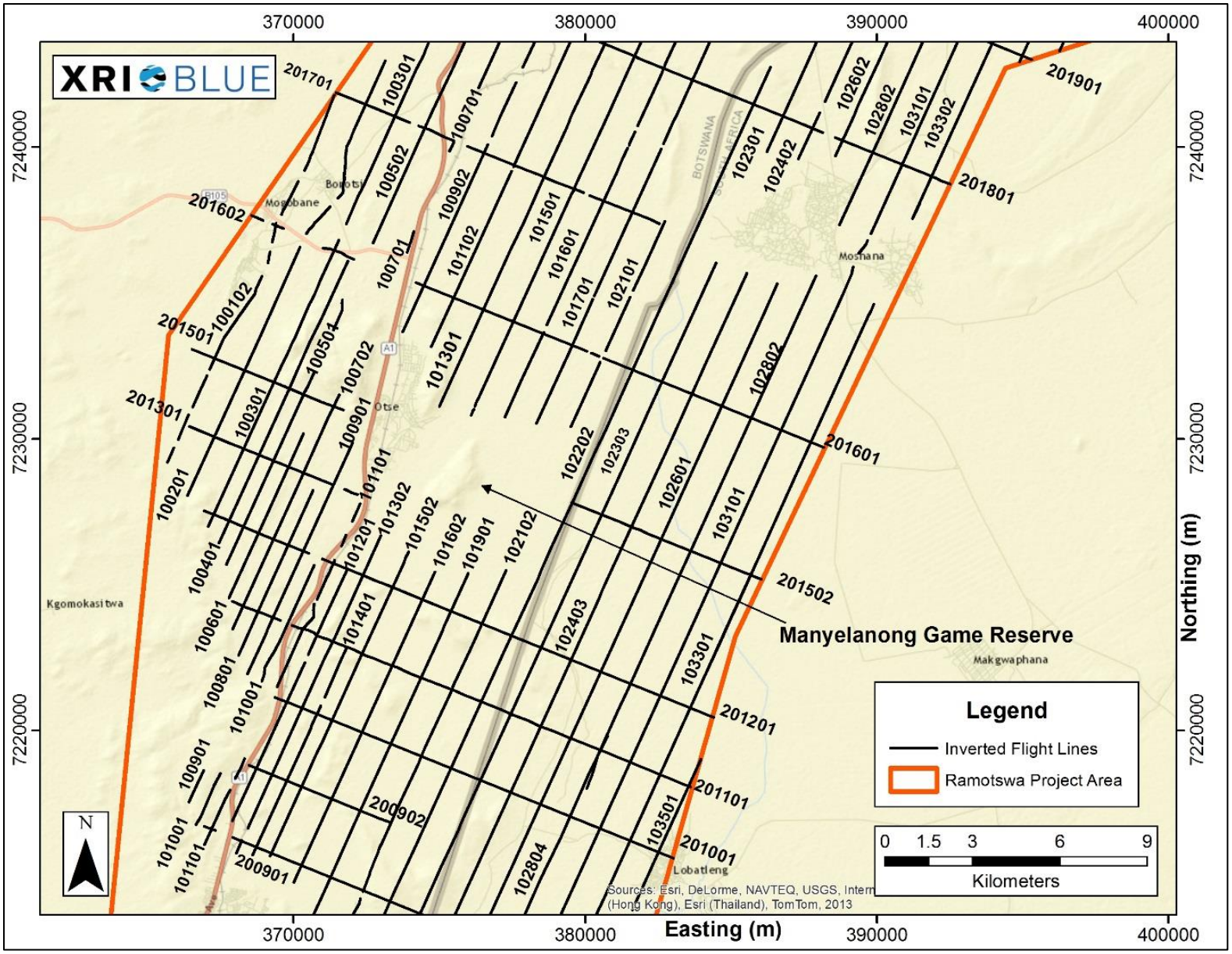

Figure 3: Labeled inverted flight lines in the Central portion of the Ramotswa Project Area.

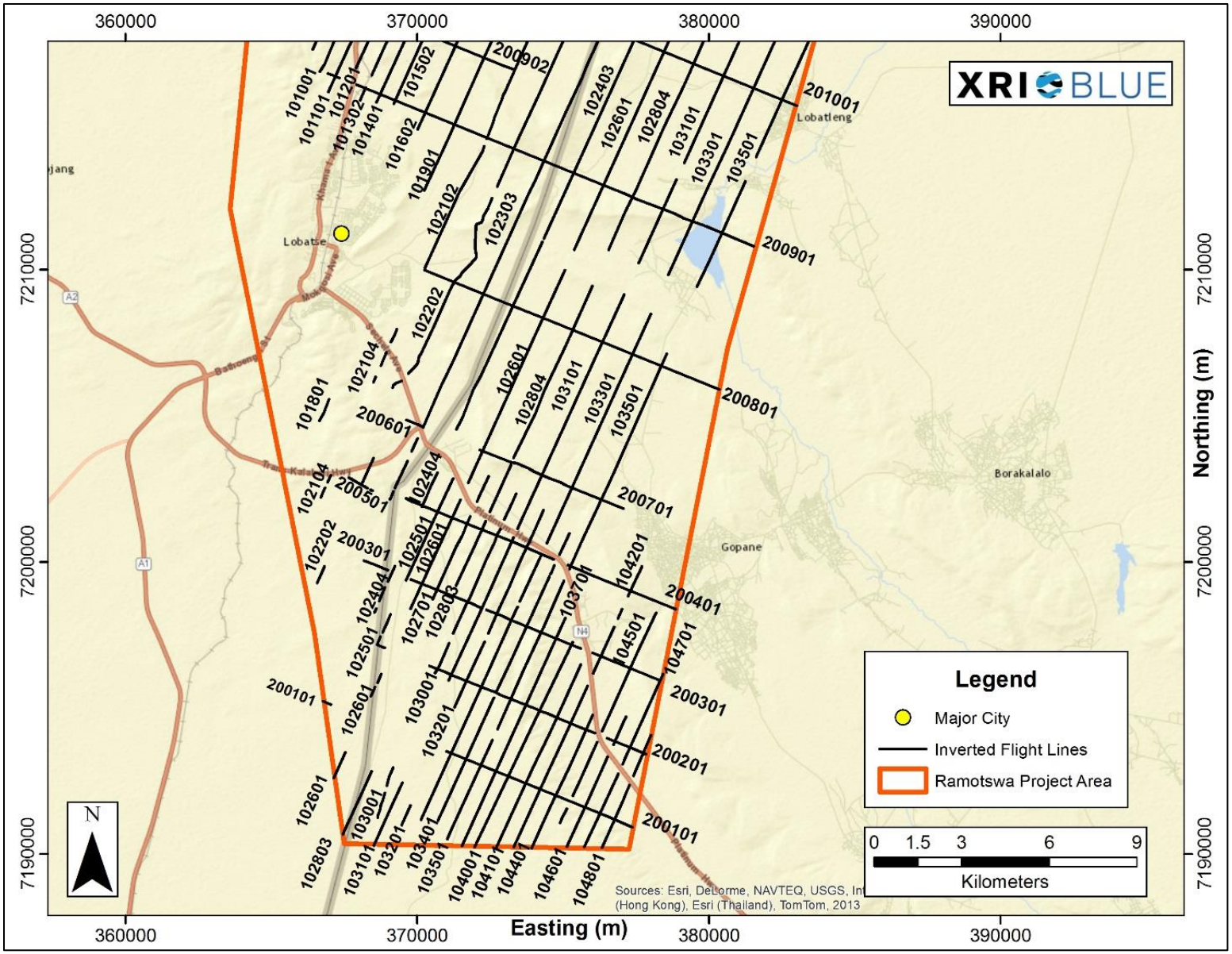

Figure 4: Labeled inverted flight lines in the Southern portion of the Ramotswa Project Area.

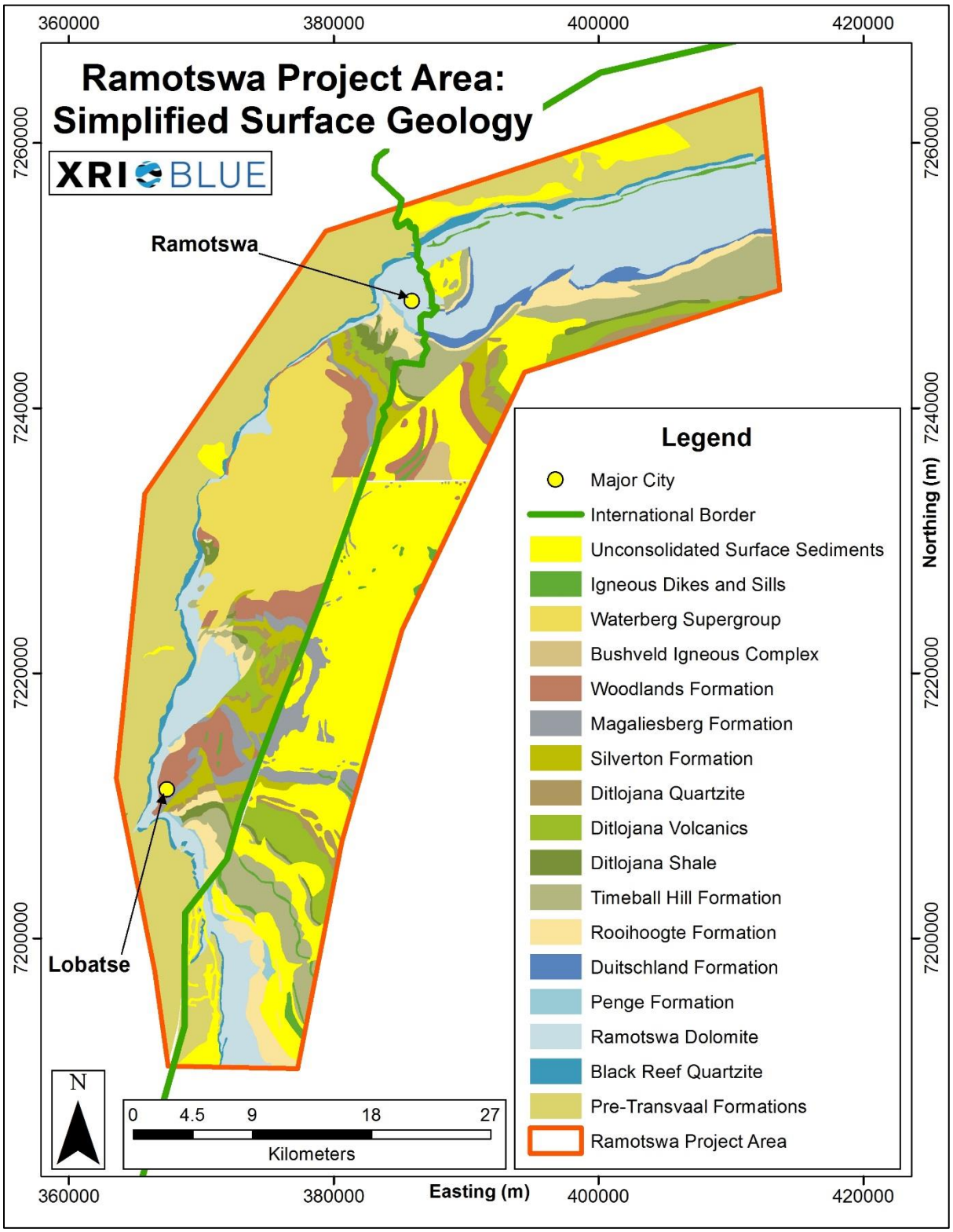

Figure 5: Simplified surface geology map of the Ramotswa Project Area.

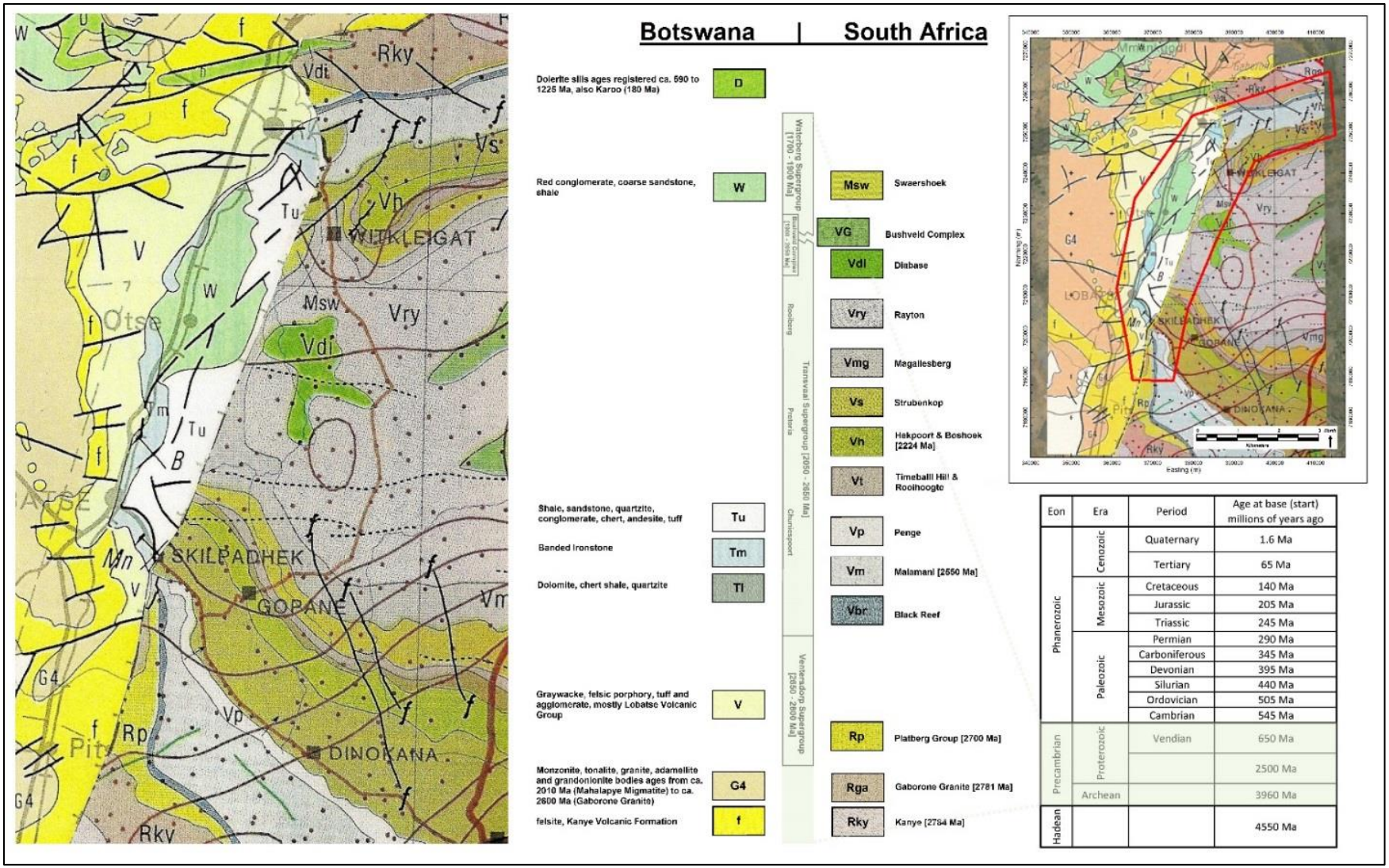

Figure 6: Merged 1:1,000,000 scale geology maps of the Ramotswa Project Area, indicating discrepancies in mapped geologic units across the international border (From XRI's Hydrogeological Report submitted January, 2016).

Figure 7: Stratigraphic column of the seventeen (17) simplified surface geologic formations in the Ramotswa Project Area.

Simplified Geologic Name	Other Geologic Formations or Units Included	General Geologic Description	Expected Resistivity Signature
Unconsolidated Surface Deposits	NA	Alluvium	Mixed
Igneous Dikes and Sills	NA	Dolerite diabases, sills, and dikes	Conductiuve
Bushveld Igneous Complex	Rooiberg Group	Volcanics and minor shales	Mixed
Waterberg Supergroup	Manyelanong, Maladiepe, Moeding, and Ditsotswane Formations	Conglomerate, sandstone, shales, and siltstones	Resistive
Woodlands Formation	Rayton Formation	Sandstones, shales, and volcanics	Mixed
Magaliesberg Formation	Sengoma Quartzite Formation	Sandstone	Resistive
Silverton Formation	Sengoma Argillite Formation	Shales and volcanics	Very Conductive
Ditlojana Quartzite	Daspoort, Strubenkop, and Dwaalheuwel Formations	Shale/siltstone and sandstone	Resistive
Ditlojana Volcanics	Hekpoort Formation	Andesite	Moderate
Ditlojana Shale	Boshoek Formation	Shale/ siltstone, sandstones and conglomerates	Moderately Conductive
Timeball Hill Formation	Tsokwane Quartzite	Shale/siltstone and sandstone	Very Resistive
Rooihoogte Formation	Lephala Formation	Conglomerate and shale/siltstone	Layered Variations
Duitschland Formation	Ramotswa Shale	Carbonaceous mudrocks, limestone, and dolomite	Very Conductive
Penge Formation	Ramotswa Shale	BIF and Shale	Very Conductive
Ramotswa Dolomite	Oaktree, Monte Christo, Lyttleton, Frisco, Eccles, Maholobota, and Magopance Formations	Dolomite	Resistive
Black Reef Quartzite	NA	Quartzite	Resistive
Pre-Transvaal Formations	Ventersdorp Supergroup,Kanye Volcanics, Lobatse Group, Mogobane, and Nmywane Formations	Clastic sediments and volcanics	Mixed

Figure 8: Table with simplified geologic unit name, other geologic formations included in a simplified geologic unit, general geologic description, and expected electrical resistivity signature of the simplified geologic unit.

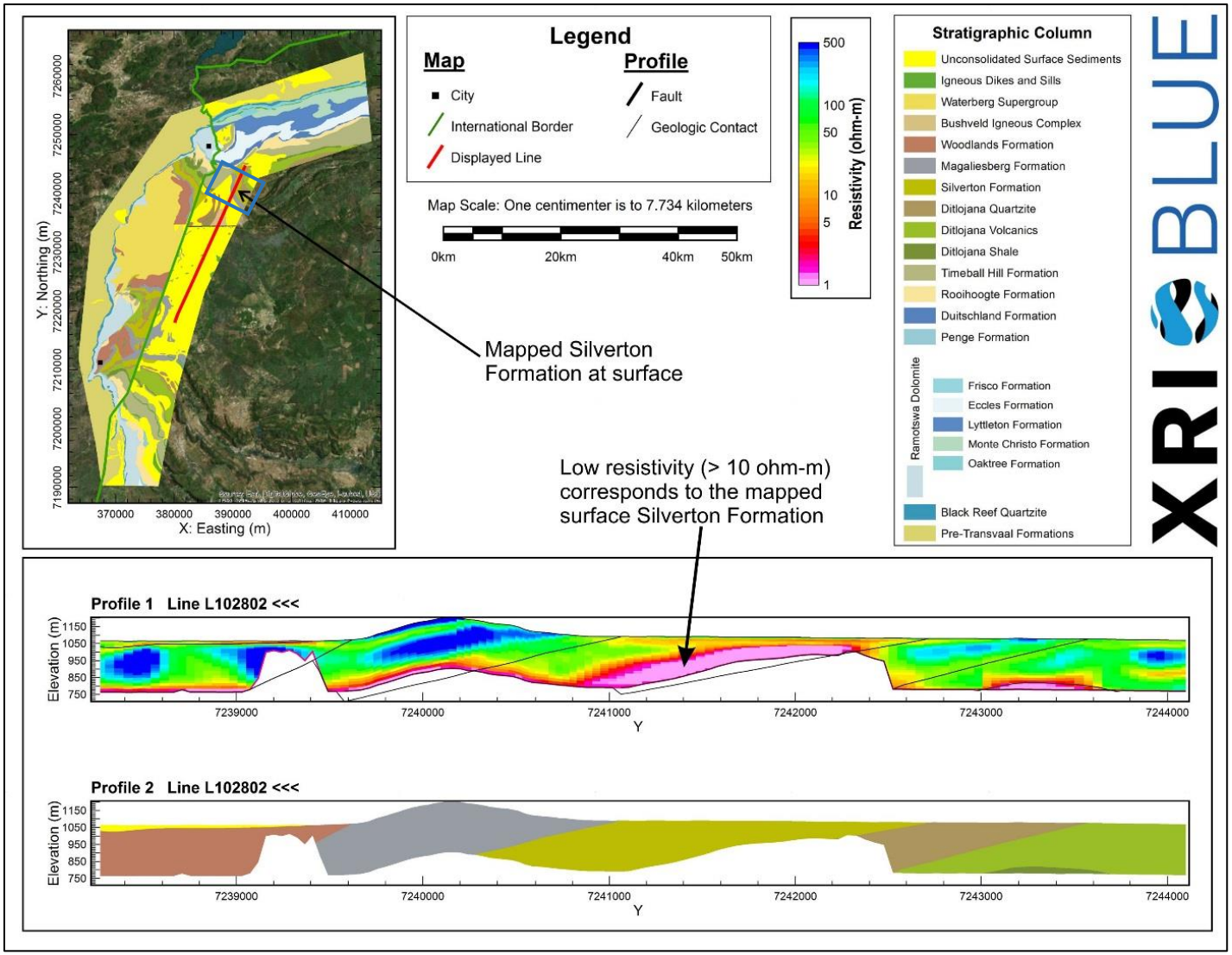

Figure 9: Interpreted conductive resistivity signature of the Silverton Formation based on surface geology mapping using AEM profile L102802. The Silverton Formation was mapped at the surface from an approximate Northing (Y) of 7,240,750 – 7,243,850 meters, and has been interpreted to have a surface expression from an approximate Northing (Y) of 7,241,060 – 7,242,710 meters. The low (> 10 Ω-m) resistivity feature that is interpreted to be the Silverton Formation is the large pink area in the AEM profile. The blue rectangle on the geologic map in the upper left of the figure, show the approximate extents of what is displayed in the resistivity and interpreted geology profiles.

Simplified Geologic Name	General Geologic Description	Interpreted Resistivity Signature	Justification of Interpreted Resistivity Signature	Corresponding Surface Feature	Representative Example
Unconsolidated Surface Deposits	Alluvium	Mixed (20-600 Ωm)	Surface sediments are commonly thin, only located in shallow subsurface, and will have a contrasting electrical signature with underlying litholgy	Little to no topographic variations	L201502 (upper 20 m of entire profile)
Igneous Dikes and Sills	Dolerite diabases, sills, and dikes	Inconclusive, indicated by high AEM data residuals	No clear resistivity signature, but due to the model being unable to recover the signal, AEM data will have higher residuals, and AEM data in the area of the dike or sill will be smoothed through the igneous features	NA	L102804 (approx. Northing of 7,204,550 - 7,204,750 meters)
Bushveld Igneous Complex	Volcanics and minor shales	Mixed (20-1000 Ωm)	Volcanics commonly have varying resistivities, and conductive shales will result in a decrease in resistivity.	NA	L101301 (approx. Northing of 7,232,350 - 7,236,8000 meters)
Waterberg Supergroup	Conglomerate, sandstone, shales, and siltstones	Resistive (20-800 Ωm)	Areas with outcropped Waterberg are highly resistivity, and areas with surface Waterberg are resistive	Some formations of this supergroup have distinct topographic highs (hill)	L101102 (approx. Northing of 7,233,150 - 7,243,600 meters)
Woodlands Formation	Sandstones, shales, and volcanics	Mixed (50-1500 Ωm)	The three lithologies comprising the Woodlands are known to have different electrical signatures: sandstones (resistive), shales (conductive), volcanics (mixed)	NA	L200901 (approx. Easting of 369,240 - 372,250 meters)
Magaliesberg Formation	Sandstone	Resistive (100-800 Ωm) in distinct layers	Sandstones are commonly resistive in resistivity data	Distinct topographic high (hill)	L102303 (approx. Northing of 7,211,210 - 7,218,430 meters)
Silverton Formation	Shales and volcanics	Very Conductive (< 10 Ωm)	Shales are commonly very conductive in resistivity data	Typically errods to a topographic low	L102802 (approx. Northing of 7,240,270 - 7,242,710 meters)
Ditlojana Quartzite	Shale/siltstone and sandstone	Resistive (As high as 1200 Ωm)	Quartzites are commonly resistive in resistivity data, no mention of unit being water bearing to decrease resistiivty	Distinct topographic high (hill)	L101501 (approx. Northing of 7,243,100 - 7,243,710 meters)
Ditlojana Volcanics	Andesite	Moderate (20-400 Ωm), with weathered shale surface	Volcanics commonly have varying resistivities, but weathered shale at top of formation yields a thin conductive signature	NA	L200801 (approx. Easting of 370,990 - 380,360 meters)
Ditlojana Shale	Shale/ siltstone, sandstones and conglomerates	Conductive (< 20 Ωm)	Shales are commonly very conductive in resistivity data	NA	L202001 (approx. Easting of 399,250 - 400,720 meters)
Timeball Hill Formation	Shale/siltstone and sandstone	Very Resistive (300-1000 Ωm)	Includes a quartzite (metamorphosed sandstone) member, quartzites are commonly resistive in resistivity data. For the purpose of this project, XRI has decided that the upper mudrocks in the Timeball Hill Formation are classified as the Ditlojana Shale	Distinct topographic high (hill)	L200701 (upper 150 - 200 meters of profile)
Rooihoogte Formation	Conglomerate and shale/siltstone	Mixed (5-500 Ωm)	Lower conglomerate member is resistive, and upper shale/siltstone member is conductive. Conglomerates are commonly resistive in resistivity data, and shales/siltstones are commonly conductive in resistivity data	Moderate topographic high in southern portion of the project area	L103301 (approx. Northing of 7,198,770 - 7,204,440 meters)
Duitschland Formation	Carbonaceous mudrocks, limestone, and dolomite	Very Conductive (< 5 Ωm)	Mudrocks are prominent in the formation, and mudrocks are commonly very conductive in resistivity data	NA	L104301 (approx Northing of 7,248,800 - 7,250,200 meters)
Penge Formation	BIF and Shale	Very Conductive (< 5 Ωm)	Shales and BIFs are commonly very conductive in resistivity data	NA	L204001 (approx. Easting of 371,360 - 376,740 meters)
Ramotswa Dolomite	Dolomite	Resistive (As great as 13000 Ωm)	Dolomites are typcially resistivite. Additionally, there is a thin layer of shale (conductive) between the base of dolomite and top of Black Reef Quartzite, which was used as an indicator of the base of Ramotswa Dolomite	NA	L102801 (approx. Northing of 7,248,470 - 7,254,800 meters)
Black Reef Quartzite	Quartzite	Resistive (As great as 900 Ωm)	Quartzites are commonly resistive in resistivity data	Distinct topographic high (hill)	L201101 (approx. Easting of 368,420 - 369,545 meters)
Pre-Transvaal Formations	Clastic sediments and volcanics	Mixed (10-800 Ωm)	Clastic sediments (resistive) and eroded volcanics (conductive) typically have mixed resistivities in resistivity data.	NA	L100102 (entire profile)

Figure 10: Table with simplified geologic name, general geologic description, interpreted resistivity signature, justification of resistivity interpretation, any corresponding surface feature, and a representative example for each of the simplified surface geologic units.

Figure 11: Mapped surface locations of the Black Reef Quartzite relative to the Ramotswa Dolomite in the Ramotswa Project Area.

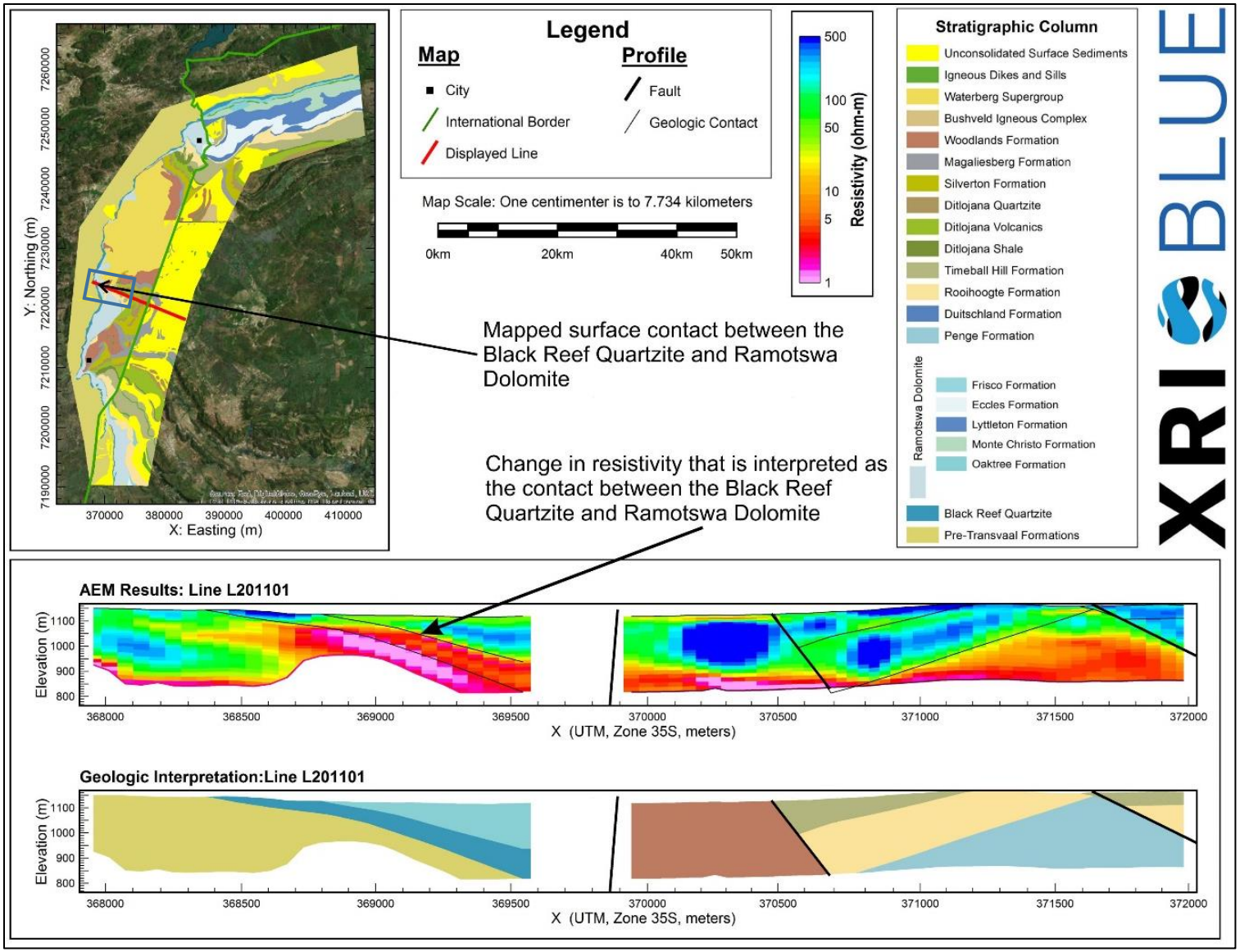

Figure 12: Example of interpreted contact between the Black Reef Quartzite and the Ramotswa Dolomite in AEM profile L201101. The contact between the Black Reef Quartzite and Ramotswa Dolomite has been interpreted to be at the change in resistivity from an approximate Easting (X) of 368,790 – 369,545 meters. The blue rectangle on the geologic map in the upper left of the figure, show the approximate extents of what is displayed in the resistivity and interpreted geology profiles.

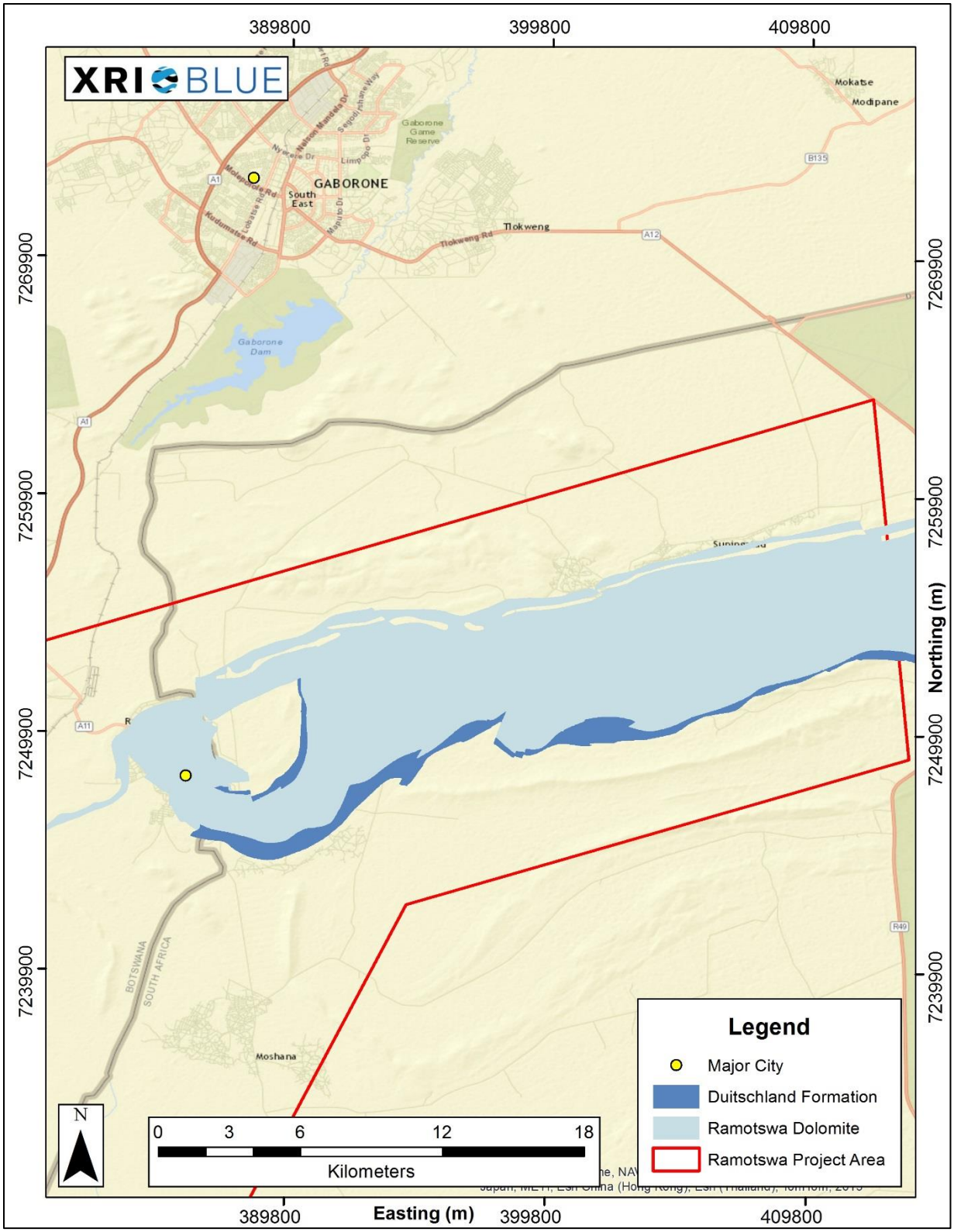

Figure 13: Mapped surface locations of the Duitschland Formation relative to the Ramotswa Dolomite in the Northern portion of the Ramotswa Project Area.

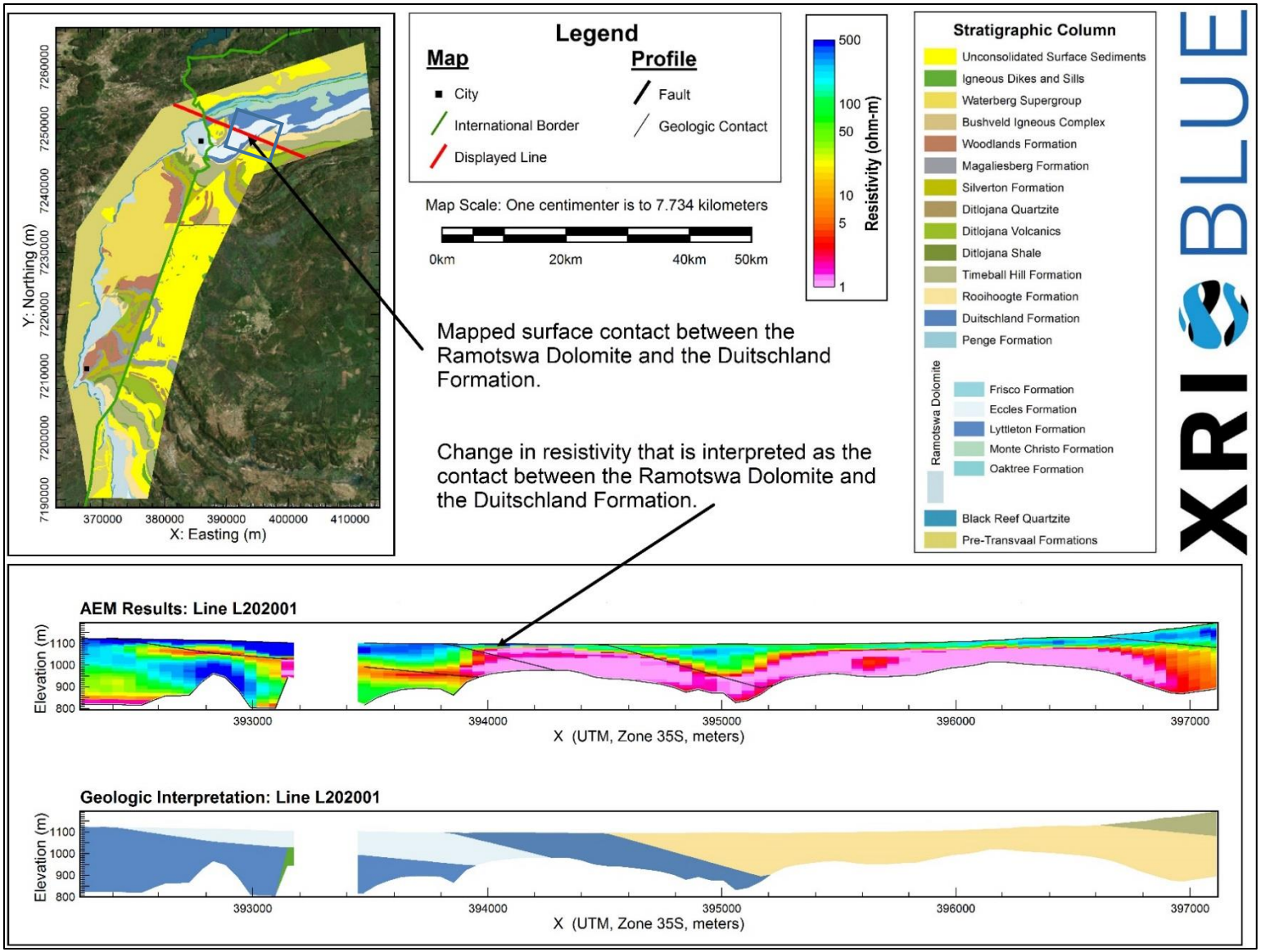

Figure 14: Example of interpreted contact between the Duitschland Formation and the Ramotswa Dolomite in AEM profile L202001. The contact has been interpreted at the change in resistivity from an approximate Easting (X) of 393,800 – 394,250 meters. The blue rectangle on the geologic map in the upper left of the figure, show the approximate extents of what is displayed in the resistivity and interpreted geology profiles.

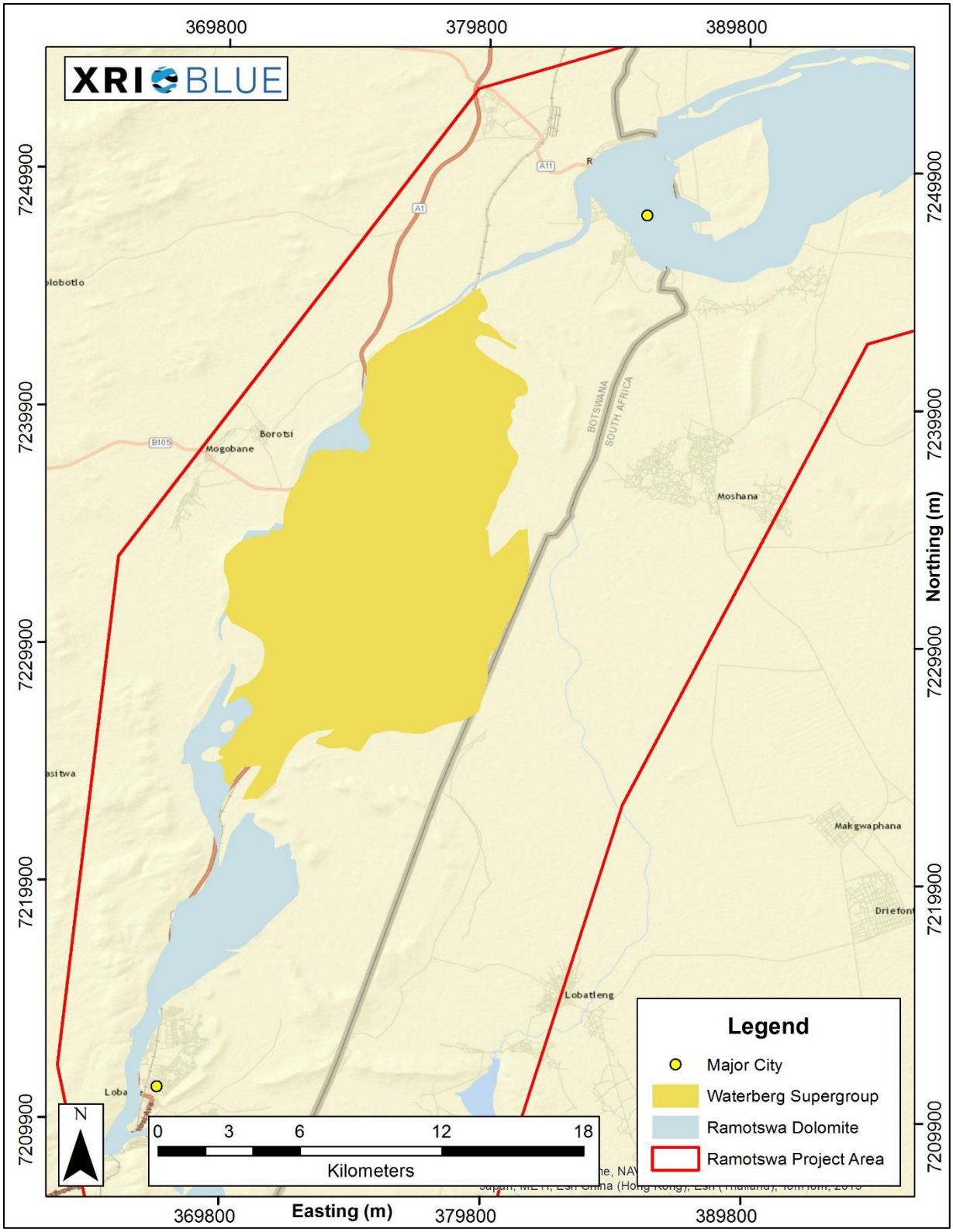

Figure 15: Mapped surface locations of the Waterberg Supergroup relative to the Ramotswa Dolomite in the Southern portion of the Ramotswa Project Area.

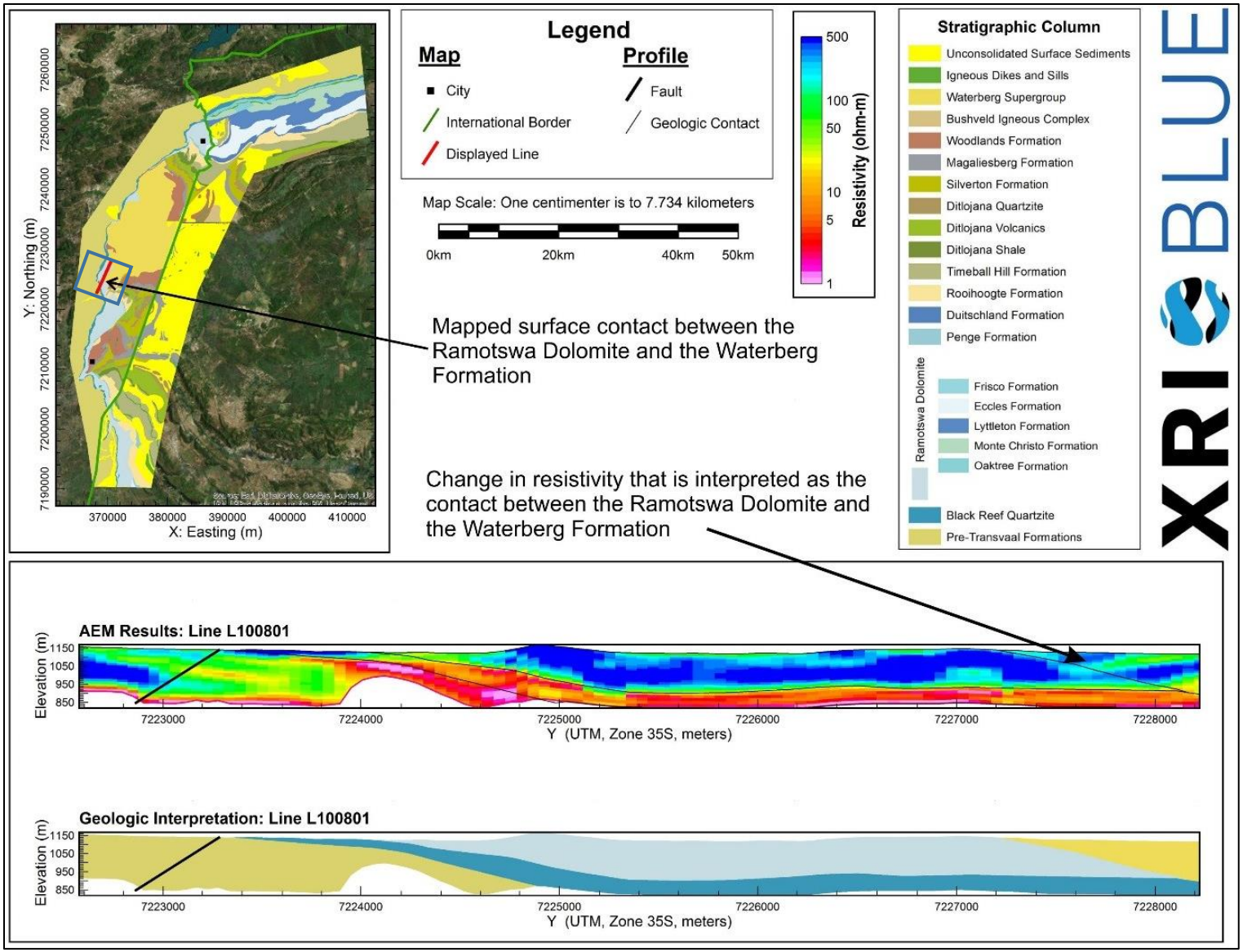

Figure 16: Example of interpreted contact between the Waterberg Formation and the Ramotswa Dolomite in AEM profile L100801. The interpreted contact is at the change in resistivity observed from an approximate Northing (Y) of 7,227,200 – 7,228,220 meters. The blue rectangle on the geologic map in the upper left of the figure, show the approximate extents of what is displayed in the resistivity and interpreted geology profiles.

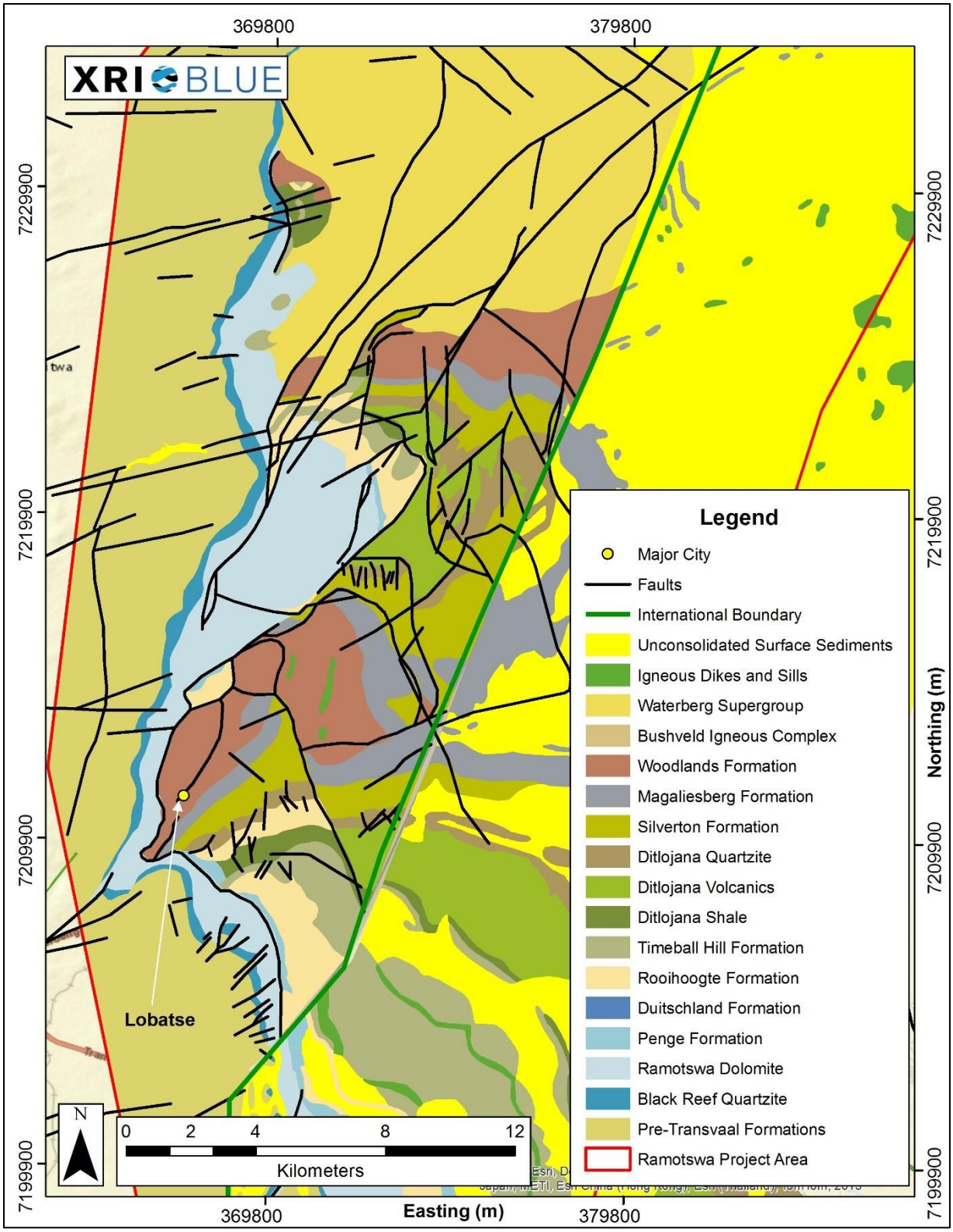

Figure 17: Mapped surface locations of the simplified geologic units and high concentration of faults relative to the Ramotswa Dolomite in the South-Central portion of the Ramotswa Project Area.

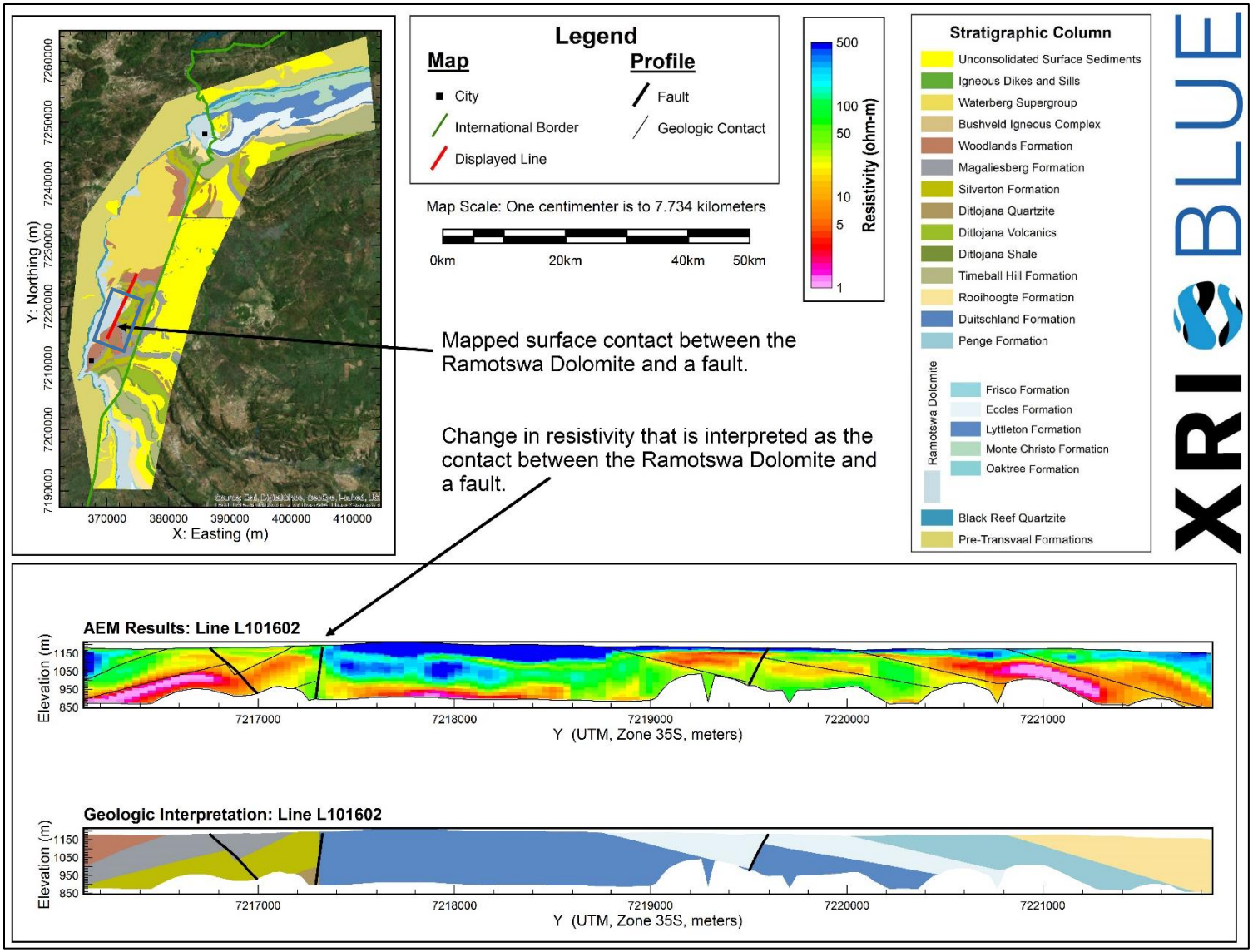

Figure 18: Example of interpreted contact in the South-Central portion of the Ramotswa Project Area between the Ramotswa Dolomite and a near vertical fault in AEM profile L101602. The interpreted fault is located at an approximate Northing (Y) of 7,217,280 meters. The blue rectangle on the geologic map in the upper left of the figure, show the approximate extents of what is displayed in the resistivity and interpreted geology profiles.

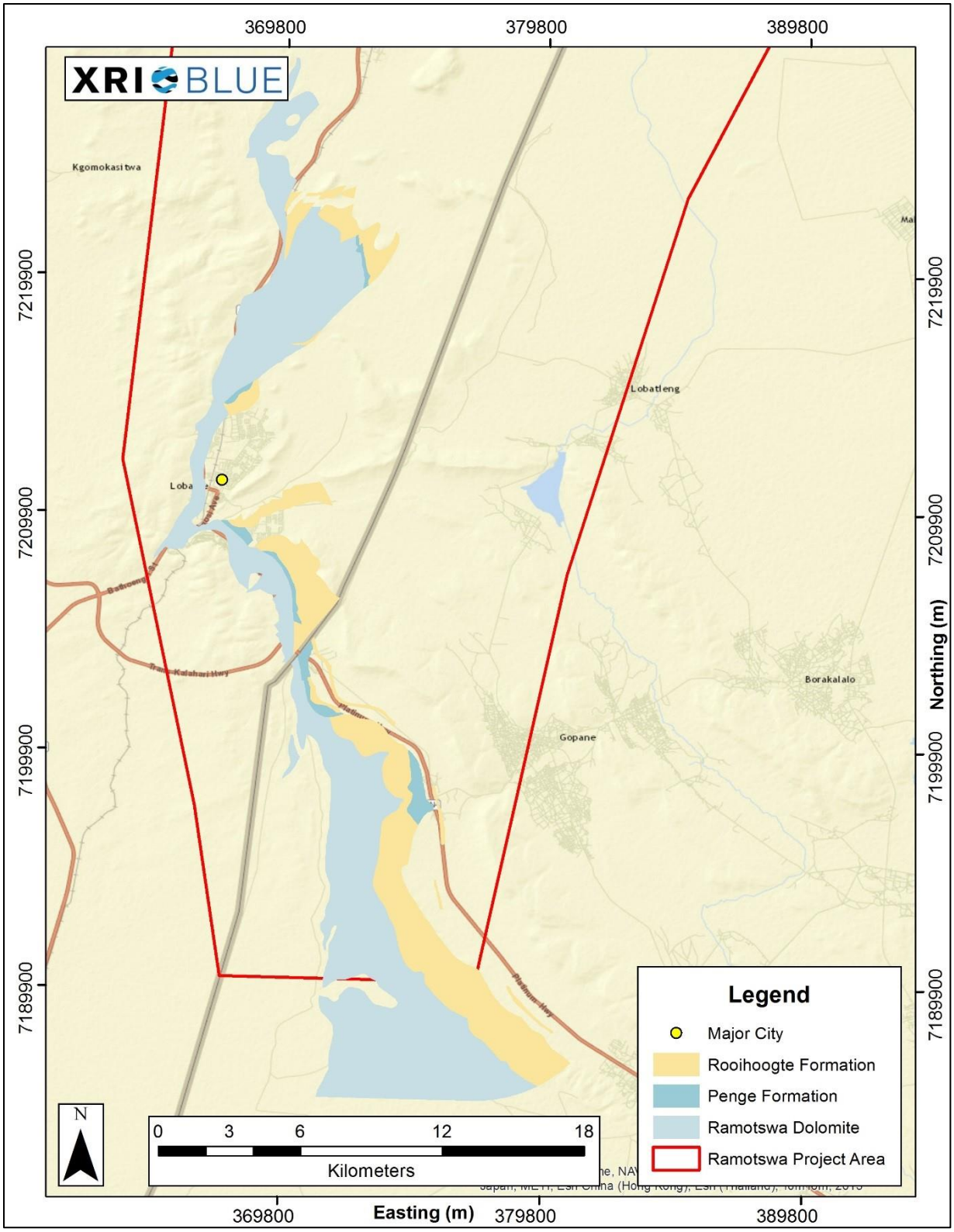

Figure 19: Mapped surface locations of the Rooihoogte and Penge Formations relative to the Ramotswa Dolomite in the Southern portion of the Ramotswa Project Area.

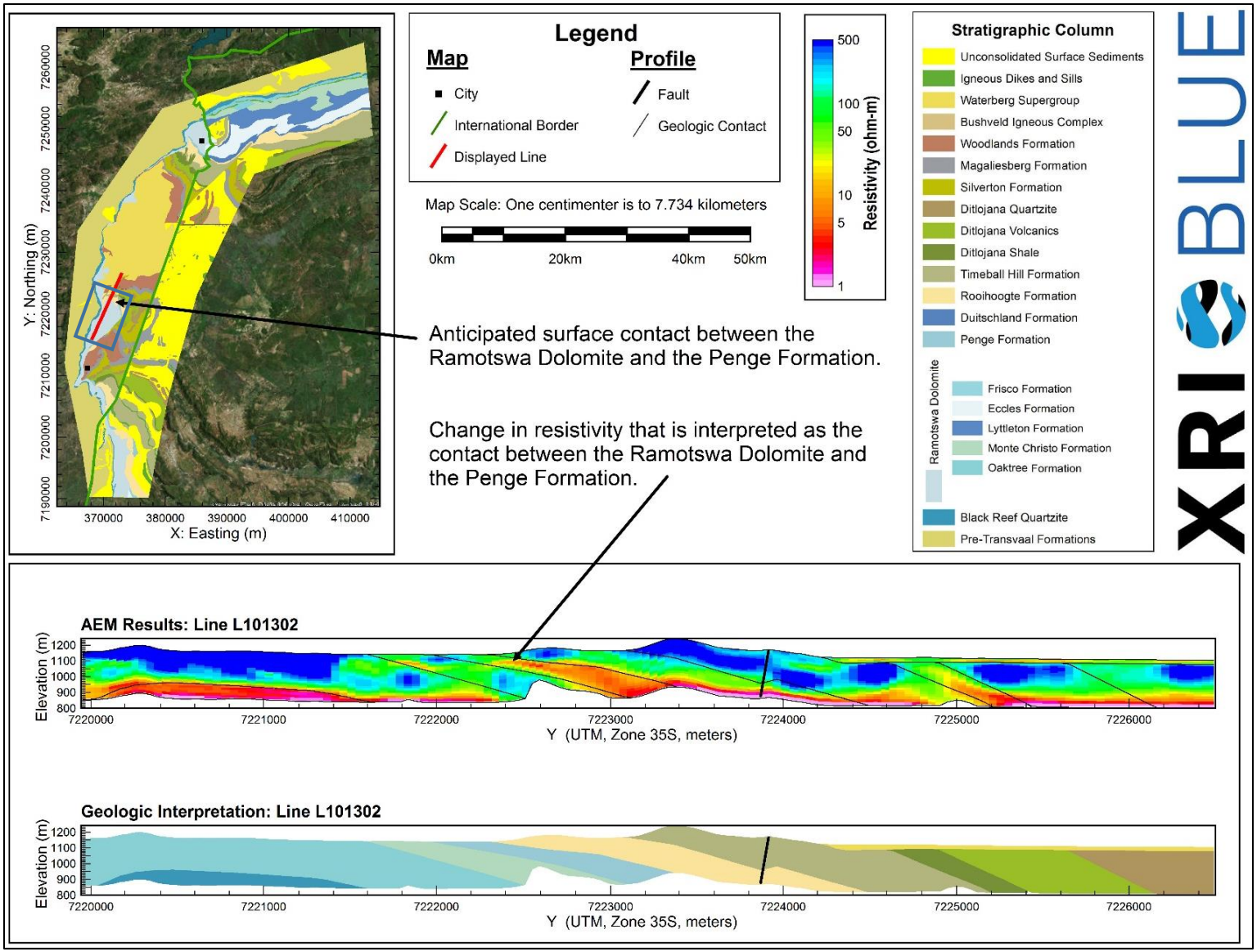

Figure 20: Example of interpreted contact between the Penge Formation and the Ramotswa Dolomite in AEM profile L101302. The interpreted contact is at the change in resistivity from an approximate Northing (Y) of 7,222,020 – 7,223,020 meters. The blue rectangle on the geologic map in the upper left of the figure, show the approximate extents of what is displayed in the resistivity and interpreted geology profiles.

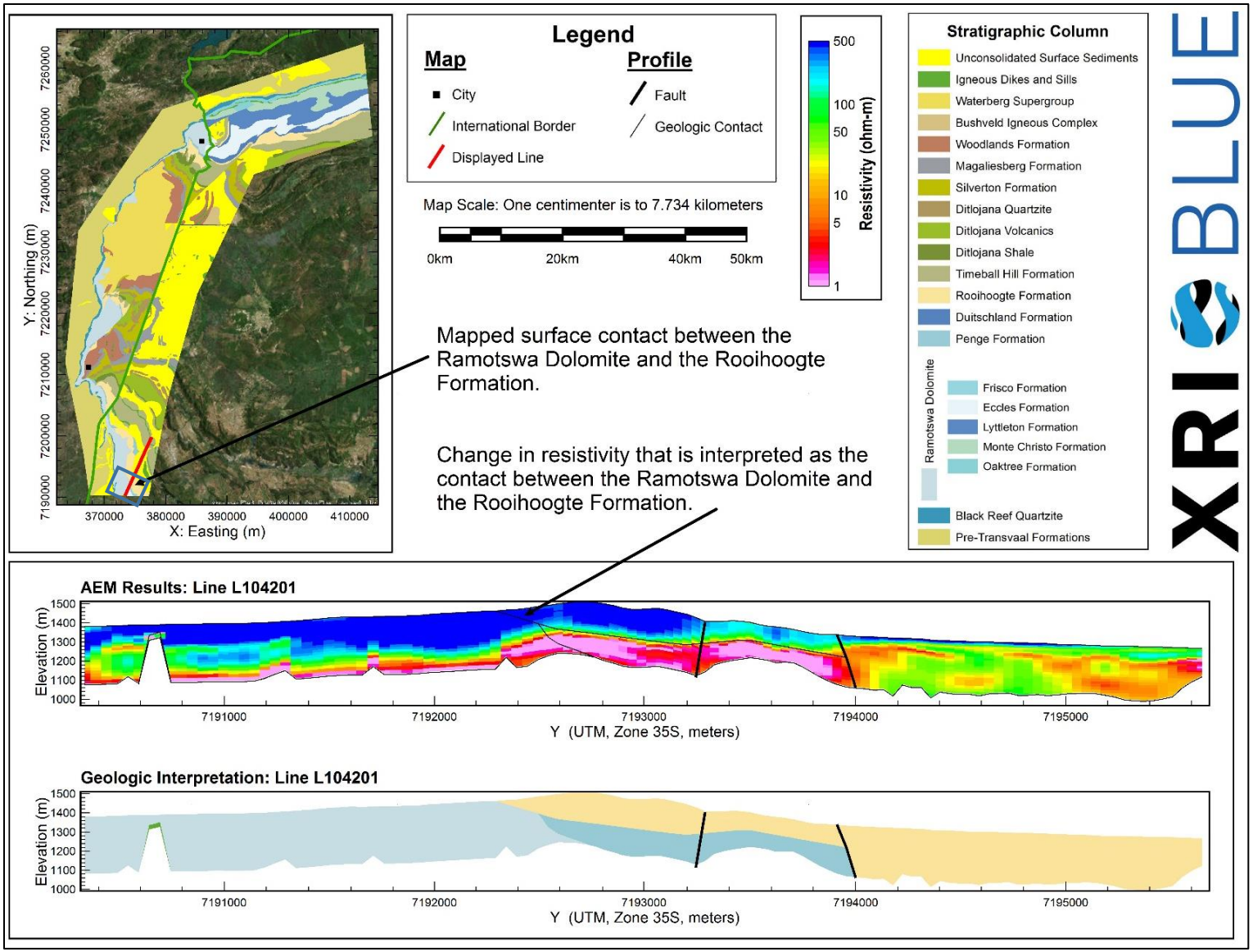

Figure 21: Example of interpreted contact between the Rooihoogte Formation and the Ramotswa Dolomite along AEM L104201. The interpreted contact is at the change in resistivity observed from an approximate Northing (Y) of 7,192,040 – 7,192,480 meters. The blue rectangle on the geologic map in the upper left of the figure, show the approximate extents of what is displayed in the resistivity and interpreted geology profiles.

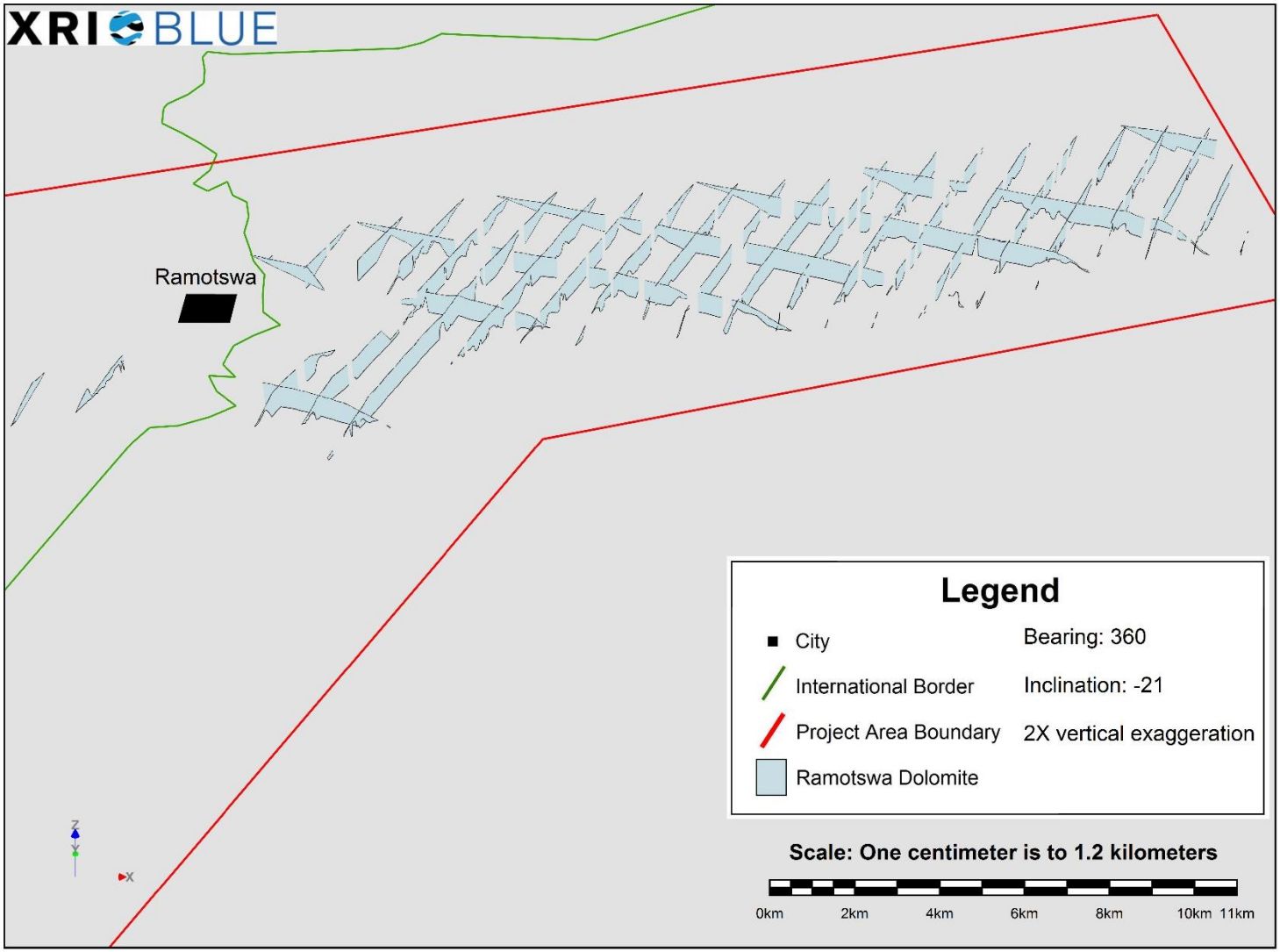

Figure 22: Three-Dimension (3D) view of the extent of the Ramotswa Dolomite in the Northern portion of Ramotswa Project Area.

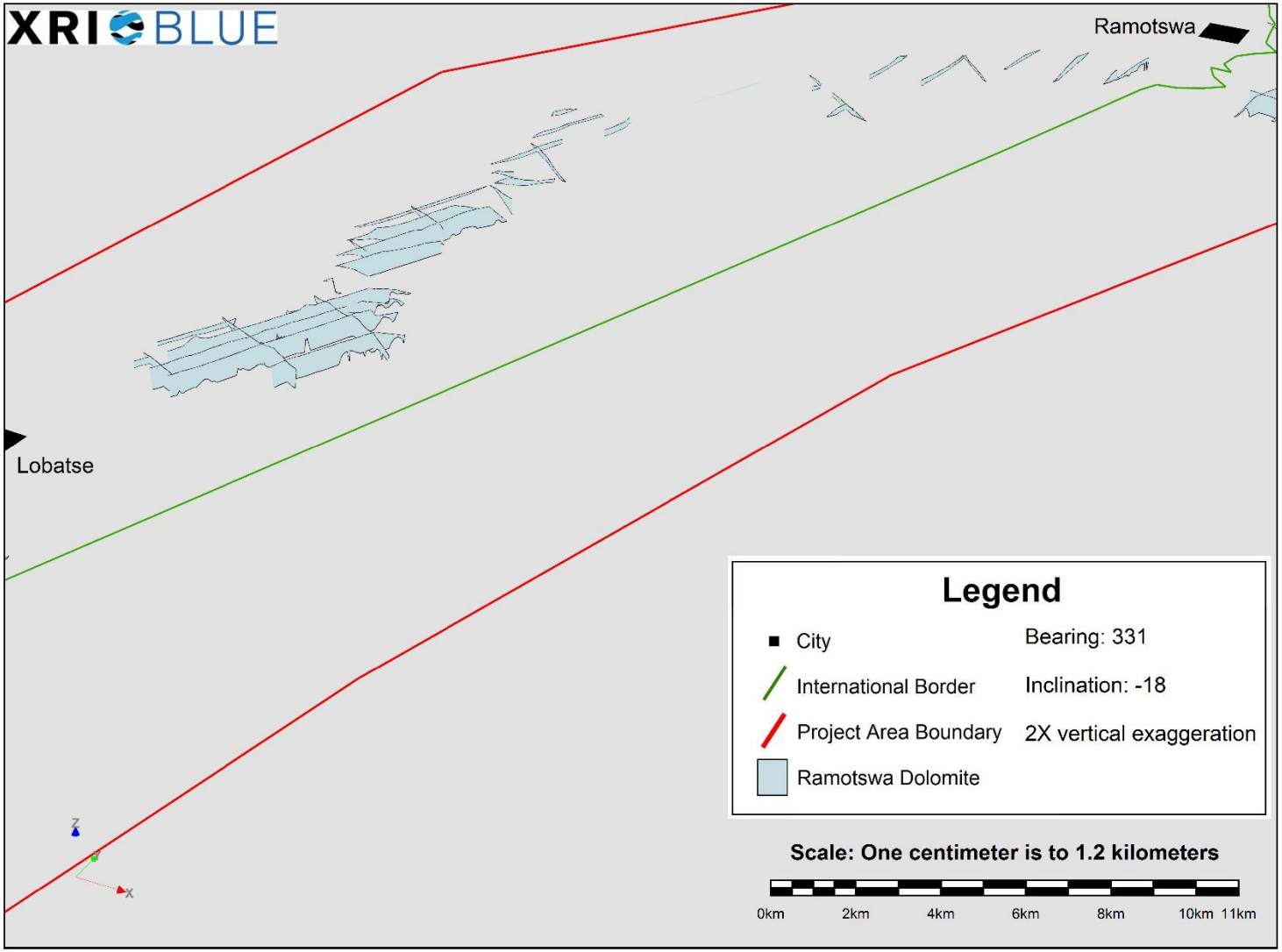

Figure 23: 3D view of the extent of the Ramotswa Dolomite in the Central portion of Ramotswa Project Area.

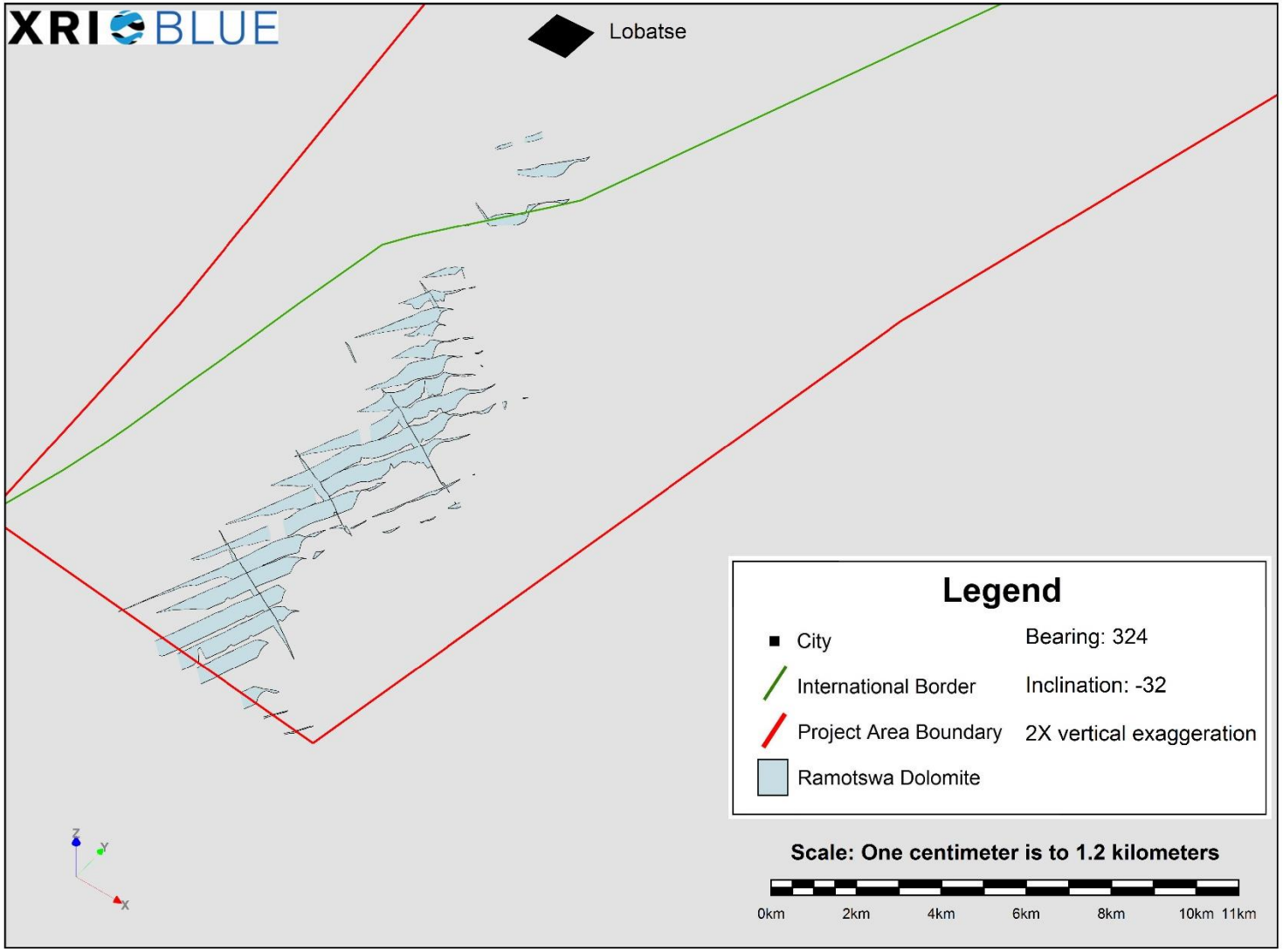

Figure 24: 3D view of the extent of the Ramotswa Dolomite in the Southern portion of Ramotswa Project Area.

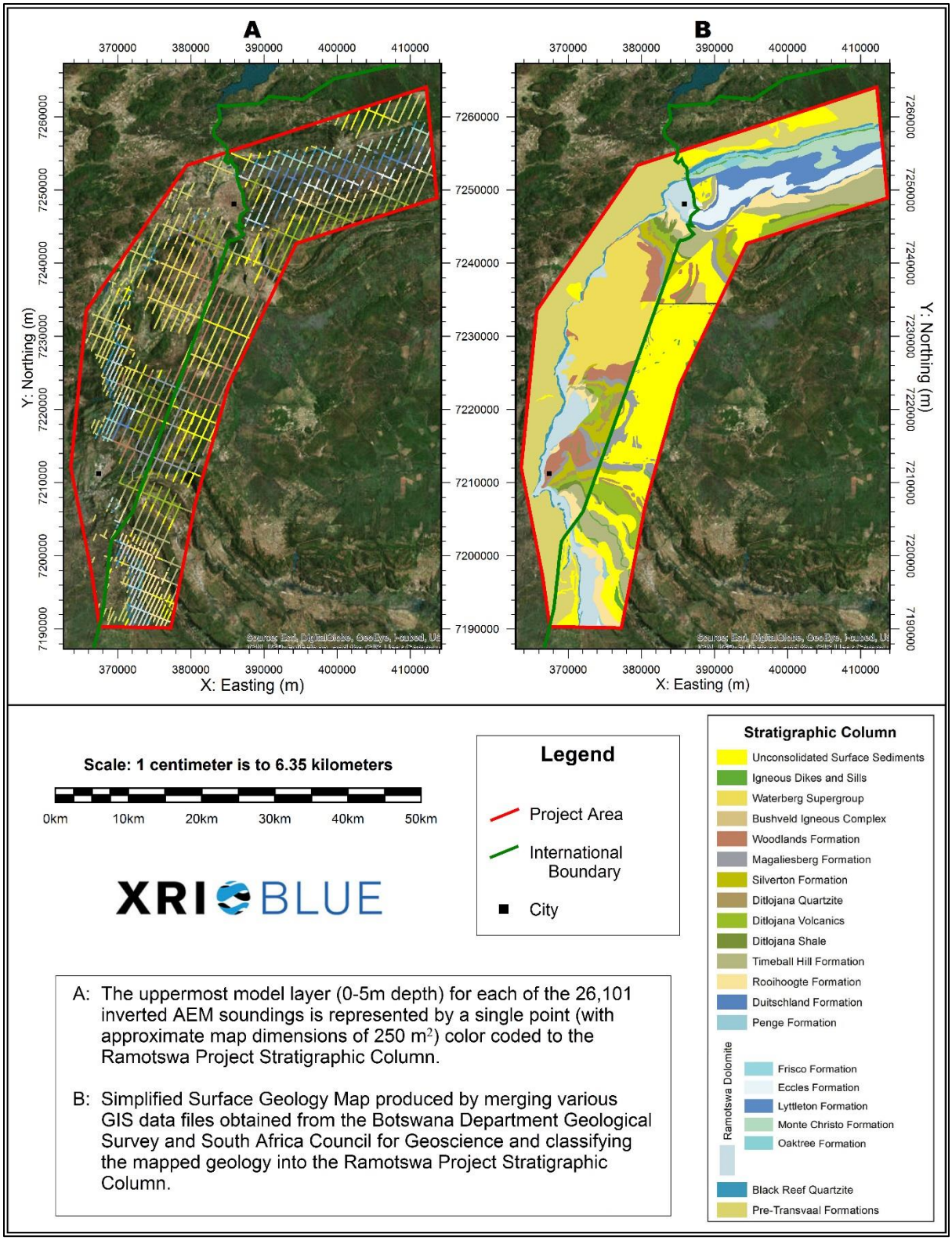

Figure 25: Comparison of interpreted surface geology extent of the top model layer from 0-5 meters depth (A) and the previously mapped surface extent (B) of the seventeen geologic formations interpreted in the Ramotswa Project Area.

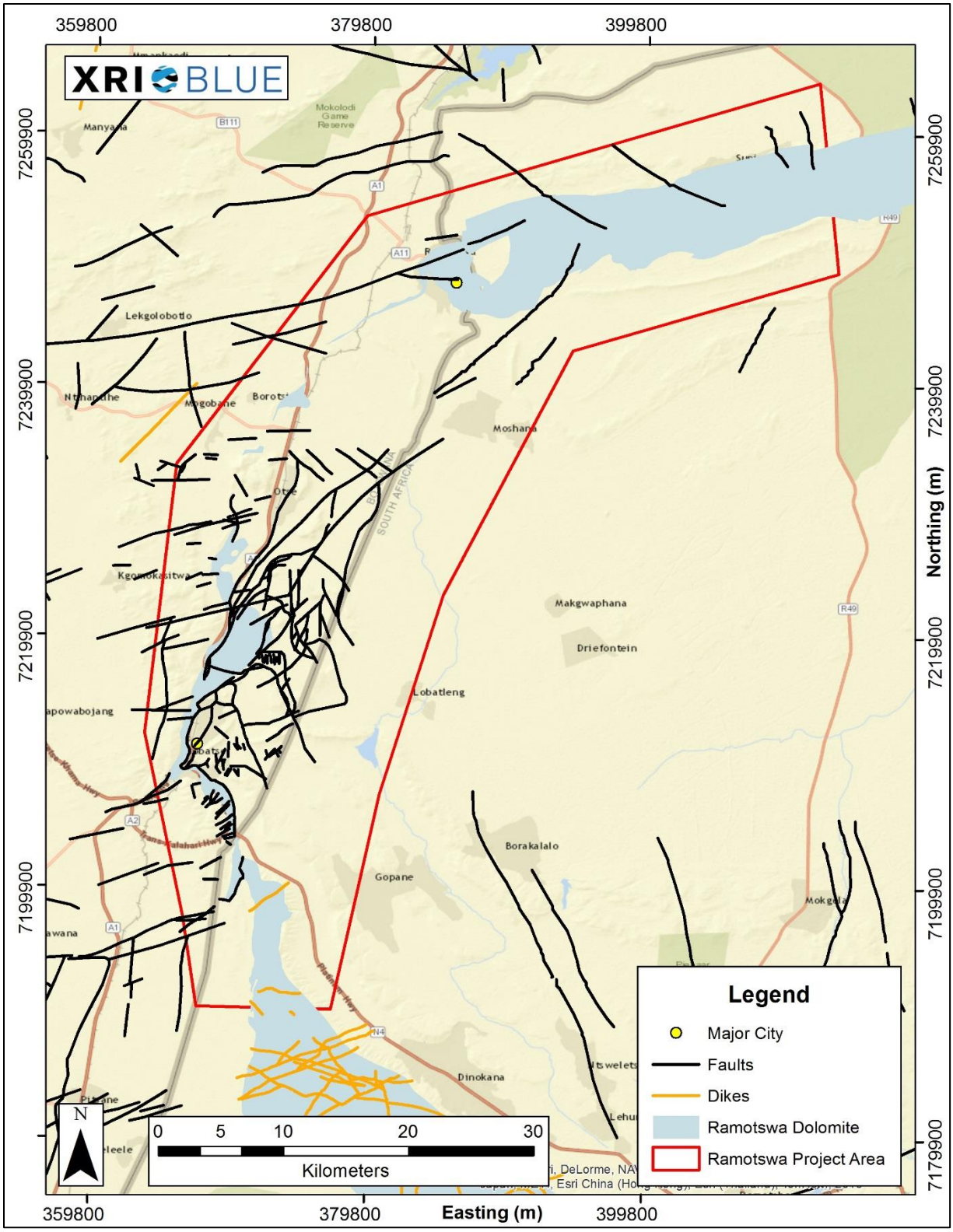

Figure 26: Mapped surface extent of the Ramotswa Dolomite, faults, and dikes in and around the Ramotswa Project Area.

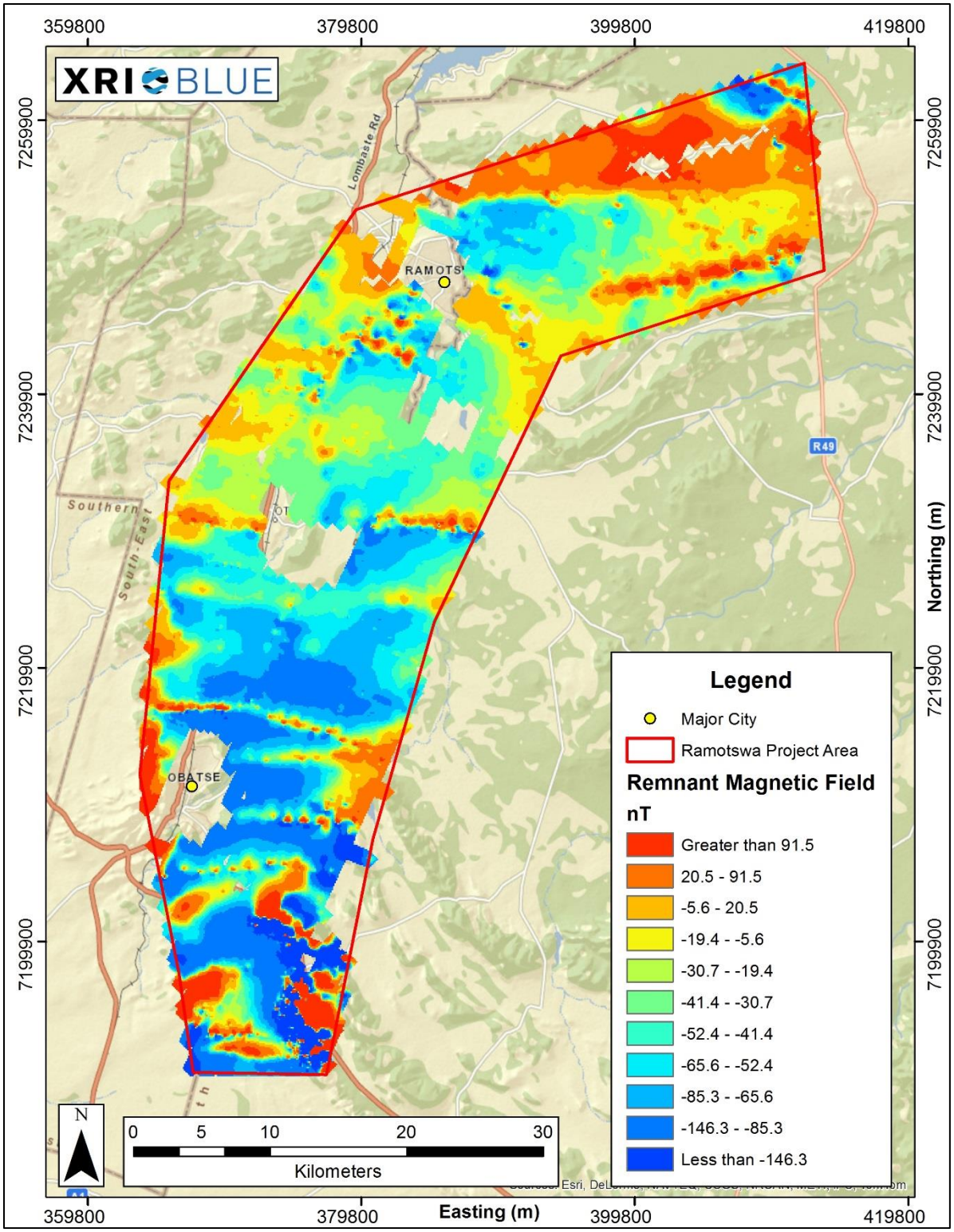

Figure 27: Remnant Magnetic Field (in nanoteslas) of the Ramotswa Project Area.

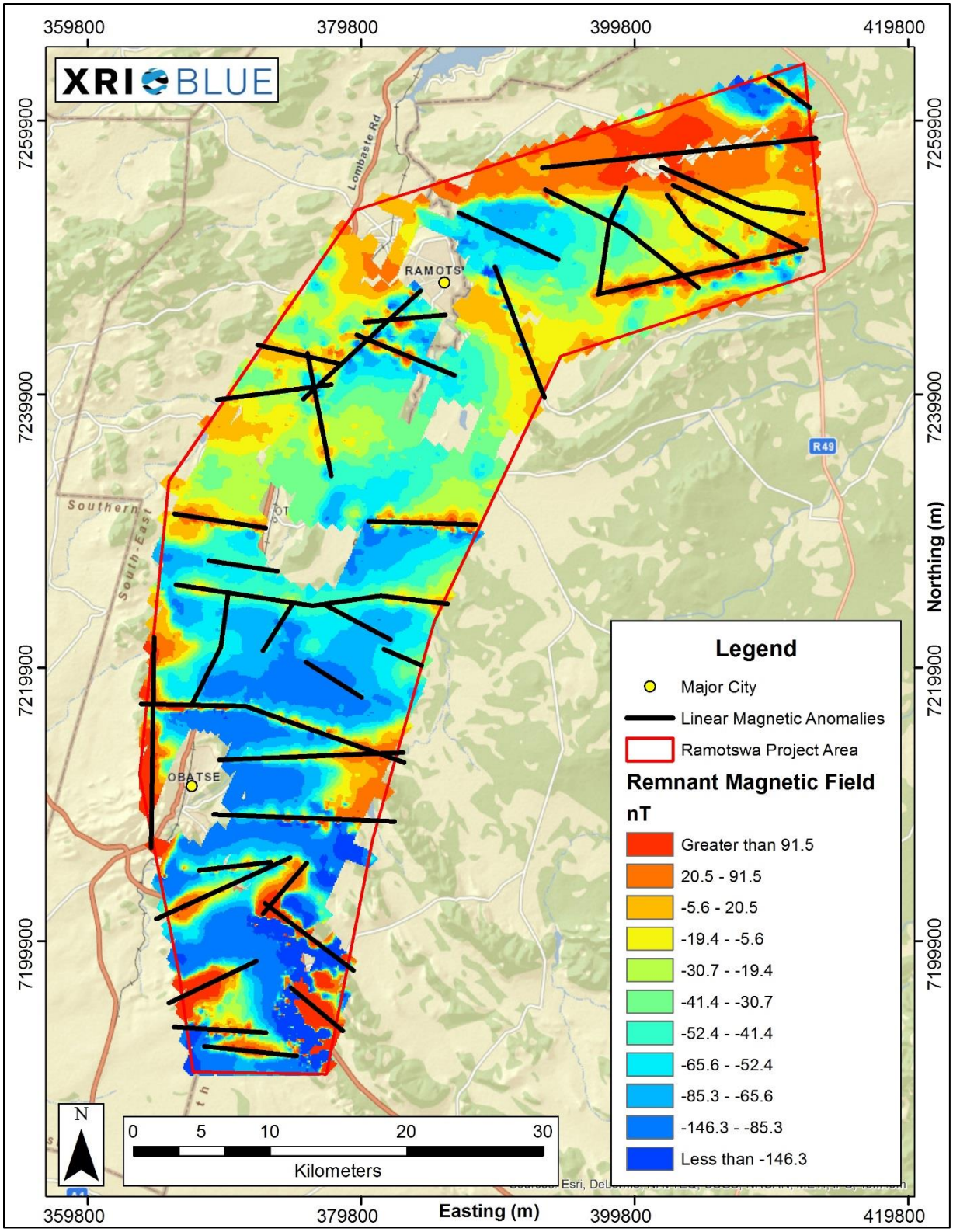

Figure 28: Remnant Magnetic Field (in nanoteslas) and linear magnetic anomalies in the Ramotswa Project Area.

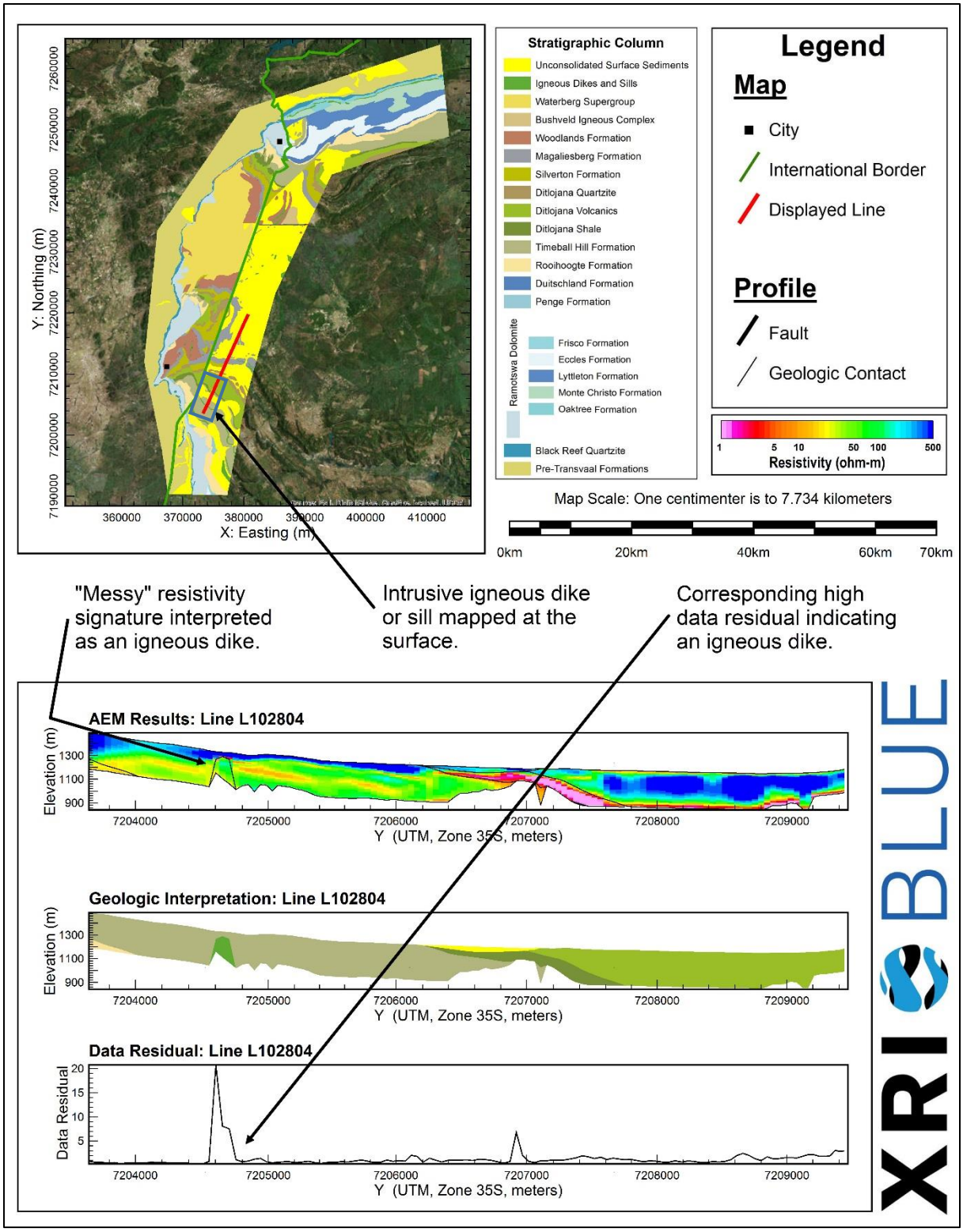

Figure 29: Example of an interpreted dike in AEM profile L102804. The interpreted dike is located from an approximate Northing (Y) of 7,204,550 – 7,204,750 meters. The blue rectangle on the geologic map in the upper left of the figure, show the approximate extents of what is displayed in the resistivity and interpreted geology profiles.

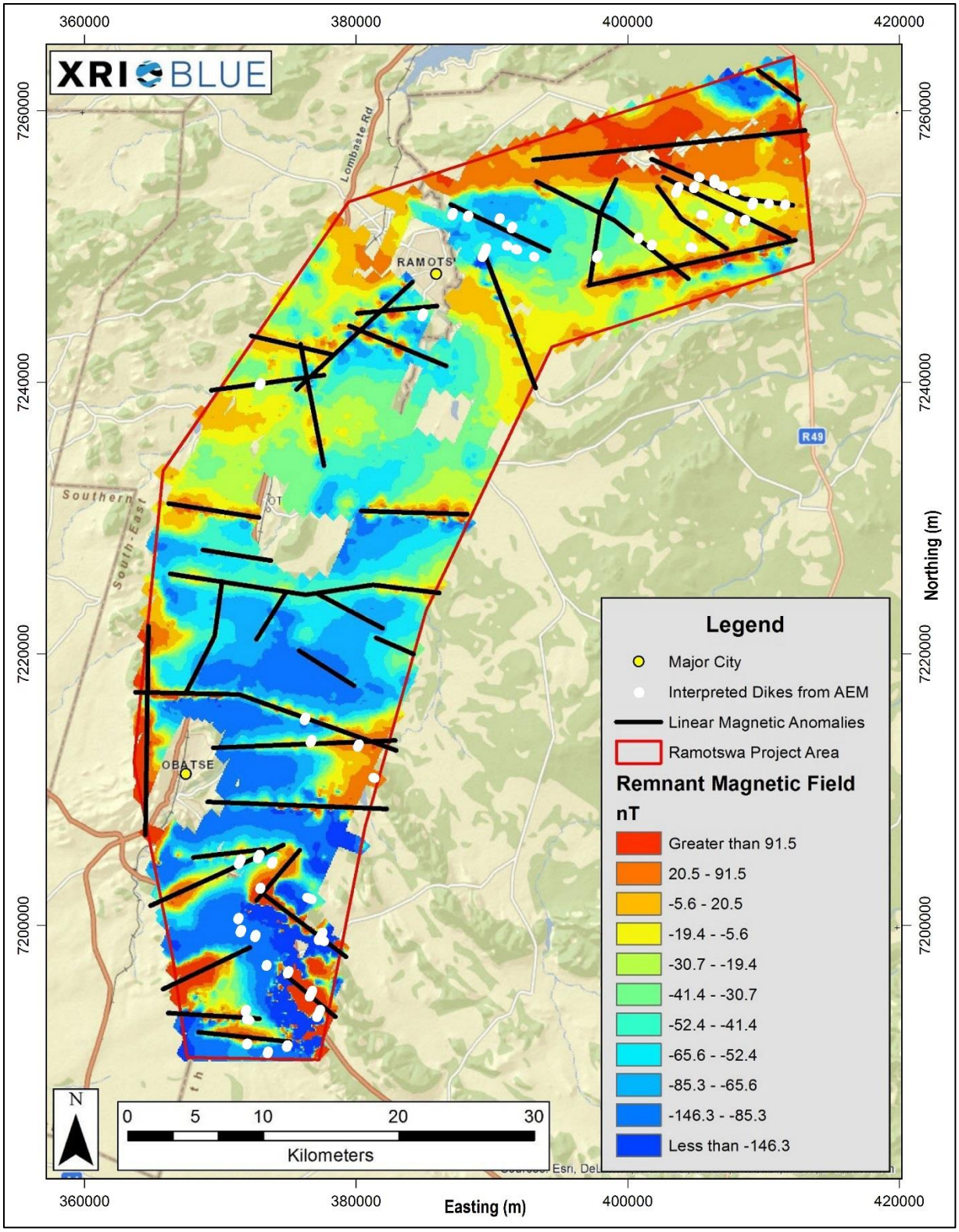

Figure 30: Remnant Magnetic Field, linear magnetic anomalies, and locations of interpreted dikes from the AEM data in the Ramotswa Project Area.

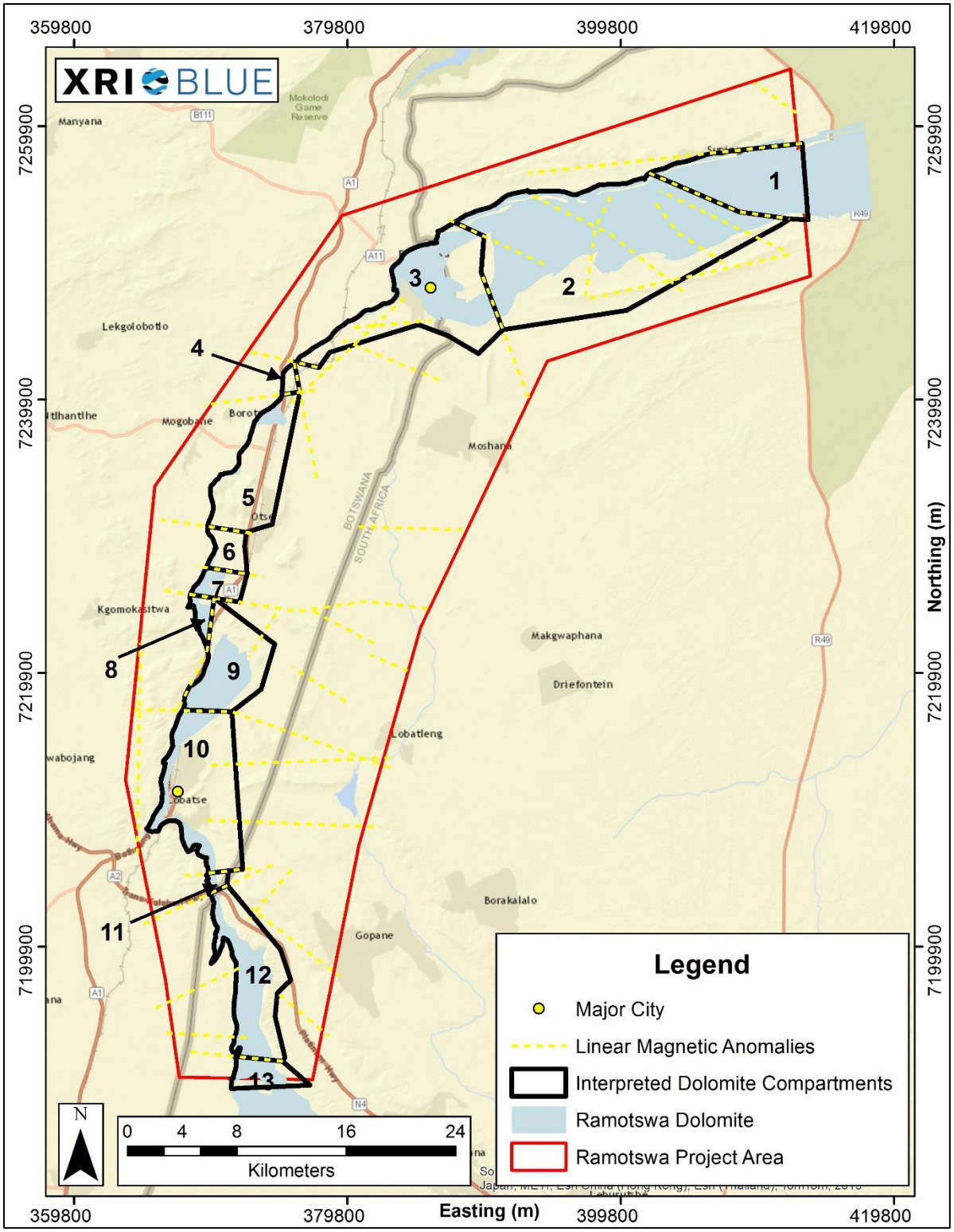

Figure 31: Interpreted Dolomite Compartments, linear magnetic anomalies, and the Ramotswa Dolomite in the Ramotswa Project Area.

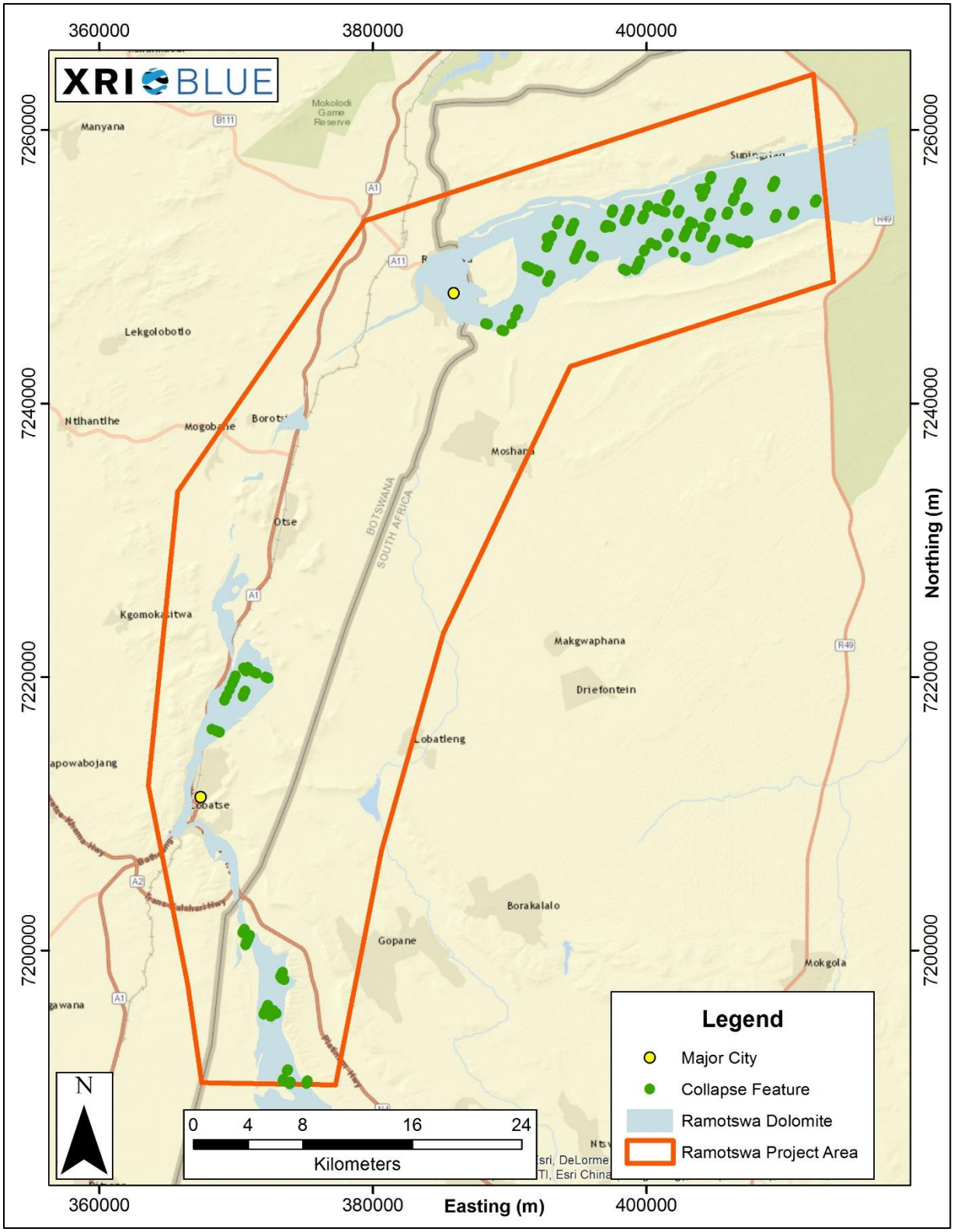

Figure 32: Location of interpreted collapse features within the Ramotswa Project Area.

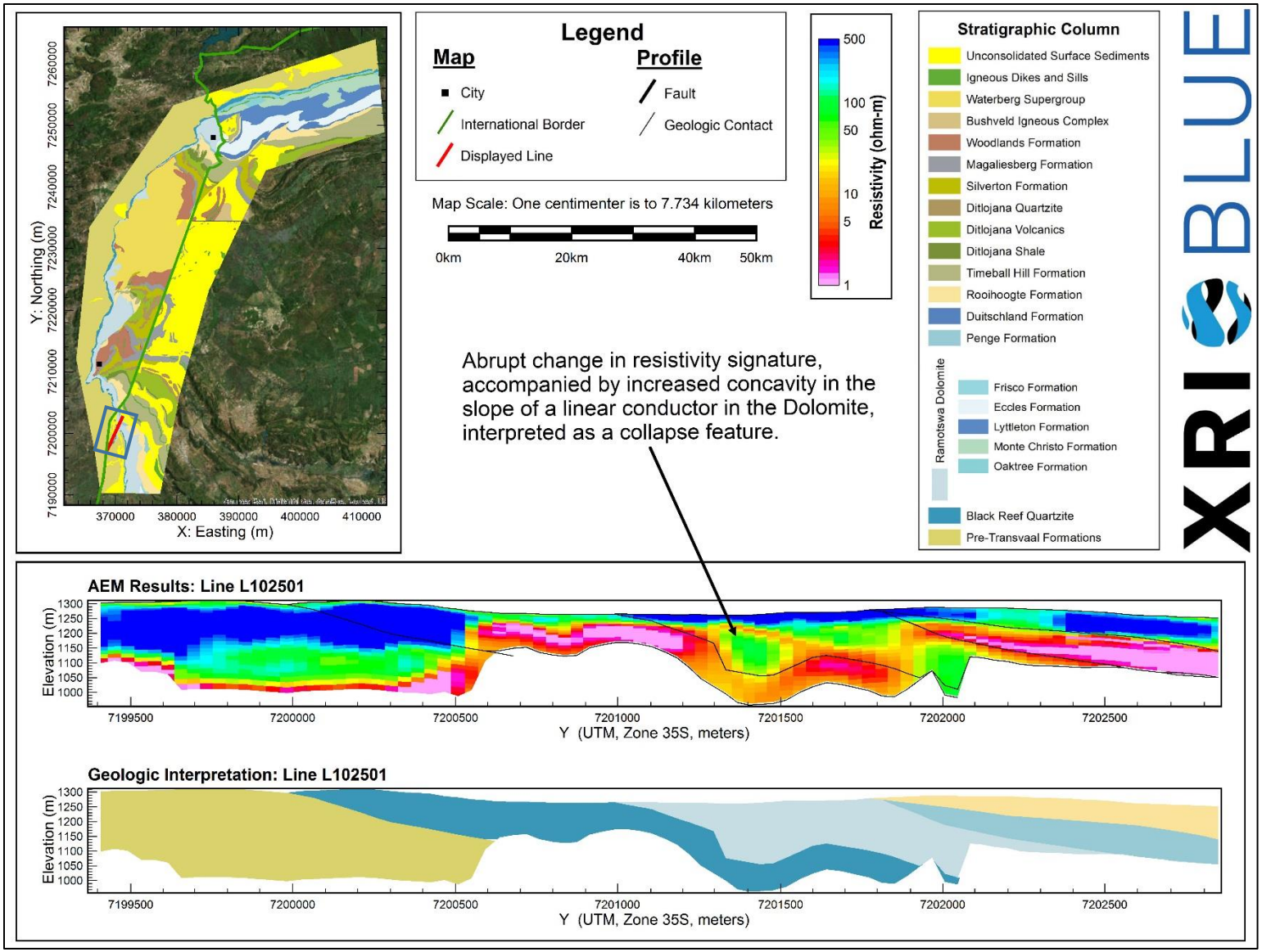

Figure 33: Example of an interpreted collapse feature in AEM profile L102501. The collapse features is interpreted to be from an approximate Northing (Y) of 7,201,290 – 7,201,590. The blue rectangle on the geologic map in the upper left of the figure, show the approximate extents of what is displayed in the resistivity and interpreted geology profiles.

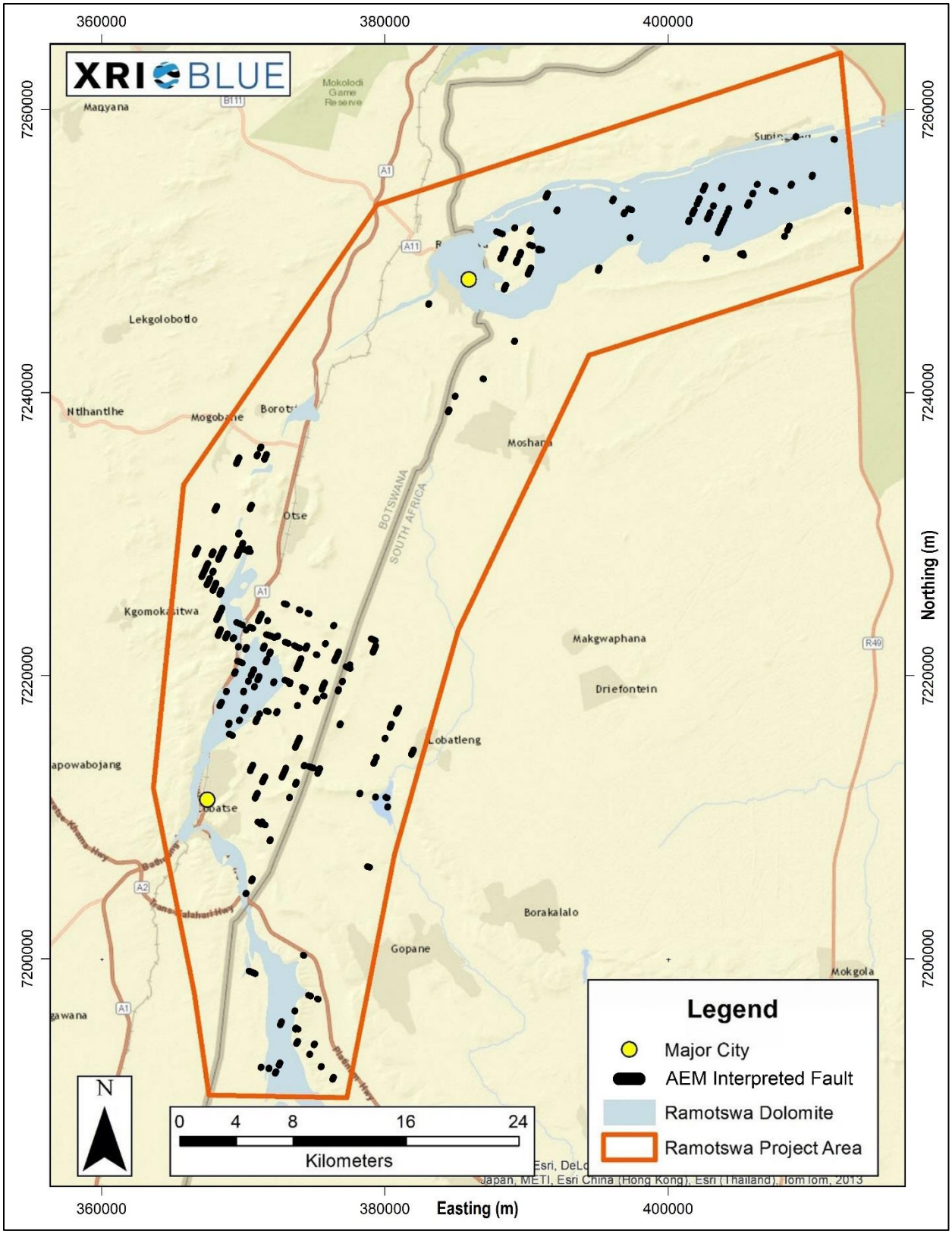

Figure 34: Location of the interpreted faults from the AEM data in the Ramotswa Project Area.

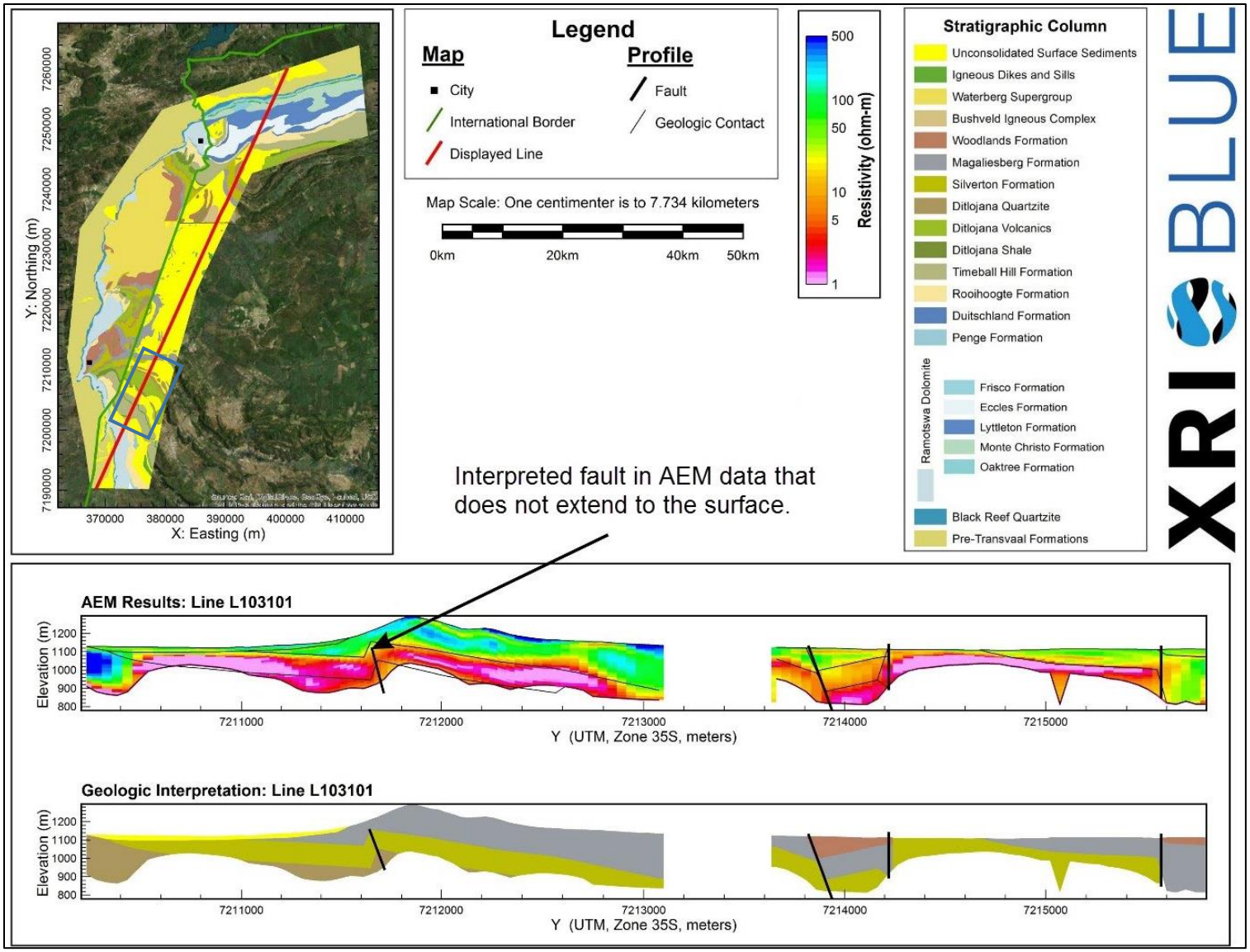

Figure 35: Example of an interpreted fault with noticeable offset in the subsurface that does not extend to the surface in AEM profile 103301. The interpreted fault is nearly vertical and located at an approximate Northing (Y) 7,211,630 meters. The blue rectangle on the geologic map in the upper left of the figure, show the approximate extents of what is displayed in the resistivity and interpreted geology profiles.

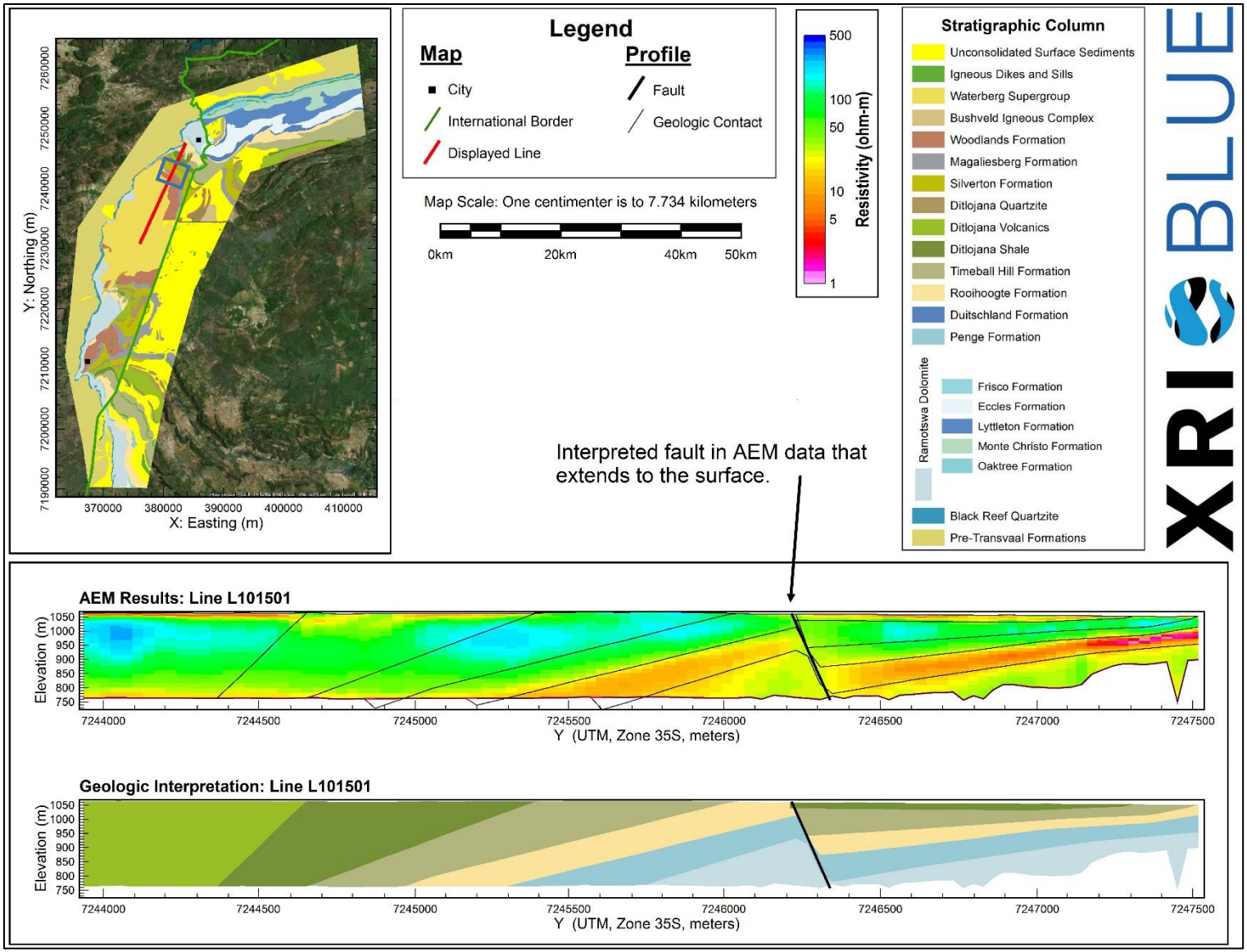

Figure 36: Example of a fault interpreted in AEM profile L101501, with noticeable offset in the subsurface that extends to the surface. The interpreted fault is nearly vertical at an approximate Northing (Y) of 7,246,430 meters. The blue rectangle on the geologic map in the upper left of the figure, show the approximate extents of what is displayed in the resistivity and interpreted geology profiles.

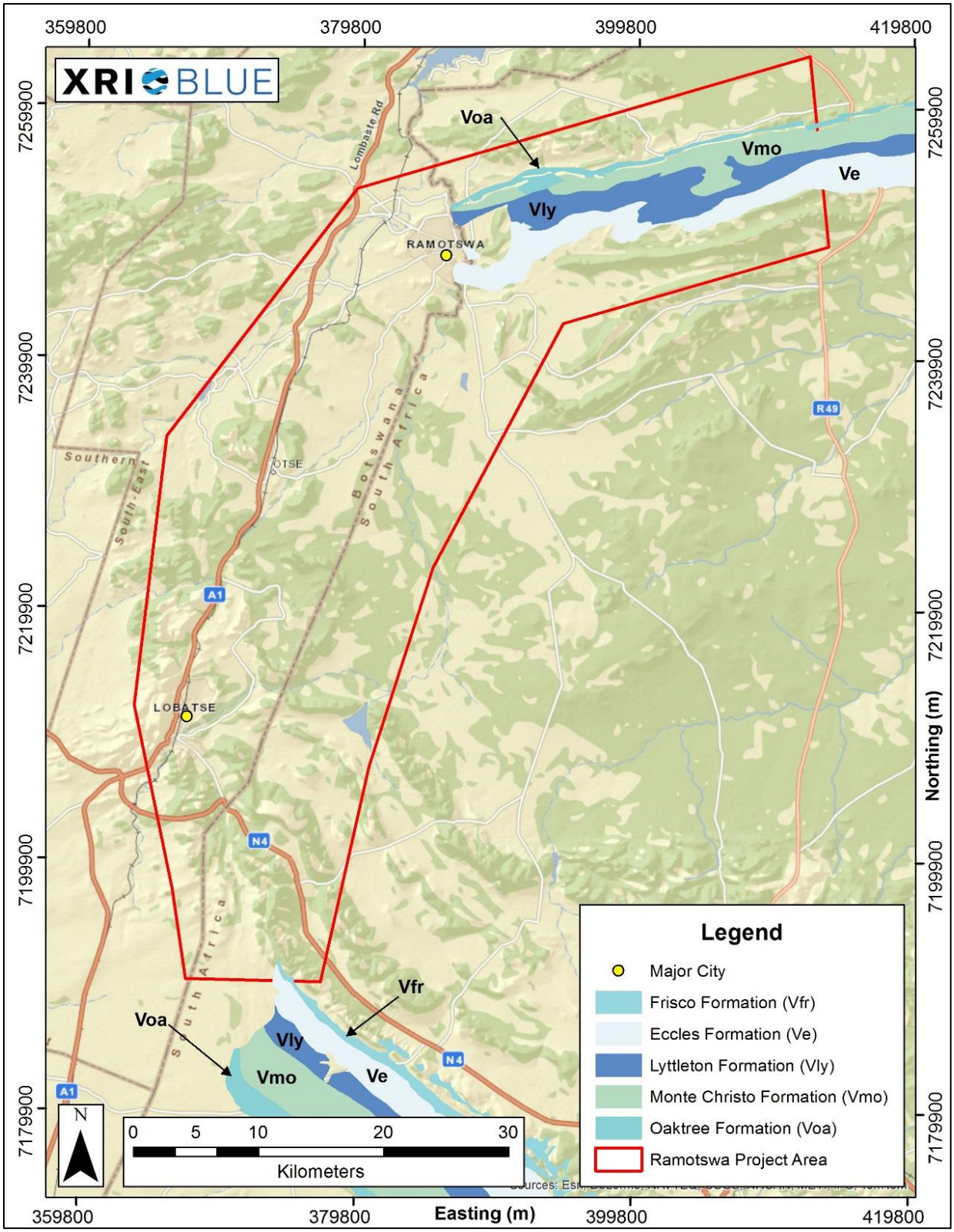

Figure 37: Mapped surface locations of the unique dolomite formations of the Ramotswa Dolomite in the Ramotswa Project Area.

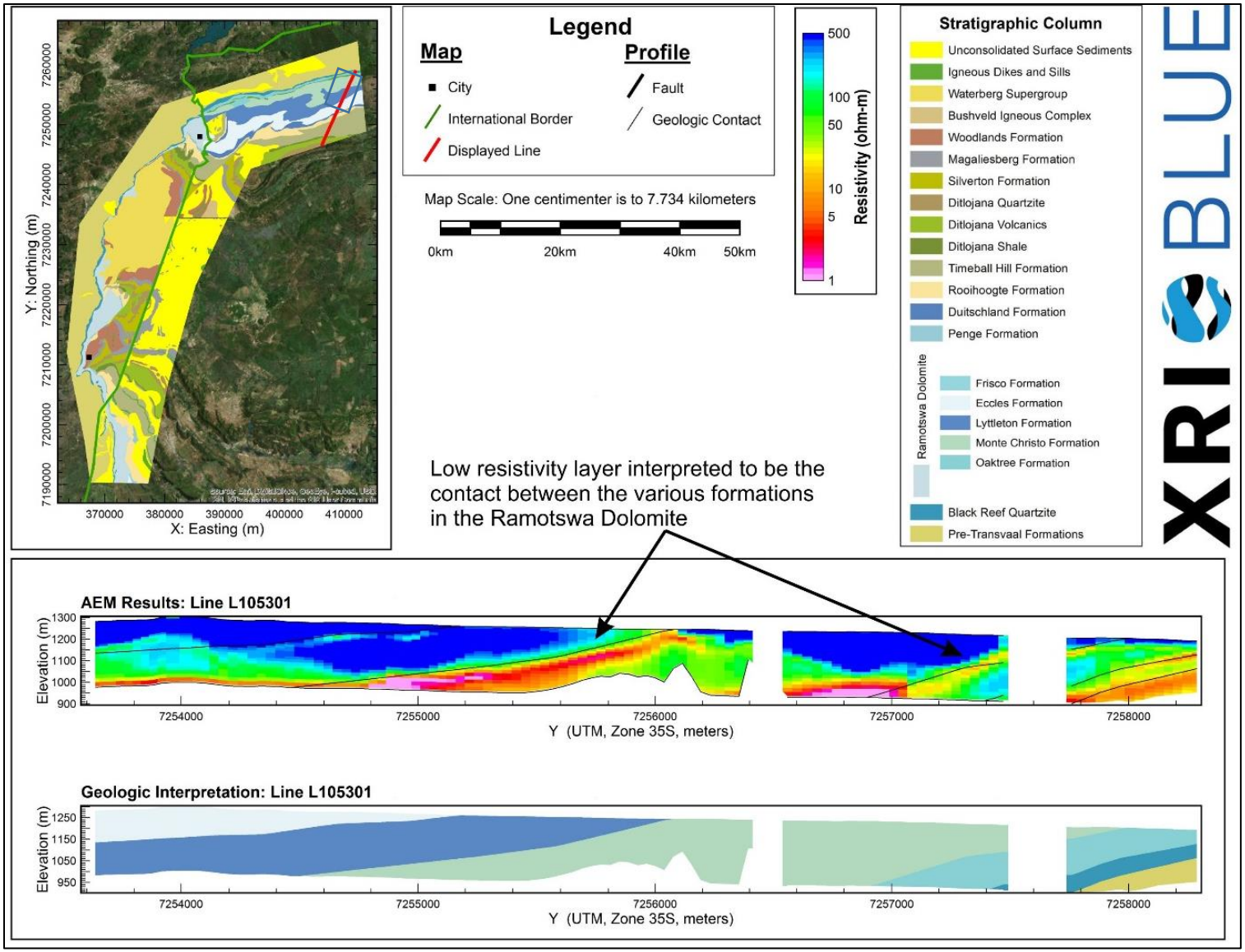

Figure 38: Example of thin low resistivity layers in the Ramotswa Dolomite, interpreted to be the contact between the unique Dolomite formations in AEM profile L105301. The blue rectangle on the geologic map in the upper left of the figure, show the approximate extents of what is displayed in the resistivity and interpreted geology profiles.

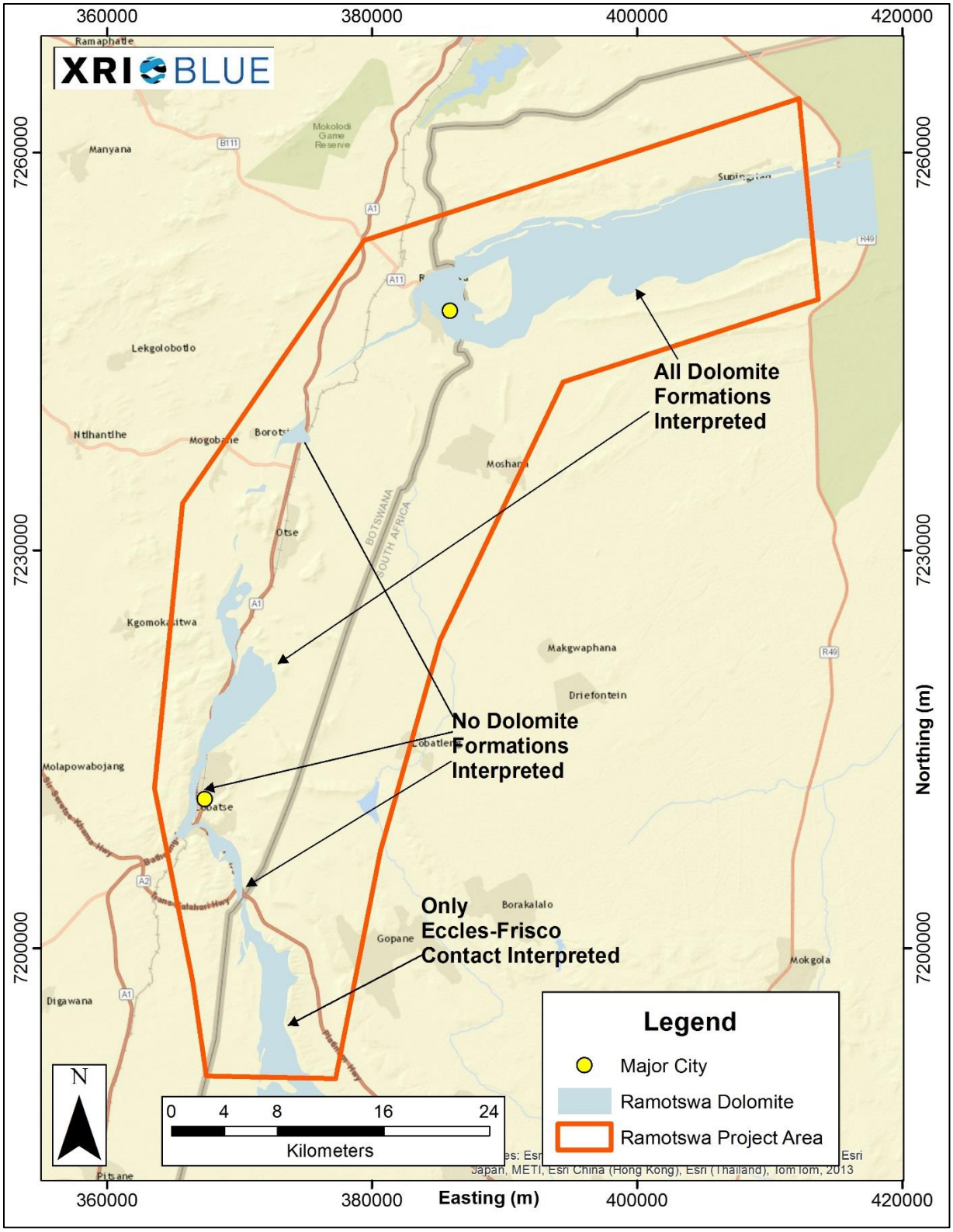

Figure 39: Map indicating what unique formations within the Ramotswa Dolomite were interpreted within the Ramotswa Project Area.

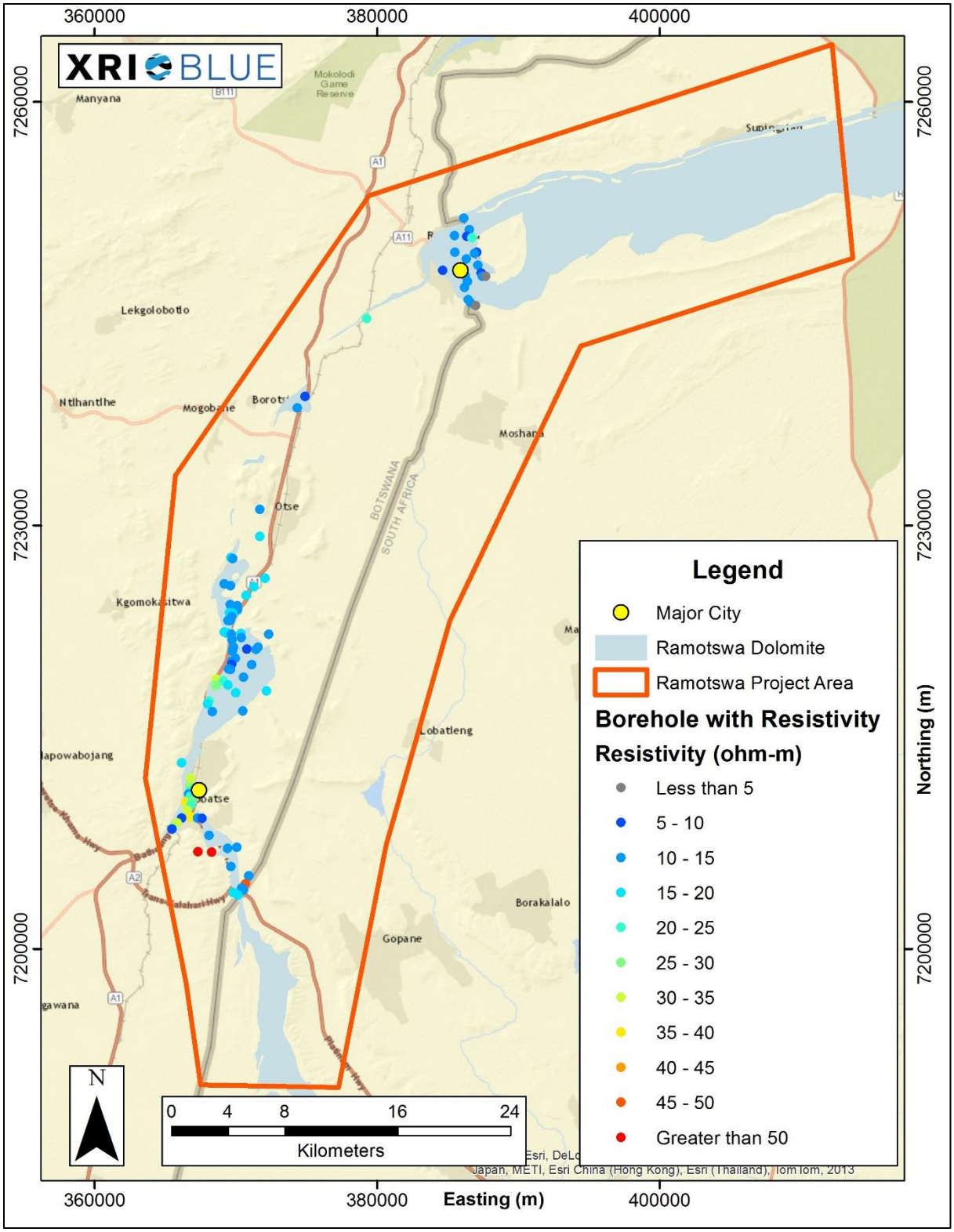

Figure 40: Pore fluid resistivity of boreholes interpreted to be within the Ramotswa Dolomite in the Ramotswa Project Area.

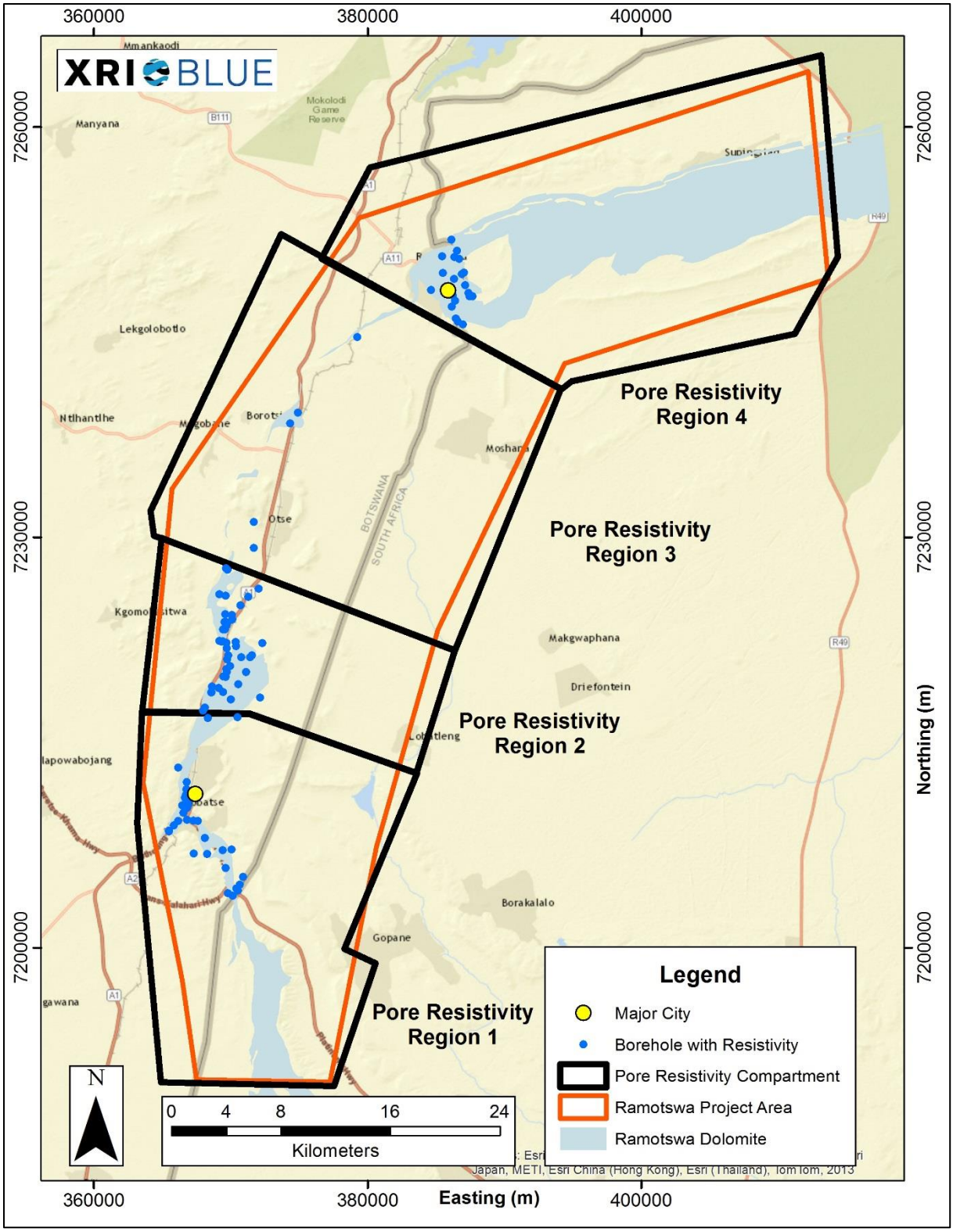

Figure 41: Four pore fluid resistivity regions delineated by XRI based on the locations of the boreholes with pore fluid resistivity in the Ramotswa Project Area.

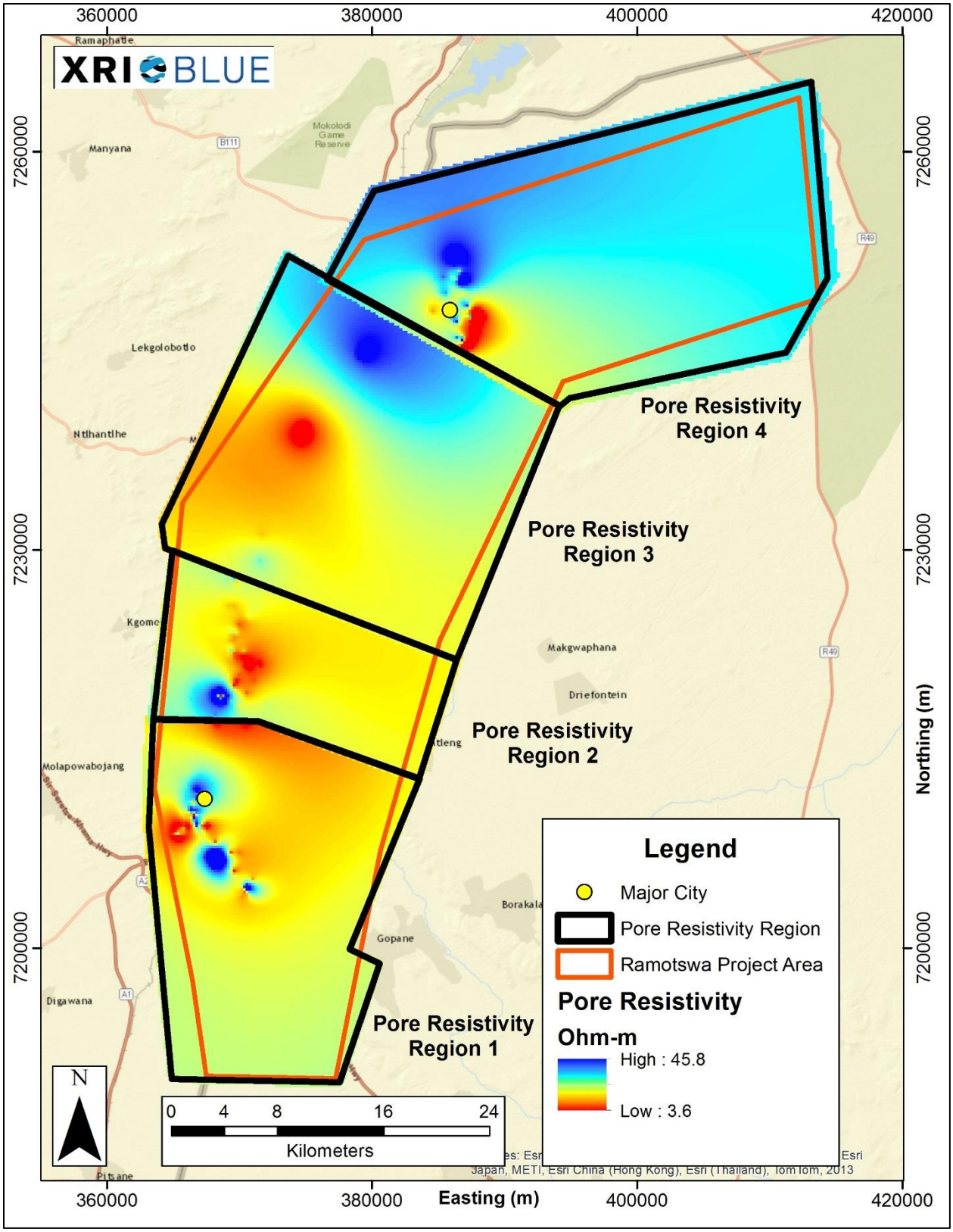

Figure 42: Gridded pore fluid resistivity of the four resistivity regions in the Ramotswa Project Area.

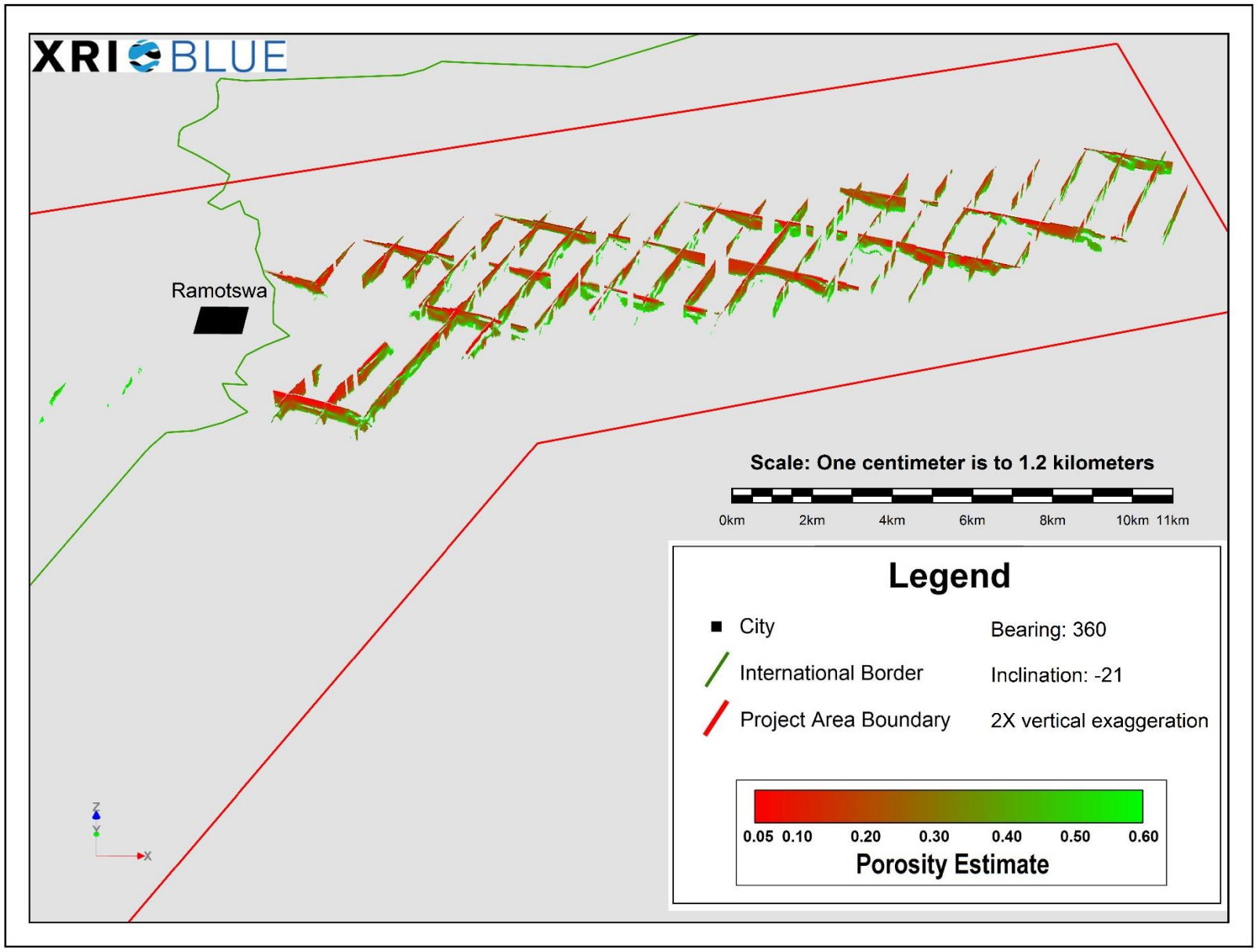

Figure 43: 3D view of the porosity estimates of the Ramotswa Dolomite in the Northern portion of the Ramotswa Project Area.

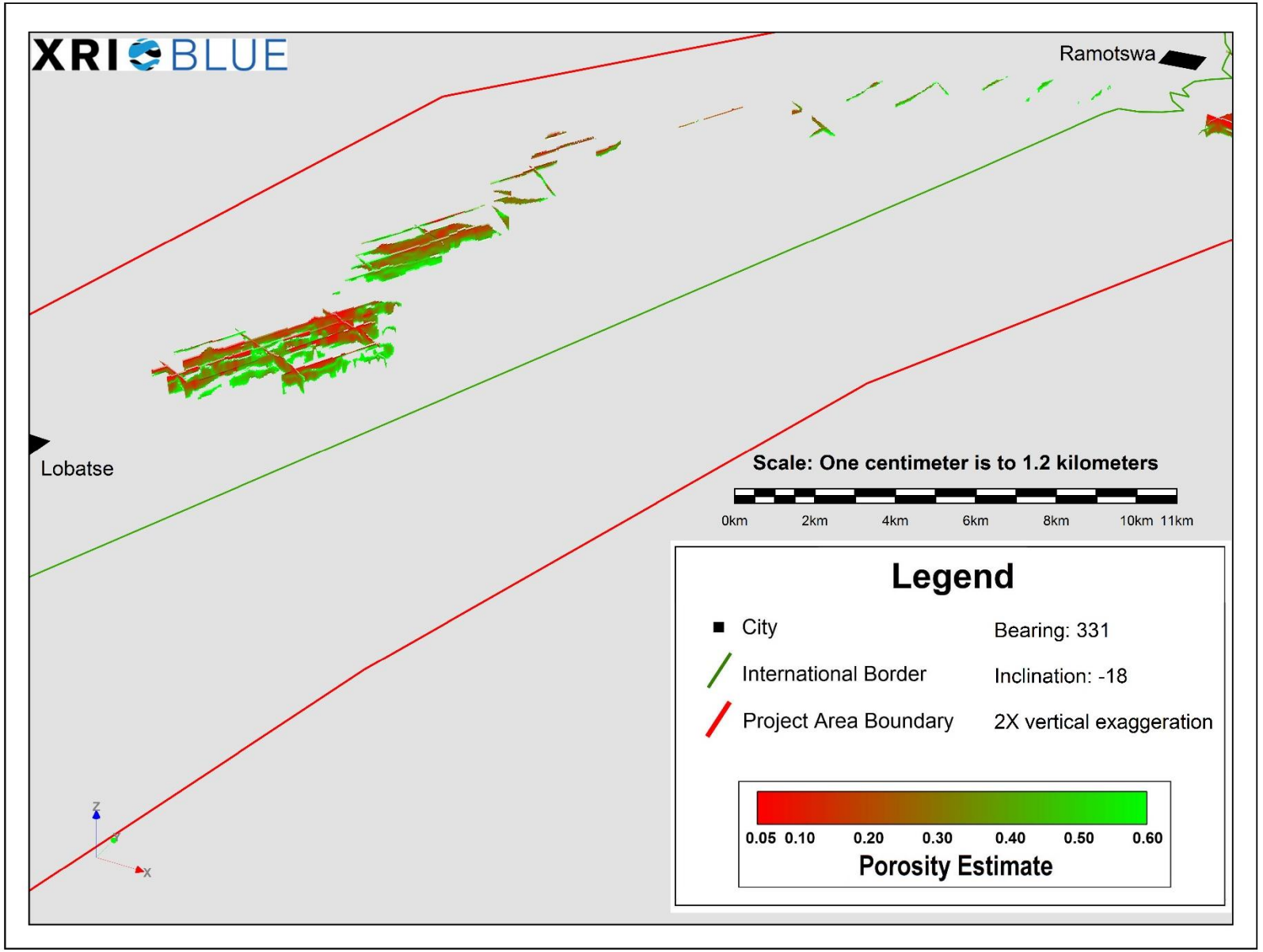

Figure 44: 3D view of the porosity estimates of the Ramotswa Dolomite in the Central portion of the Ramotswa Project Area.

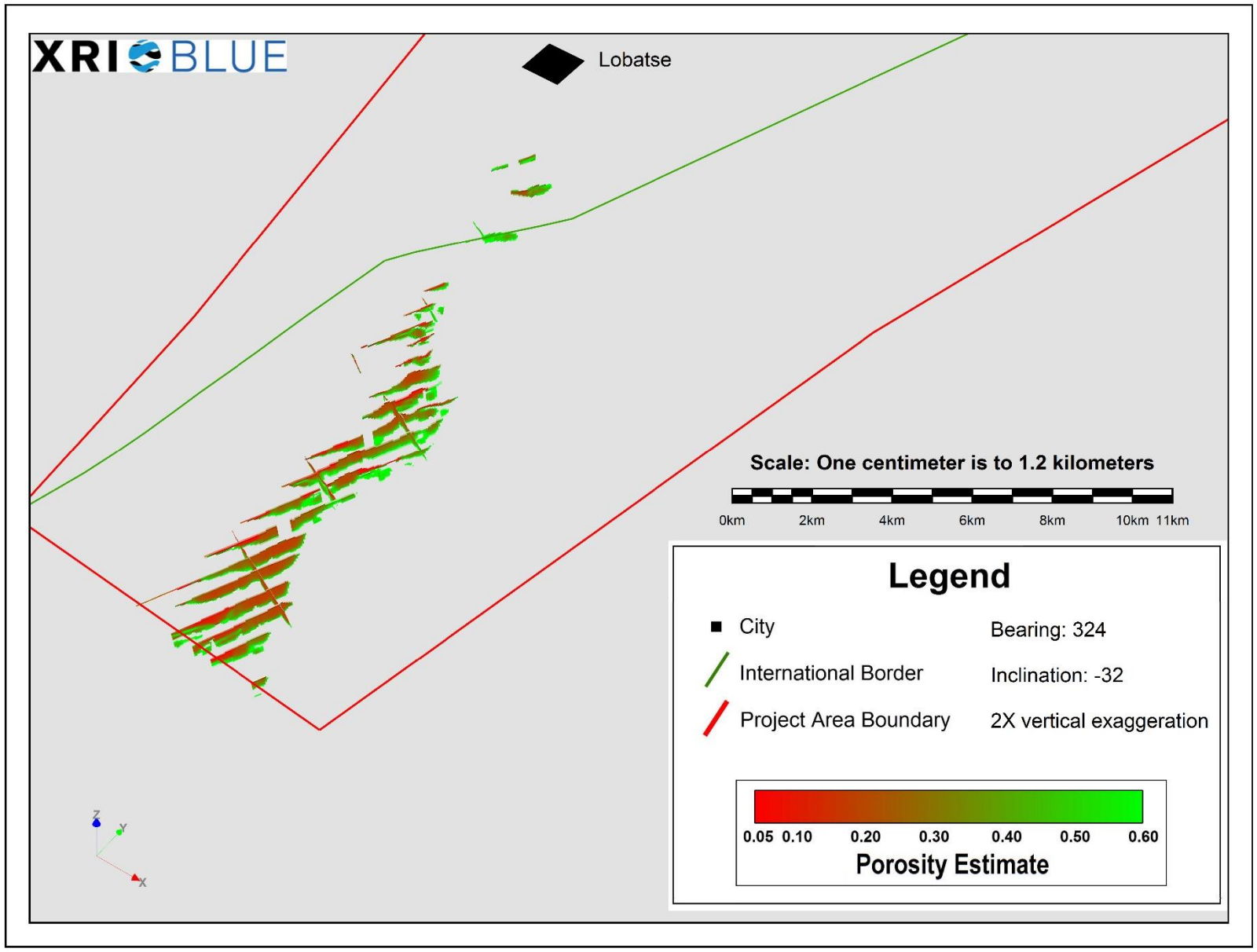

Figure 45: 3D view of the porosity estimates of the Ramotswa Dolomite in the Southern portion of the Ramotswa Project Area.

Pump Test Borehole No.	Easting [m] UTM 35 S *	Northing [m] UTM 35 S *	Elevation [m] *	Transmissivity [m^2/d]	Well Depth [m]	Resting Water Level [m bgl] *	Saturated Thickness (b) **	Calculated Hydraulic Conductivity (K) [m/d] | [m/s])		Extrapolated AEM derived Electrical Resistivity [ohm-m]	Extrapolated AEM Electrical Conductivity (σ [S/m])	Nearest AEM Flight Line	Distance to nearest AEM Sounding [m]
4336	385636	7247484	1030.7	800	102	13.2	88.8	9.0	1.04E-04	394.55	0.00253	102001	3487
4337	387656	7247733	1022.3	500	118	6.2	111.8	4.5	5.18E-05	210.63	0.00475	102201	875
4422	387385	7248087	1018.7	12	120	1.8	114	0.1	1.22E-06	156.65	0.00638	102001	1262
4423	386791	7245992	1023.3	210	120	8.3	111.7	1.9	2.18E-05	456.92	0.00219	102201	939
Z4400	386462	7247365	1023.7	500	102	6.6	95.4	5.2	6.07E-05	394.55	0.00253	101701	2190
4349	387338	7247344	1021.6	550	120	5.8	114.2	4.8	5.57E-05	516.01	0.00194	102201	1007

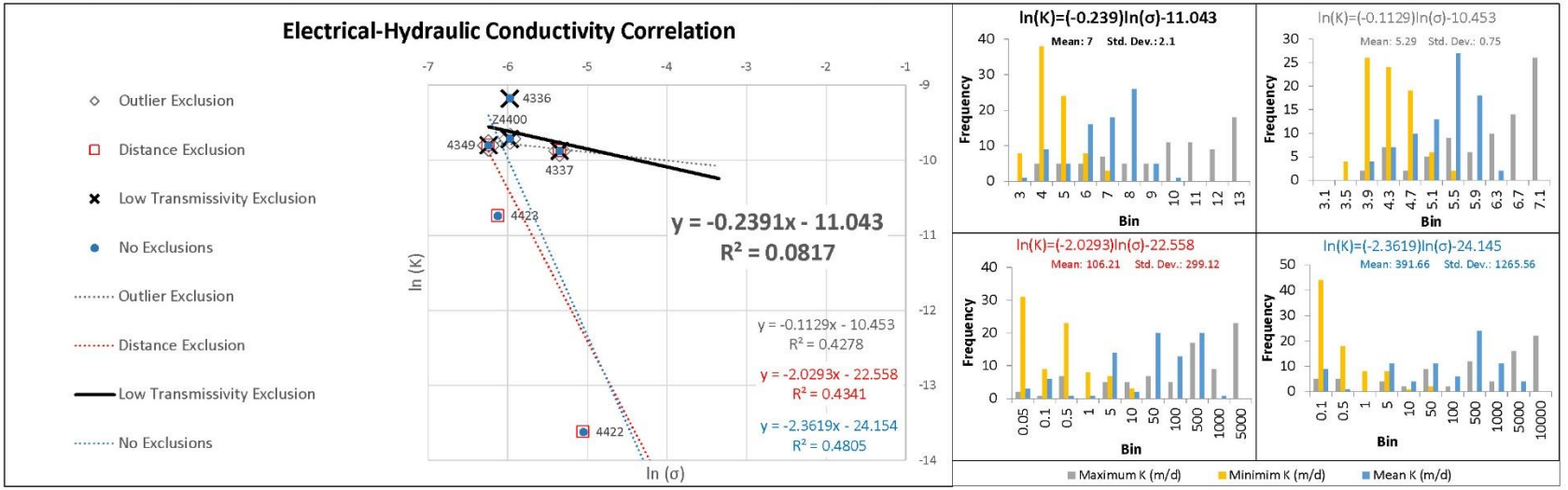

* As reported from pump test information (Carlsson, 2006), which may differ from other informatonn presented throughout the Ramostwa AEM Project

** Ground water level to well depth, with the exception of well 4422 in which 6m thick surface clay layer has been accounted for

Figure 46: Locations, elevations, provided transmissivity values, well depths, resting water level at the time of pump testing, saturated thickness of the aquifer, calculated hydraulic conductivity, extrapolated bulk resistivity & conductivity values and distance from the nearest AEM flight line for all boreholes used in the hydraulic conductivity distribution estimations and as well as the graphical and statistical analysis of various well data subsets.

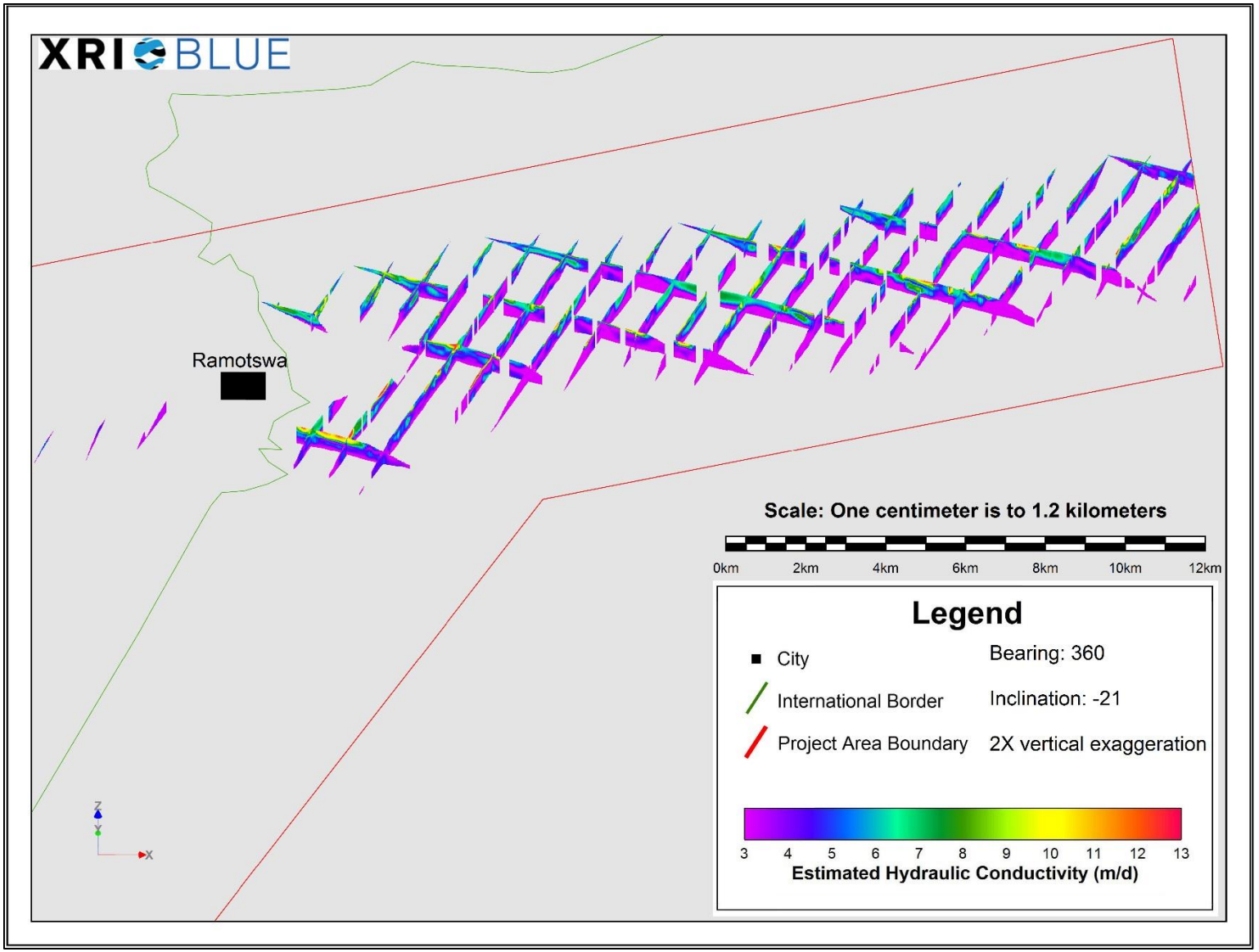

Figure 47: 3D view of the hydraulic conductivity estimates of the Ramotswa Dolomite in the Northern portion of the Ramotswa Project Area.

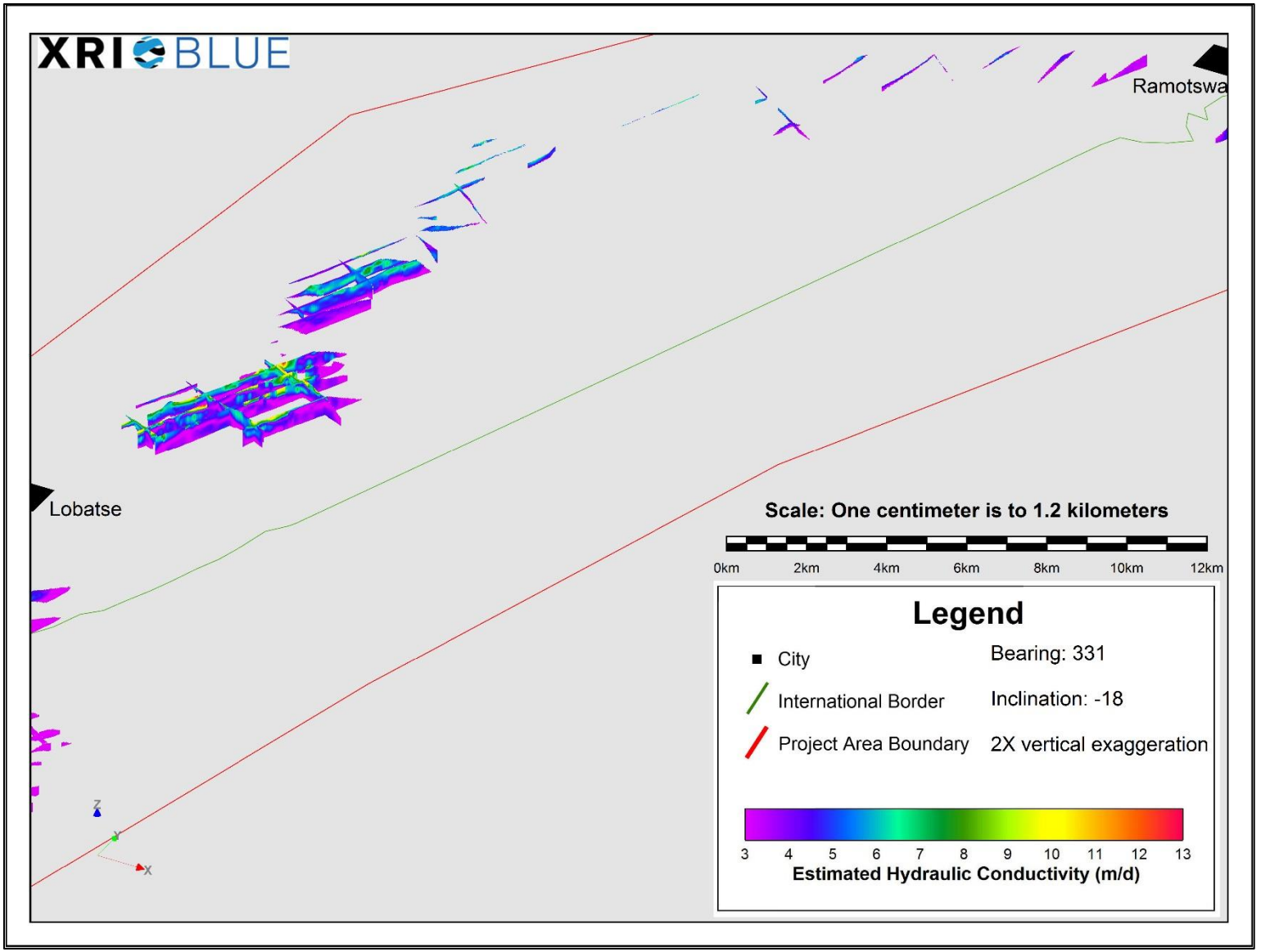

Figure 48: 3D view of the hydraulic conductivity estimates of the Ramotswa Dolomite in the Central portion of the Ramotswa Project Area.

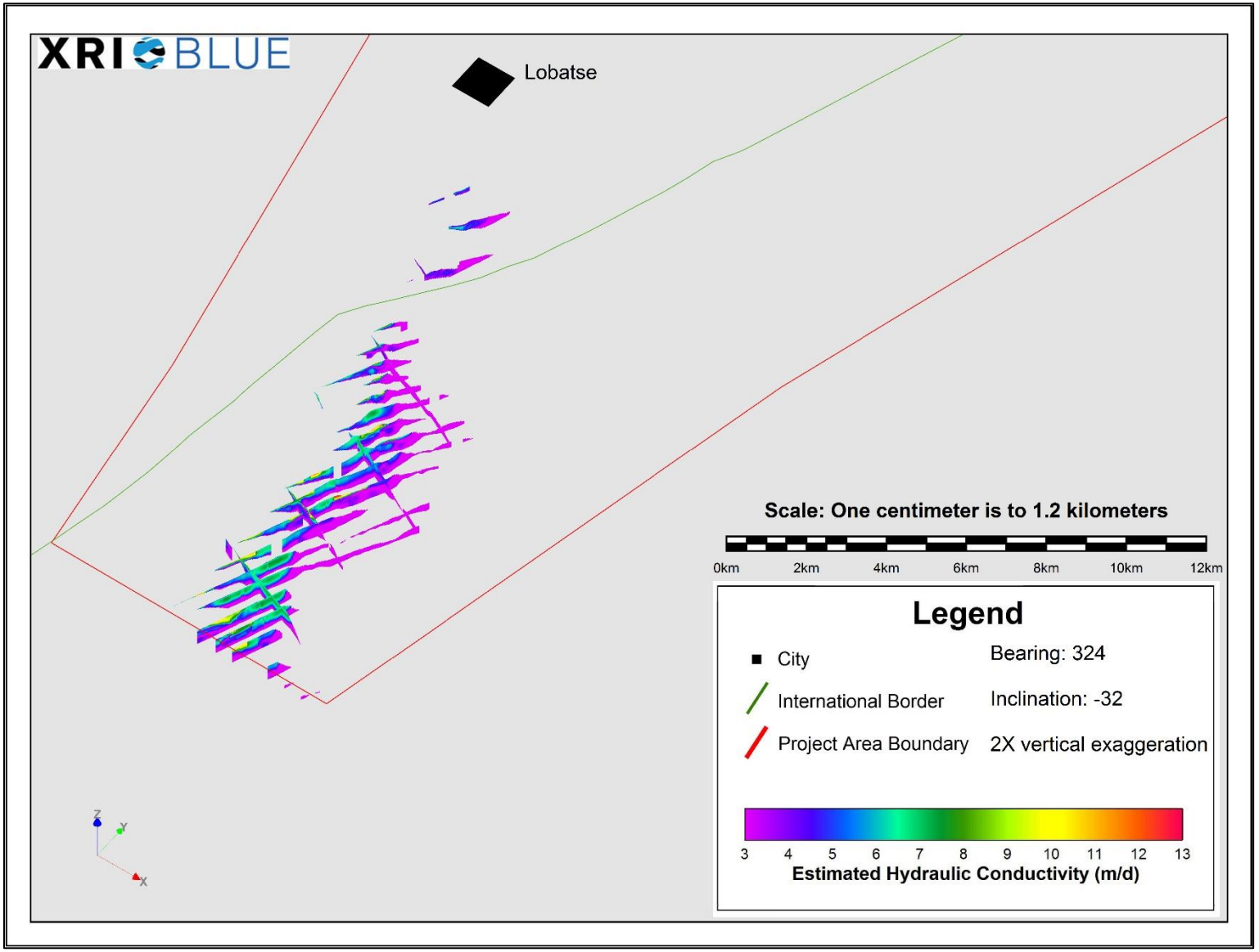

Figure 49: 3D view of the hydraulic conductivity estimates of the Ramotswa Dolomite in the Southern portion of the Ramotswa Project Area.

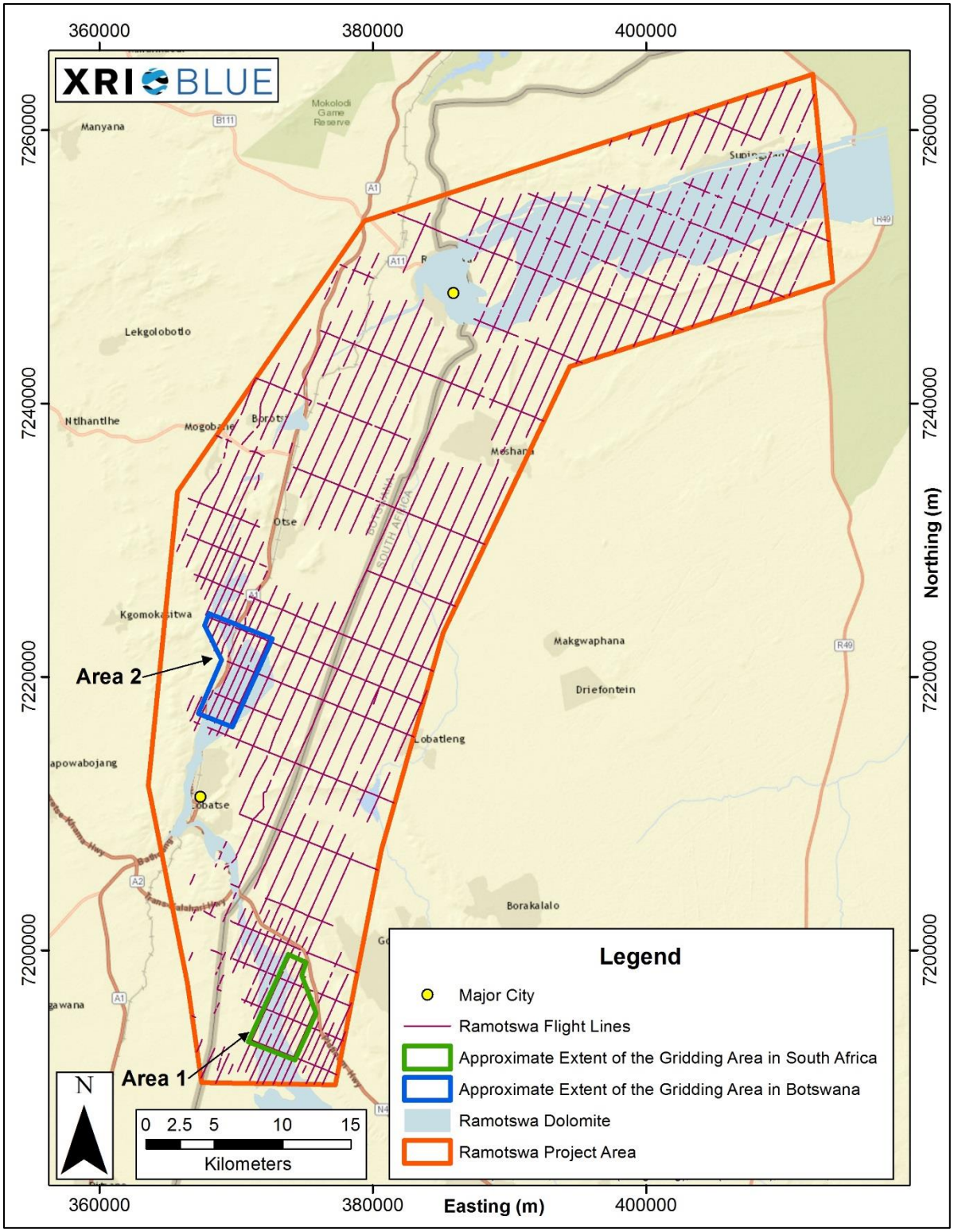

Figure 50: Two areas within the Ramotswa Project Area, where the minimal geologic complexity in the subsurface allowed for realistic and geologically valid gridding of the present geologic formations.

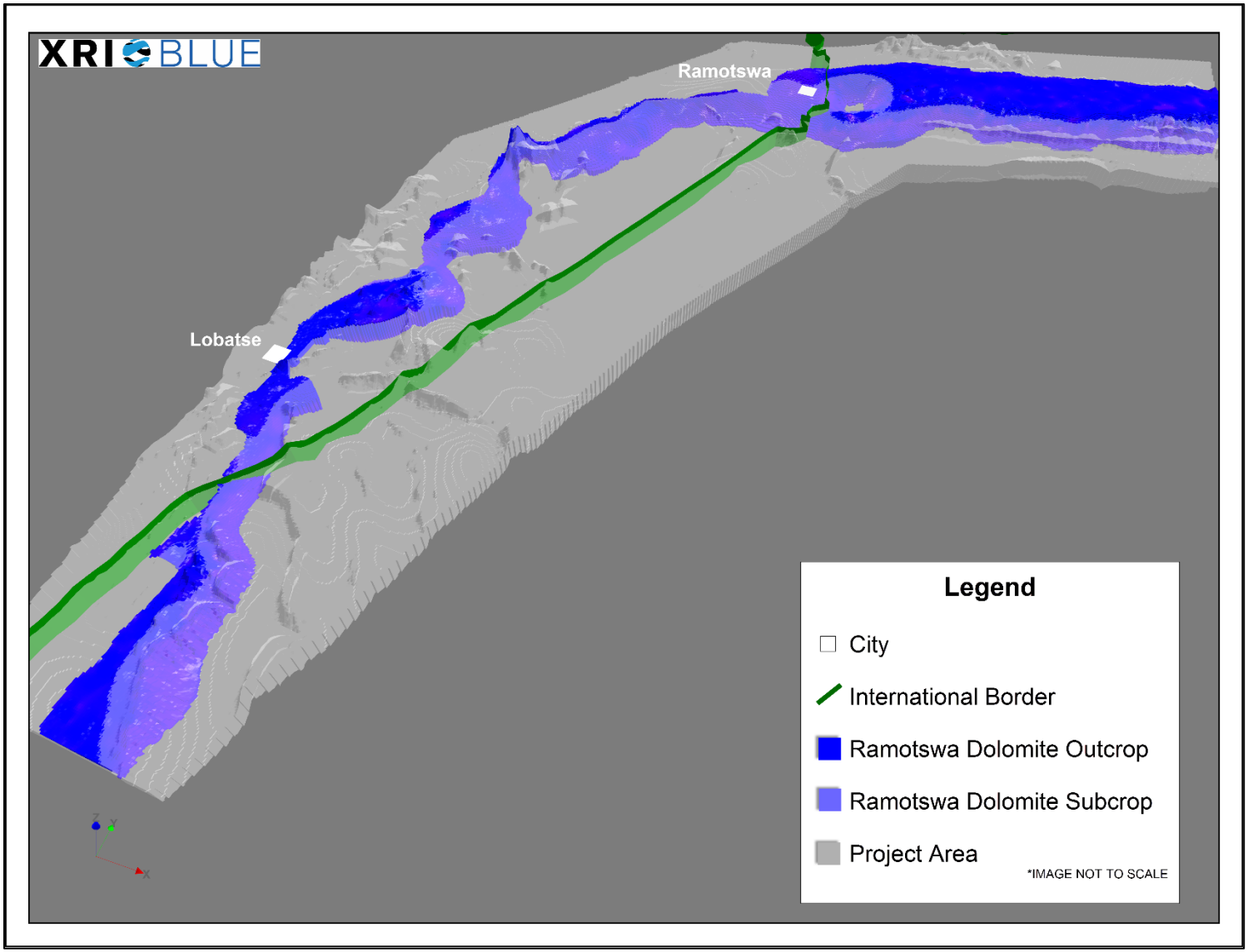

Figure 51: Representative schematic of the Ramotswa Dolomite.

Appendix B: AEM and Interpreted Geology Profiles

Table 1 provides the details of the interpreted geology .xyz file for the Ramotswa Project Area. Specifically the first column in Table 1 is the Header or name for each unique column in the .xyz file, the second column in Table 1 is the type of data that is presented, and the third column in Table 1 is a brief description of the data that is provided for each specific column (with units).

To view this .xyz file in Microsoft Excel, the user should open the file, which will cause a "Text Import Wizard" Popup Box to be displayed. For Step 1, make sure that the box for "Delimited" is checked, and that the "Start import at row" is set to "6", then click the "Next" button. For Step 2, the "Tab" and "Comma" Delimiters boxes should be checked, then click the "Next" button. For the Step 3, all the defaults can be left alone, and the "Finish" button can be clicked. Following these steps should allow the file to be correctly imported into Microsoft Excel with all the correct headers.

XRI used both Geosoft's Oasis Montaj (http://www.geosoft.com/products/oasis-montaj/overview) and Encom's PA (https://www.pitneybowes.com/pbencom/products/geophysics/encom-pa.html) software packages to view and interpret data for this project. An alternative software option for 3D viewing of this data that is Golden Software's Voxler (http://www.goldensoftware.com/products/voxler).

This .xyz file is the basis of the Interpreted Geology Profiles included in Appendix B. Within the .xyz file if the symbol "*" is observed that indicates that the formation has not been interpreted to be present at that location. The remainder of Appendix B is used to display all the unique AEM and Interpreted Geology Profiles for the Ramotswa Project Area. The AEM and Interpreted Geology Profiles are displayed with a 1:1 horizontal and vertical ratio, each profile is uniquely scaled so that the information for an entire flight line is displayed in one figure. While the specifics of each profile may be difficult to view in the figure, the Ramotswa_Geologic_Interpretations.xyz file provided along with this report give all of the necessary data to understand the subsurface geology of the Ramotswa Project Area.

Table 1: Explanation of the Interpreted Geology .xyz file of the Ramotswa Project Area.

Header	Data Type	Description
LINE	Point	Line Number
X	Point	X Coordinate of Data Point (WGS84 UTM Zone 35S meters)
Y	Point	Y Coordinate of Data Point (WGS84 UTM Zone 35S meters)
Z	Point	Surface elevation based on USGS SRTM Digital Elevation Model (meters)
DOI_UPPER	Point	Shallow DOI estimate for data point (meters)
DOI_LOWER	Point	Deep DOI estimate for data point (meters)
RESDATA	Point	Calculated data residual for each inverted AEM sounding (unitless)
SurfaceDeposits_top	Point	Interpreted top of the Surface Deposits (meters)
SurfaceDeposits_base	Point	Interpreted base of the Surface Deposits (meters)
IgneousIntrusions_top	Point	Interpreted top of an Igneous Intrusion (meters)
IgneousIntrusions_base	Point	Interpreted base of an Igneous Intrusion (meters)
Waterberg_top	Point	Interpreted top of the Waterberg Formation (meters)
Waterberg_base	Point	Interpreted base of the Waterberg Formation (meters)
BushveldComplex_top	Point	Interpreted top of the Bushveld Igneous Complex (meters)
BushveldComplex_base	Point	Interpreted base of the Bushveld Igneous Complex (meters)

Woodlands_top	Point	Interpreted top of the Woodlands Formation (meters)
Woodlands_base	Point	Interpreted base of the Woodlands Formation (meters)
Magaliesberg_top	Point	Interpreted top of the Magaliesberg Formation (meters)
Magaliesberg_base	Point	Interpreted base of the Magaliesberg Formation (meters)
Silverton_top	Point	Interpreted top of the Silverton Formation (meters)
Silverton_base	Point	Interpreted base of the Silverton Formation (meters)
DitlojanaQuartzite_top	Point	Interpreted top of the Ditlojana Quartzite (meters)
DitlojanaQuartzite_base	Point	Interpreted base of the Ditlojana Quartzite (meters)
DitlojanaVolcanics_top	Point	Interpreted top of the Ditlojana Volcanics (meters)
DitlojanaVolcanics_base	Point	Interpreted base of the Ditlojana Volcanics (meters)
DitlojanaShale_top	Point	Interpreted top of the Ditlojana Shale (meters)
DitlojanaShale_base	Point	Interpreted base of the Ditlojana Shale (meters)
TimeballHill_top	Point	Interpreted top of the Timeball Hill Formation (meters)
TimbeballHill_base	Point	Interpreted base of the Timeball Hill Formation (meters)
Rooihoogte_top	Point	Interpreted top of the Rooihoogte Formation (meters)
Rooihoogte_base	Point	Interpreted base of the Rooihoogte Formation (meters)
Duitschland_top	Point	Interpreted top of the Duitschland Formation (meters)
Duitschland_base	Point	Interpreted base of the Duitschland Formation (meters)
Penge_top	Point	Interpreted top of the Penge Formation (meters)
Penge_base	Point	Interpreted base of the Penge Formation (meters)
Frisco_base	Point	Interpreted base of the Frisco Formation of the Ramotswa Dolomite (meters)
Frisco_top	Point	Interpreted top of the Frisco Formation of the Ramotswa Dolomite (meters)
Eccles_top	Point	Interpreted top of the Eccles formation within the Ramotswa Dolomite (meters)
Eccles_base	Point	Interpreted base of the Eccles formation within the Ramotswa Dolomite (meters)
Lyttleton_top	Point	Interpreted top of the Lyttleton formation within the Ramotswa Dolomite (meters)
Lyttleton_base	Point	Interpreted base of the Lyttleton formation within the Ramotswa Dolomite (meters)
MonteChristo_top	Point	Interpreted top of the Monte Christo formation within the Ramotswa Dolomite (meters)
MonteChristo_base	Point	Interpreted base of the Monte Christo formation within the Ramotswa Dolomite (meters)
Oaktree_top	Point	Interpreted top of the Oaktree formation within the Ramotswa Dolomite (meters)
Oaktree_base	Point	Interpreted base of the Oaktree formation within the Ramotswa Dolomite (meters)
RamotswaDolomite_top	Point	Interpreted top of the Ramotswa Dolomite (meters)
RamotswaDolomite_base	Point	Interpreted base of the Ramotswa Dolomite (meters)
BlackReef_top	Point	Interpreted top of the Black Reef Quartzite (meters)
BlackReef_base	Point	Interpreted base of the Black Reef Quartzite (meters)
preTransvaal_top	Point	Interpreted top of the Pre-Transvaal Formations (meters)

Fault	Point	Interpreted fault (meters)

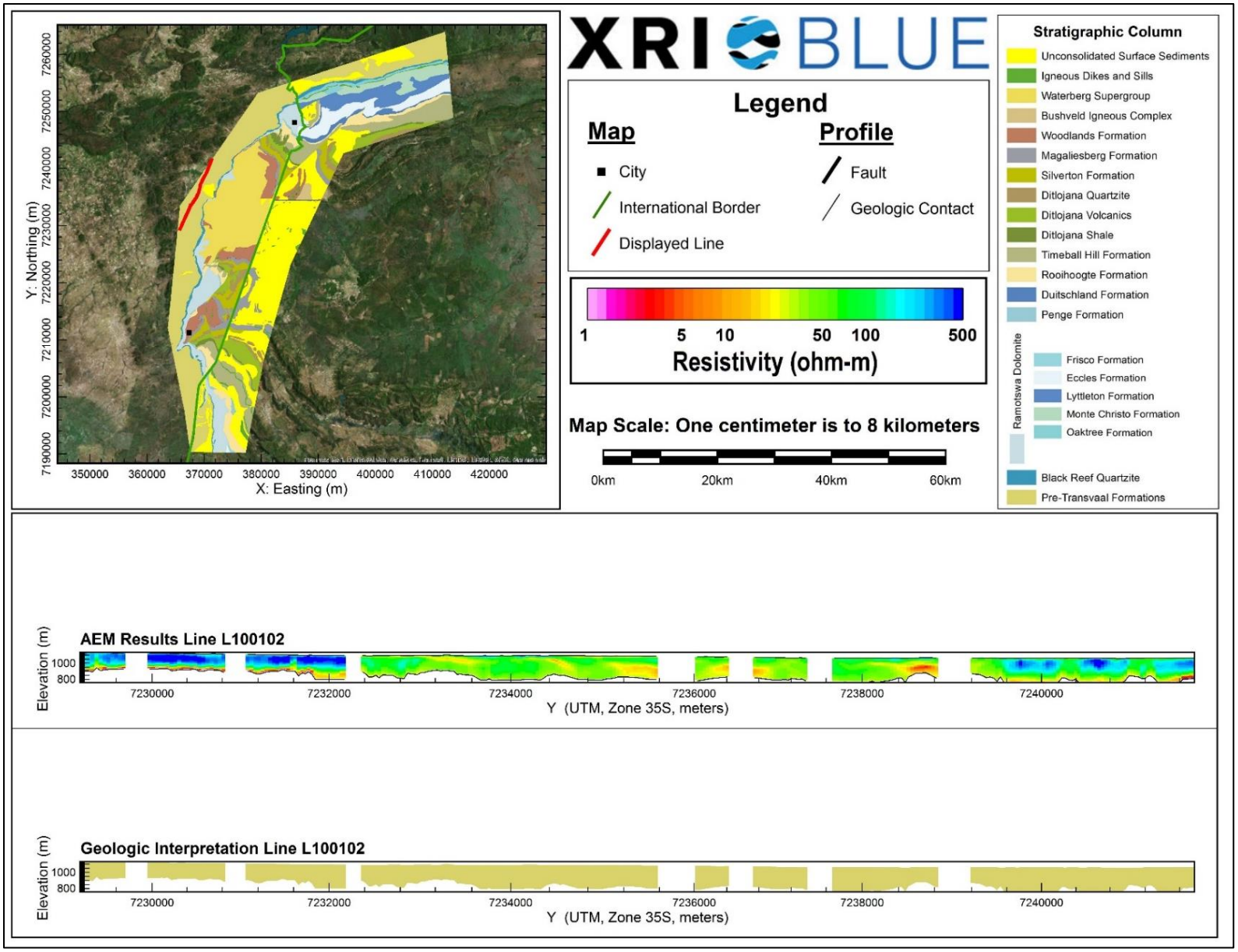

AEM and Interpreted Geology Profile for L100102.

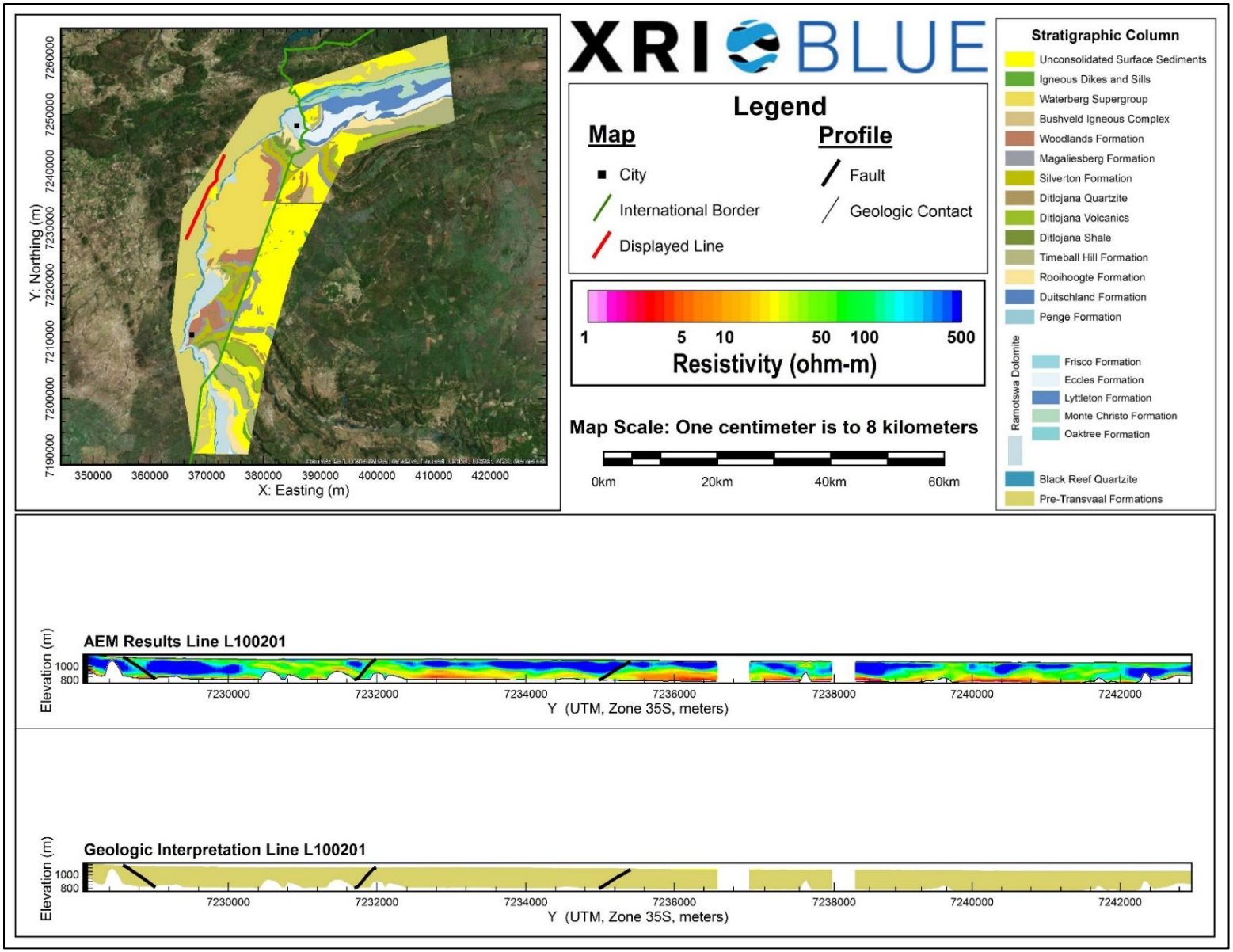

AEM and Interpreted Geology Profile for L100201.

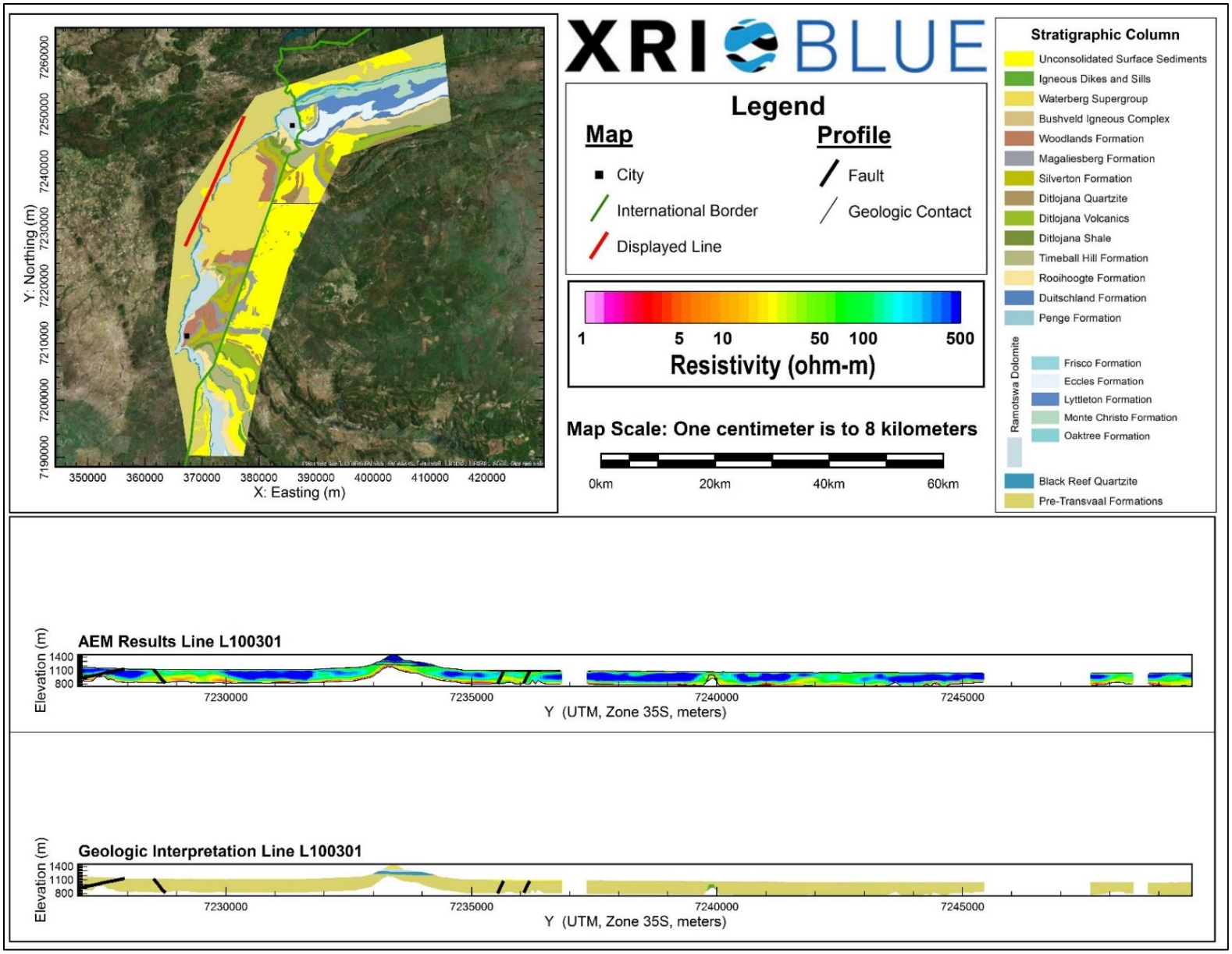

AEM and Interpreted Geology Profile for L100301.

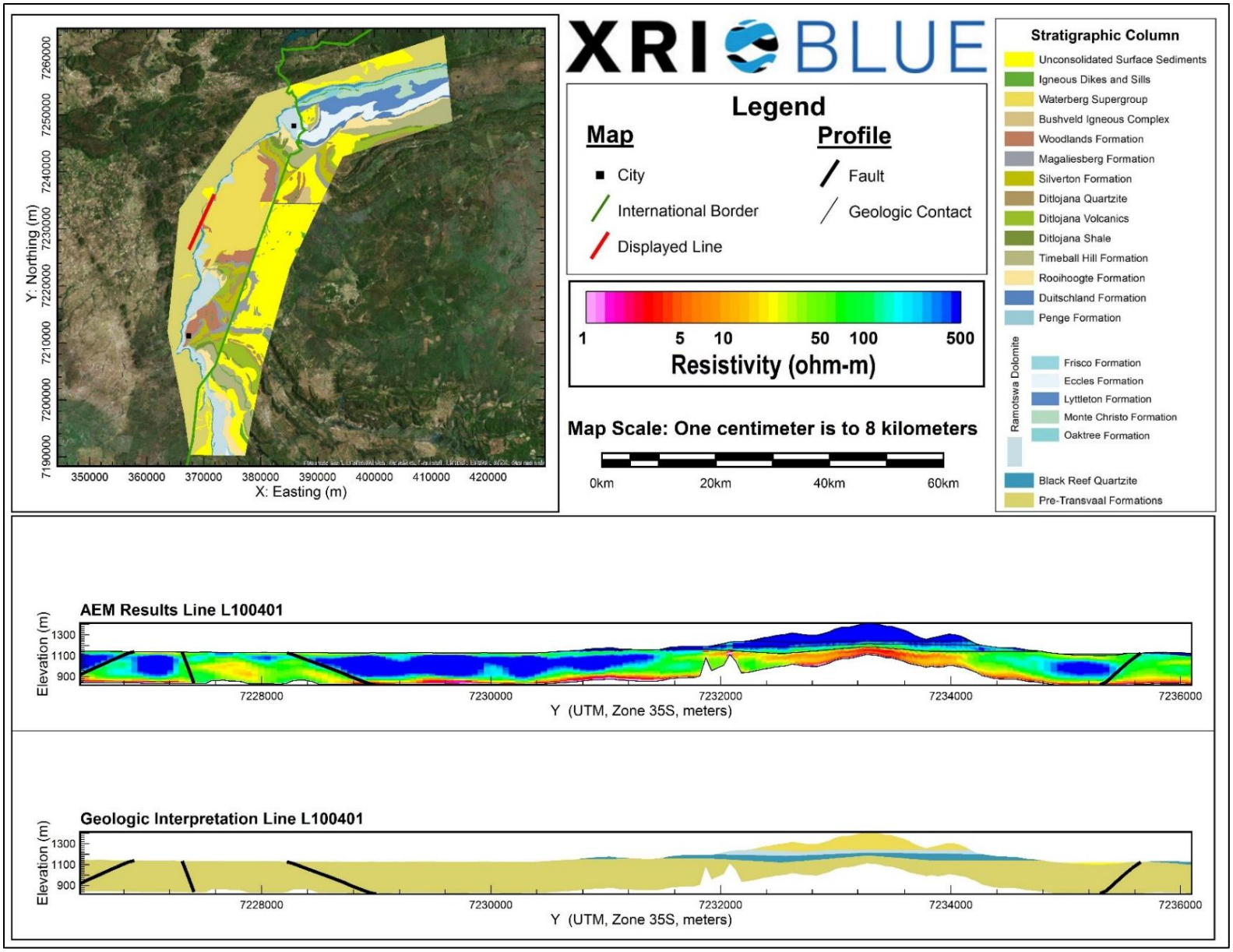

AEM and Interpreted Geology Profile for L100401.

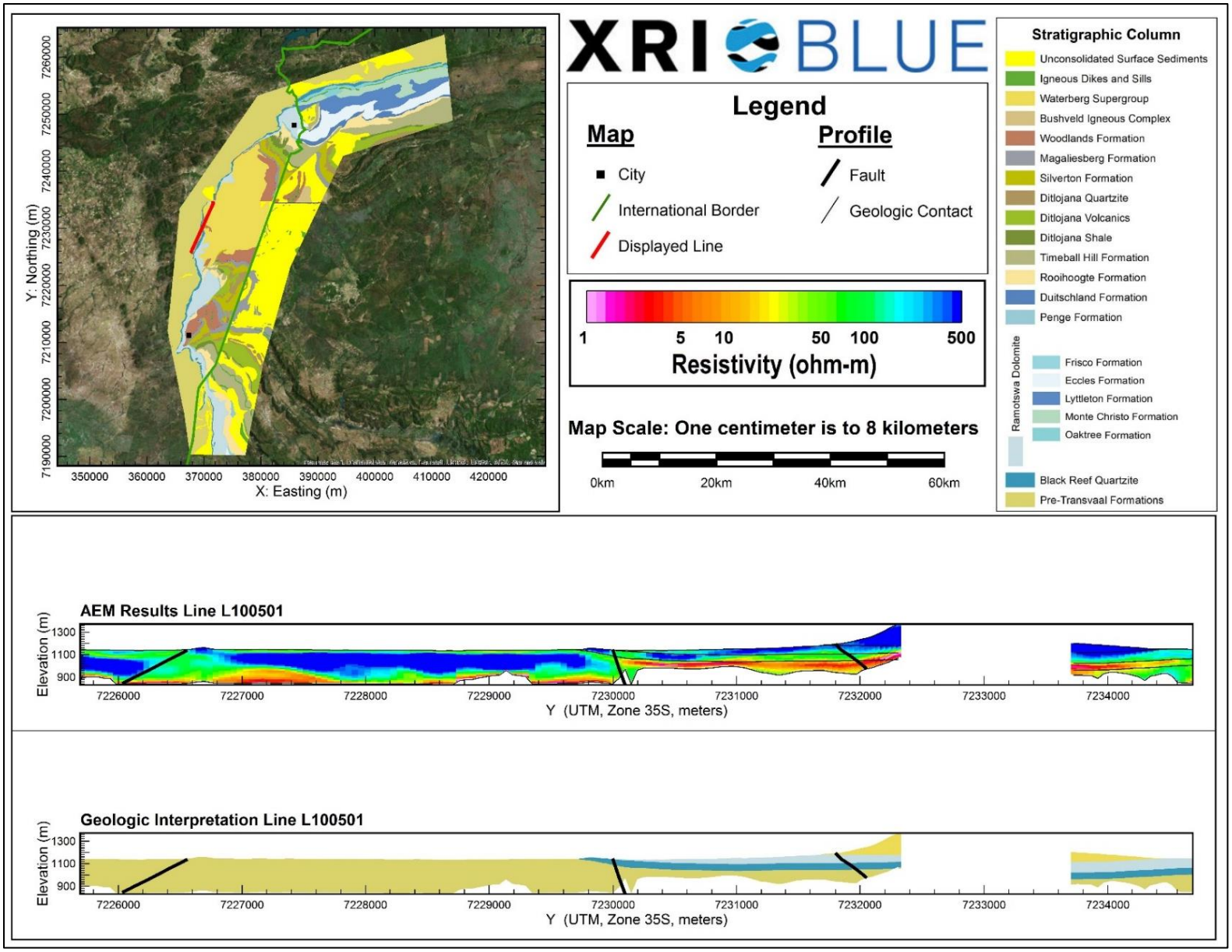

AEM and Interpreted Geology Profile for L100501.

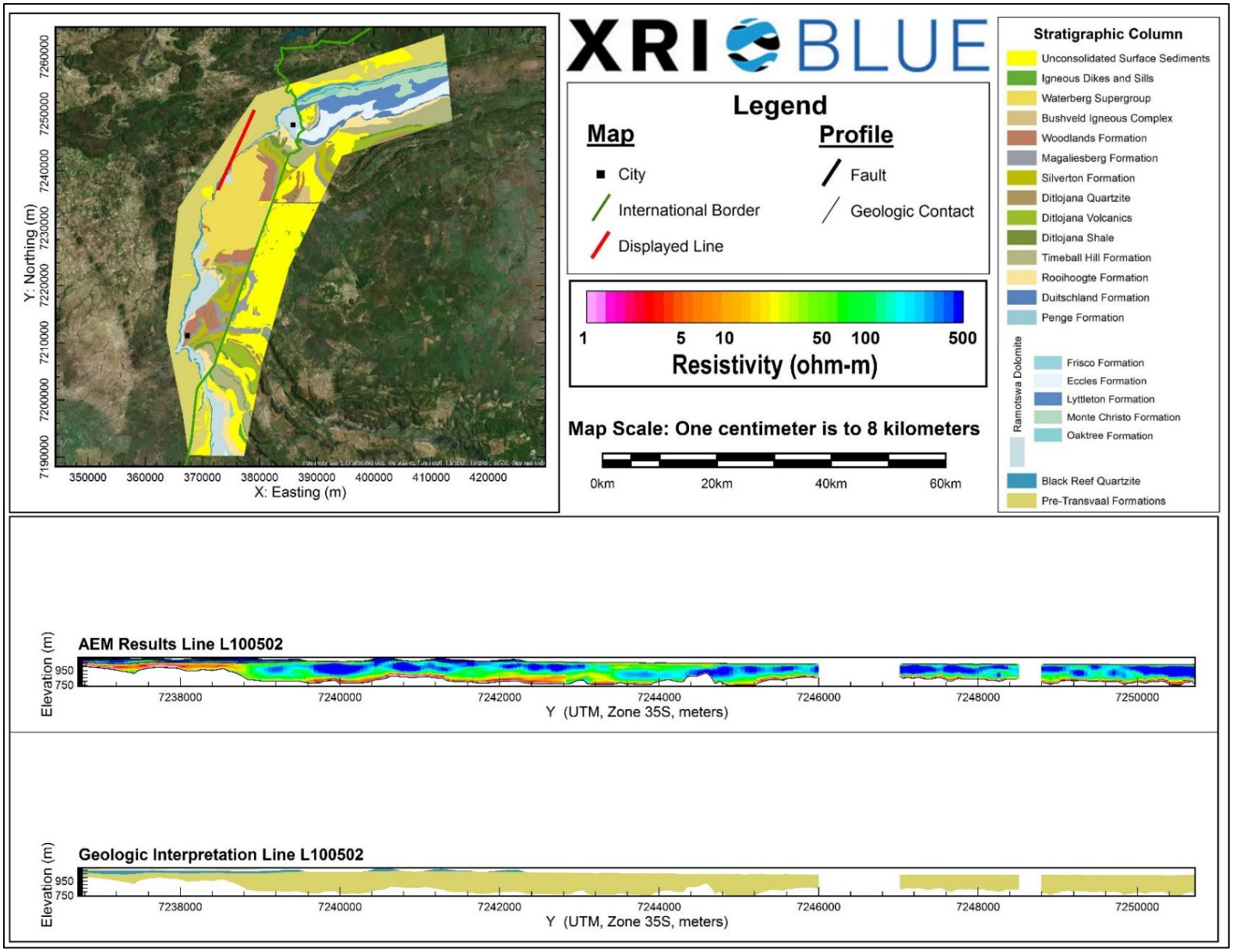

AEM and Interpreted Geology Profile for L100502.

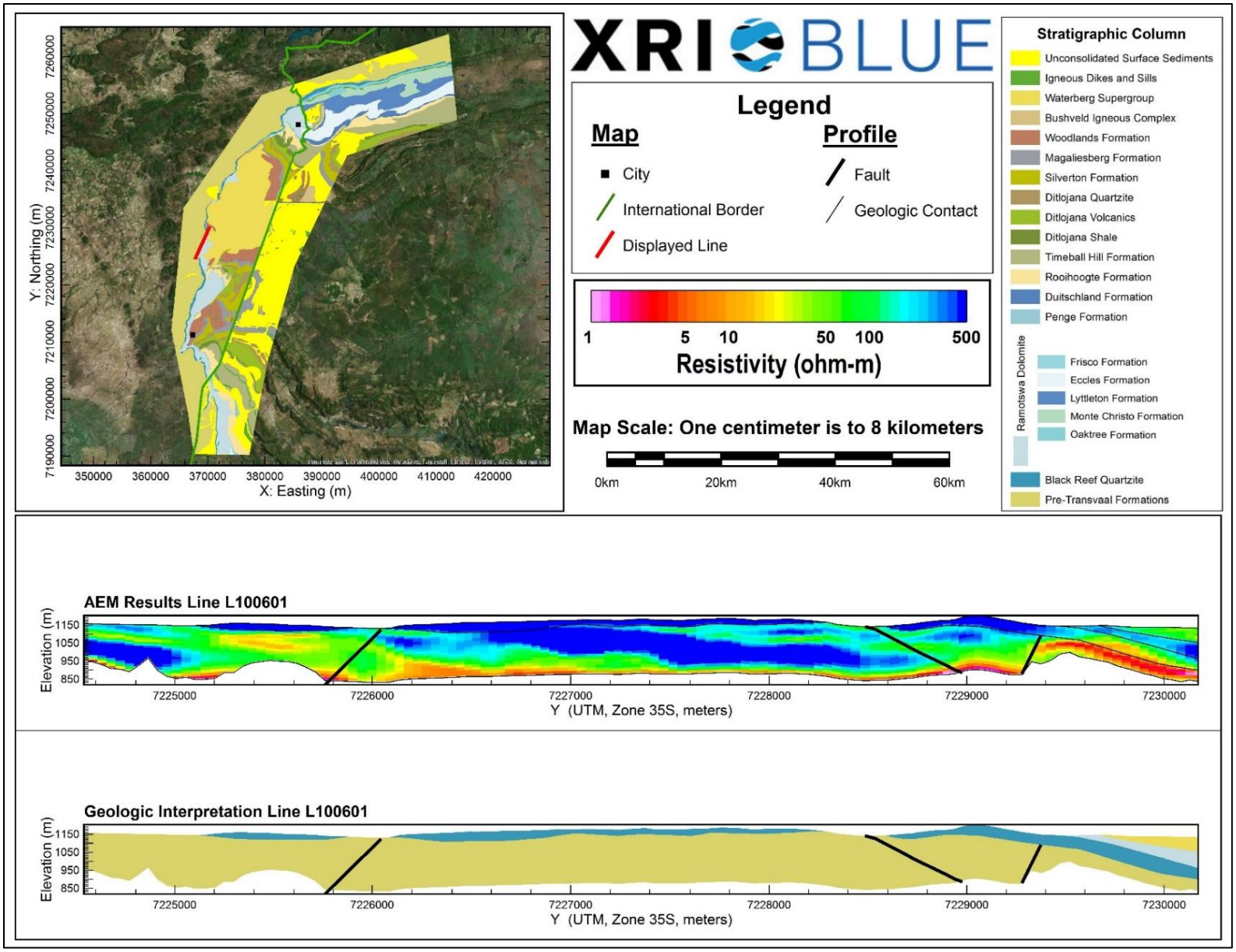

AEM and Interpreted Geology Profile for L100601.

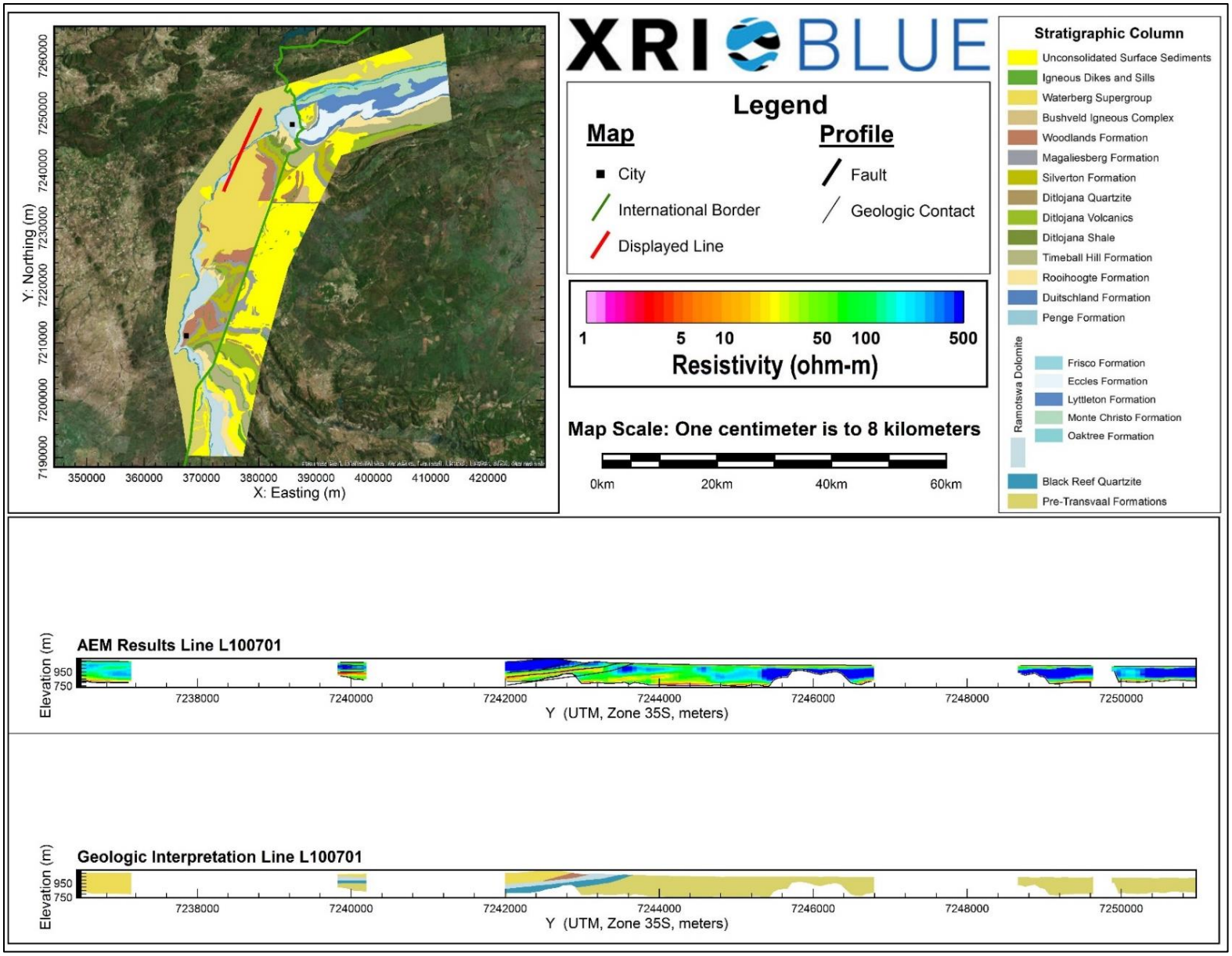

AEM and Interpreted Geology Profile for L100701.

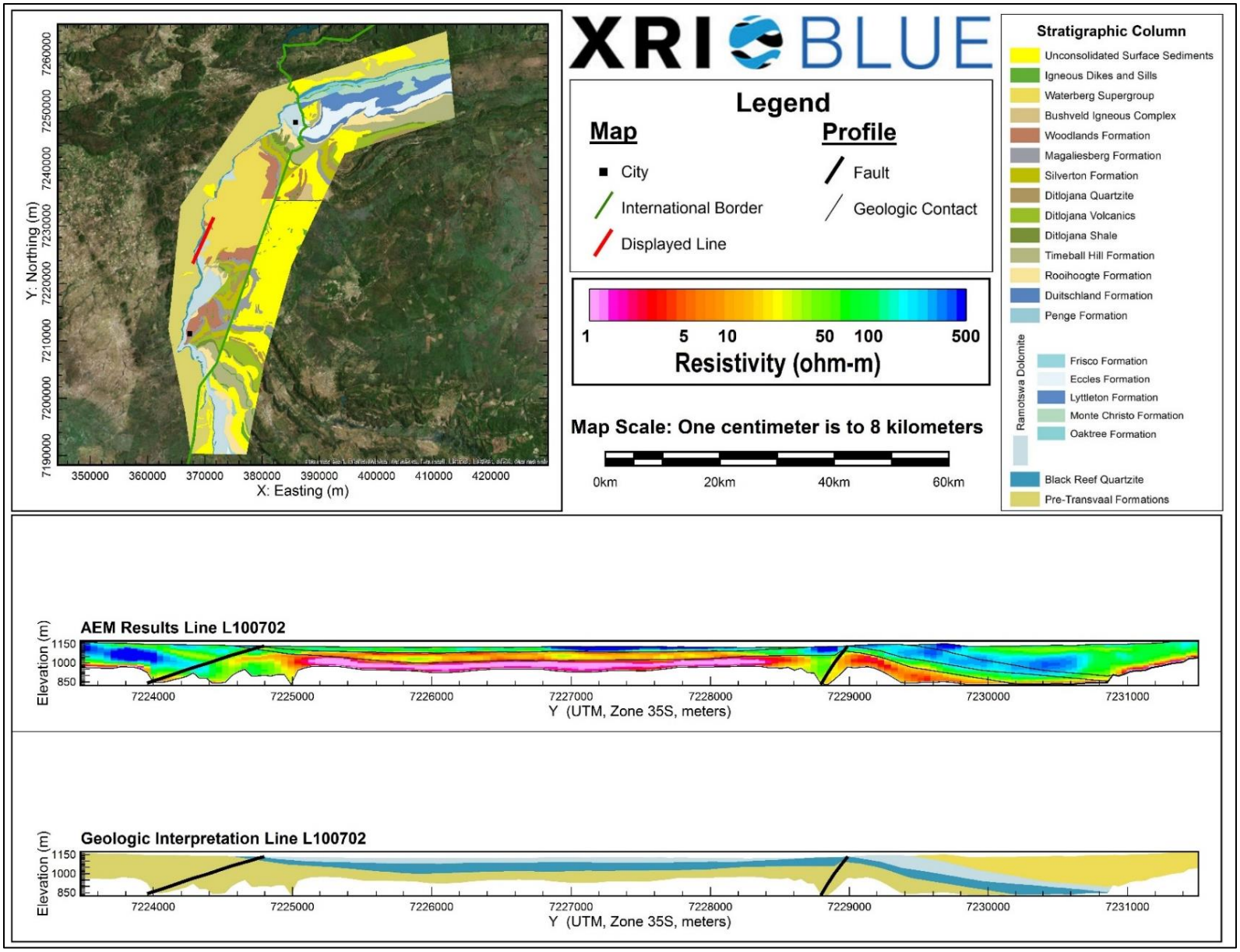

AEM and Interpreted Geology Profile for L100702.

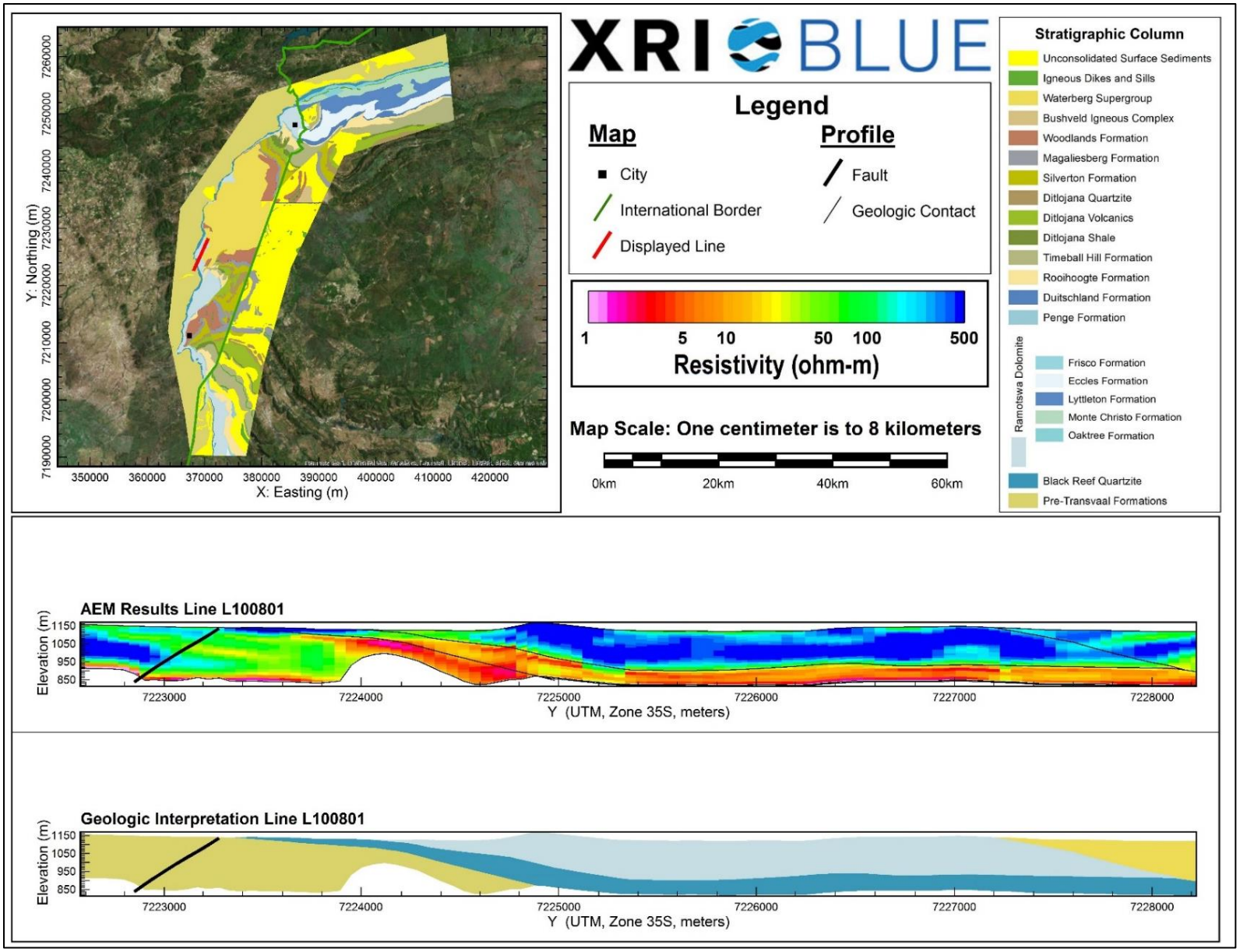

AEM and Interpreted Geology Profile for L100801.

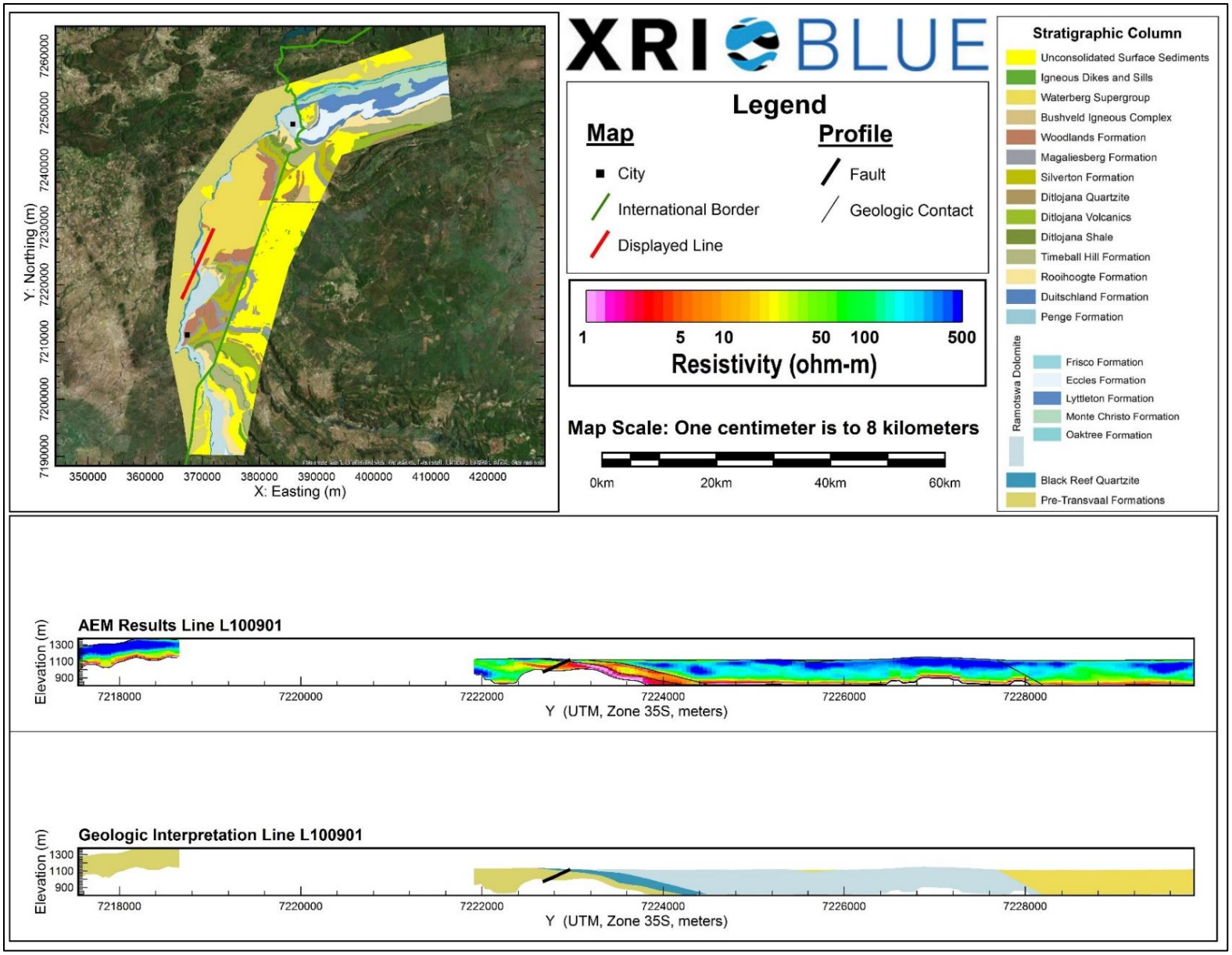

AEM and Interpreted Geology Profile for L100901.

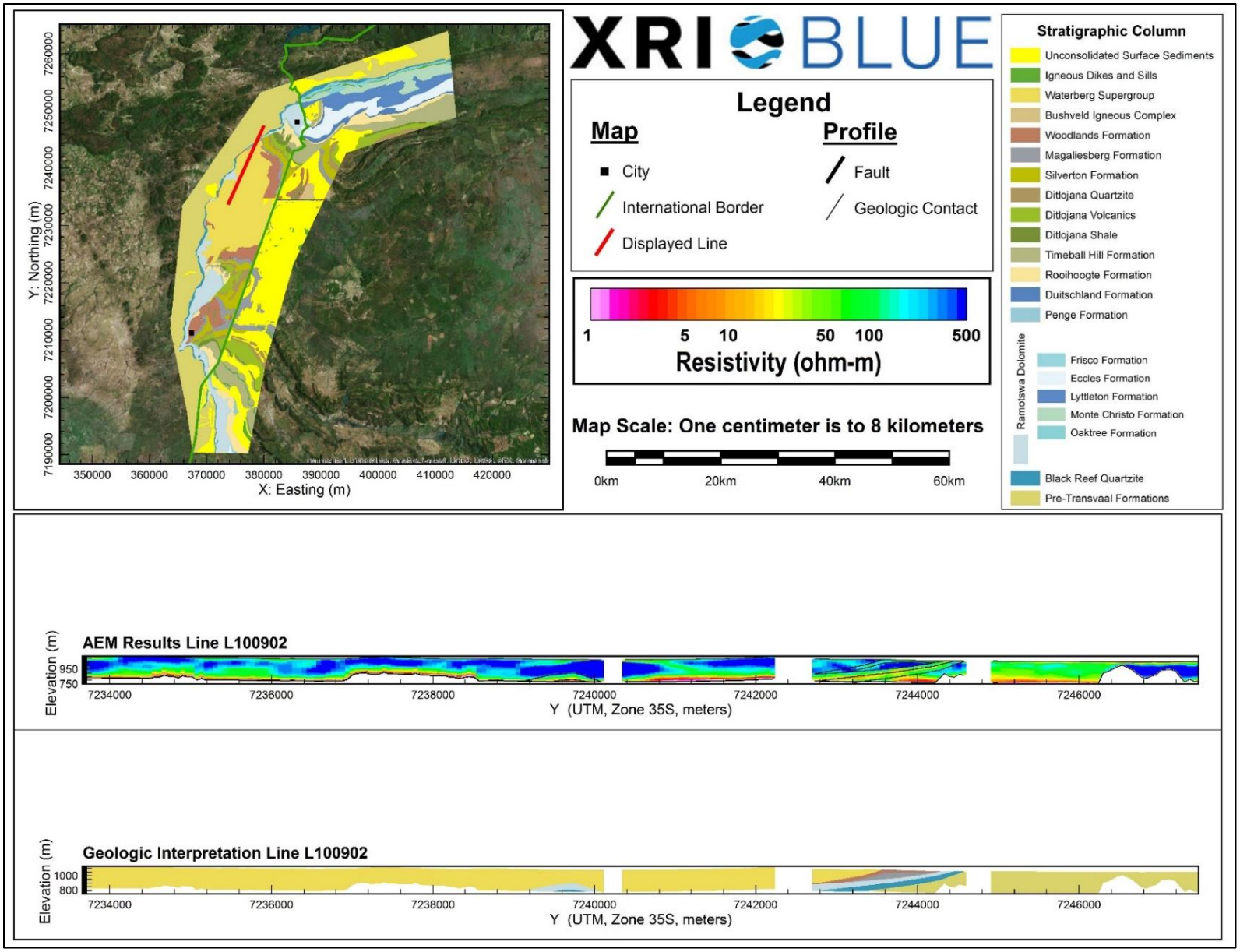

AEM and Interpreted Geology Profile for L100902.

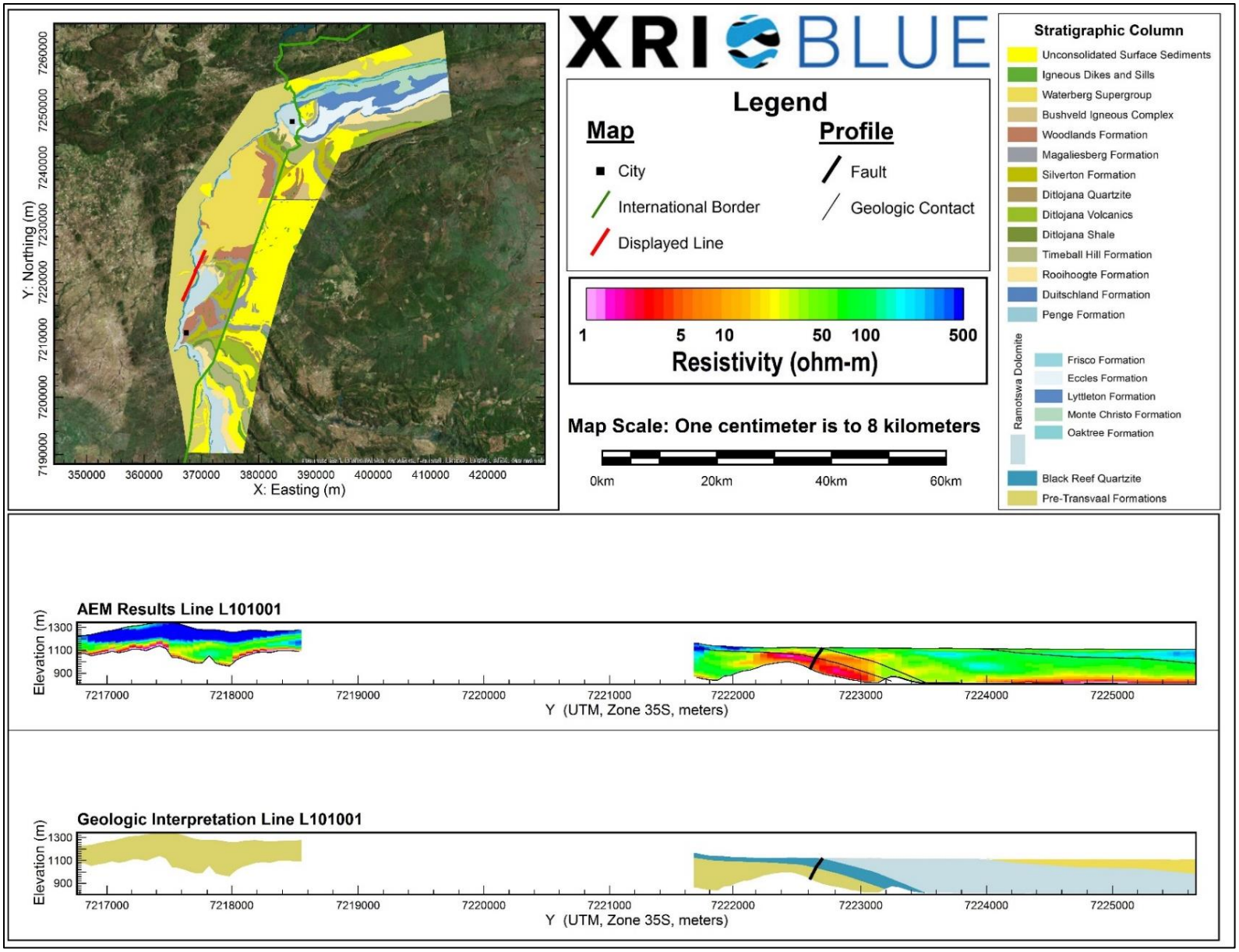

AEM and Interpreted Geology Profile for L1010001.

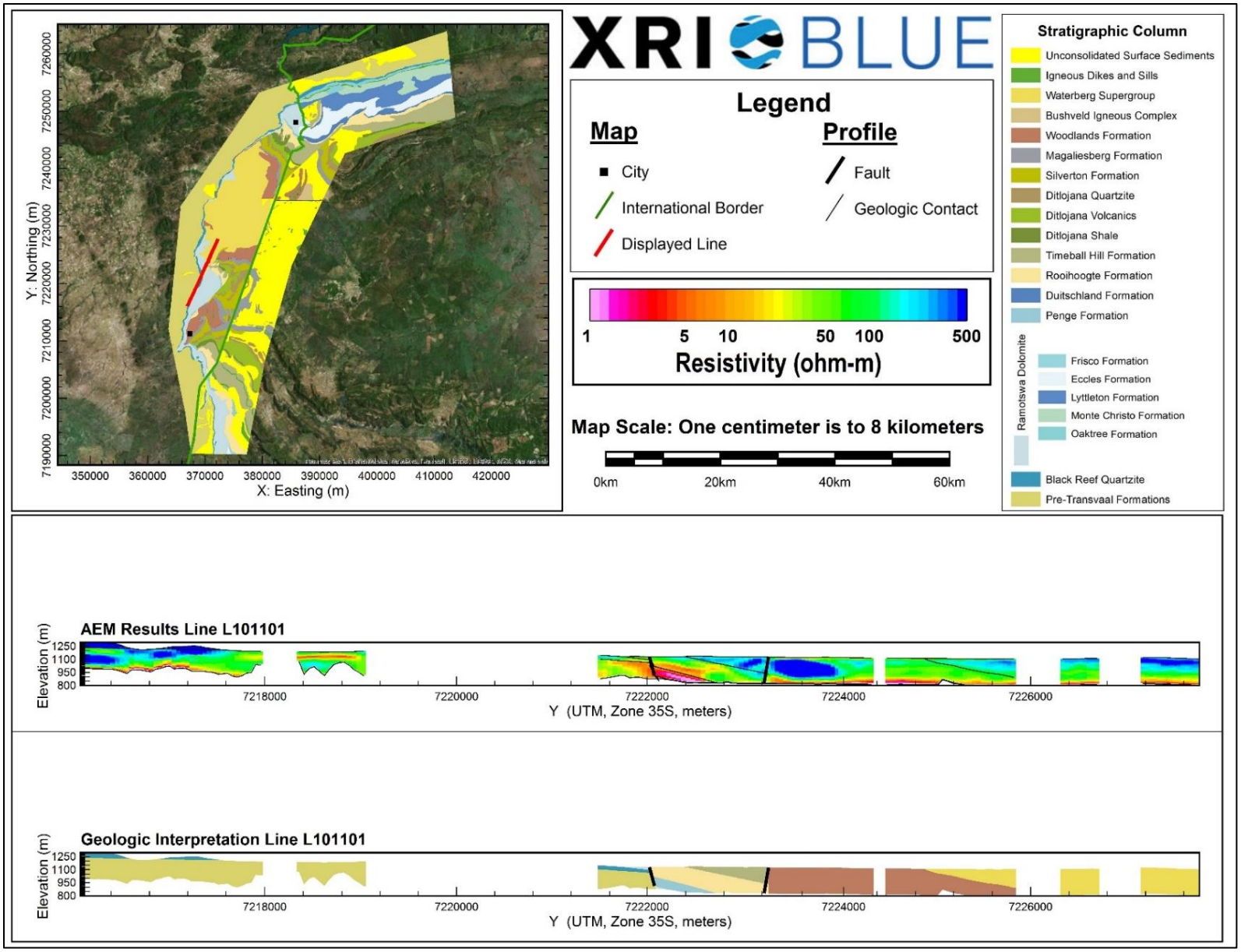

AEM and Interpreted Geology Profile for L101101.

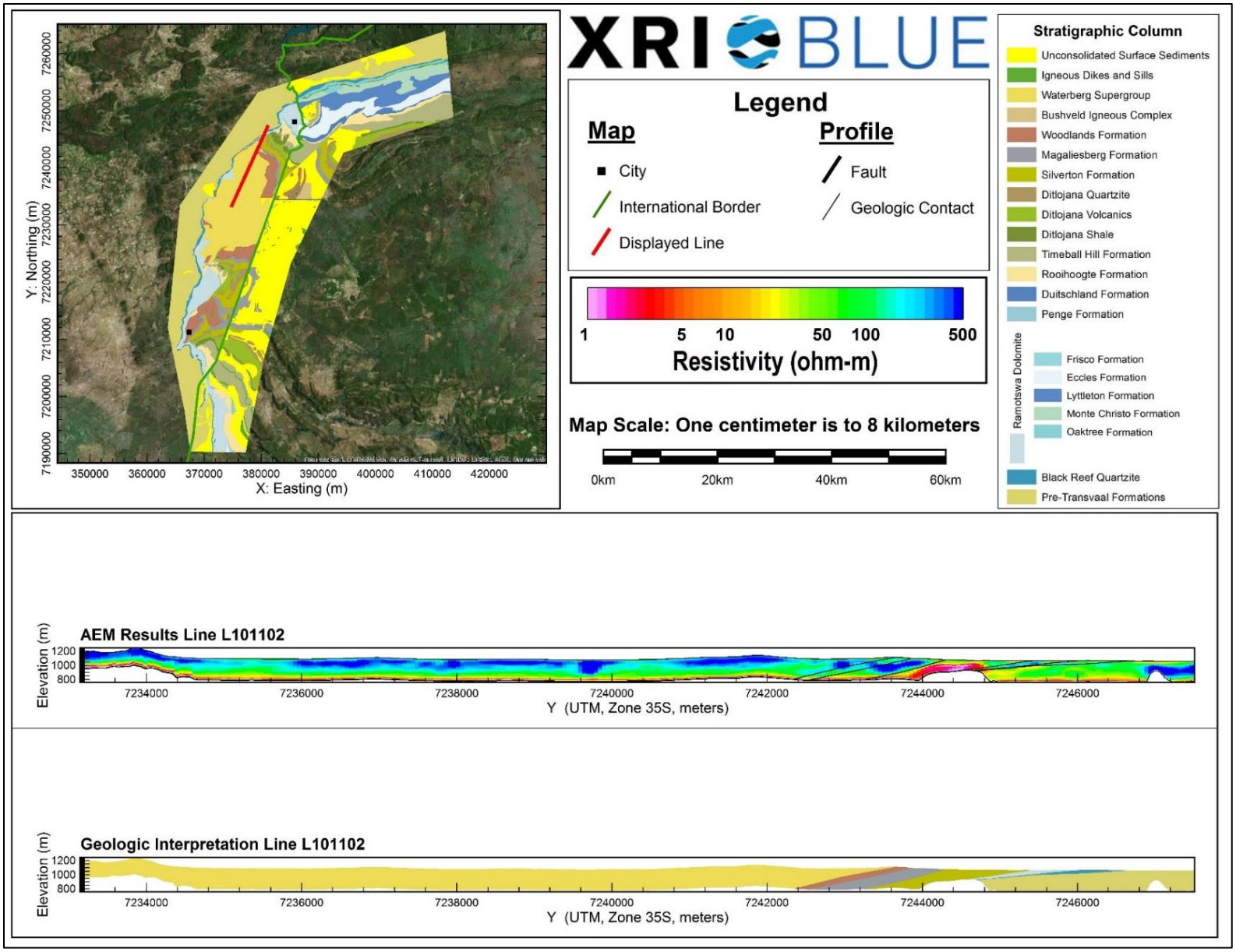

AEM and Interpreted Geology Profile for L101102.

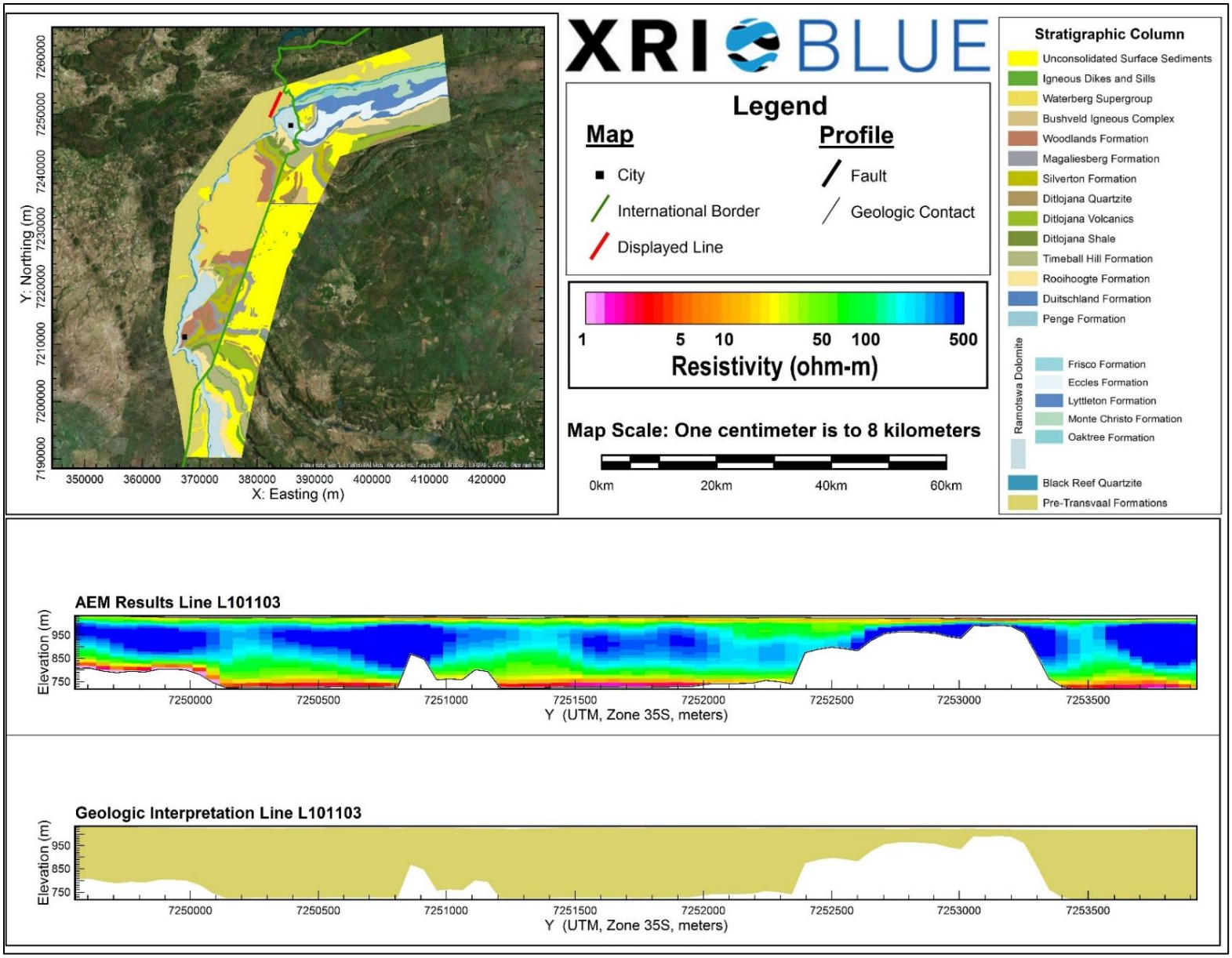

AEM and Interpreted Geology Profile for L101103.

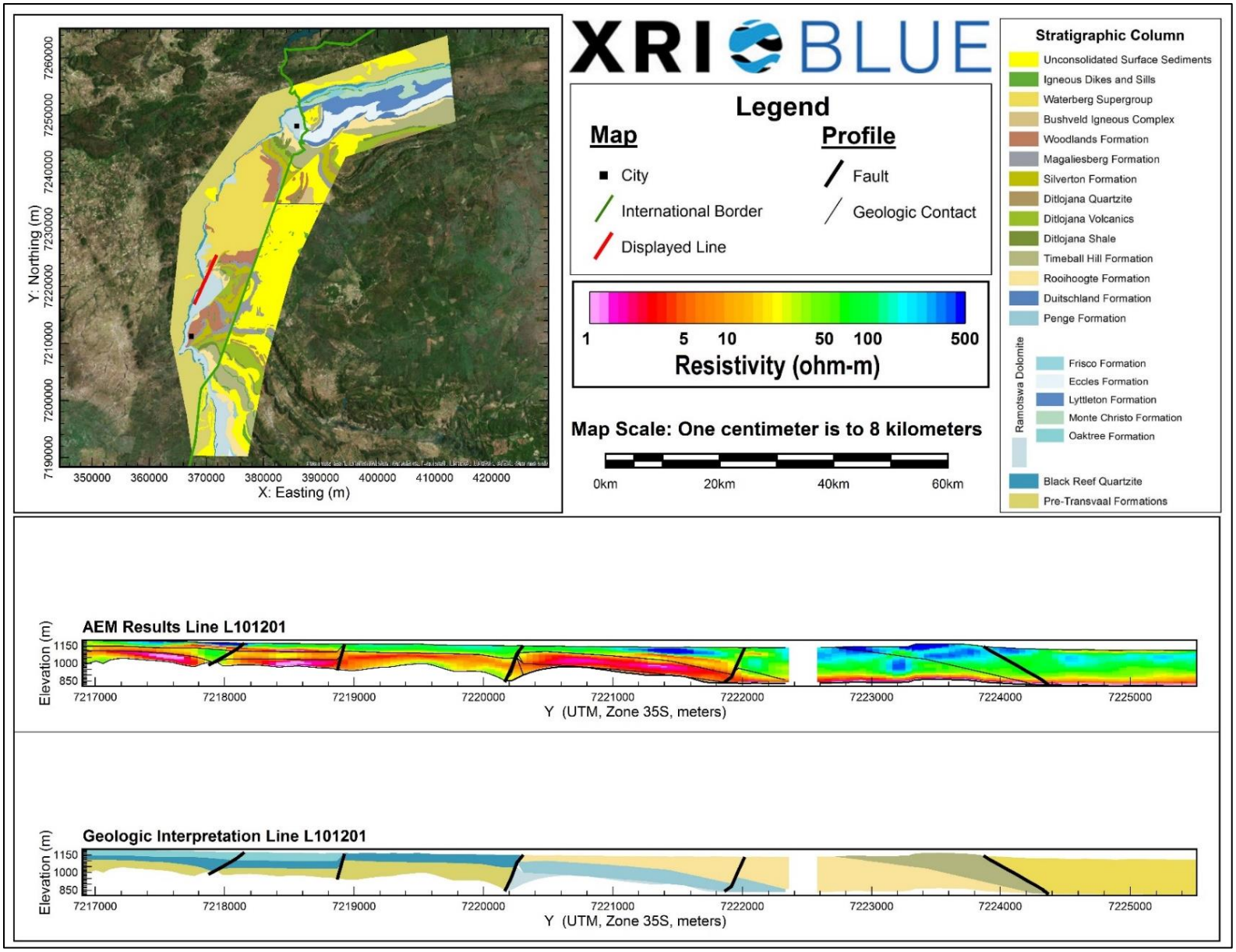

AEM and Interpreted Geology Profile for L101201.

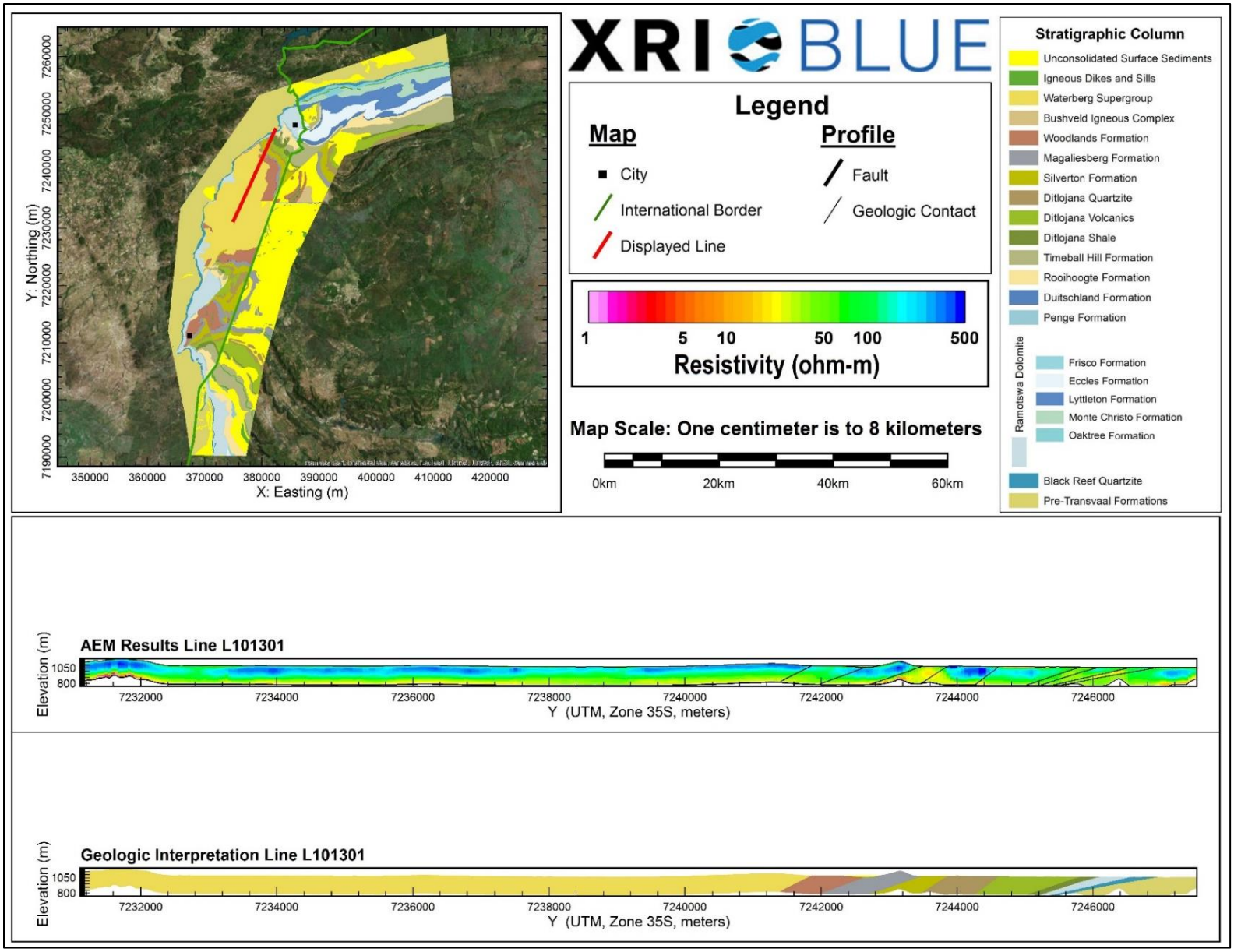

AEM and Interpreted Geology Profile for L101301.

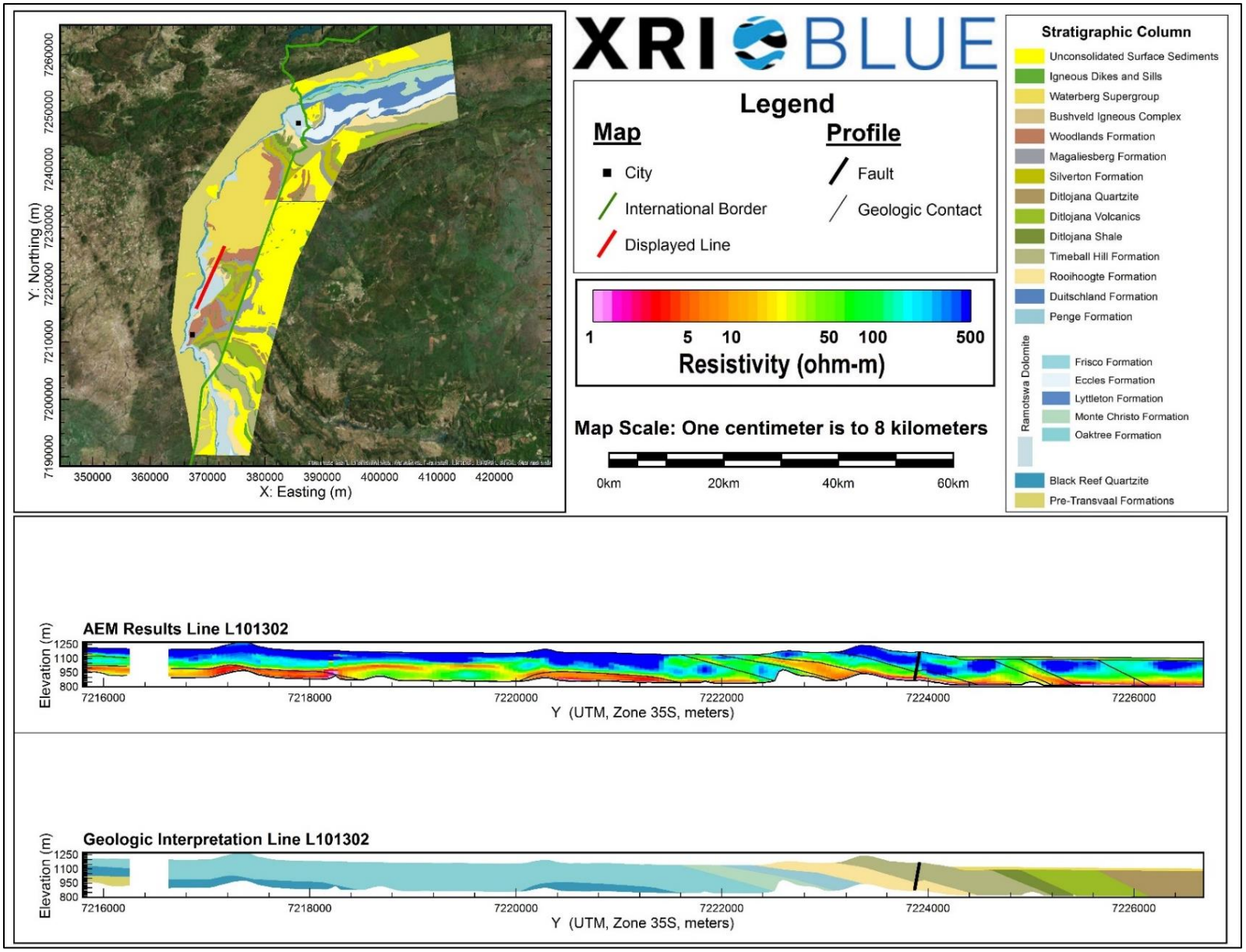

AEM and Interpreted Geology Profile for L101302.

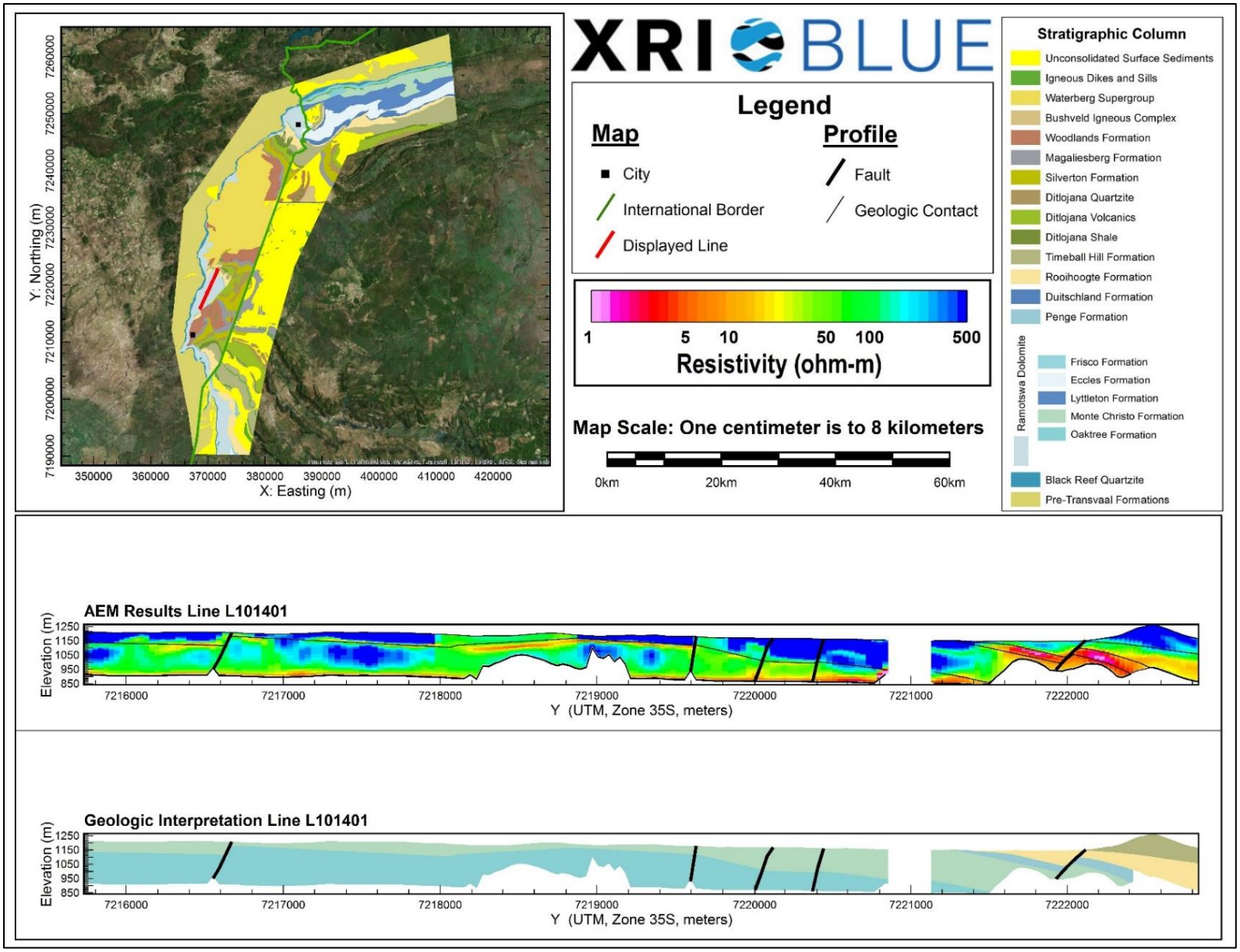

AEM and Interpreted Geology Profile for L101401.

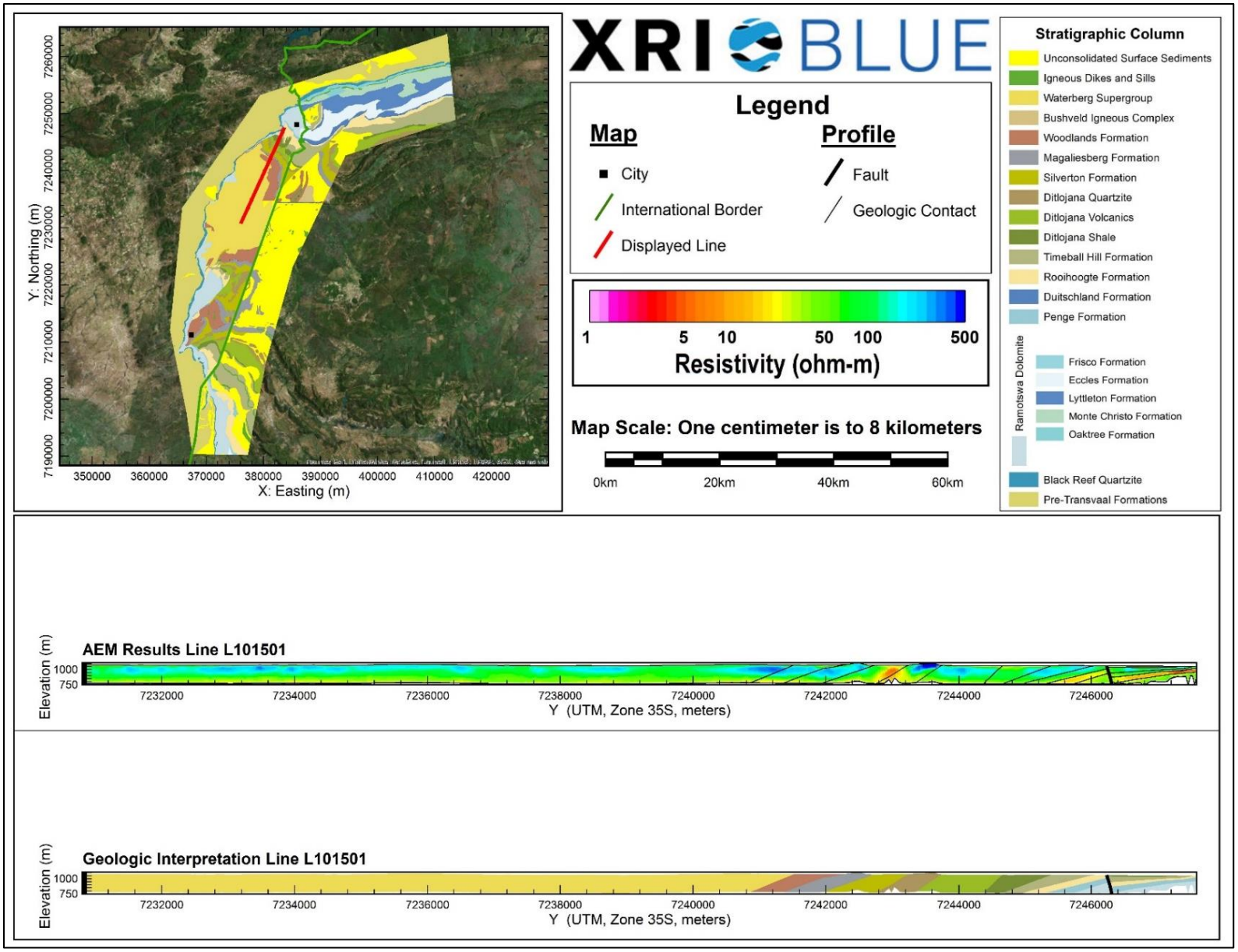

AEM and Interpreted Geology Profile for L101501.

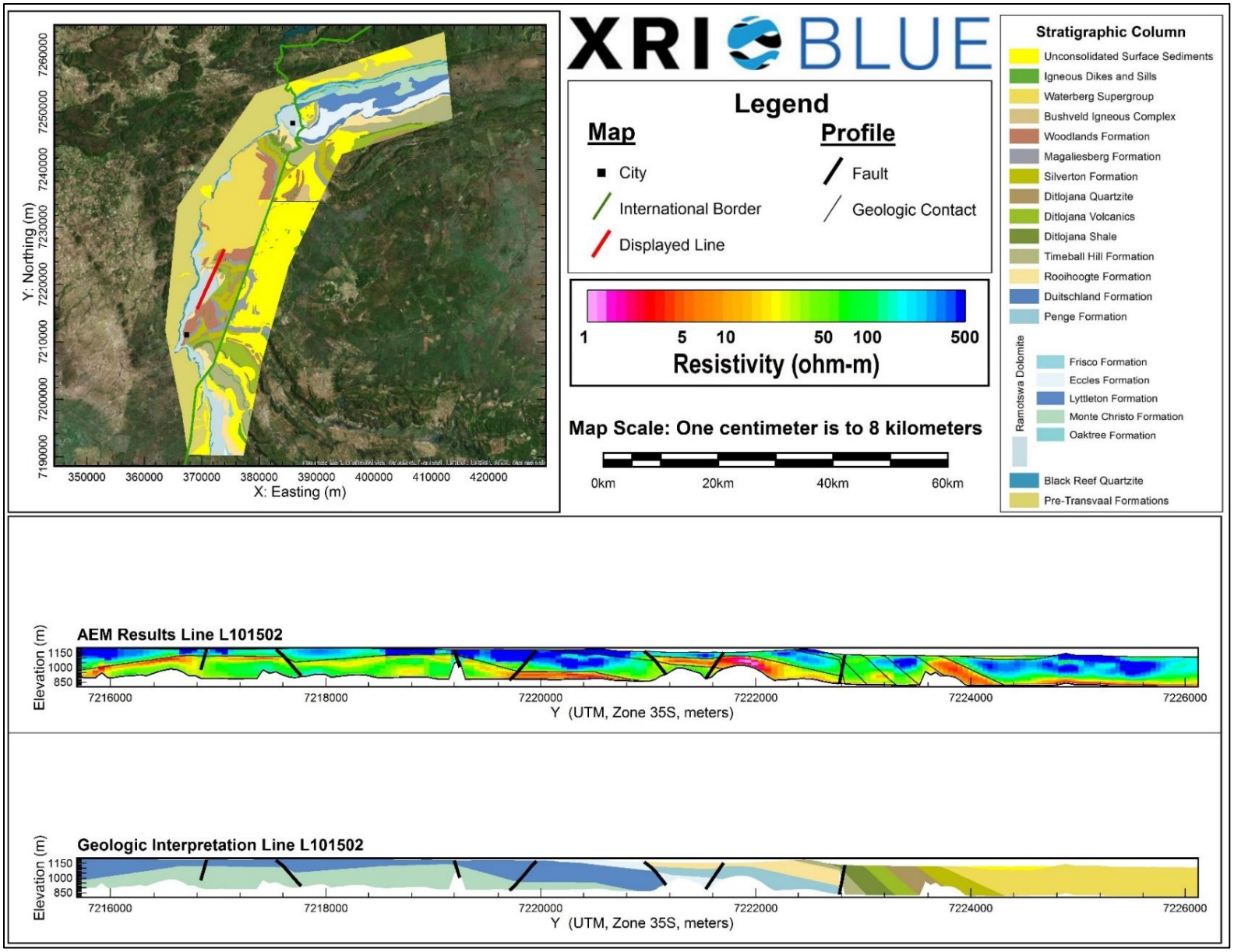

AEM and Interpreted Geology Profile for L101502.

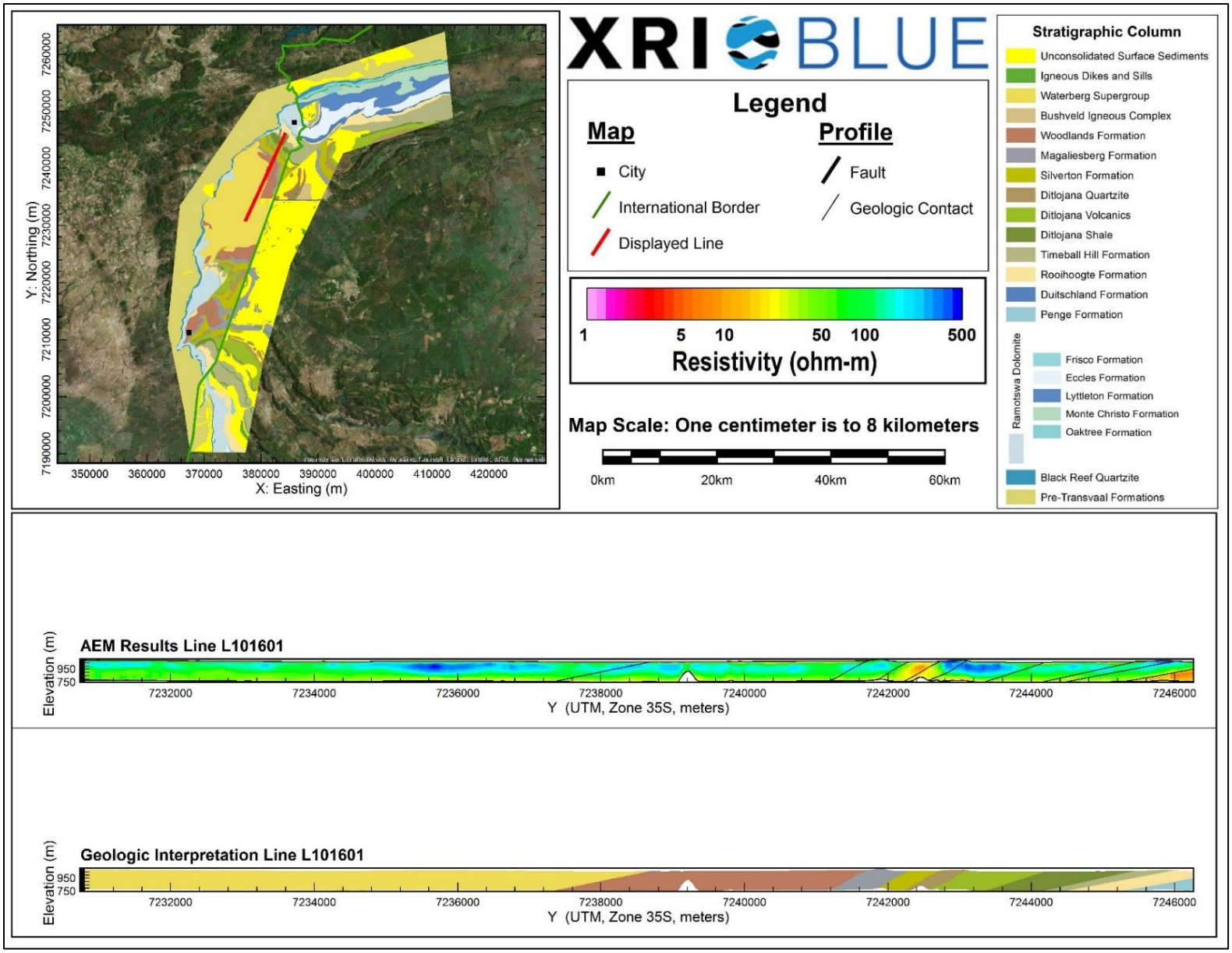

AEM and Interpreted Geology Profile for L101601.

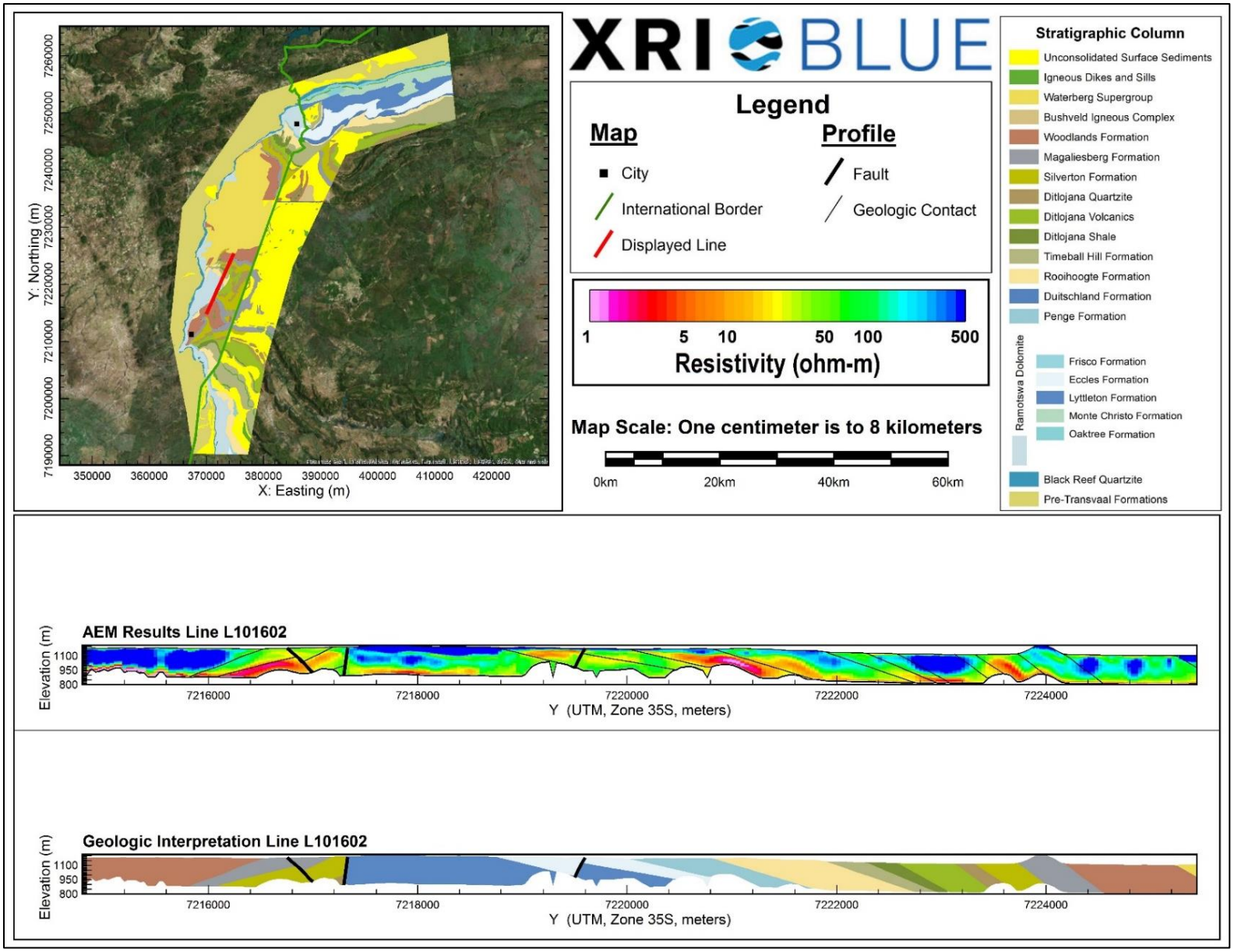

AEM and Interpreted Geology Profile for L101602.

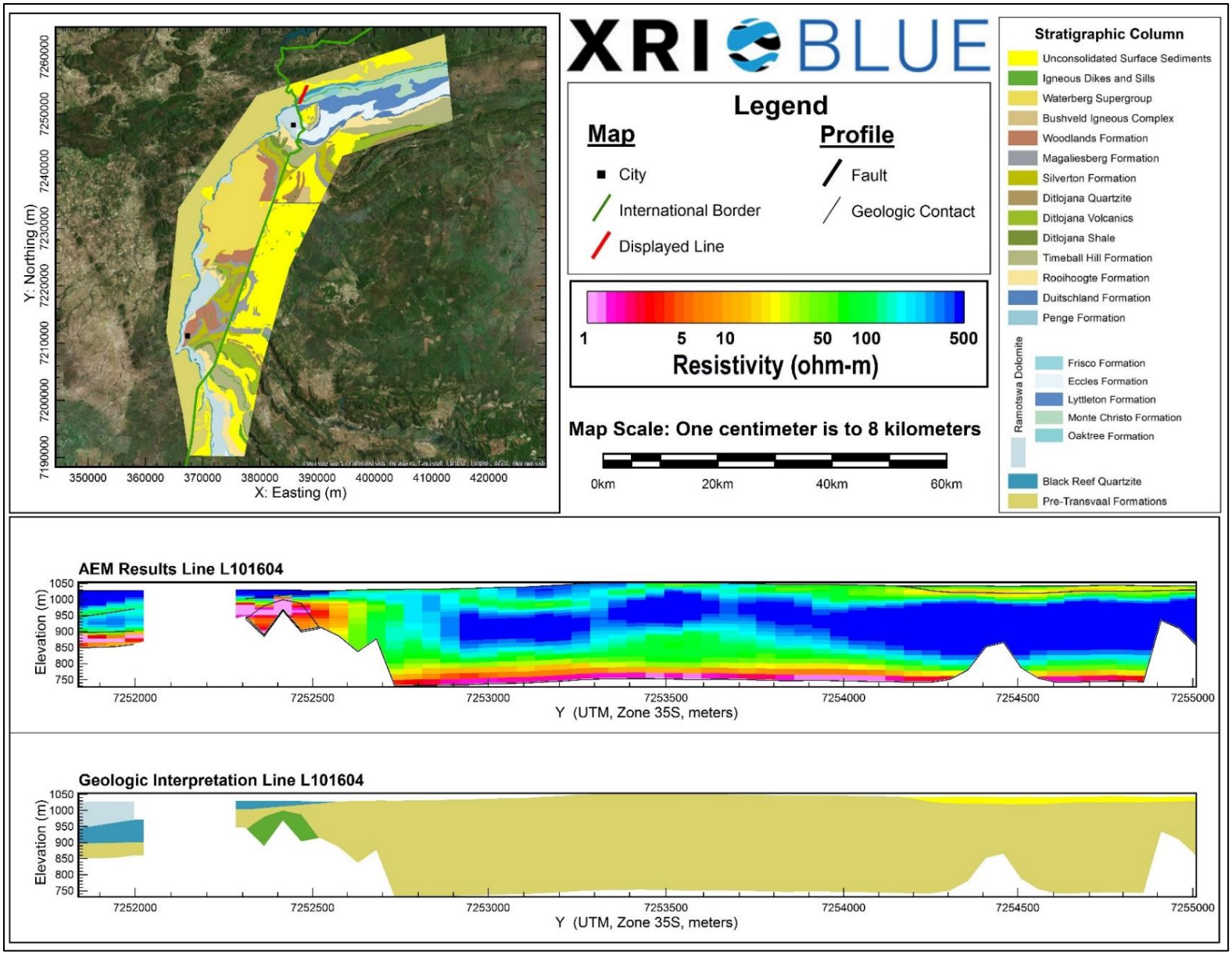

AEM and Interpreted Geology Profile for L101604.

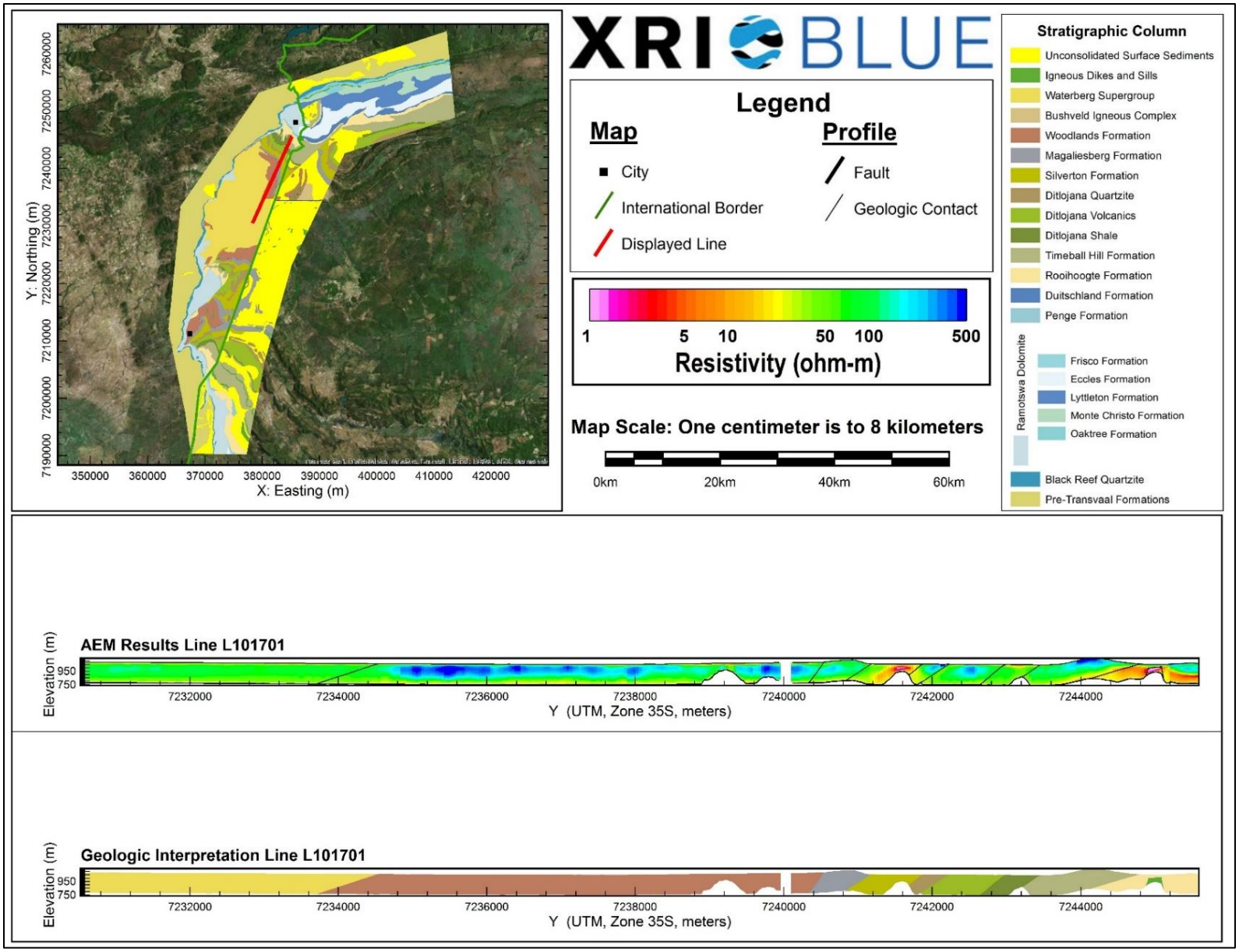

AEM and Interpreted Geology Profile for L101701.

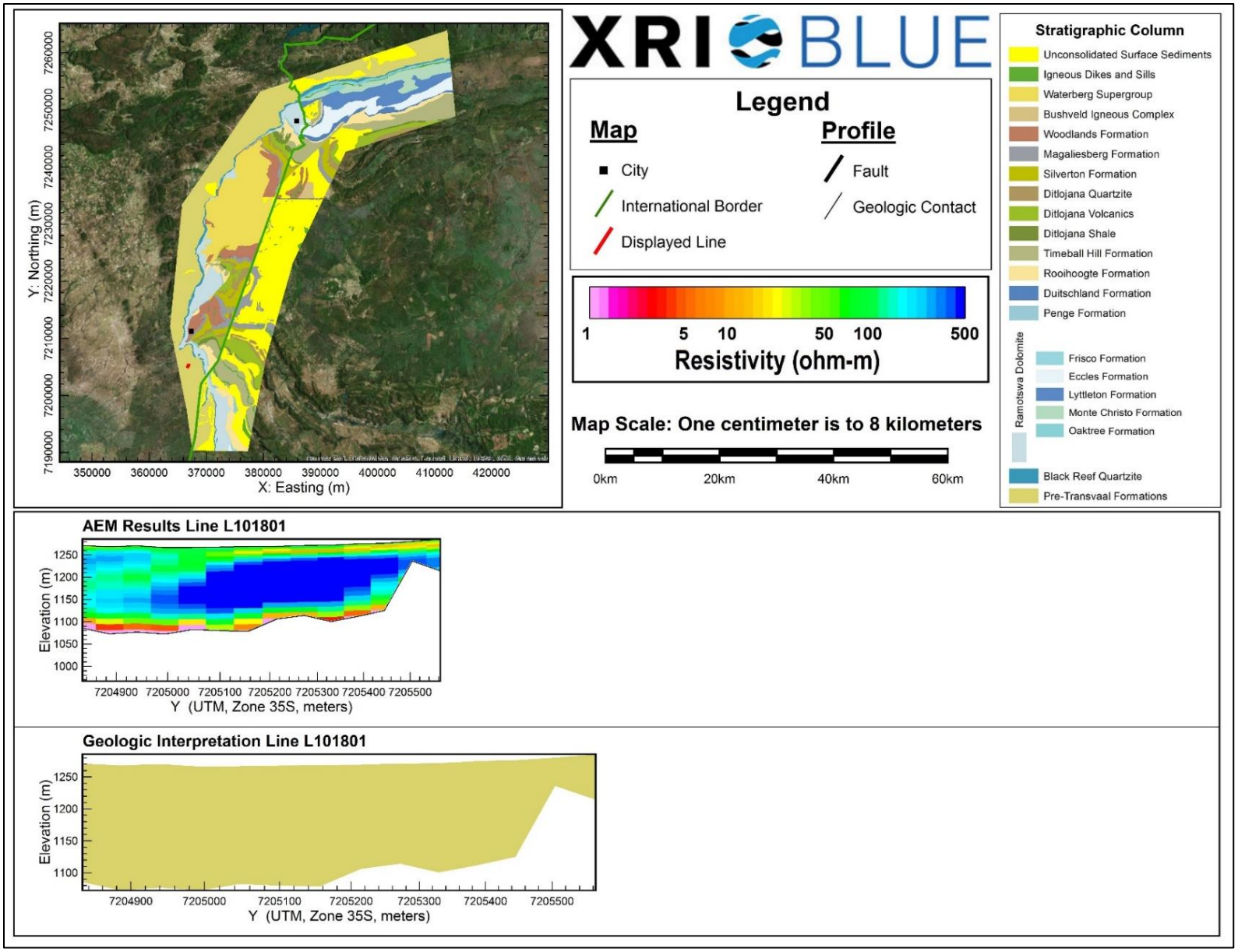

AEM and Interpreted Geology Profile for L101801.

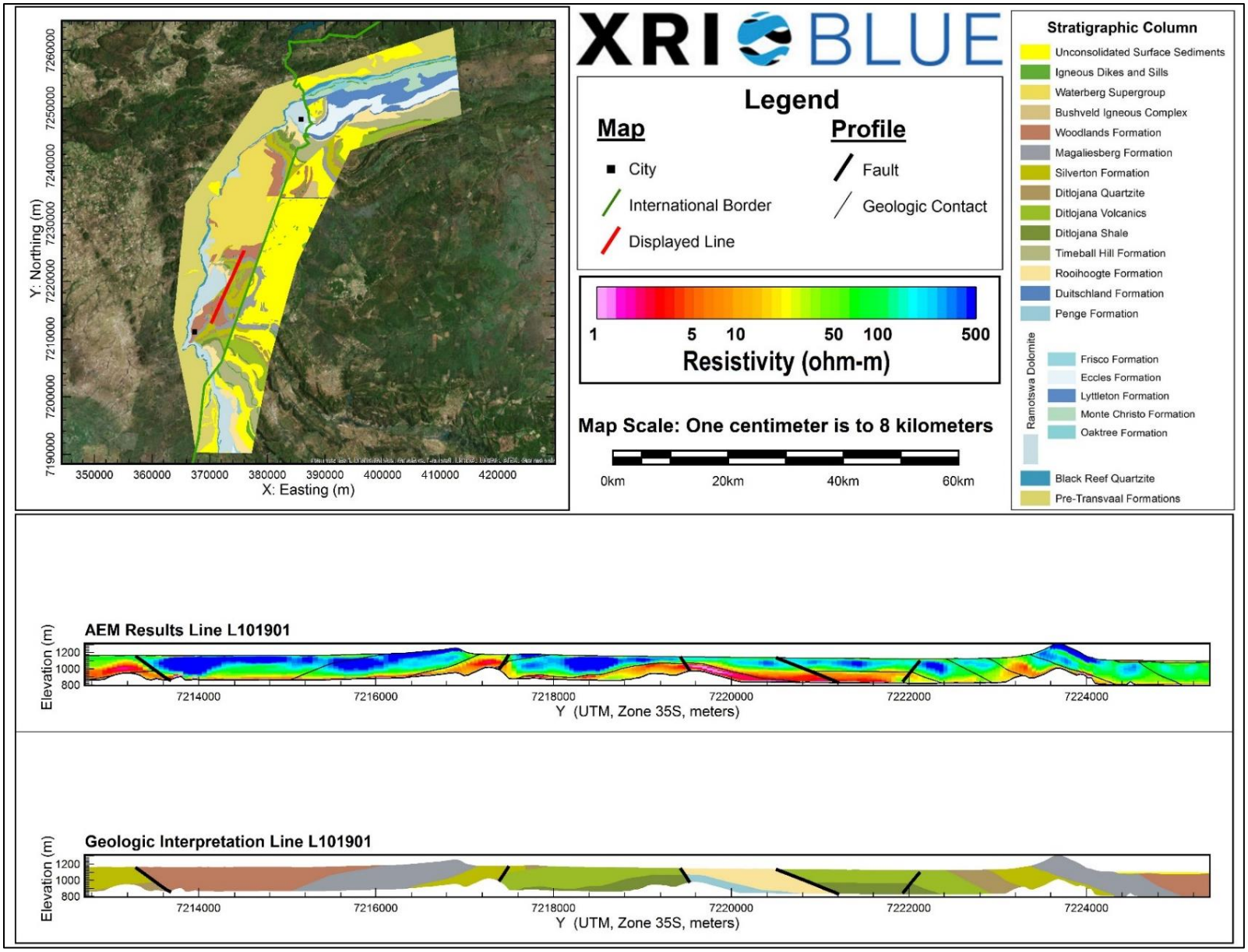

AEM and Interpreted Geology Profile for L101901.

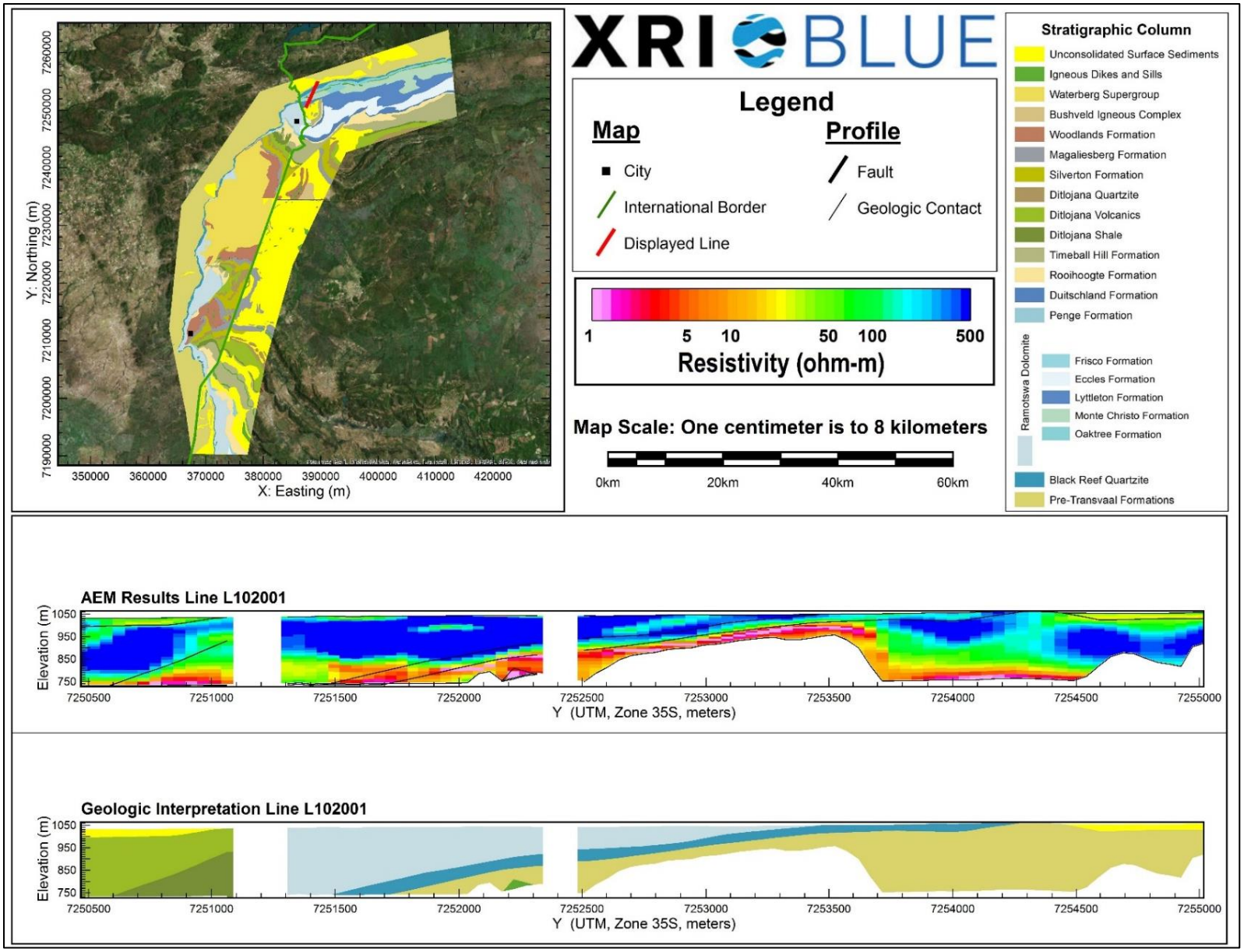

AEM and Interpreted Geology Profile for L102001.

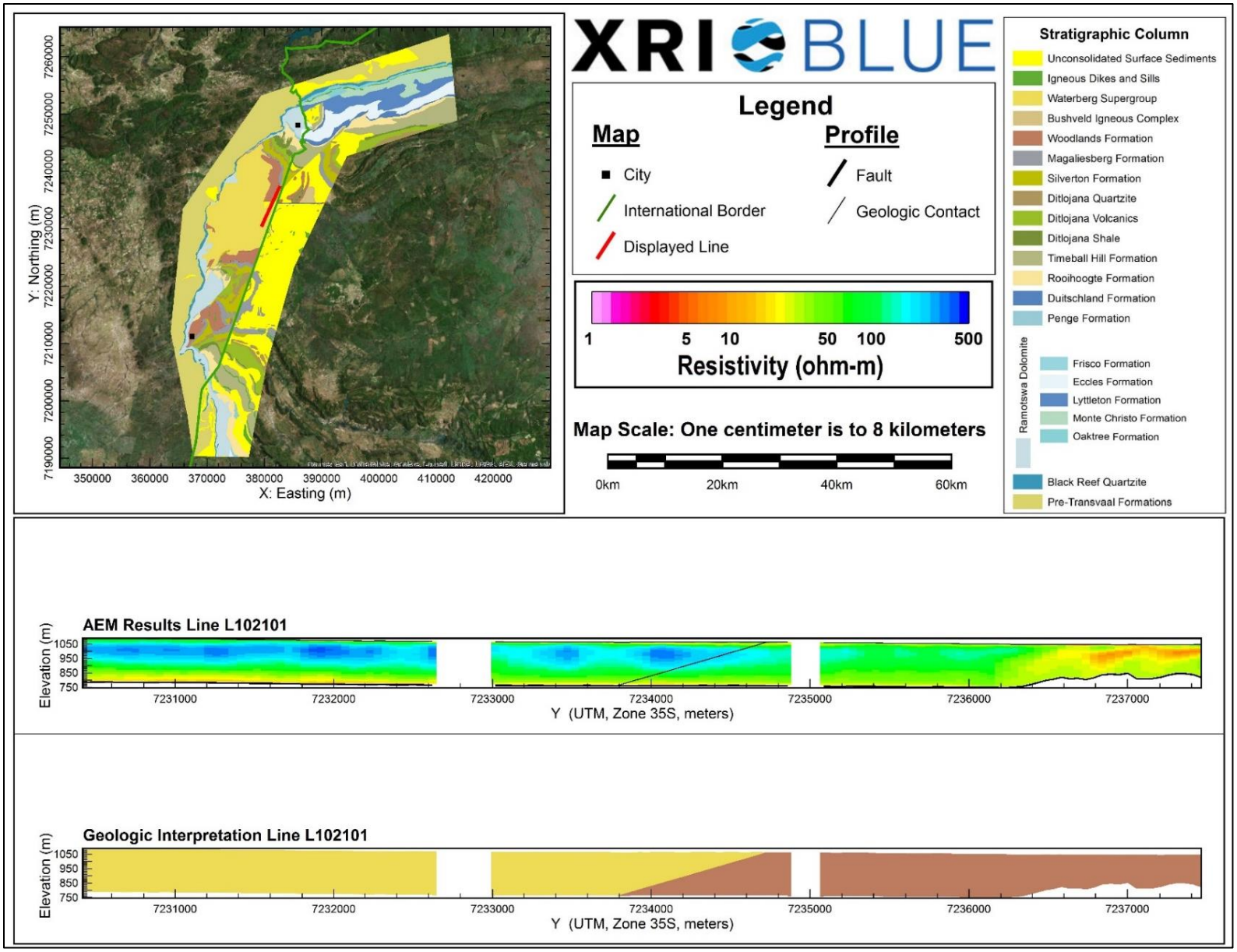

AEM and Interpreted Geology Profile for L102101.

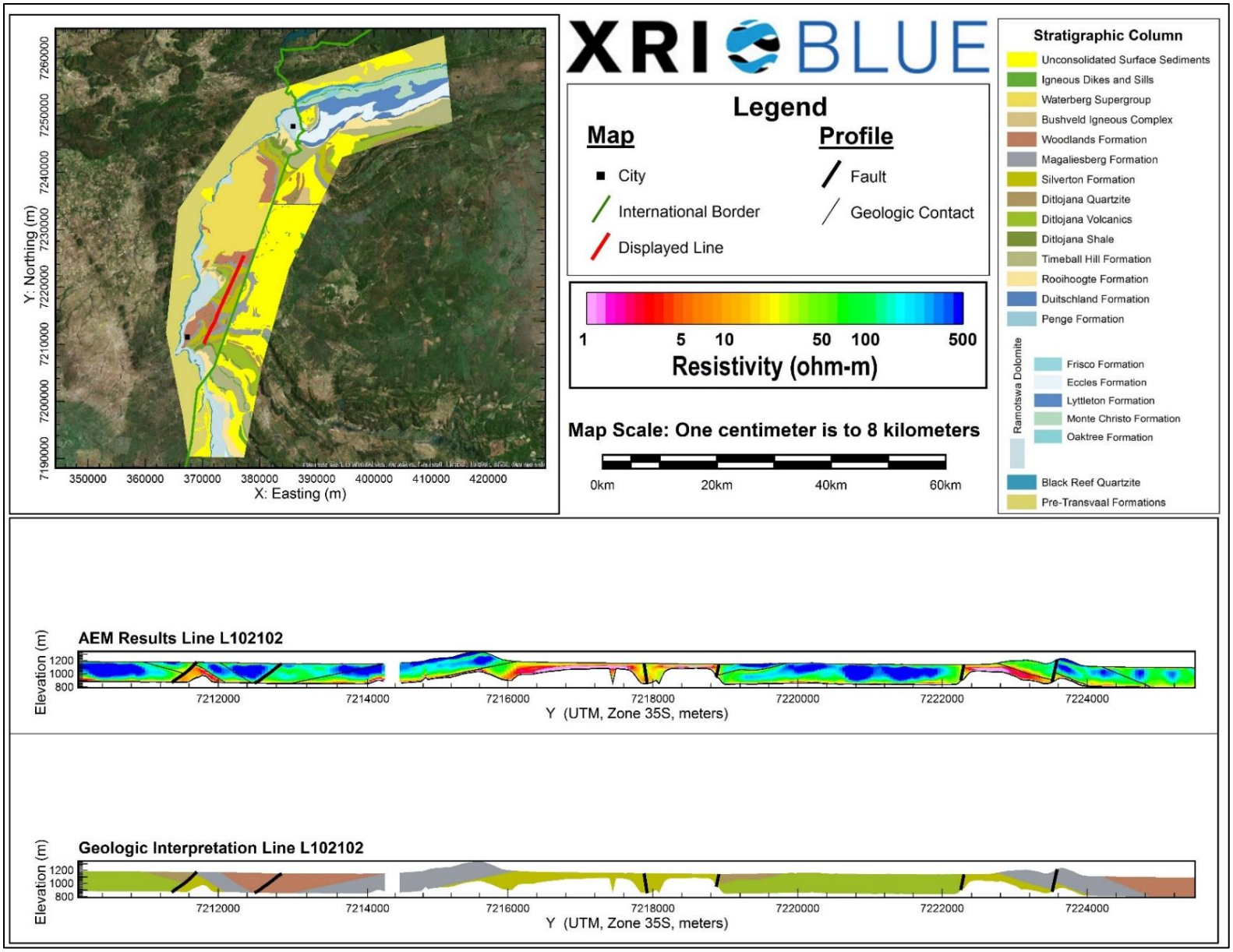

AEM and Interpreted Geology Profile for L102102.

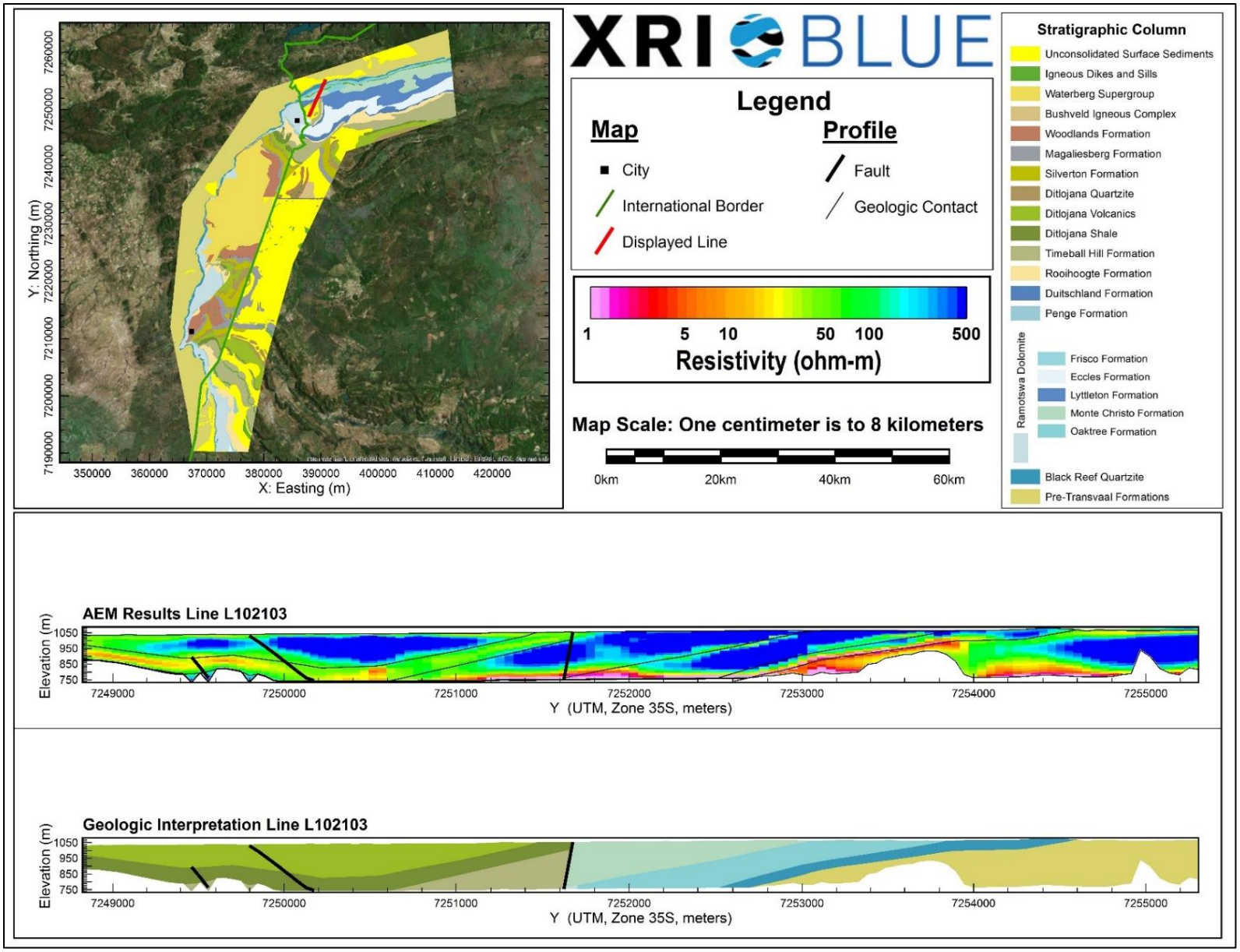

AEM and Interpreted Geology Profile for L102103.

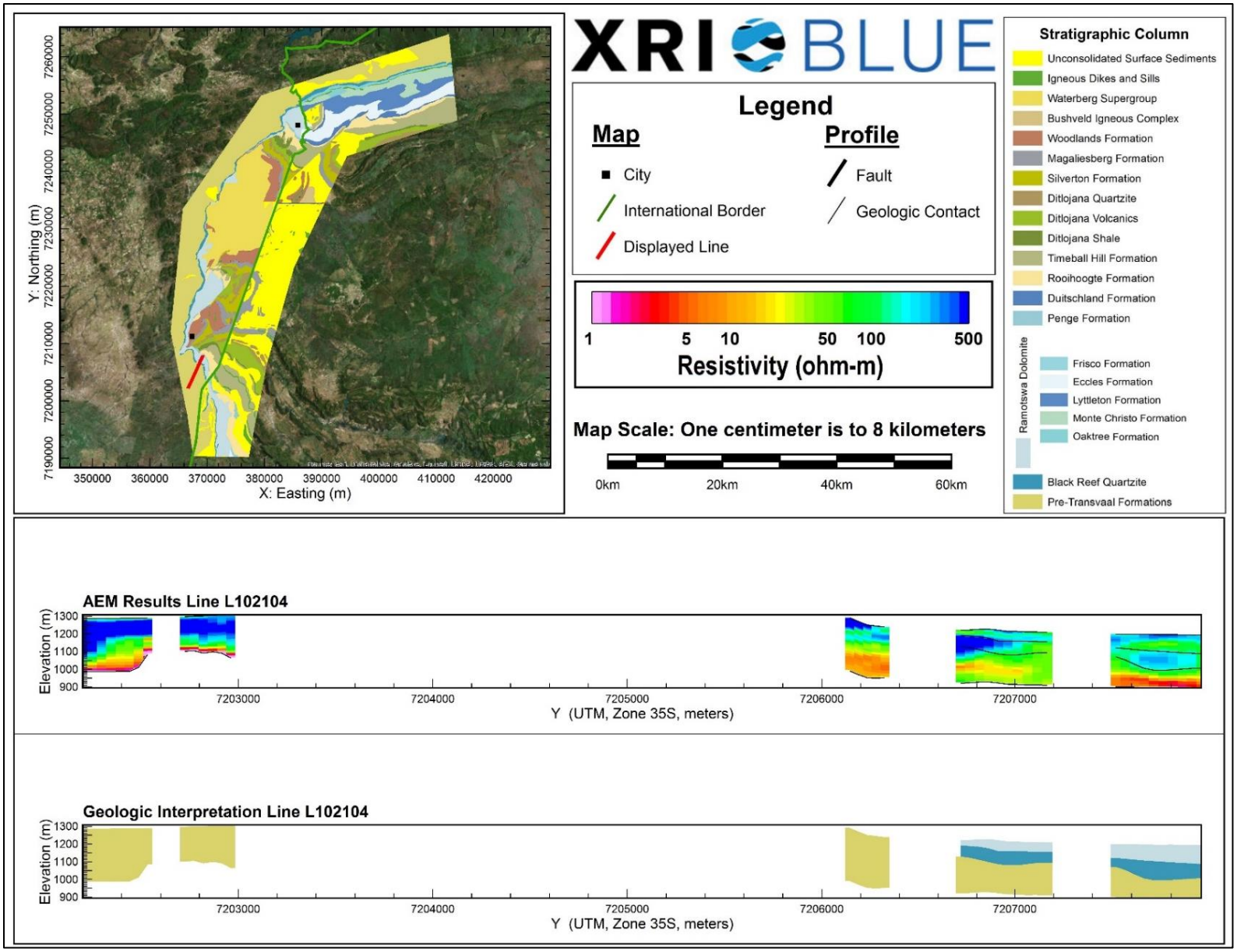

AEM and Interpreted Geology Profile for L102104.

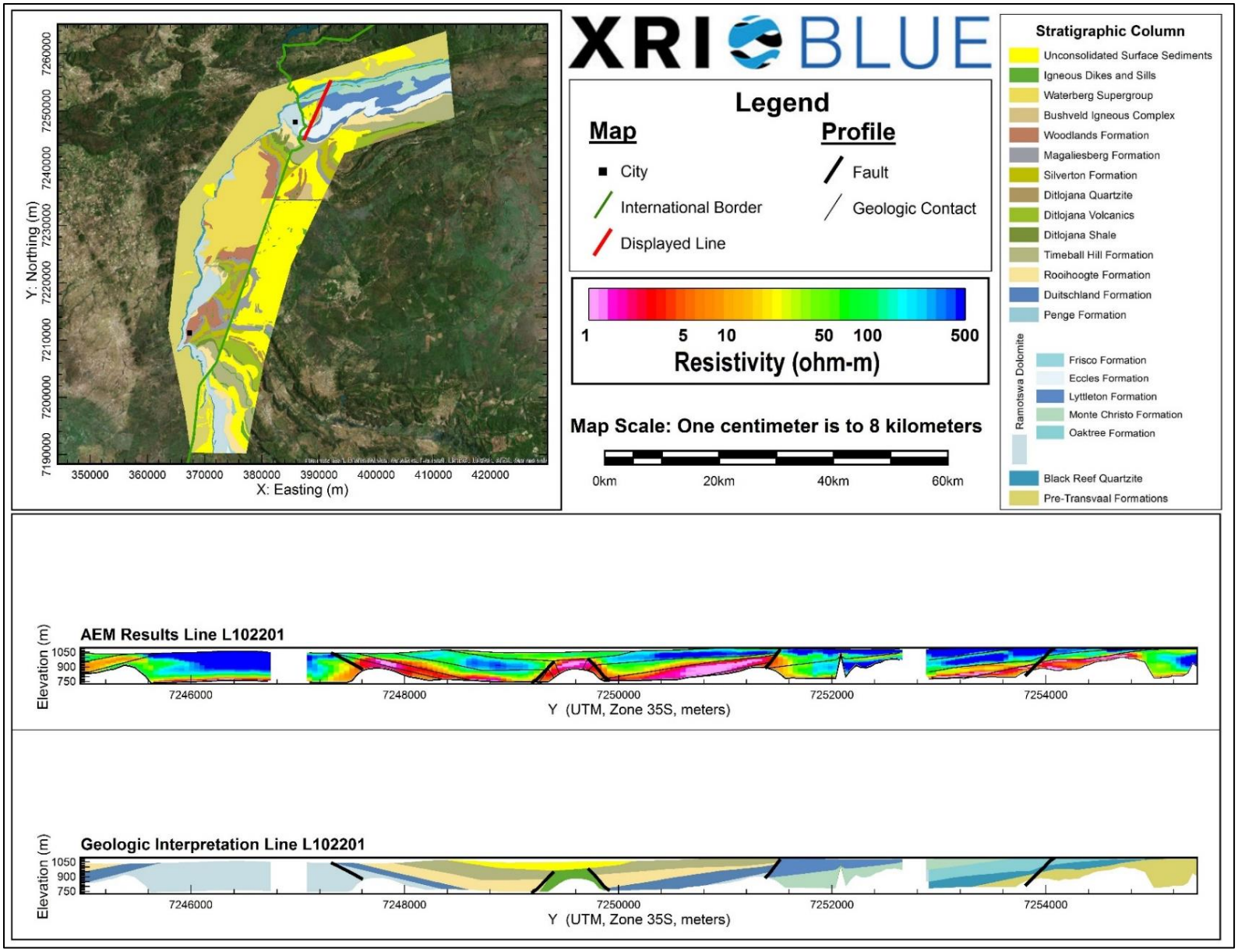

AEM and Interpreted Geology Profile for L102201.

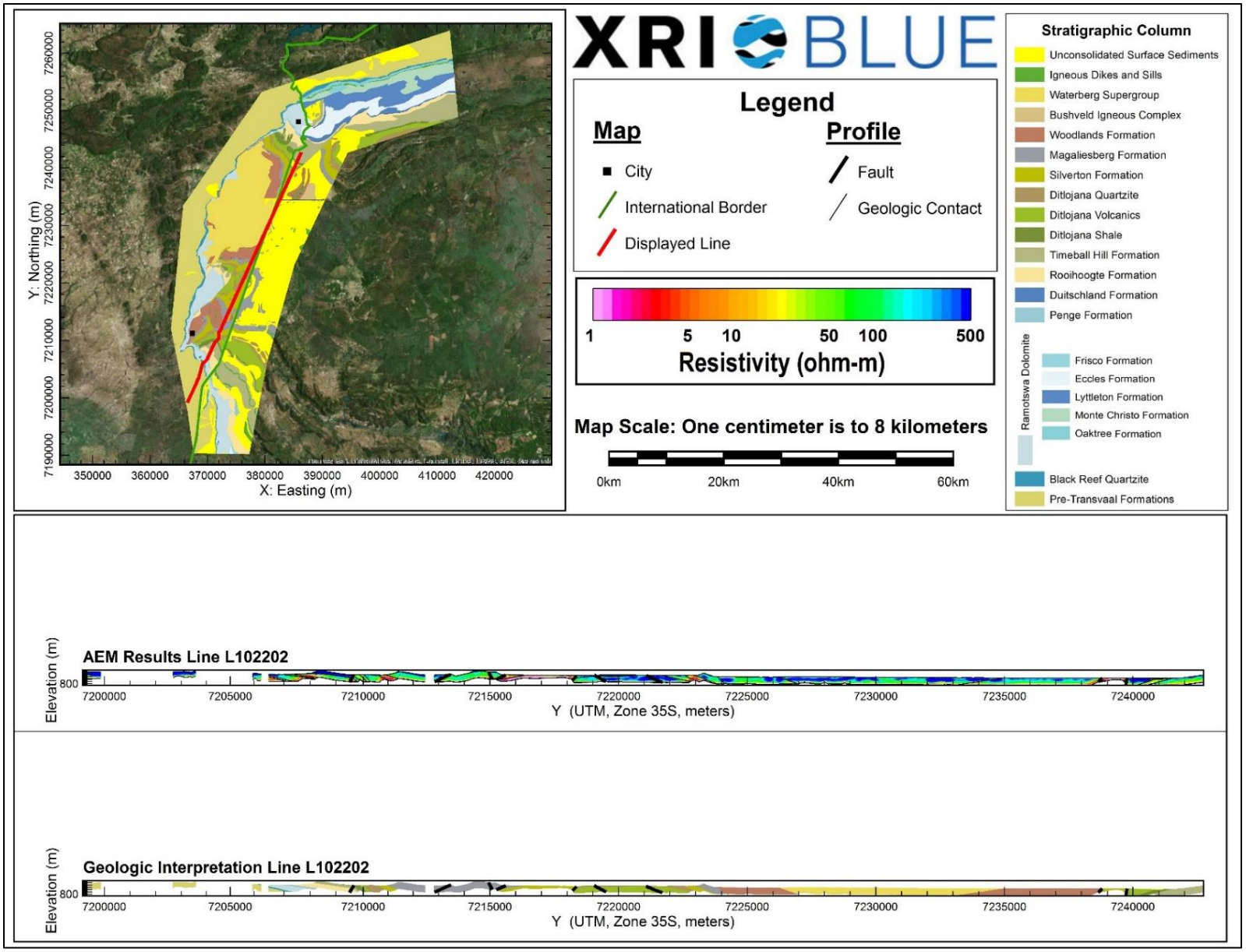

AEM and Interpreted Geology Profile for L102202.

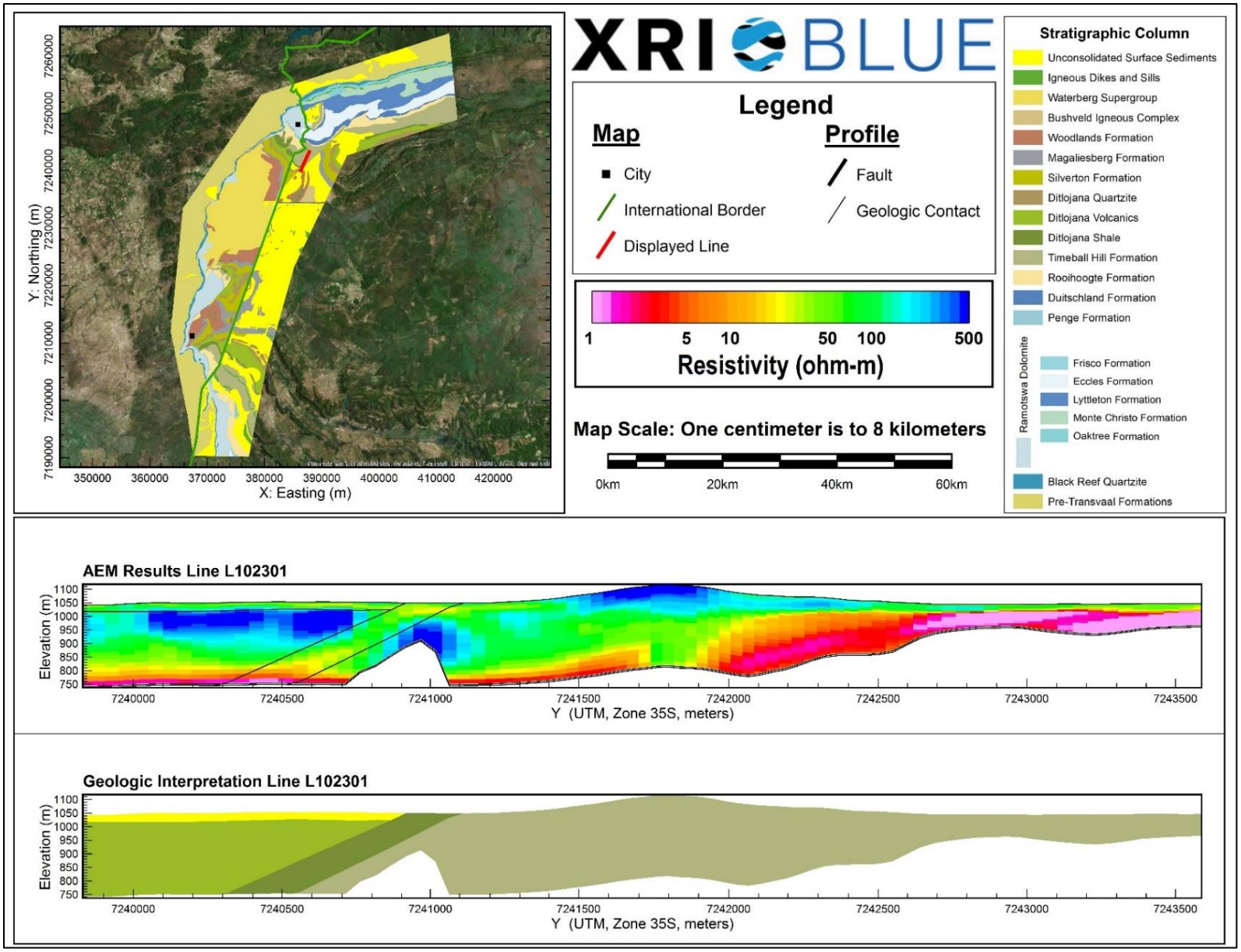

AEM and Interpreted Geology Profile for L102301.

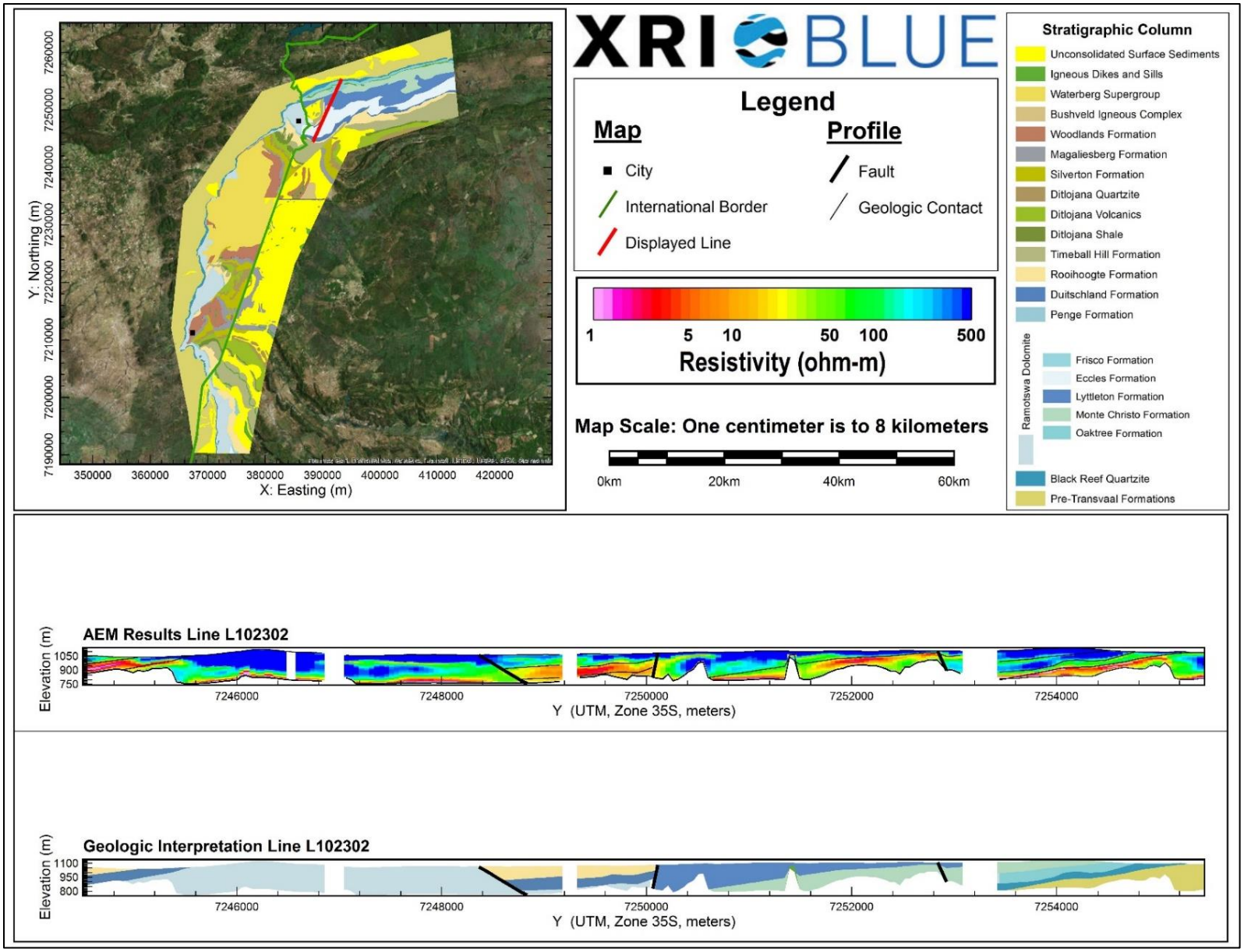

AEM and Interpreted Geology Profile for L102302.

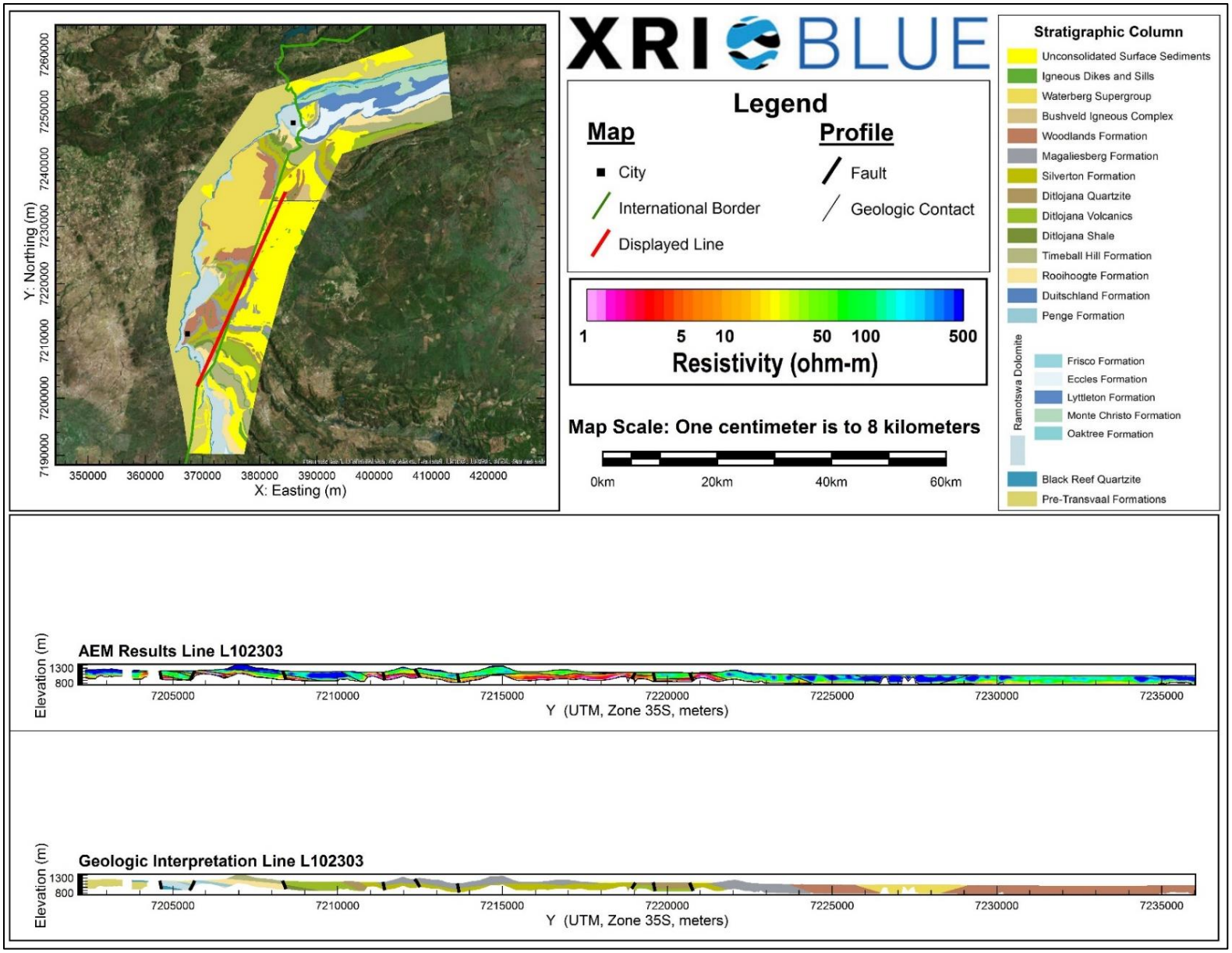

AEM and Interpreted Geology Profile for L102303.

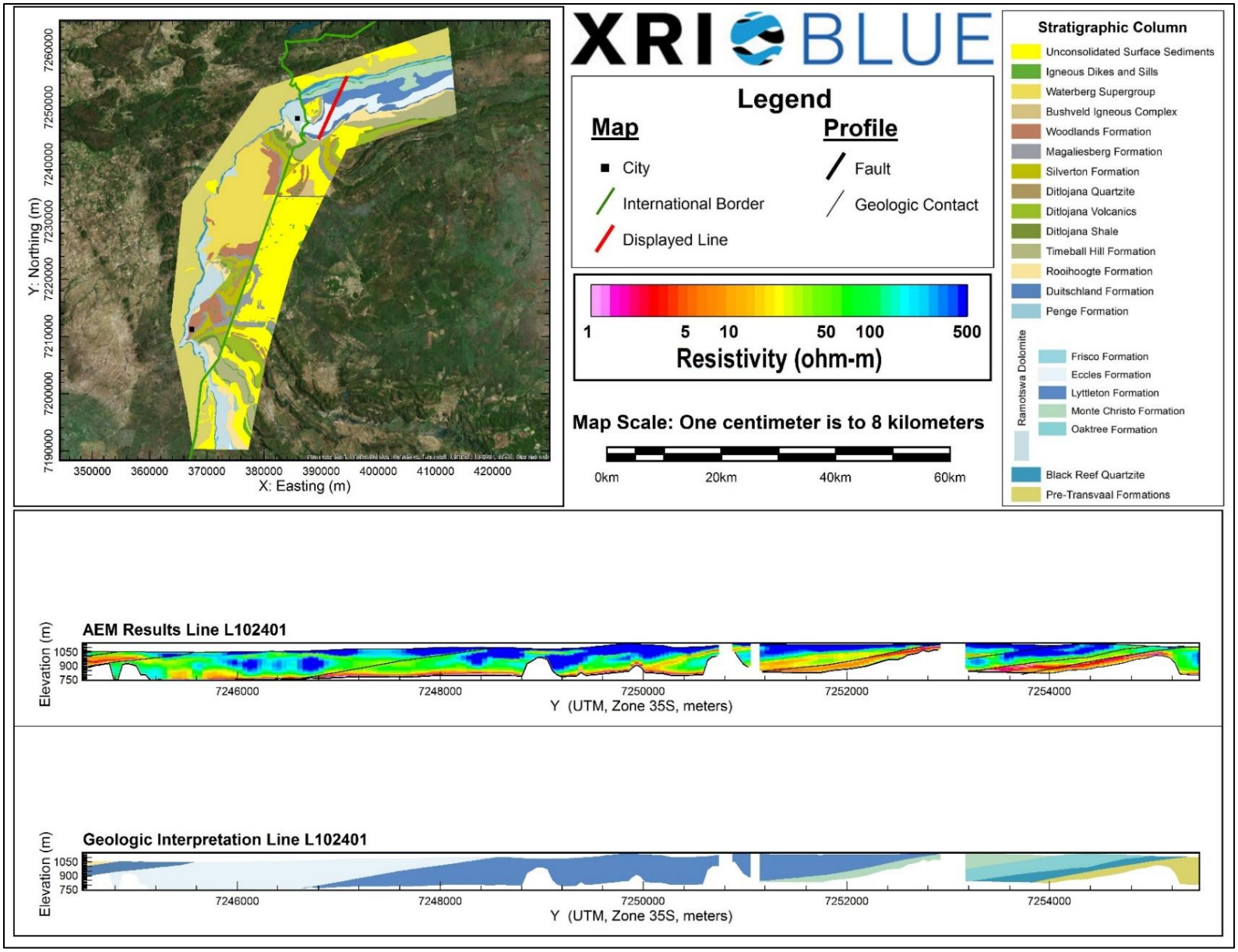

AEM and Interpreted Geology Profile for L102401.

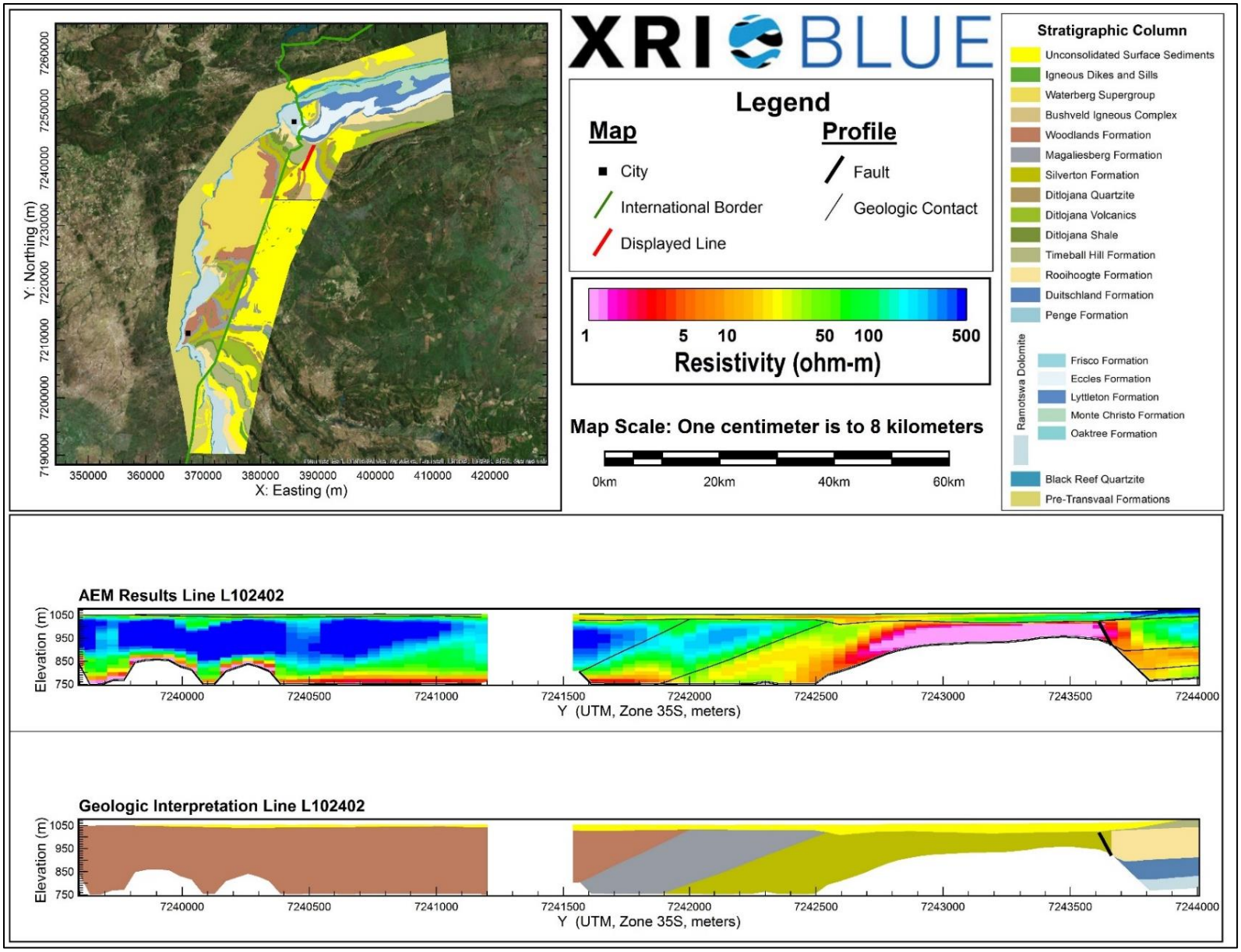

AEM and Interpreted Geology Profile for L102402.

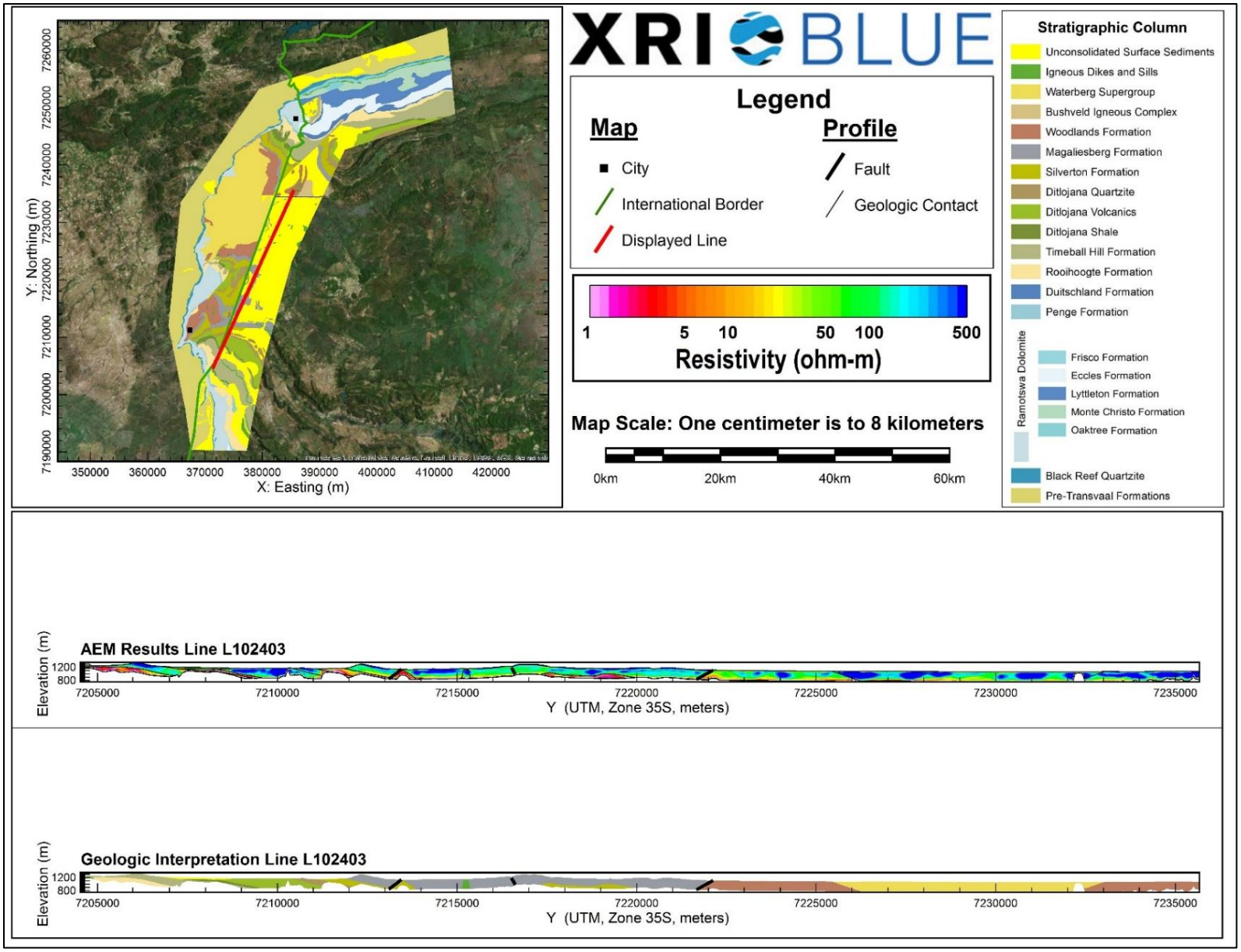

AEM and Interpreted Geology Profile for L102403.

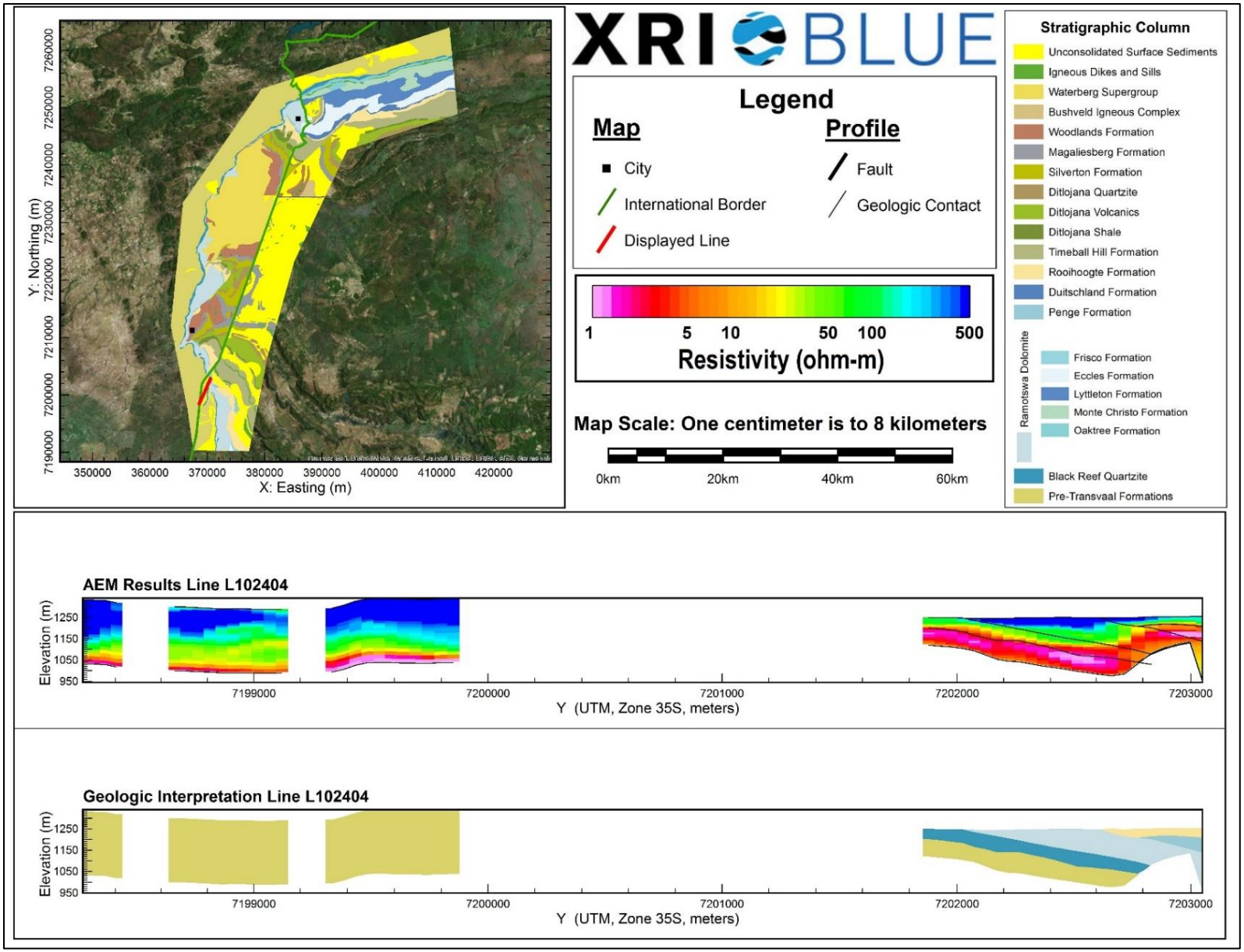

AEM and Interpreted Geology Profile for L102404.

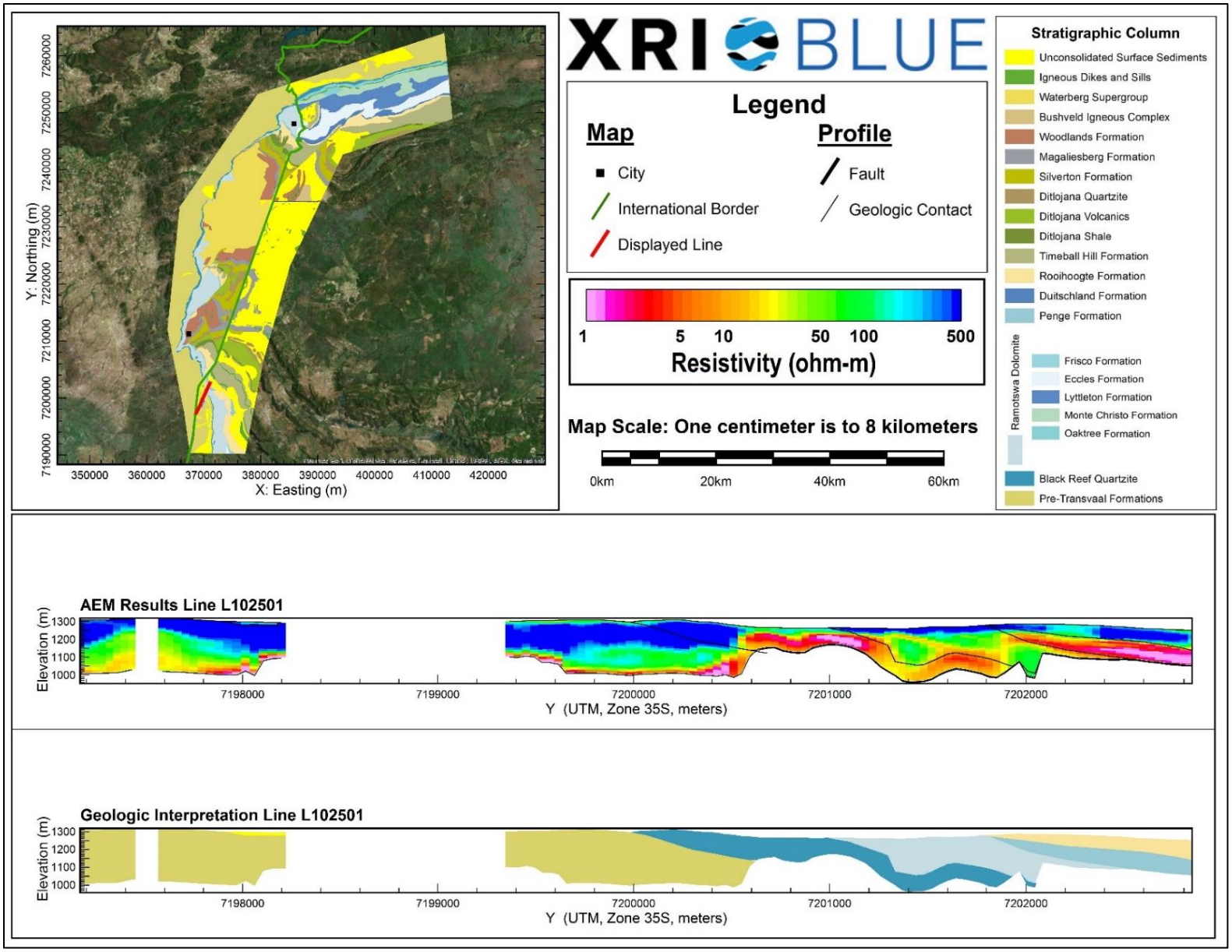

AEM and Interpreted Geology Profile for L102501.

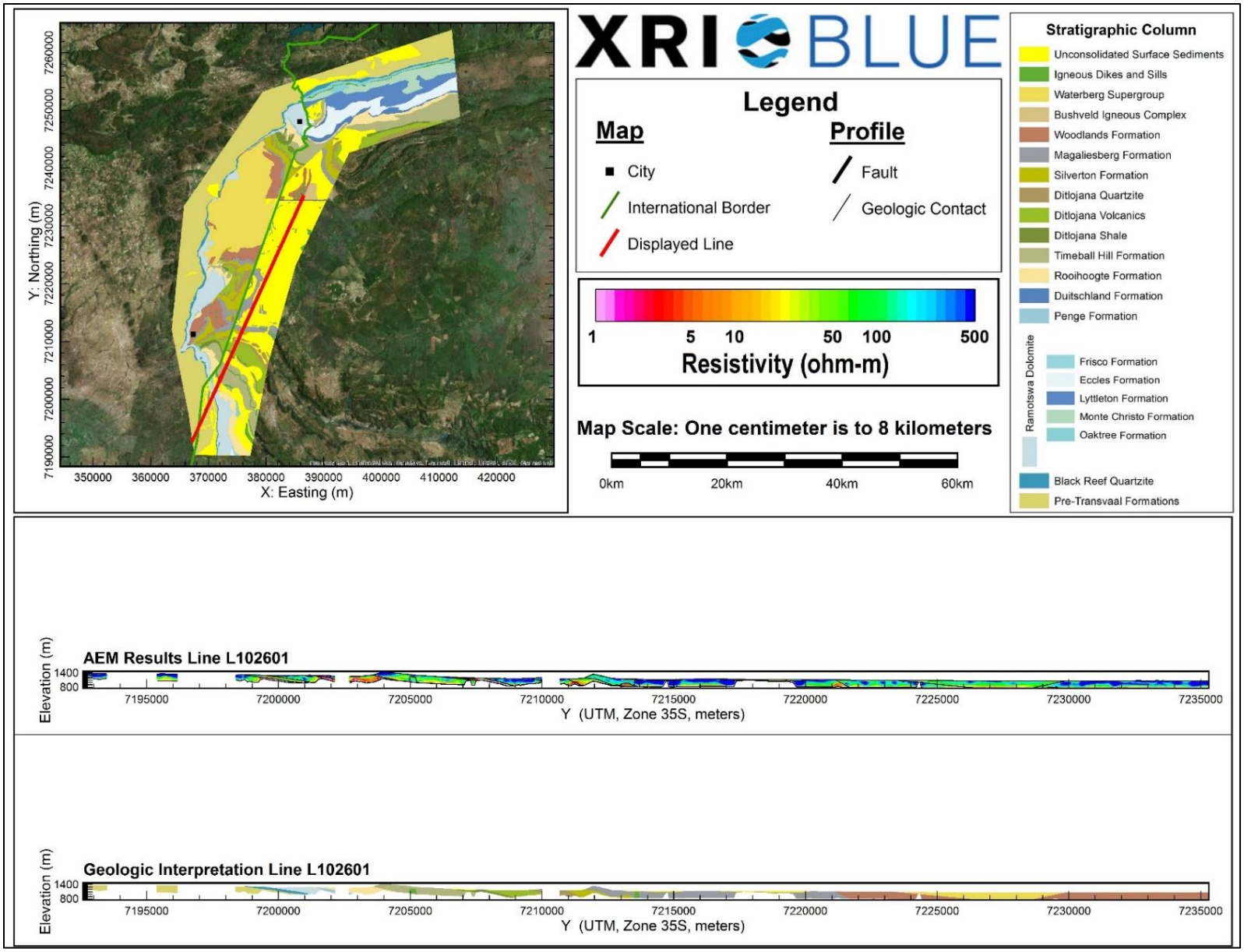

AEM and Interpreted Geology Profile for L102601.

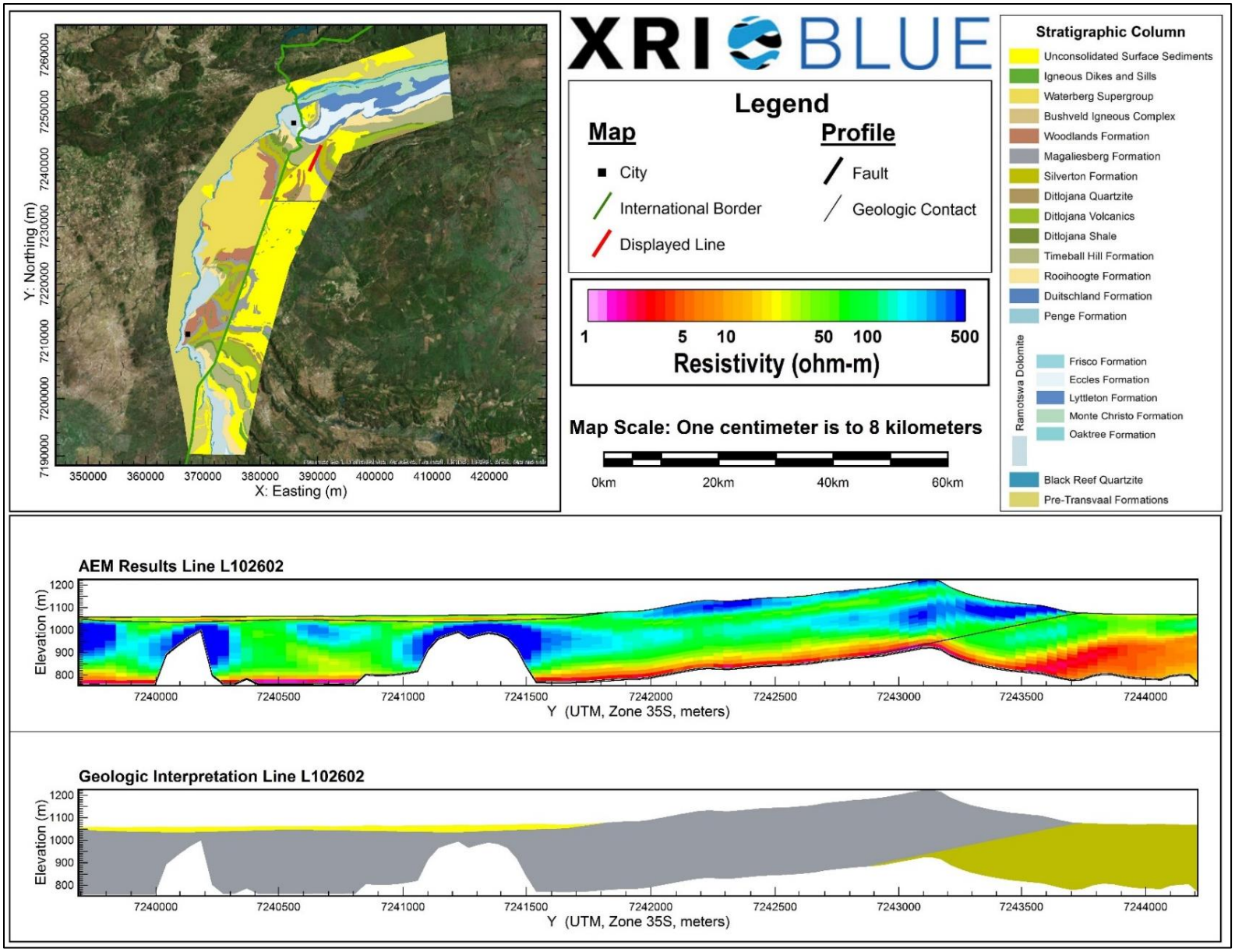

AEM and Interpreted Geology Profile for L102602.

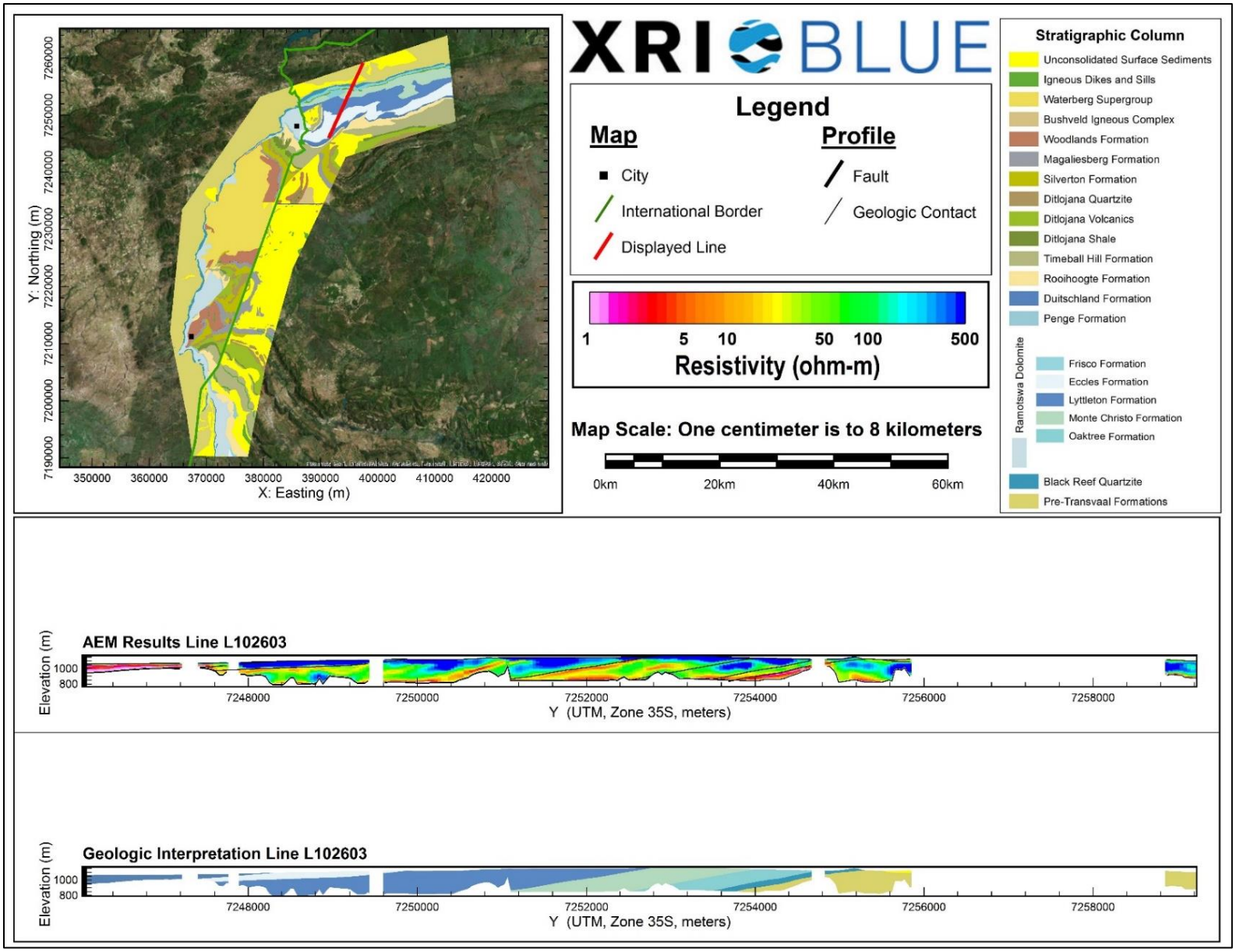

AEM and Interpreted Geology Profile for L102603.

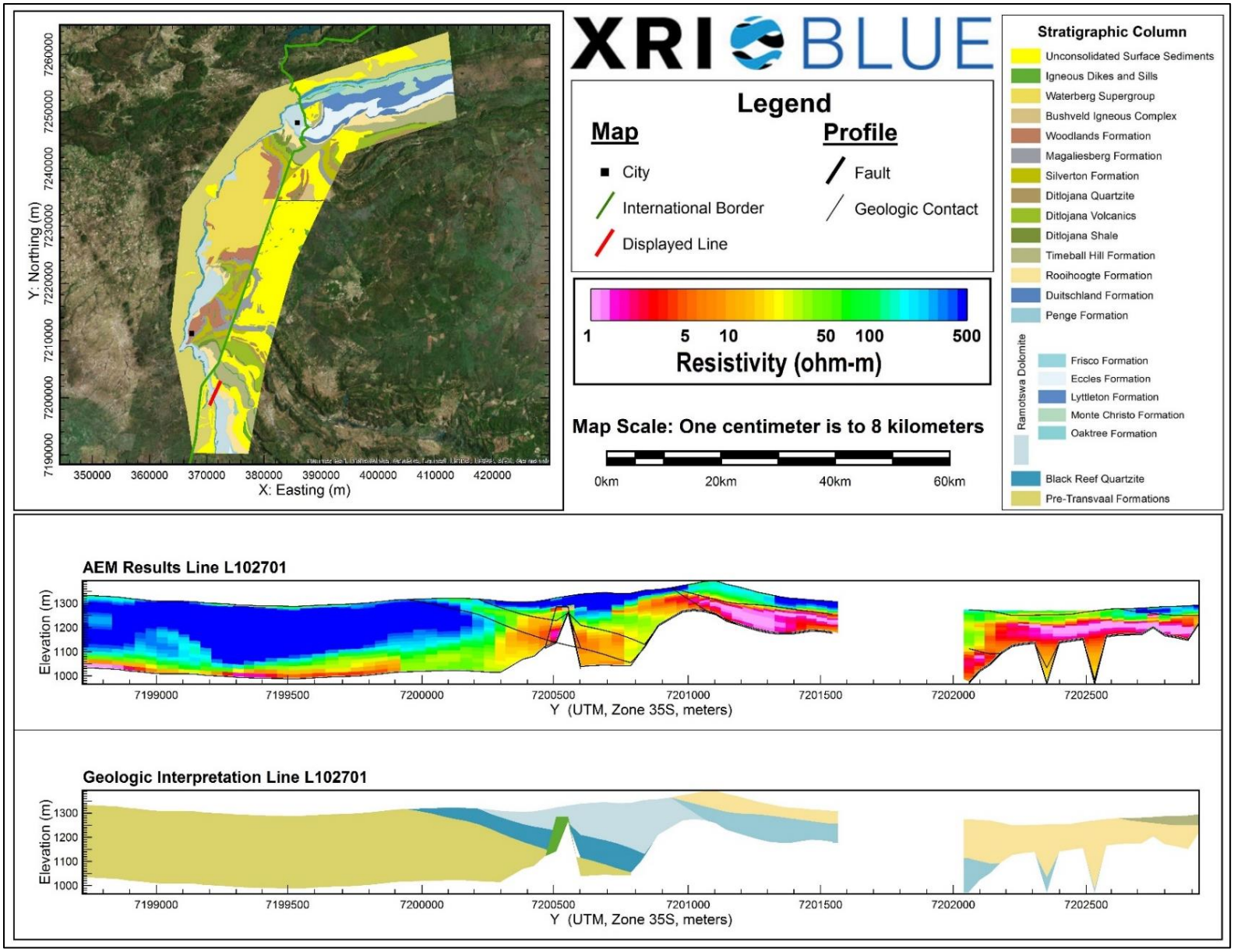

AEM and Interpreted Geology Profile for L102701.

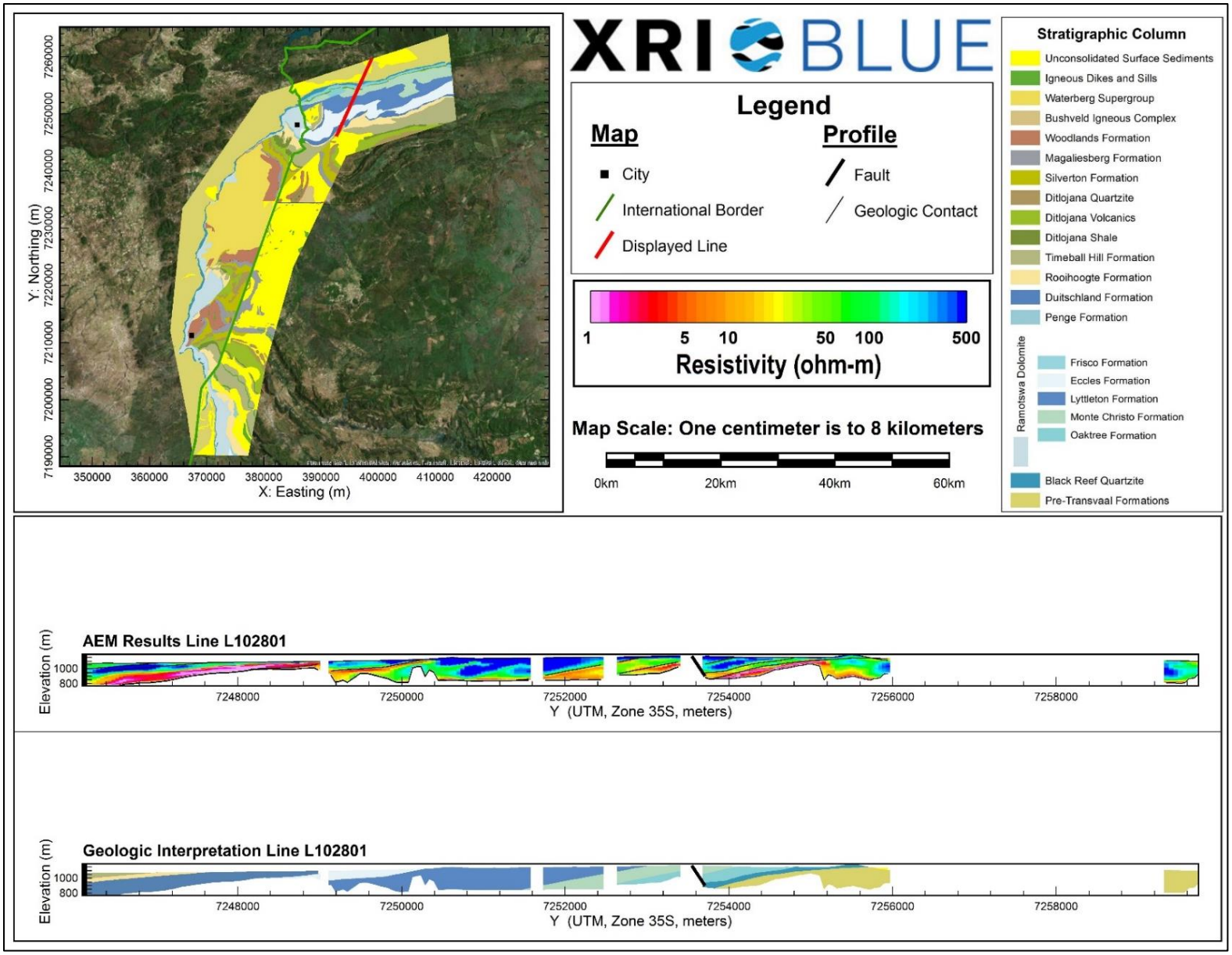

AEM and Interpreted Geology Profile for L102801.

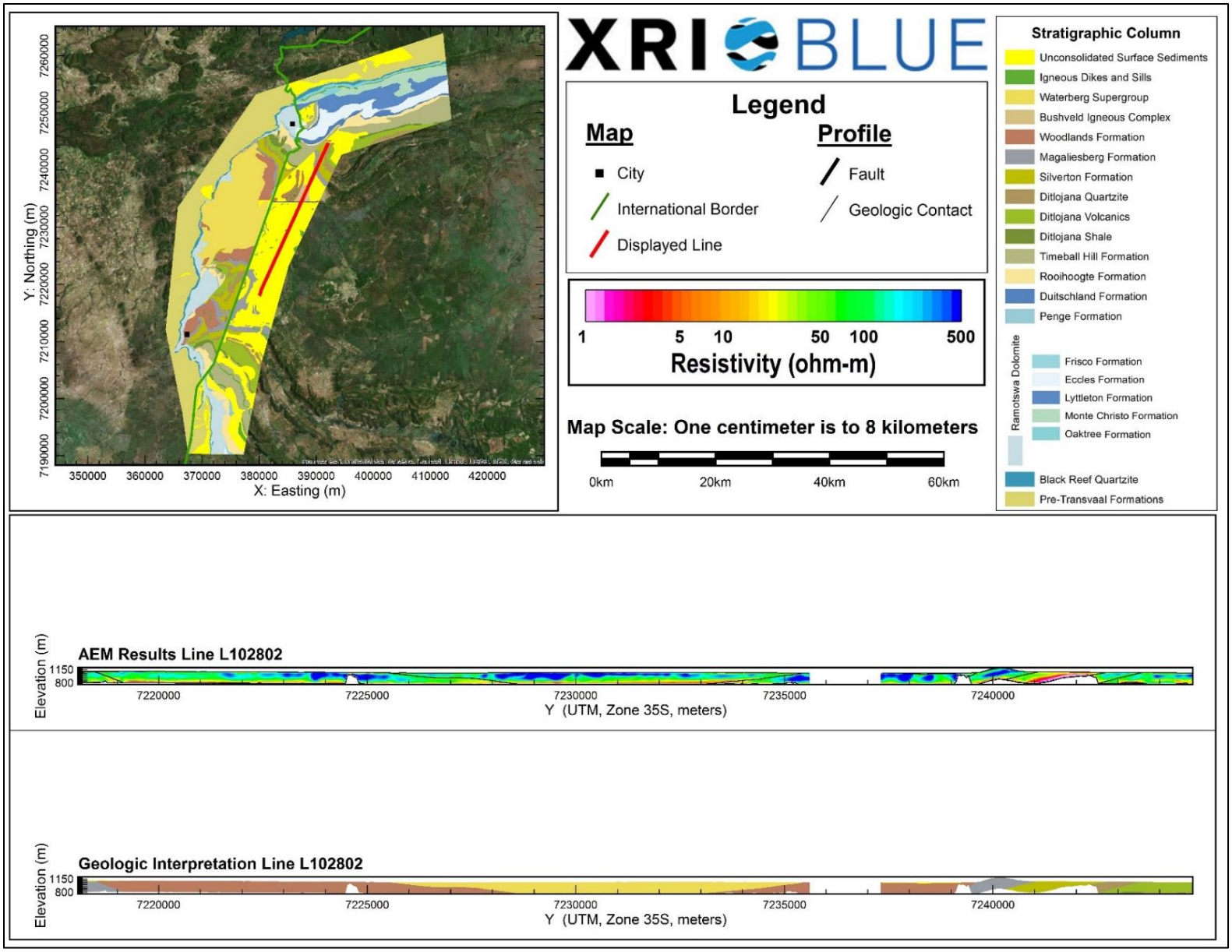

AEM and Interpreted Geology Profile for L102802.

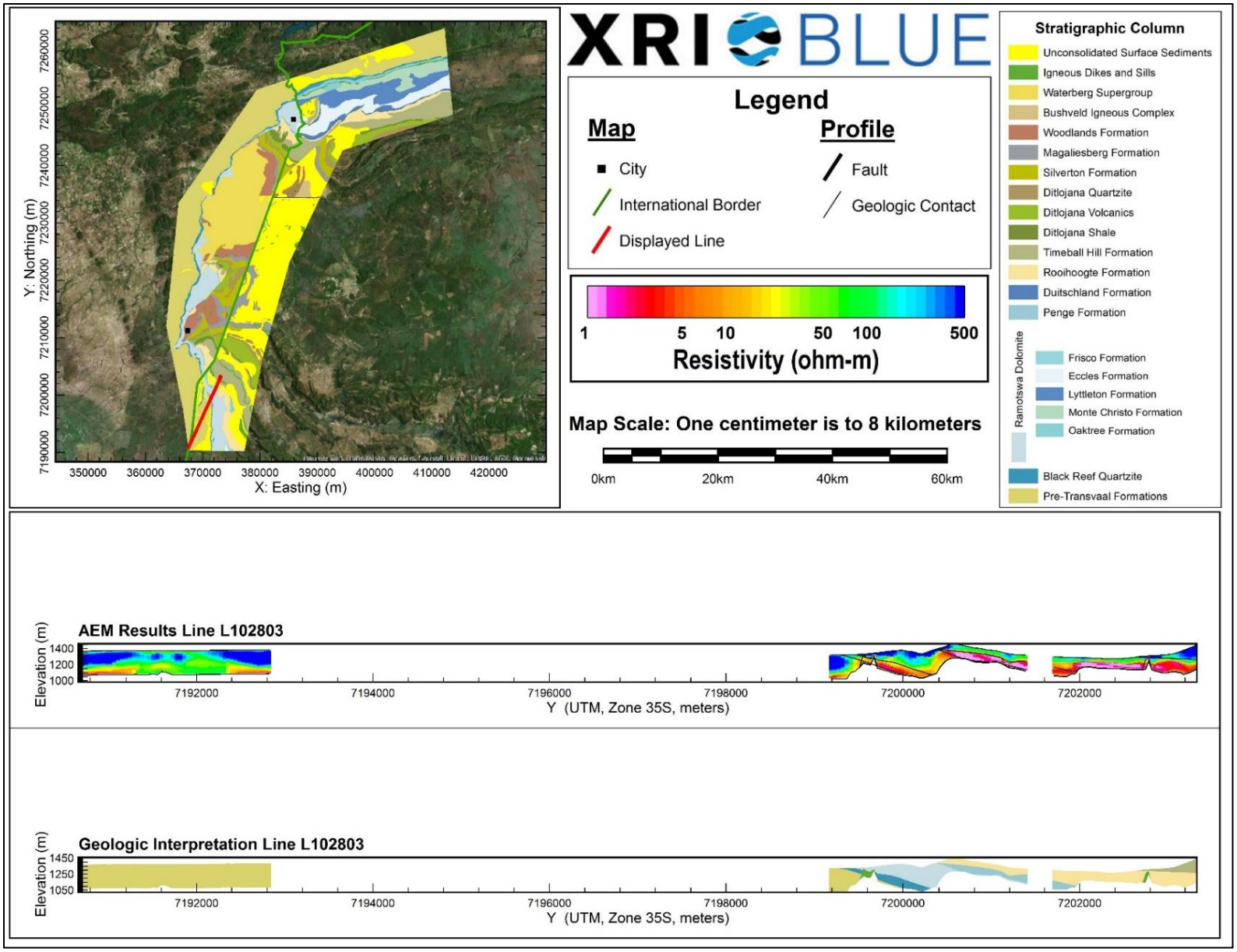

AEM and Interpreted Geology Profile for L102803.

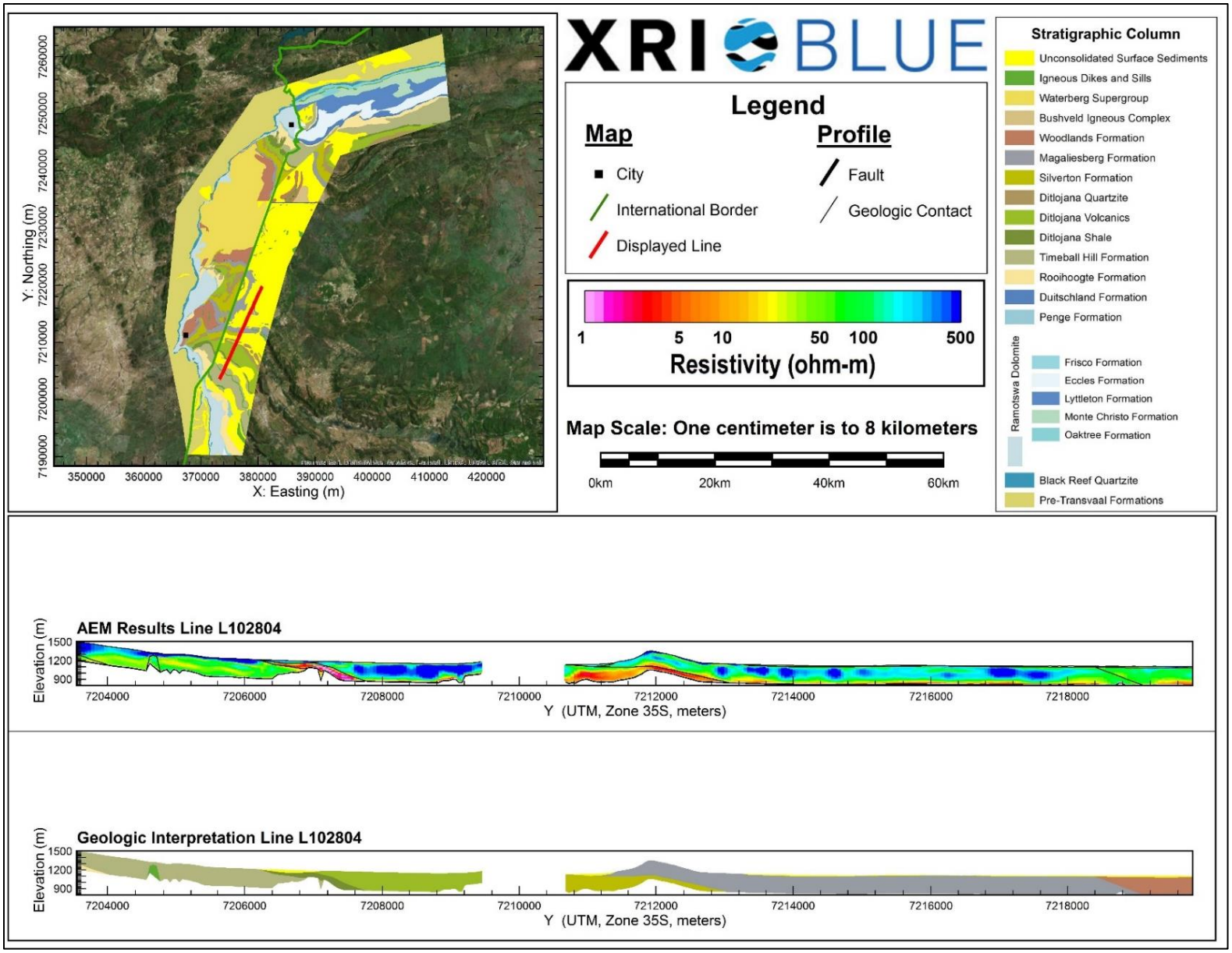

AEM and Interpreted Geology Profile for L102804.

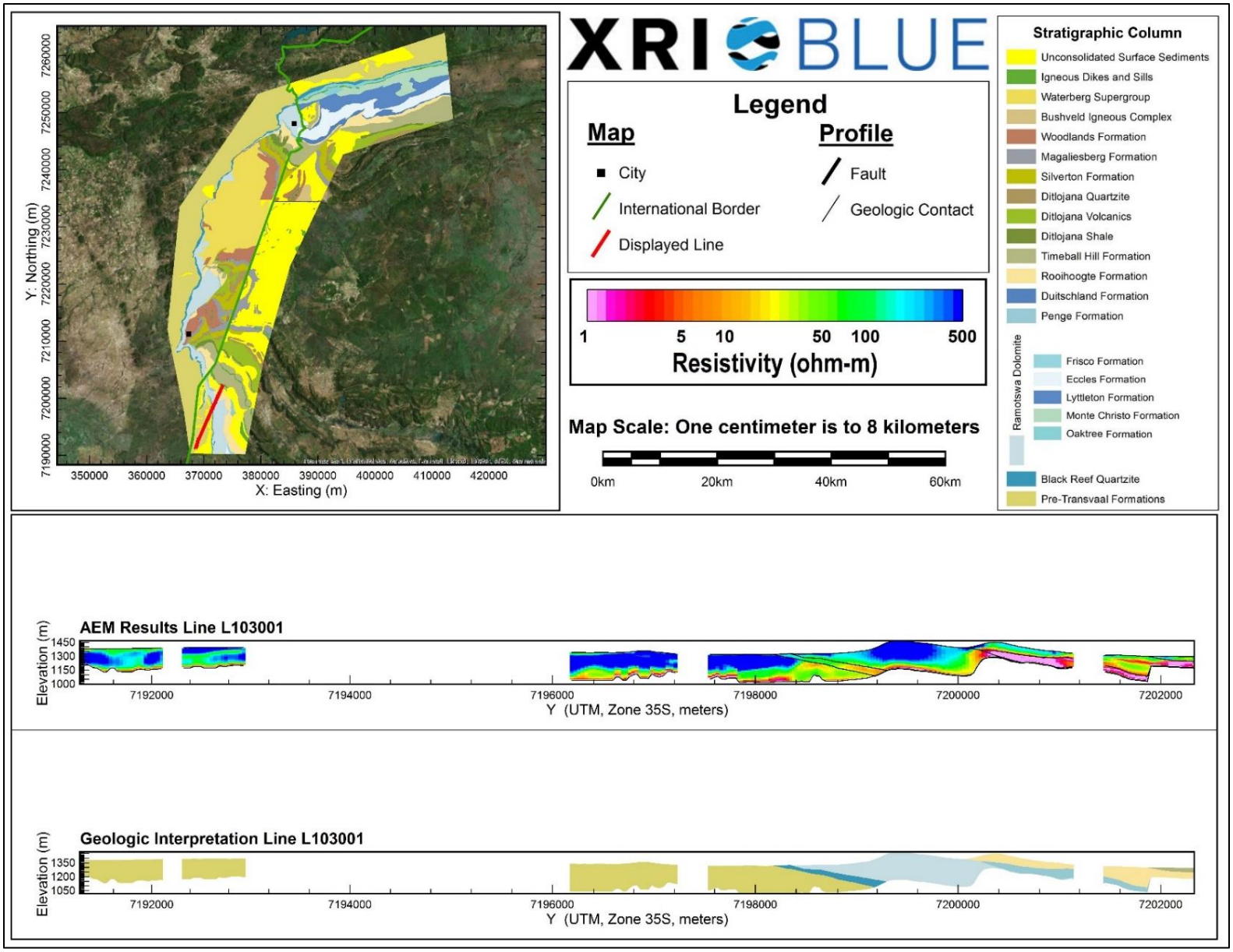

AEM and Interpreted Geology Profile for L103001.

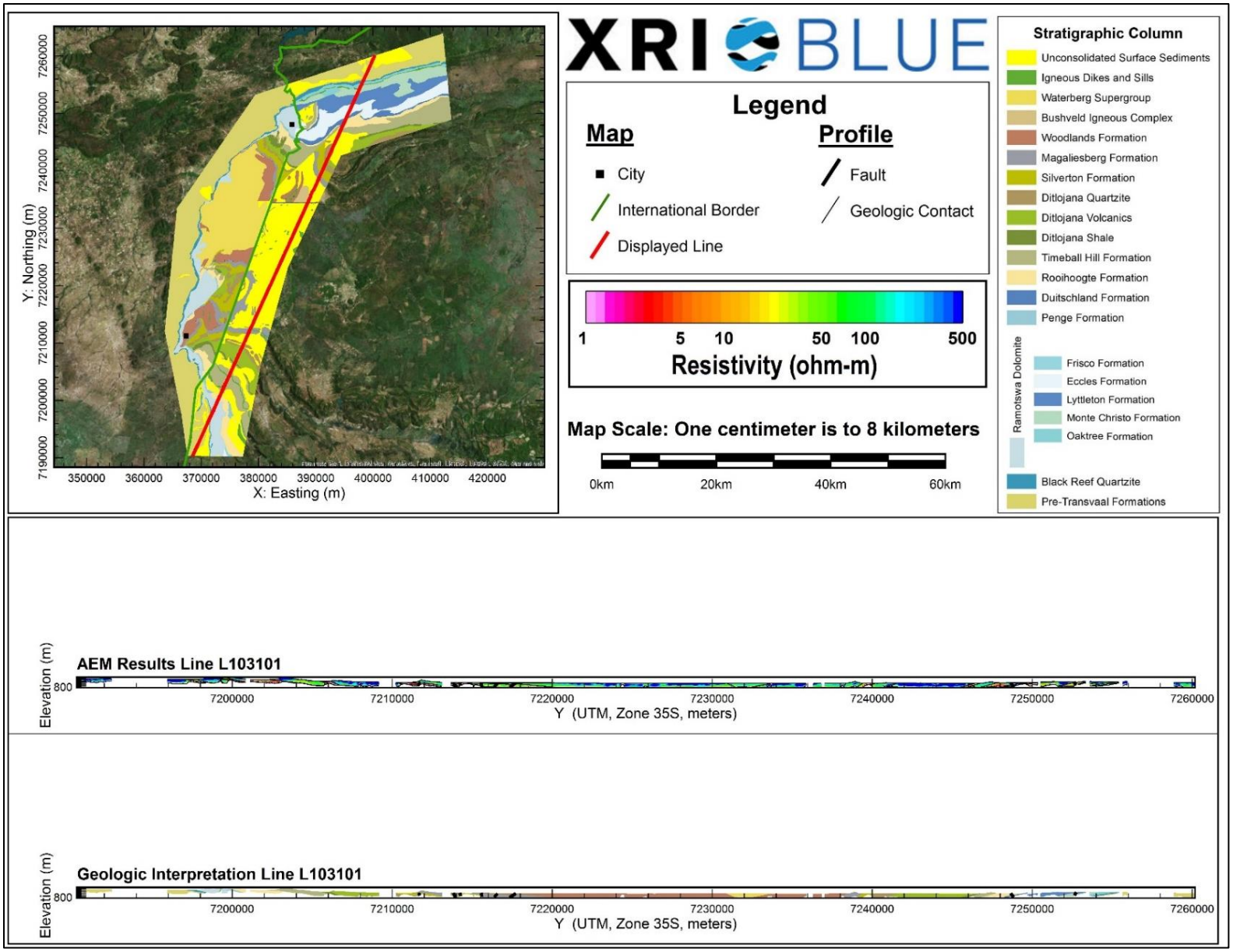

AEM and Interpreted Geology Profile for L103101.

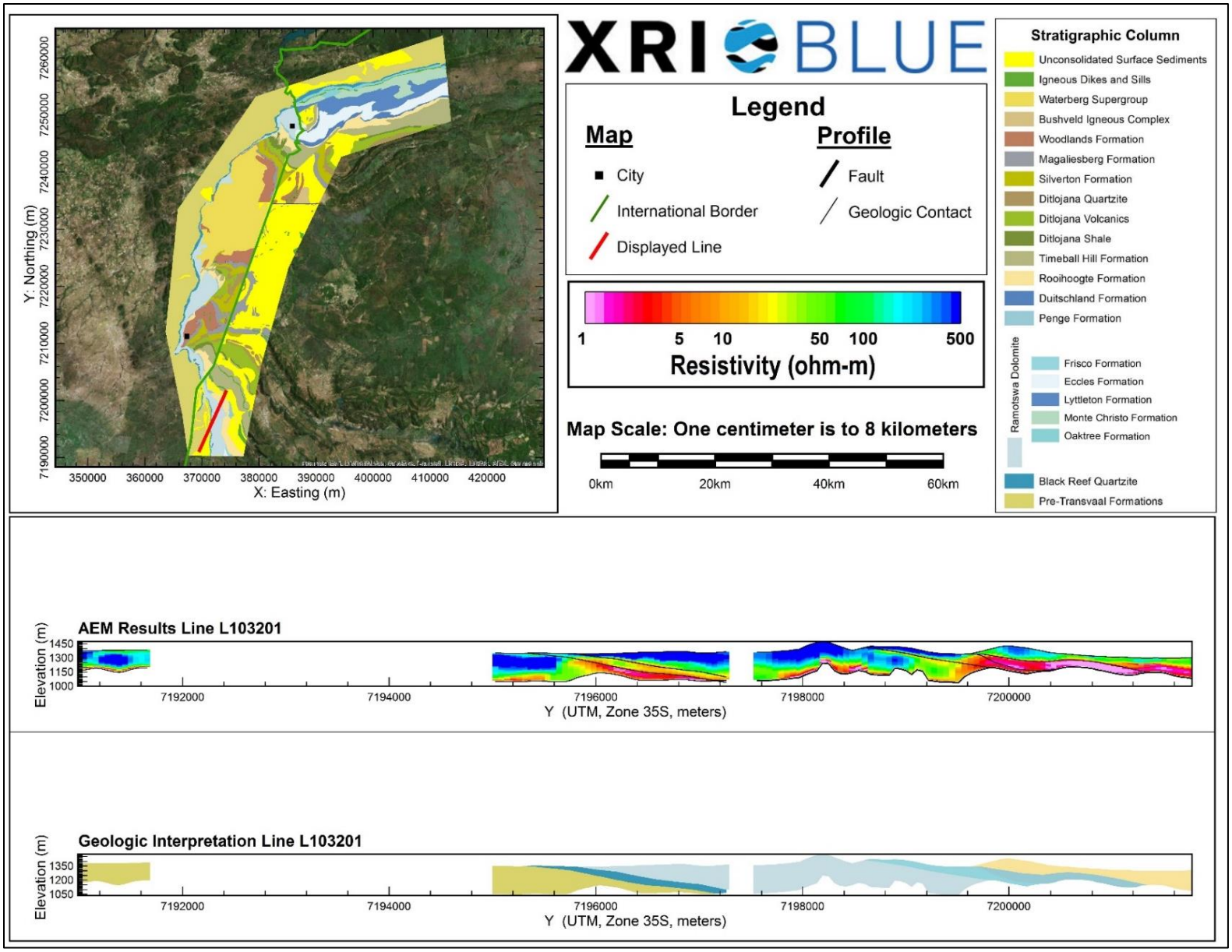

AEM and Interpreted Geology Profile for L103201.

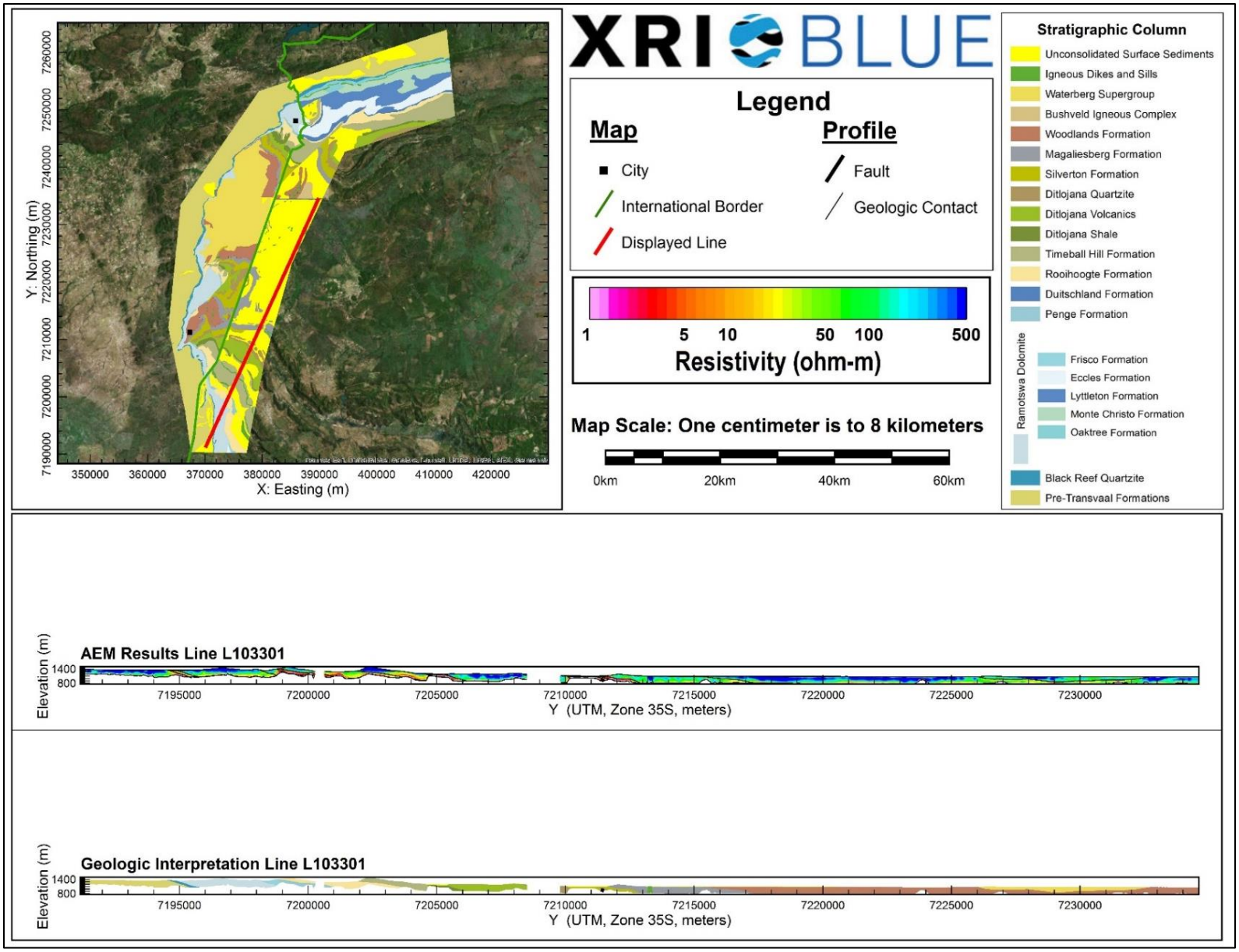

AEM and Interpreted Geology Profile for L103301.

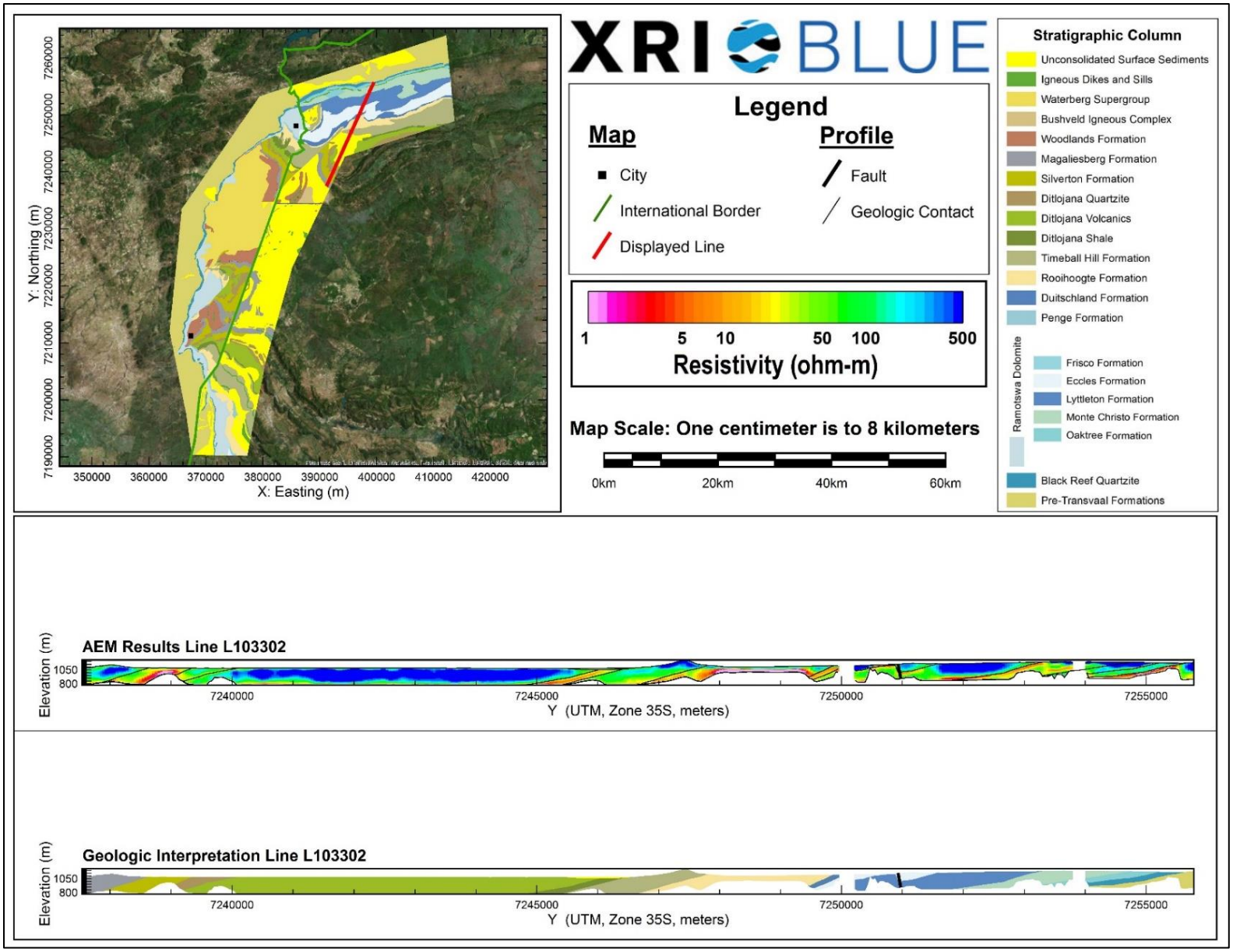

AEM and Interpreted Geology Profile for L103302.

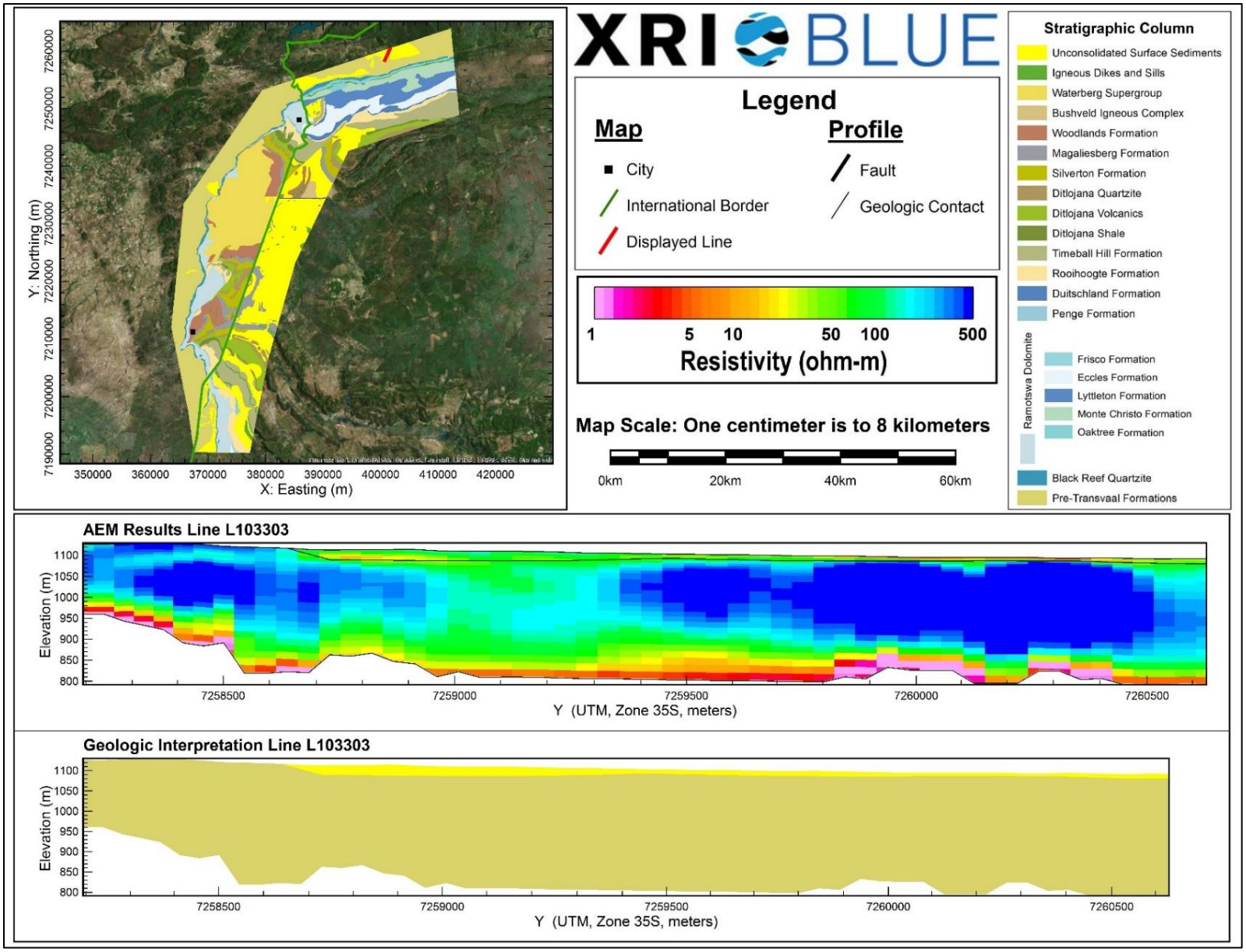

AEM and Interpreted Geology Profile for L103303.

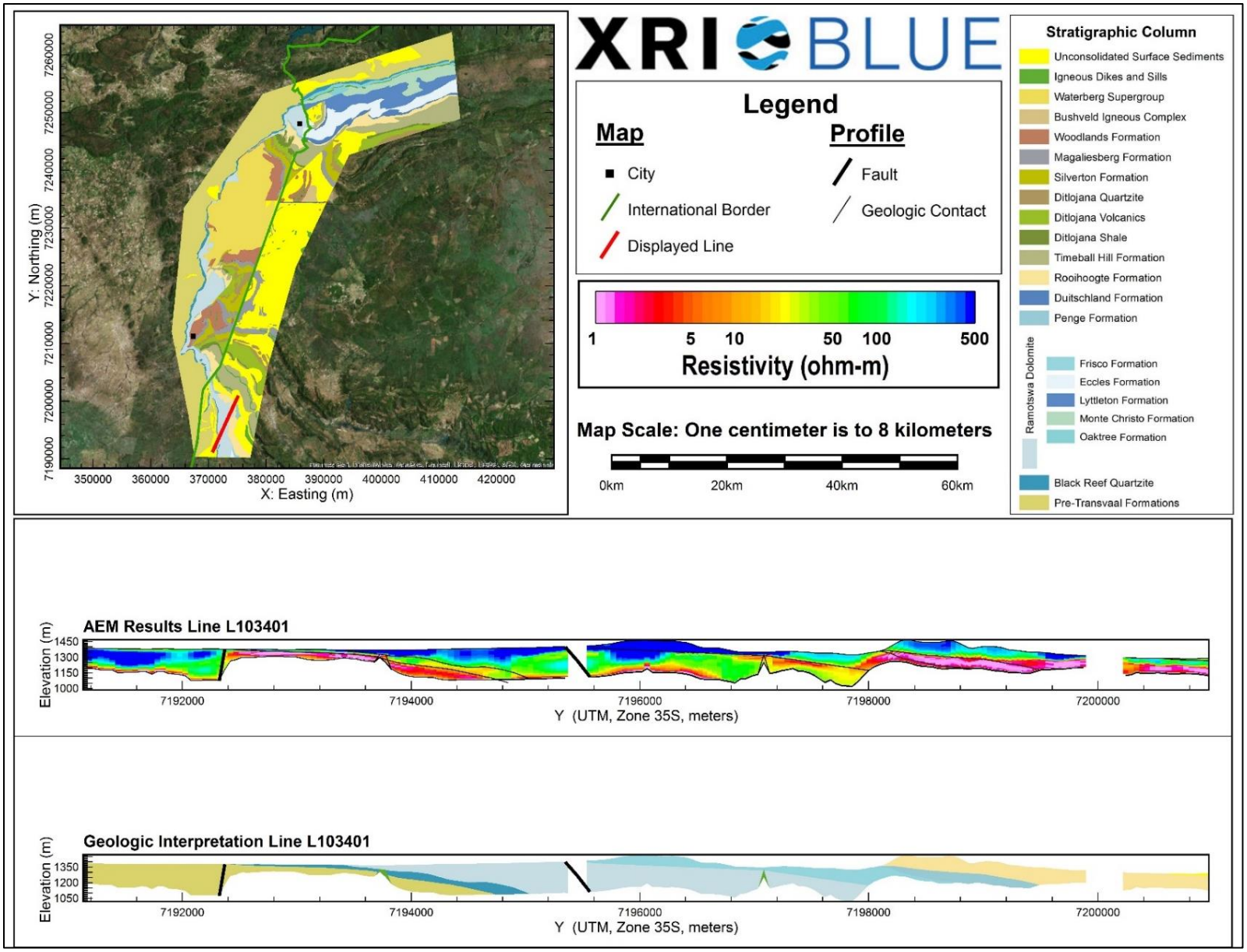

AEM and Interpreted Geology Profile for L103401.

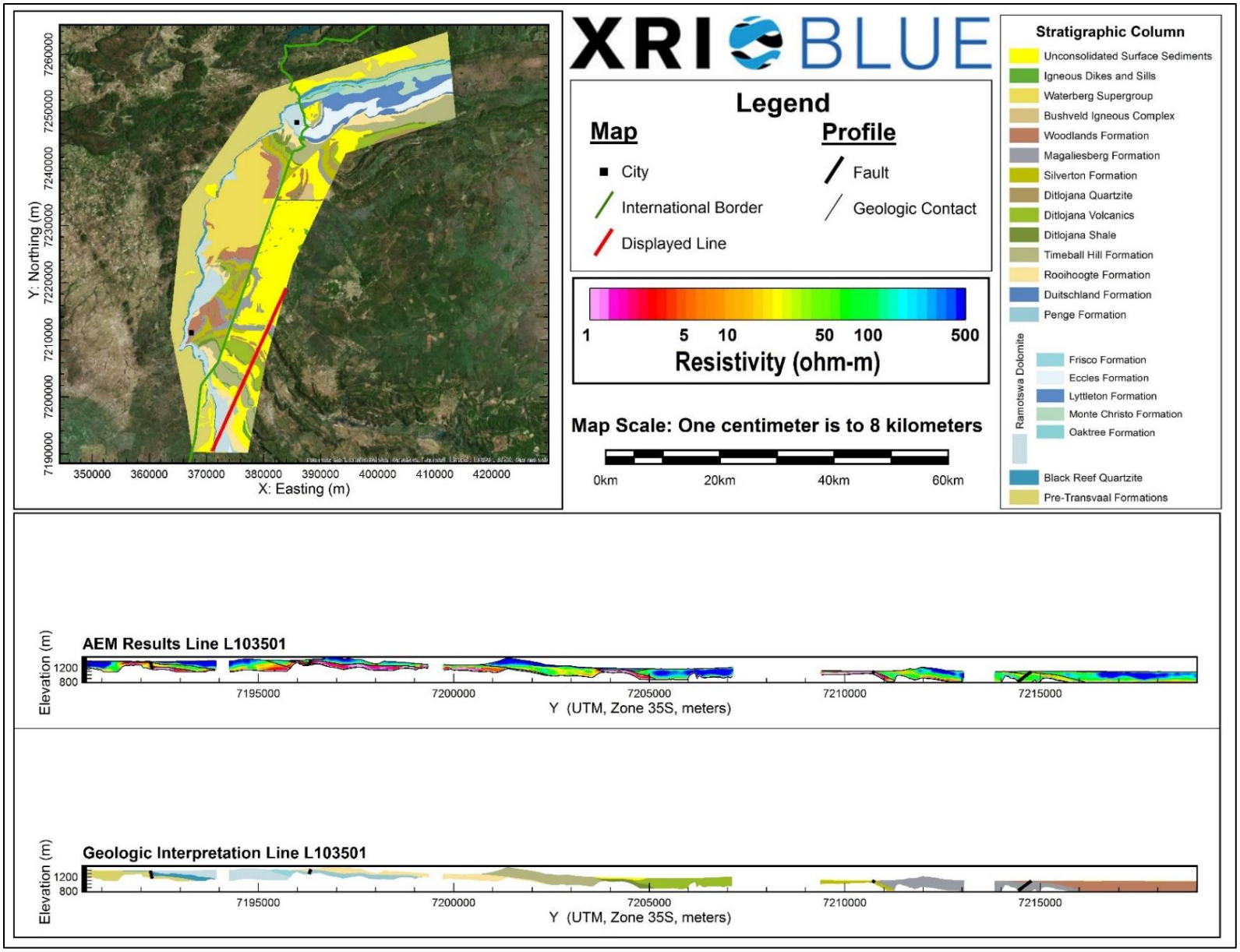

AEM and Interpreted Geology Profile for L103501.

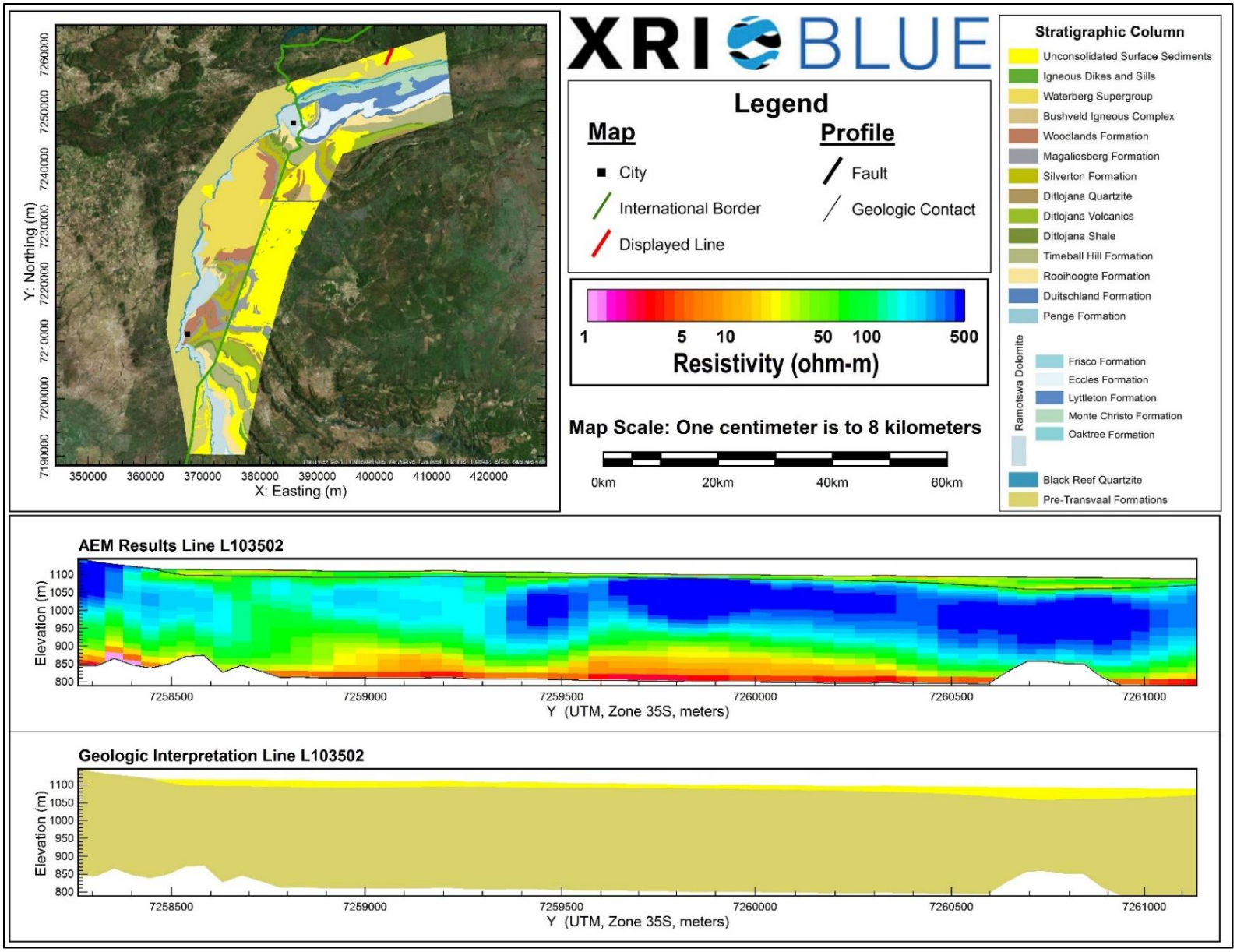

AEM and Interpreted Geology Profile for L103502.

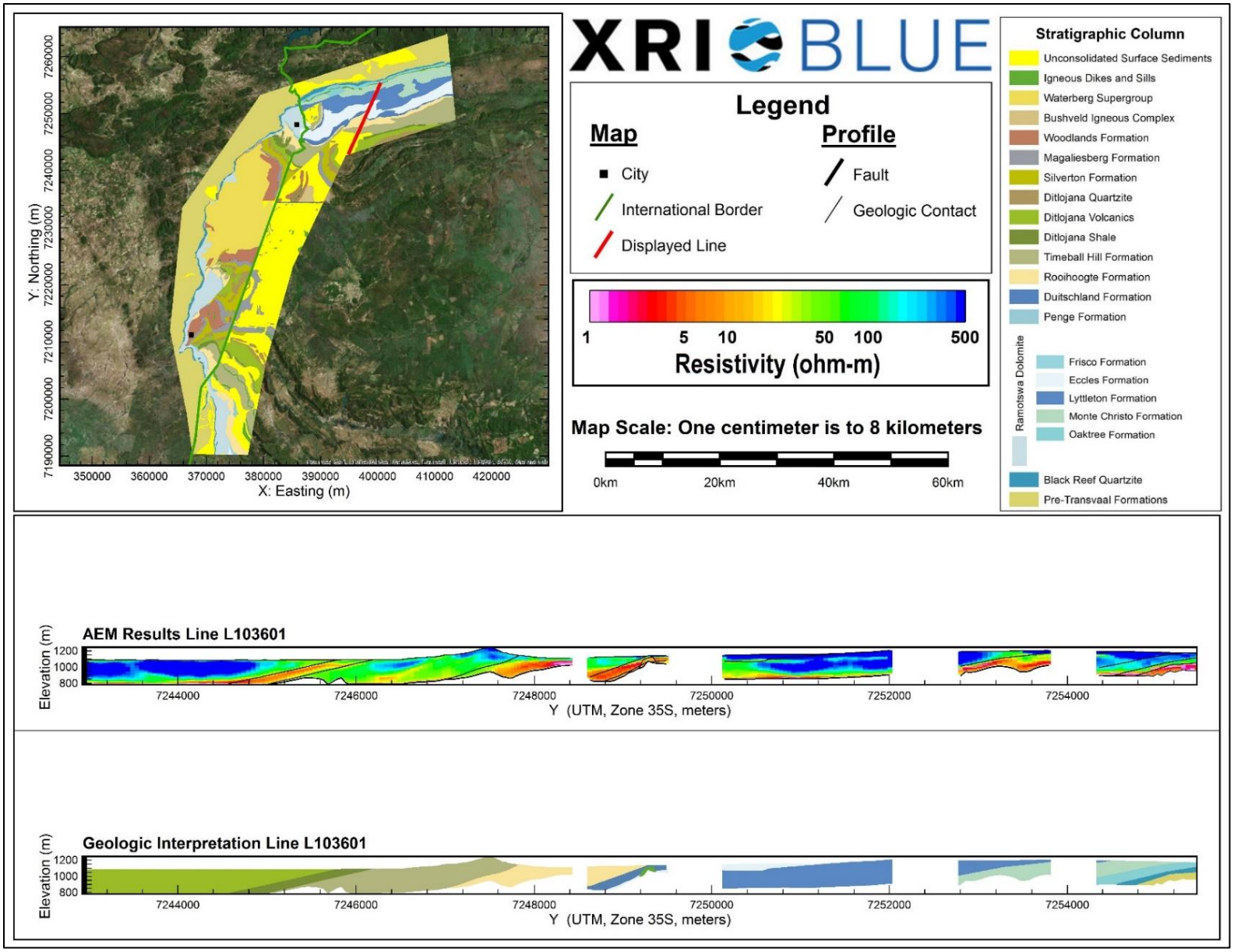

AEM and Interpreted Geology Profile for L103601.

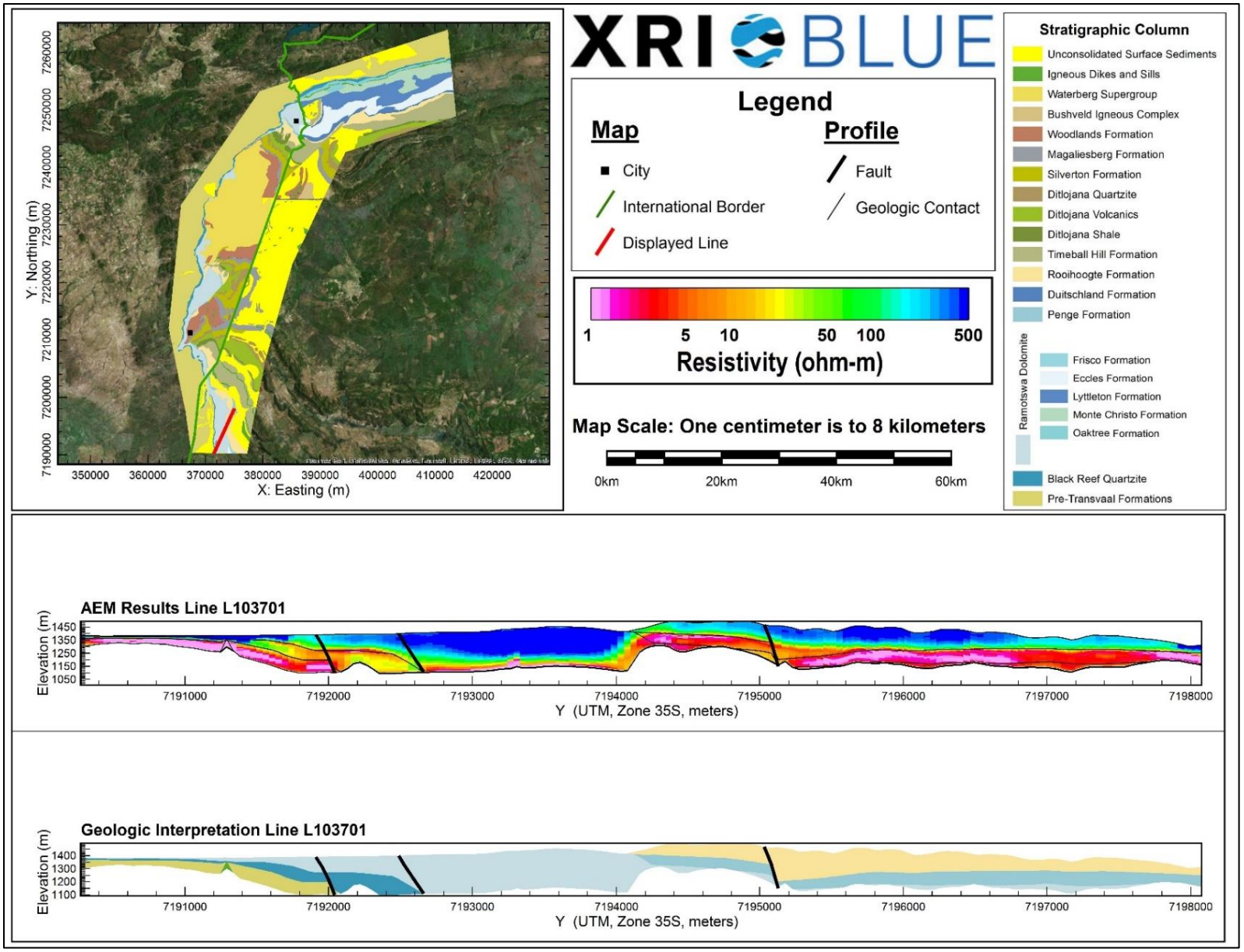

AEM and Interpreted Geology Profile for L103701.

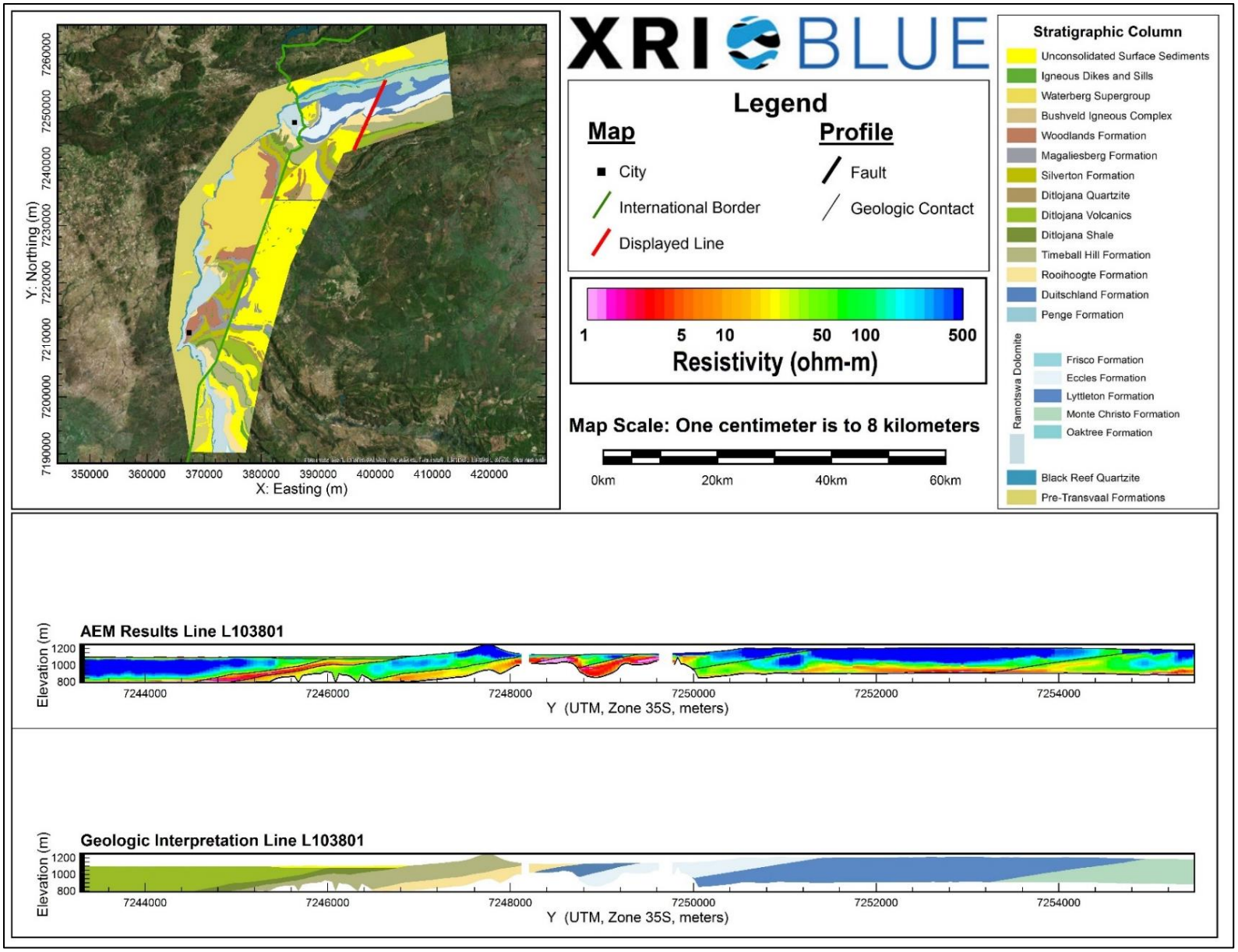

AEM and Interpreted Geology Profile for L103801.

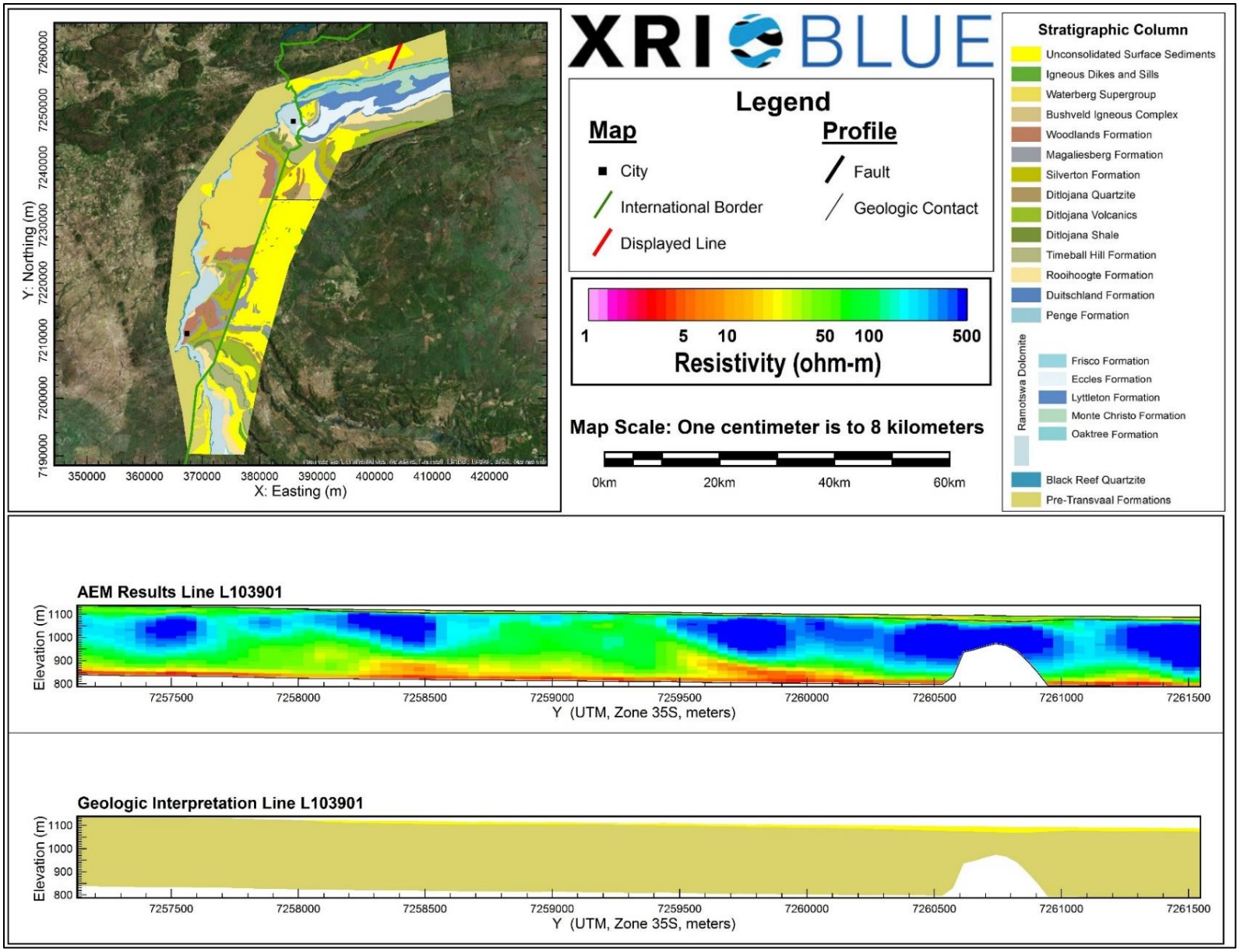

AEM and Interpreted Geology Profile for L103901.

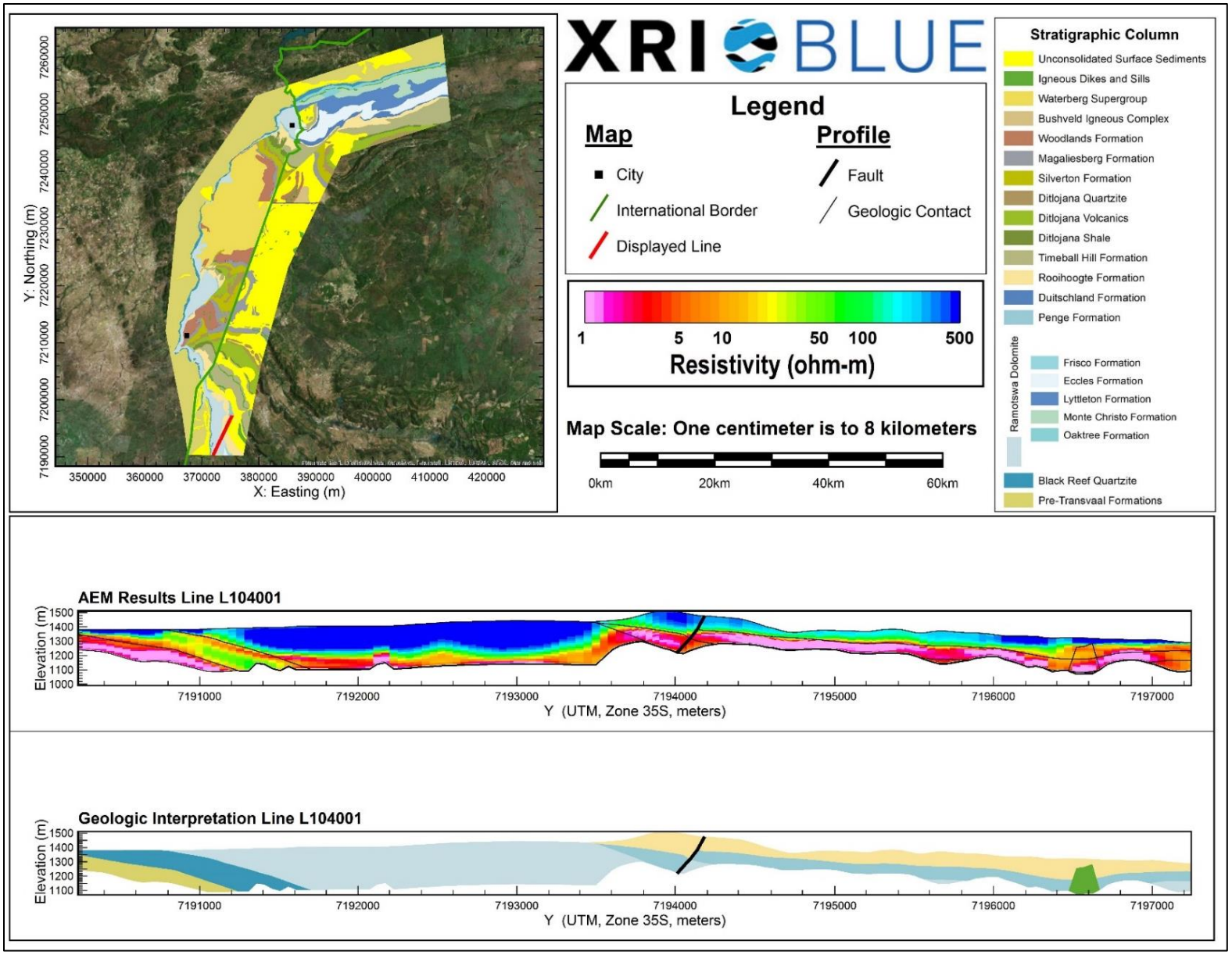

AEM and Interpreted Geology Profile for L104001.

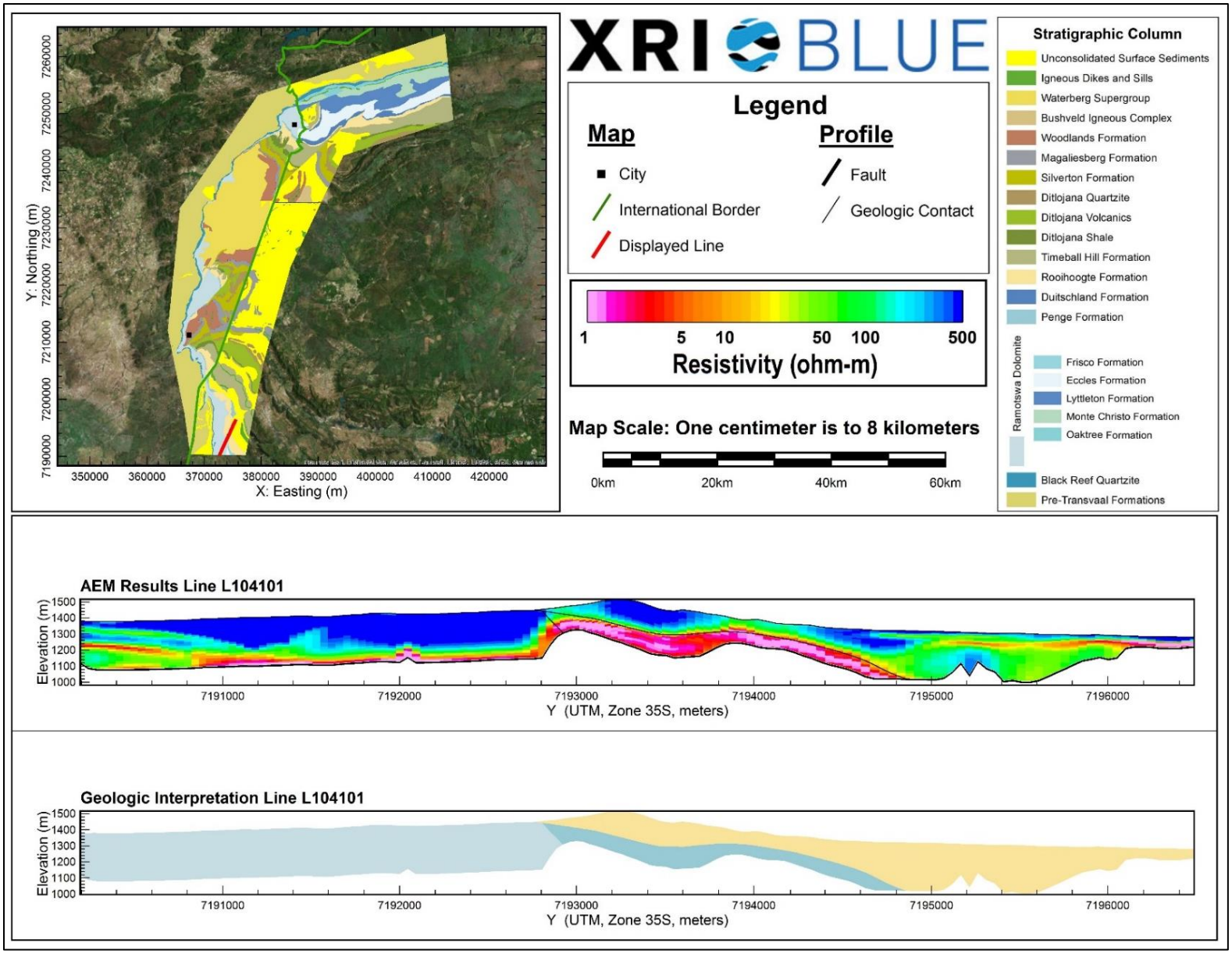

AEM and Interpreted Geology Profile for L104101.

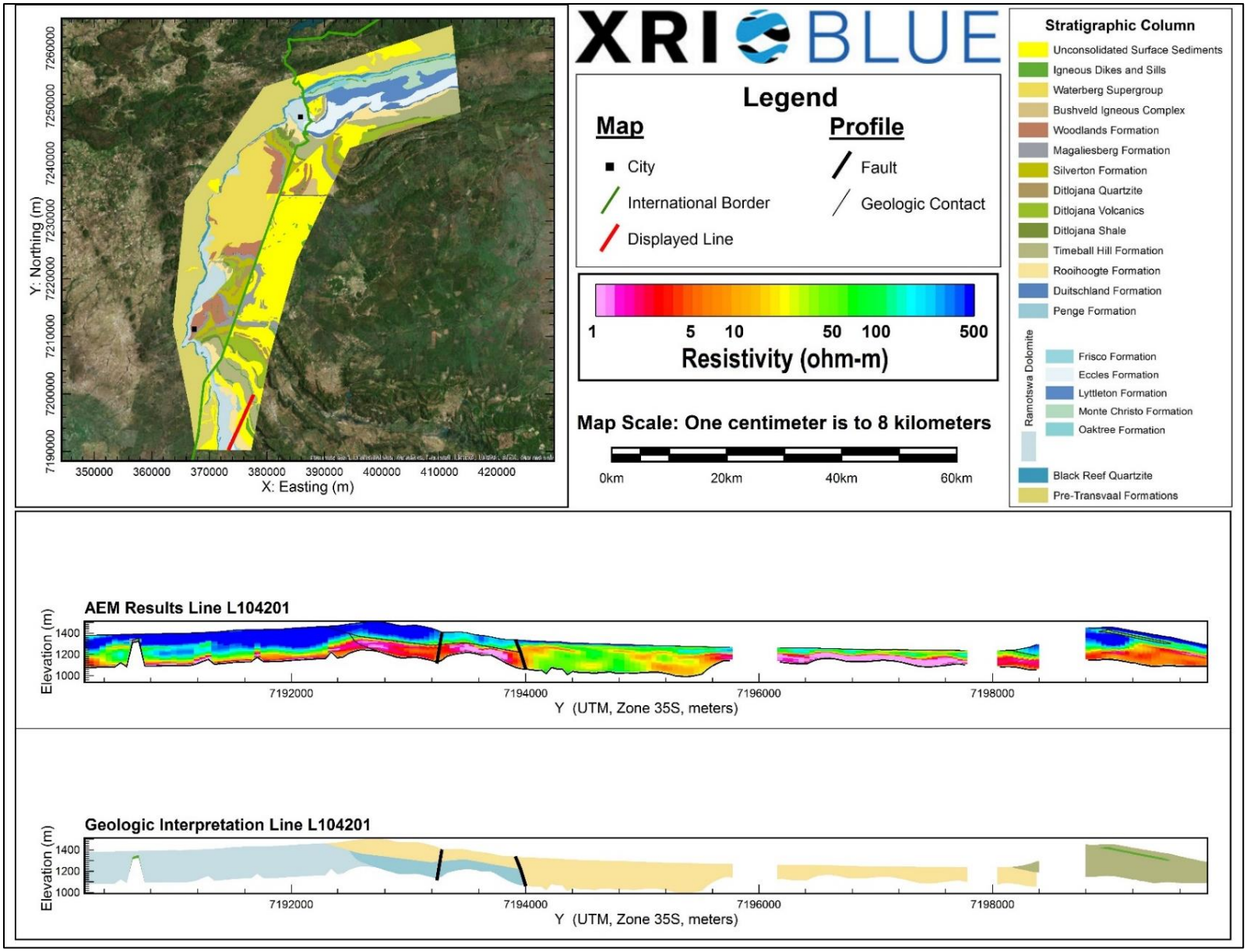

AEM and Interpreted Geology Profile for L104201.

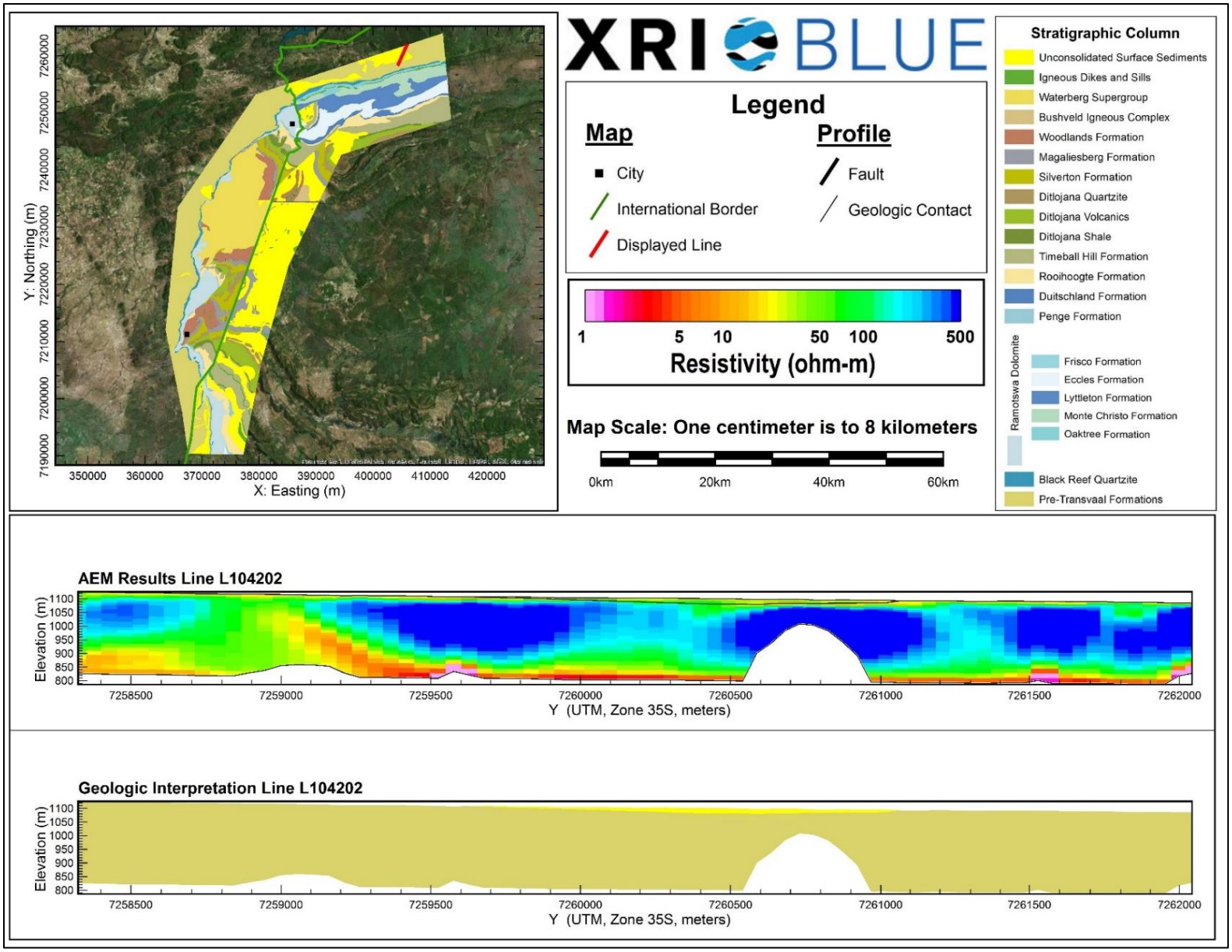

AEM and Interpreted Geology Profile for L104202.

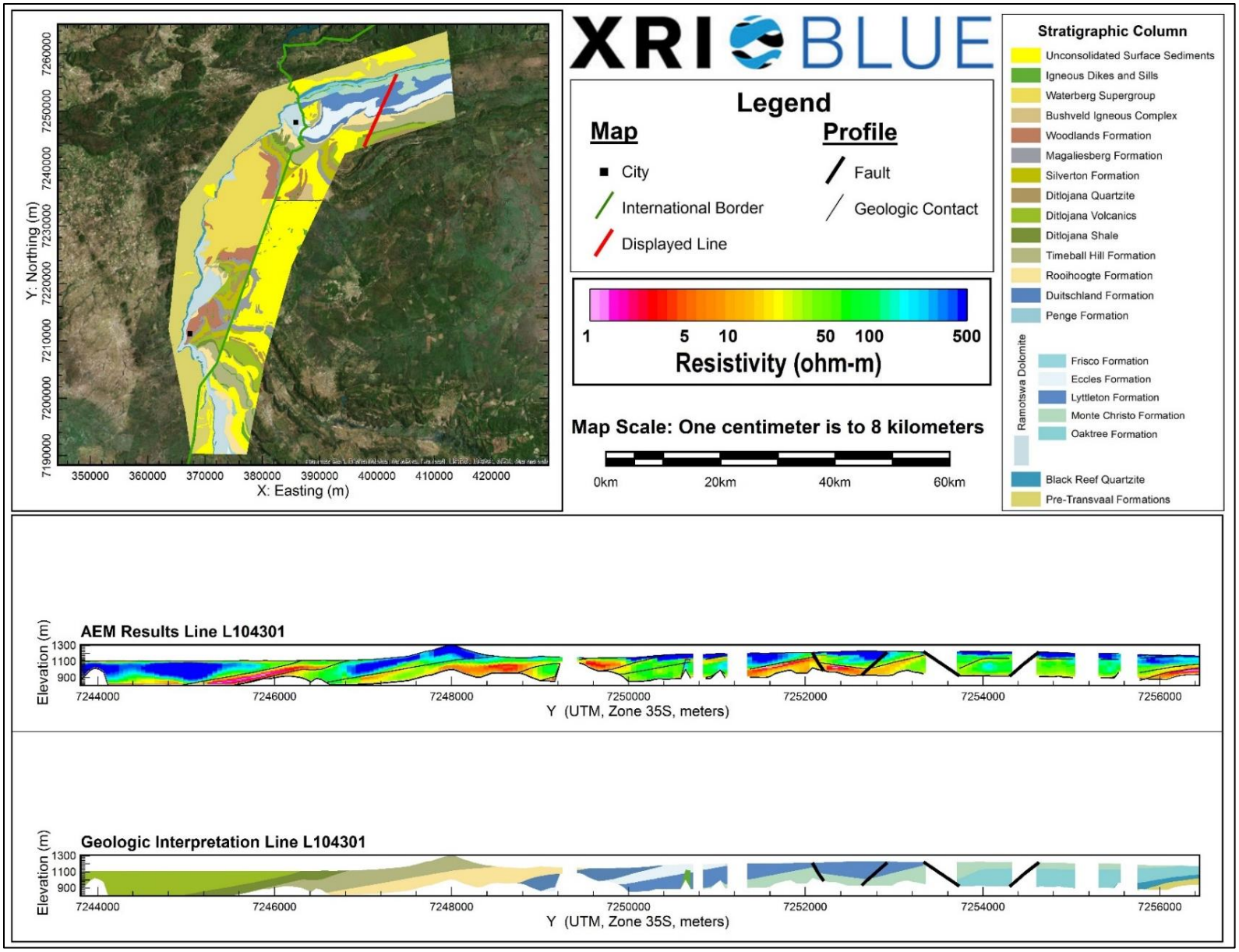

AEM and Interpreted Geology Profile for L104301.

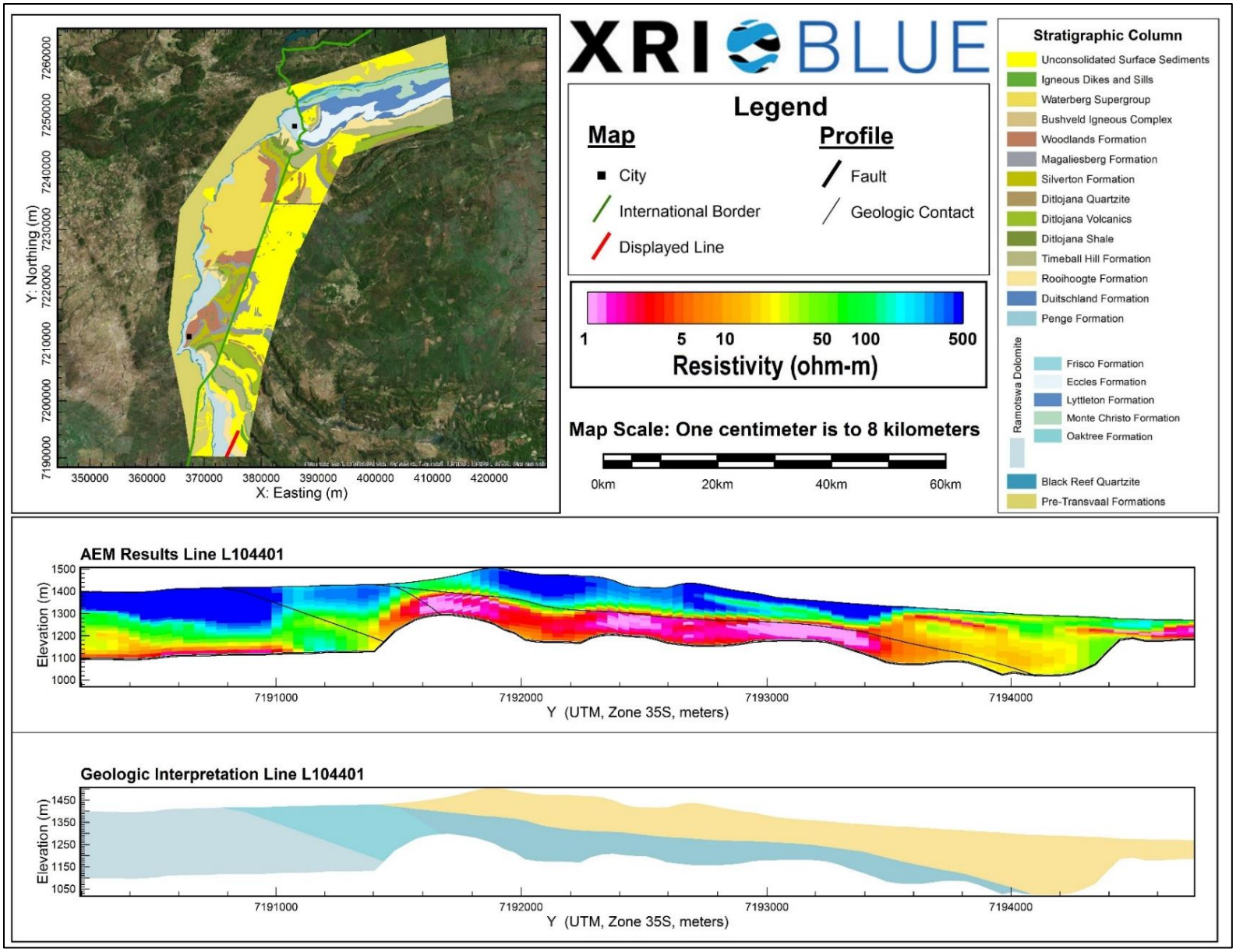

AEM and Interpreted Geology Profile for L104401.

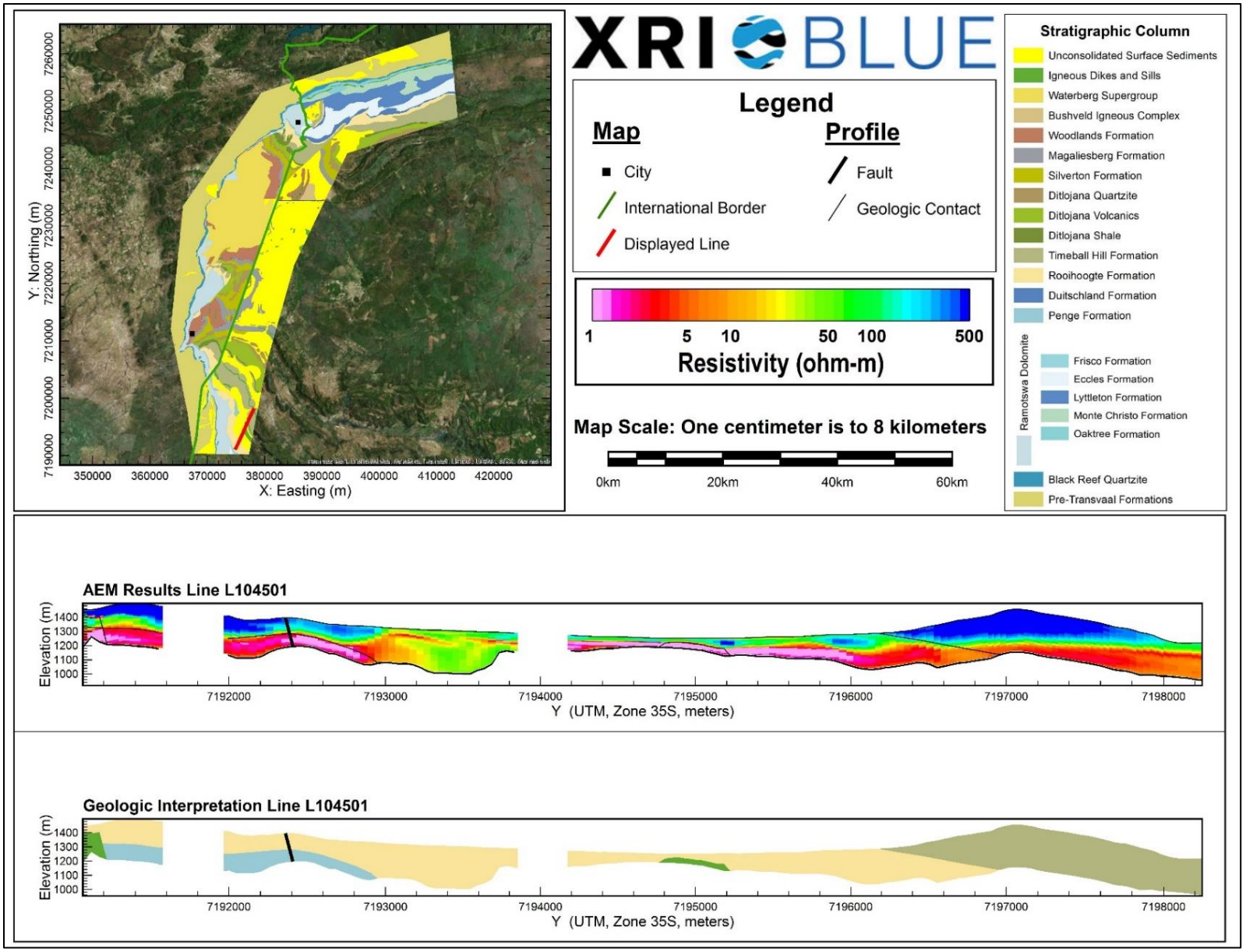

AEM and Interpreted Geology Profile for L104501.

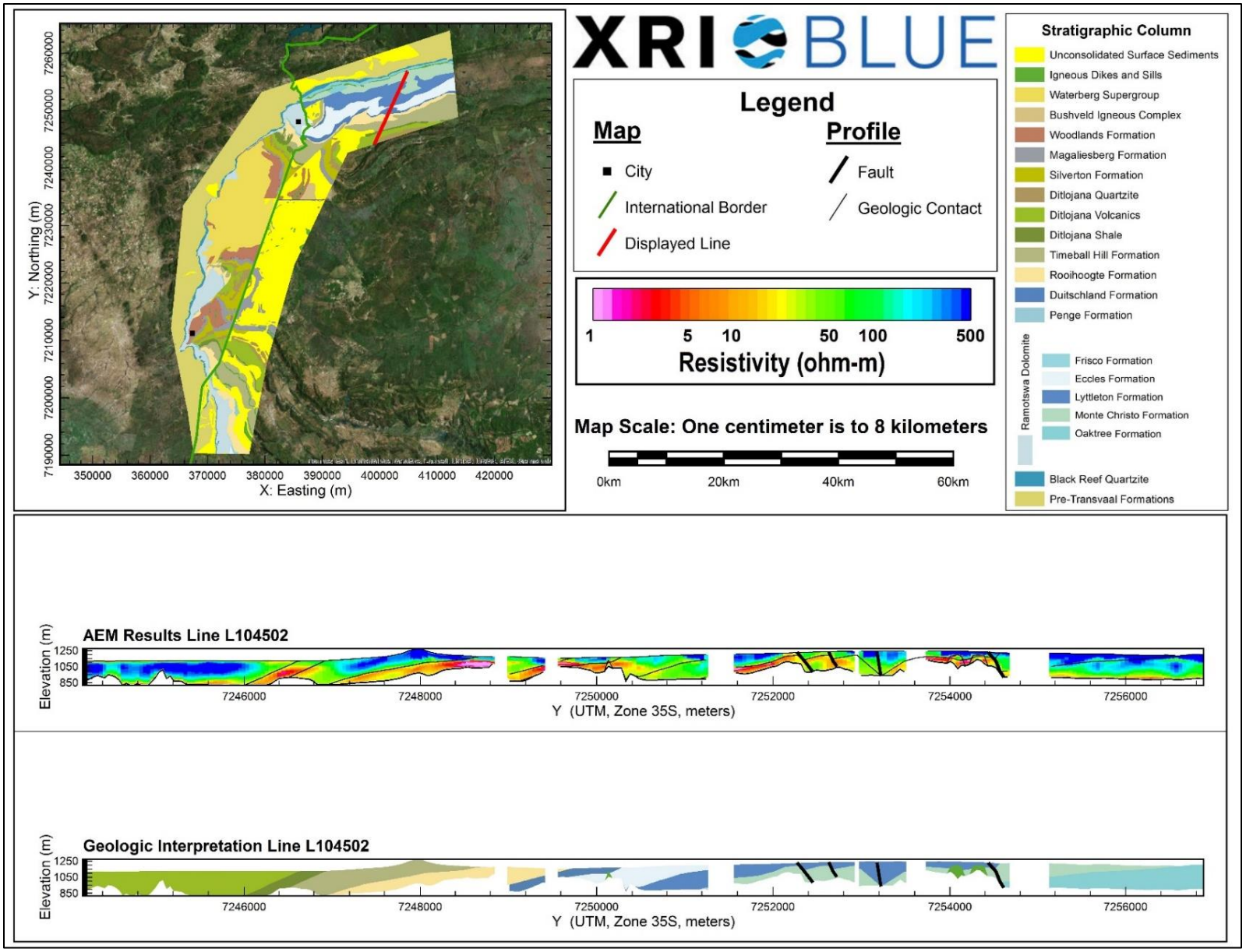

AEM and Interpreted Geology Profile for L104502.

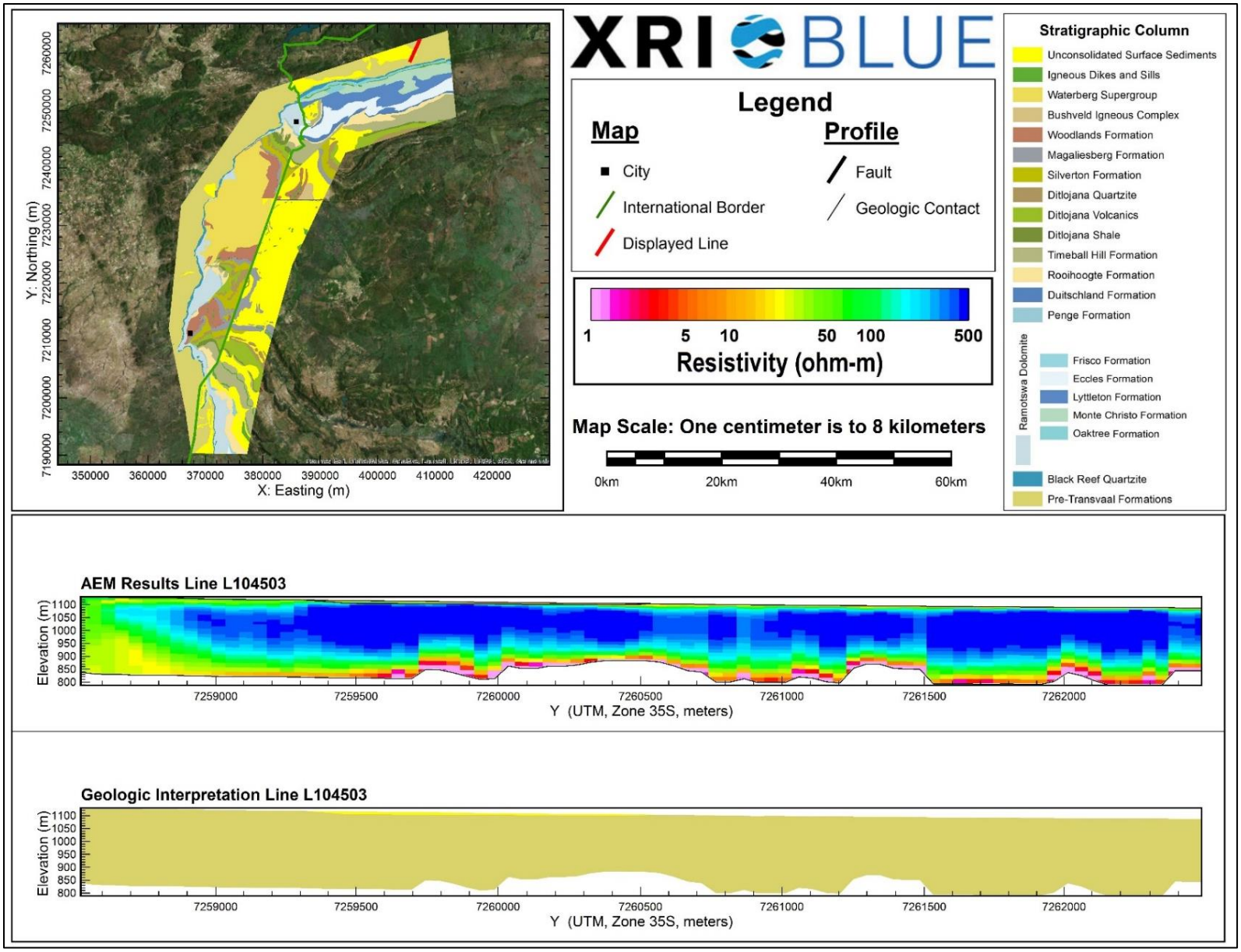

AEM and Interpreted Geology Profile for L104503.

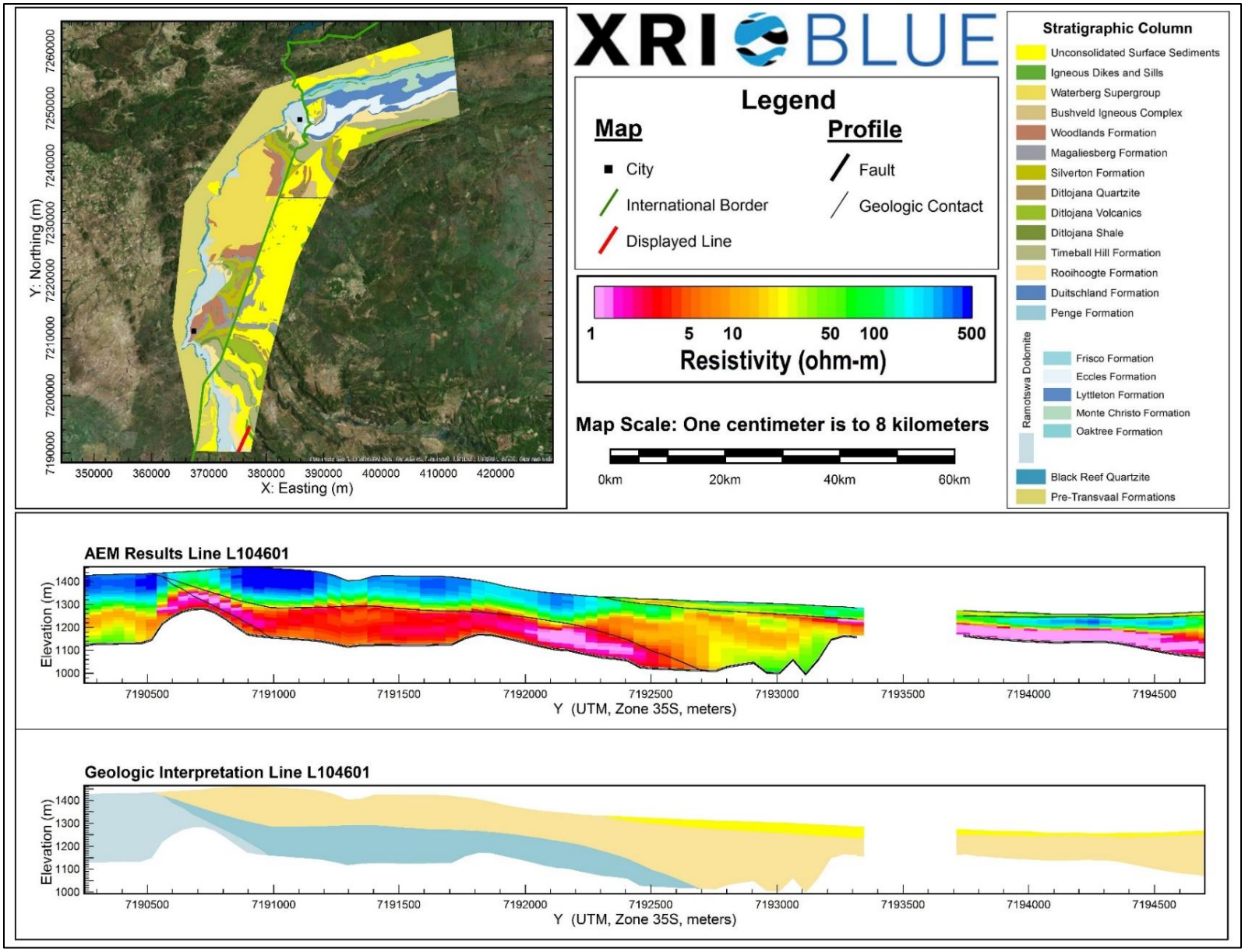

AEM and Interpreted Geology Profile for L104601.

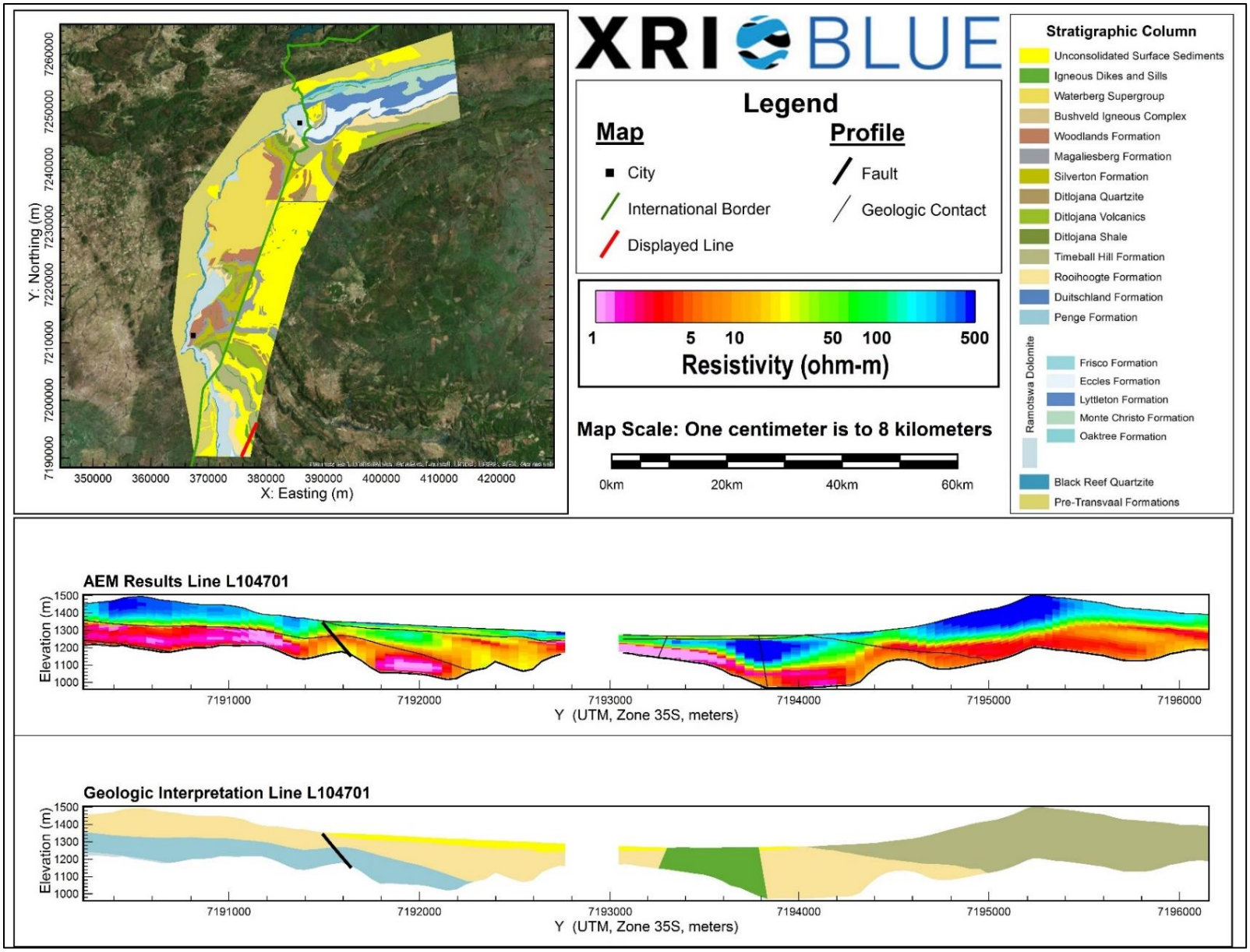

AEM and Interpreted Geology Profile for L104701.

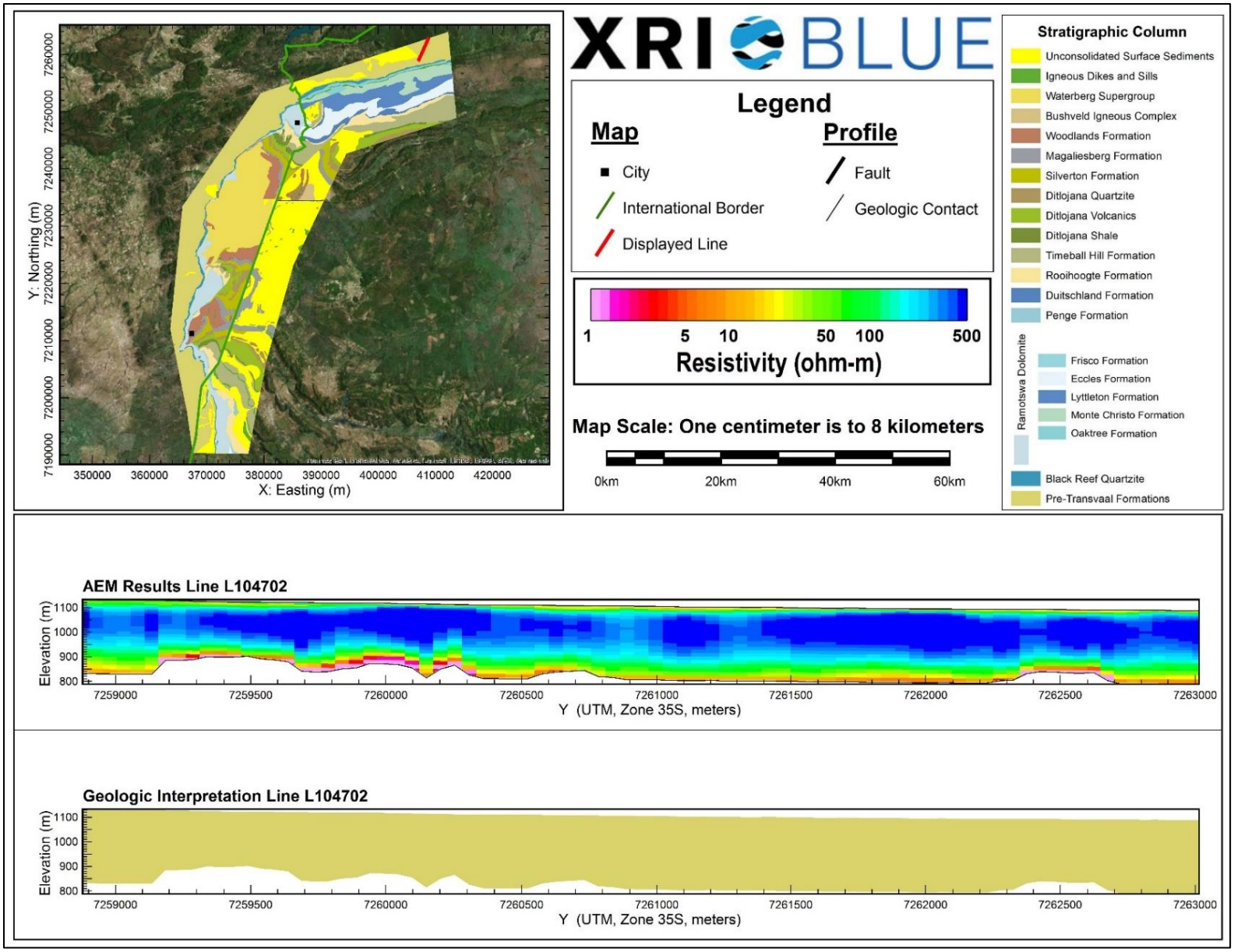

AEM and Interpreted Geology Profile for L104702.

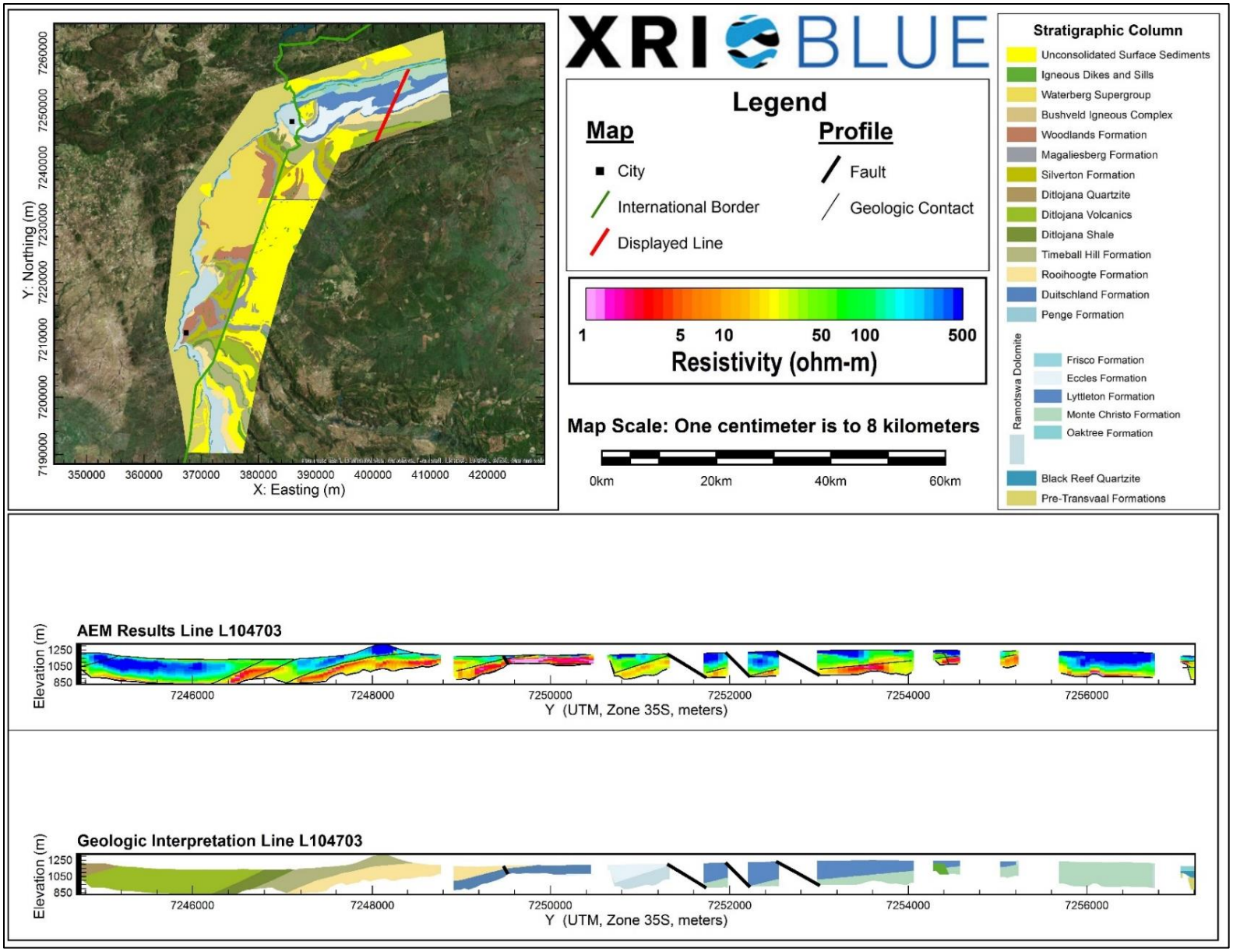

AEM and Interpreted Geology Profile for L104703.

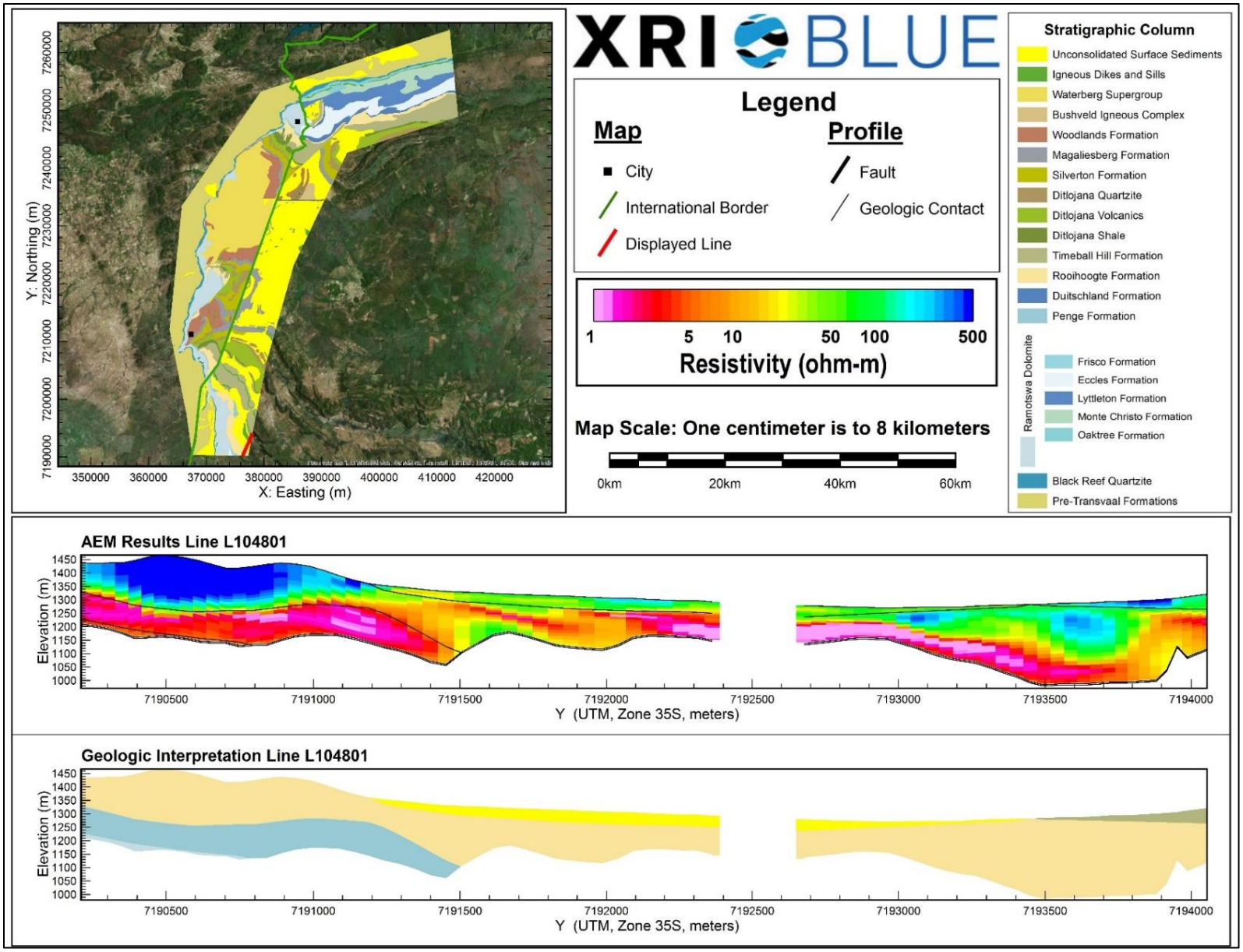

AEM and Interpreted Geology Profile for L104801.

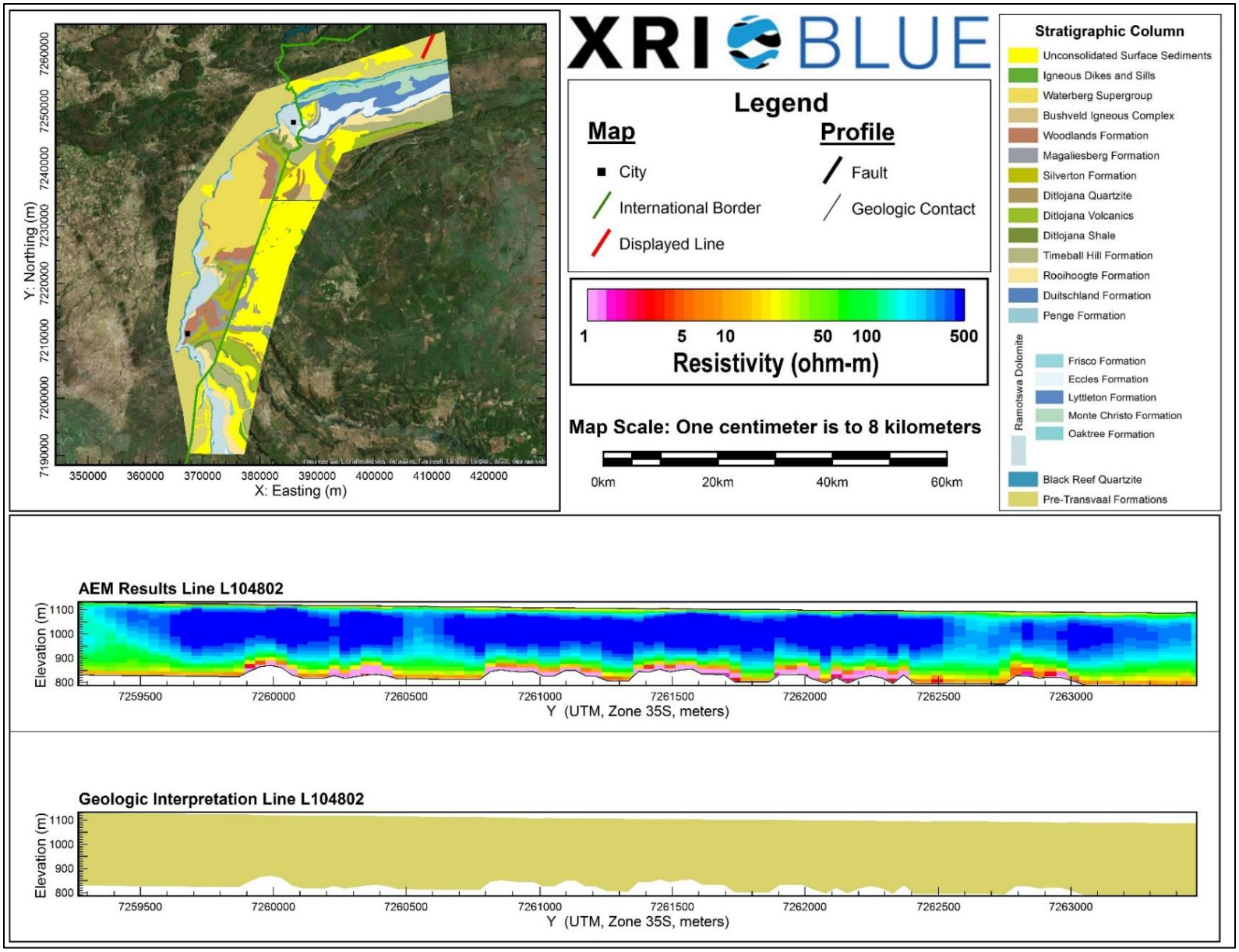

AEM and Interpreted Geology Profile for L104802.

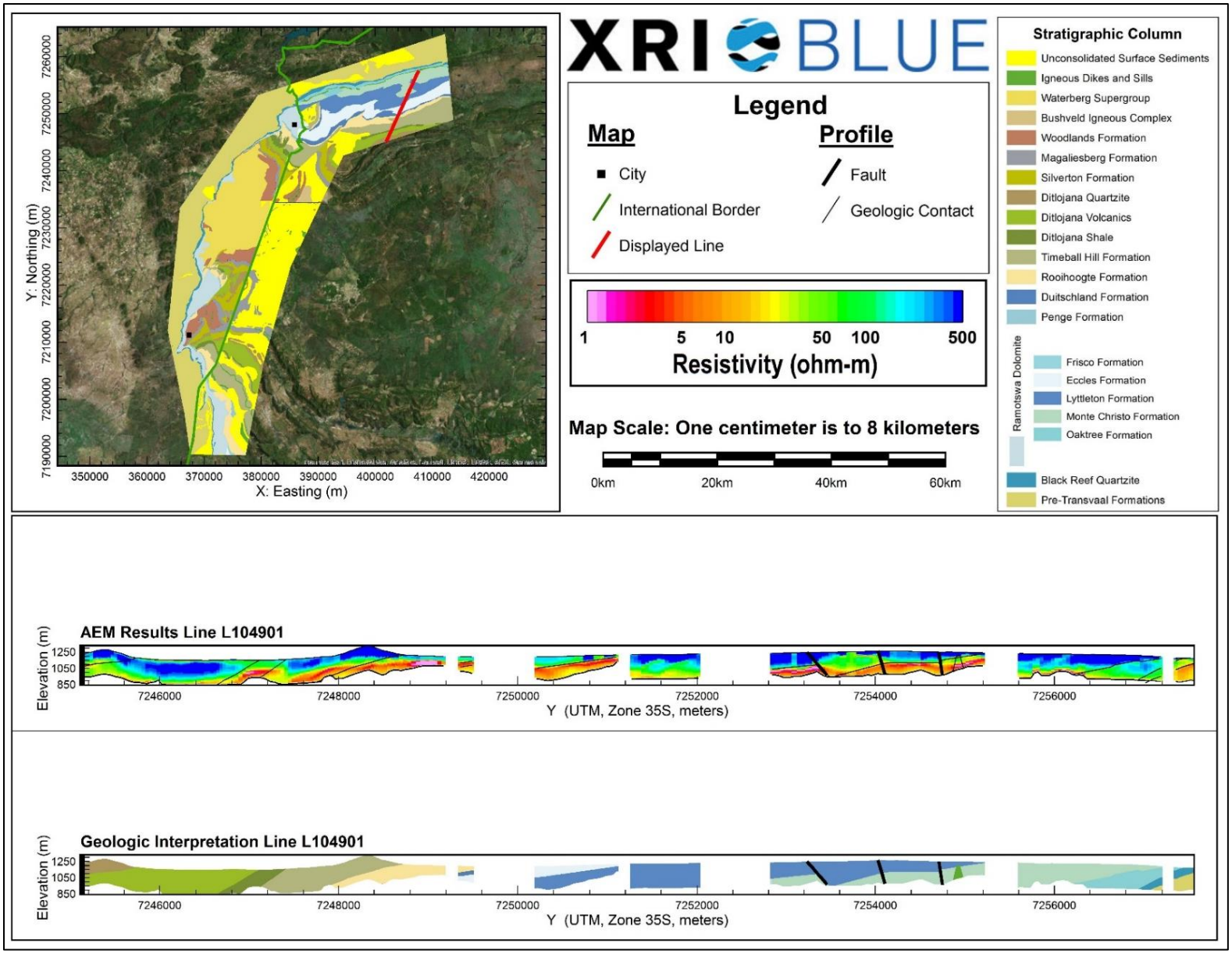

AEM and Interpreted Geology Profile for L104901.

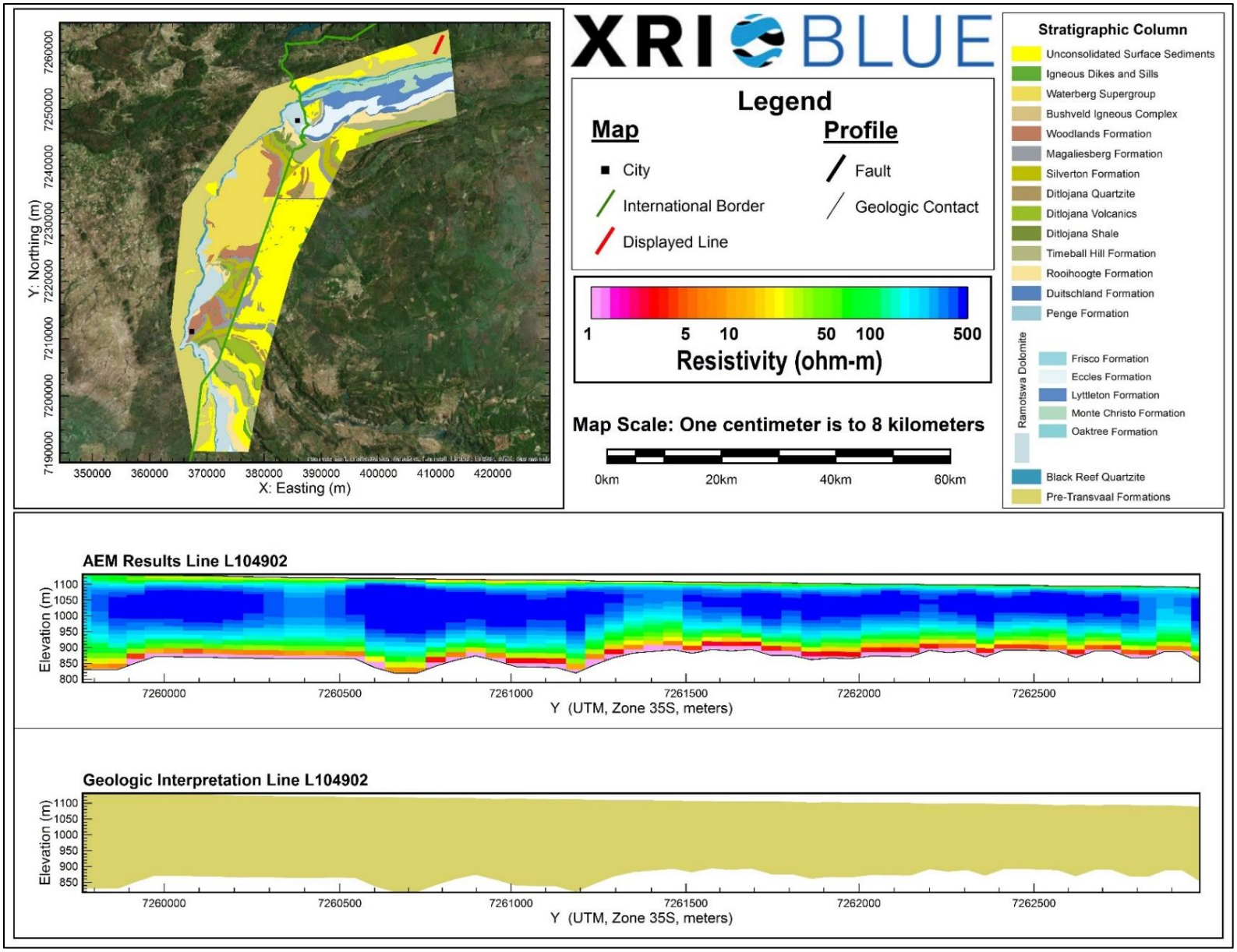

AEM and Interpreted Geology Profile for L104902.

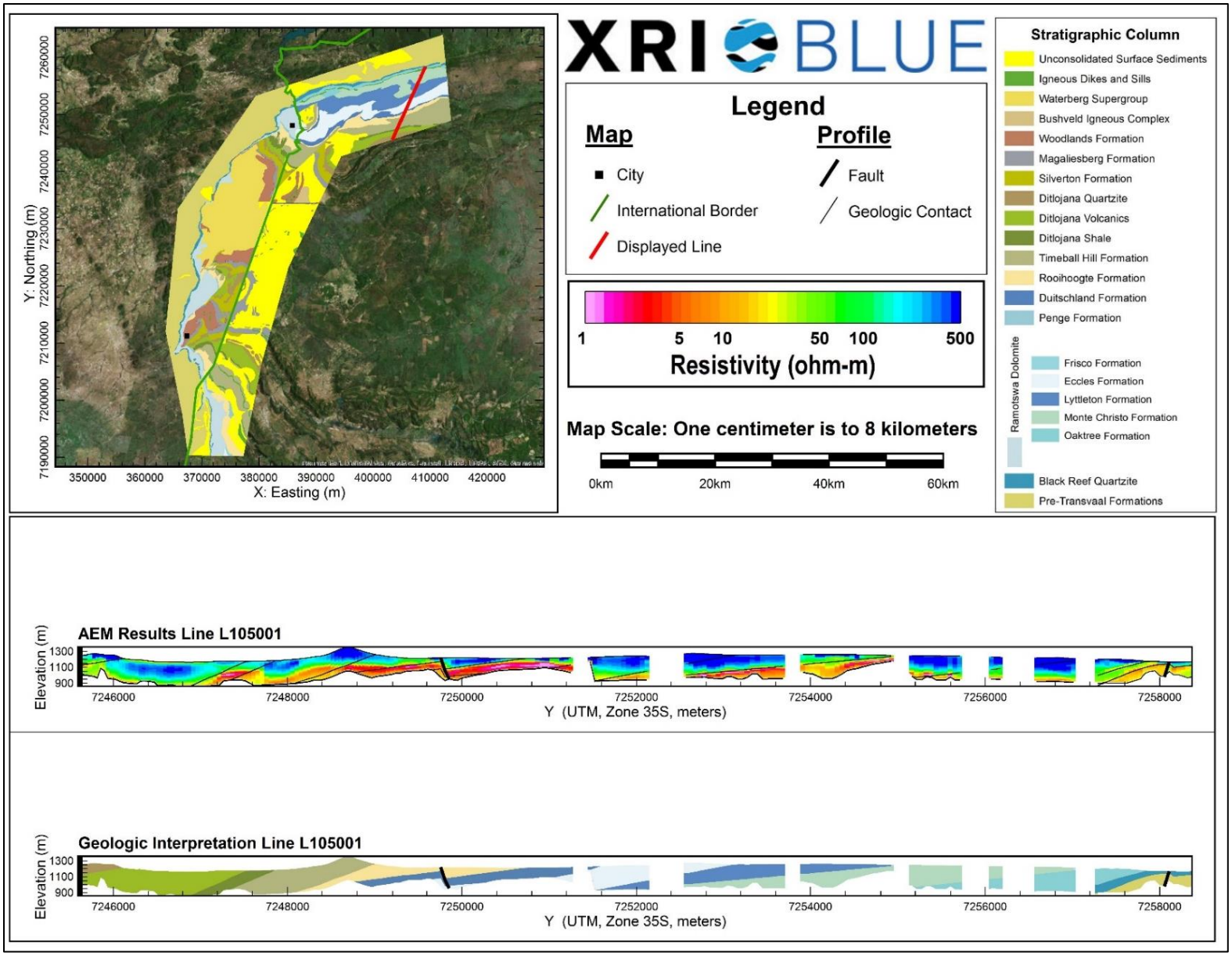

AEM and Interpreted Geology Profile for L105001.

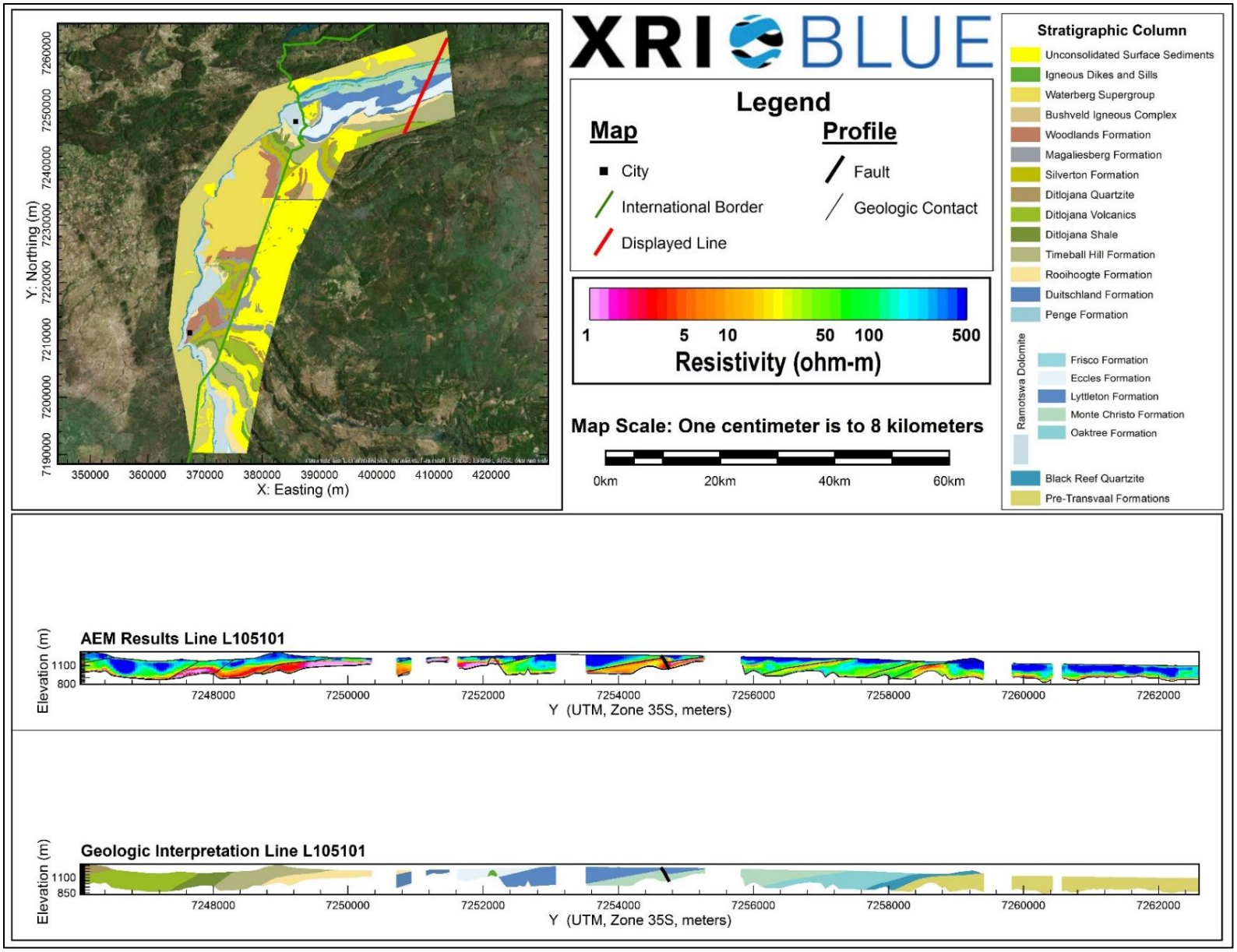

AEM and Interpreted Geology Profile for L105101.

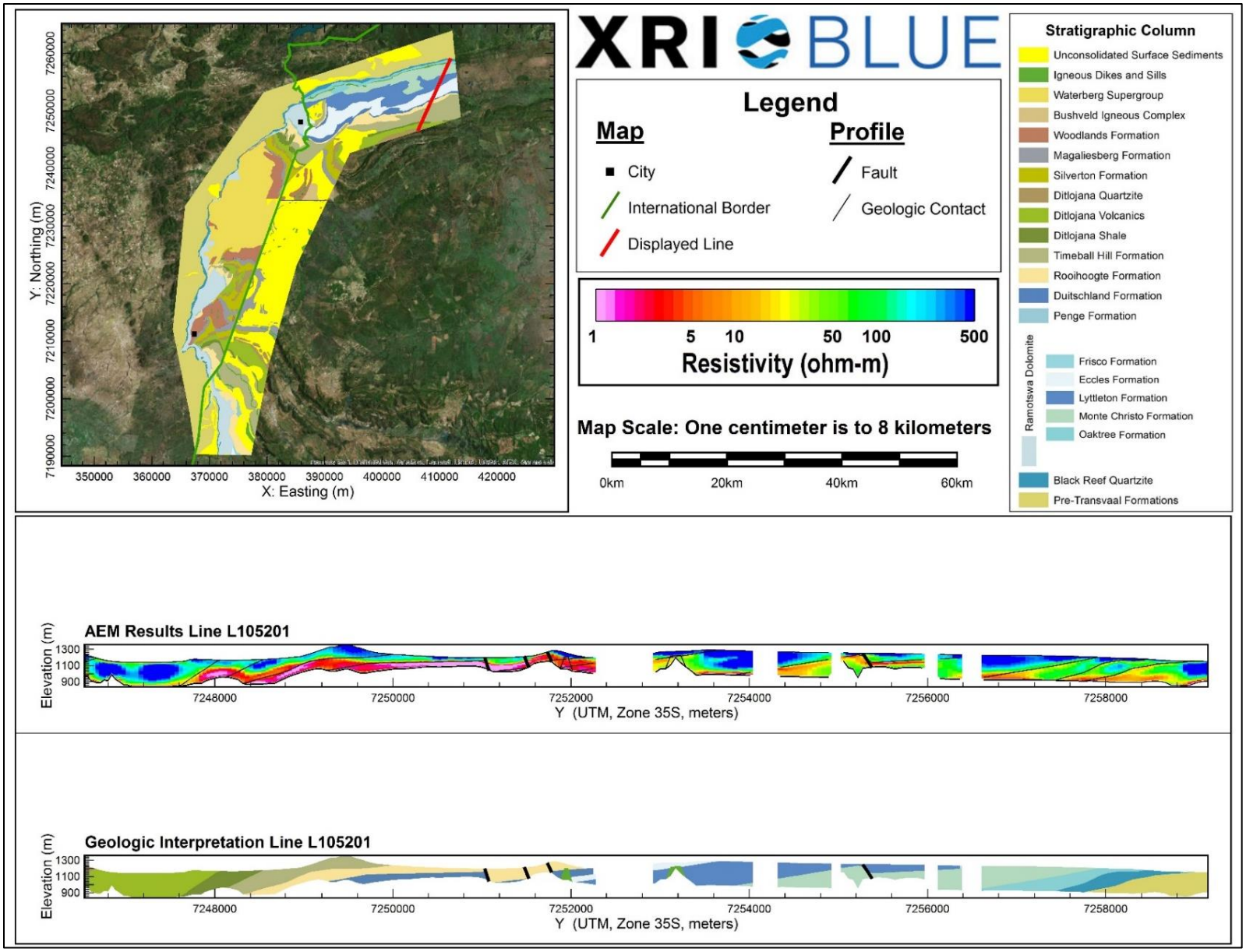

AEM and Interpreted Geology Profile for L105201.

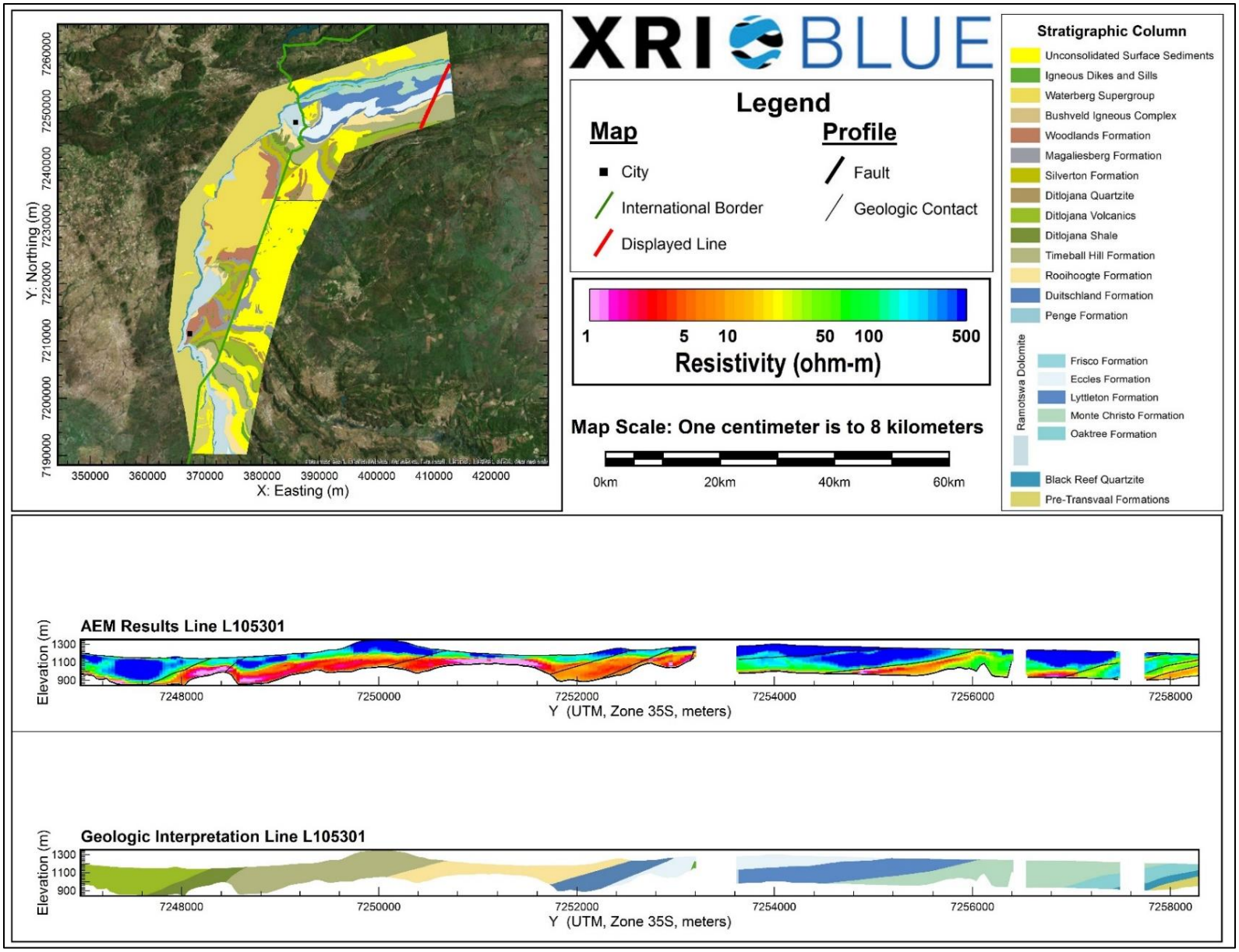

AEM and Interpreted Geology Profile for L105301.

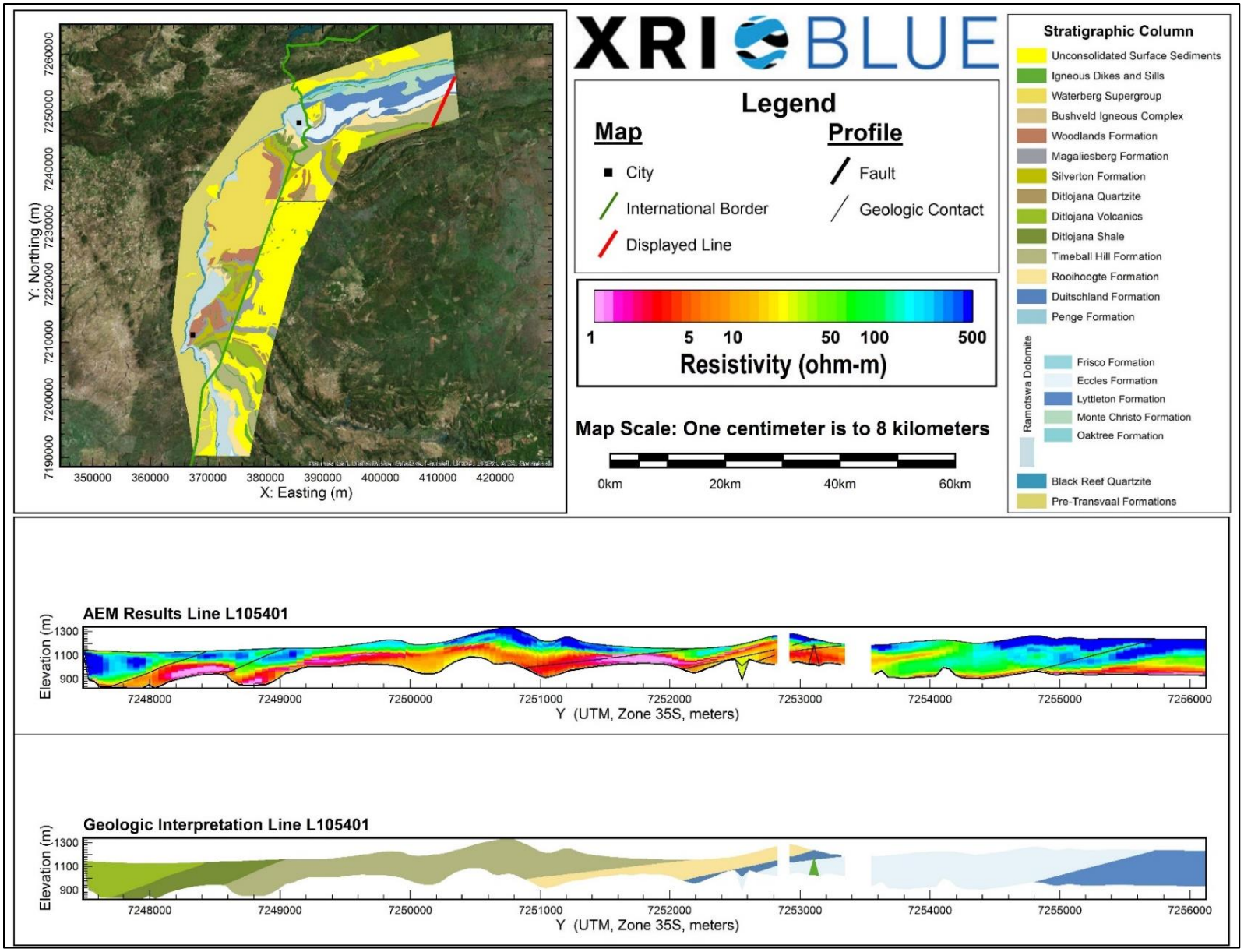

AEM and Interpreted Geology Profile for L105401.

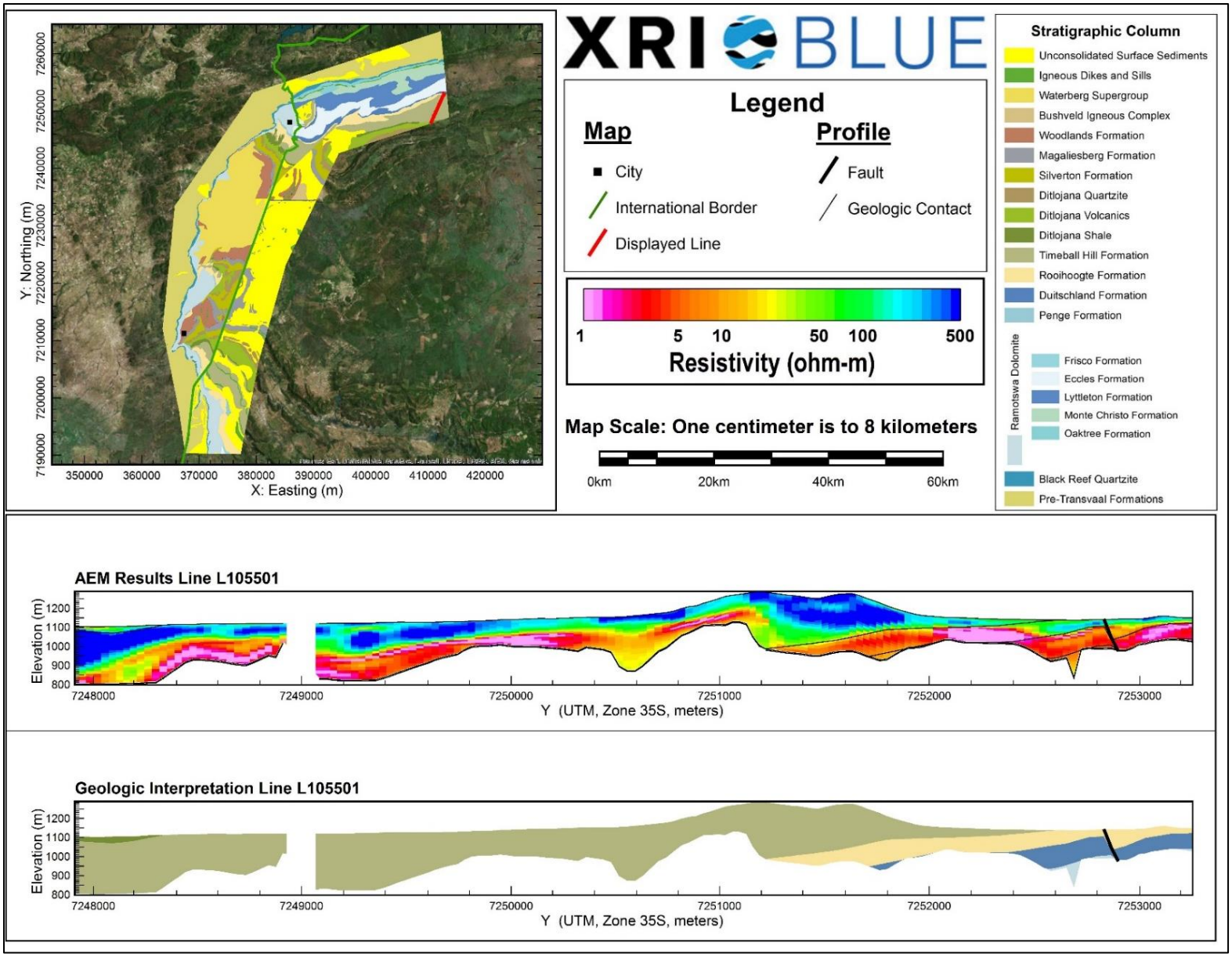

AEM and Interpreted Geology Profile for L105501.

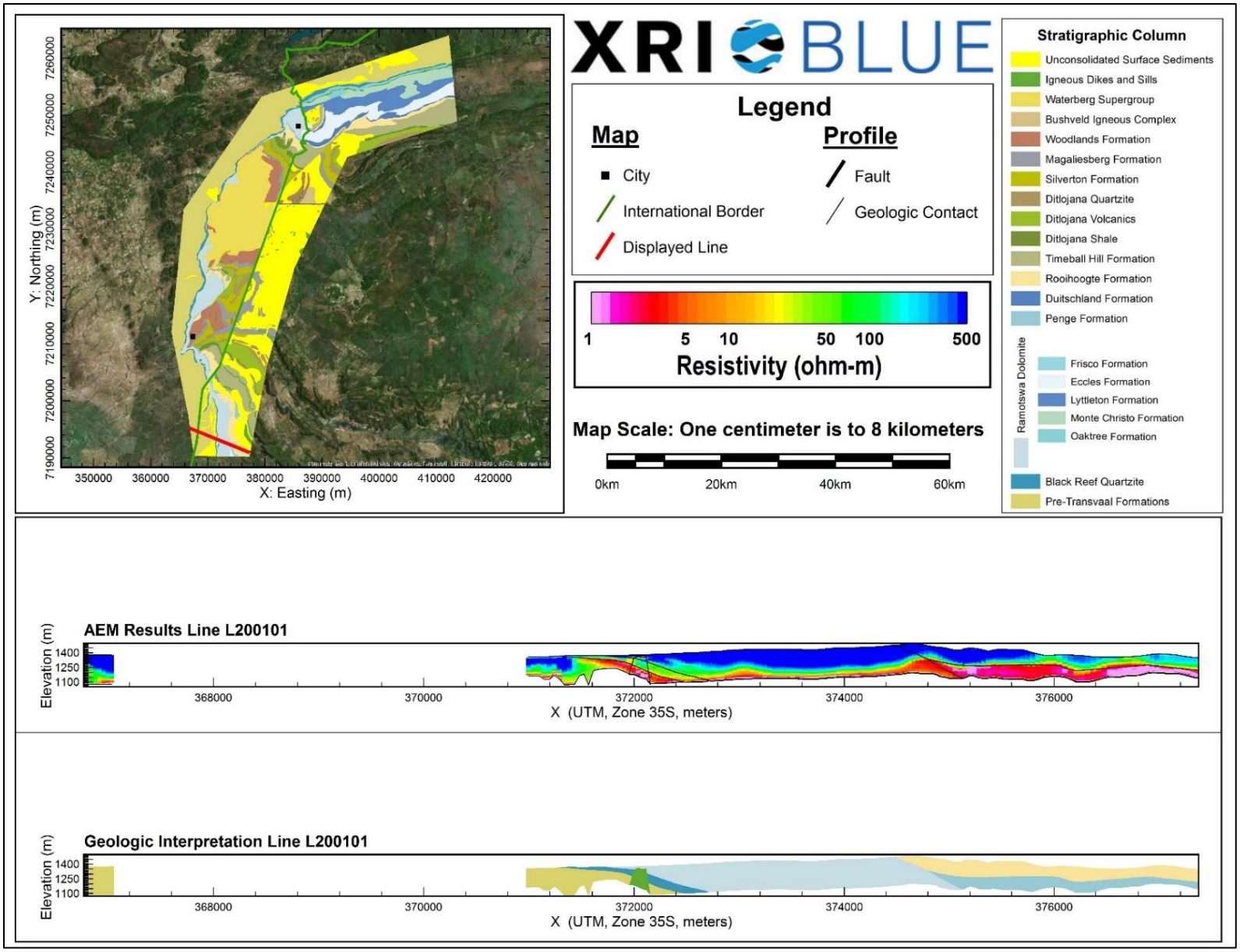

AEM and Interpreted Geology Profile for L200101.

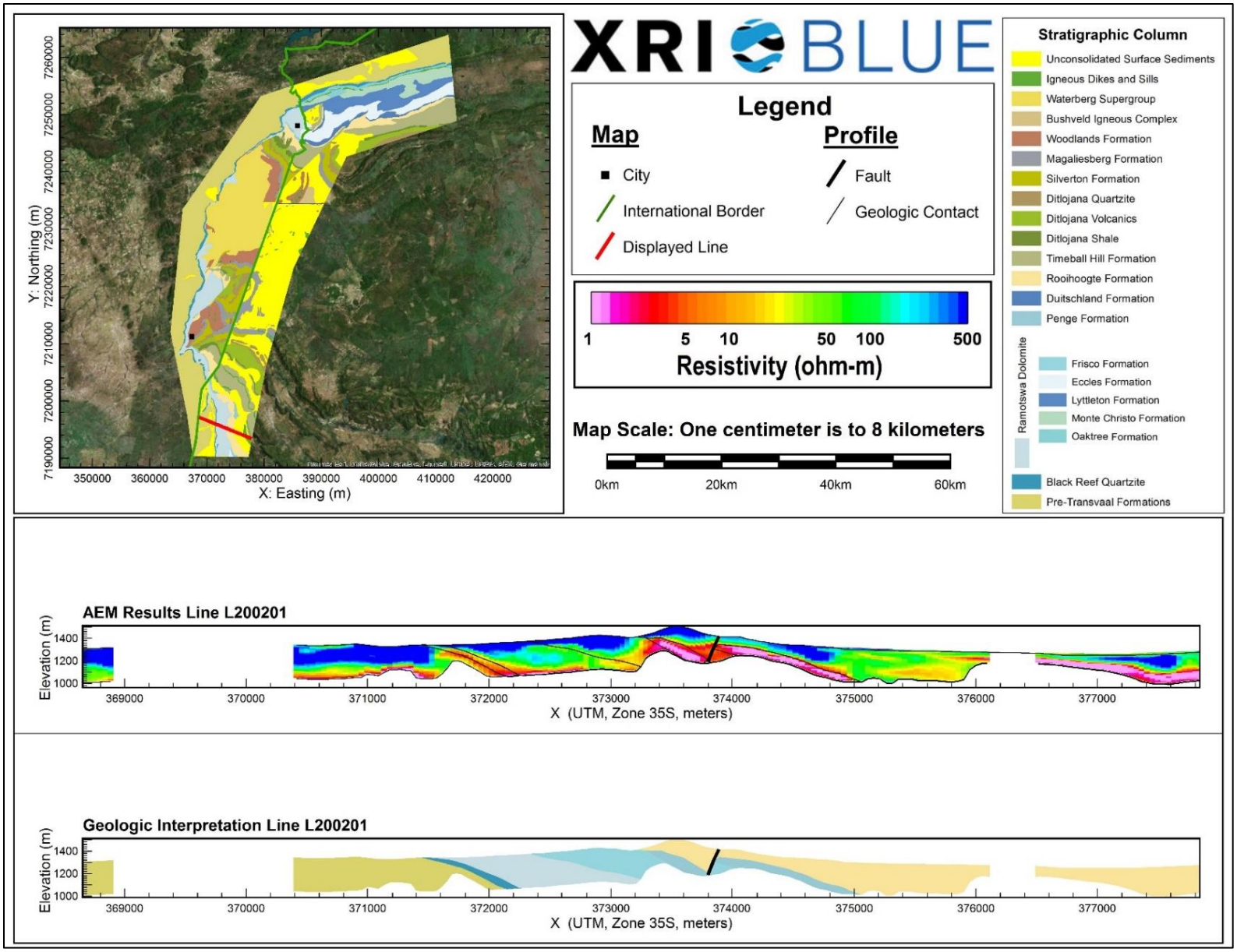

AEM and Interpreted Geology Profile for L200201.

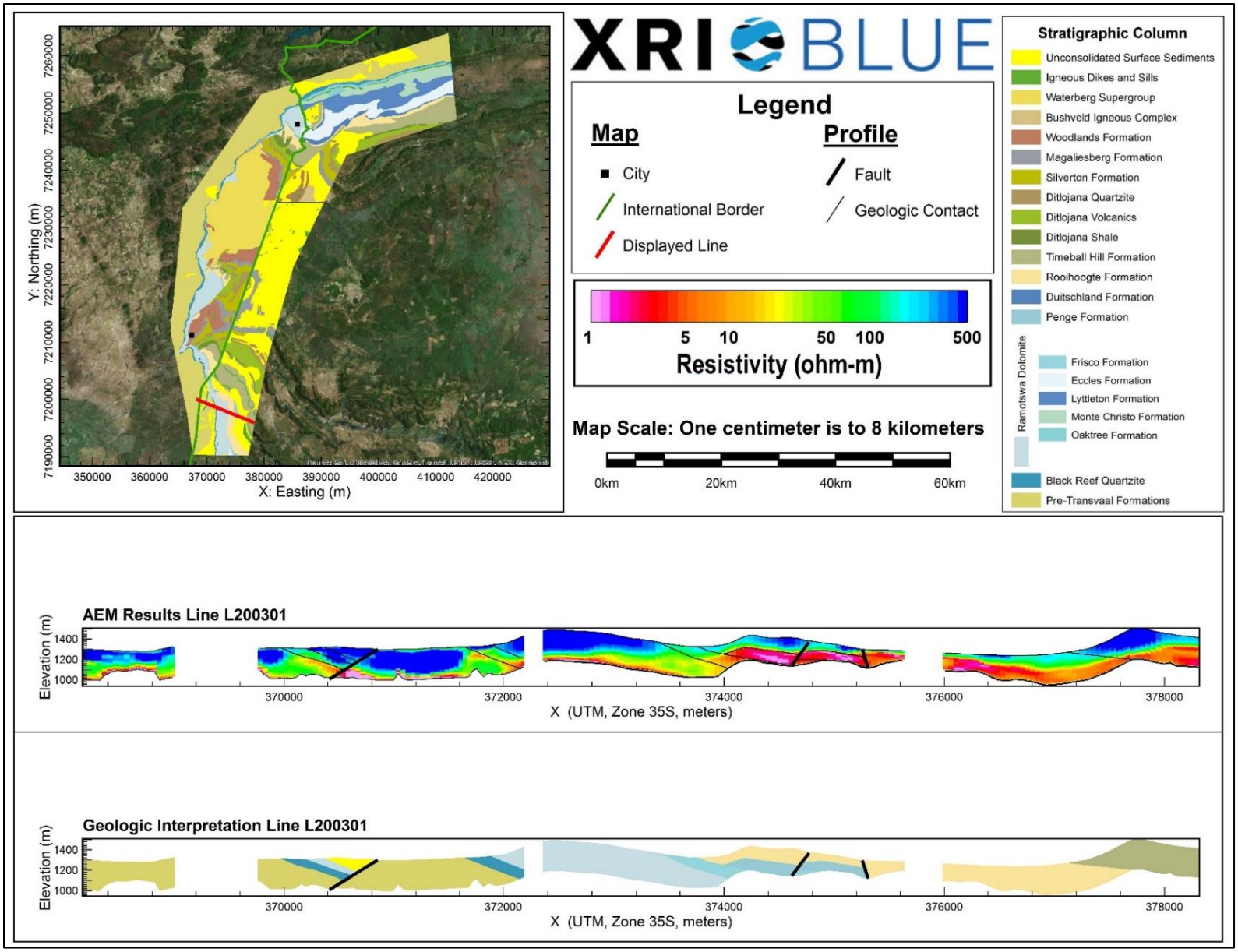

AEM and Interpreted Geology Profile for L200301.

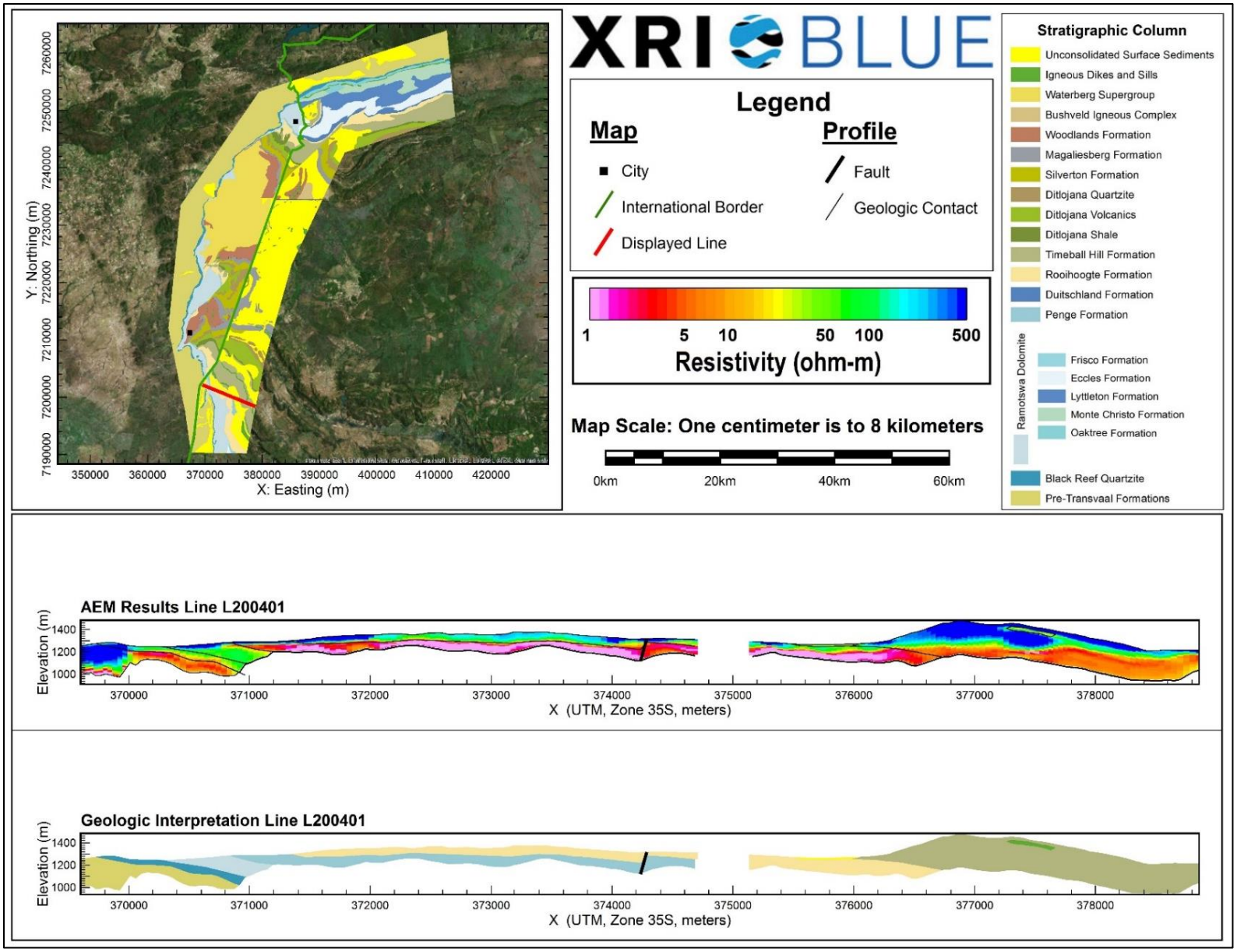

AEM and Interpreted Geology Profile for L200401.

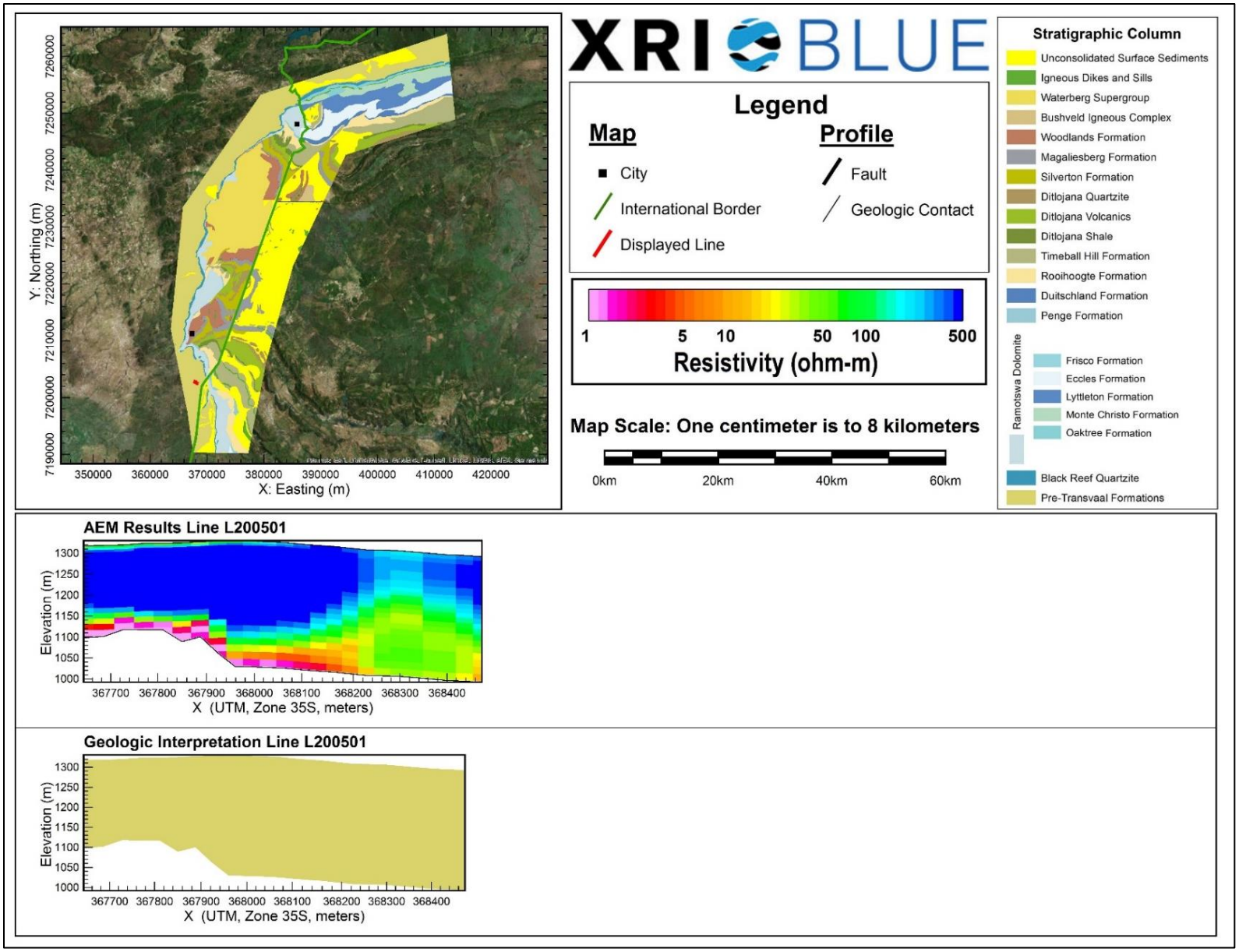

AEM and Interpreted Geology Profile for L200501.

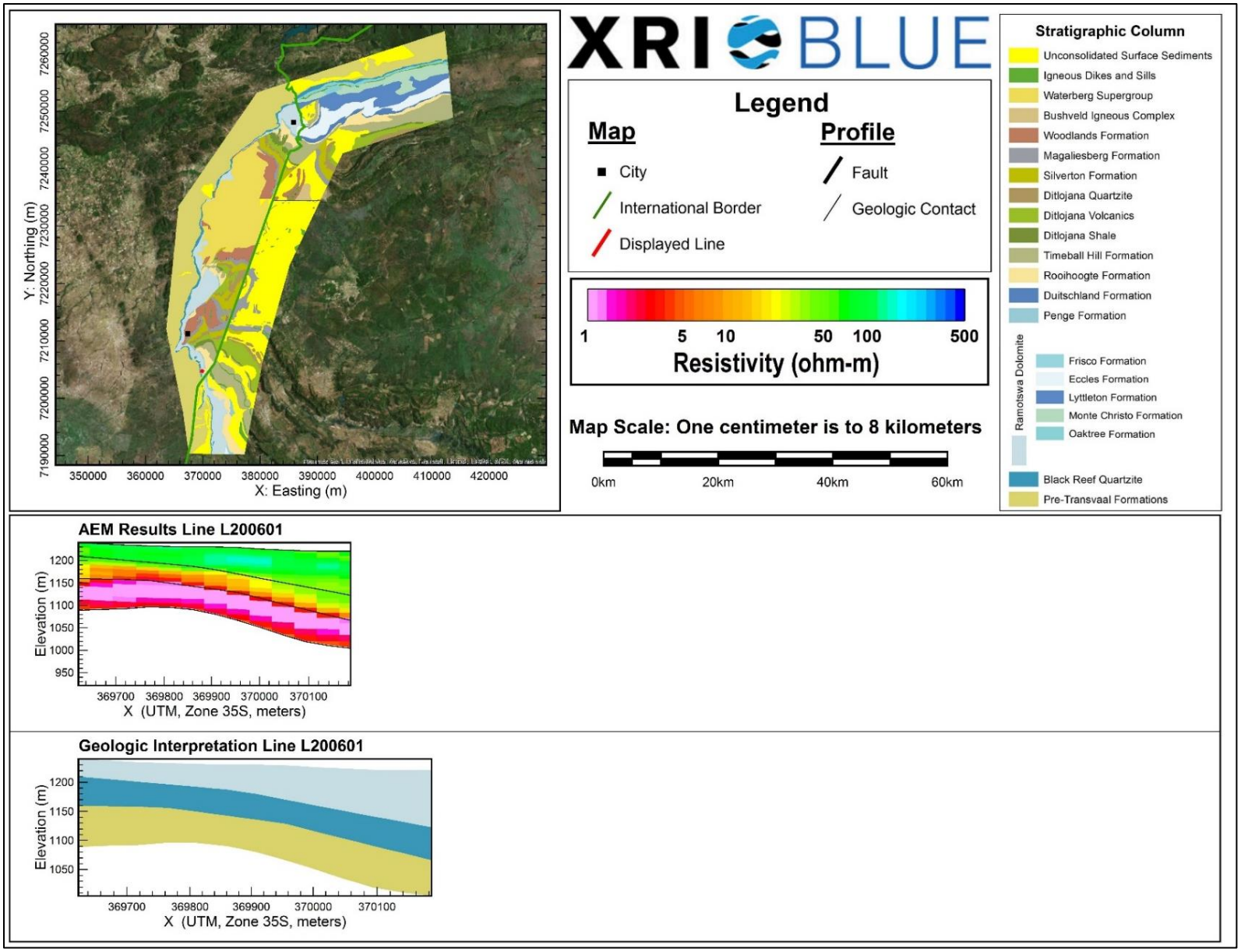

AEM and Interpreted Geology Profile for L200601.

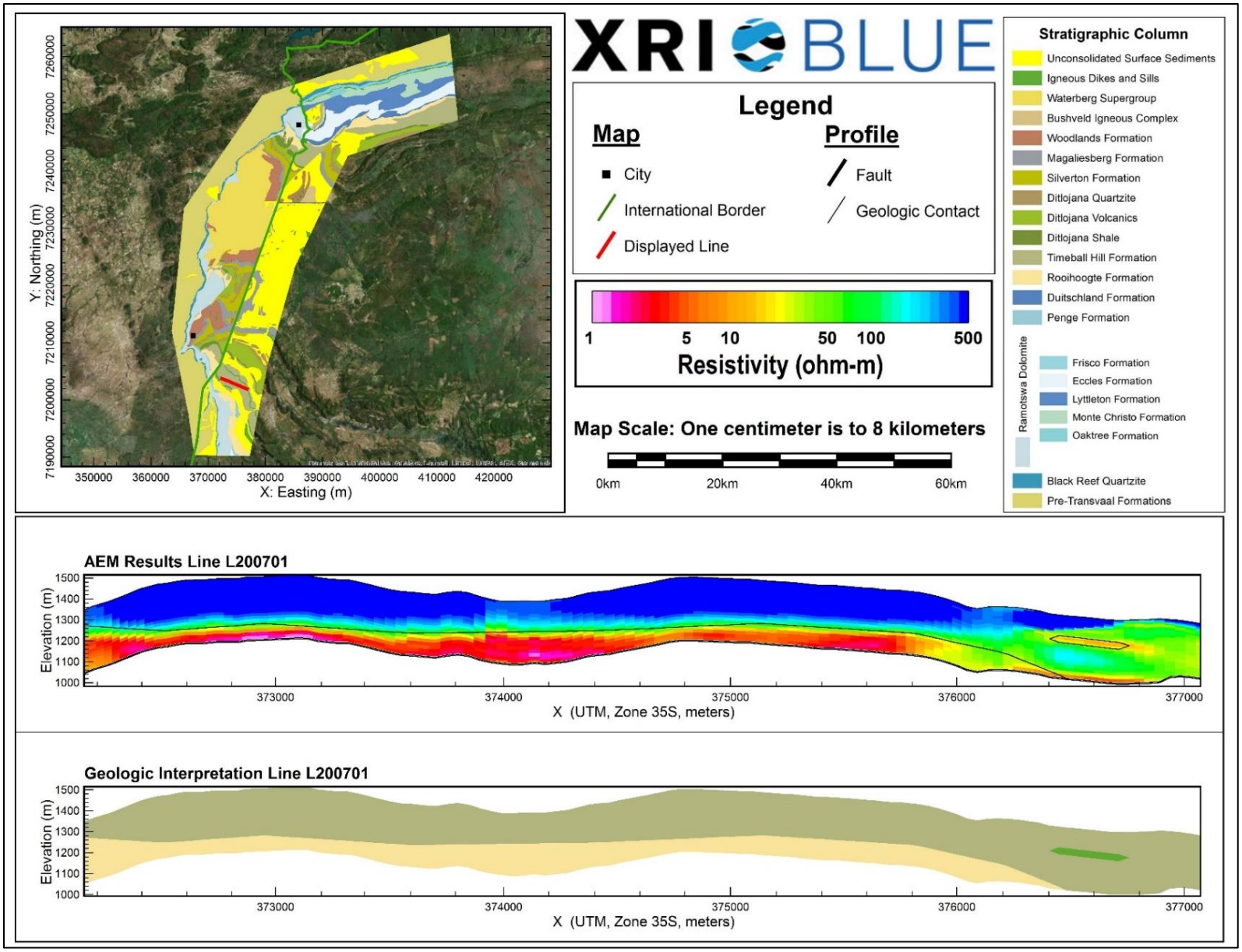

AEM and Interpreted Geology Profile for L200701.

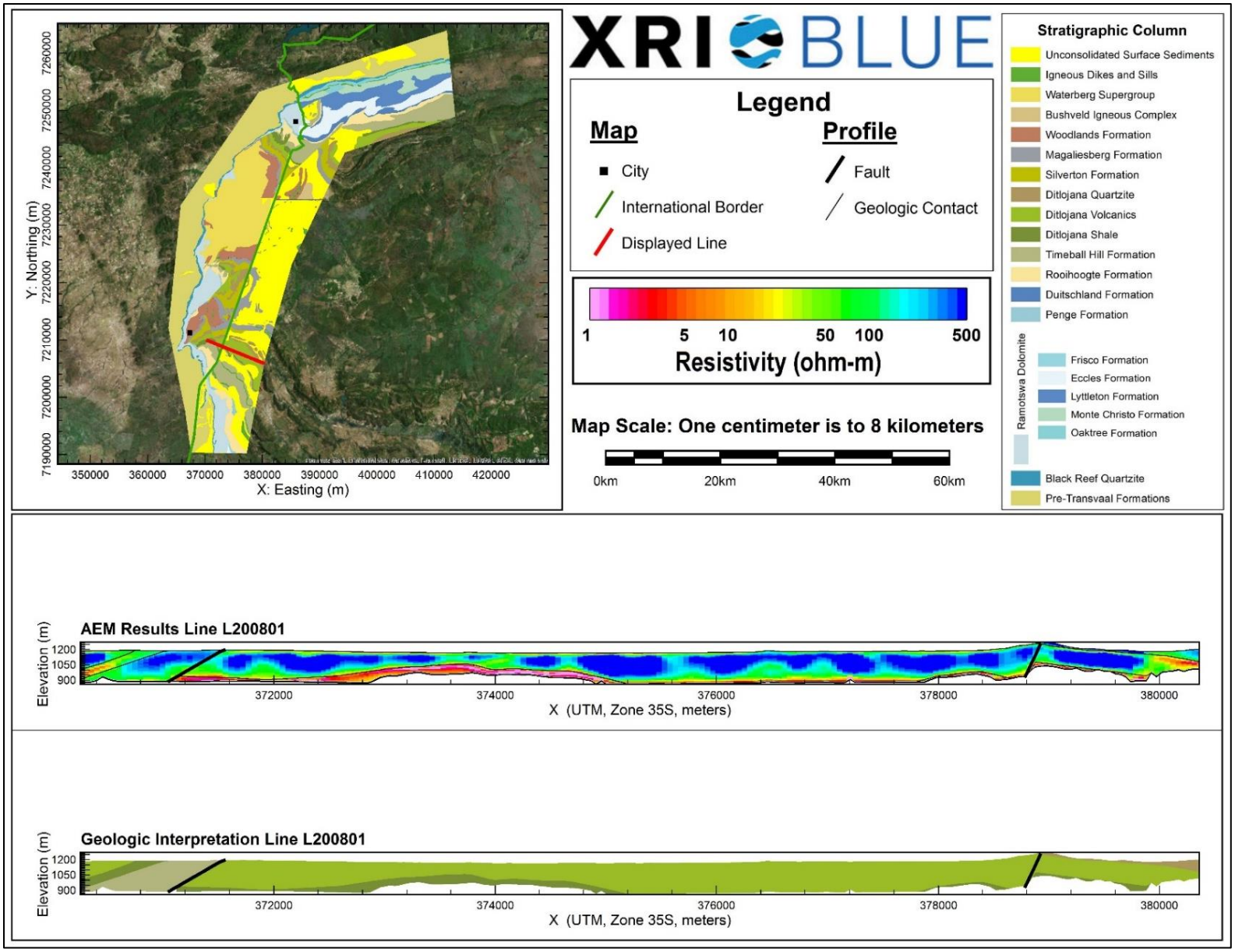

AEM and Interpreted Geology Profile for L200801.

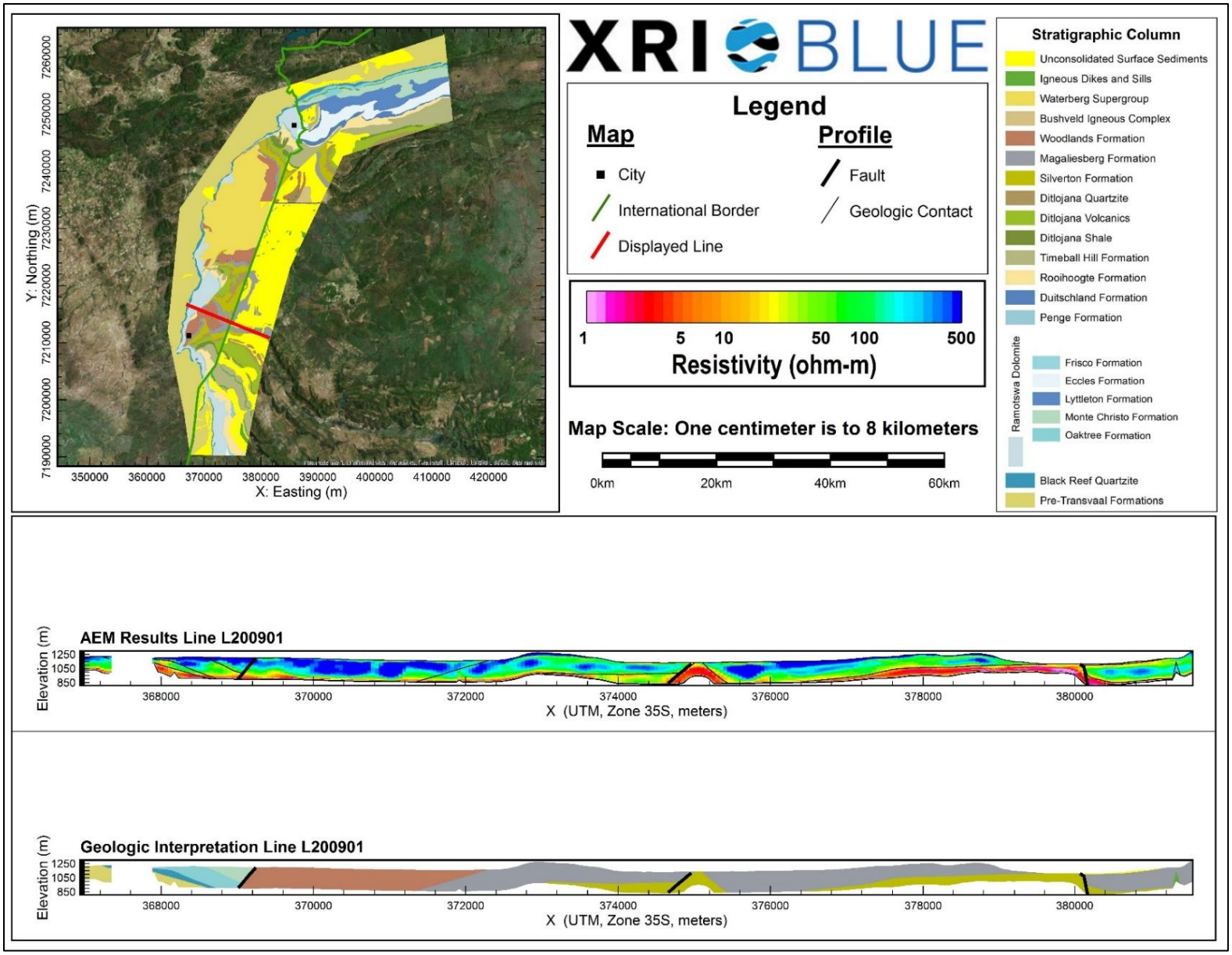

AEM and Interpreted Geology Profile for L200901.

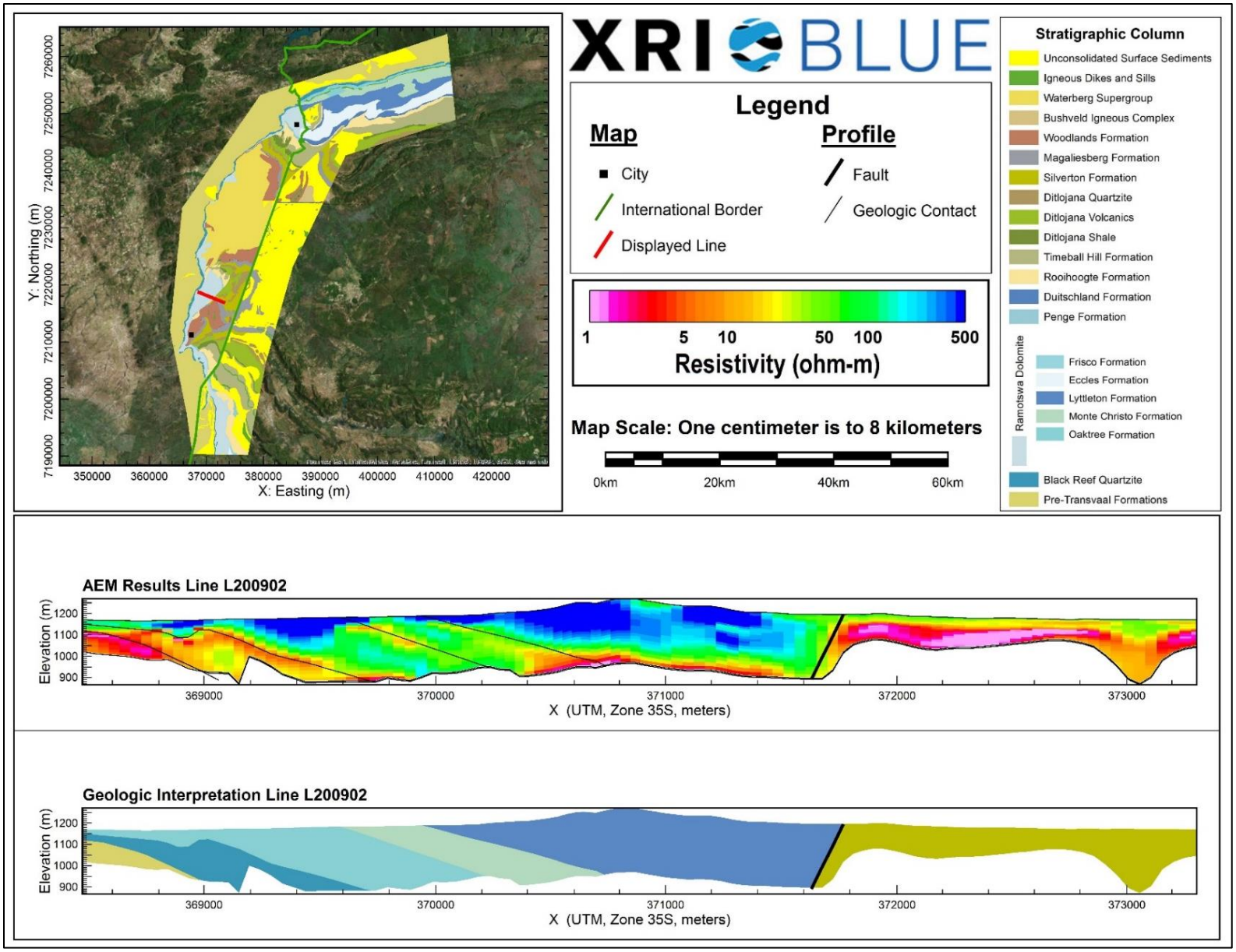

AEM and Interpreted Geology Profile for L200902.

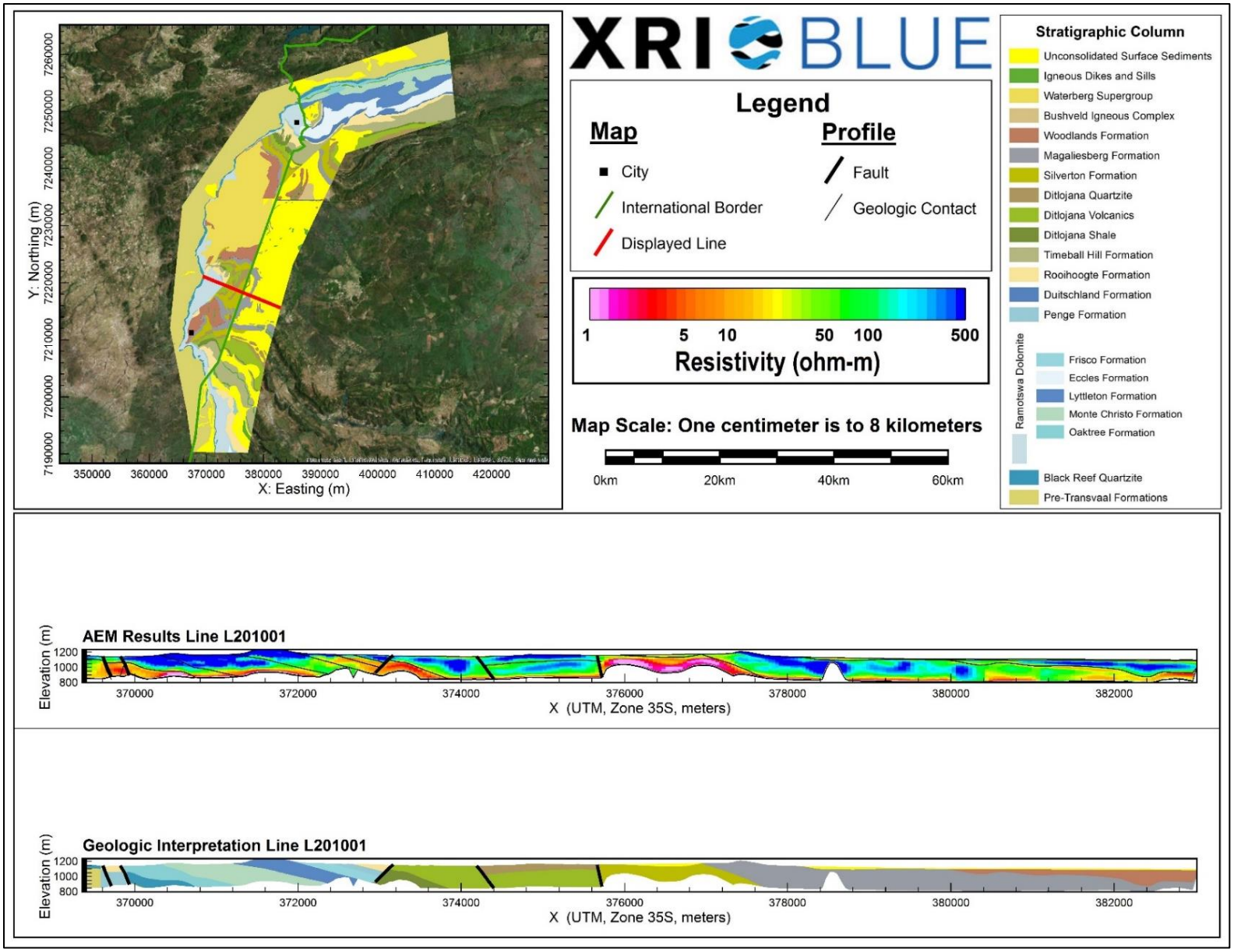

AEM and Interpreted Geology Profile for L201001.

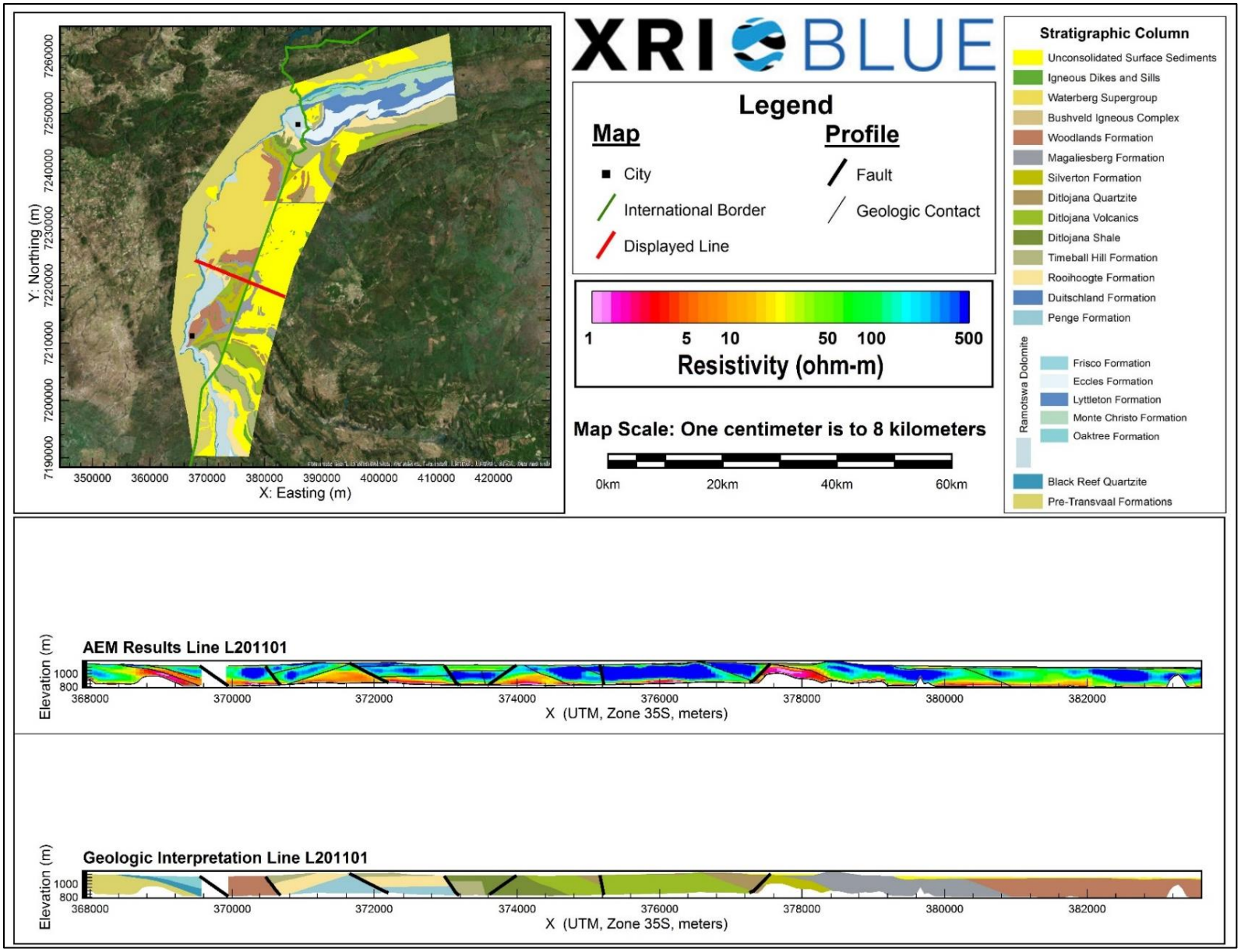

AEM and Interpreted Geology Profile for L201101.

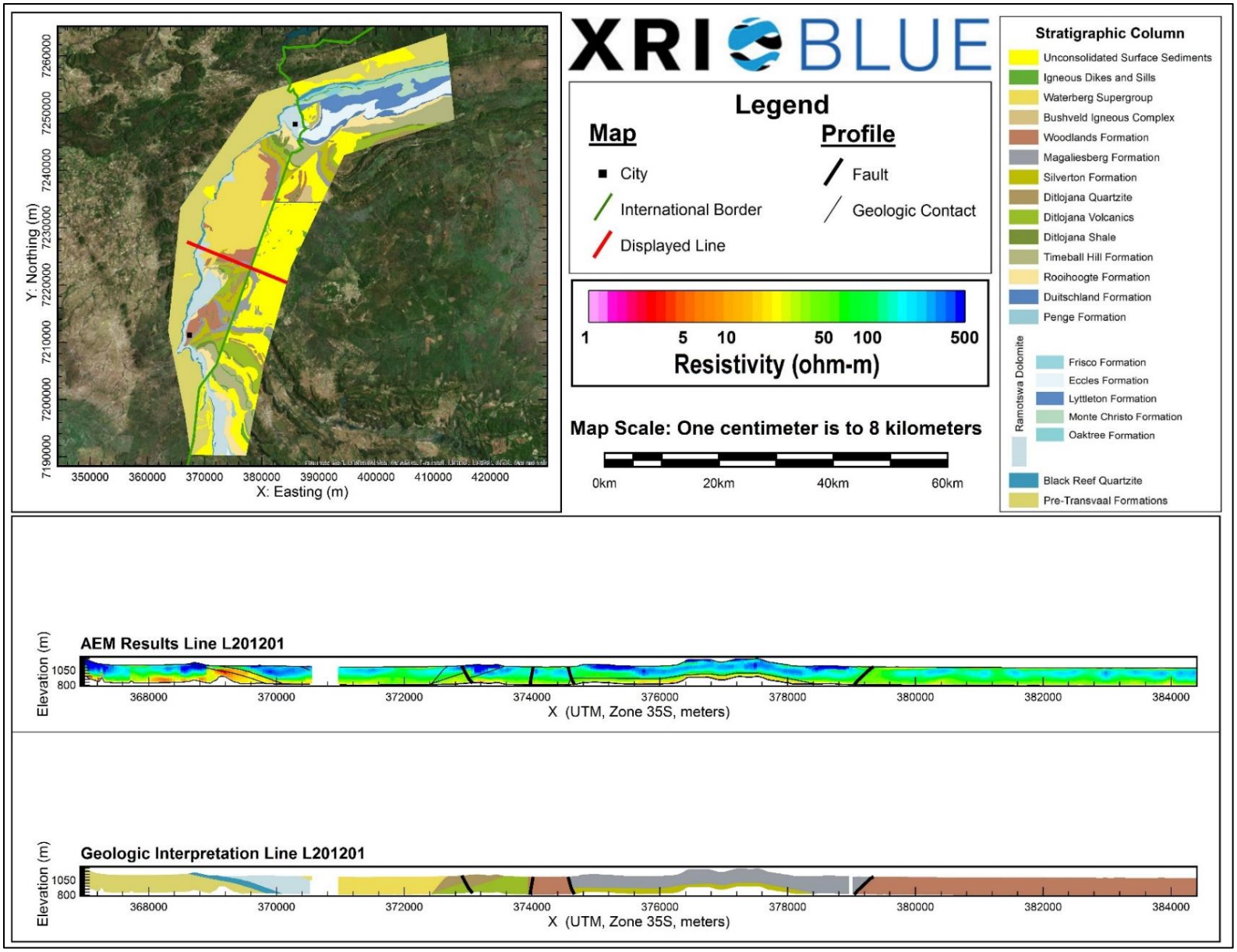

AEM and Interpreted Geology Profile for L201201.

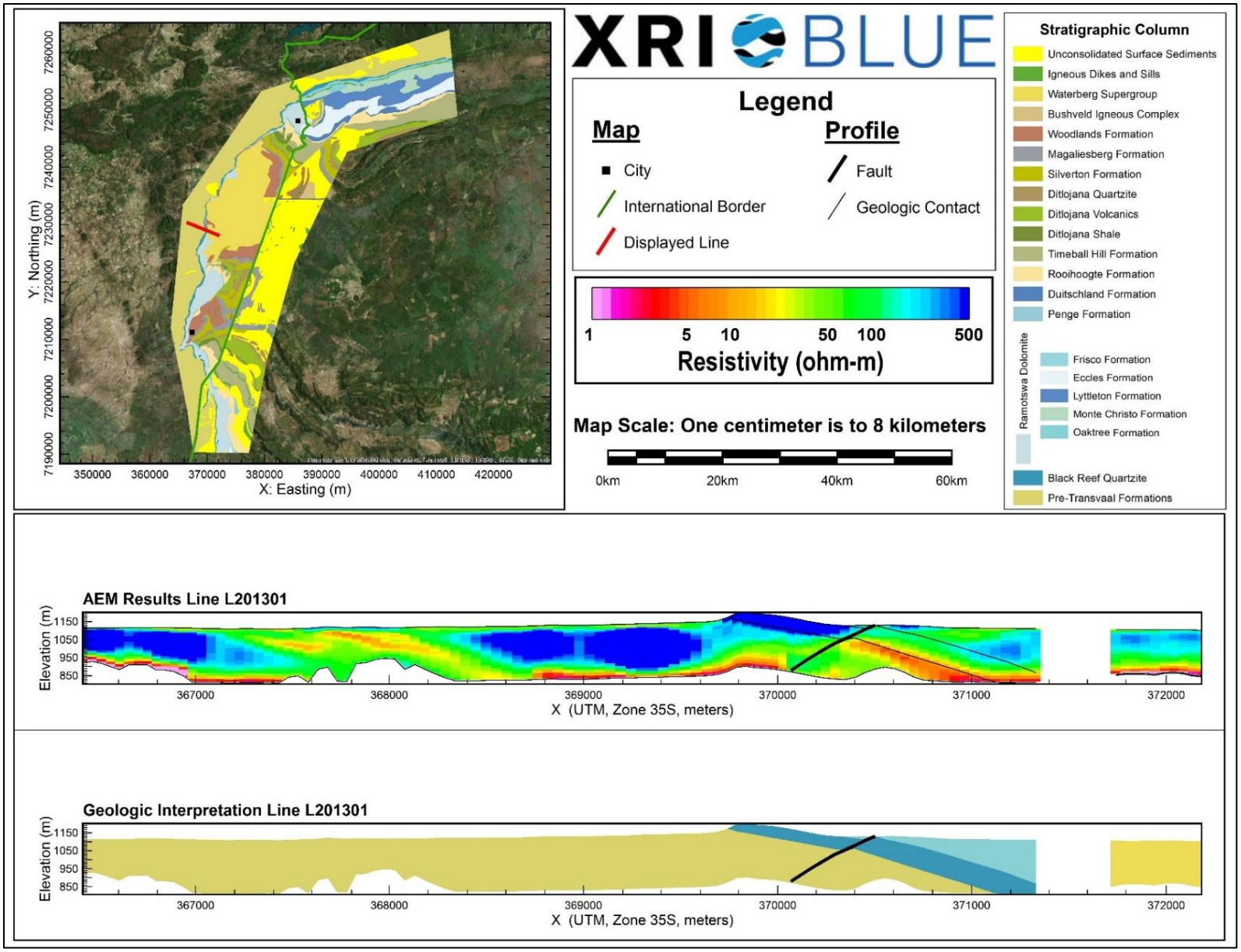

AEM and Interpreted Geology Profile for L201301.

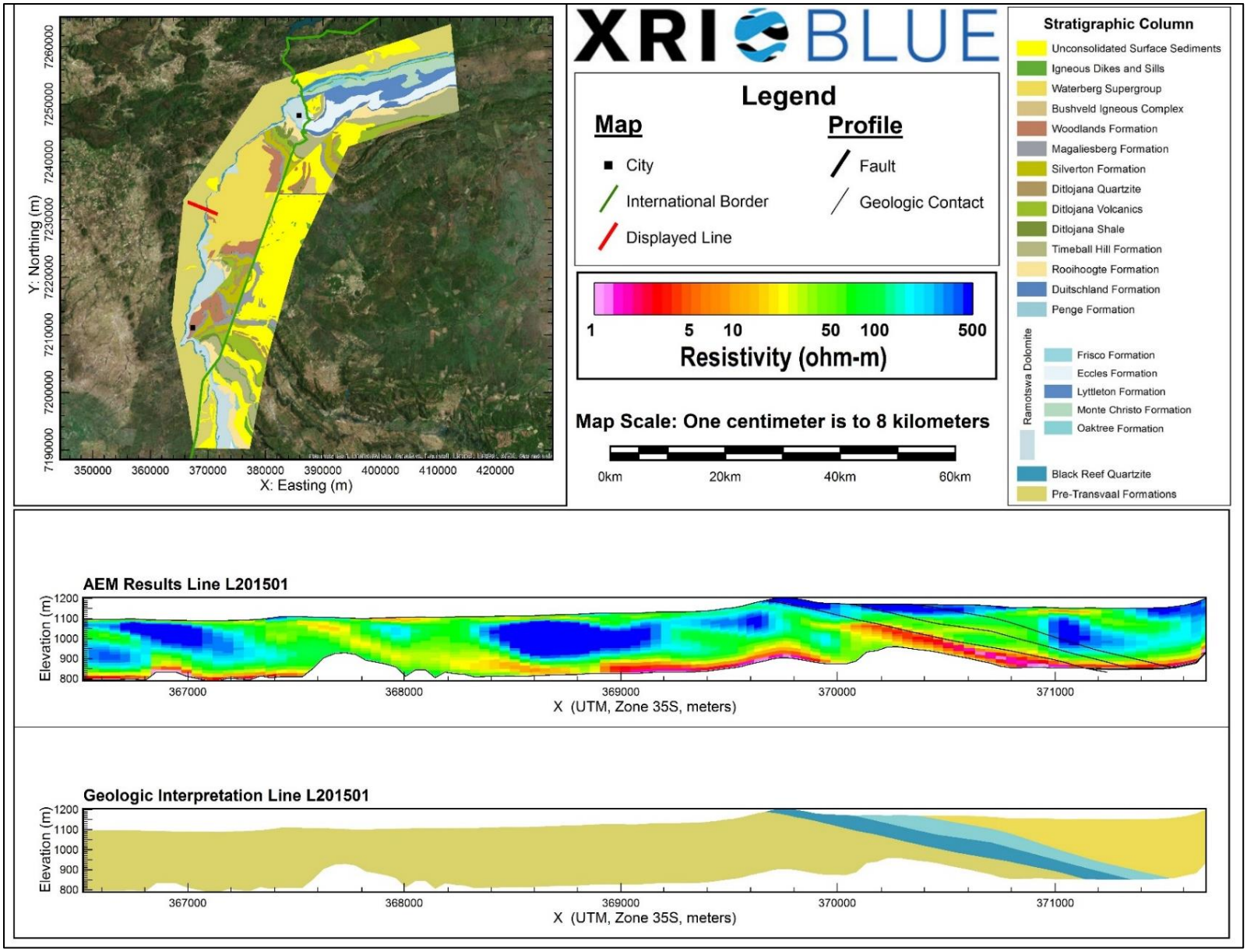

AEM and Interpreted Geology Profile for L201501.

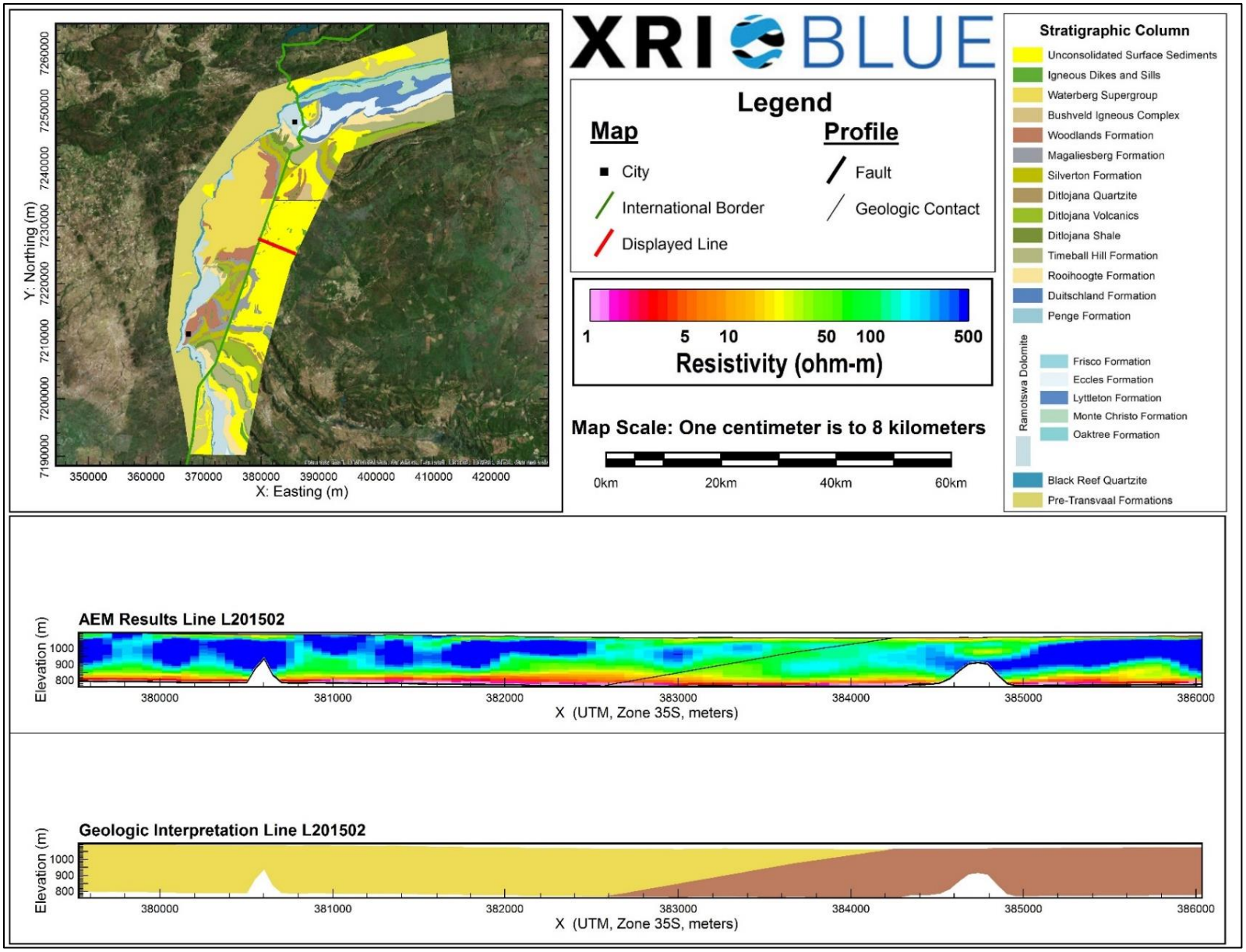

AEM and Interpreted Geology Profile for L201502.

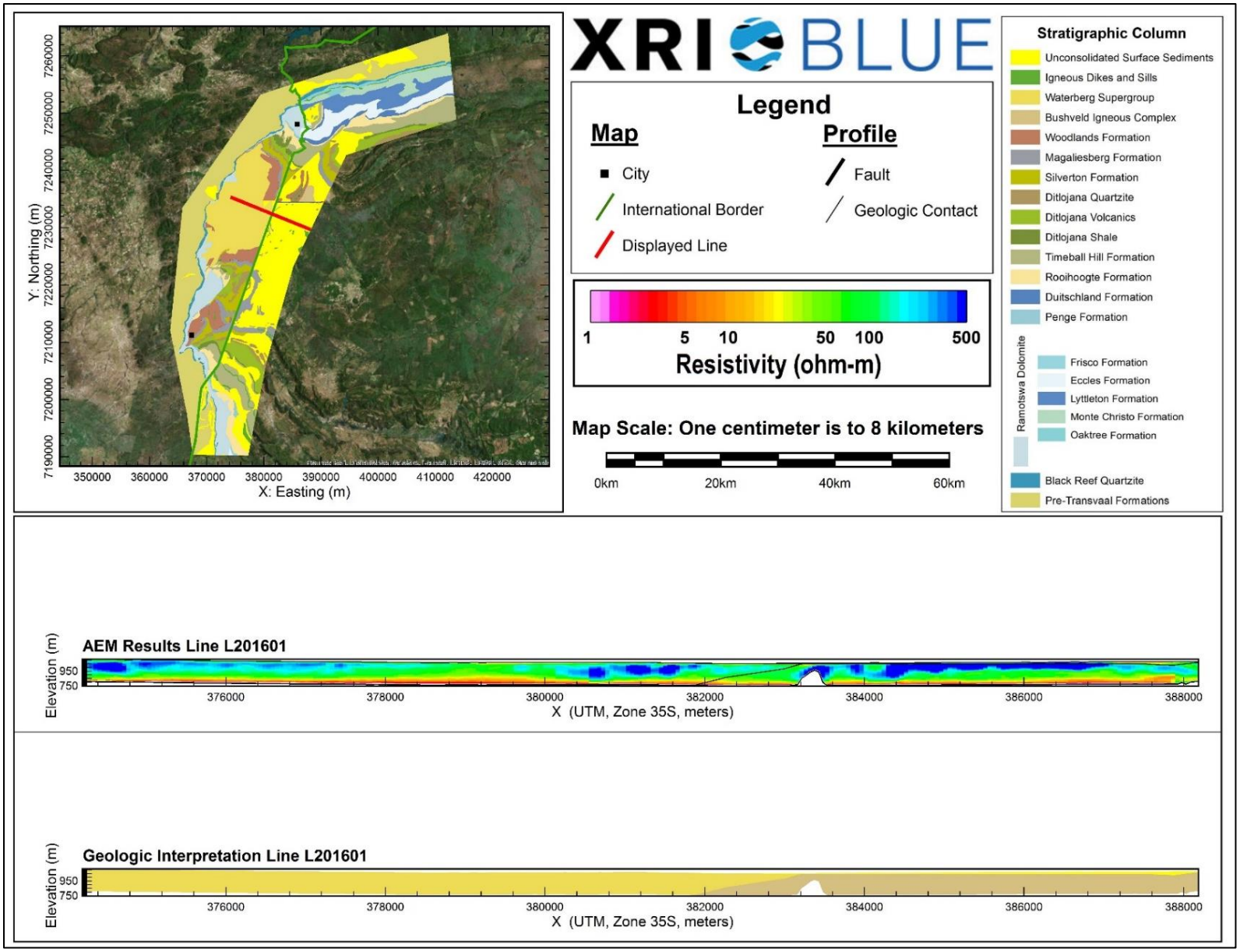

AEM and Interpreted Geology Profile for L201601.

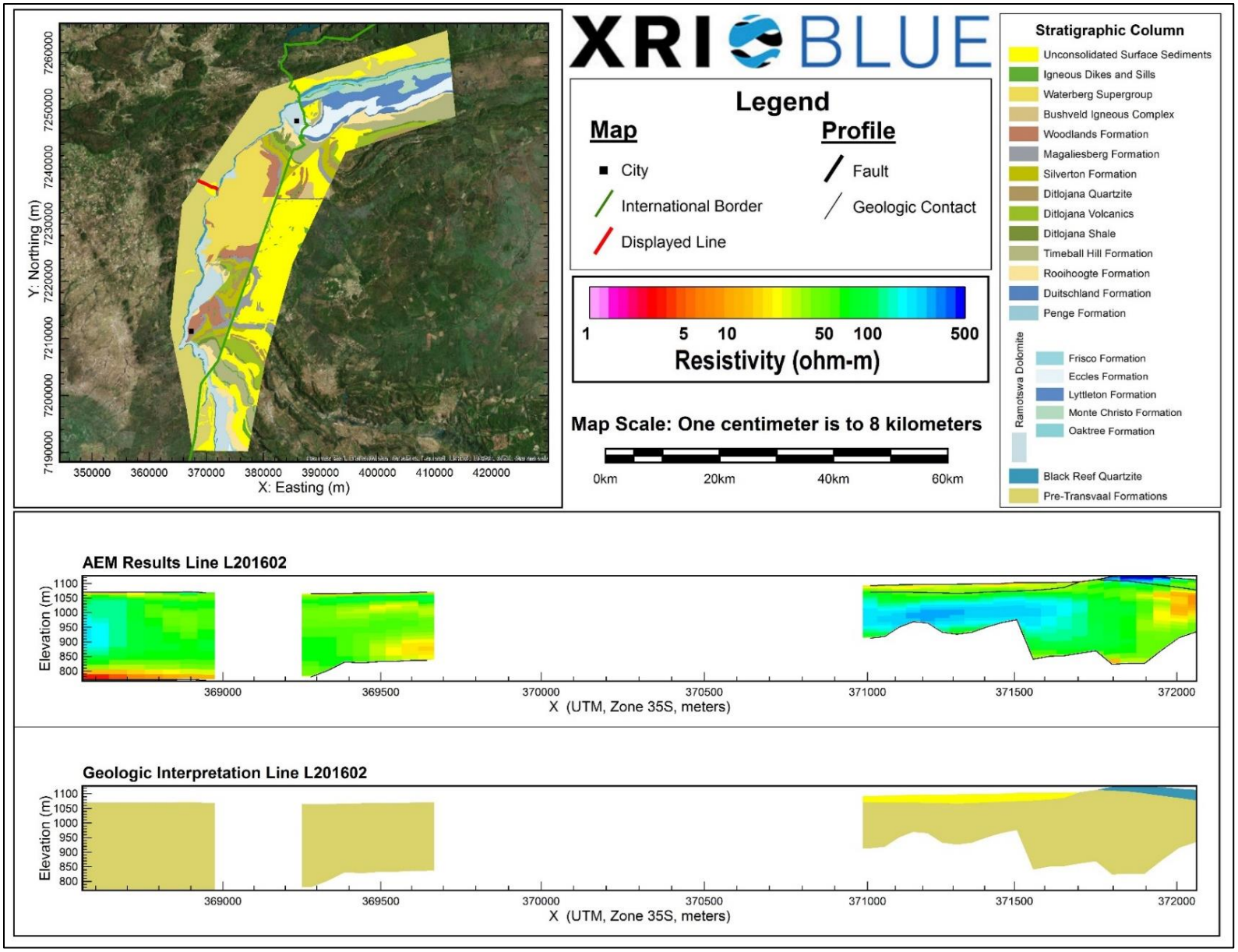

AEM and Interpreted Geology Profile for L201602.

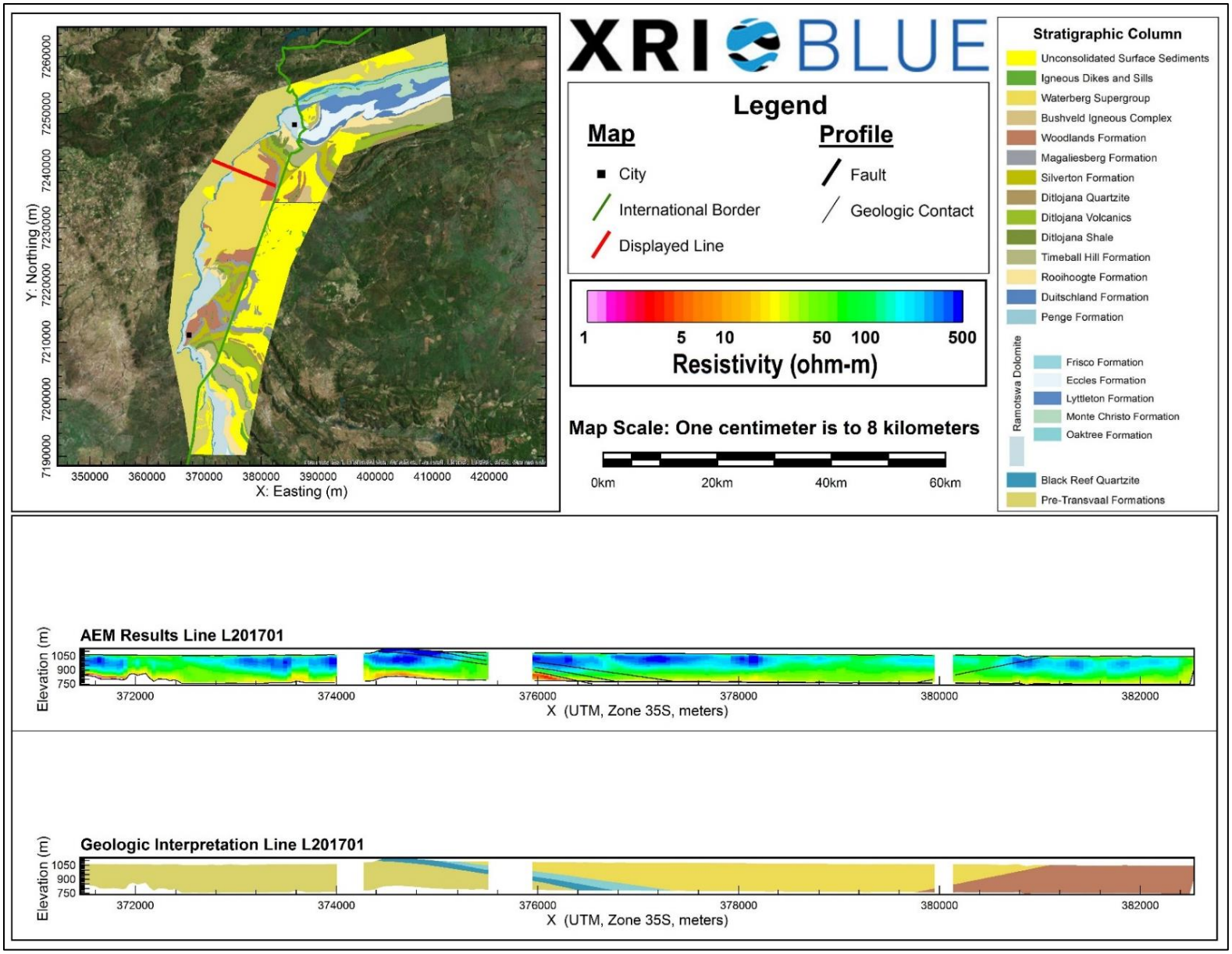

AEM and Interpreted Geology Profile for L201701.

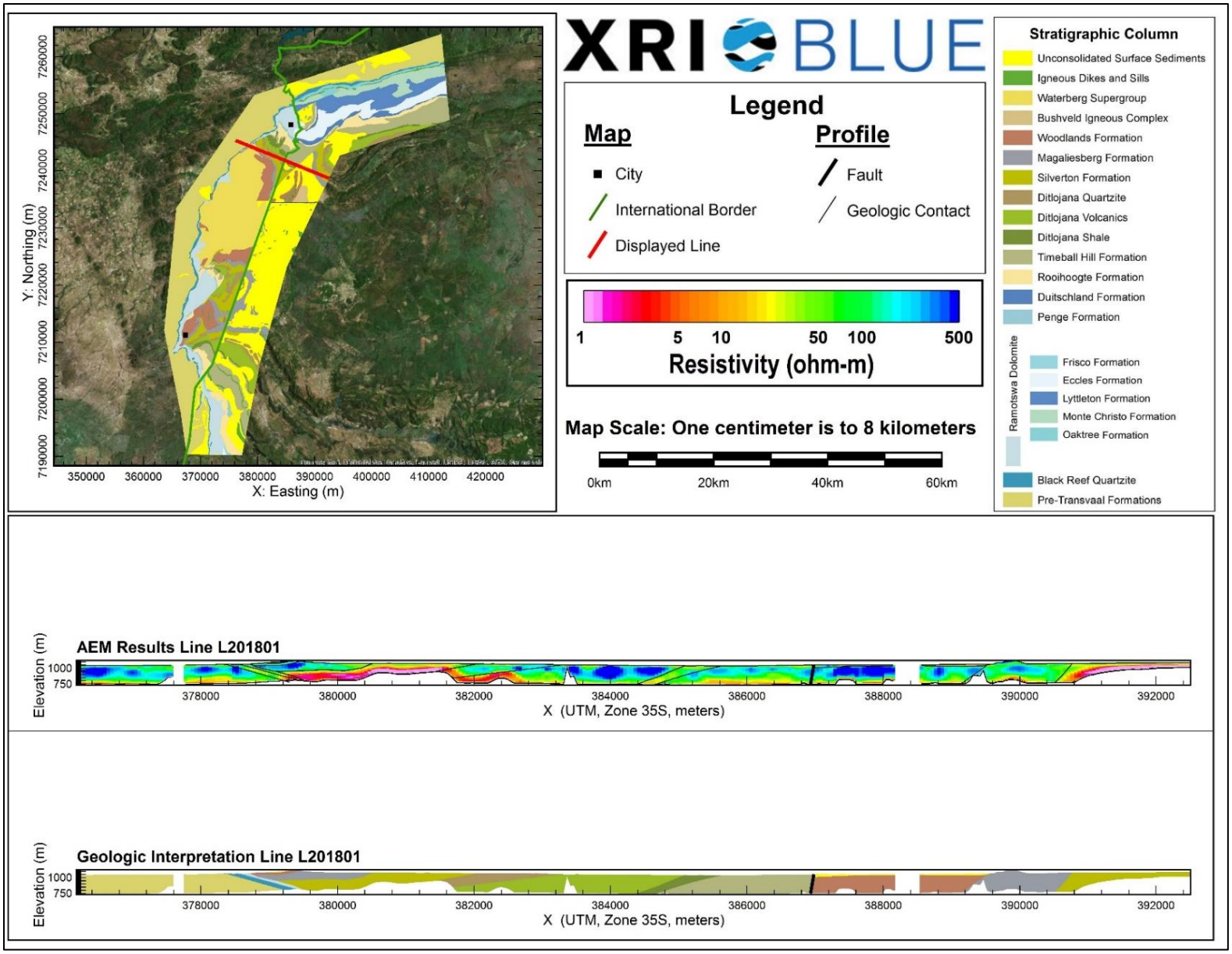

AEM and Interpreted Geology Profile for L201801.

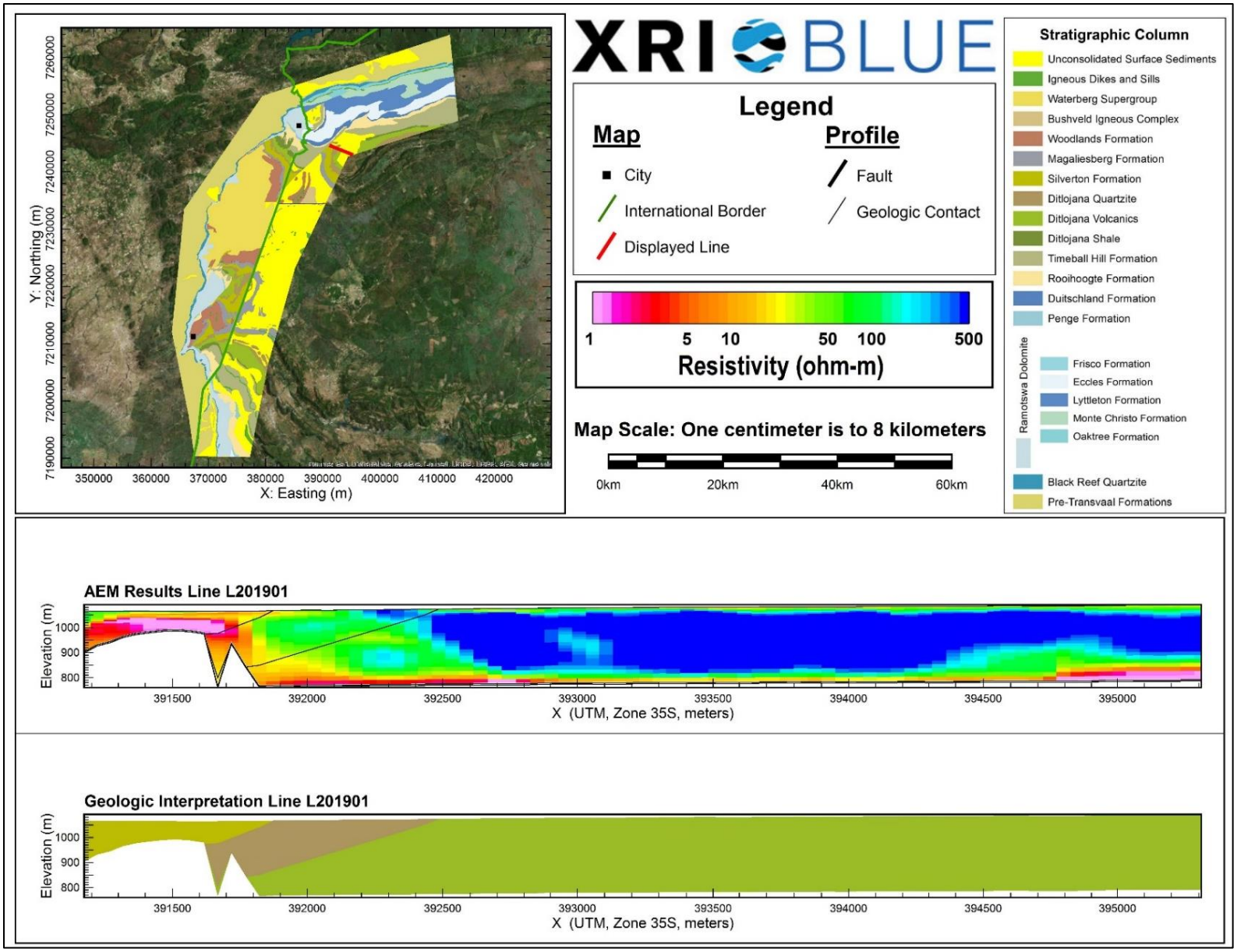

AEM and Interpreted Geology Profile for L201901.

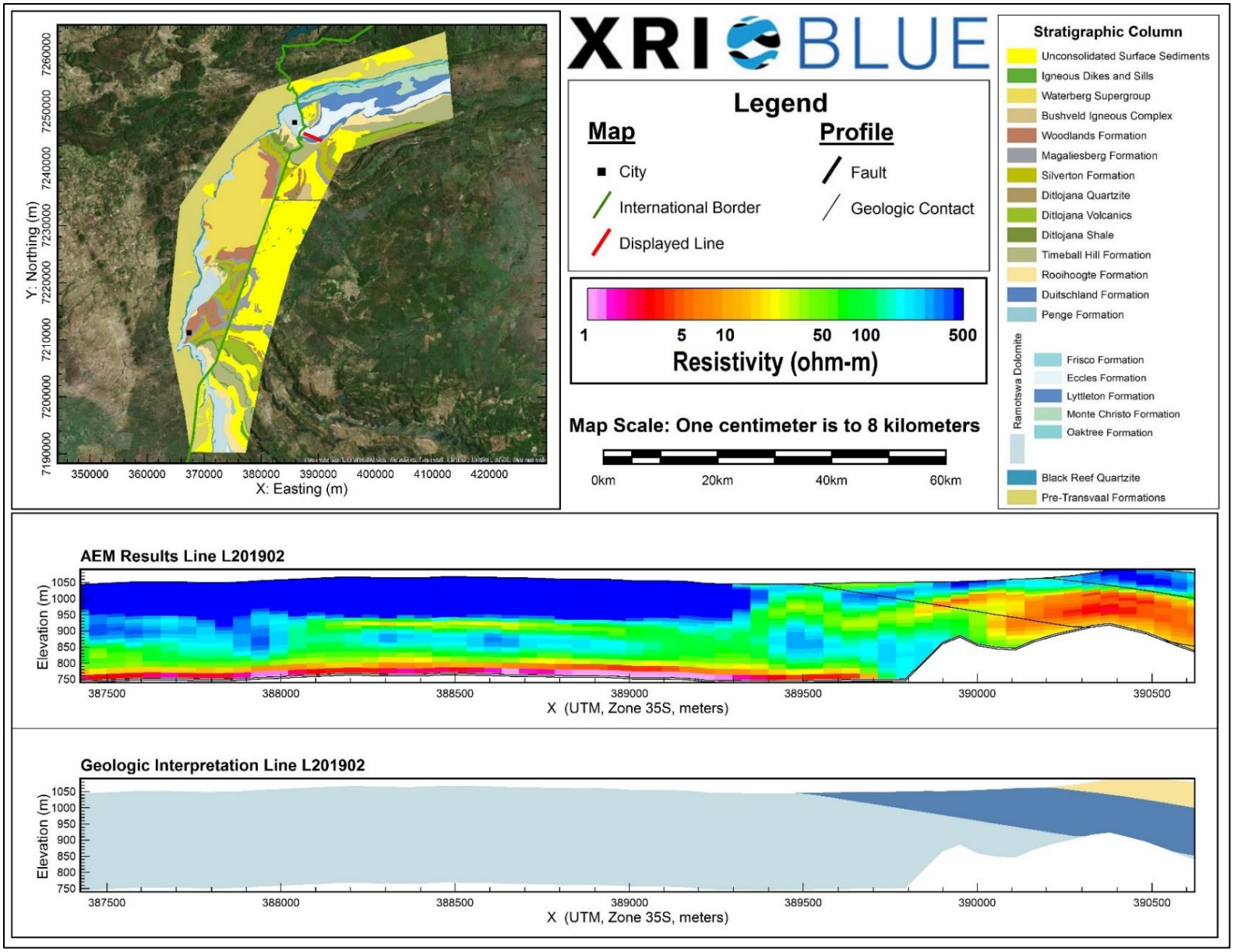

AEM and Interpreted Geology Profile for L201902.

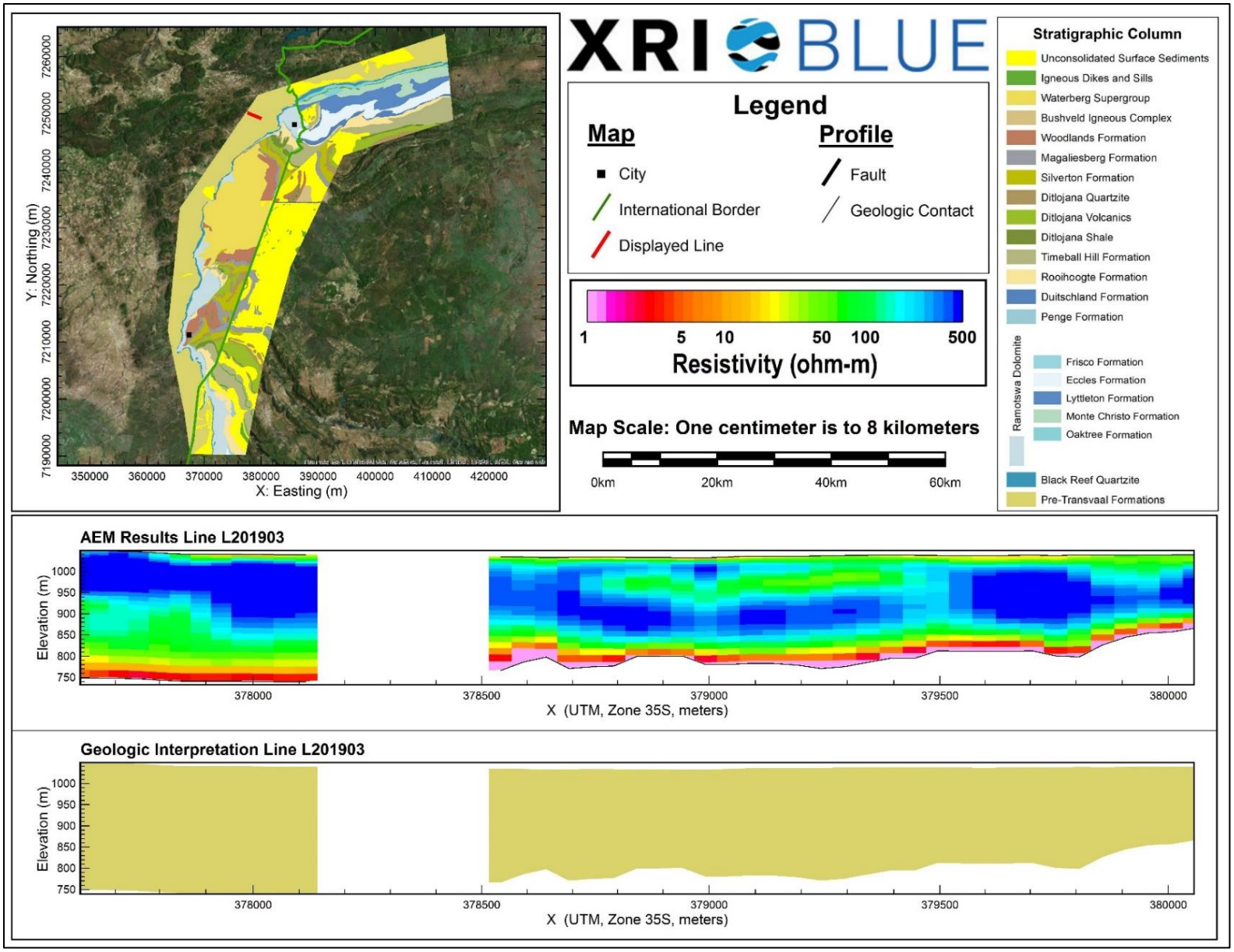

AEM and Interpreted Geology Profile for L201903.

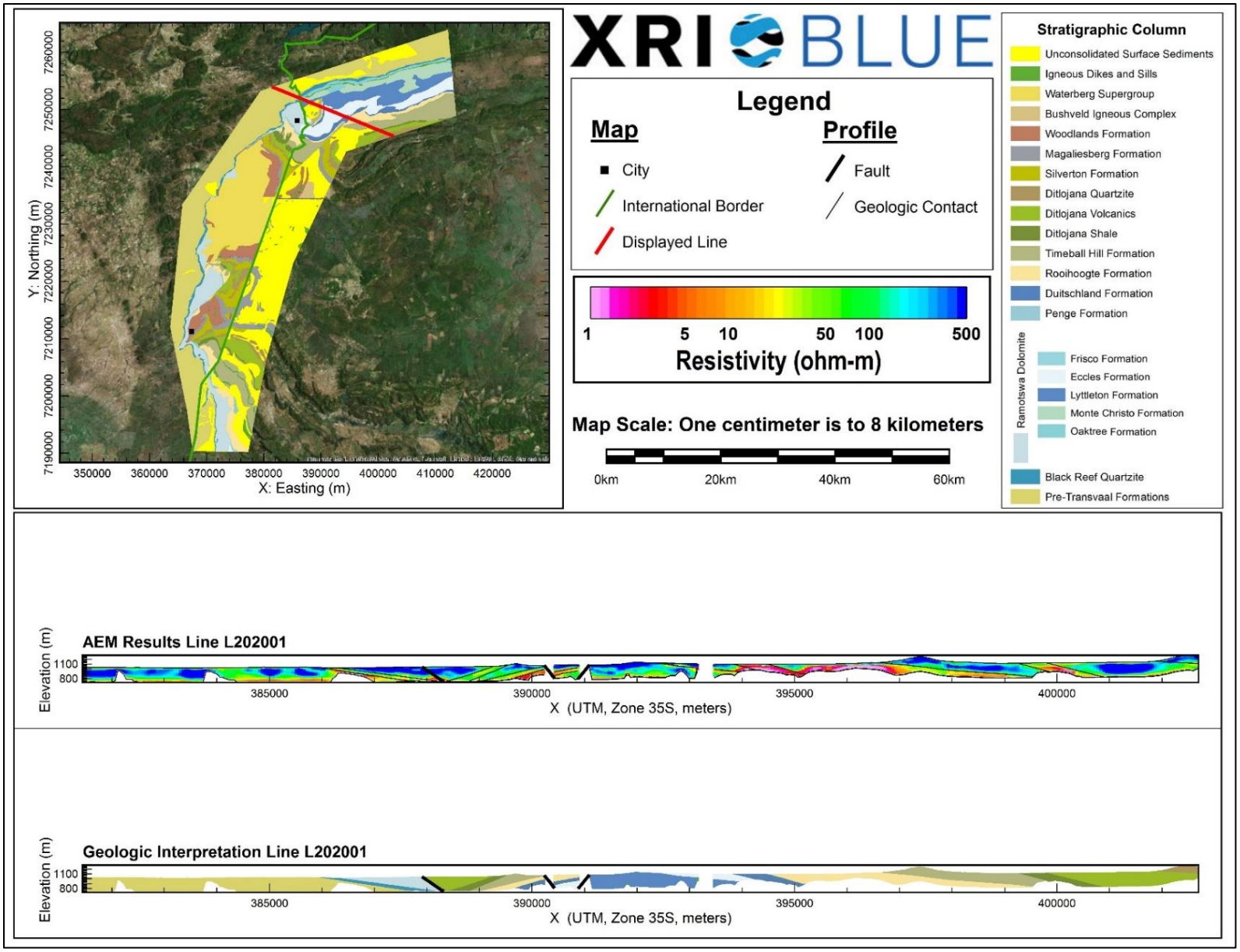

AEM and Interpreted Geology Profile for L202001.

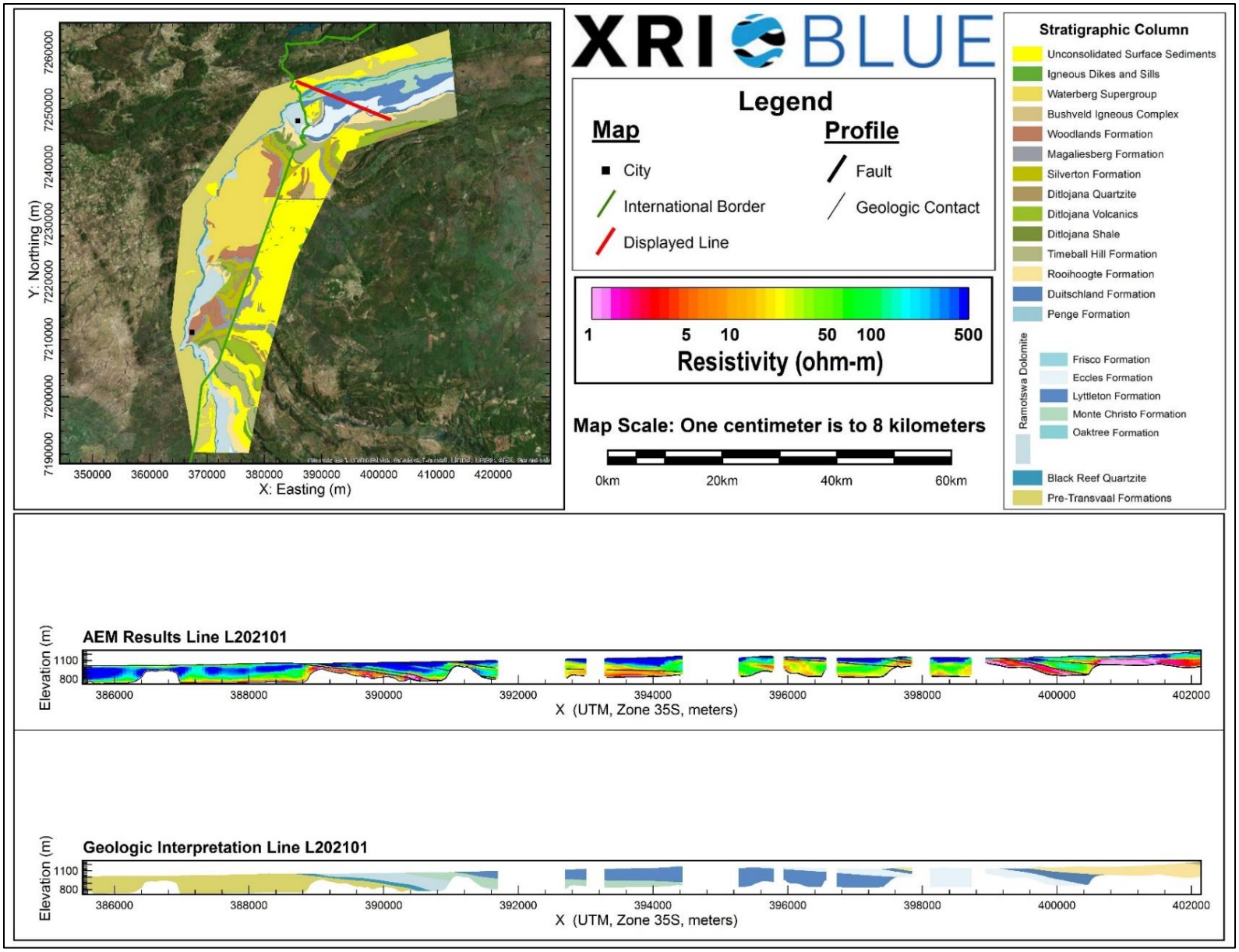

AEM and Interpreted Geology Profile for L202101.

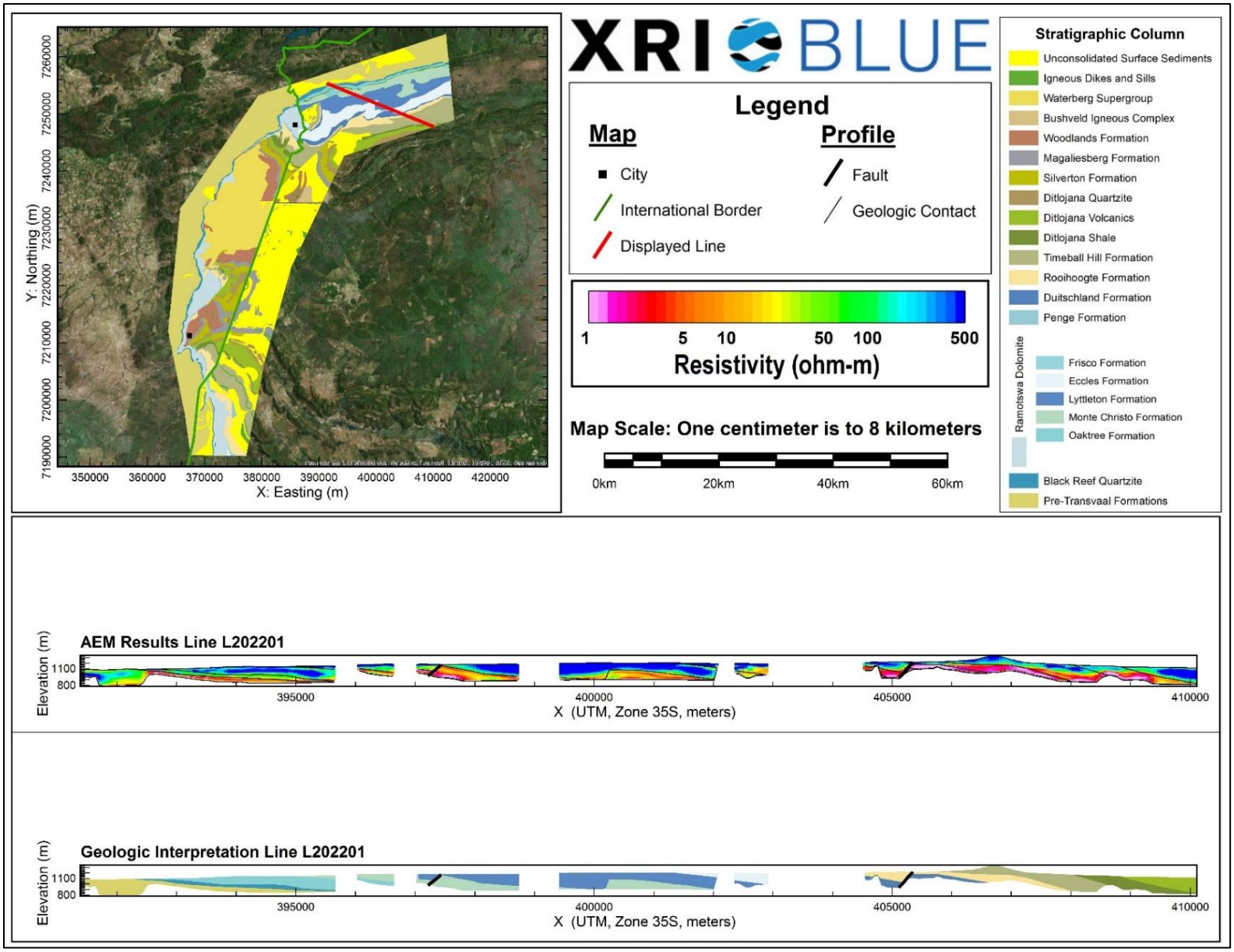

AEM and Interpreted Geology Profile for L202201.

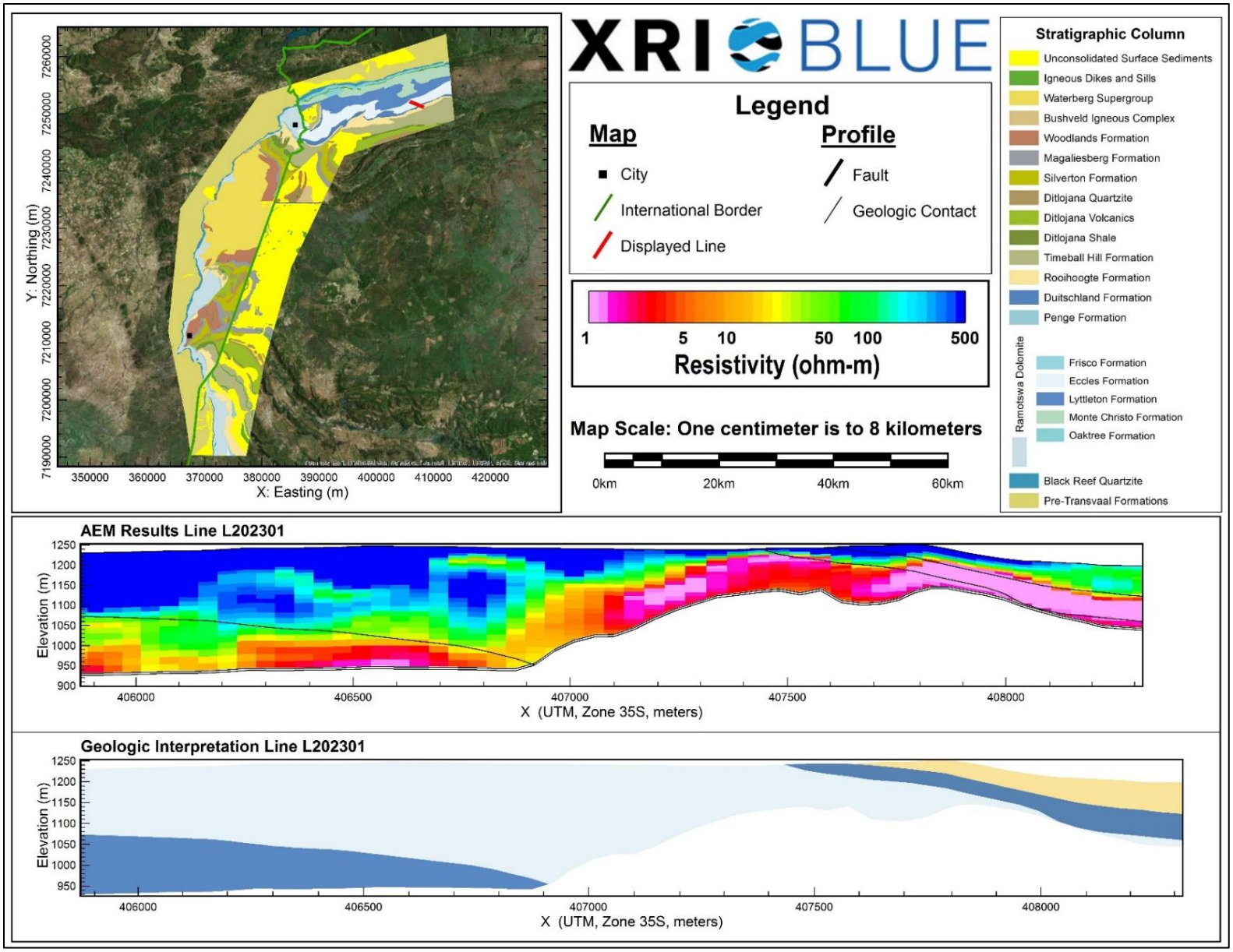

AEM and Interpreted Geology Profile for L202301.

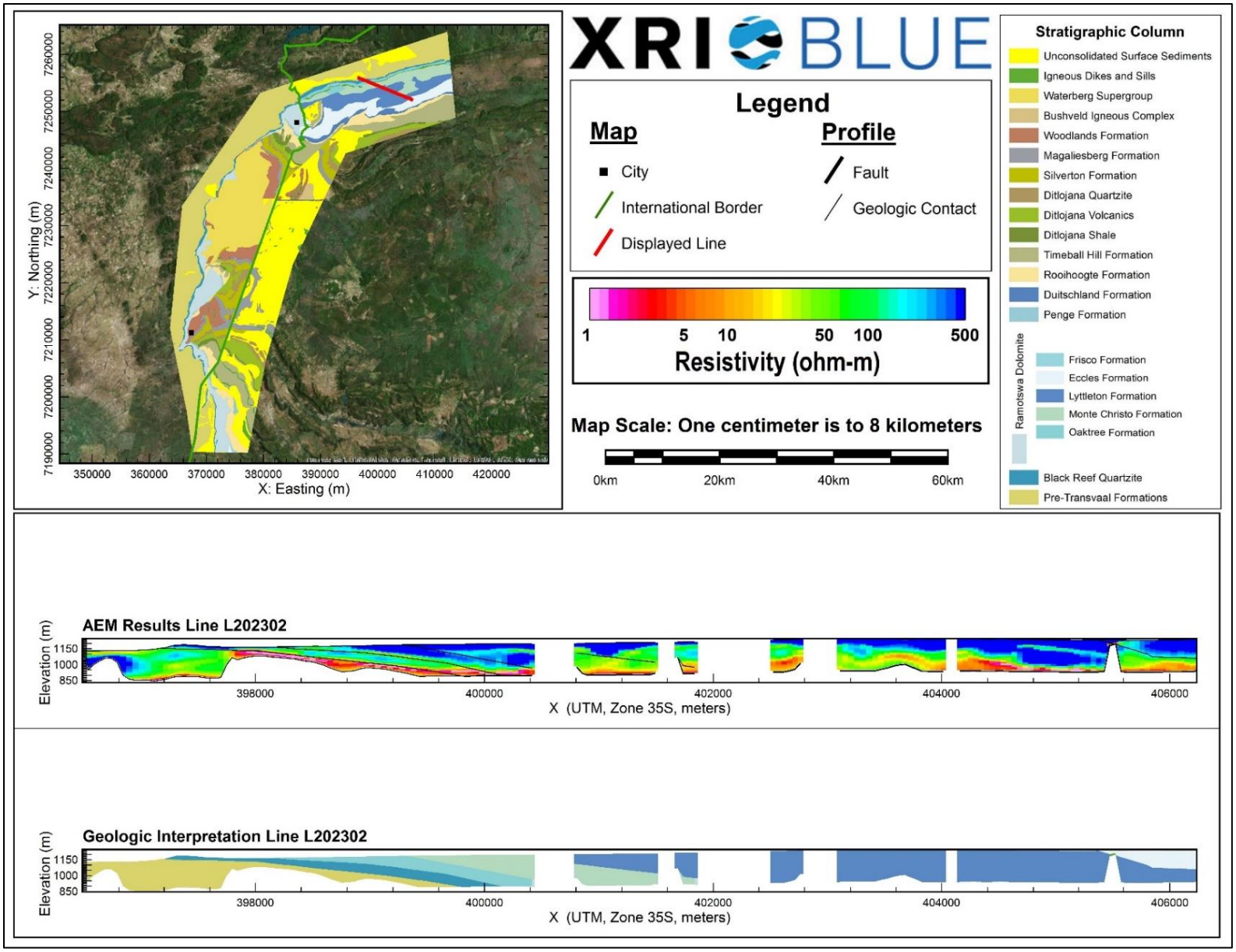

AEM and Interpreted Geology Profile for L202302.

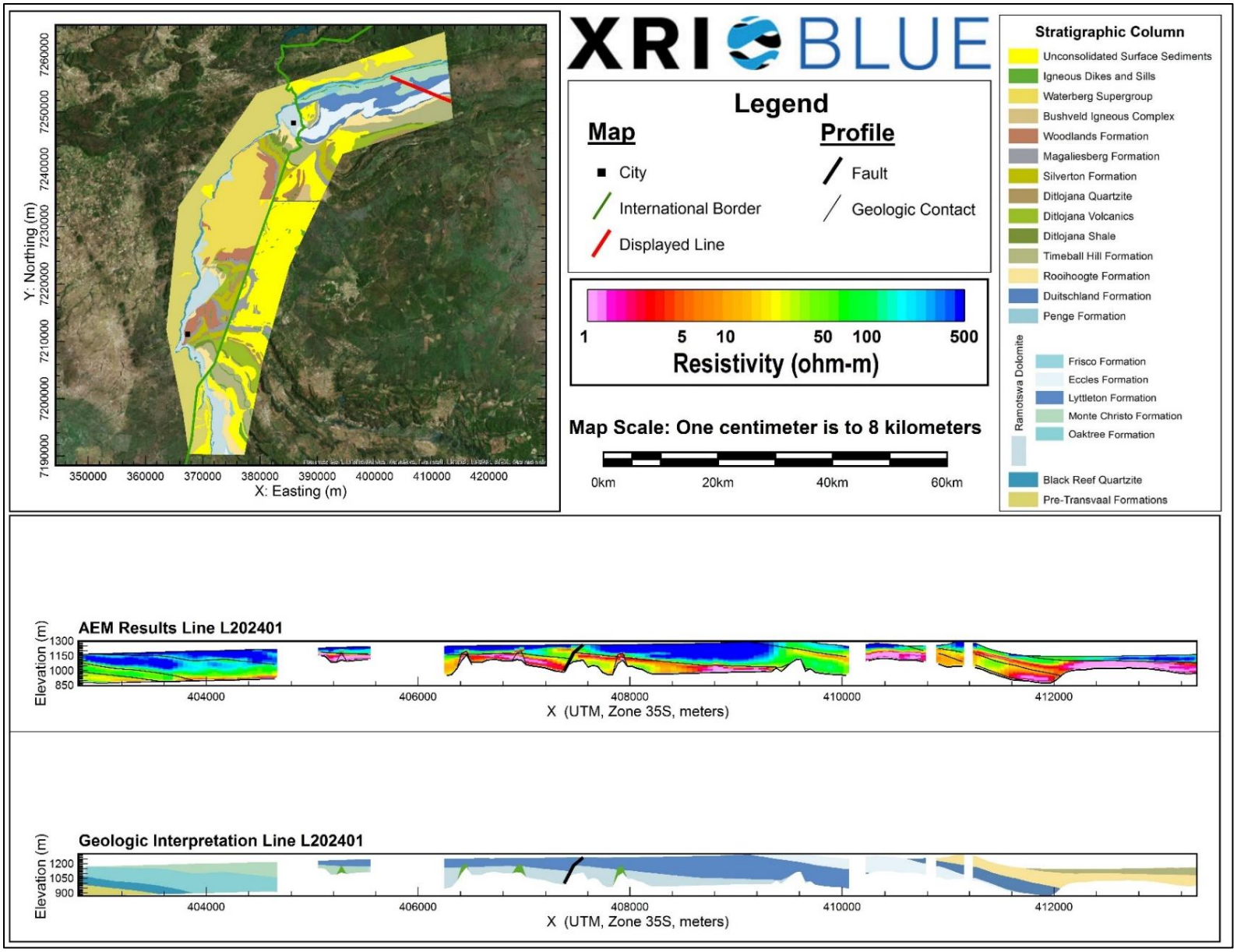

AEM and Interpreted Geology Profile for L202401.

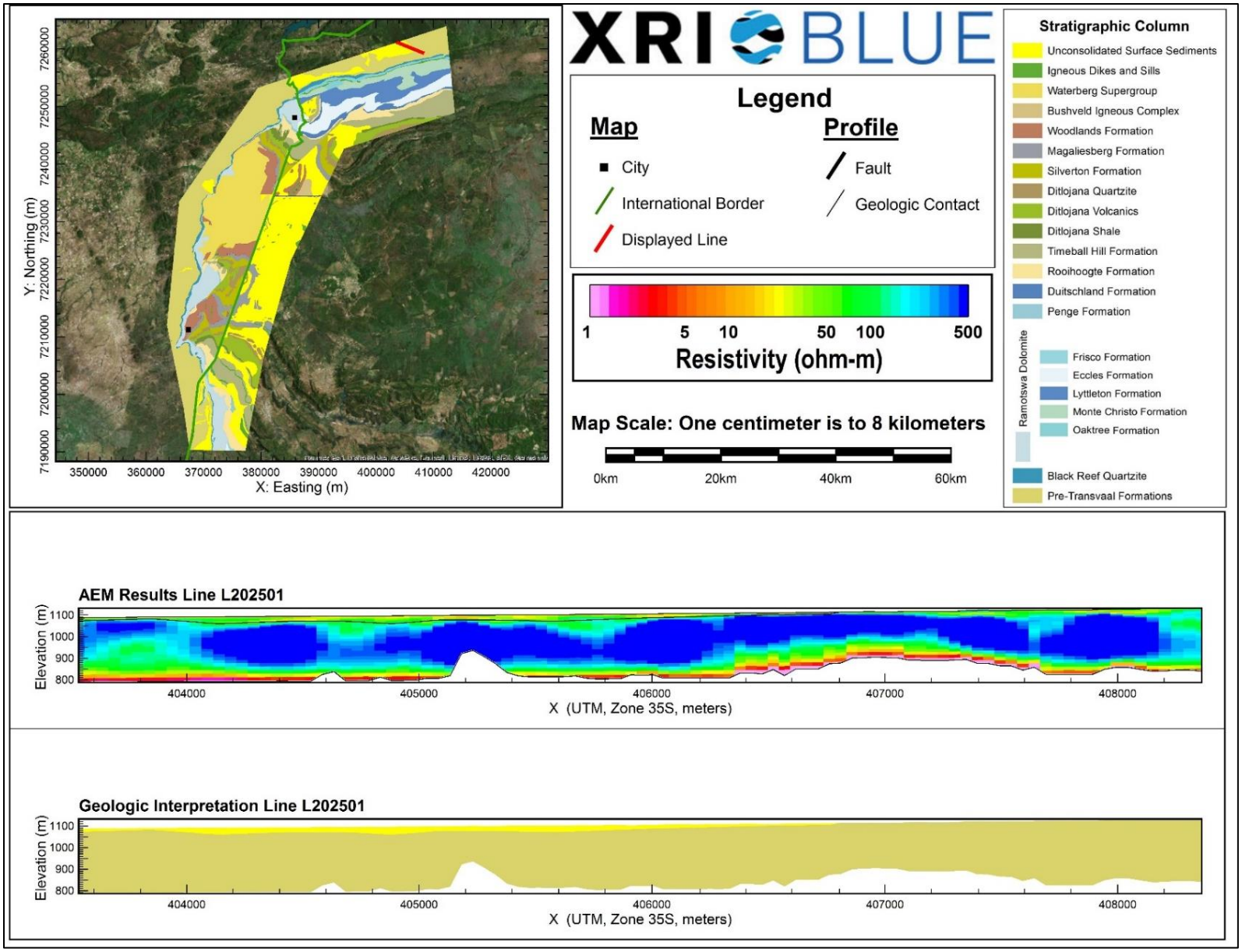

AEM and Interpreted Geology Profile for L202501.

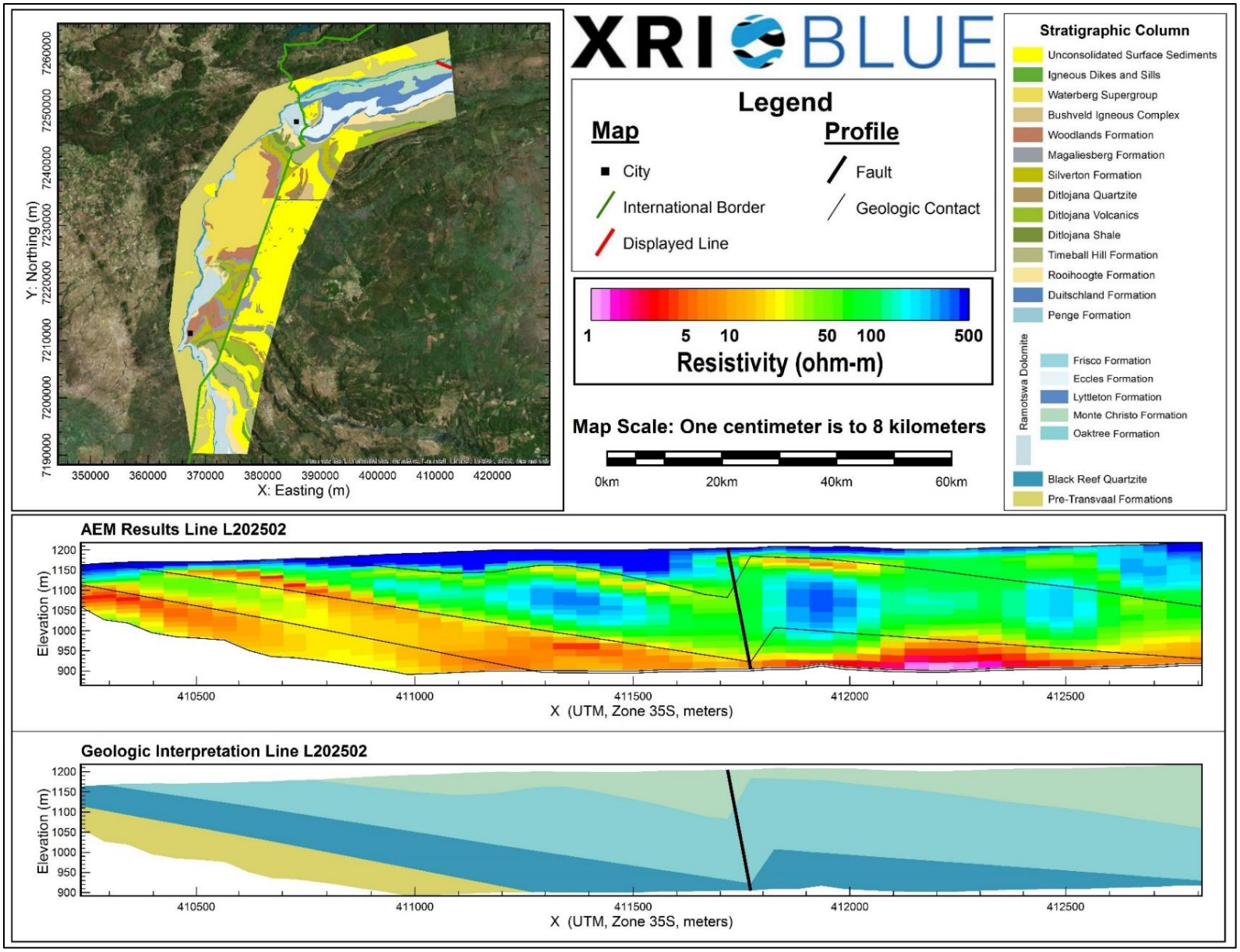

AEM and Interpreted Geology Profile for L202502.

Appendix C: Estimated Porosity Profiles

Table 2 provides the details of the interpreted geology .xyz file for the Ramotswa Project Area. Specifically the first column in Table 1 is the Header or name for each unique column in the .xyz file, the second column in Table 1 is the type of data that is presented, and the third column in Table 1 is a brief description of the data that is provided for each specific column (with units).

To view this .xyz file in Microsoft Excel, the user should open the file, which will cause a "Text Import Wizard" Popup Box to be displayed. For Step 1, make sure that the box for "Delimited" is checked, and that the "Start import at row" is set to "6", then click the "Next" button. For Step 2, the "Tab" and "Comma" Delimiters boxes should be checked, then click the "Next" button. For the Step 3, all the defaults can be left alone, and the "Finish" button can be clicked. Following these steps should allow the file to be correctly imported into Microsoft Excel with all the correct headers.

XRI used both Geosoft's Oasis Montaj (http://www.geosoft.com/products/oasis-montaj/overview) and Encom's PA (https://www.pitneybowes.com/pbencom/products/geophysics/encom-pa.html) software packages to view and interpret data for this project. An alternative software option for 3D viewing of this data that is Golden Software's Voxler (http://www.goldensoftware.com/products/voxler).

This .xyz file is the basis of the Estimated Porosity Profiles included in Appendix C. The only resistivity data included in the .xyz file is resistivity that is greater than the resistivity threshold of 40 Ω-m. The porosity estimates included in the .xyz file are porosity estimates that are within the interpreted extent of the Dolomite. Any porosity estimates that are beneath the DOI Upper or Lower values should be interpreted with a degree of skepticism. Within the .xyz file if the symbol "*" is observed that indicates that the porosity estimate has not been calculated at that specific location and depth due to the fact that either the Dolomite is not interpreted to be present at that location, or the resistivity of the Dolomite is below the resistivity threshold of 40 Ω-m. The remainder of Appendix C is used to display all the unique Estimated Porosity Profiles for the Ramotswa Project Area. The Estimated Porosity Profiles are displayed with a 1:1 horizontal and vertical ratio, each profile is uniquely scaled so that the information for an entire flight line is displayed in one figure. While the specifics of each profile may be difficult to view in the figure, the Ramotswa_Dolomite_Porosity_Estimates.xyz file provided along with this report give all of the necessary data to understand the estimated porosity of the Dolomite aquifer in the Ramotswa Project Area.

Table 2: Explanation of the Estimated Porosity .xyz file of the Ramotswa Project Area.

Database Header	Data Type	Description
LINE	Point	Line Number
X	Point	X Coordinate of Data Point (WGS84 UTM Zone 35S meters)
Y	Point	Y Coordinate of Data Point (WGS84 UTM Zone 35S meters)
Z	Point	Surface elevation based on USGS SRTM Digital Elevation Model (meters)
RHO_I_clip0	Point	Clipped Resistivity for data point of model layer 1 (ohm-meters)
RHO_I_clip 1	Point	Clipped Resistivity for data point of model layer 2 (ohm-meters)
RHO_I_clip 2	Point	Clipped Resistivity for data point of model layer 3 (ohm-meters)
RHO_I_clip 3	Point	Clipped Resistivity for data point of model layer 4 (ohm-meters)
RHO_I_clip 4	Point	Clipped Resistivity for data point of model layer 5 (ohm-meters)
RHO_I_clip 5	Point	Clipped Resistivity for data point of model layer 6 (ohm-meters)
RHO_I_clip 6	Point	Clipped Resistivity for data point of model layer 7 (ohm-meters)

RHO_I_clip 7	Point	Clipped Resistivity for data point of model layer 8 (ohm-meters)
RHO_I_clip 8	Point	Clipped Resistivity for data point of model layer 9 (ohm-meters)
RHO_I_clip 9	Point	Clipped Resistivity for data point of model layer 10 (ohm-meters)
RHO_I_clip 10	Point	Clipped Resistivity for data point of model layer 11 (ohm-meters)
RHO_I_clip 11	Point	Clipped Resistivity for data point of model layer 12 (ohm-meters)
RHO_I_clip 12	Point	Clipped Resistivity for data point of model layer 13 (ohm-meters)
RHO_I_clip 13	Point	Clipped Resistivity for data point of model layer 14 (ohm-meters)
RHO_I_clip 14	Point	Clipped Resistivity for data point of model layer 15 (ohm-meters)
RHO_I_clip 15	Point	Clipped Resistivity for data point of model layer 16 (ohm-meters)
RHO_I_clip 16	Point	Clipped Resistivity for data point of model layer 17 (ohm-meters)
RHO_I_clip 17	Point	Clipped Resistivity for data point of model layer 18 (ohm-meters)
RHO_I_clip 18	Point	Clipped Resistivity for data point of model layer 19 (ohm-meters)
RHO_I_clip 19	Point	Clipped Resistivity for data point of model layer 20 (ohm-meters)
RHO_I_clip 20	Point	Clipped Resistivity for data point of model layer 21 (ohm-meters)
RHO_I_clip 21	Point	Clipped Resistivity for data point of model layer 22 (ohm-meters)
RHO_I_clip 22	Point	Clipped Resistivity for data point of model layer 23 (ohm-meters)
RHO_I_clip 23	Point	Clipped Resistivity for data point of model layer 24 (ohm-meters)
RHO_I_clip 24	Point	Clipped Resistivity for data point of model layer 25 (ohm-meters)
RHO_I_clip 25	Point	Clipped Resistivity for data point of model layer 26 (ohm-meters)
RHO_I_clip 26	Point	Clipped Resistivity for data point of model layer 27 (ohm-meters)
RHO_I_clip 27	Point	Clipped Resistivity for data point of model layer 28 (ohm-meters)
RHO_I_clip 28	Point	Clipped Resistivity for data point of model layer 29 (ohm-meters)
RHO_I_clip 29	Point	Clipped Resistivity for data point of model layer 30 (ohm-meters)
DEP_BOT0	Point	Depth to the bottom of model layer 1 in the AEM model (meters)
DEP_BOT1	Point	Depth to the bottom of model layer 2 in the AEM model (meters)
DEP_BOT2	Point	Depth to the bottom of model layer 3 in the AEM model (meters)
DEP_BOT3	Point	Depth to the bottom of model layer 4 in the AEM model (meters)
DEP_BOT4	Point	Depth to the bottom of model layer 5 in the AEM model (meters)
DEP_BOT5	Point	Depth to the bottom of model layer 6 in the AEM model (meters)
DEP_BOT6	Point	Depth to the bottom of model layer 7 in the AEM model (meters)
DEP_BOT7	Point	Depth to the bottom of model layer 8 in the AEM model (meters)
DEP_BOT8	Point	Depth to the bottom of model layer 9 in the AEM model (meters)
DEP_BOT9	Point	Depth to the bottom of model layer 10 in the AEM model (meters)
DEP_BOT10	Point	Depth to the bottom of model layer 11 in the AEM model (meters)
DEP_BOT11	Point	Depth to the bottom of model layer 12 in the AEM model (meters)
DEP_BOT12	Point	Depth to the bottom of model layer 13 in the AEM model (meters)
DEP_BOT13	Point	Depth to the bottom of model layer 14 in the AEM model (meters)
DEP_BOT14	Point	Depth to the bottom of model layer 15 in the AEM model (meters)
DEP_BOT15	Point	Depth to the bottom of model layer 16 in the AEM model (meters)
DEP_BOT16	Point	Depth to the bottom of model layer 17 in the AEM model (meters)
DEP_BOT17	Point	Depth to the bottom of model layer 18 in the AEM model (meters)
DEP_BOT18	Point	Depth to the bottom of model layer 19 in the AEM model (meters)
DEP_BOT19	Point	Depth to the bottom of model layer 20 in the AEM model (meters)

DEP_BOT20	Point	Depth to the bottom of model layer 21 in the AEM model (meters)
DEP_BOT21	Point	Depth to the bottom of model layer 22 in the AEM model (meters)
DEP_BOT22	Point	Depth to the bottom of model layer 23 in the AEM model (meters)
DEP_BOT23	Point	Depth to the bottom of model layer 24 in the AEM model (meters)
DEP_BOT24	Point	Depth to the bottom of model layer 25 in the AEM model (meters)
DEP_BOT25	Point	Depth to the bottom of model layer 26 in the AEM model (meters)
DEP_BOT26	Point	Depth to the bottom of model layer 27 in the AEM model (meters)
DEP_BOT27	Point	Depth to the bottom of model layer 28 in the AEM model (meters)
DEP_BOT28	Point	Depth to the bottom of model layer 29 in the AEM model (meters)
DOI_UPPER	Point	Shallow DOI estimate for data point (meters)
DOI_LOWER	Point	Deep DOI estimate for data point (meters)
RD_Top	Point	Interpreted top of the Ramotswa Dolomite (meters)
RD_Base	Point	Interpreted base of the Ramotswa Dolomite (meters)
FluidRes	Point	Calculated Pore Fluid Resistivity (ohm-meters)
m_value	Point	“m” value used in modified version of Archie’s Law for carbonates
Porosity_Estimate0	Point	Estimated porosity of model layer 1 in the AEM model (unitless)
Porosity_Estimate1	Point	Estimated porosity of model layer 2 in the AEM model (unitless)
Porosity_Estimate2	Point	Estimated porosity of model layer 3 in the AEM model (unitless)
Porosity_Estimate3	Point	Estimated porosity of model layer 4 in the AEM model (unitless)
Porosity_Estimate4	Point	Estimated porosity of model layer 5 in the AEM model (unitless)
Porosity_Estimate5	Point	Estimated porosity of model layer 6 in the AEM model (unitless)
Porosity_Estimate6	Point	Estimated porosity of model layer 7 in the AEM model (unitless)
Porosity_Estimate7	Point	Estimated porosity of model layer 8 in the AEM model (unitless)
Porosity_Estimate8	Point	Estimated porosity of model layer 9 in the AEM model (unitless)
Porosity_Estimate9	Point	Estimated porosity of model layer 10 in the AEM model (unitless)
Porosity_Estimate10	Point	Estimated porosity of model layer 11 in the AEM model (unitless)
Porosity_Estimate11	Point	Estimated porosity of model layer 12 in the AEM model (unitless)
Porosity_Estimate12	Point	Estimated porosity of model layer 13 in the AEM model (unitless)
Porosity_Estimate13	Point	Estimated porosity of model layer 14 in the AEM model (unitless)
Porosity_Estimate14	Point	Estimated porosity of model layer 15 in the AEM model (unitless)
Porosity_Estimate15	Point	Estimated porosity of model layer 16 in the AEM model (unitless)
Porosity_Estimate16	Point	Estimated porosity of model layer 17 in the AEM model (unitless)
Porosity_Estimate17	Point	Estimated porosity of model layer 18 in the AEM model (unitless)
Porosity_Estimate18	Point	Estimated porosity of model layer 19 in the AEM model (unitless)
Porosity_Estimate19	Point	Estimated porosity of model layer 20 in the AEM model (unitless)
Porosity_Estimate20	Point	Estimated porosity of model layer 21 in the AEM model (unitless)
Porosity_Estimate21	Point	Estimated porosity of model layer 22 in the AEM model (unitless)
Porosity_Estimate22	Point	Estimated porosity of model layer 23 in the AEM model (unitless)
Porosity_Estimate23	Point	Estimated porosity of model layer 24 in the AEM model (unitless)
Porosity_Estimate24	Point	Estimated porosity of model layer 25 in the AEM model (unitless)
Porosity_Estimate25	Point	Estimated porosity of model layer 26 in the AEM model (unitless)
Porosity_Estimate26	Point	Estimated porosity of model layer 27 in the AEM model (unitless)
Porosity_Estimate27	Point	Estimated porosity of model layer 28 in the AEM model (unitless)
Porosity_Estimate28	Point	Estimated porosity of model layer 29 in the AEM model (unitless)
Porosity_Estimate29	Point	Estimated porosity of model layer 30 in the AEM model (unitless)

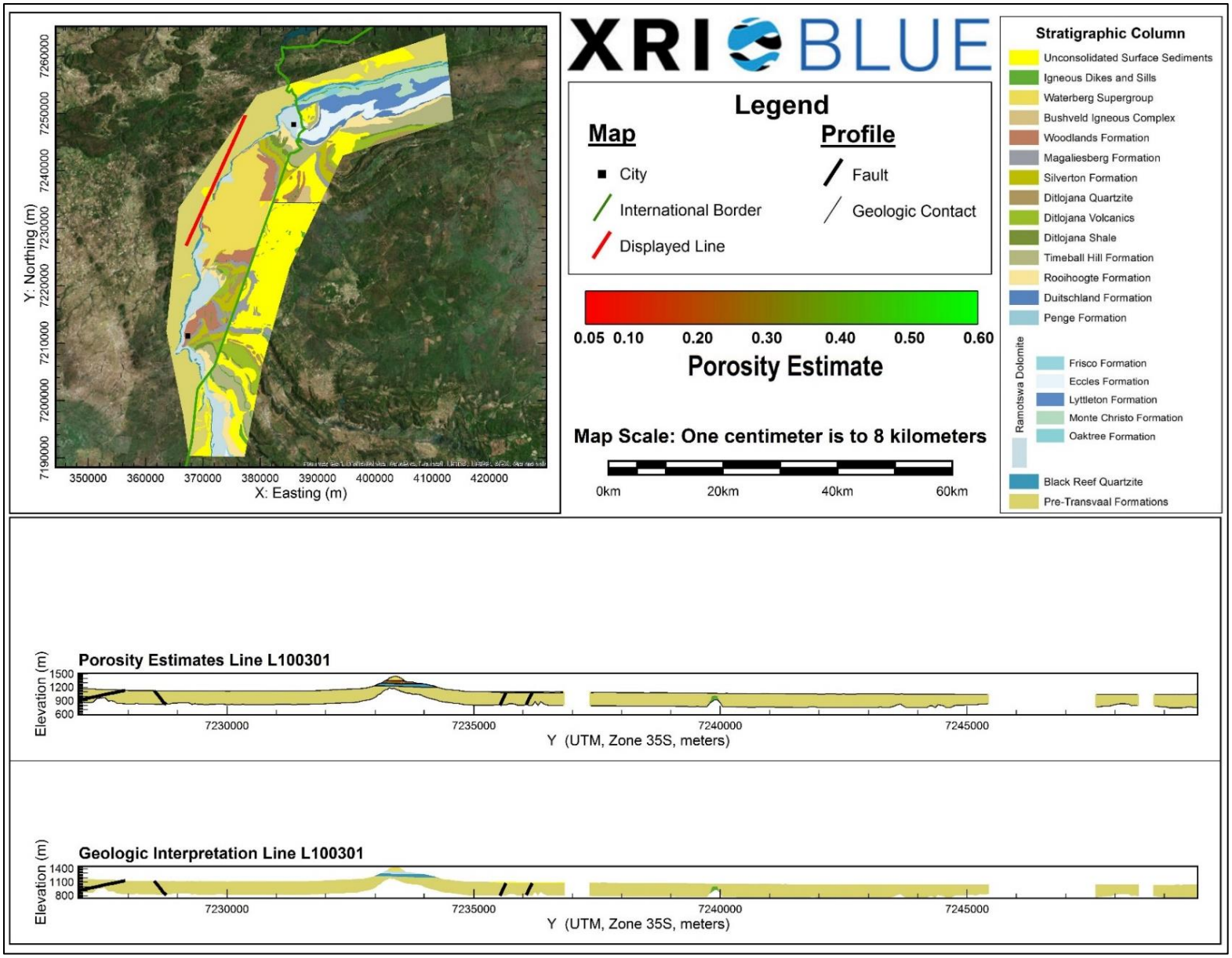

Porosity Estimates and Interpreted Geology Profile for L100301.

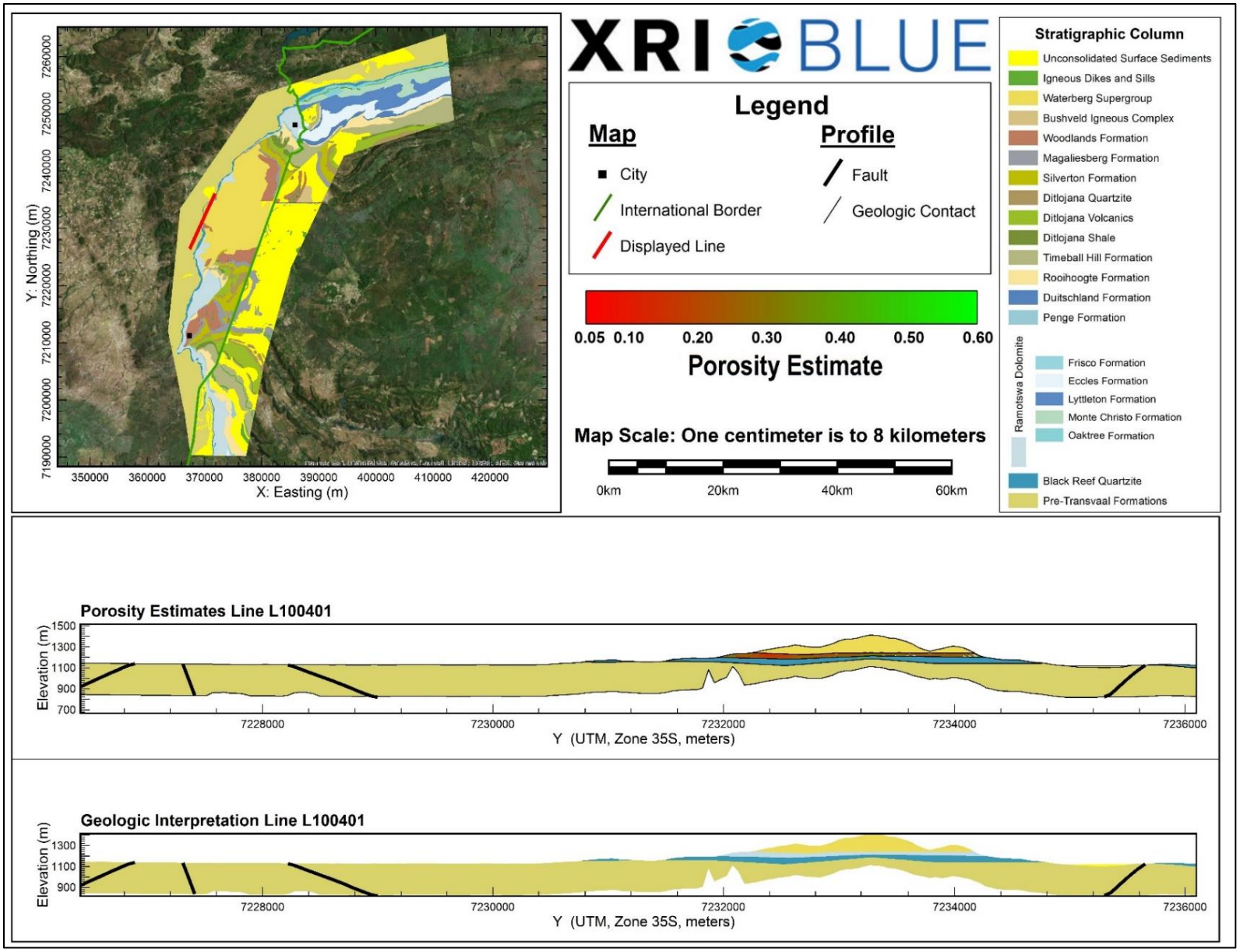

Porosity Estimates and Interpreted Geology Profile for L100401.

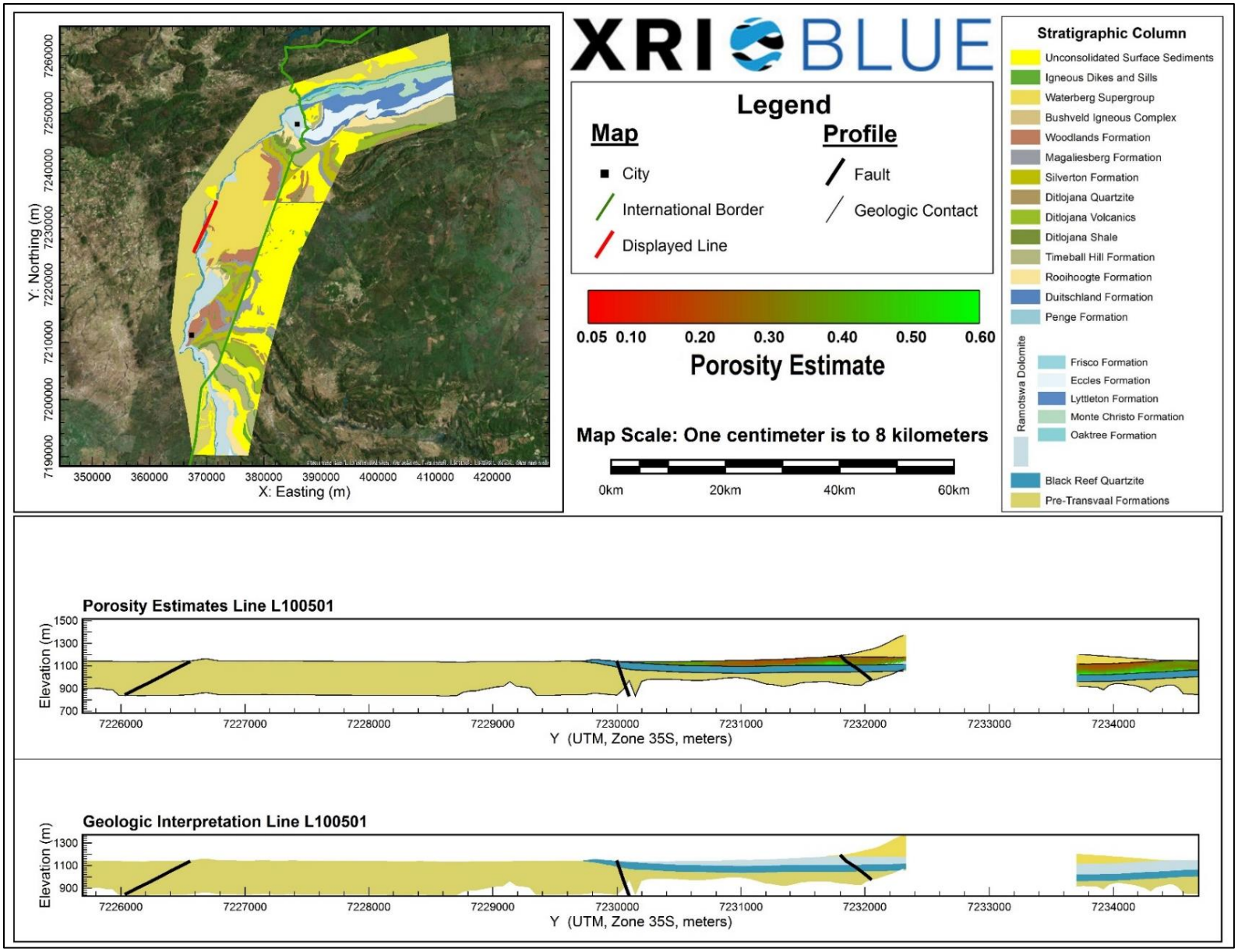

Porosity Estimates and Interpreted Geology Profile for L100501.

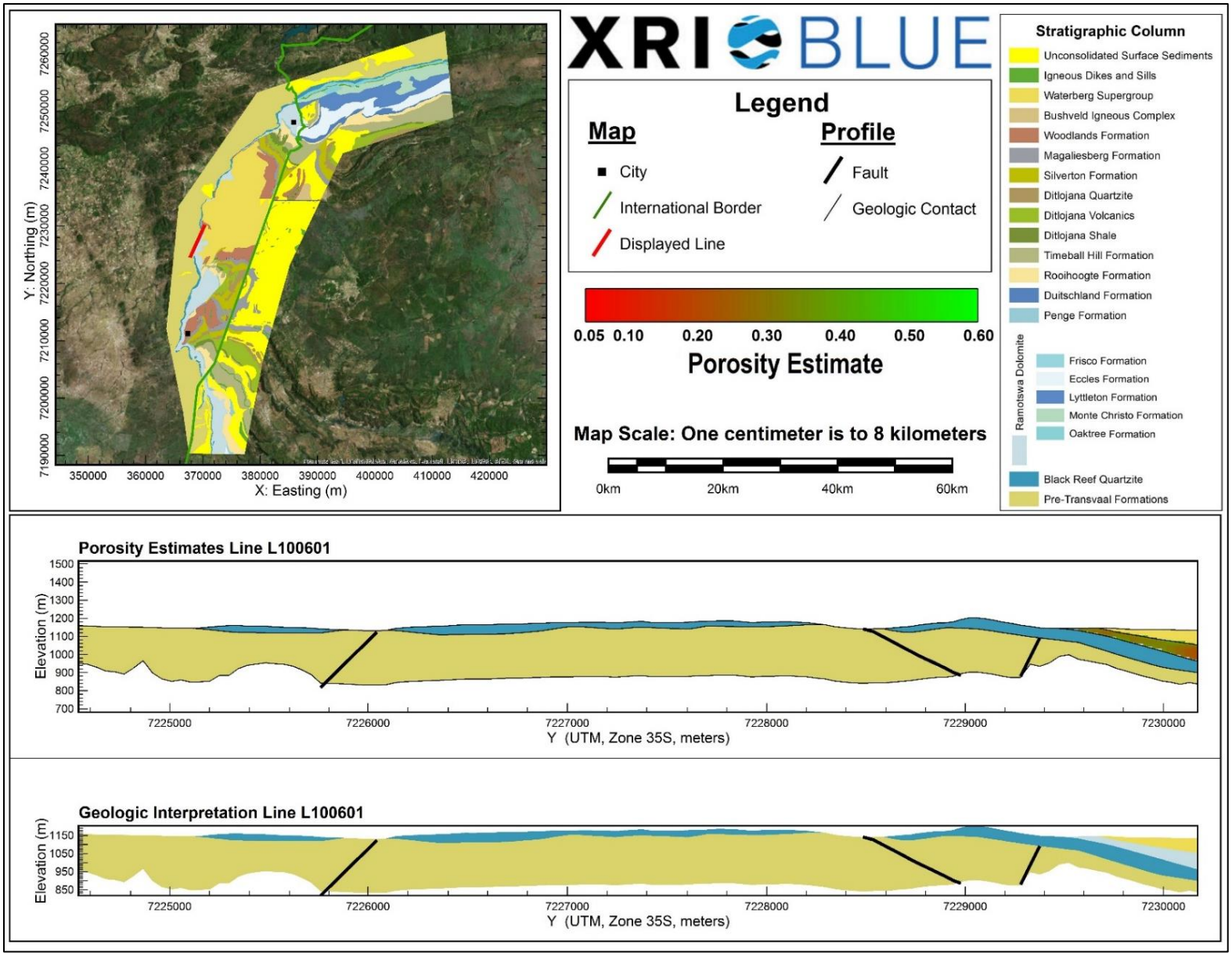

Porosity Estimates and Interpreted Geology Profile for L100601.

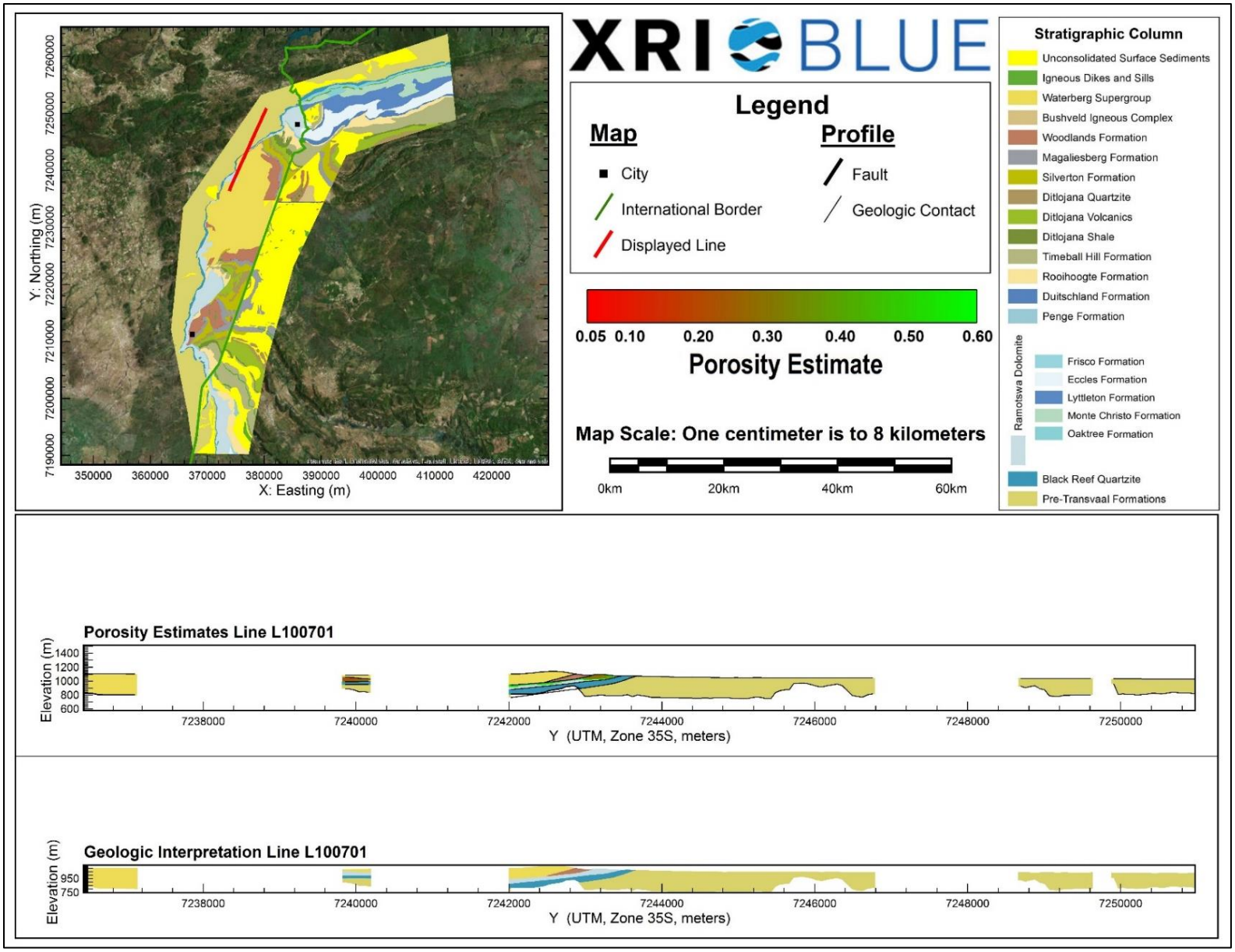

Porosity Estimates and Interpreted Geology Profile for L100701.

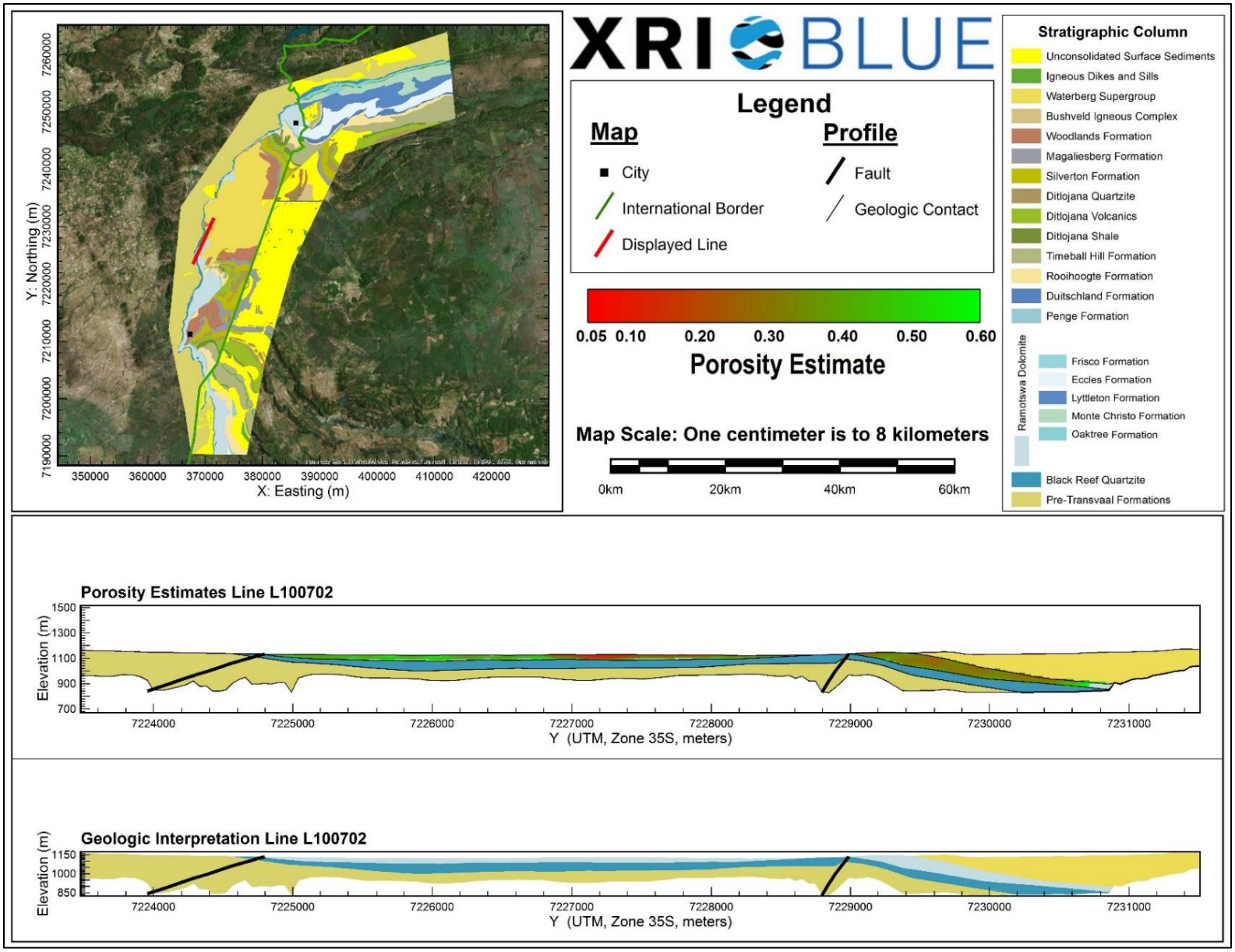

Porosity Estimates and Interpreted Geology Profile for L100702.

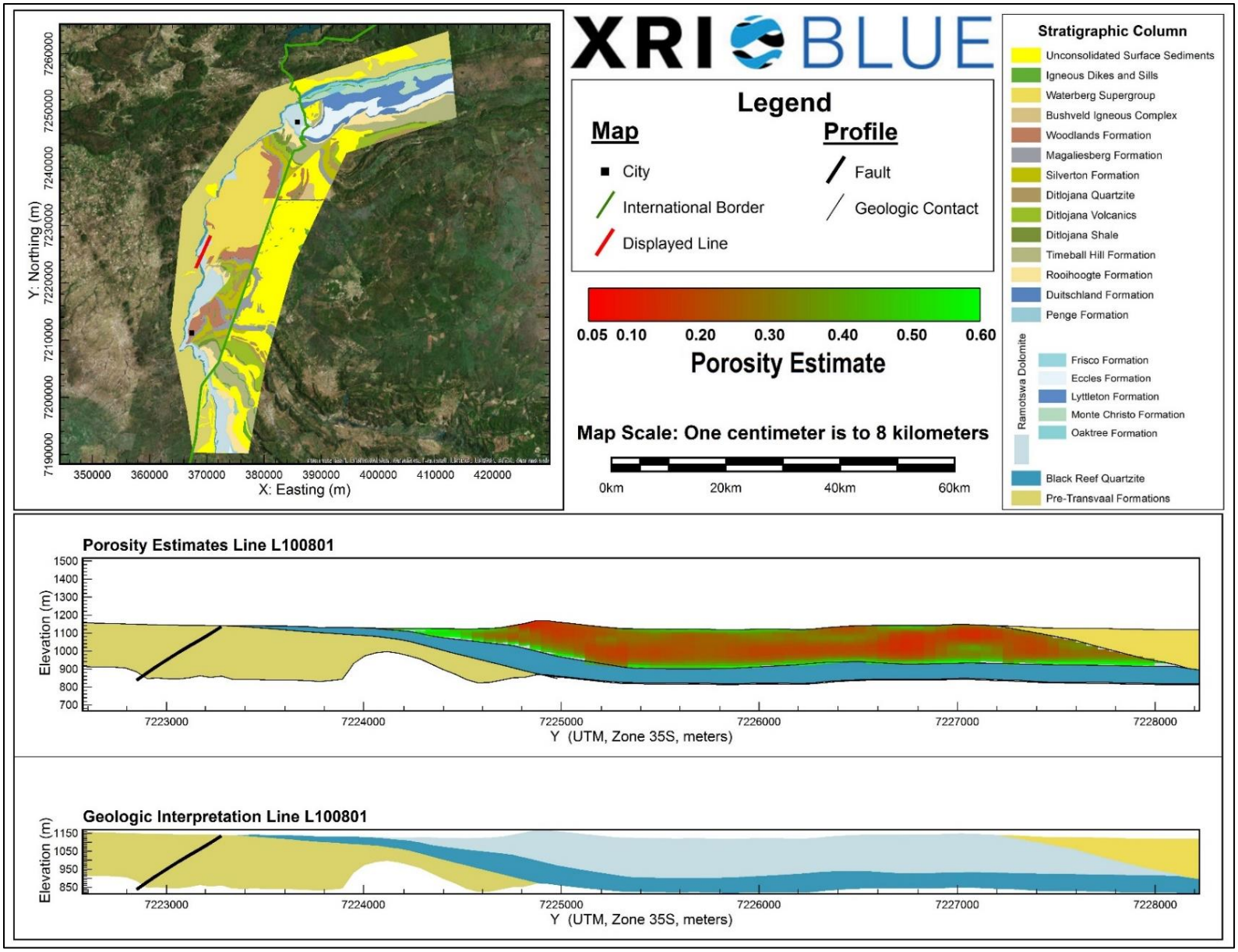

Porosity Estimates and Interpreted Geology Profile for L100801.

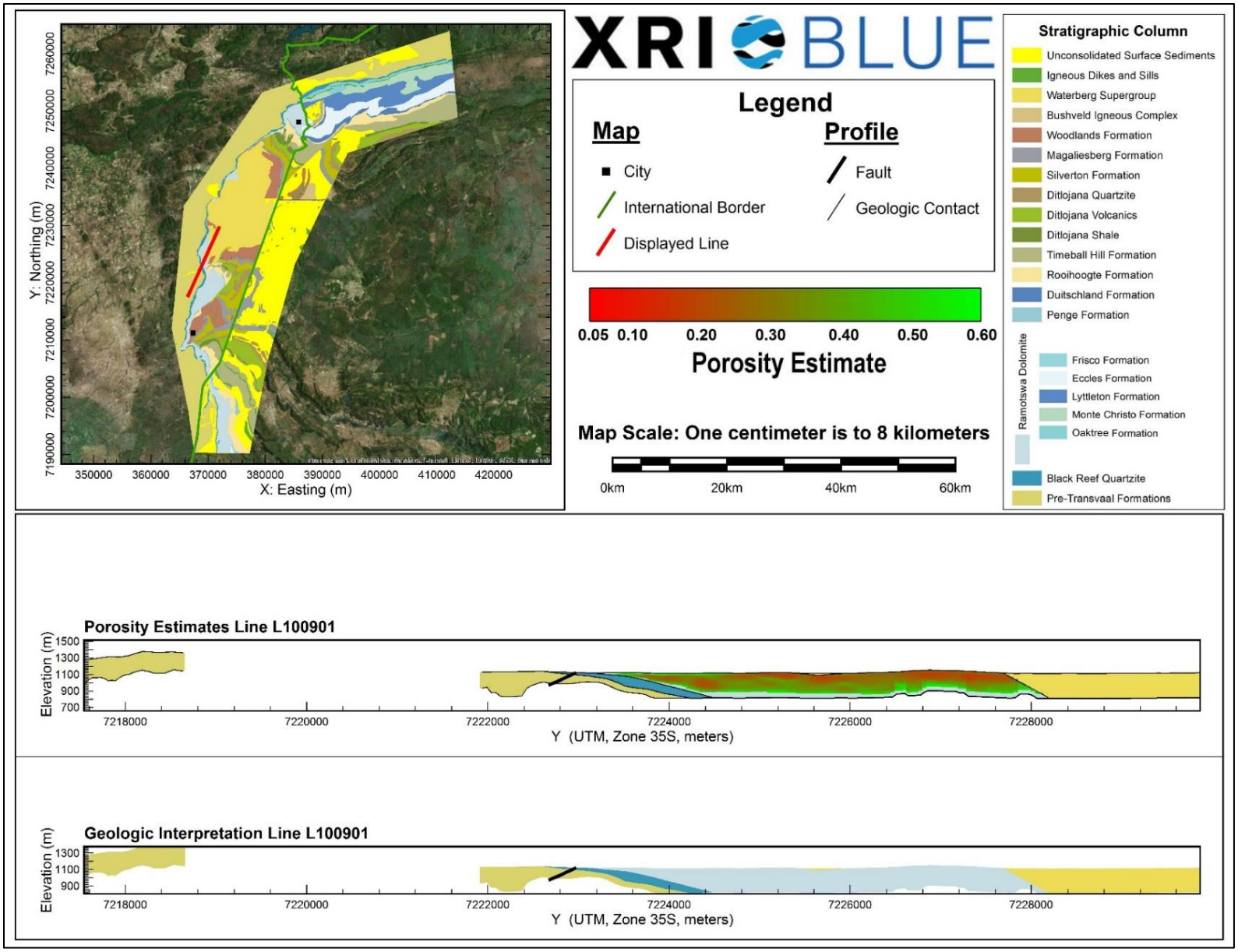

Porosity Estimates and Interpreted Geology Profile for L100901.

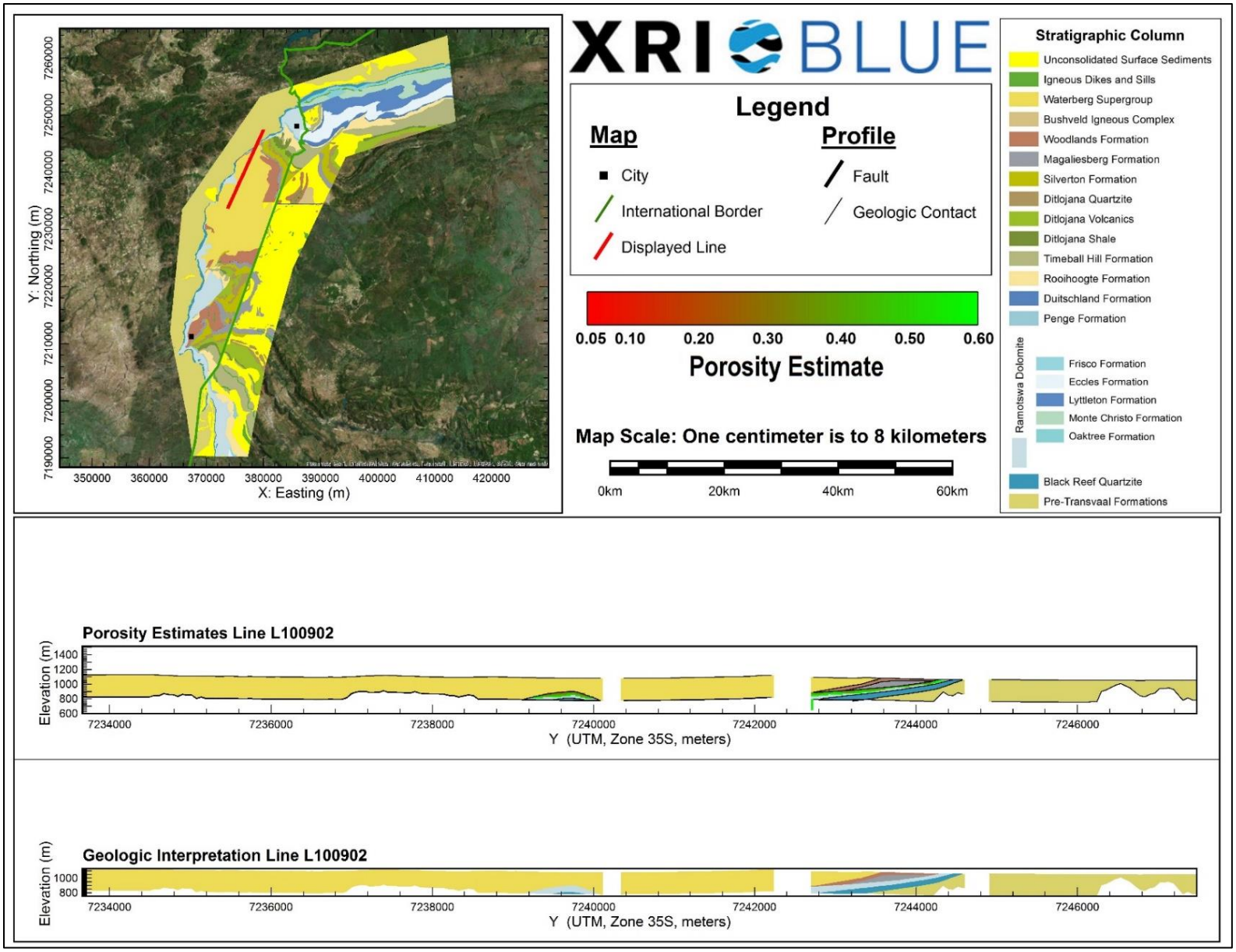

Porosity Estimates and Interpreted Geology Profile for L100902.

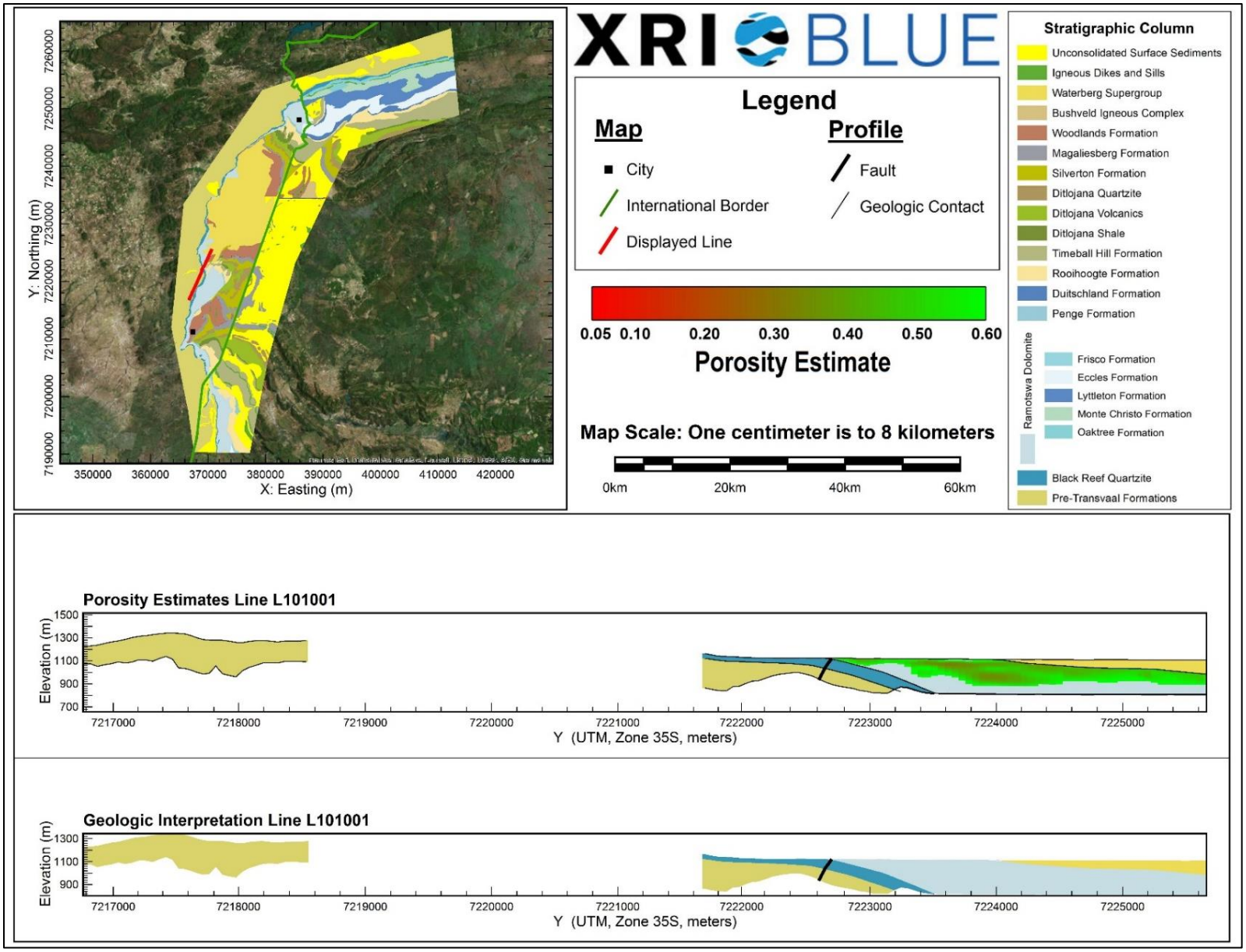

Porosity Estimates and Interpreted Geology Profile for L101001.

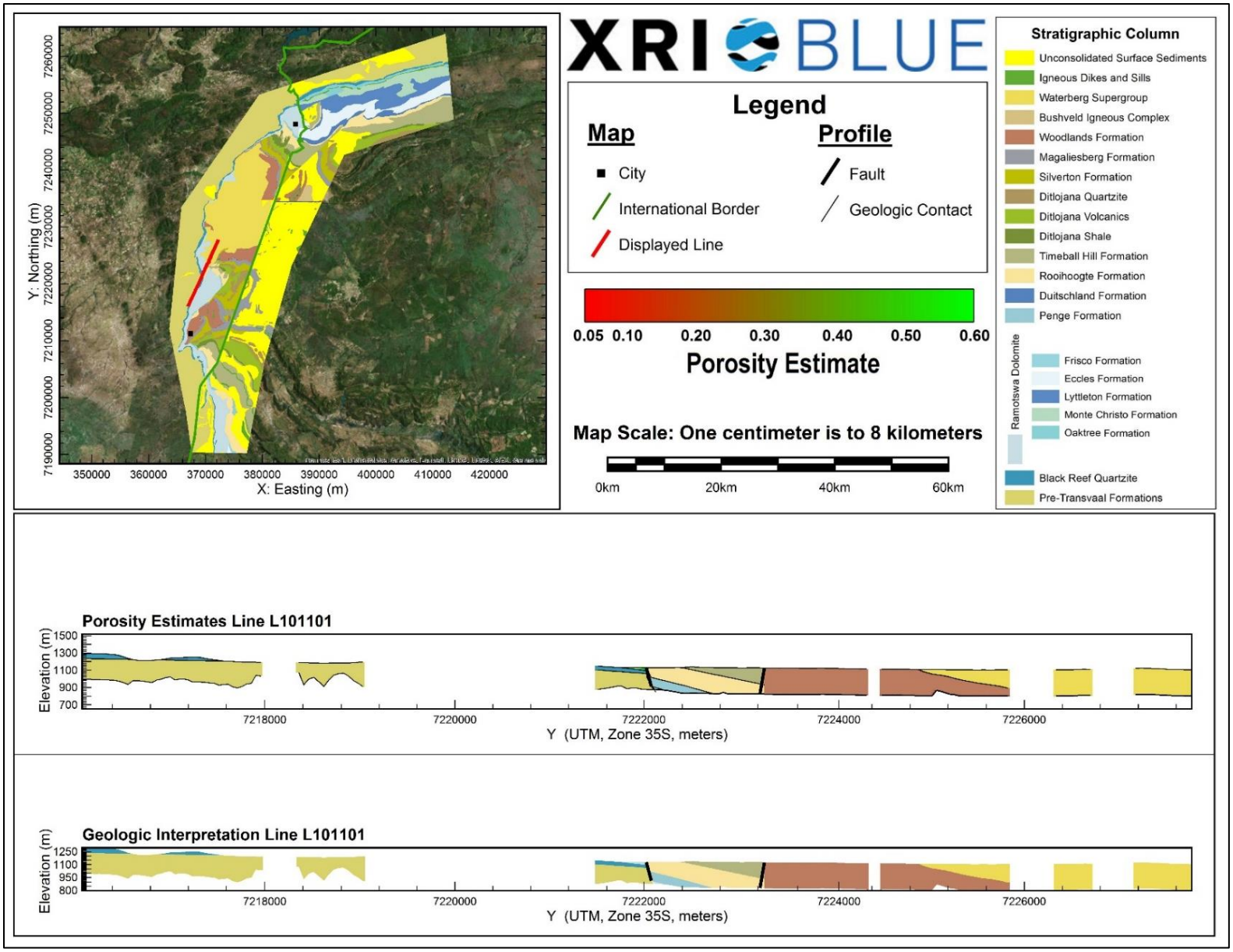

Porosity Estimates and Interpreted Geology Profile for L101101.

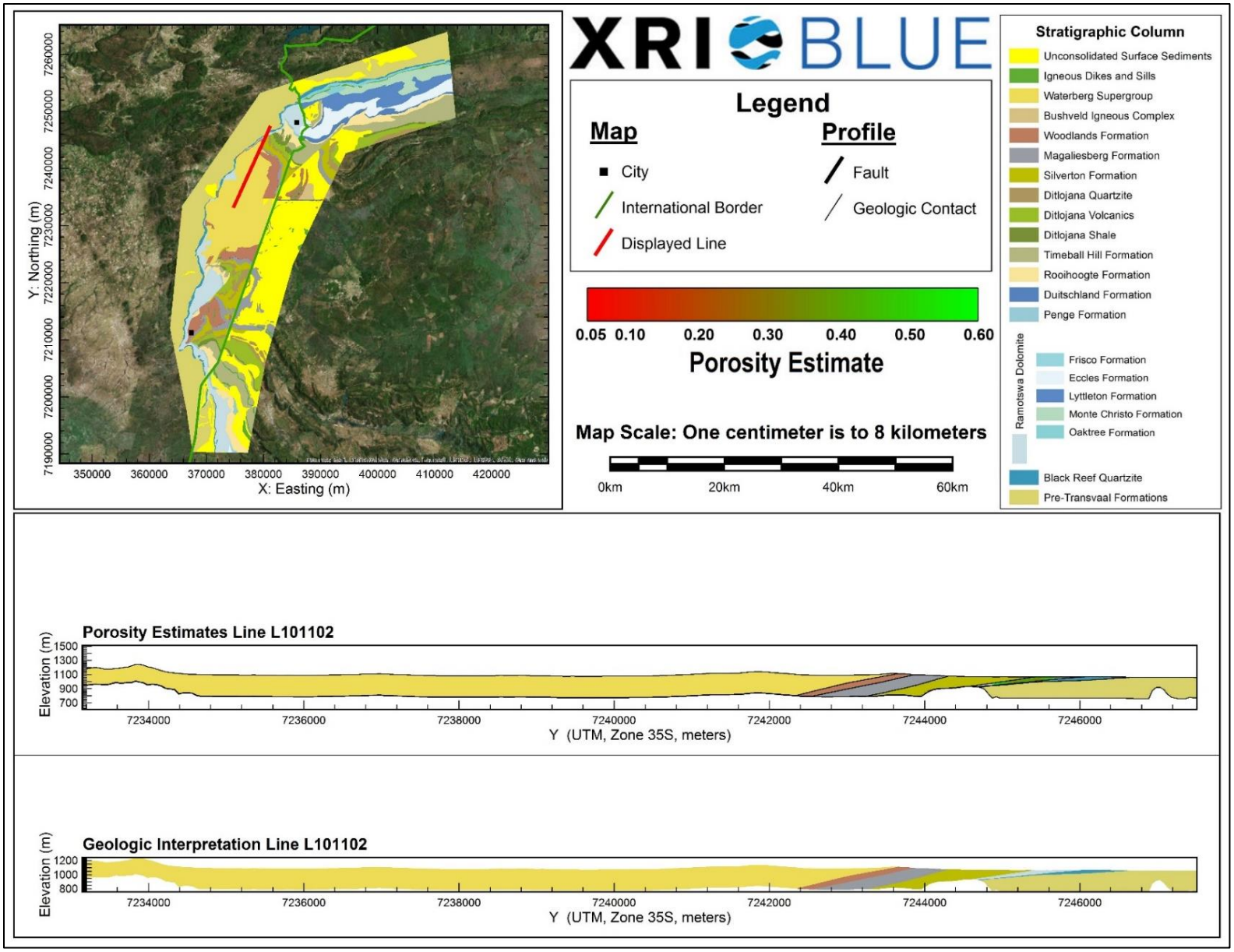

Porosity Estimates and Interpreted Geology Profile for L101102.

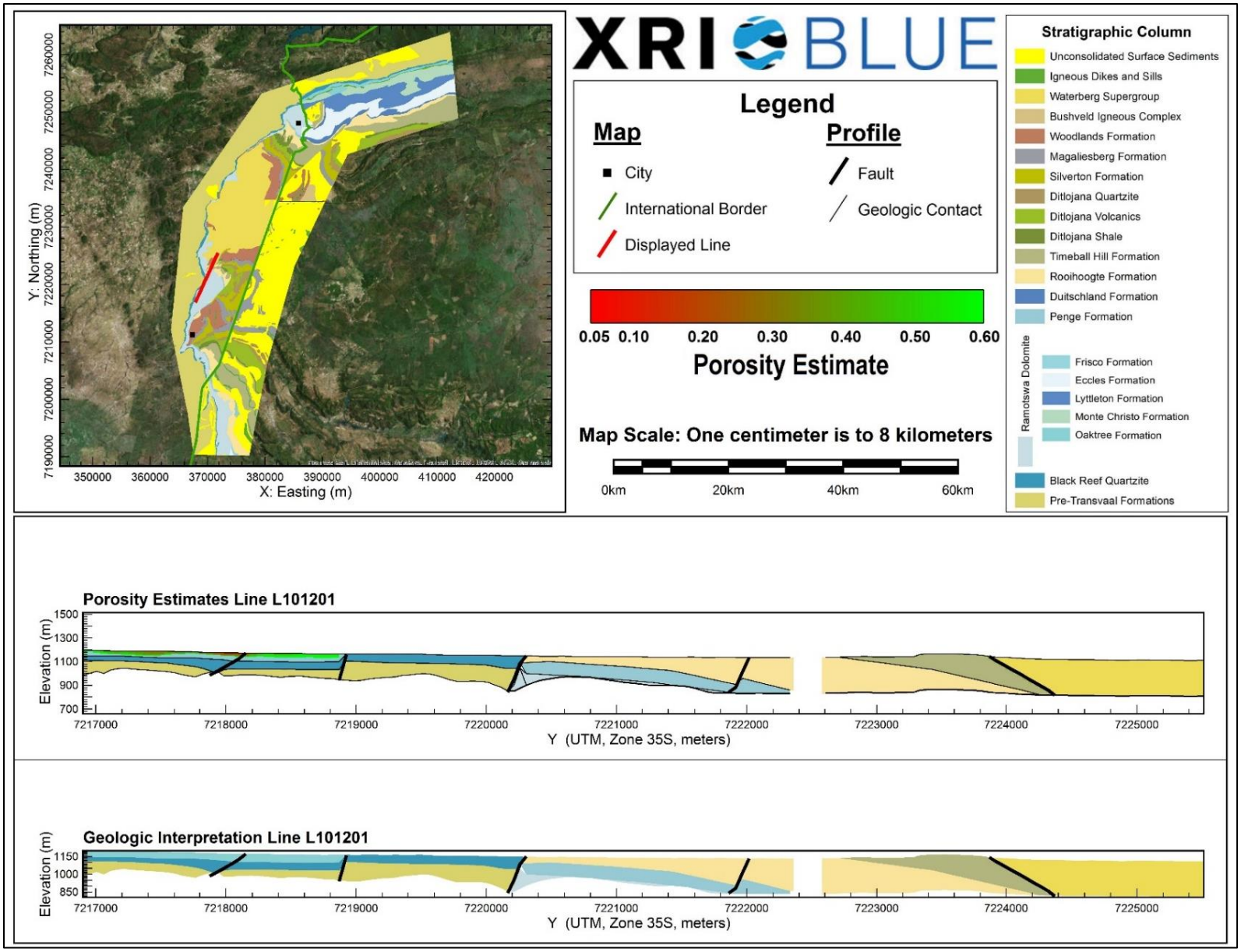

Porosity Estimates and Interpreted Geology Profile for L101201.

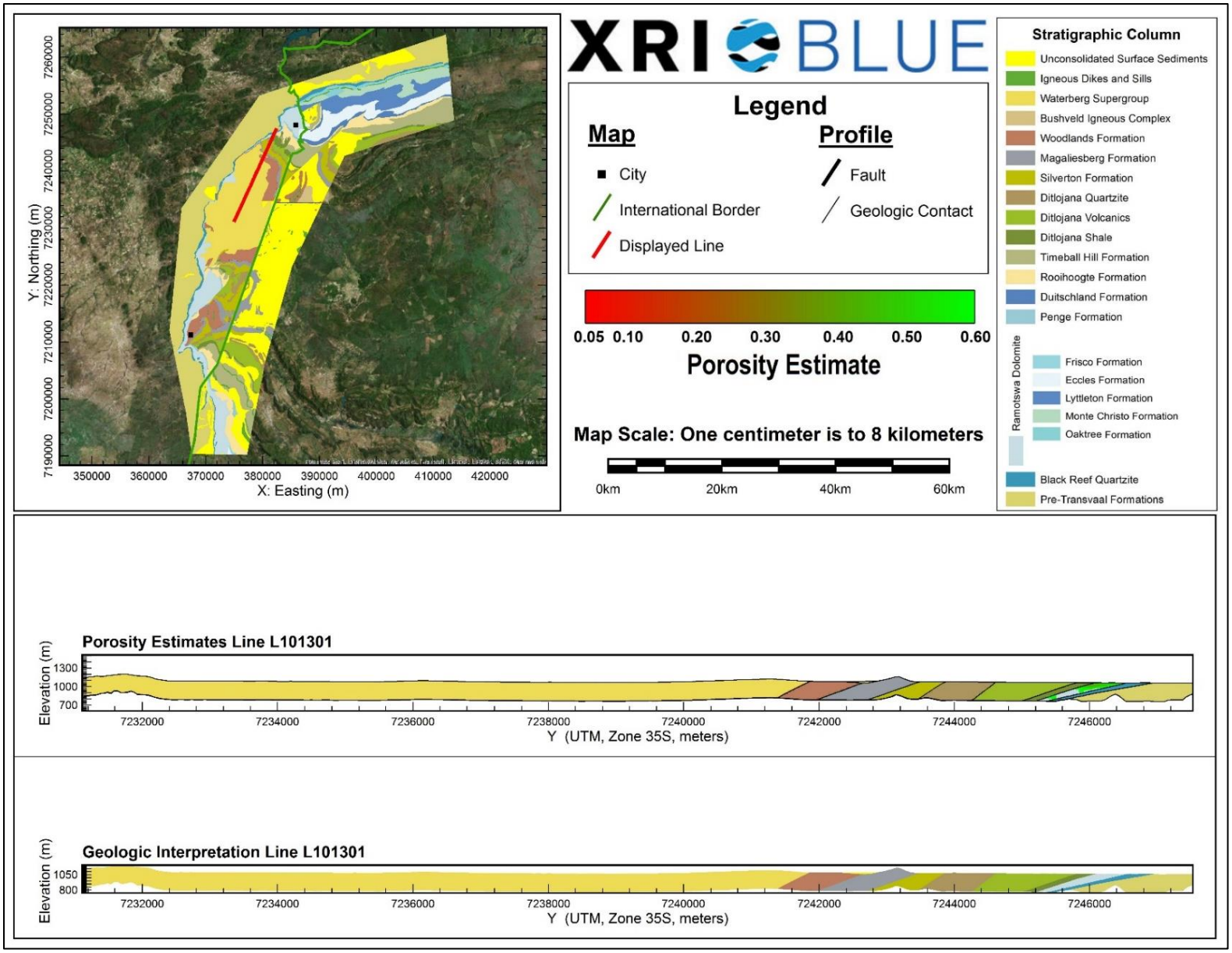

Porosity Estimates and Interpreted Geology Profile for L101301.

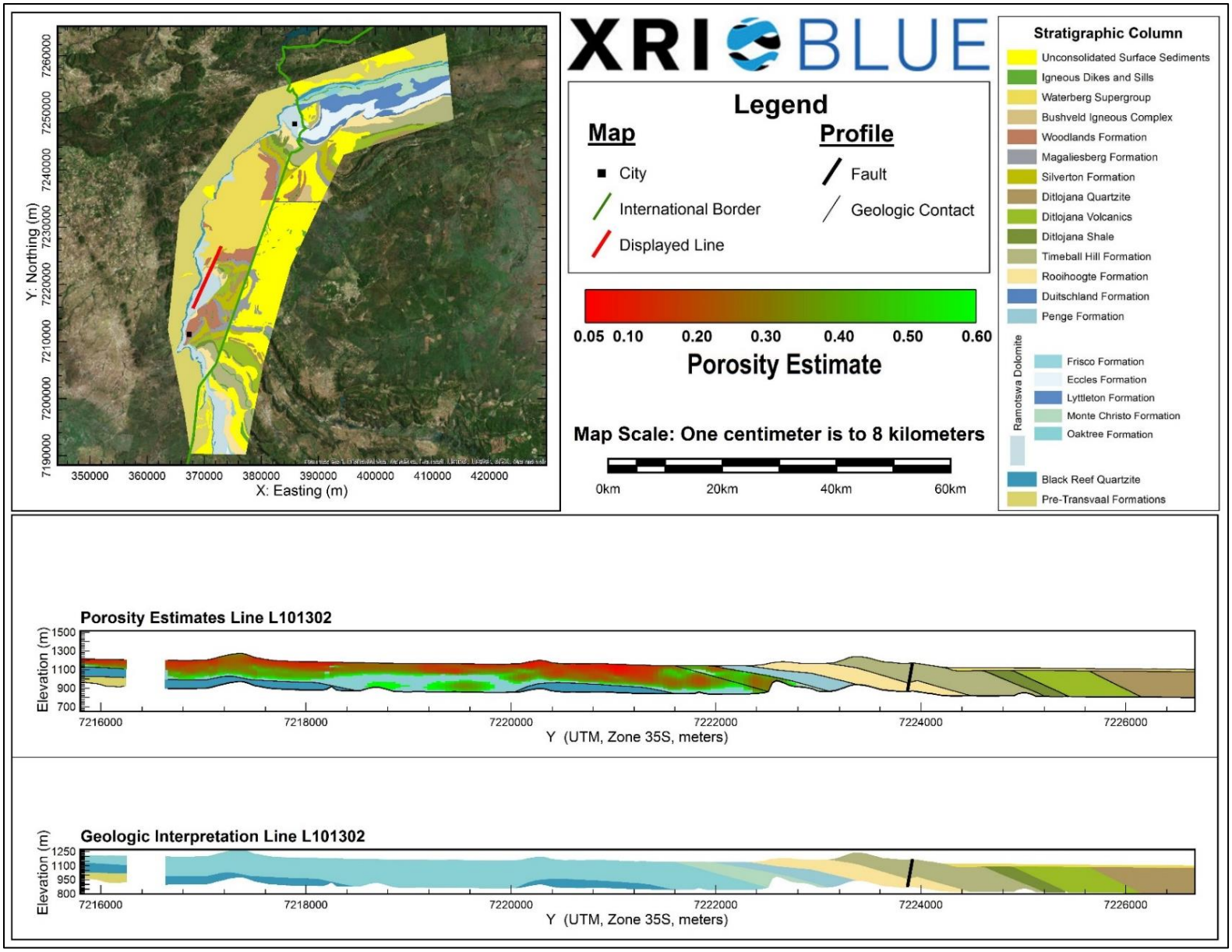

Porosity Estimates and Interpreted Geology Profile for L101302.

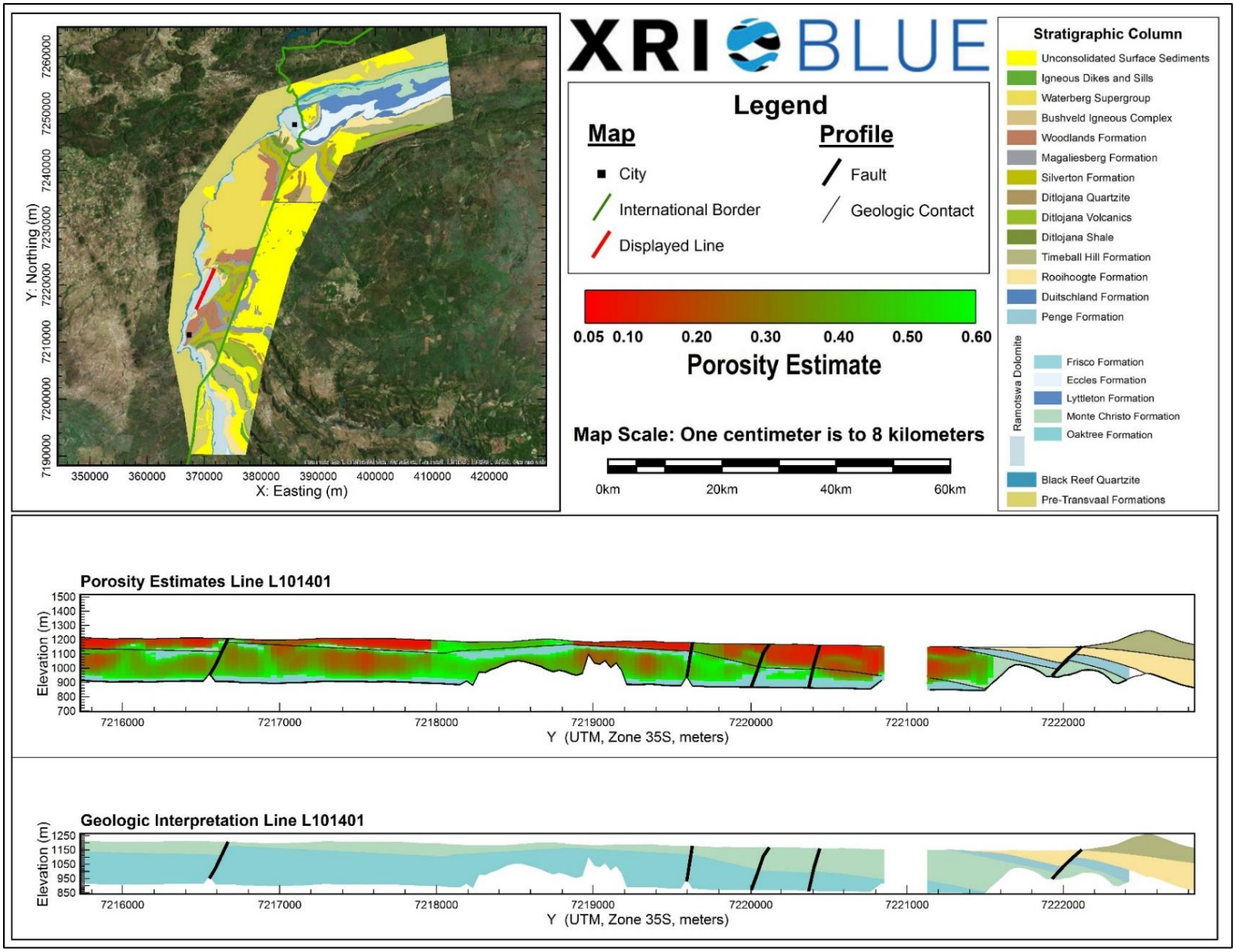

Porosity Estimates and Interpreted Geology Profile for L101401.

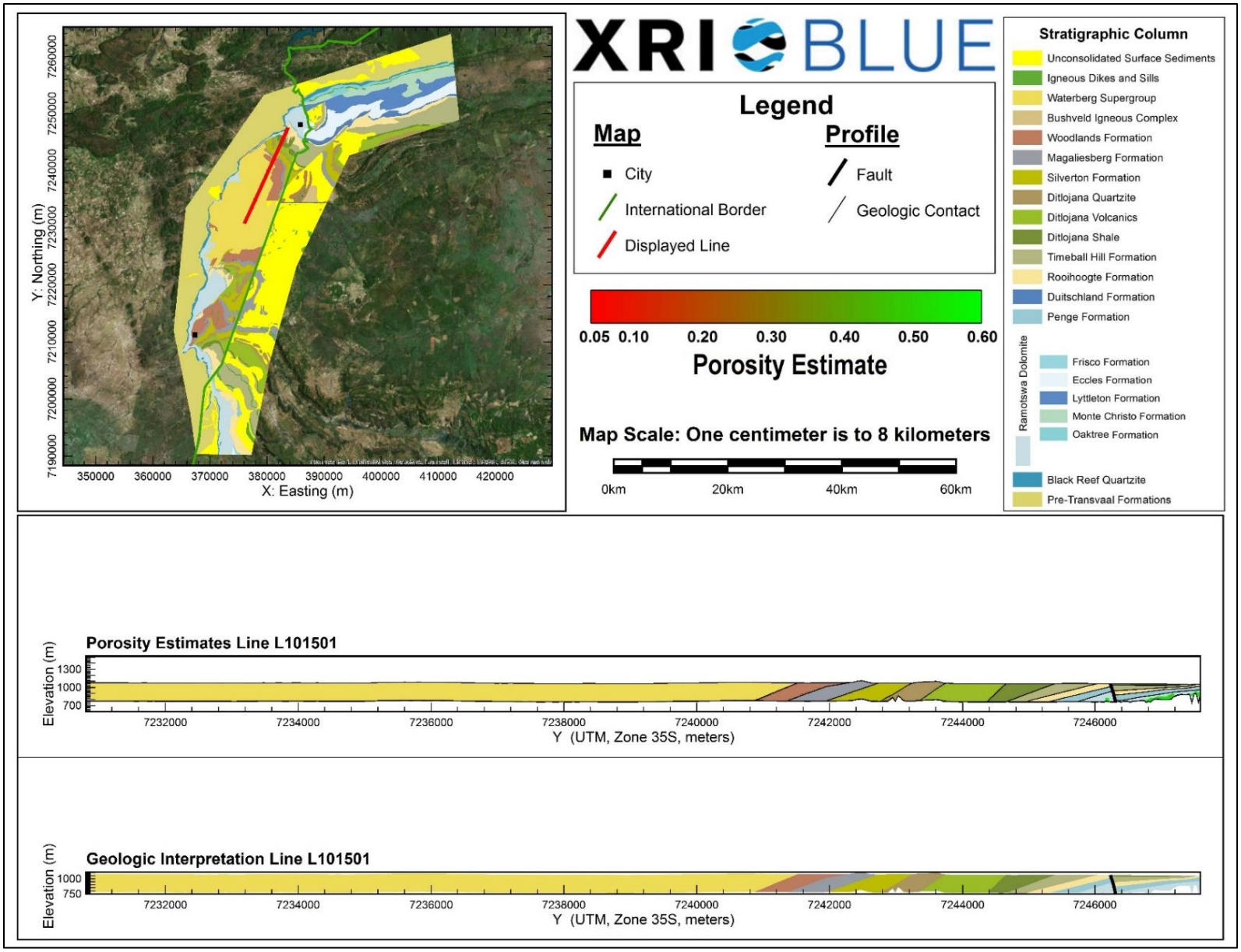

Porosity Estimates and Interpreted Geology Profile for L101501.

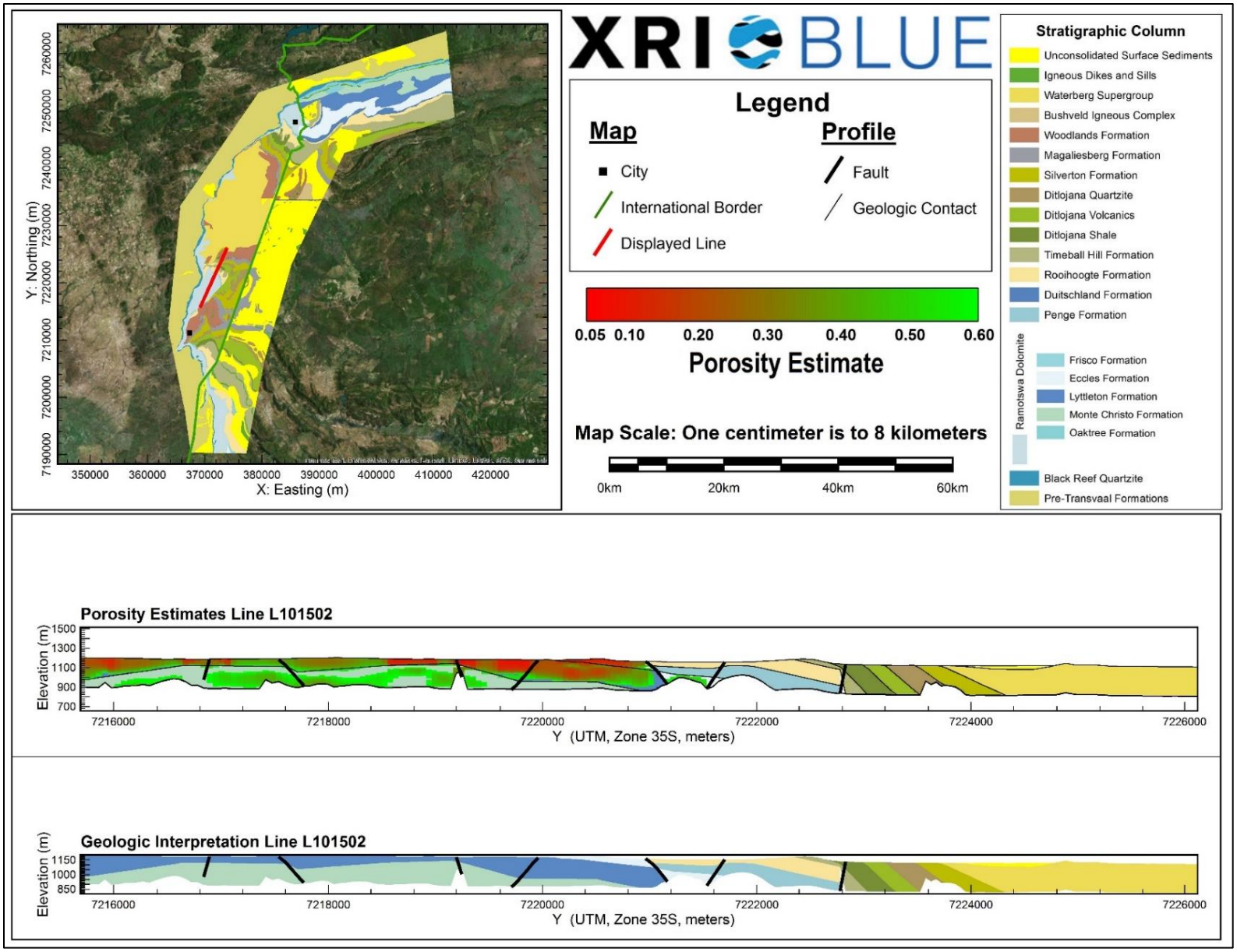

Porosity Estimates and Interpreted Geology Profile for L101502.

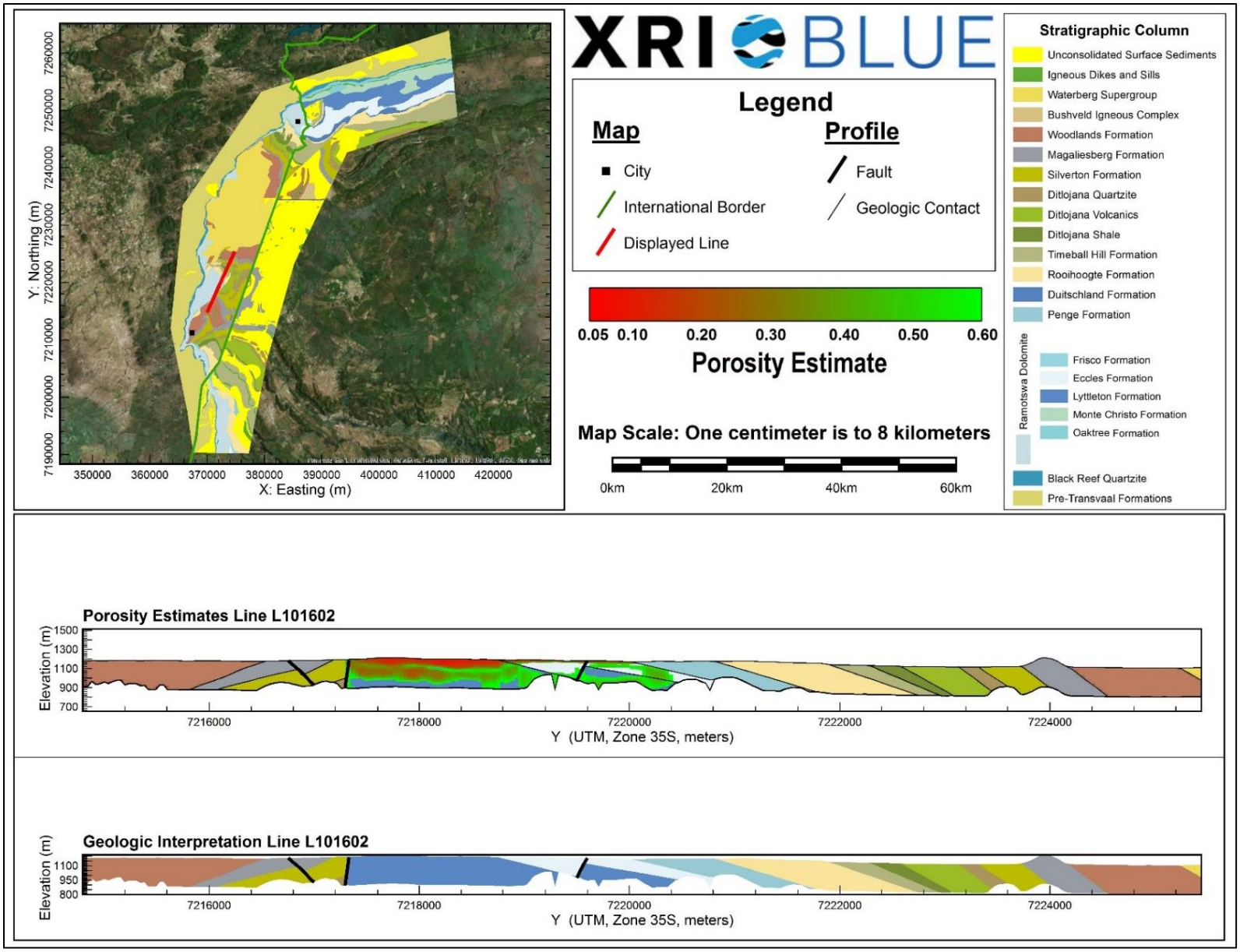

Porosity Estimates and Interpreted Geology Profile for L101602.

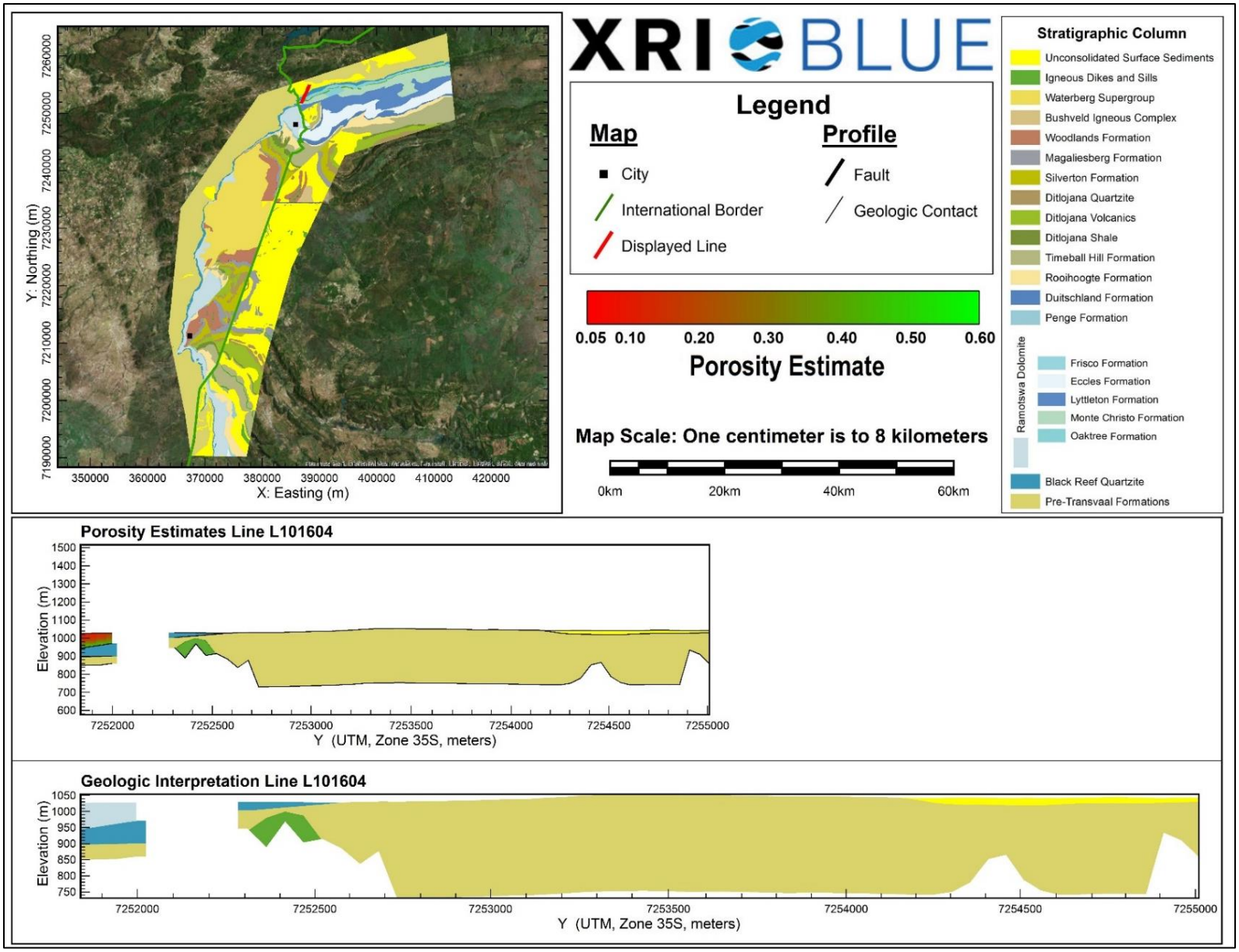

Porosity Estimates and Interpreted Geology Profile for L101604.

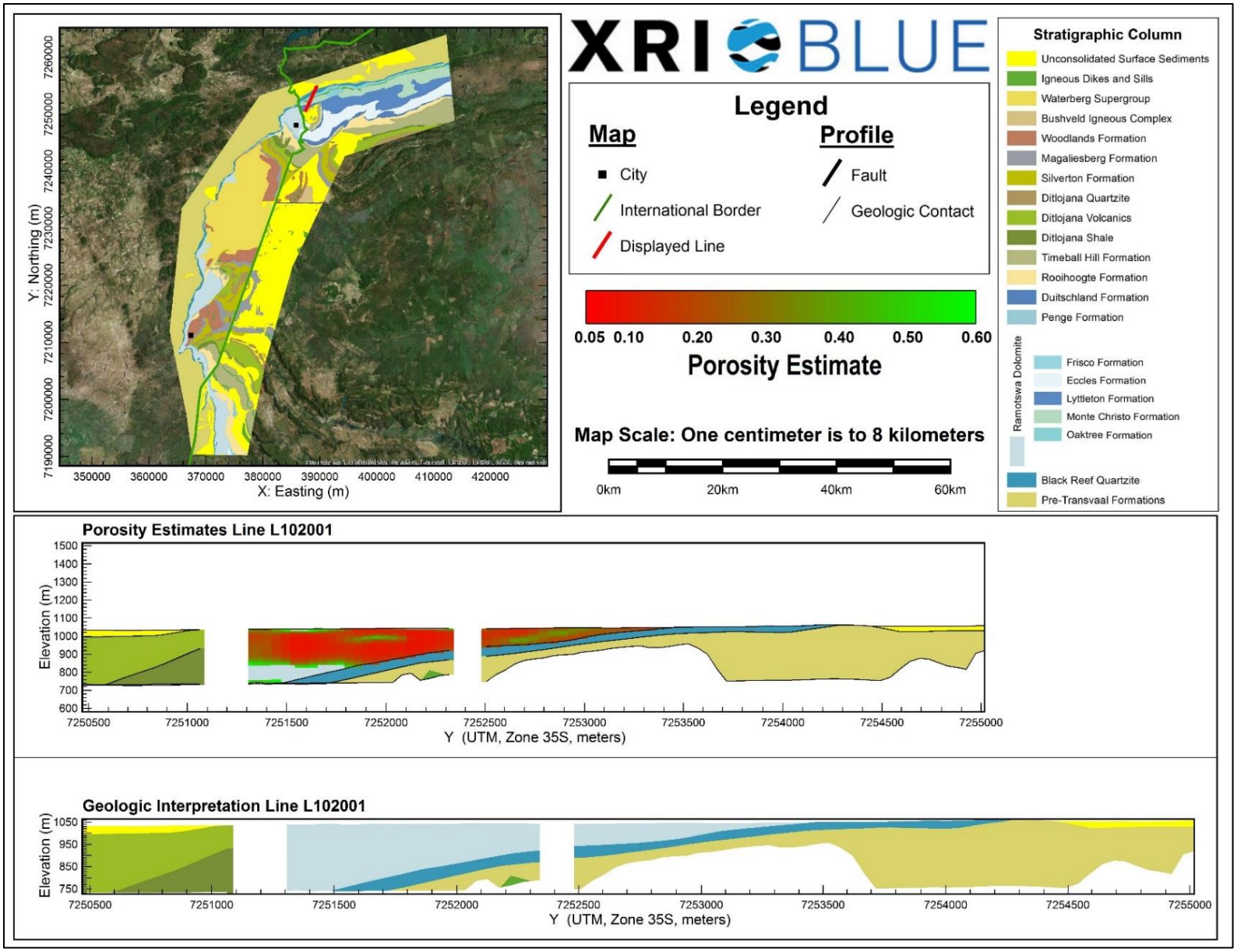

Porosity Estimates and Interpreted Geology Profile for L102001.

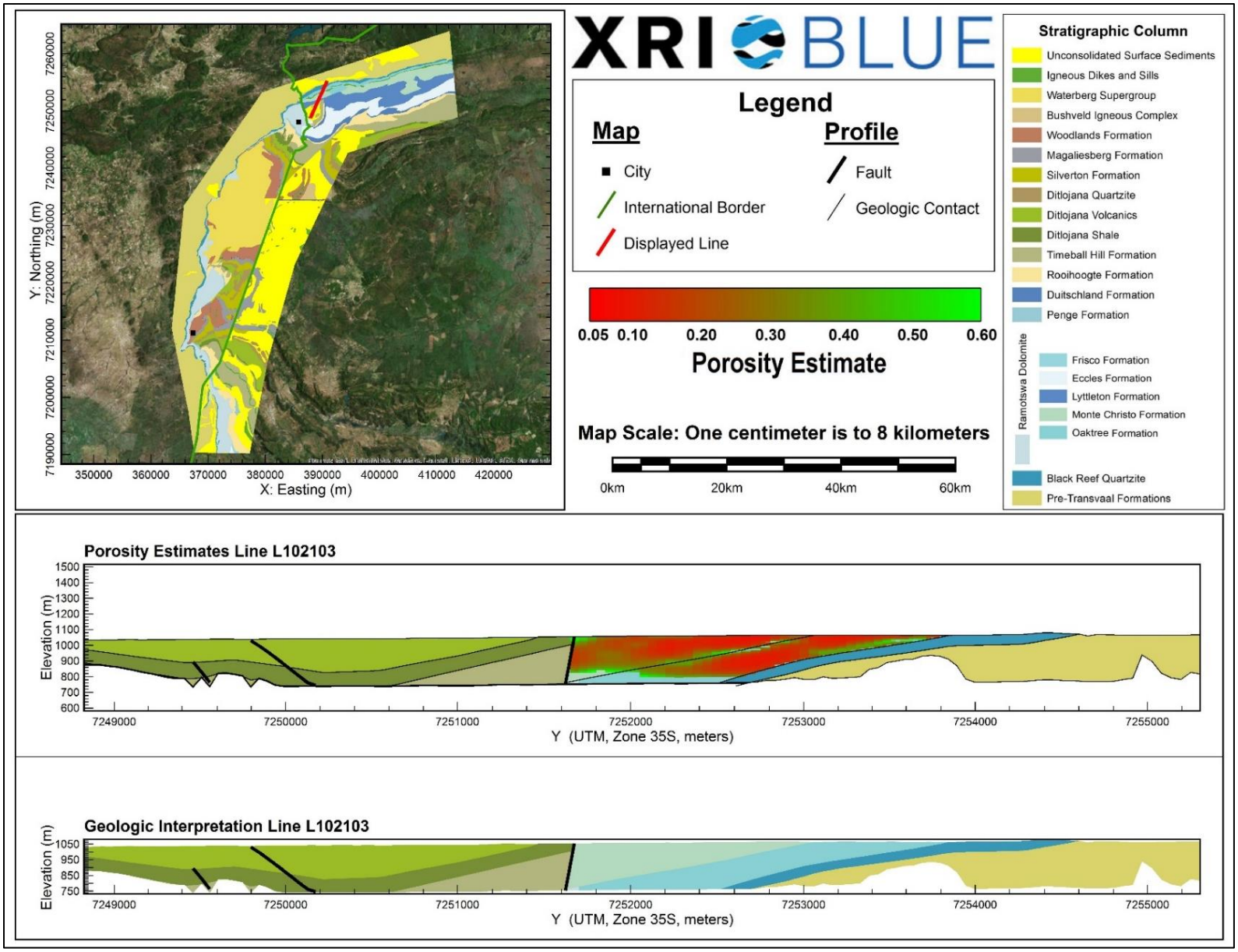

Porosity Estimates and Interpreted Geology Profile for L102103.

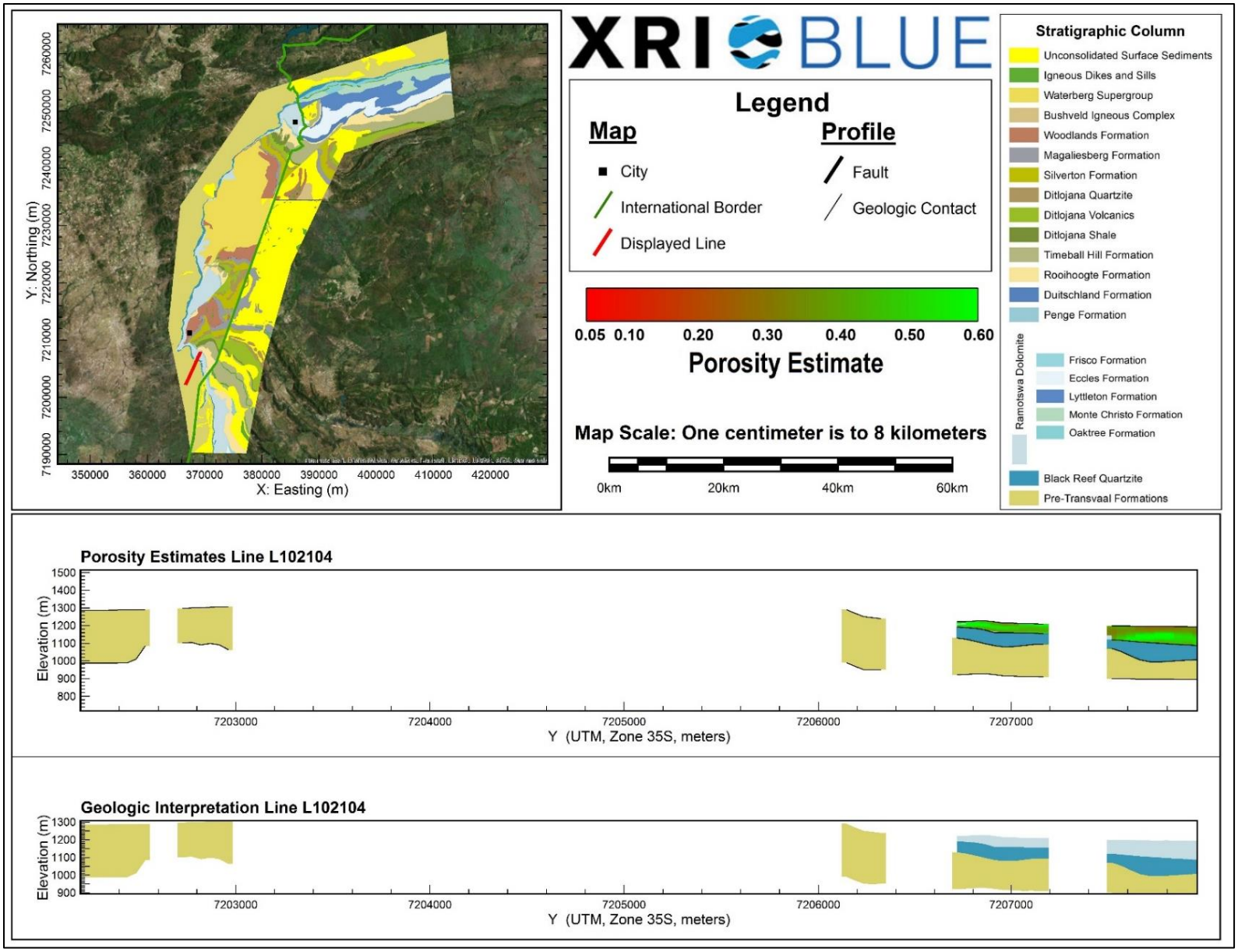

Porosity Estimates and Interpreted Geology Profile for L102104.

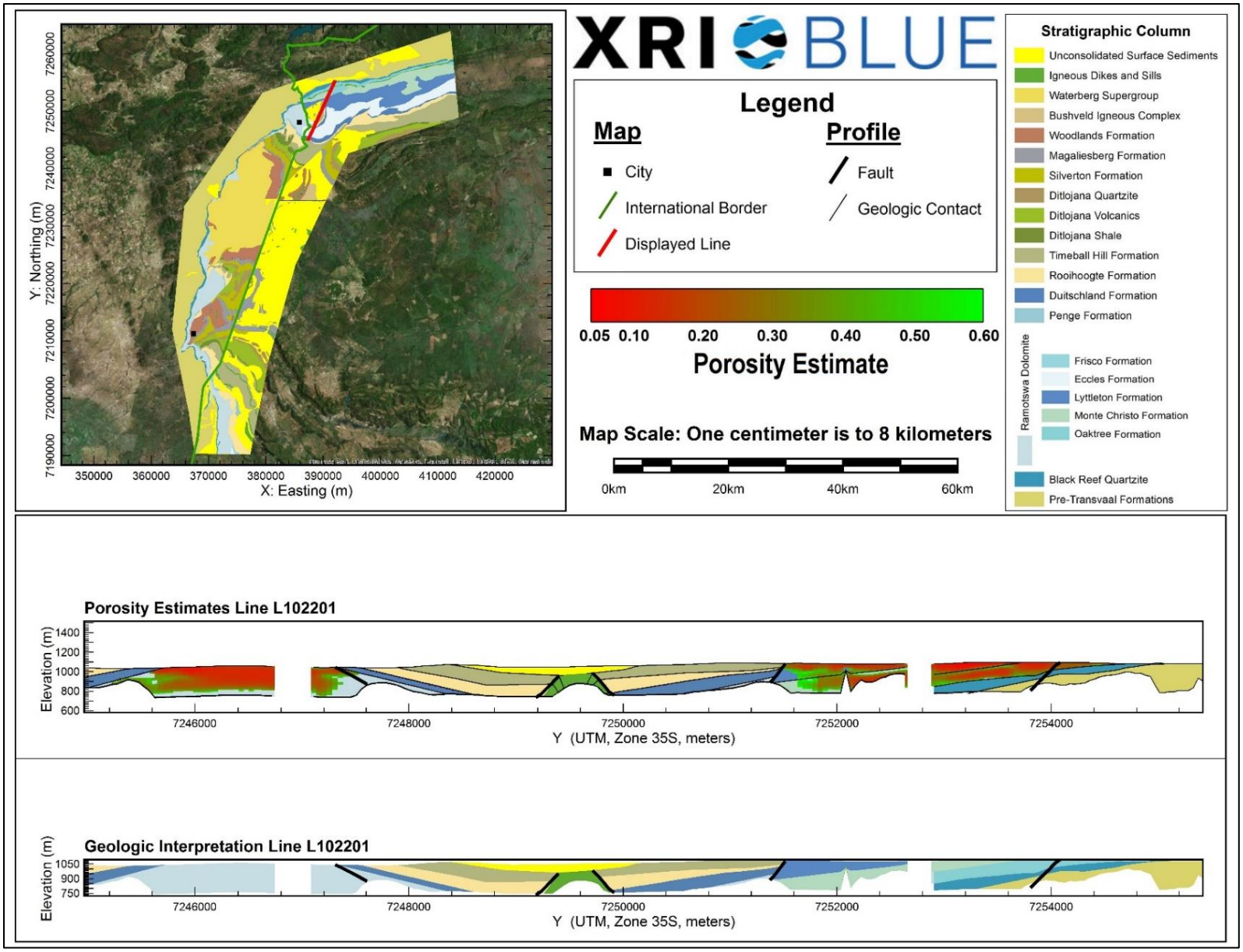

Porosity Estimates and Interpreted Geology Profile for L102201.

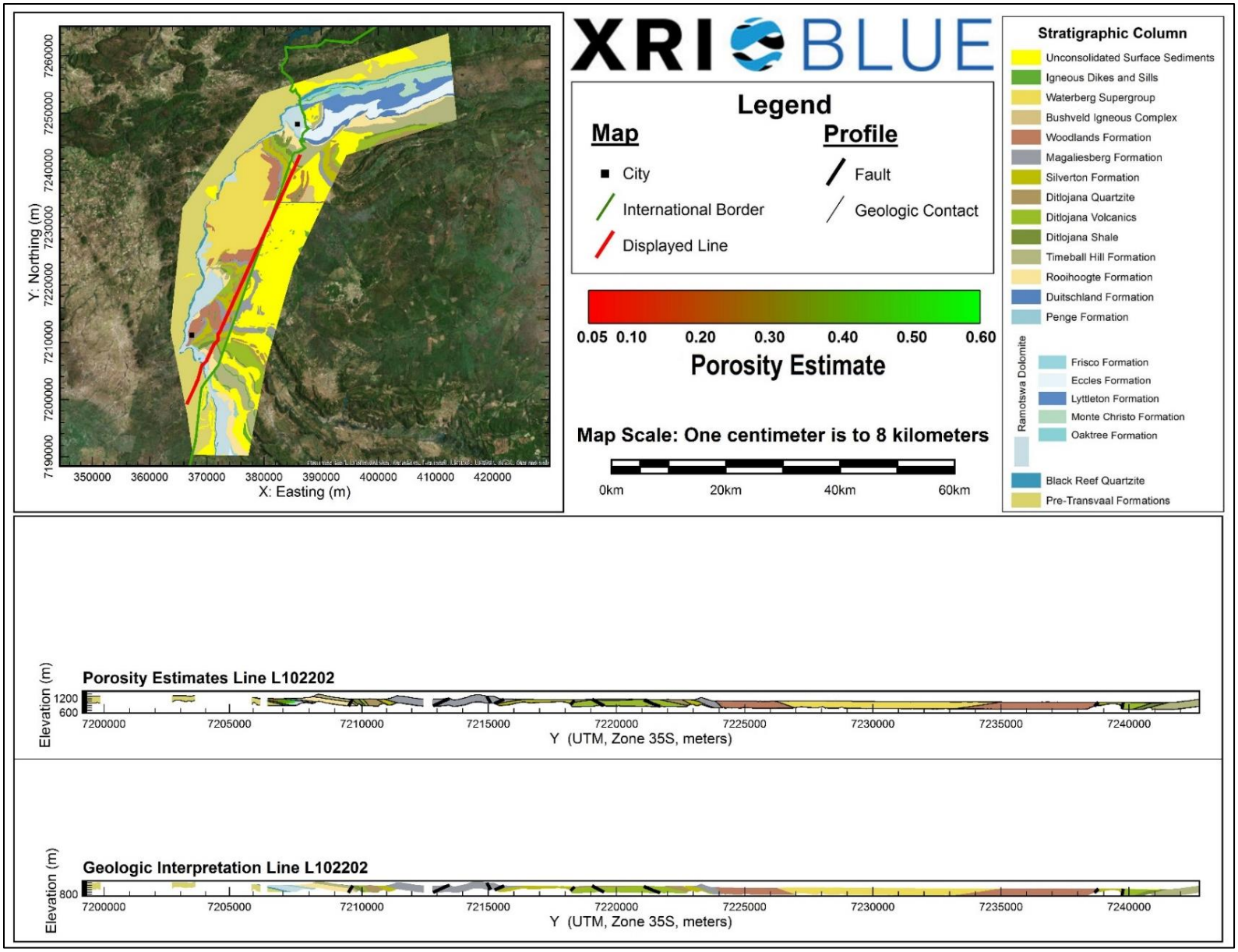

Porosity Estimates and Interpreted Geology Profile for L102202.

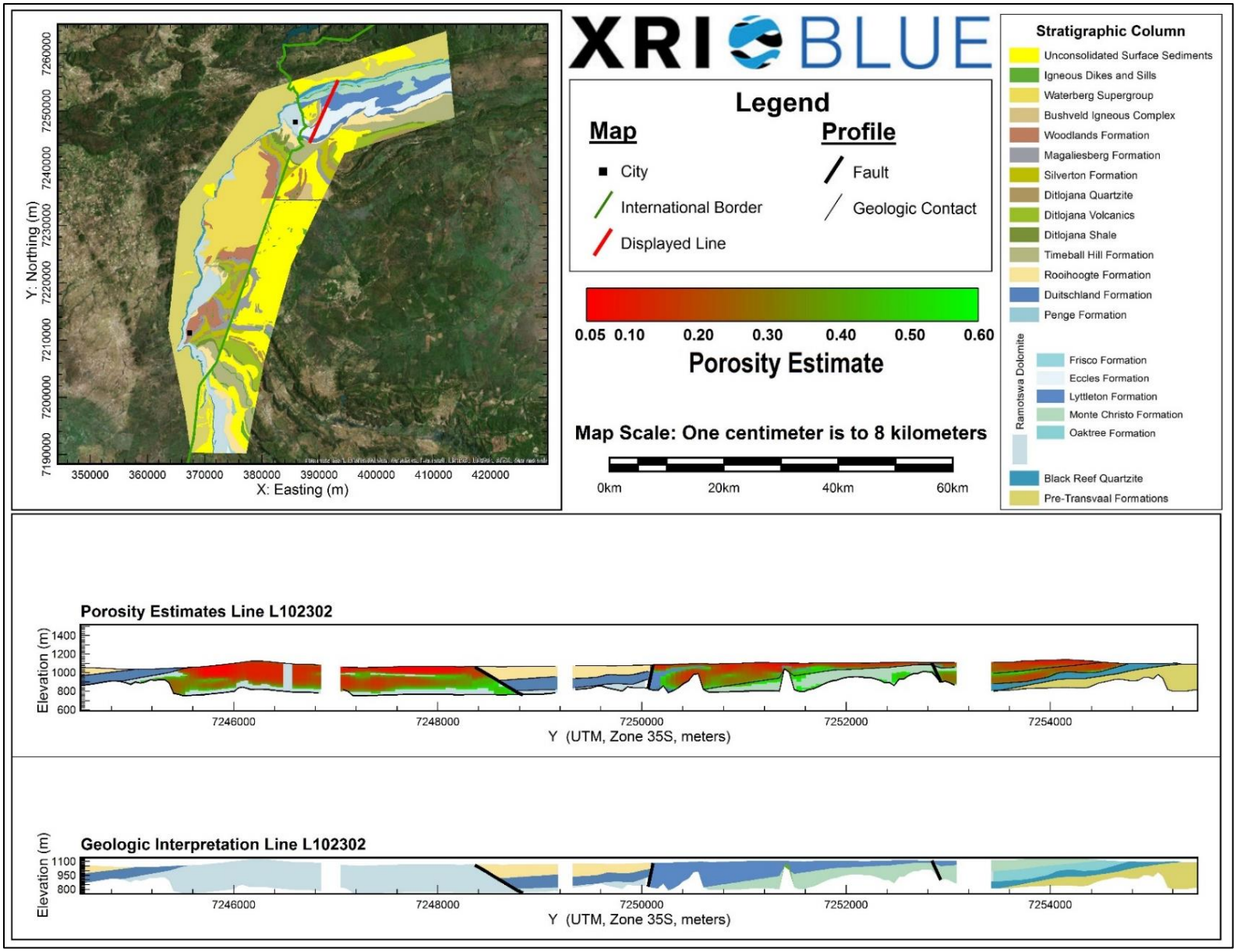

Porosity Estimates and Interpreted Geology Profile for L102302.

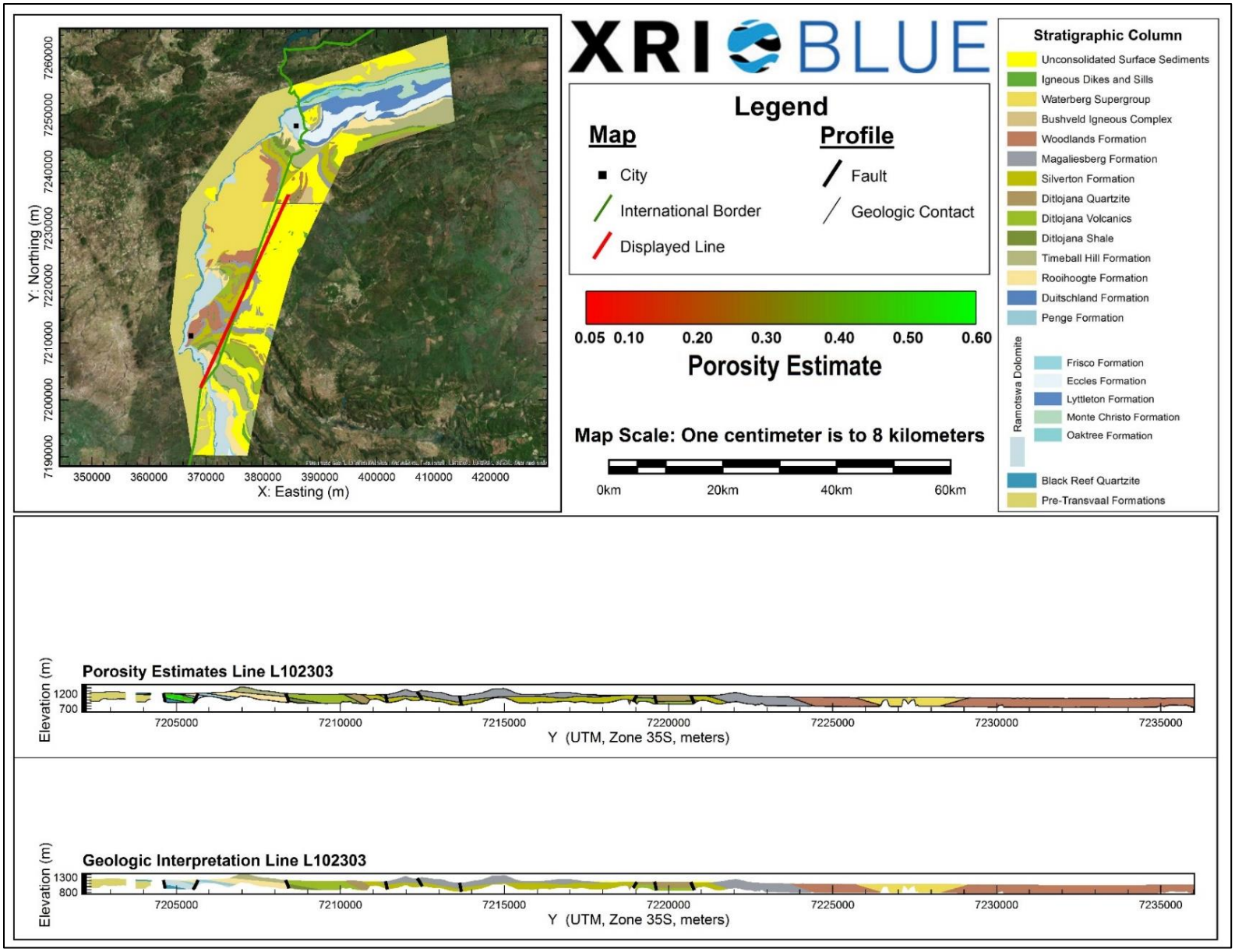

Porosity Estimates and Interpreted Geology Profile for L102303.

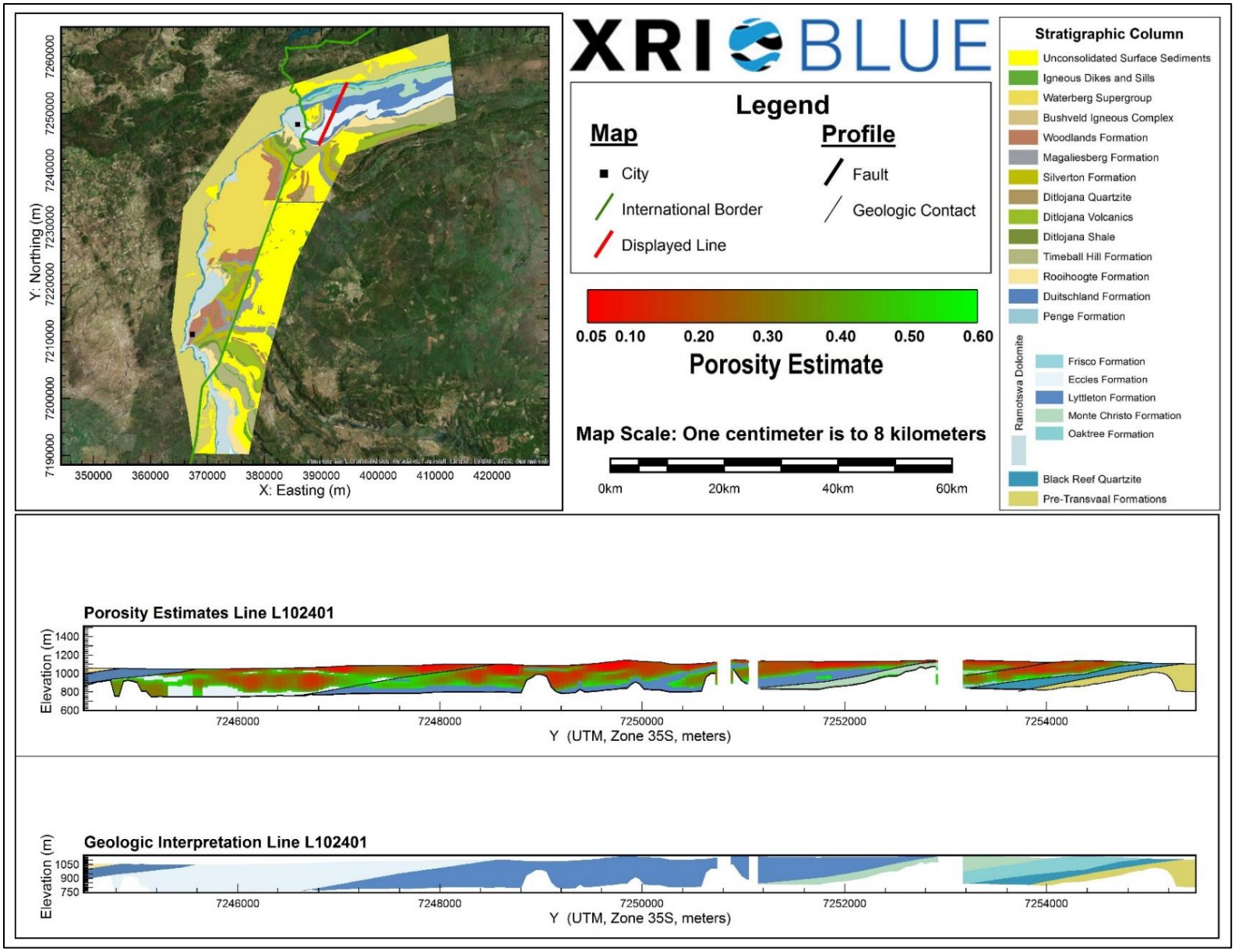

Porosity Estimates and Interpreted Geology Profile for L102401.

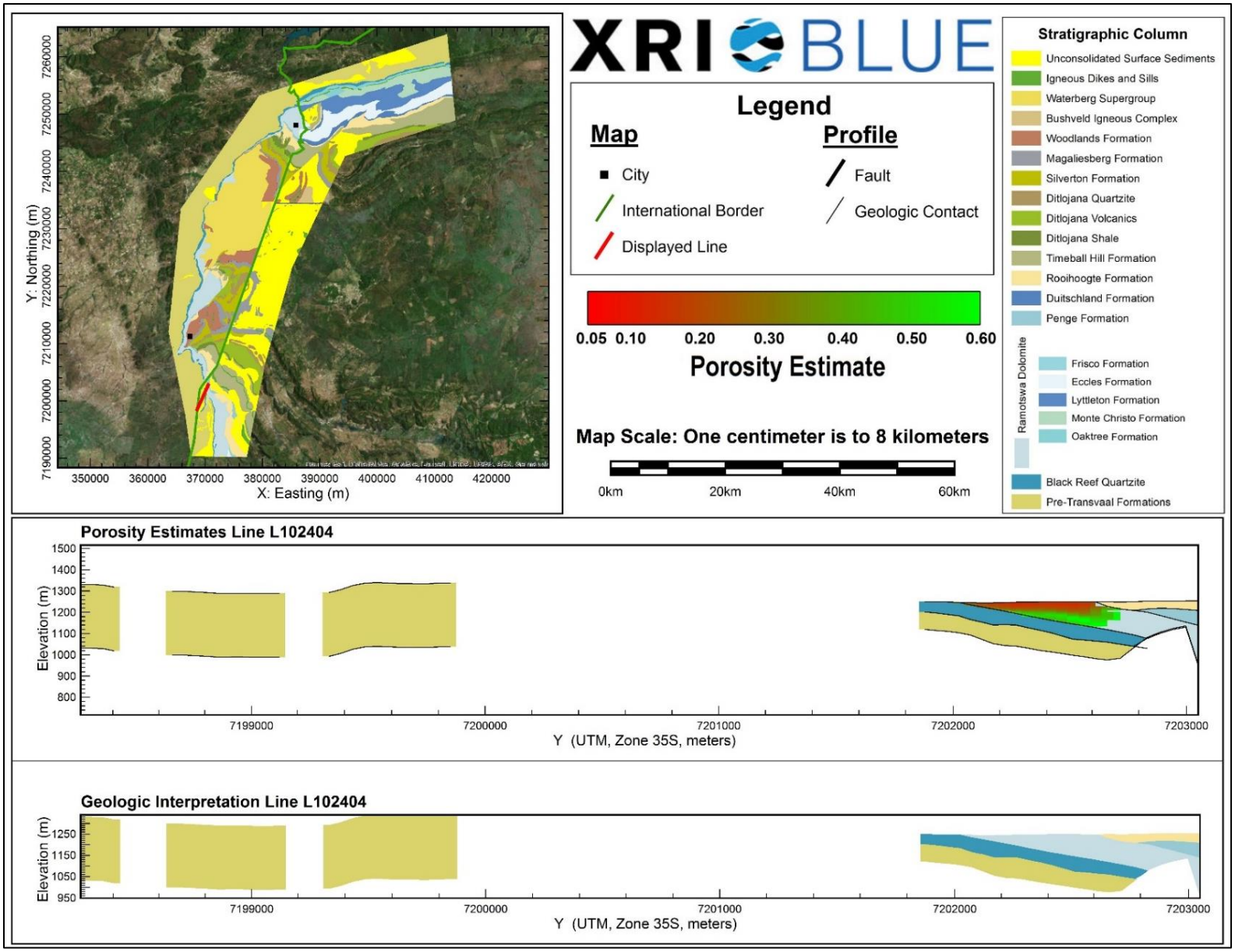

Porosity Estimates and Interpreted Geology Profile for L102404.

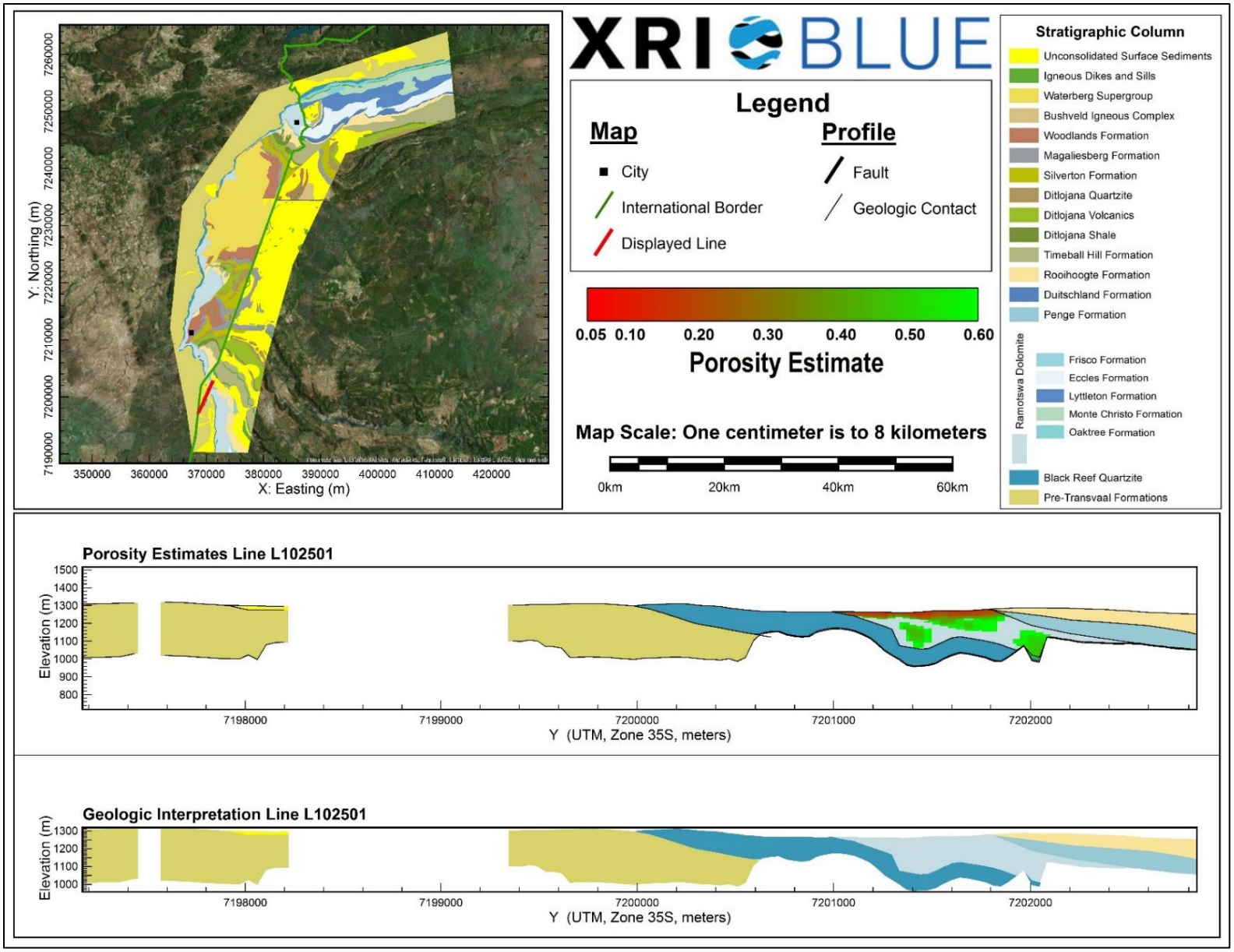

Porosity Estimates and Interpreted Geology Profile for L102501.

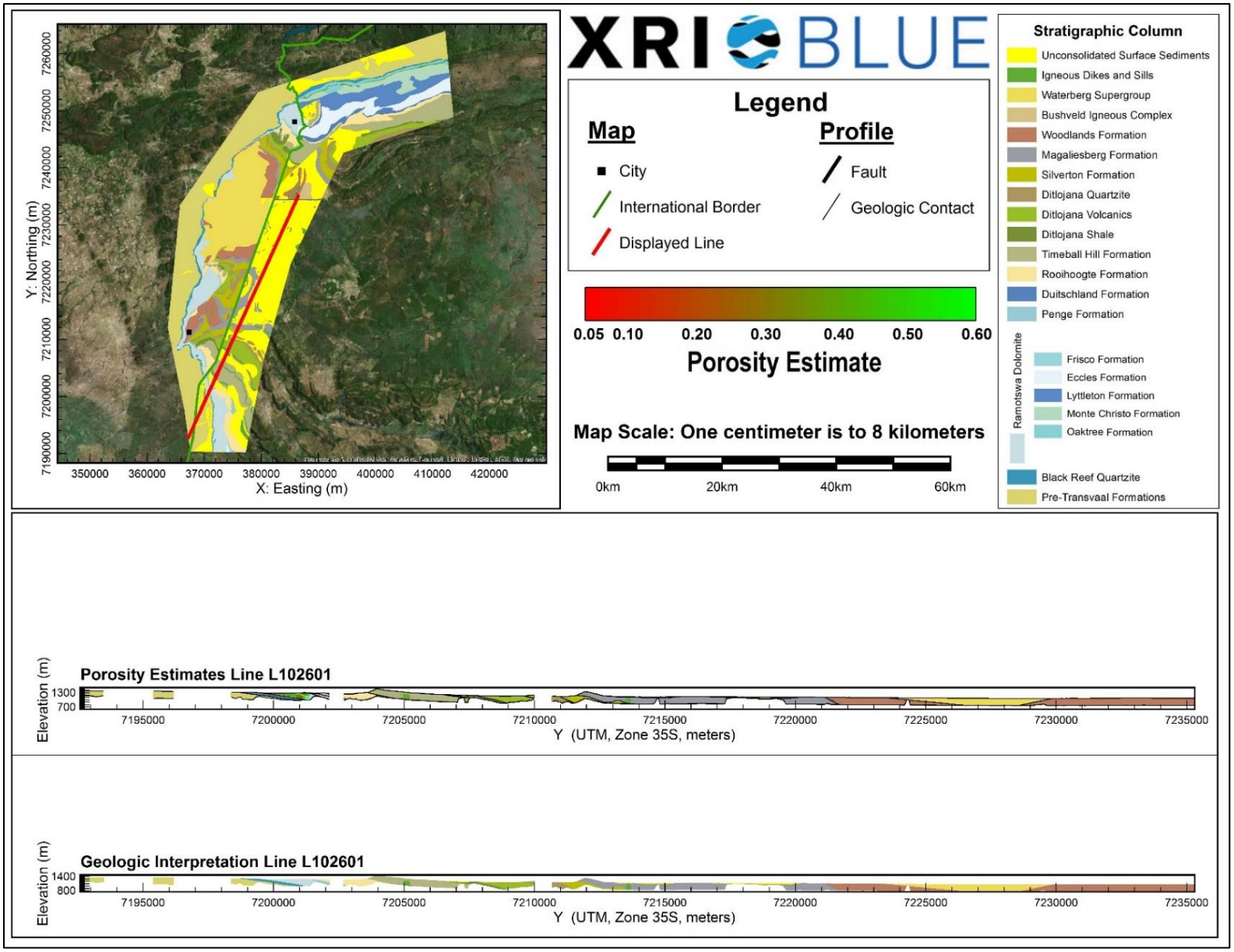

Porosity Estimates and Interpreted Geology Profile for L102601.

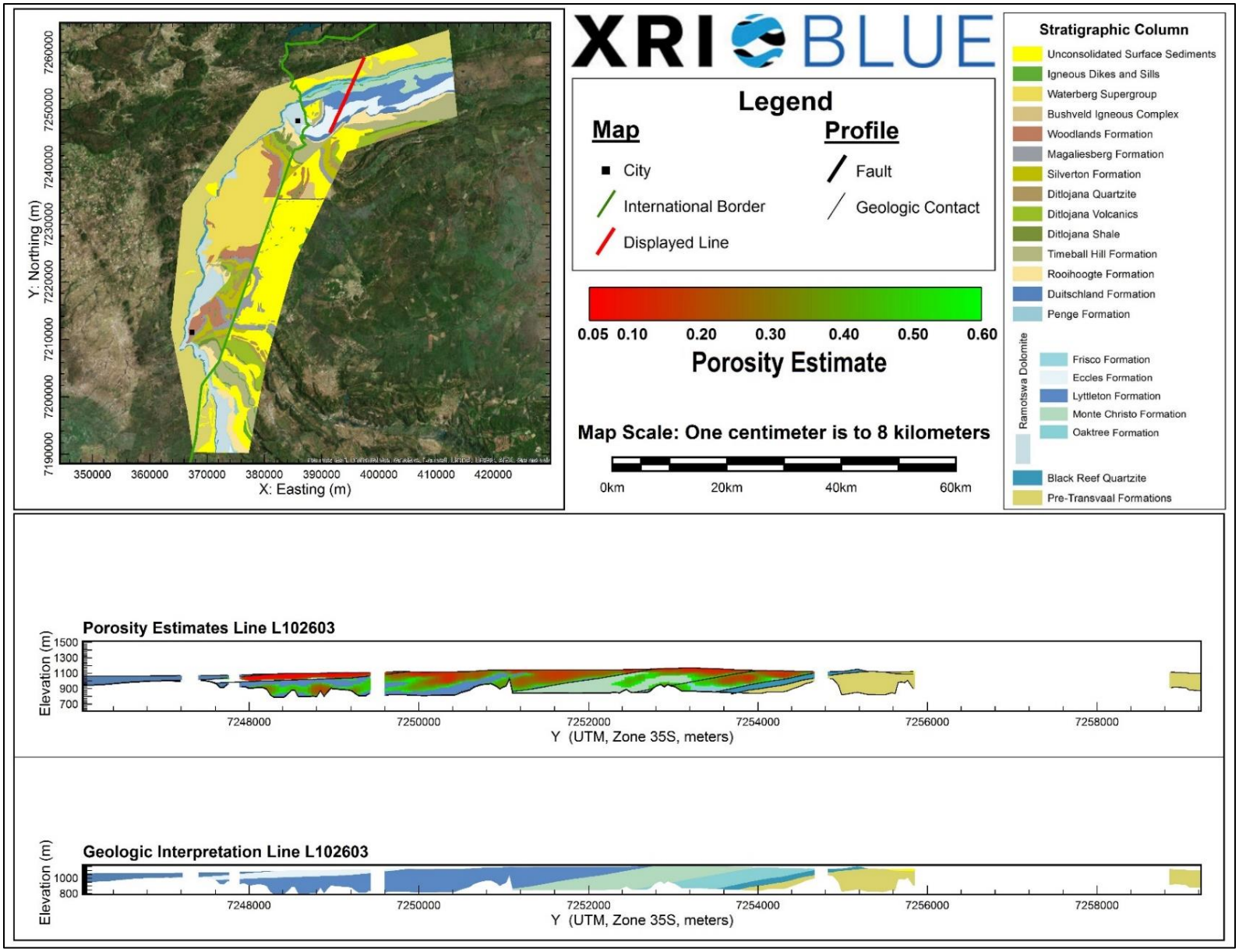

Porosity Estimates and Interpreted Geology Profile for L102603.

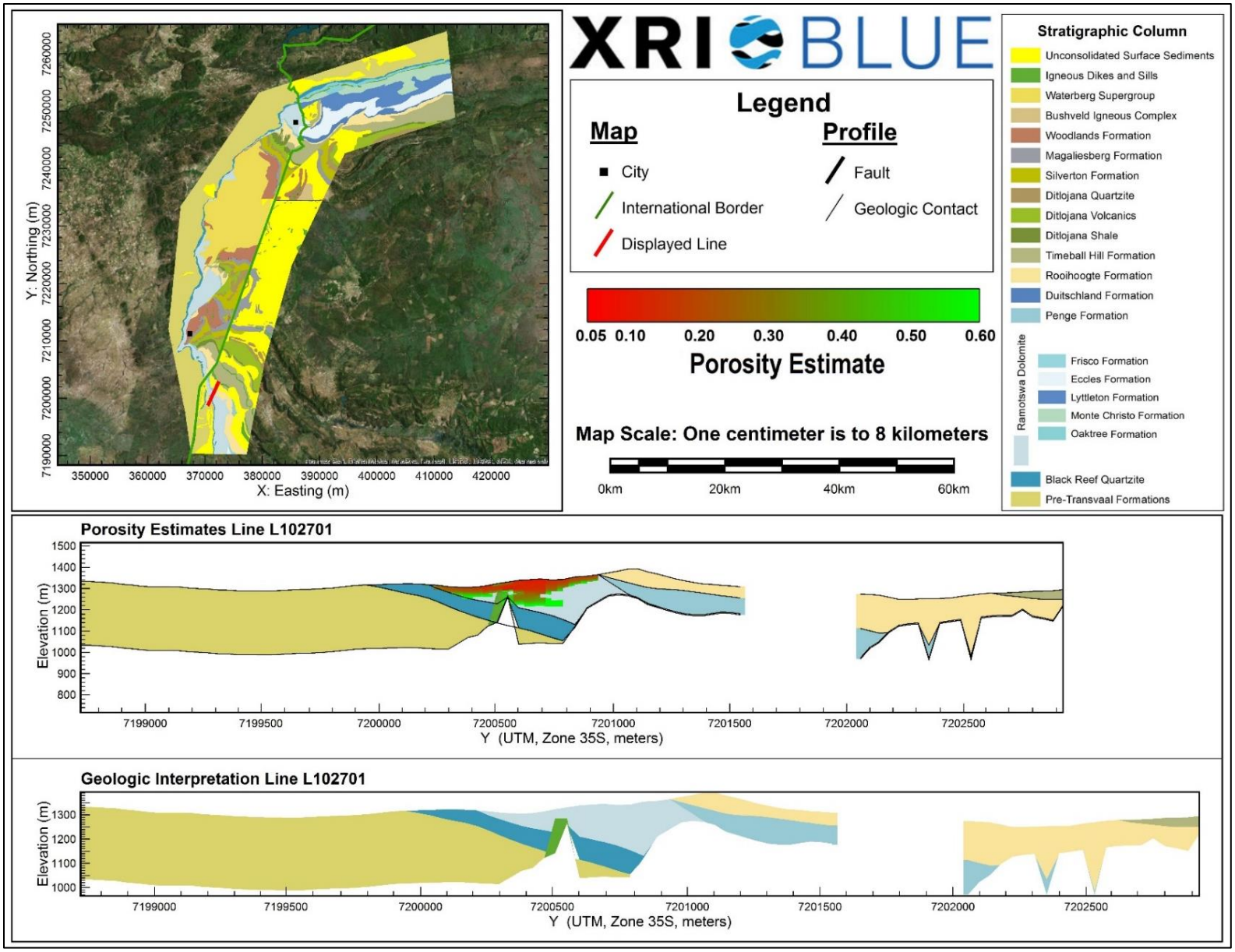

Porosity Estimates and Interpreted Geology Profile for L102701.

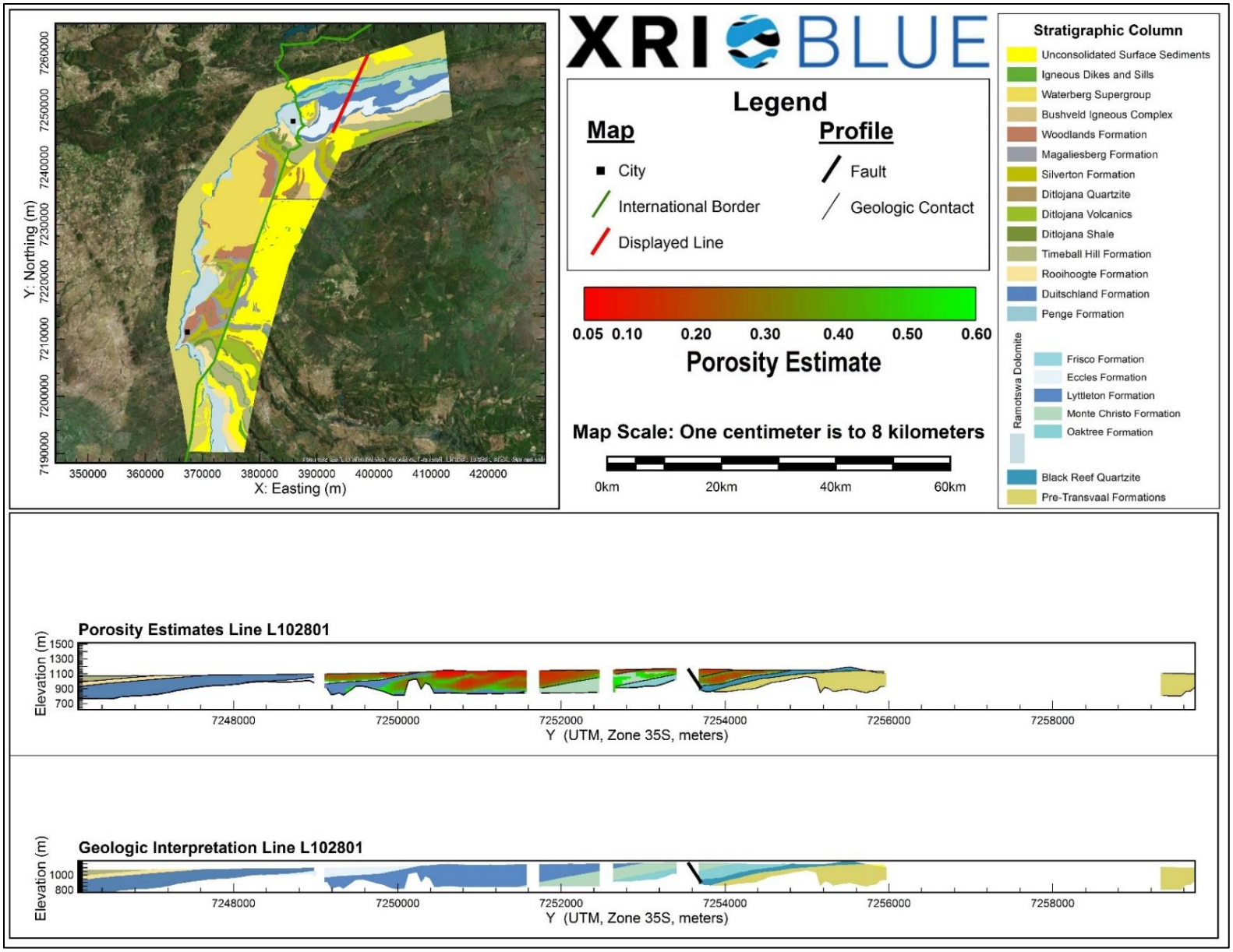

Porosity Estimates and Interpreted Geology Profile for L102801.

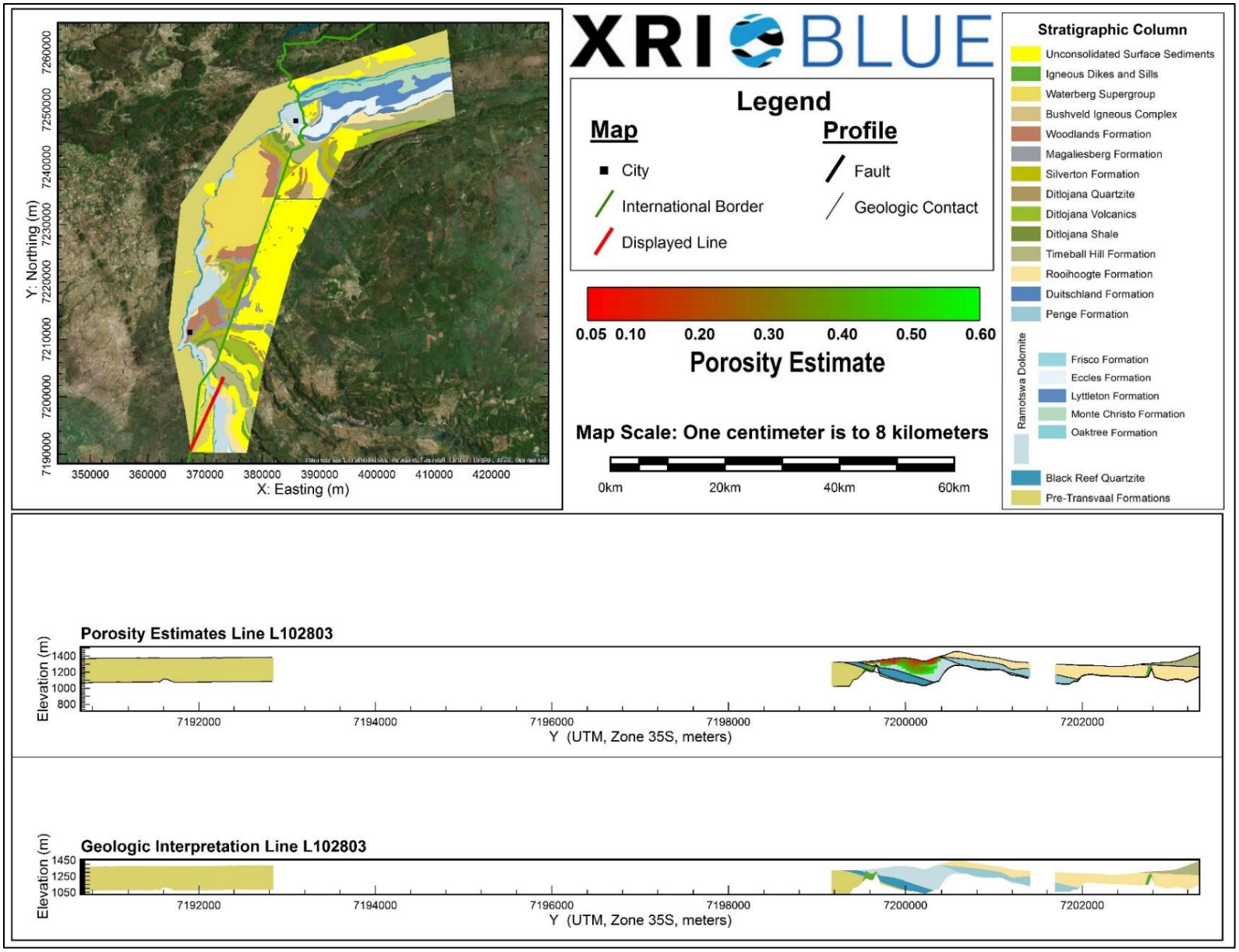

Porosity Estimates and Interpreted Geology Profile for L102803.

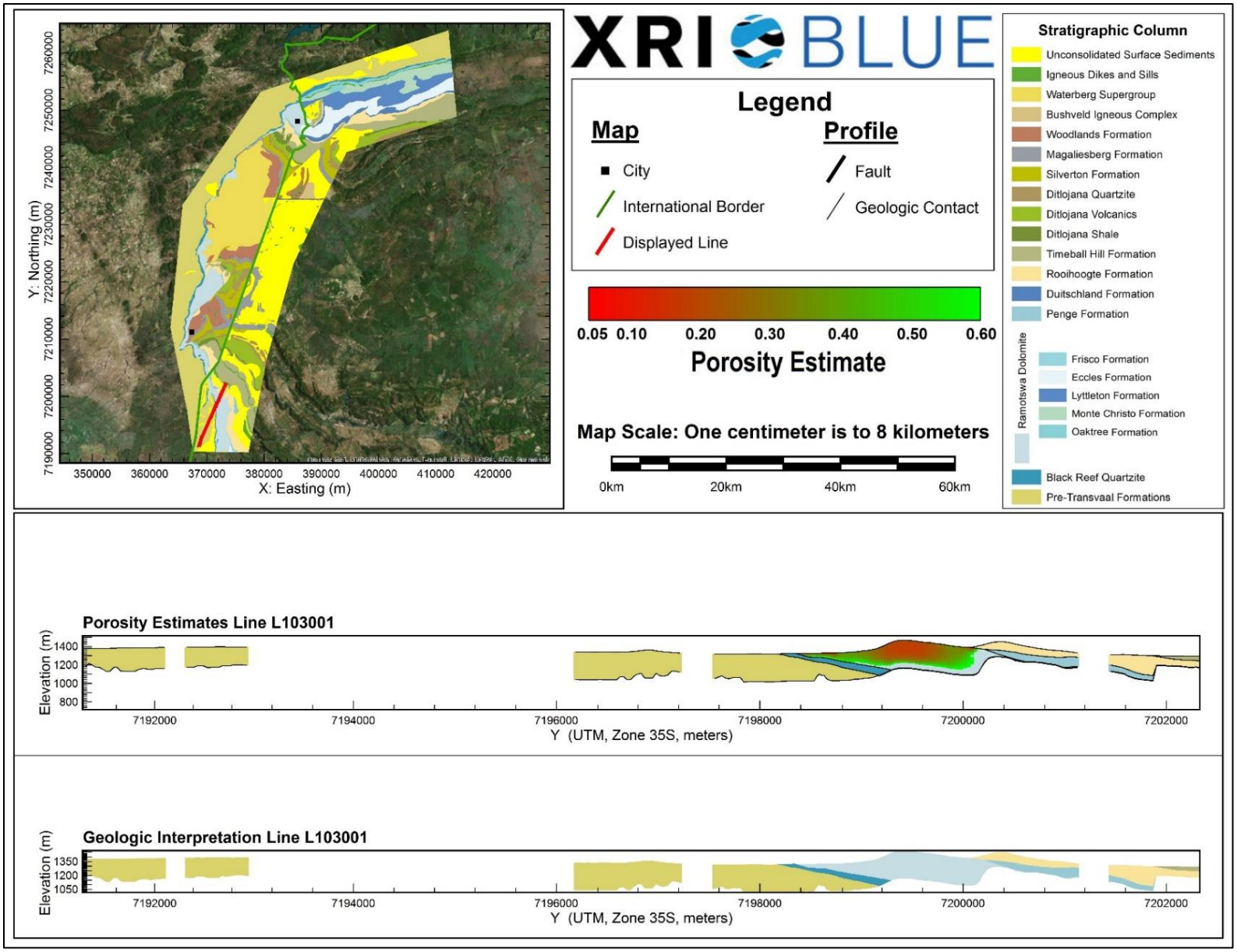

Porosity Estimates and Interpreted Geology Profile for L103001.

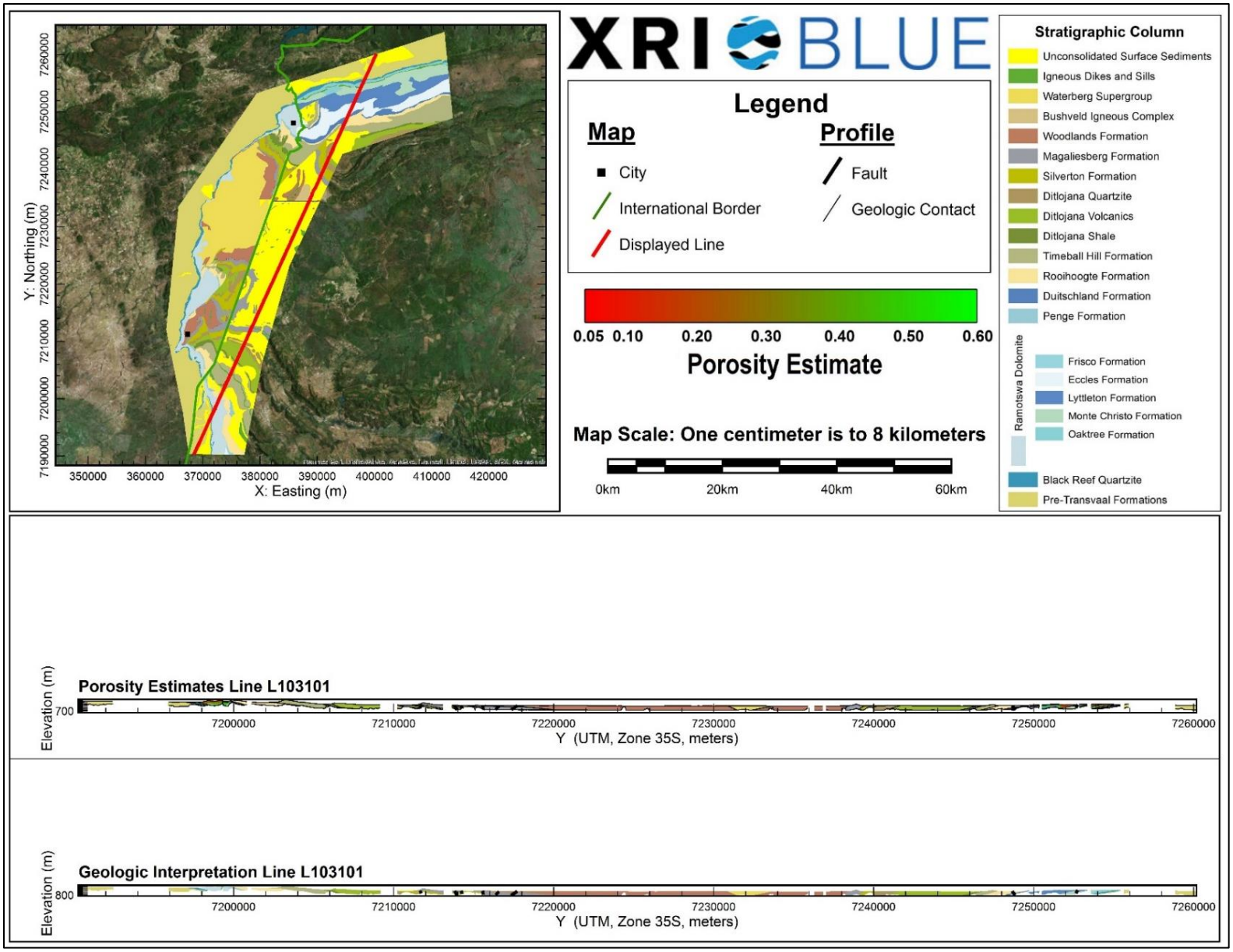

Porosity Estimates and Interpreted Geology Profile for L103101.

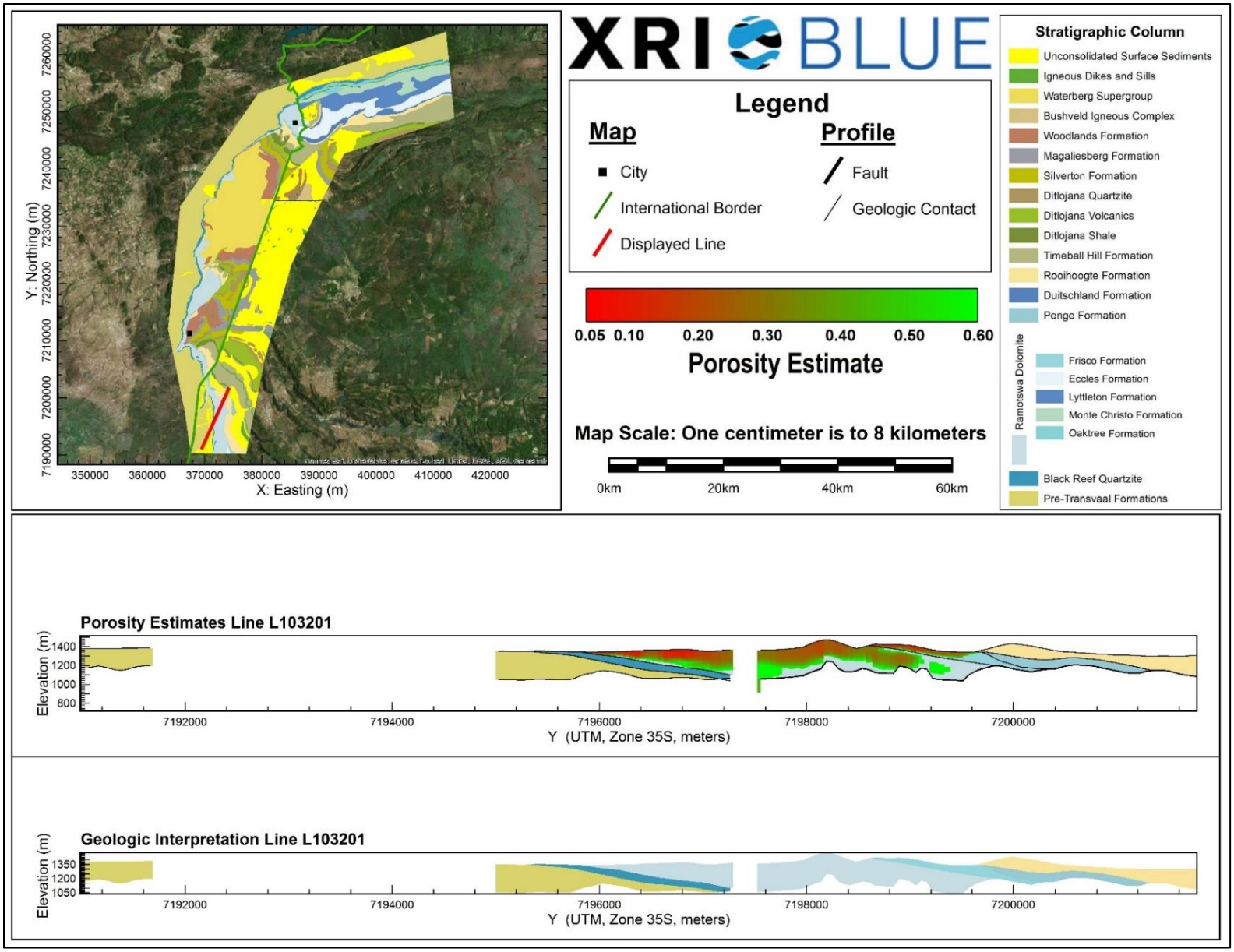

Porosity Estimates and Interpreted Geology Profile for L103201.

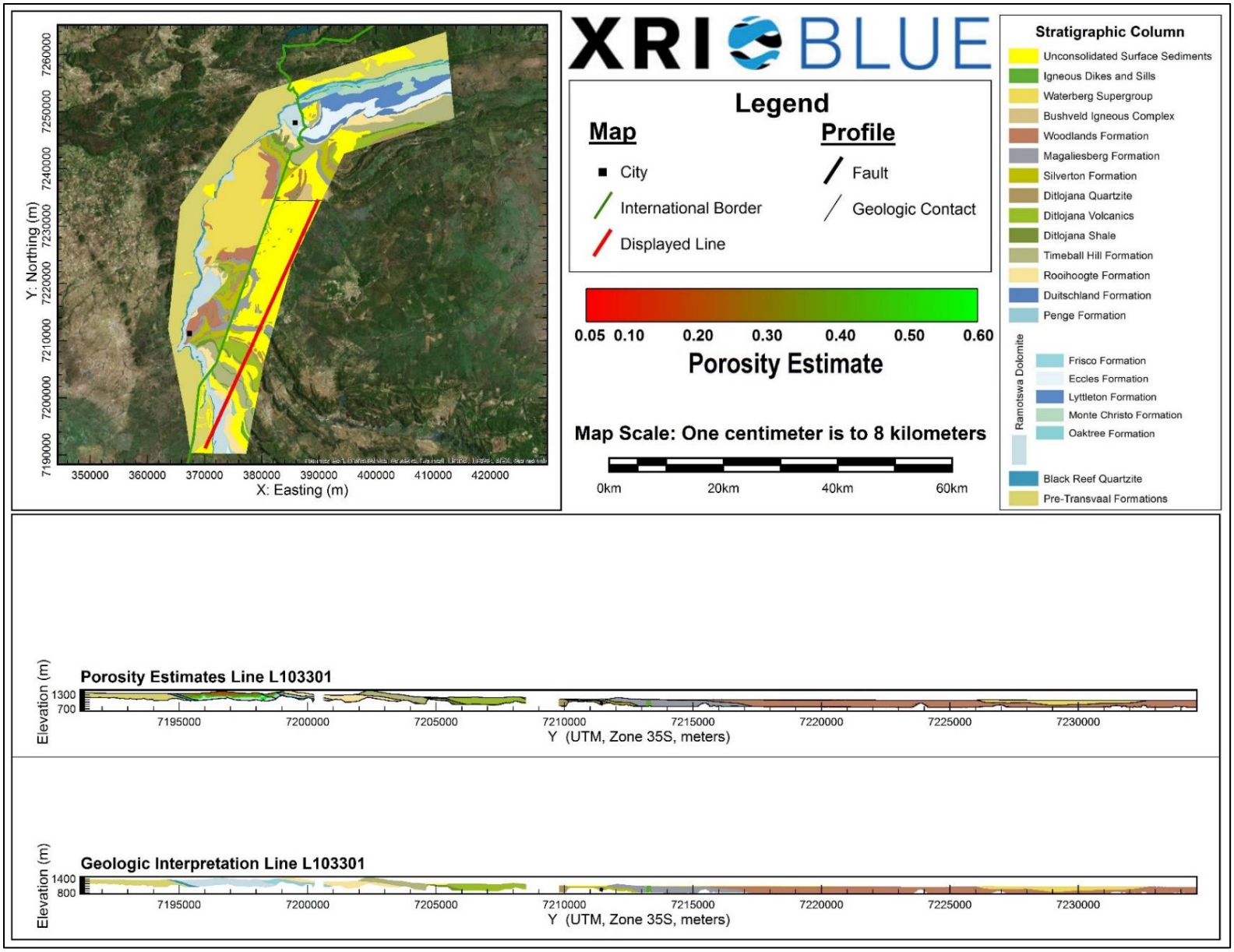

Porosity Estimates and Interpreted Geology Profile for L103301.

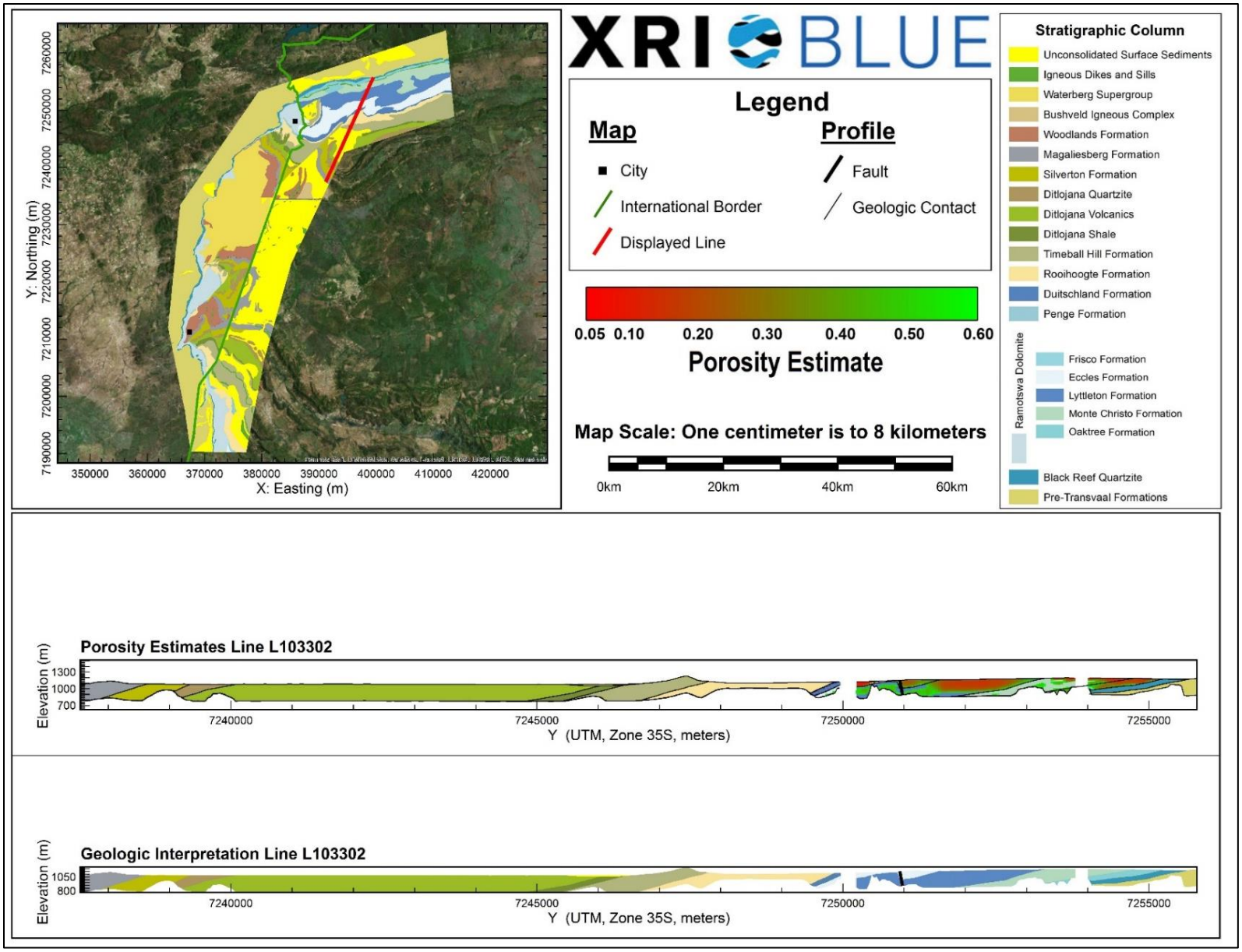

Porosity Estimates and Interpreted Geology Profile for L103302.

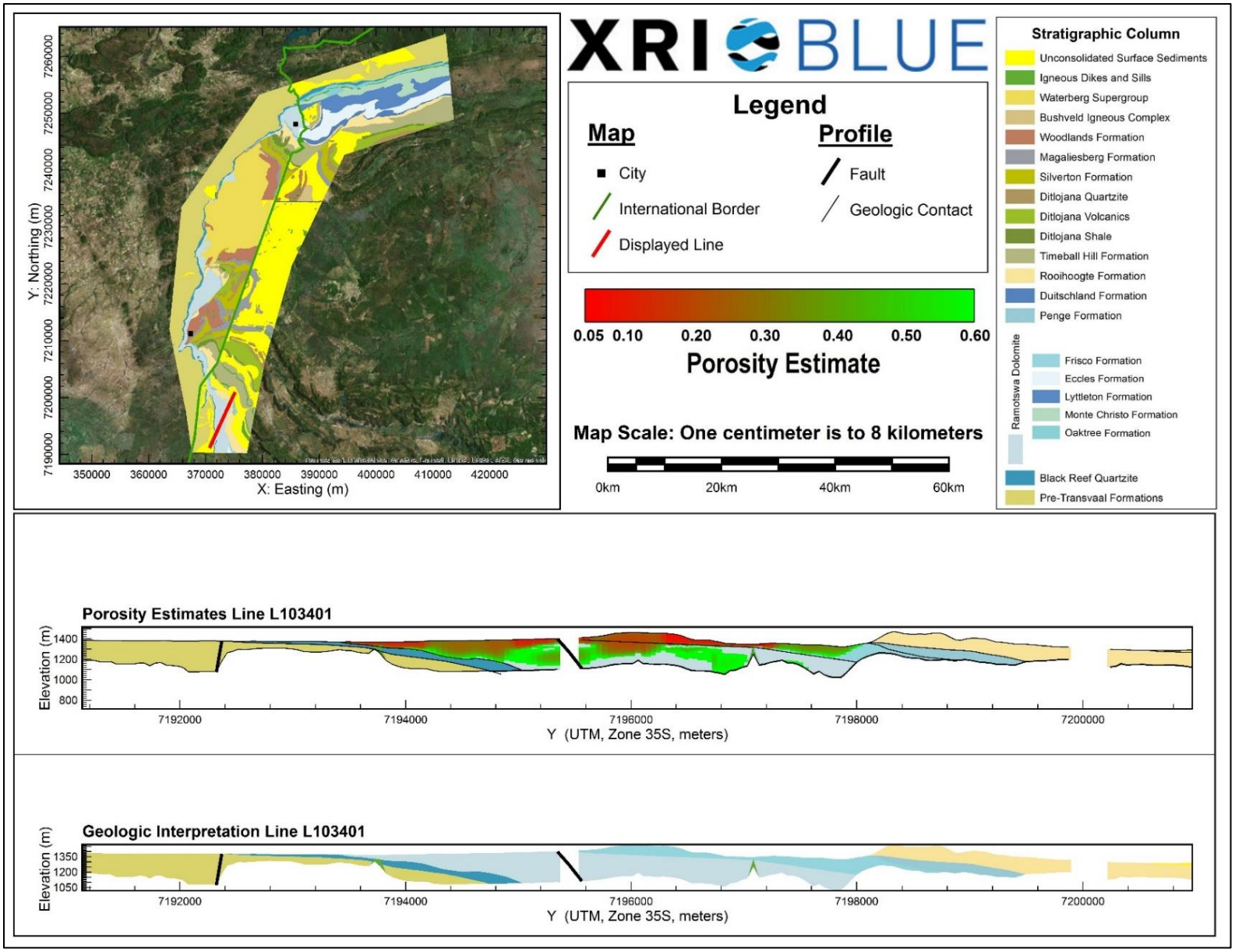

Porosity Estimates and Interpreted Geology Profile for L103401.

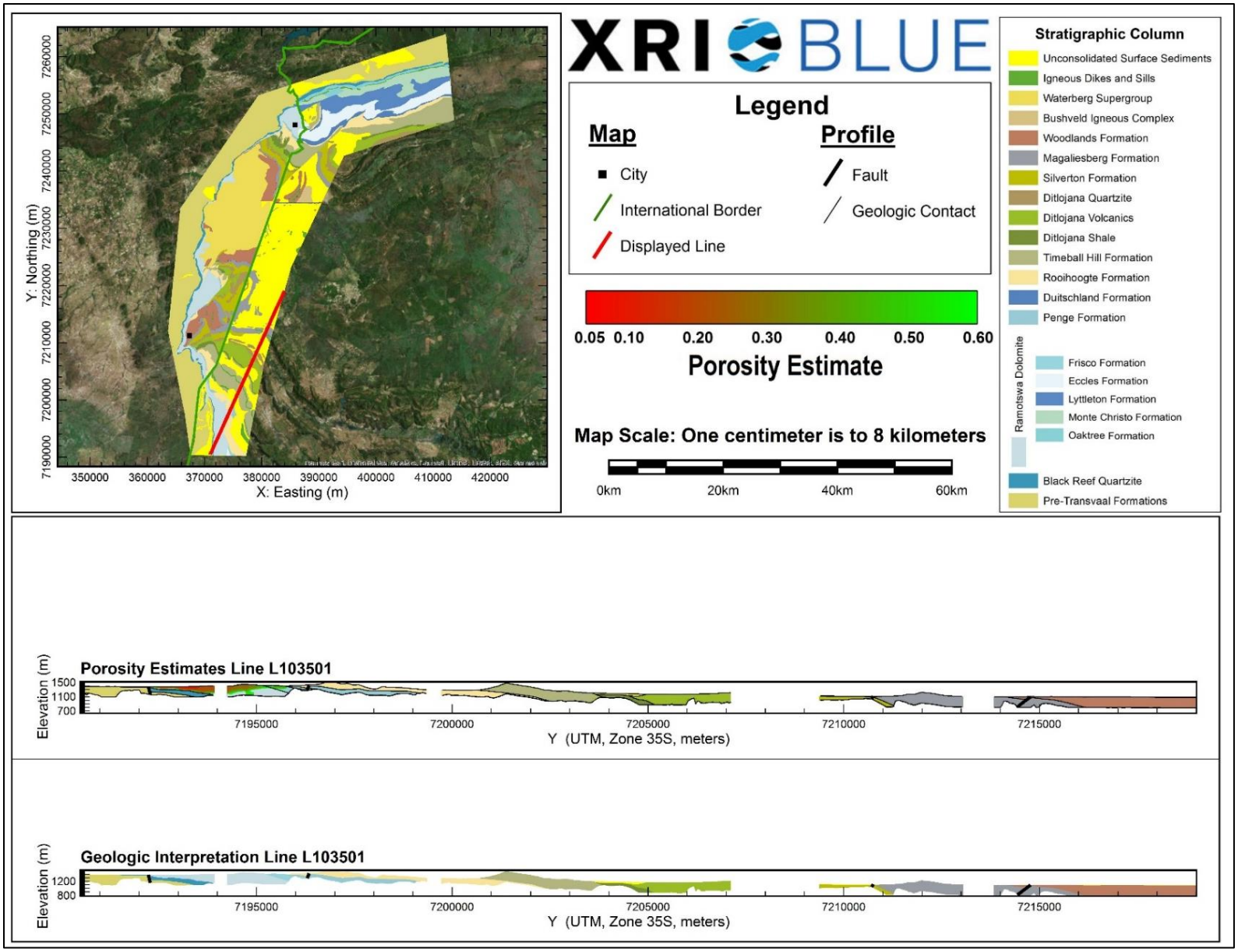

Porosity Estimates and Interpreted Geology Profile for L103501.

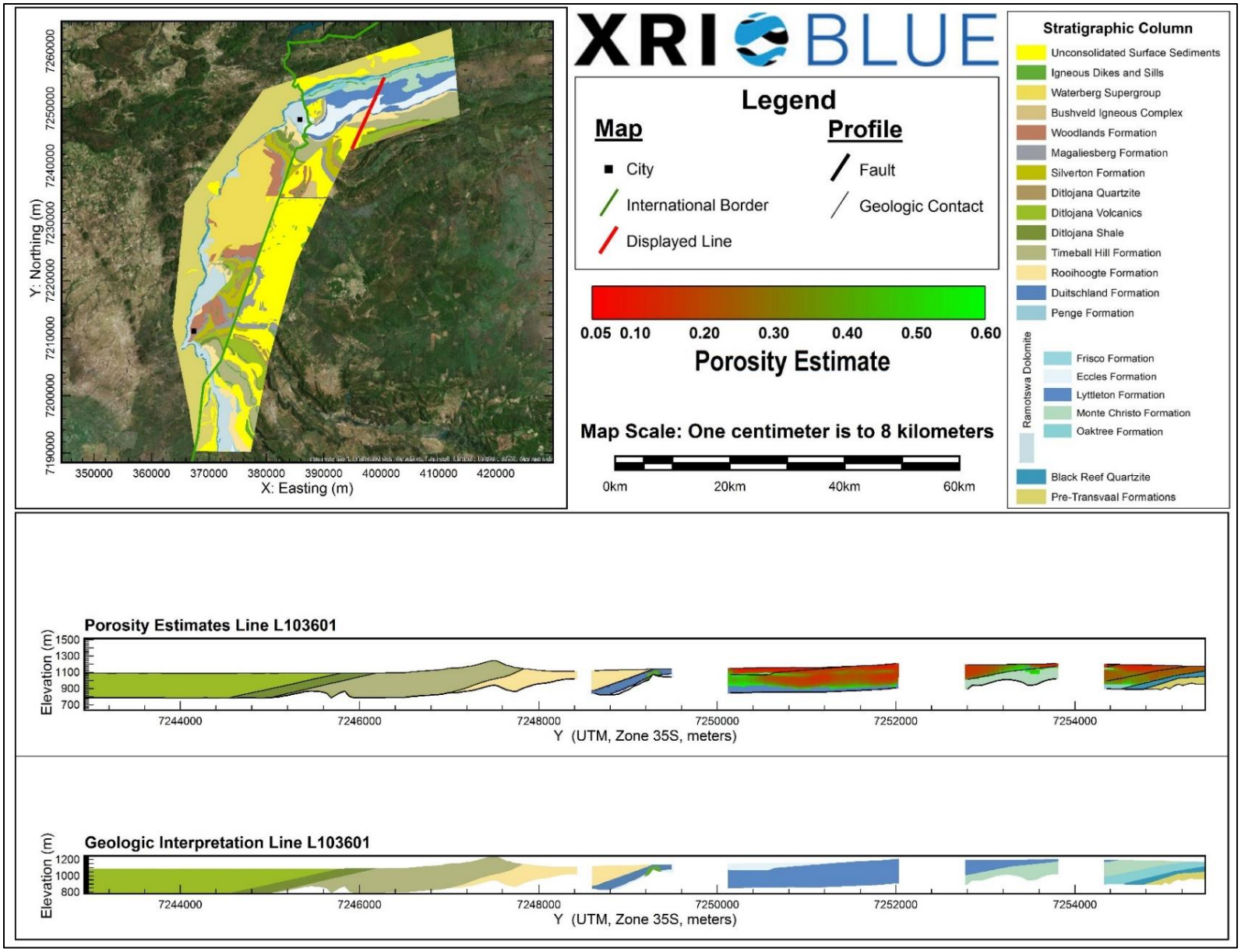

Porosity Estimates and Interpreted Geology Profile for L103601.

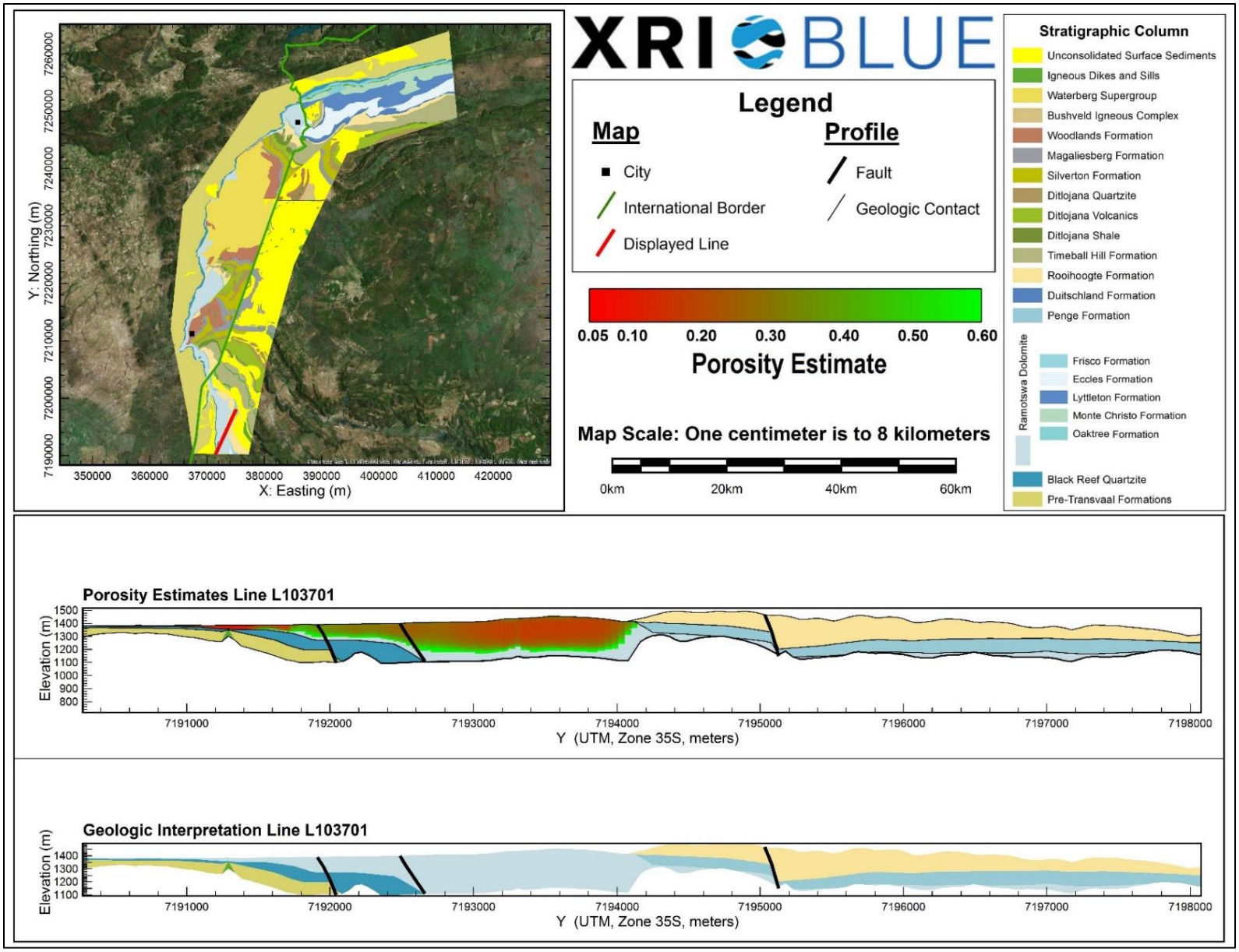

Porosity Estimates and Interpreted Geology Profile for L103701.

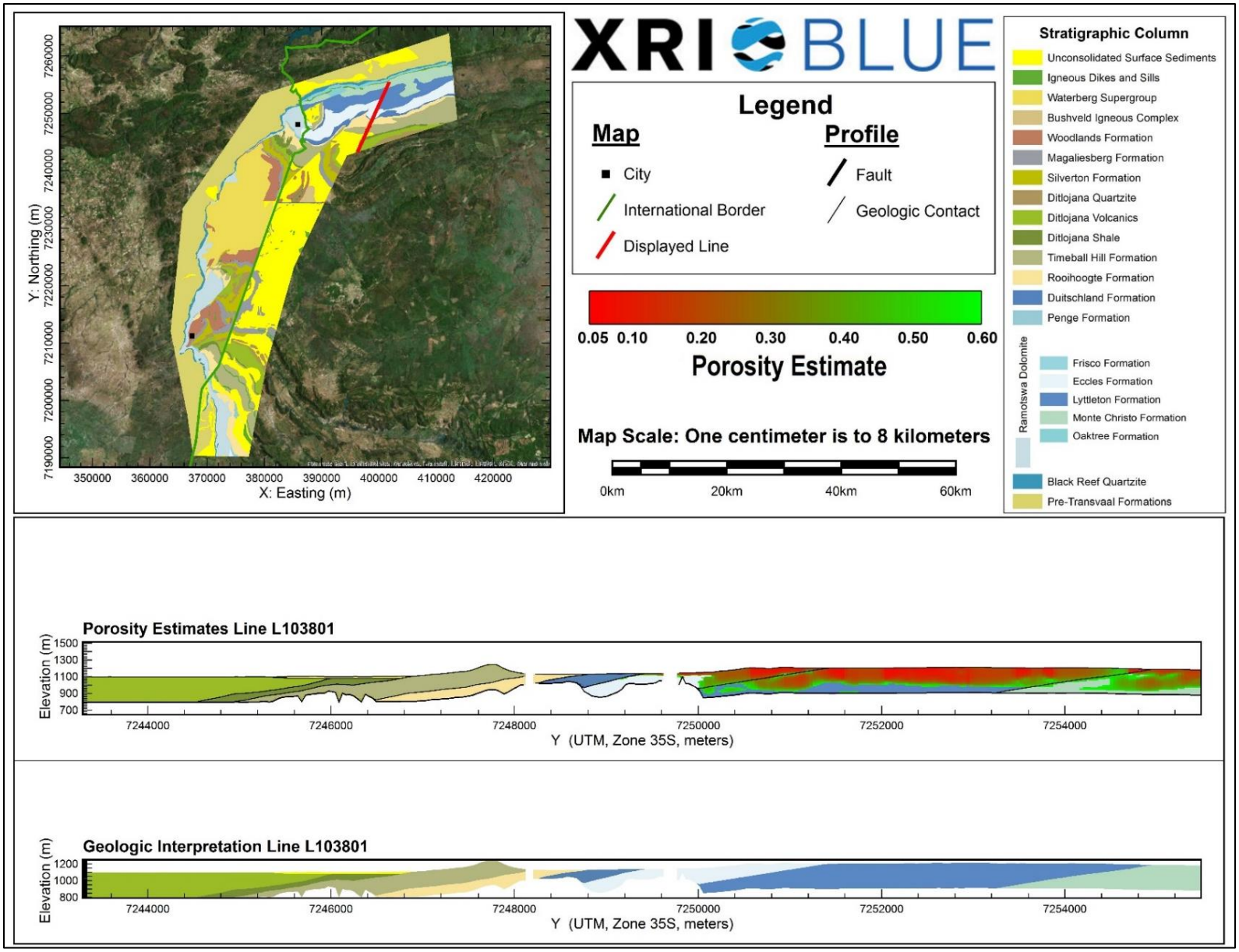

Porosity Estimates and Interpreted Geology Profile for L103801.

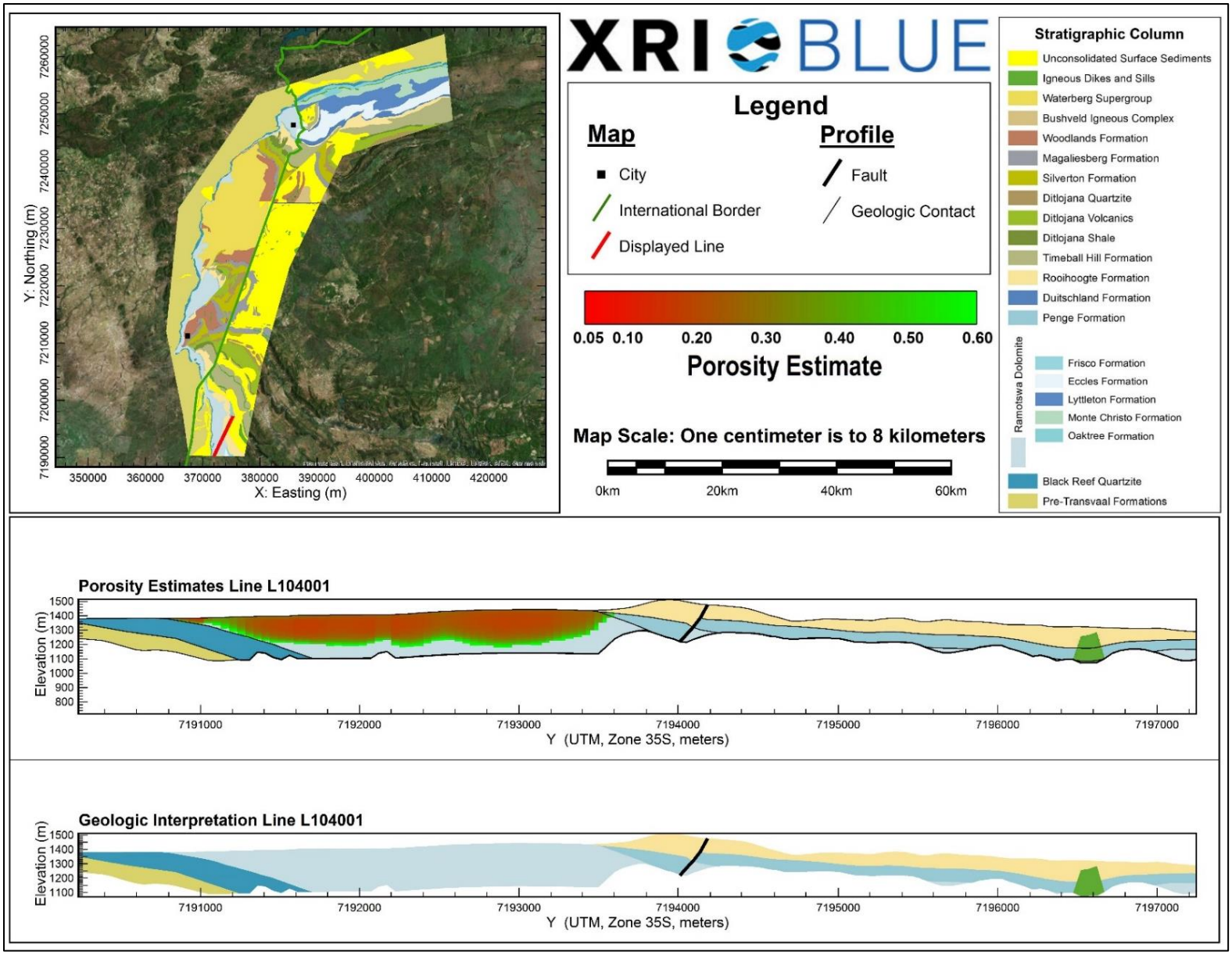

Porosity Estimates and Interpreted Geology Profile for L104001.

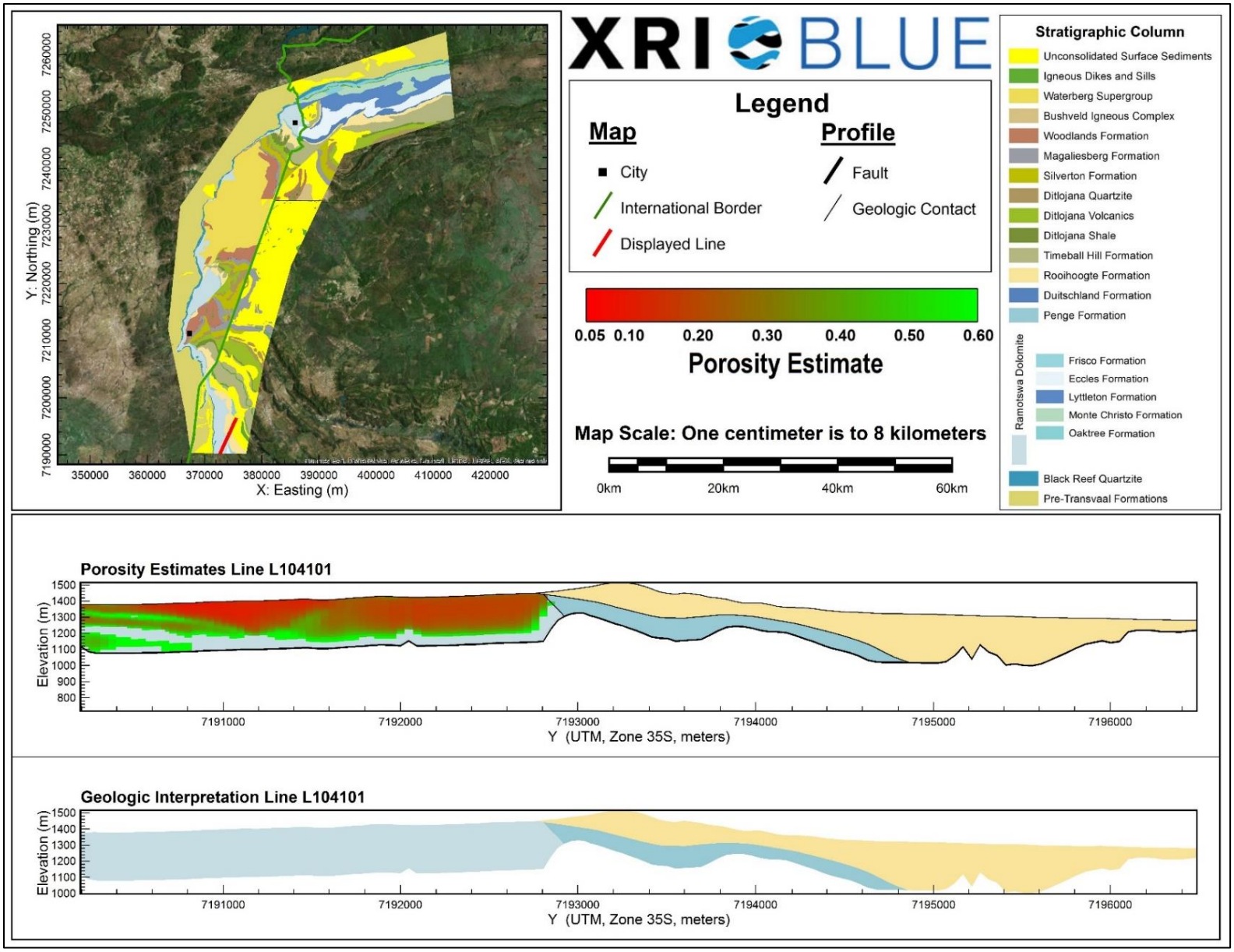

Porosity Estimates and Interpreted Geology Profile for L104101.

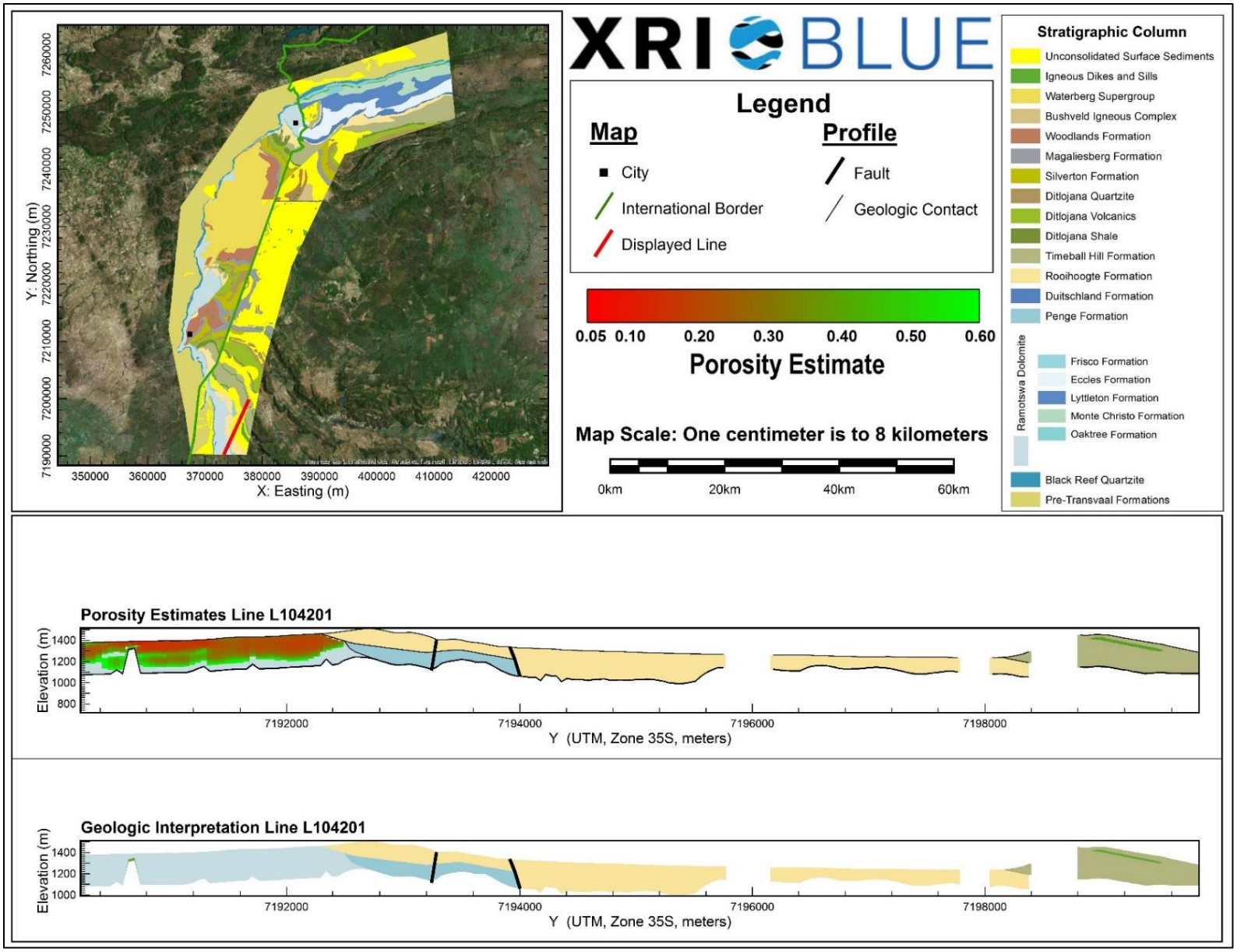

Porosity Estimates and Interpreted Geology Profile for L104201.

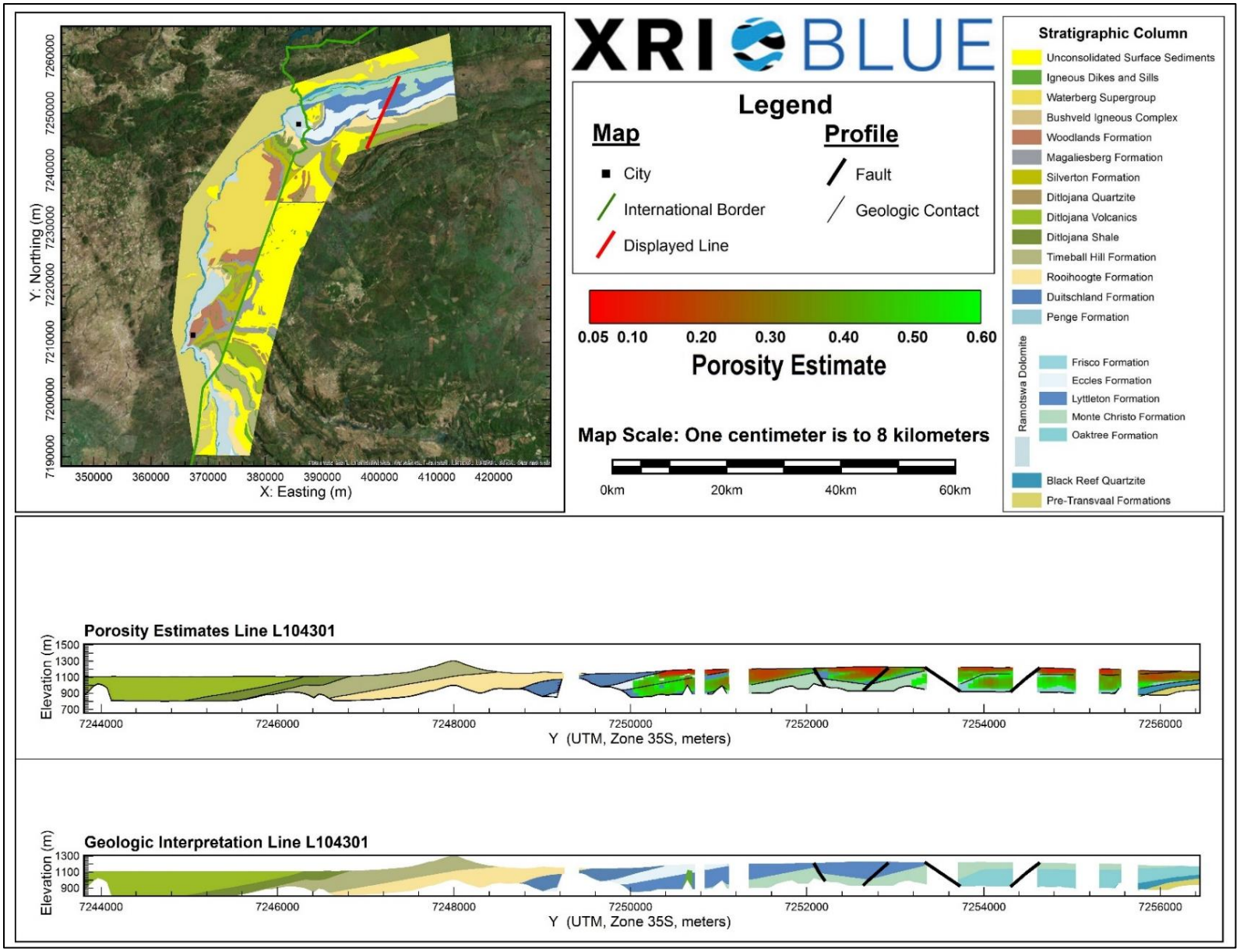

Porosity Estimates and Interpreted Geology Profile for L104301.

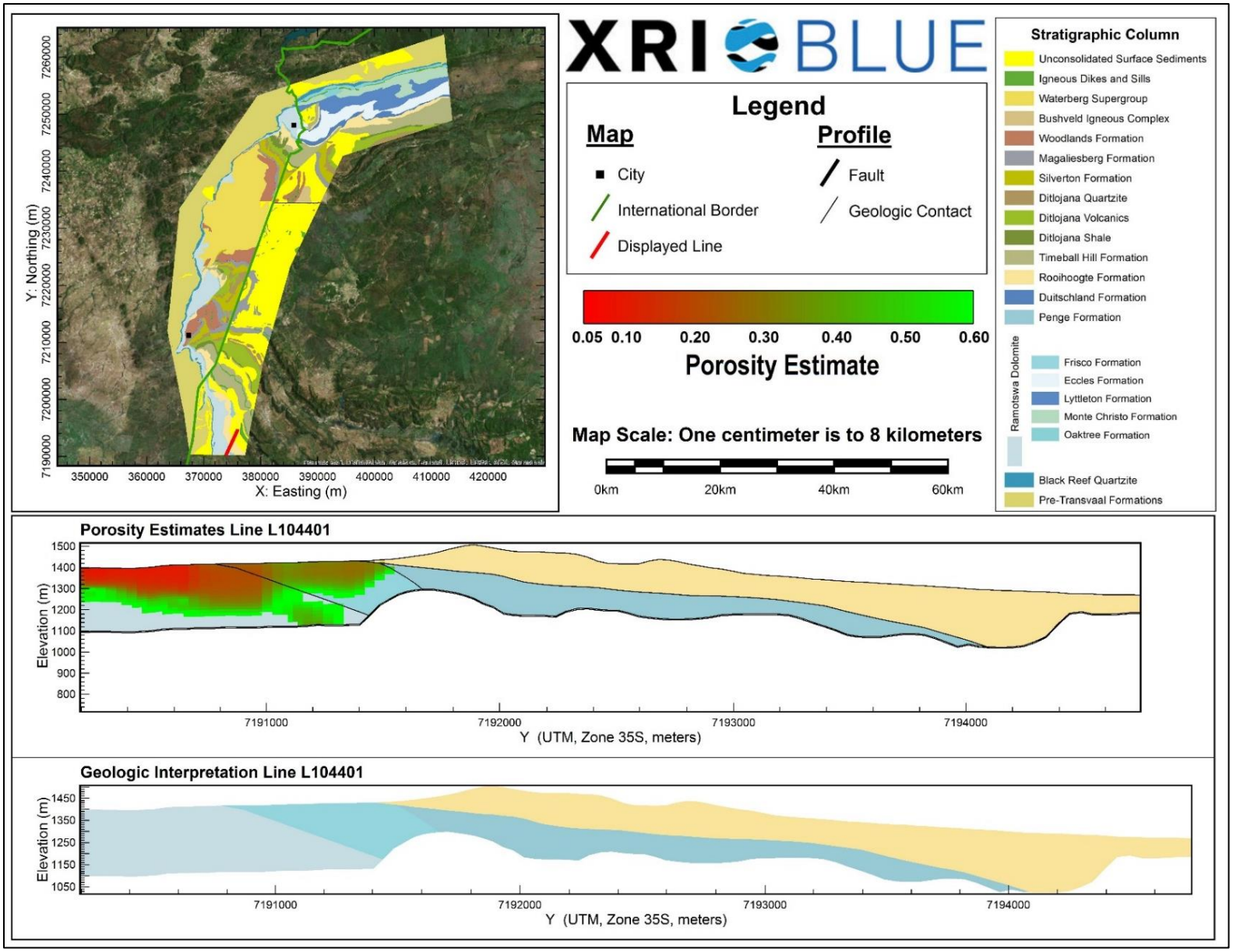

Porosity Estimates and Interpreted Geology Profile for L104401.

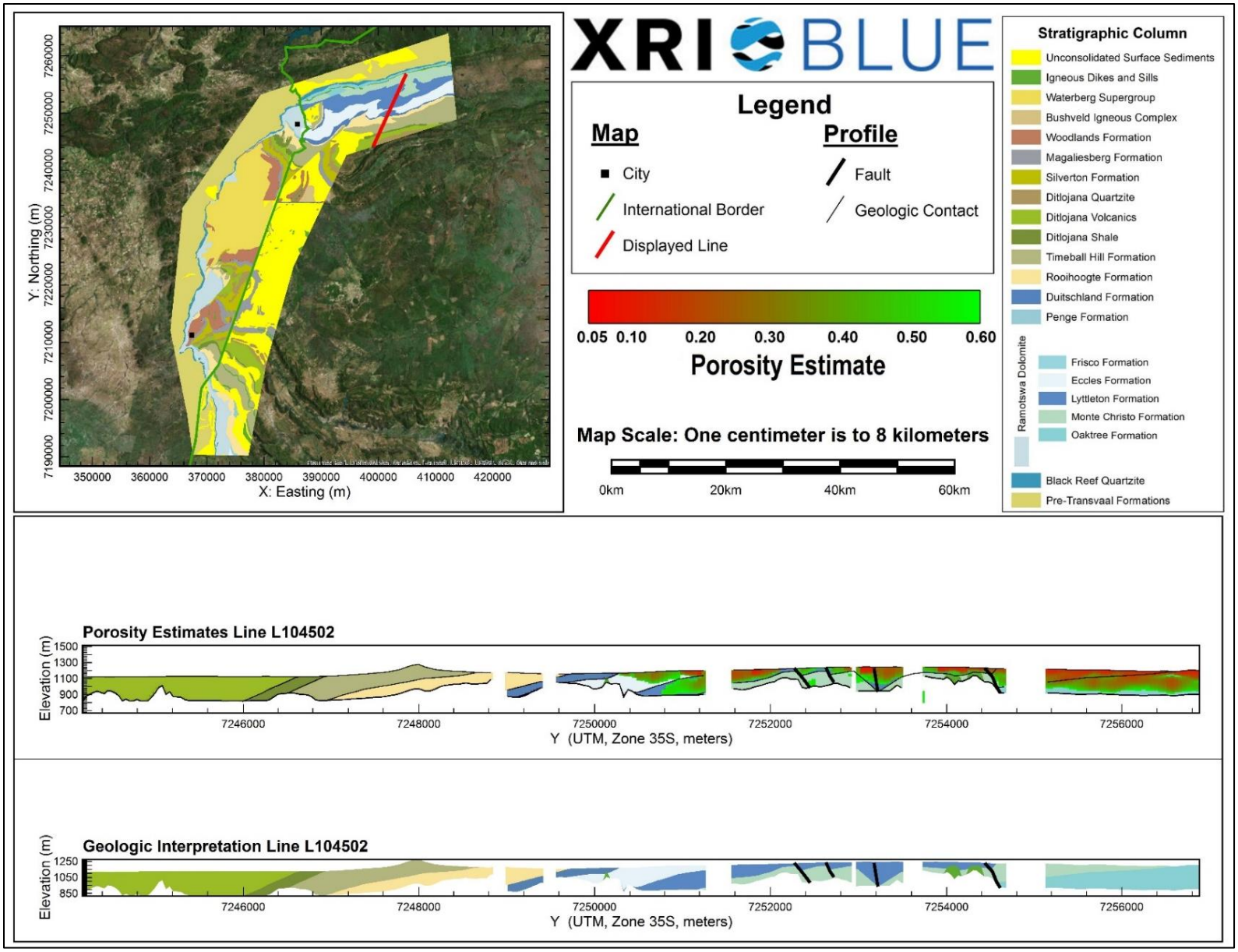

Porosity Estimates and Interpreted Geology Profile for L104502.

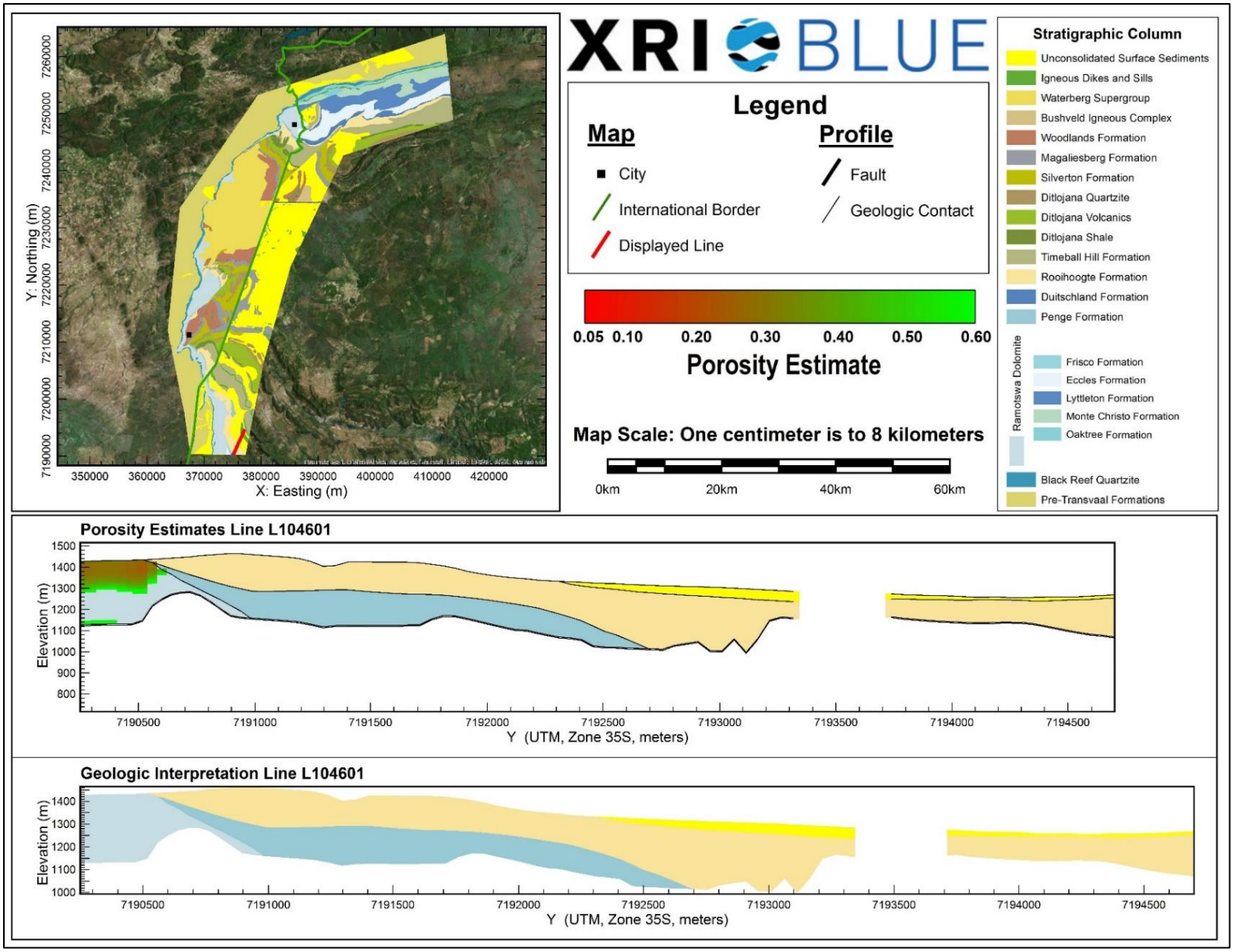

Porosity Estimates and Interpreted Geology Profile for L104601.

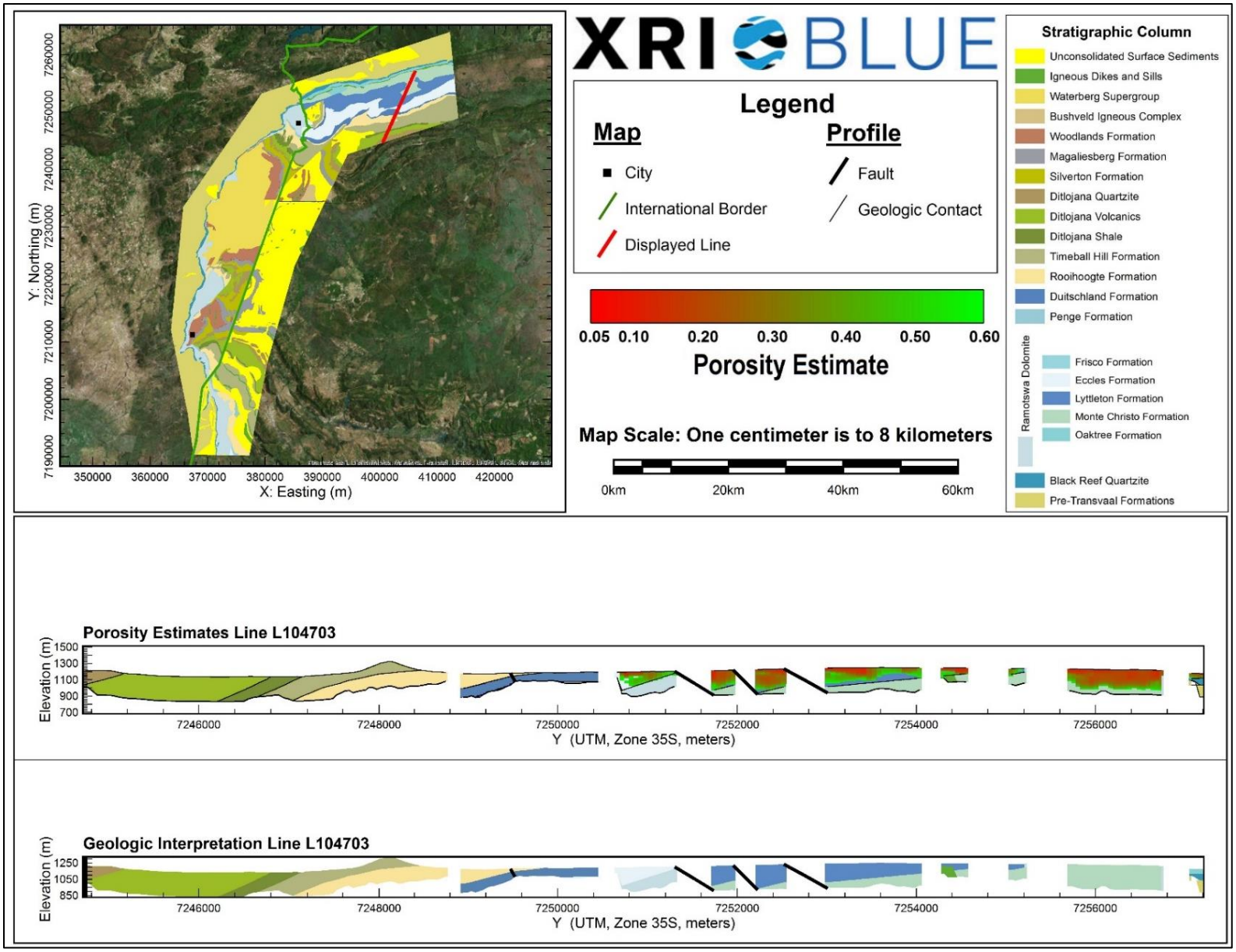

Porosity Estimates and Interpreted Geology Profile for L104703.

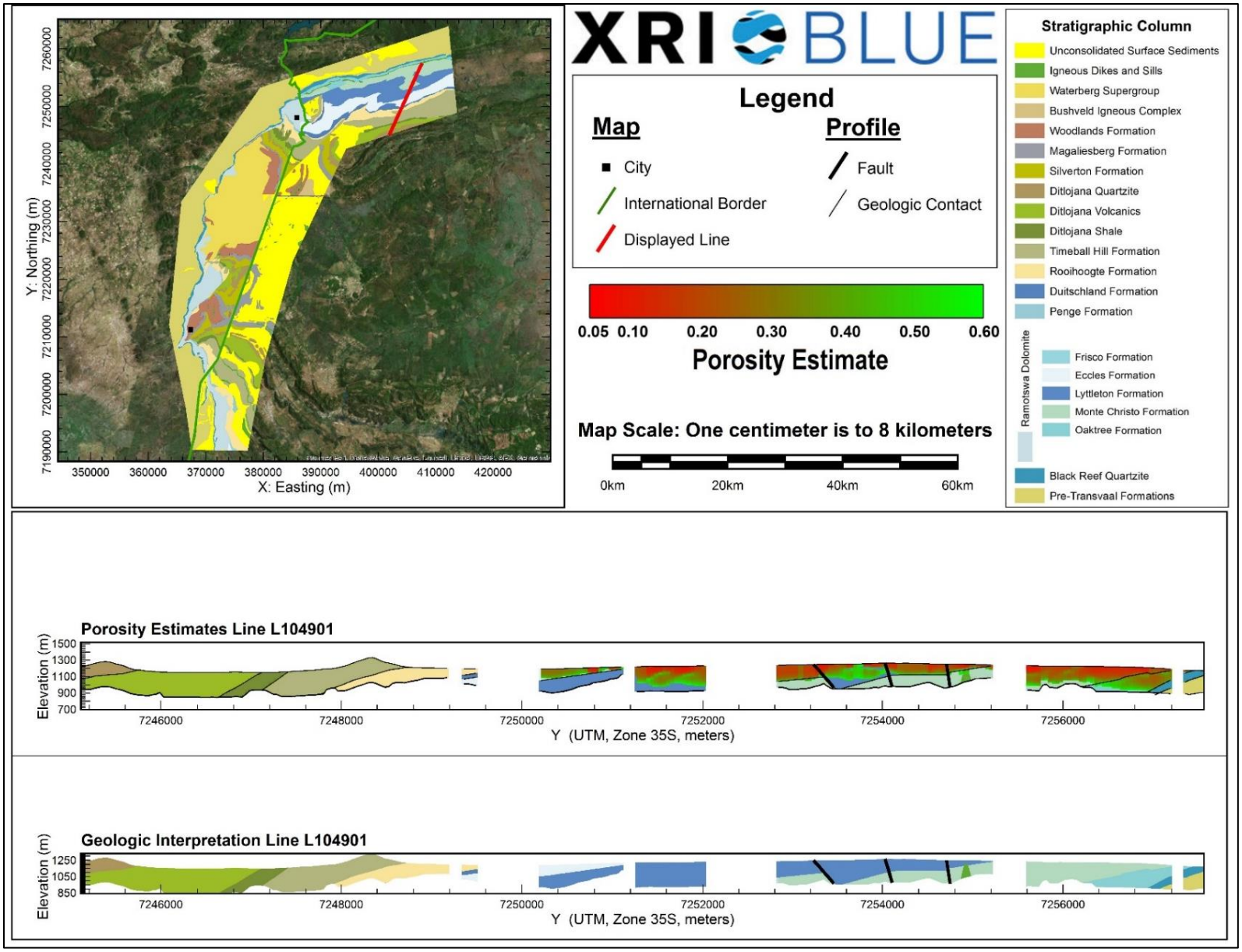

Porosity Estimates and Interpreted Geology Profile for L104901.

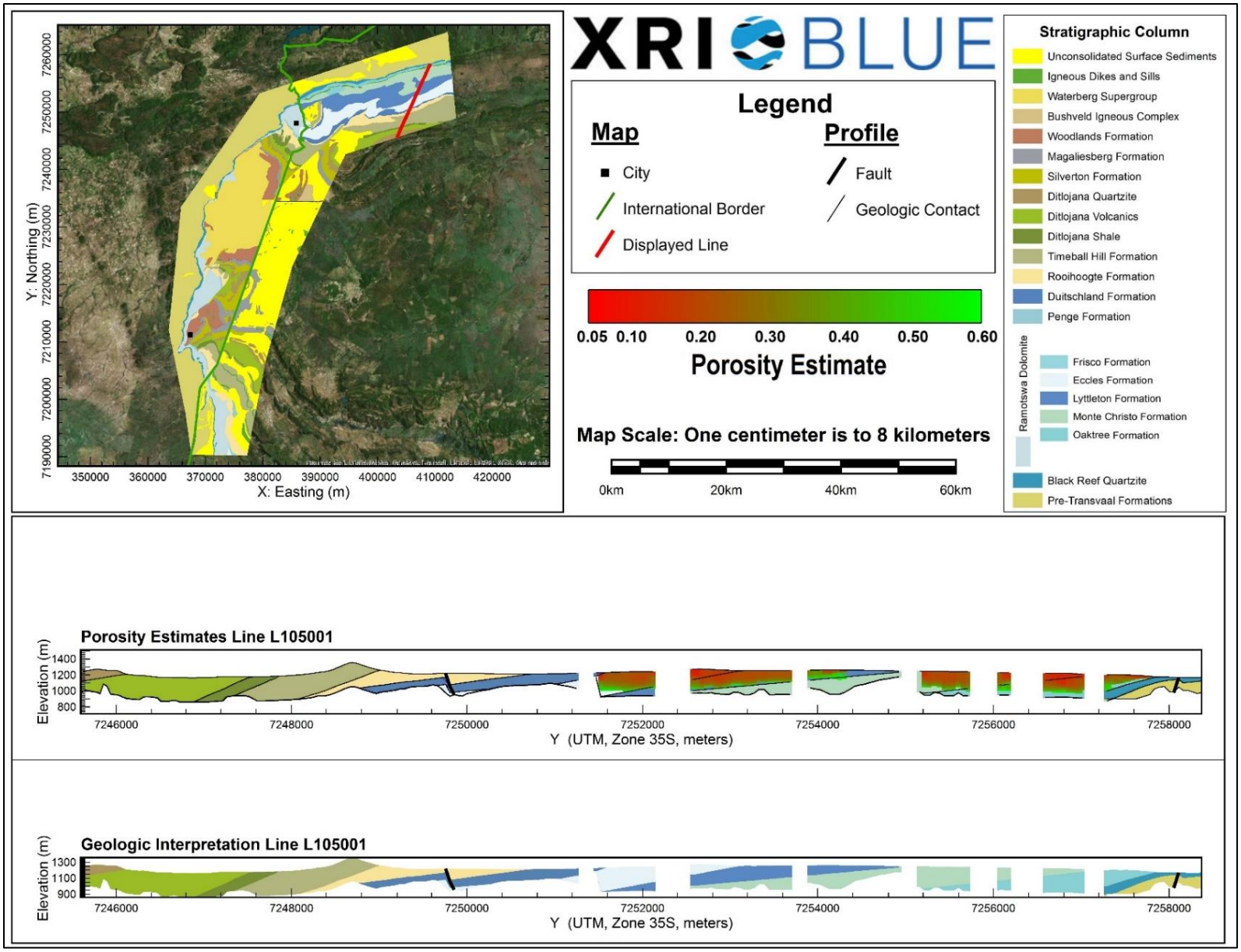

Porosity Estimates and Interpreted Geology Profile for L105001.

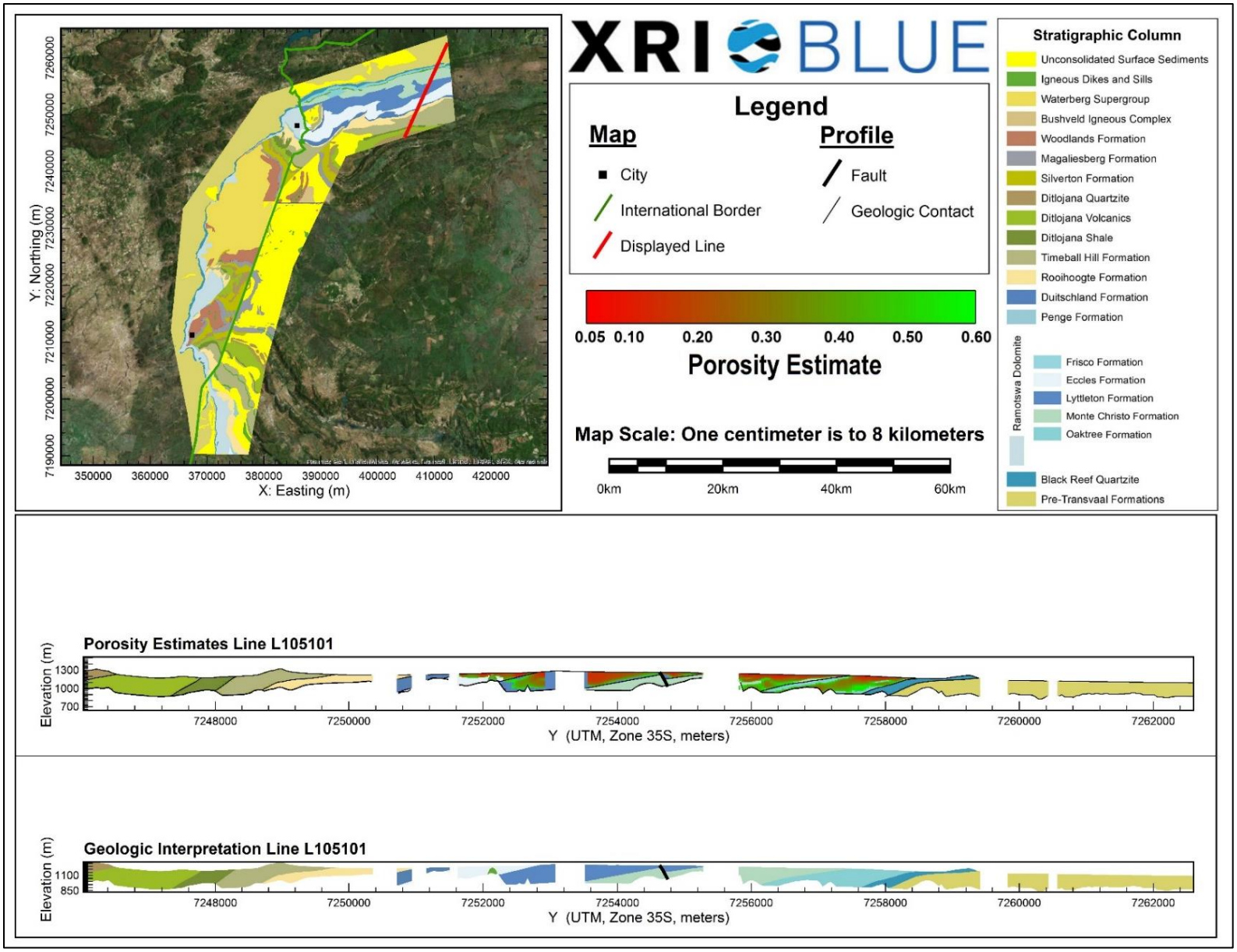

Porosity Estimates and Interpreted Geology Profile for L105101.

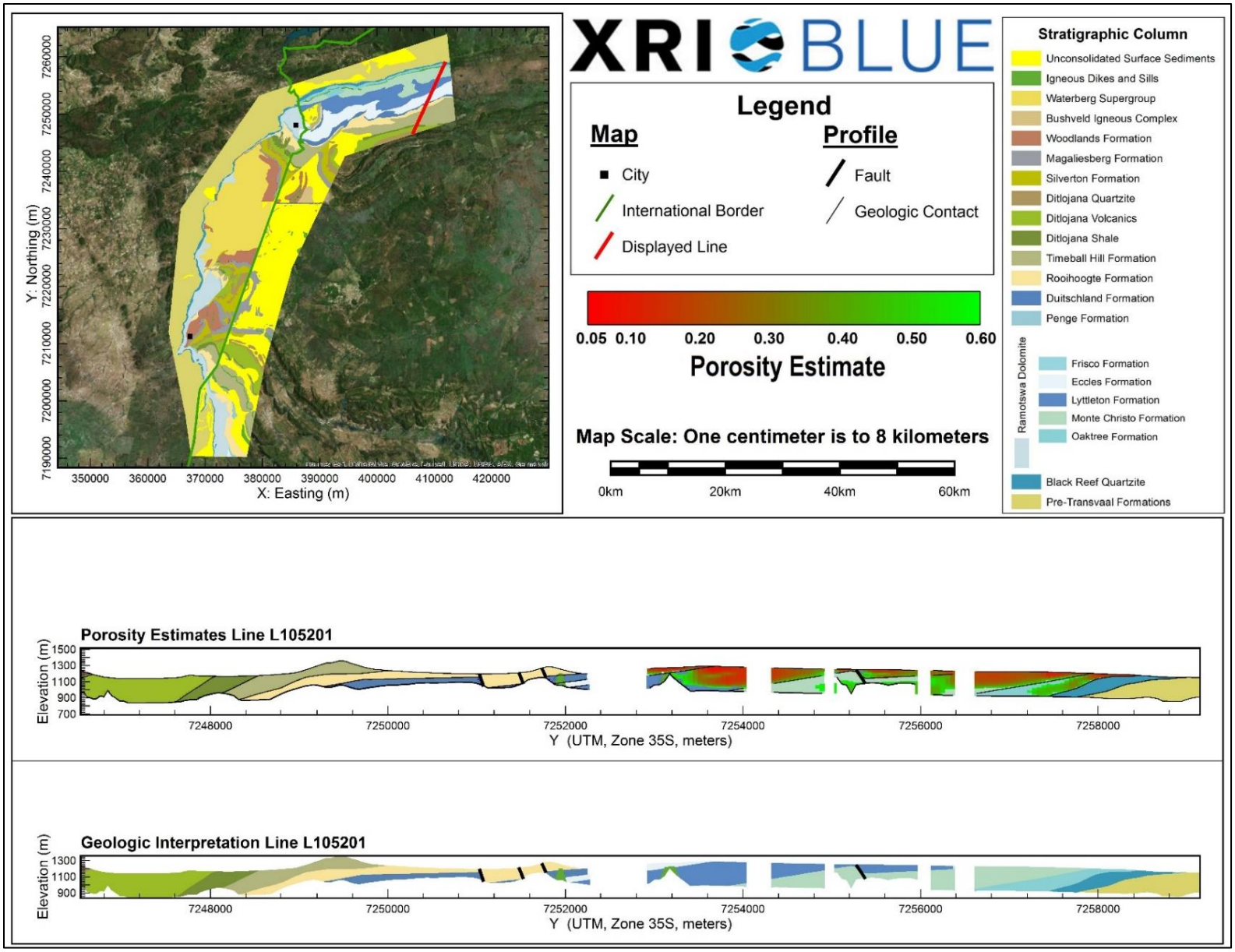

Porosity Estimates and Interpreted Geology Profile for L105201.

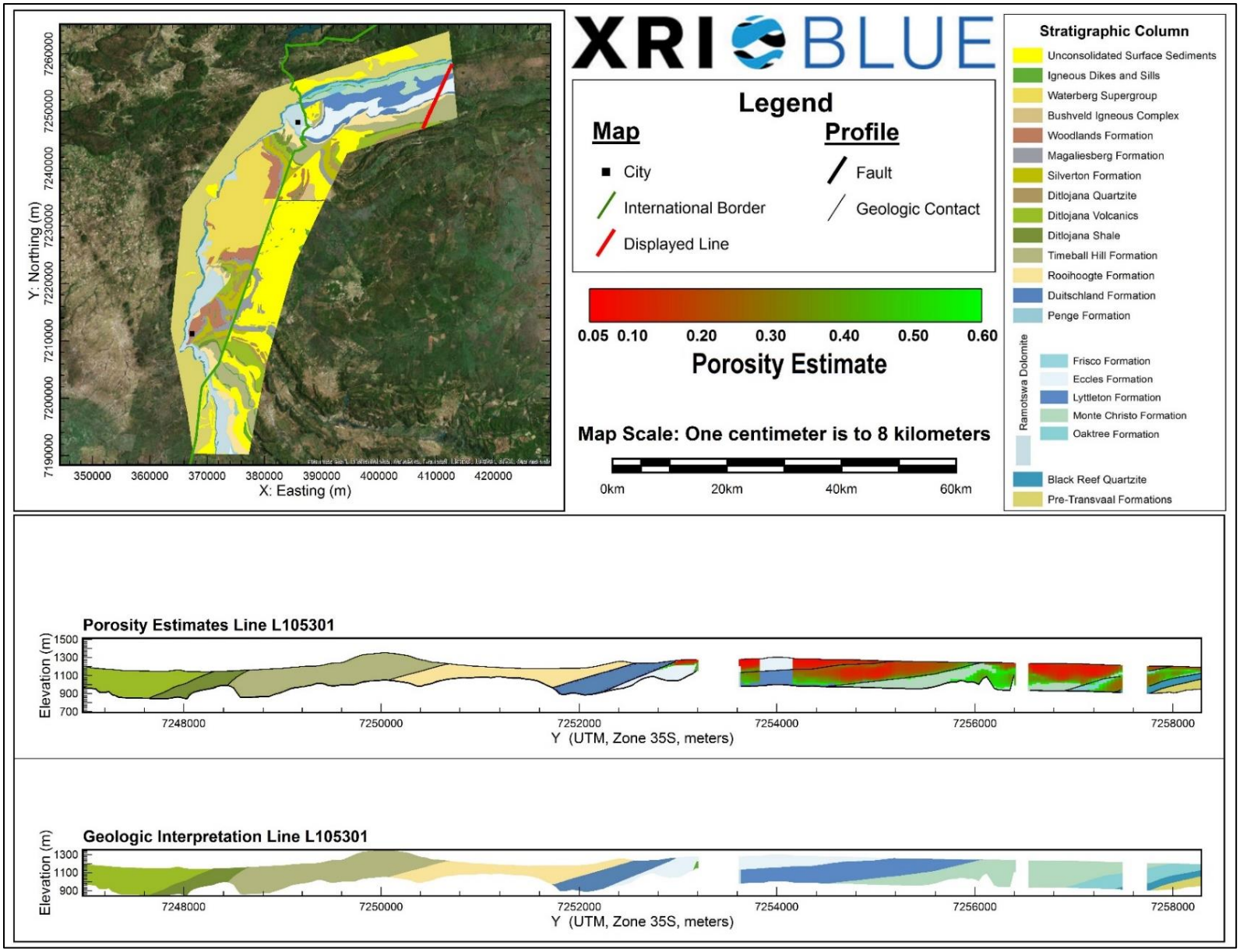

Porosity Estimates and Interpreted Geology Profile for L105301.

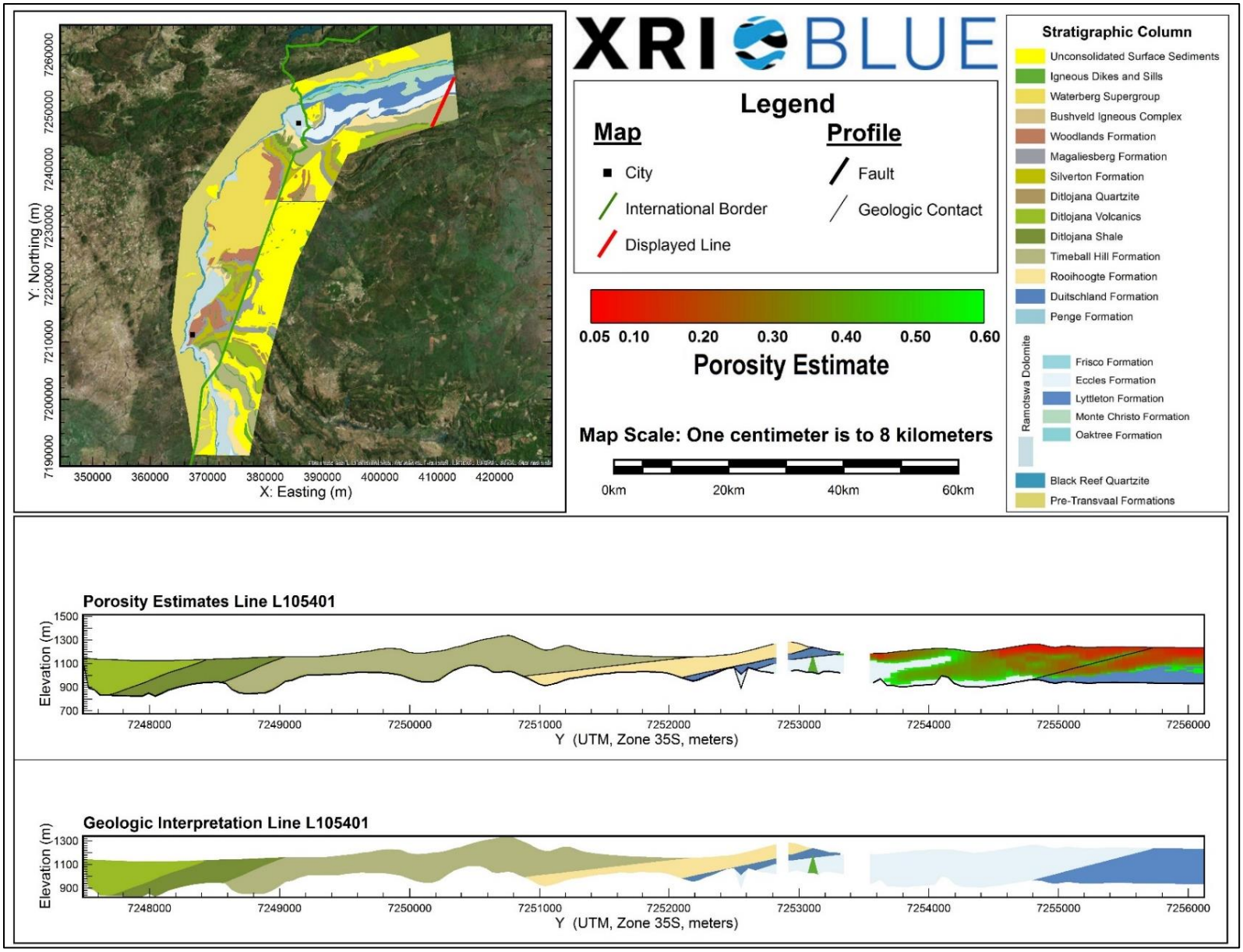

Porosity Estimates and Interpreted Geology Profile for L105401.

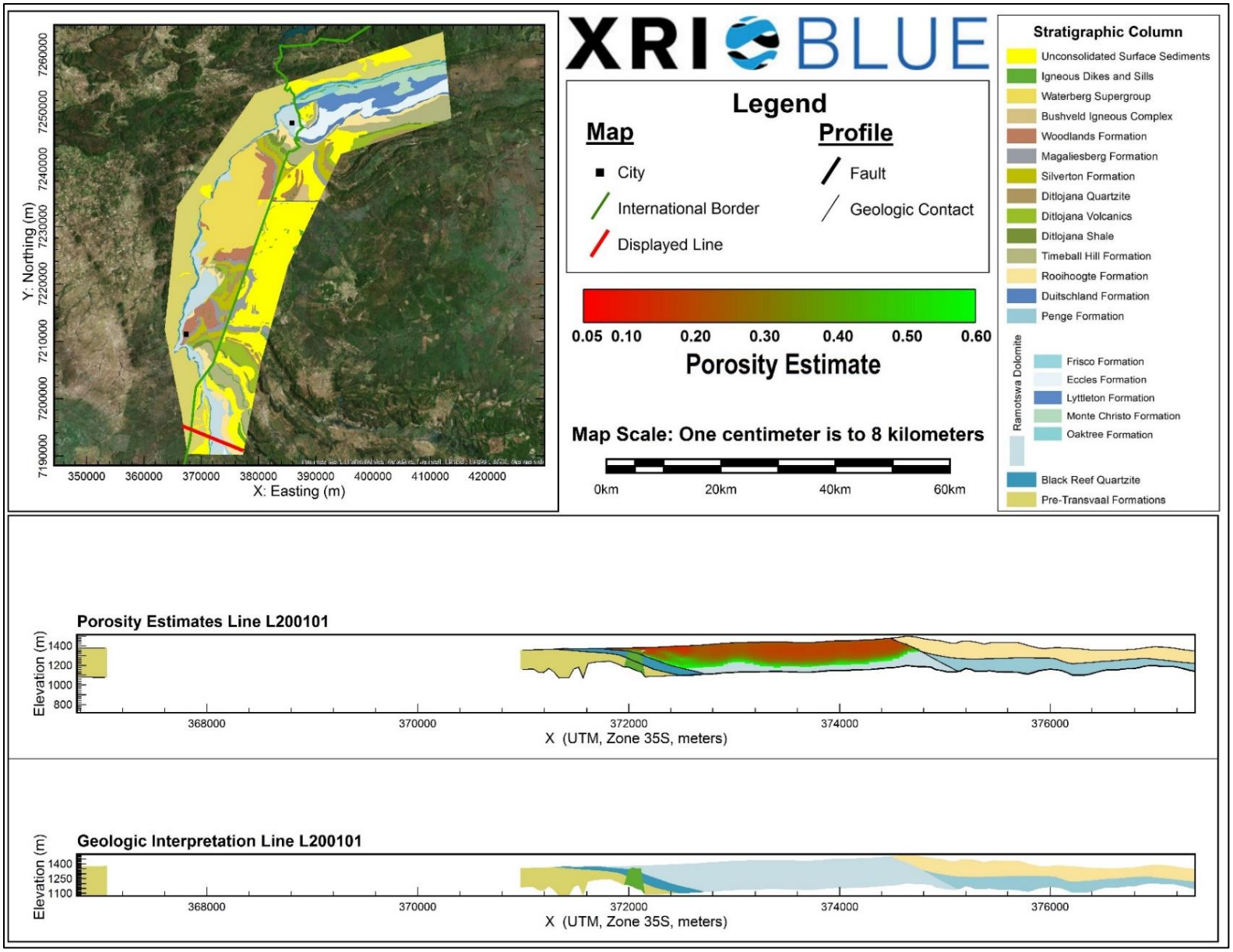

Porosity Estimates and Interpreted Geology Profile for L200101.

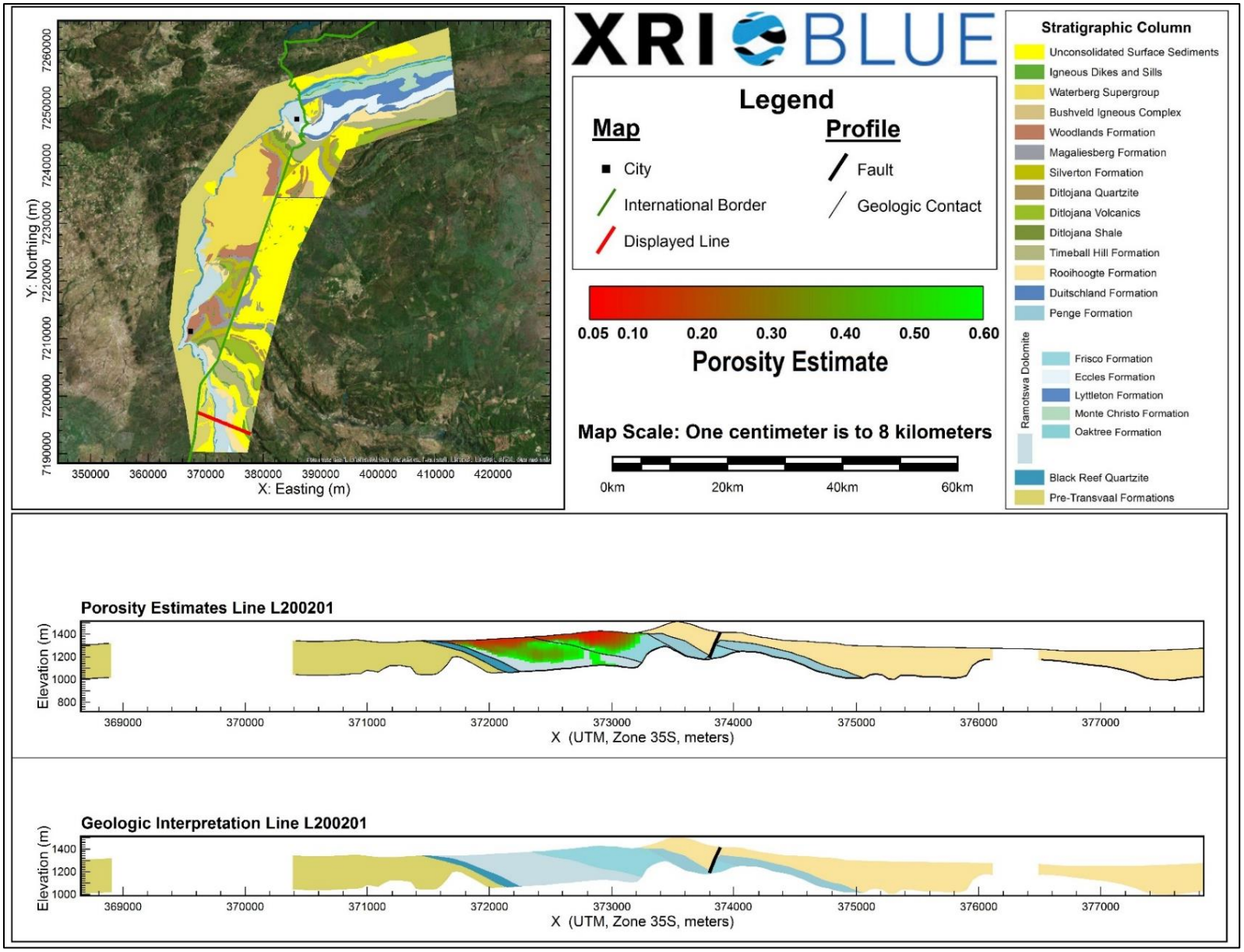

Porosity Estimates and Interpreted Geology Profile for L200201.

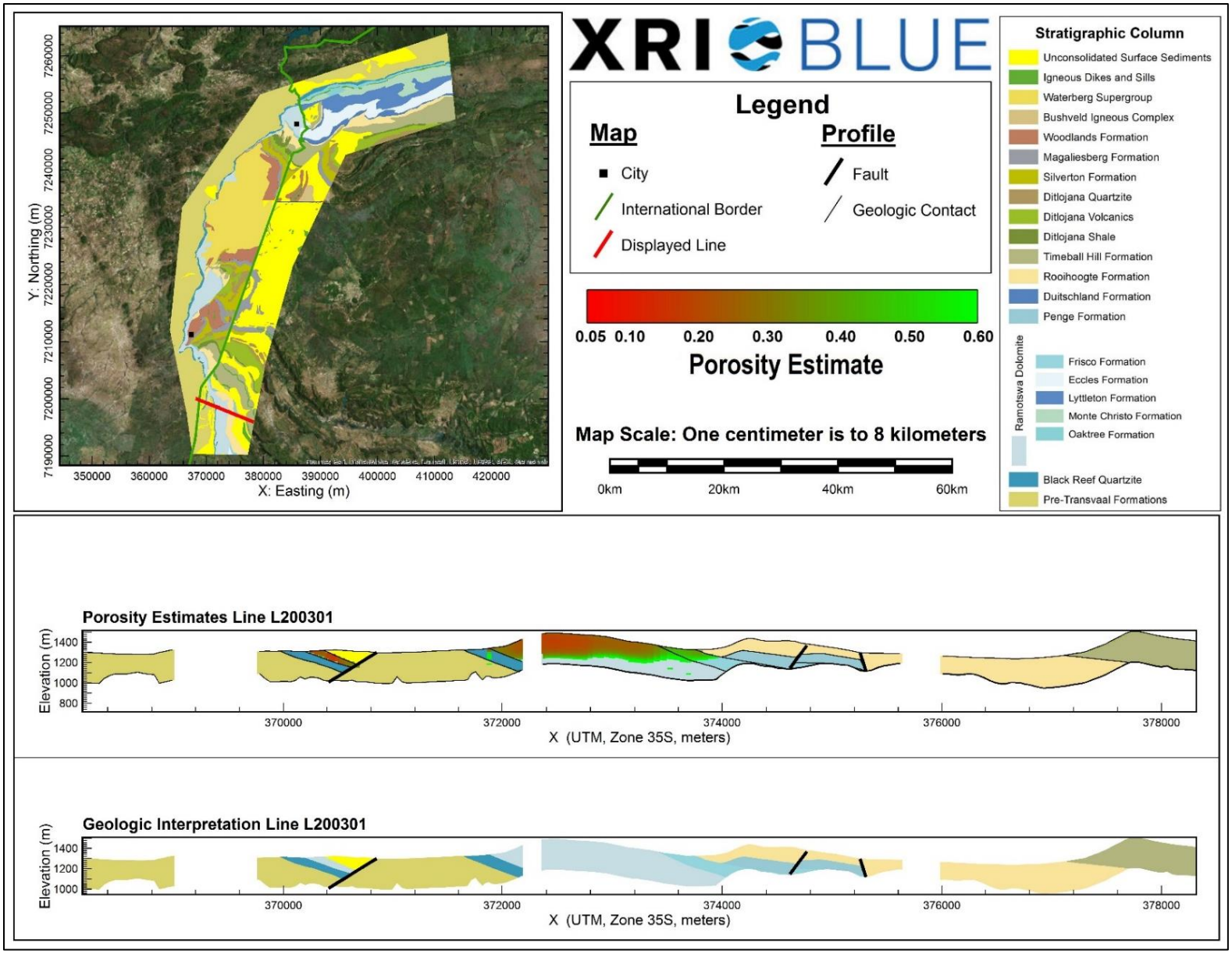

Porosity Estimates and Interpreted Geology Profile for L200301.

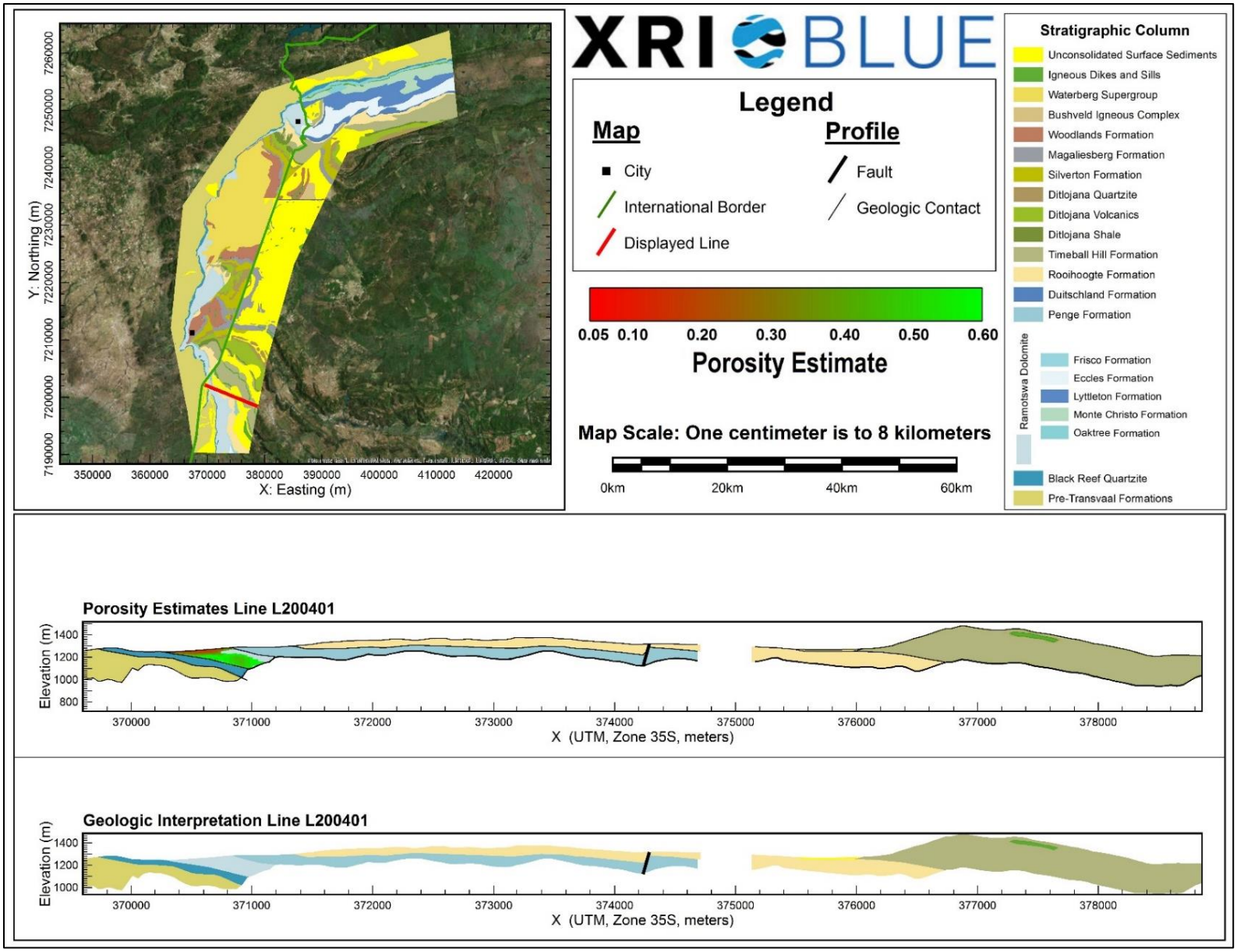

Porosity Estimates and Interpreted Geology Profile for L200401.

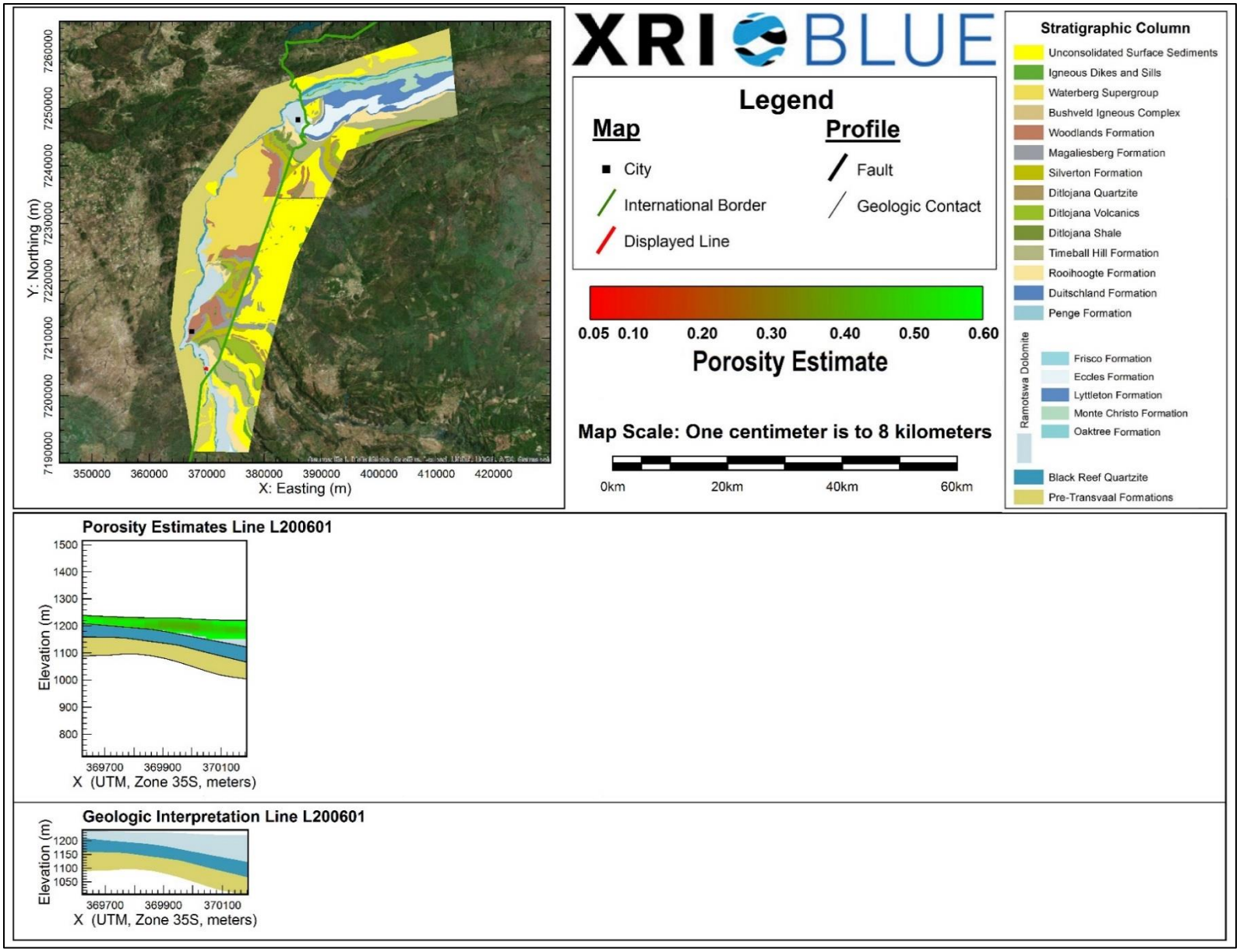

Porosity Estimates and Interpreted Geology Profile for L200601.

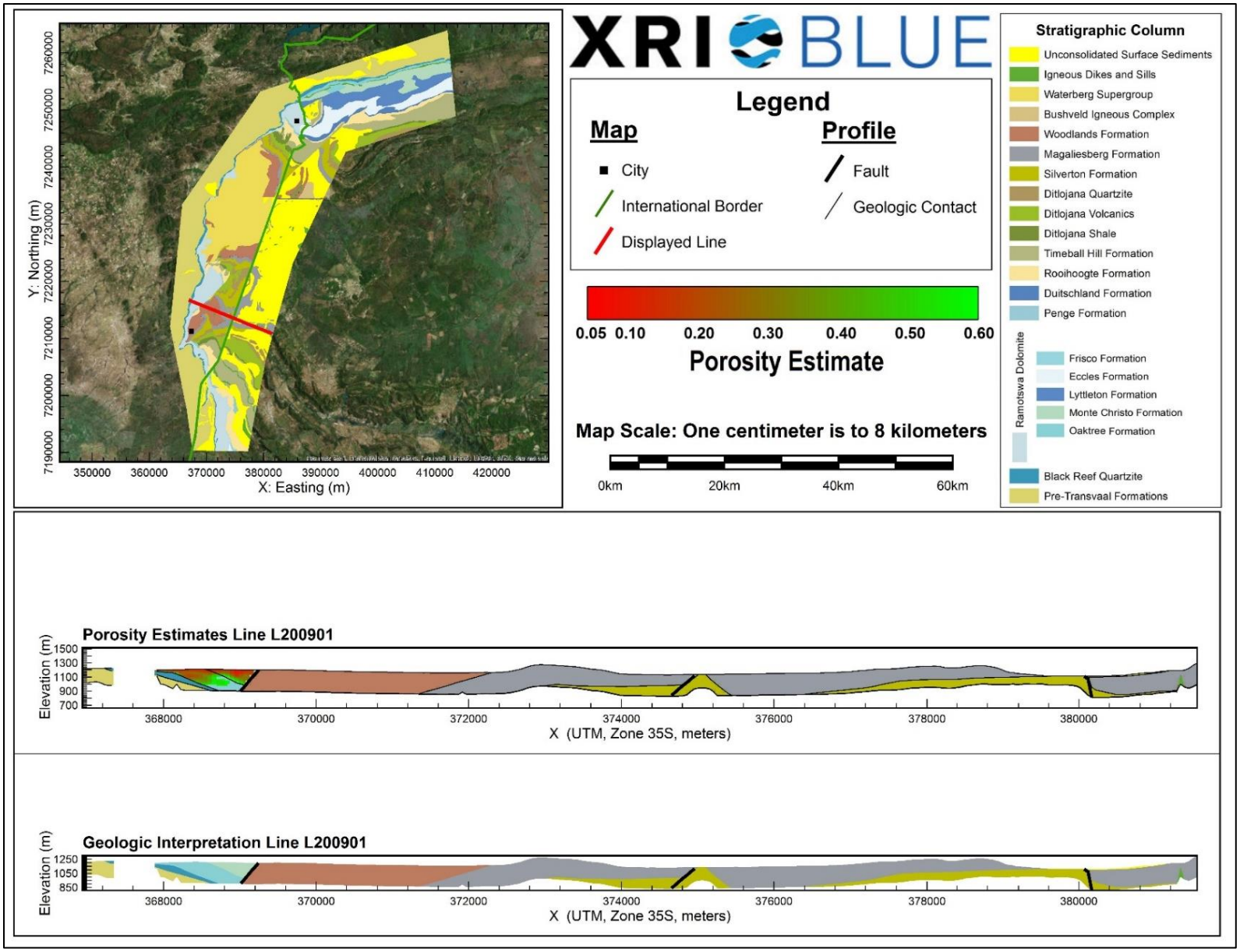

Porosity Estimates and Interpreted Geology Profile for L200901.

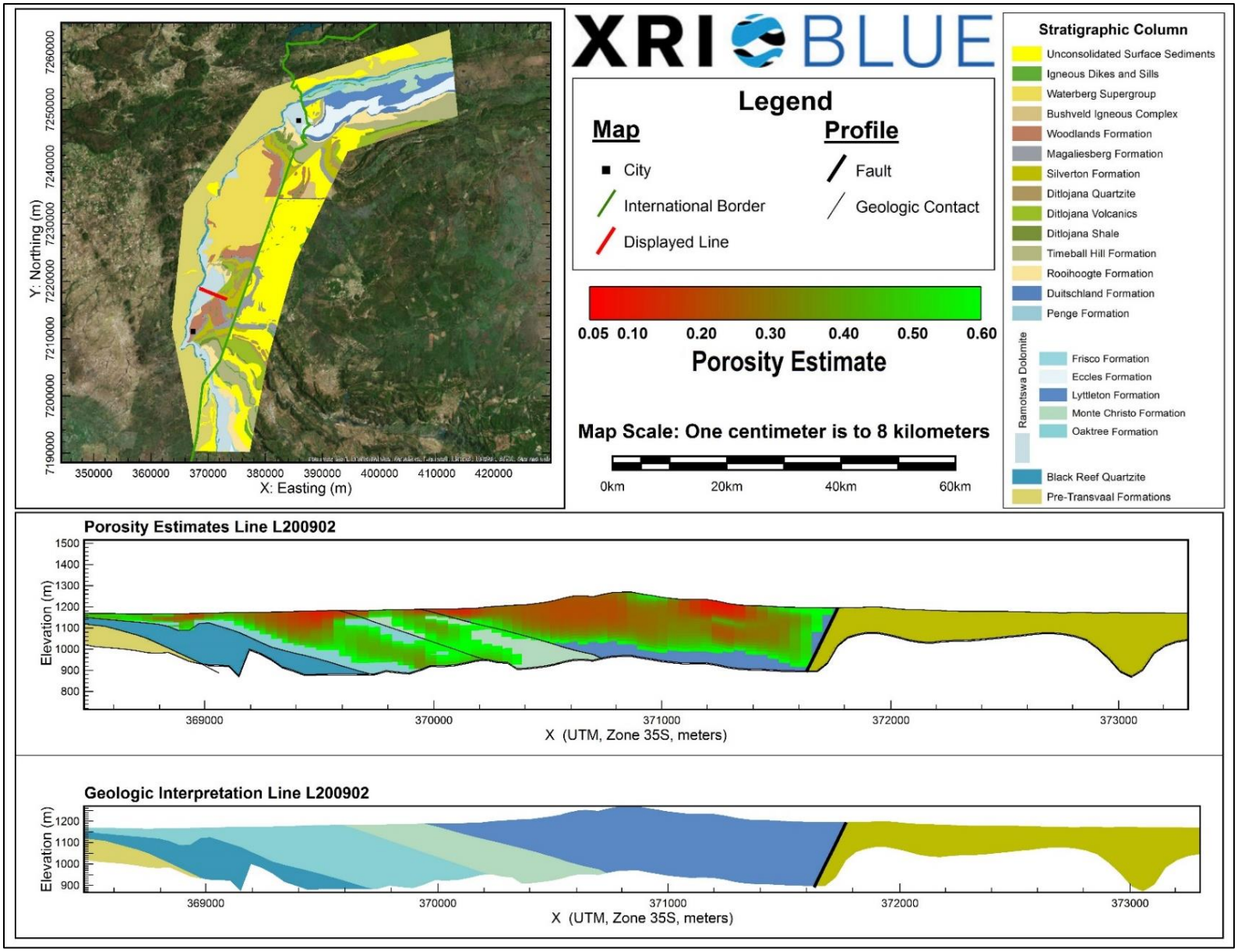

Porosity Estimates and Interpreted Geology Profile for L200902.

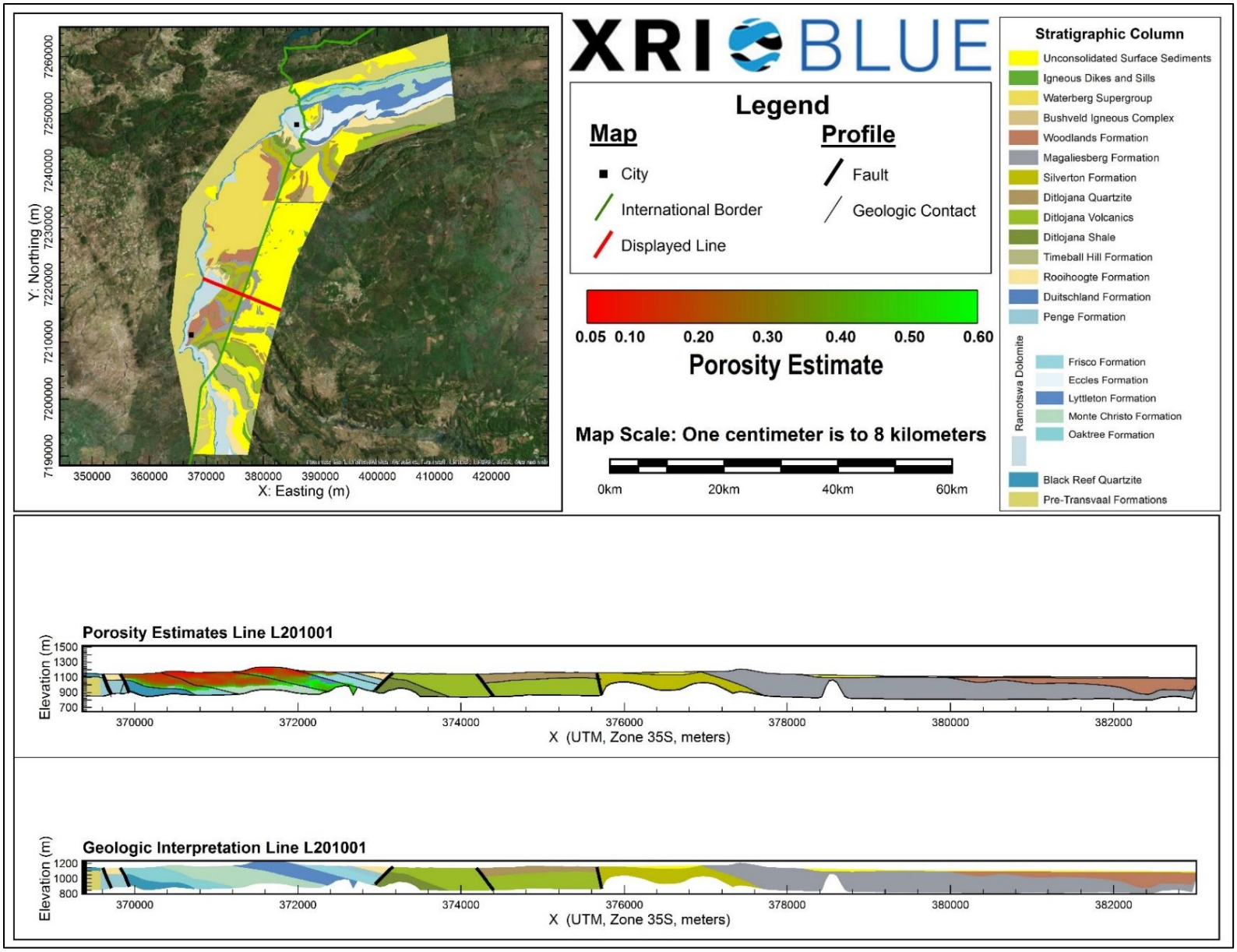

Porosity Estimates and Interpreted Geology Profile for L201001.

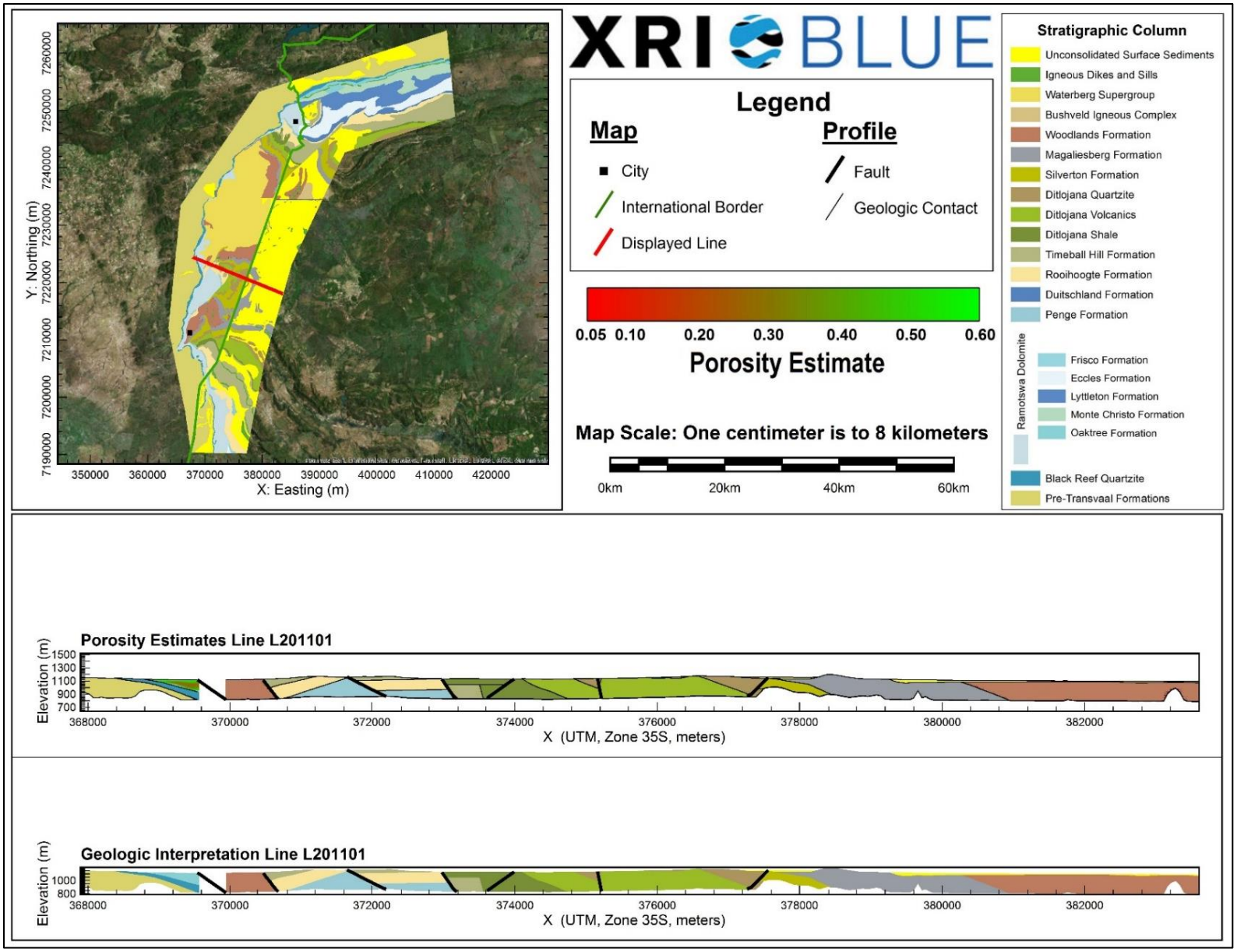

Porosity Estimates and Interpreted Geology Profile for L201101.

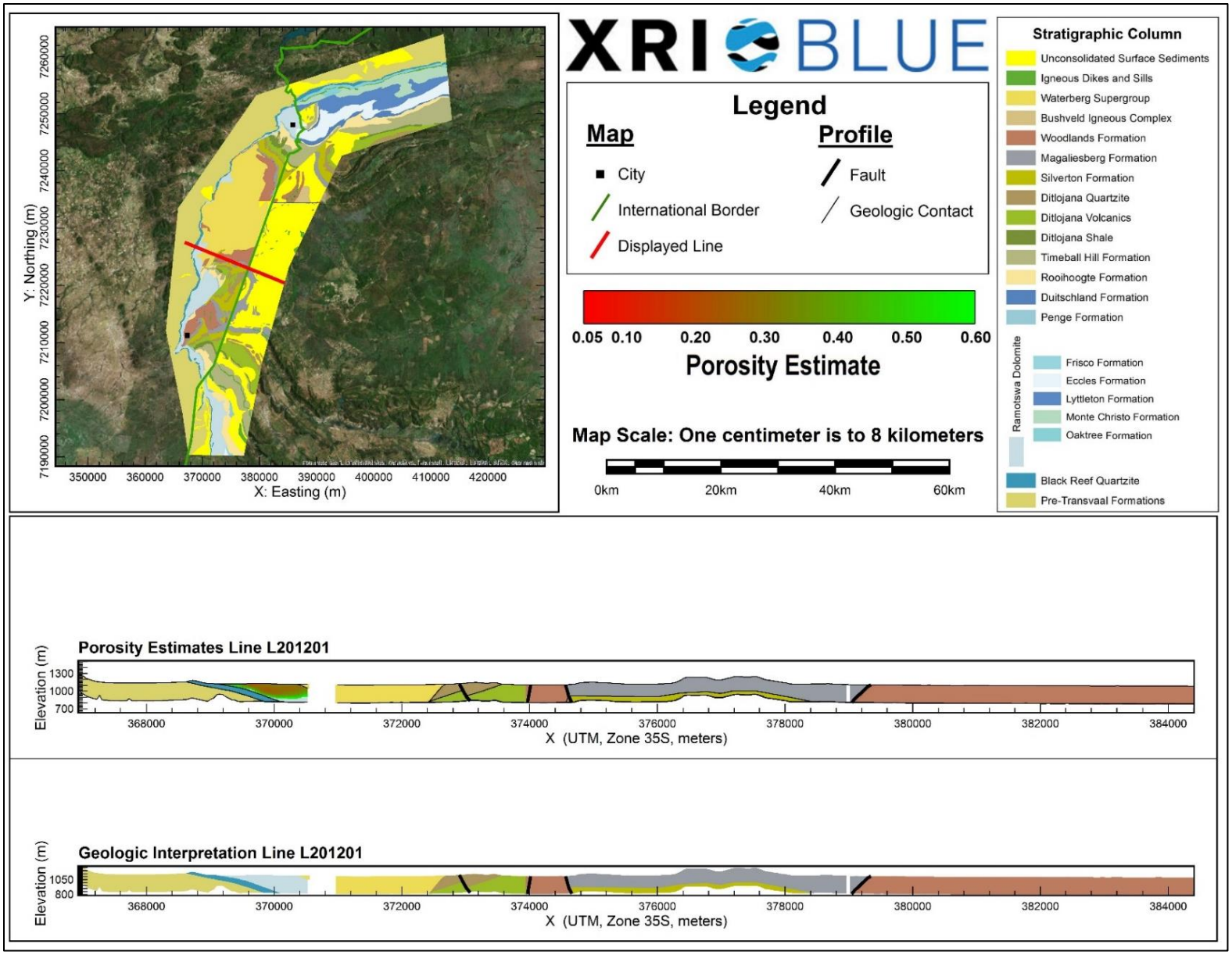

Porosity Estimates and Interpreted Geology Profile for L201201.

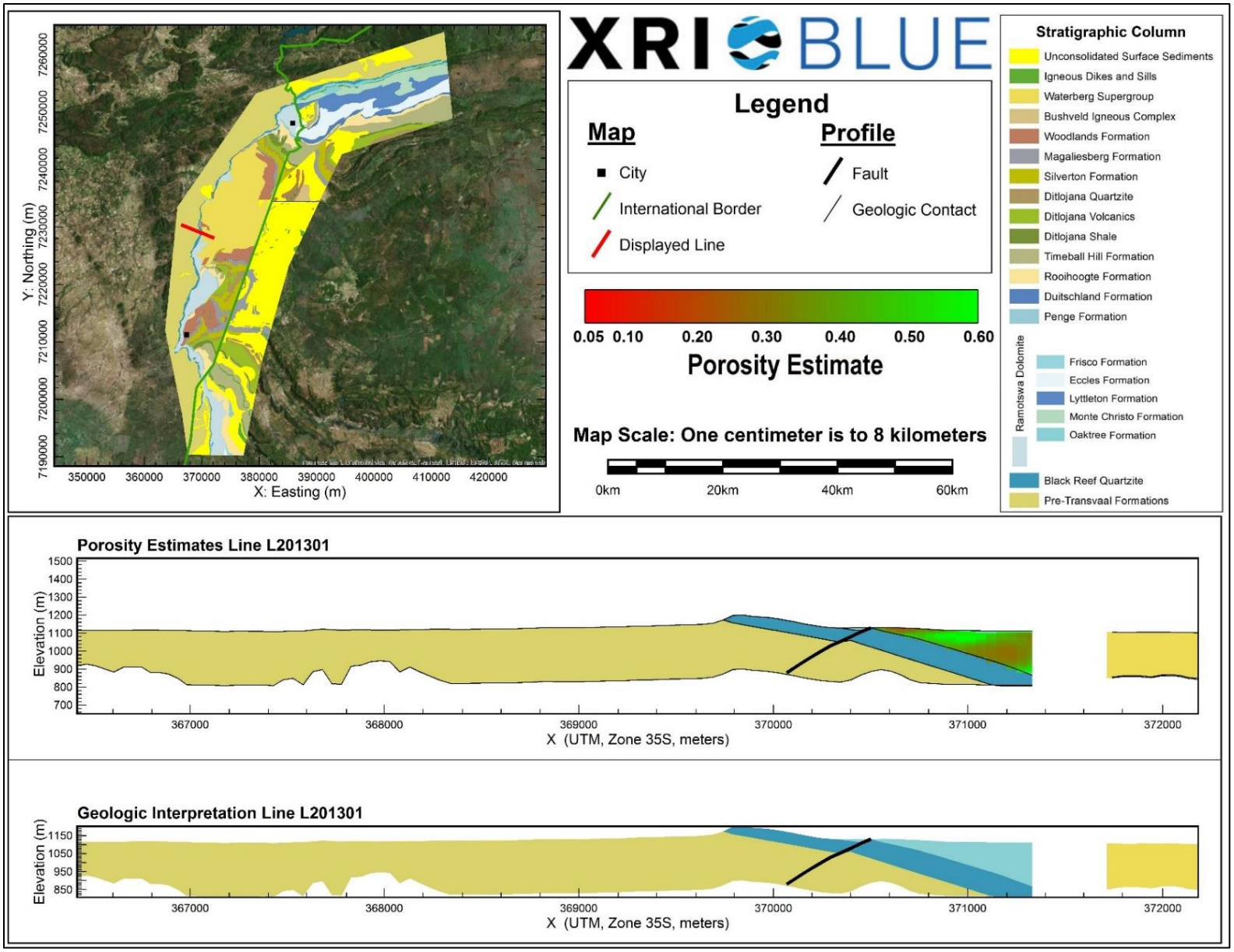

Porosity Estimates and Interpreted Geology Profile for L201301.

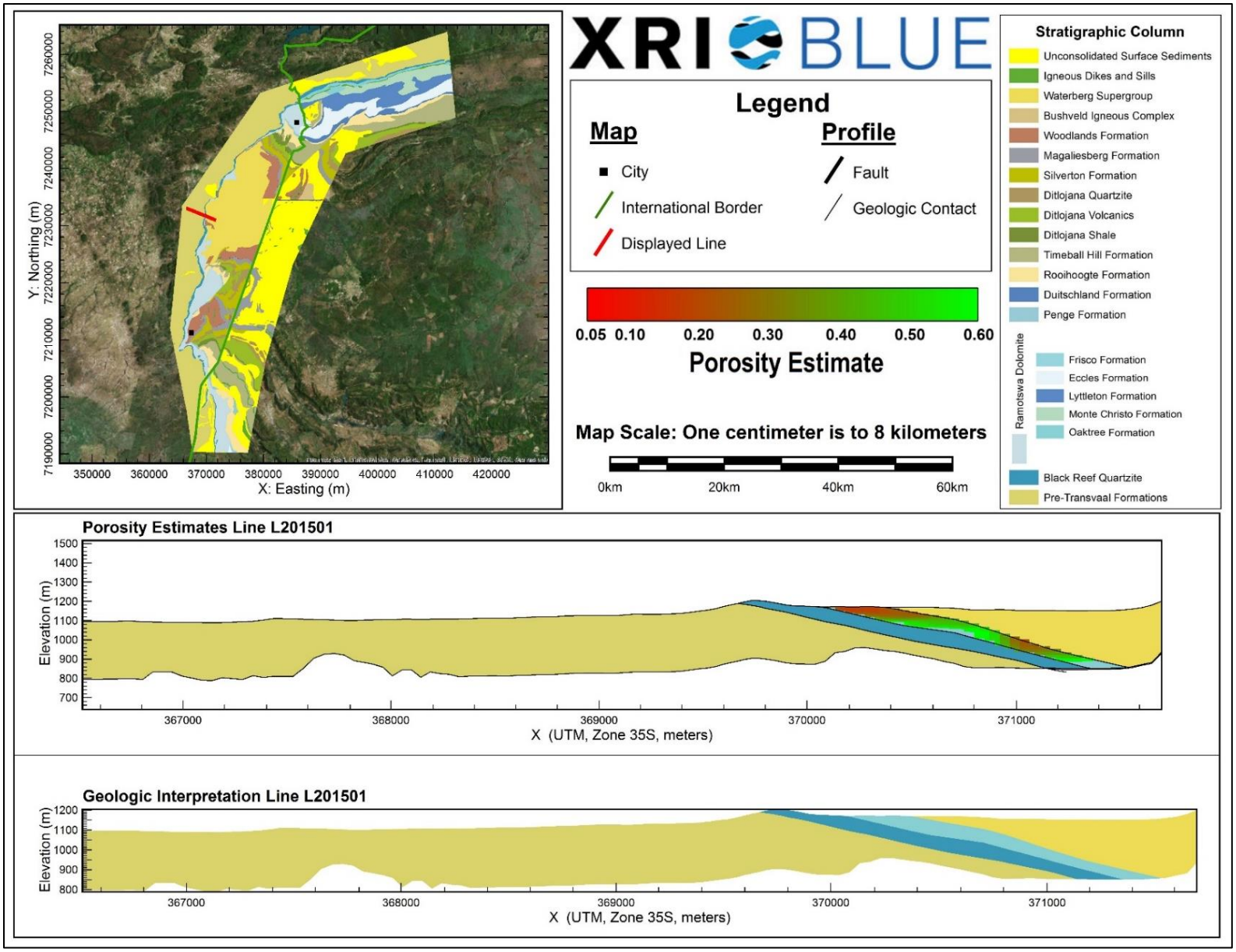

Porosity Estimates and Interpreted Geology Profile for L201501.

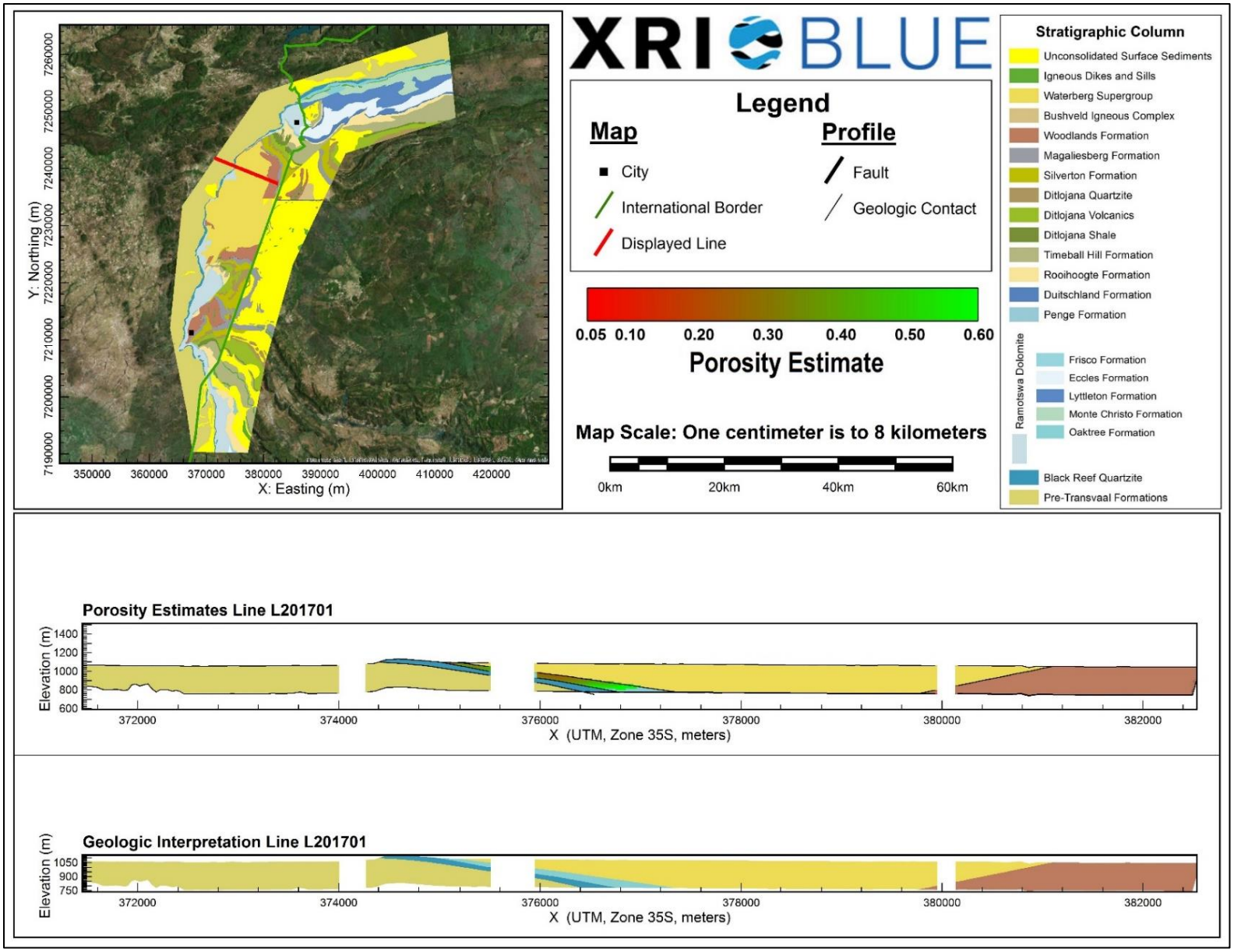

Porosity Estimates and Interpreted Geology Profile for L201701.

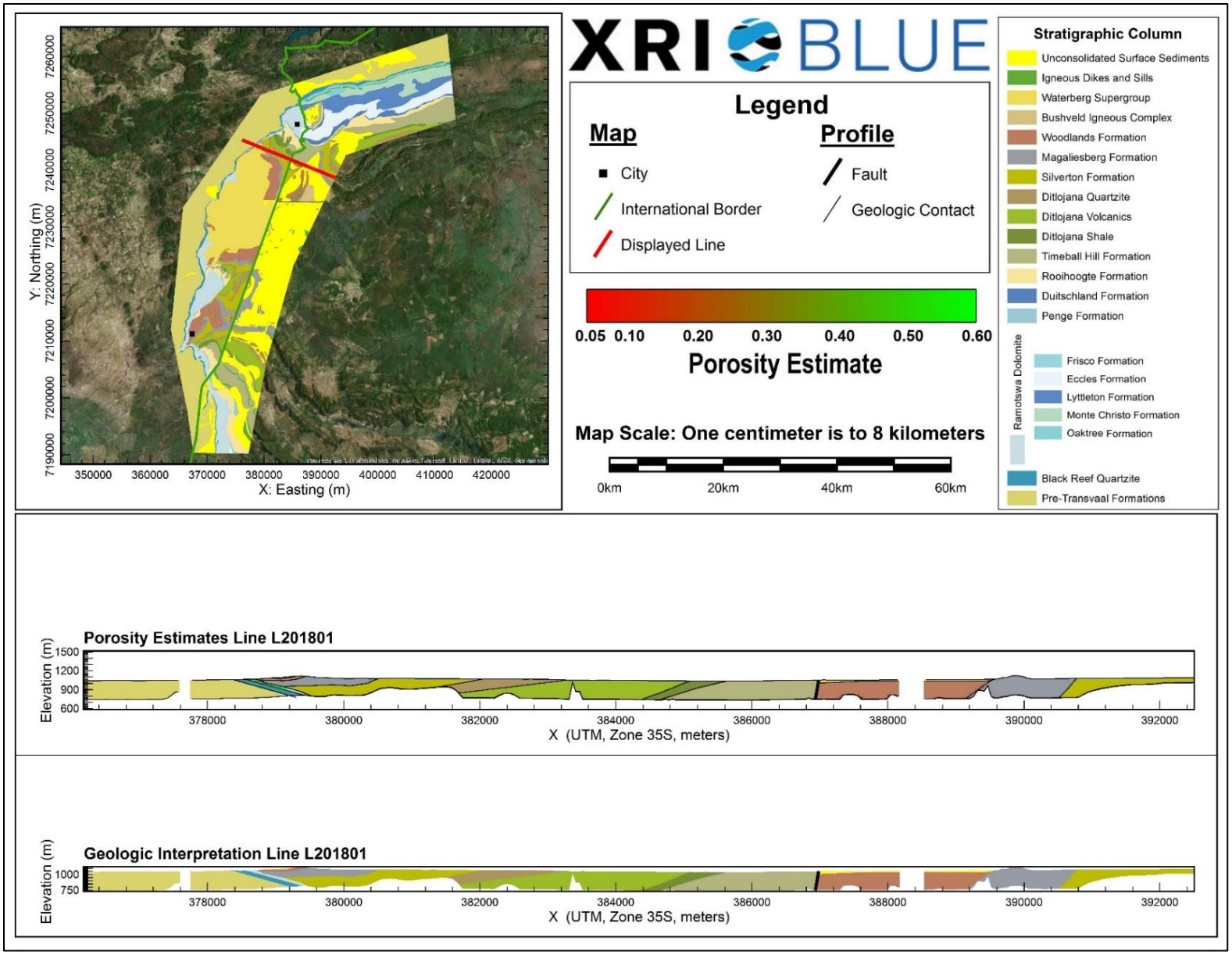

Porosity Estimates and Interpreted Geology Profile for L201801.

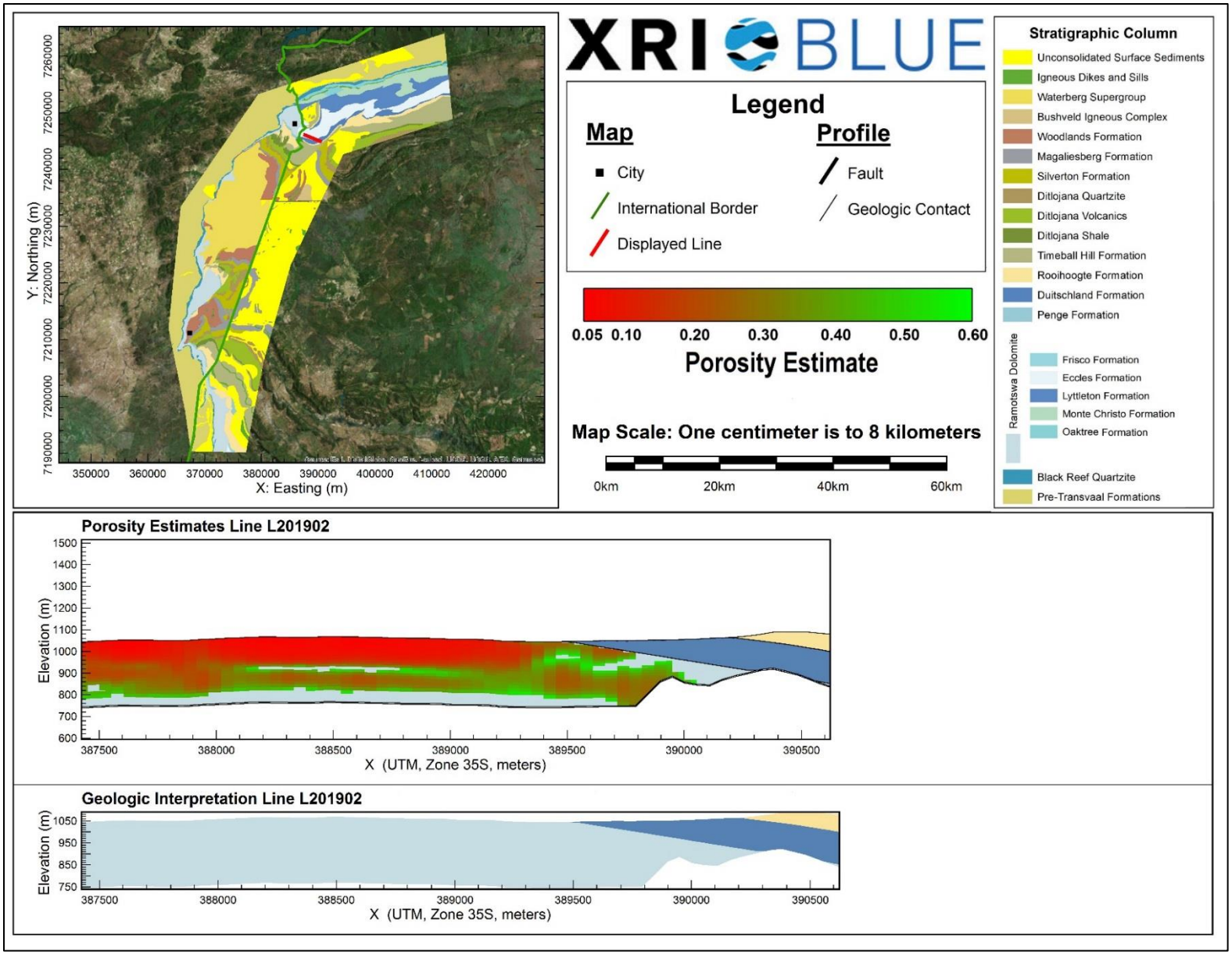

Porosity Estimates and Interpreted Geology Profile for L201902.

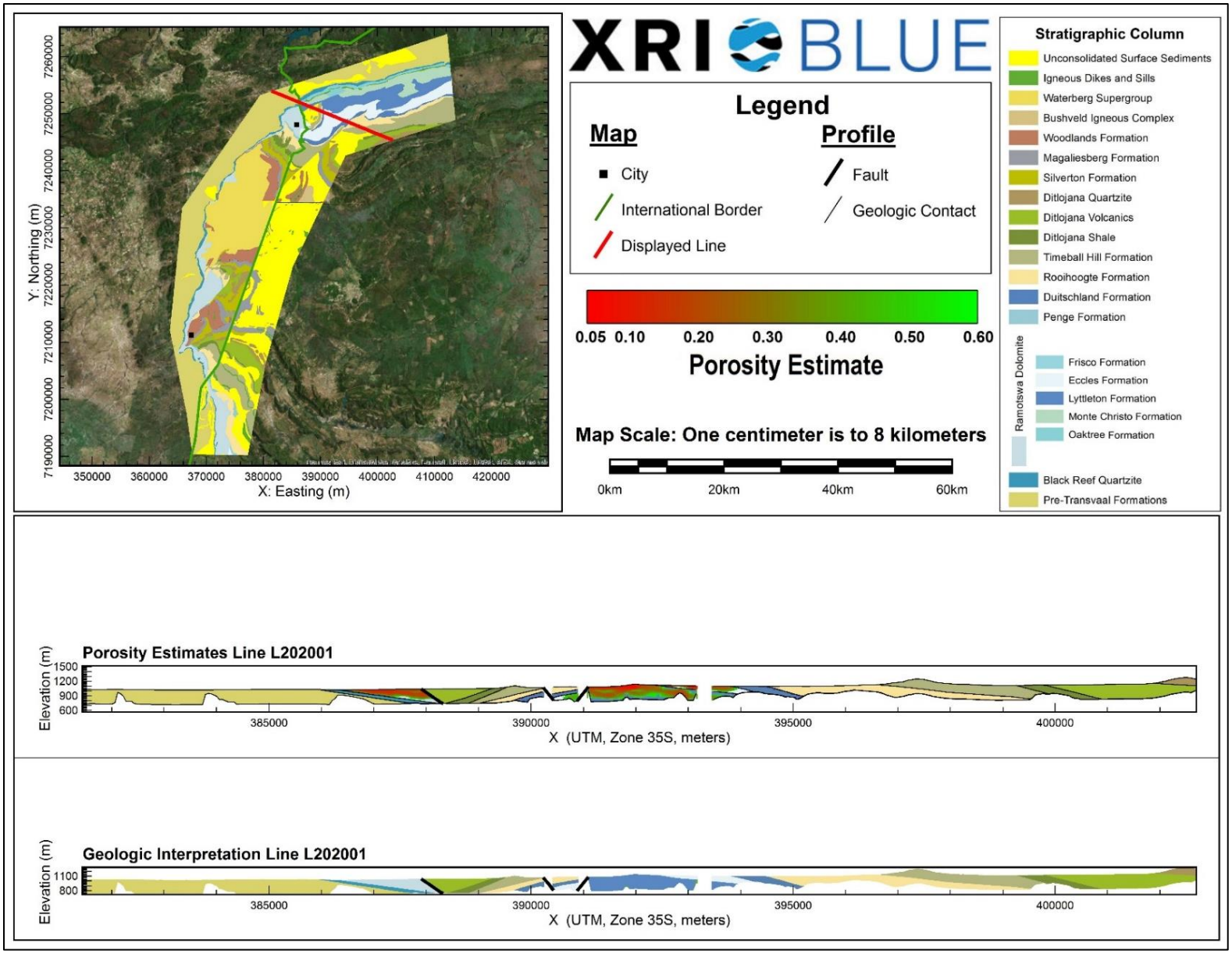

Porosity Estimates and Interpreted Geology Profile for L202001.

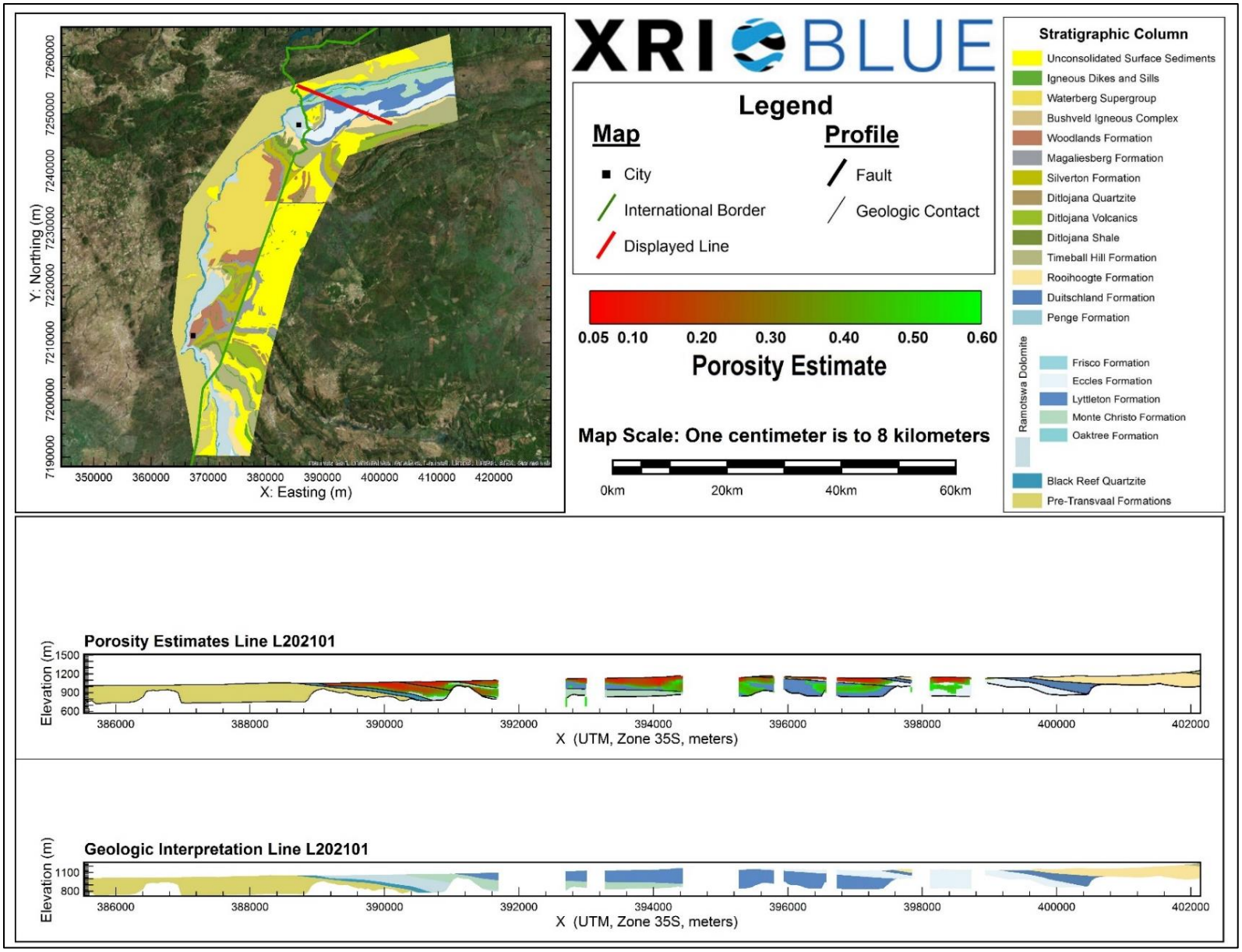

Porosity Estimates and Interpreted Geology Profile for L202101.

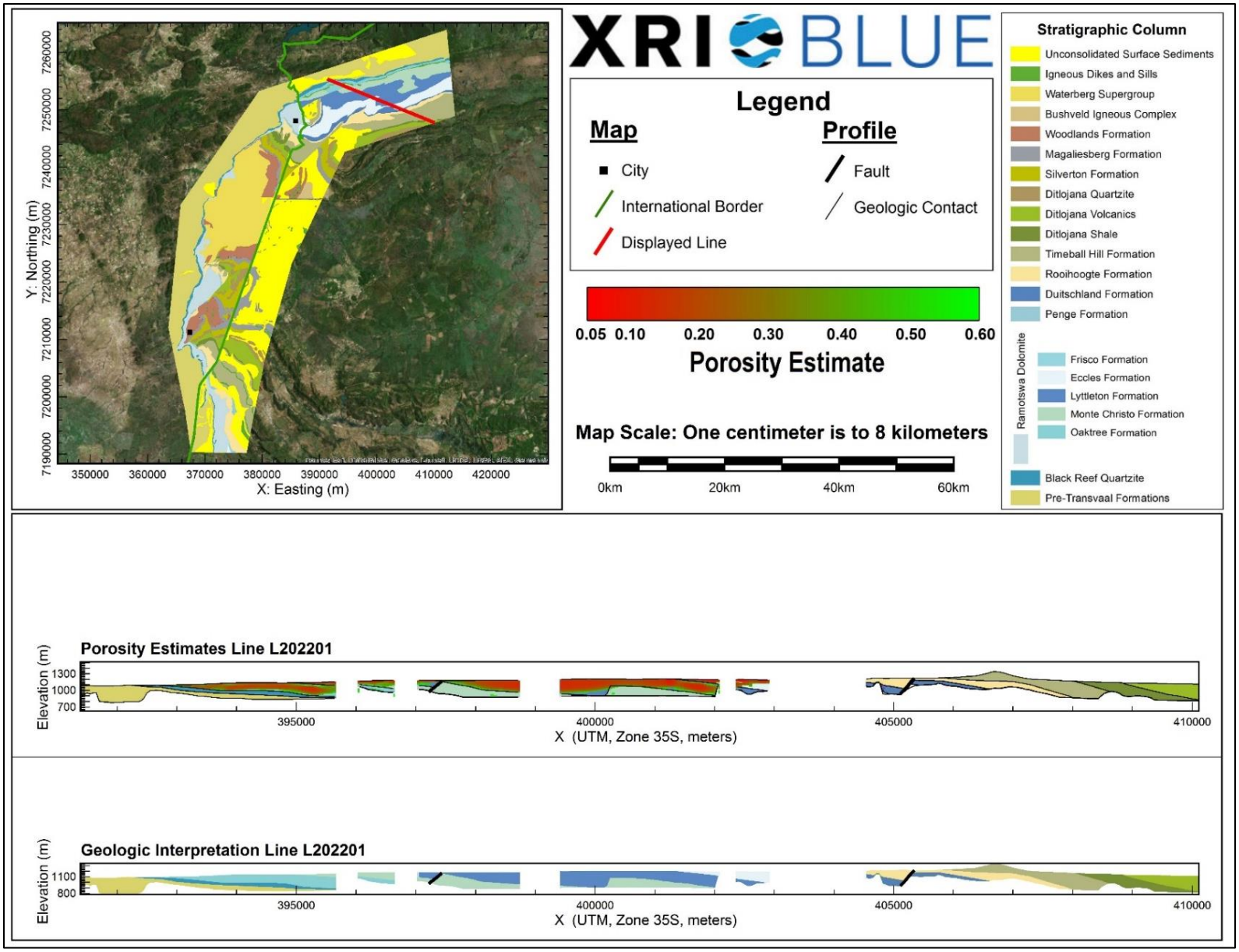

Porosity Estimates and Interpreted Geology Profile for L202201.

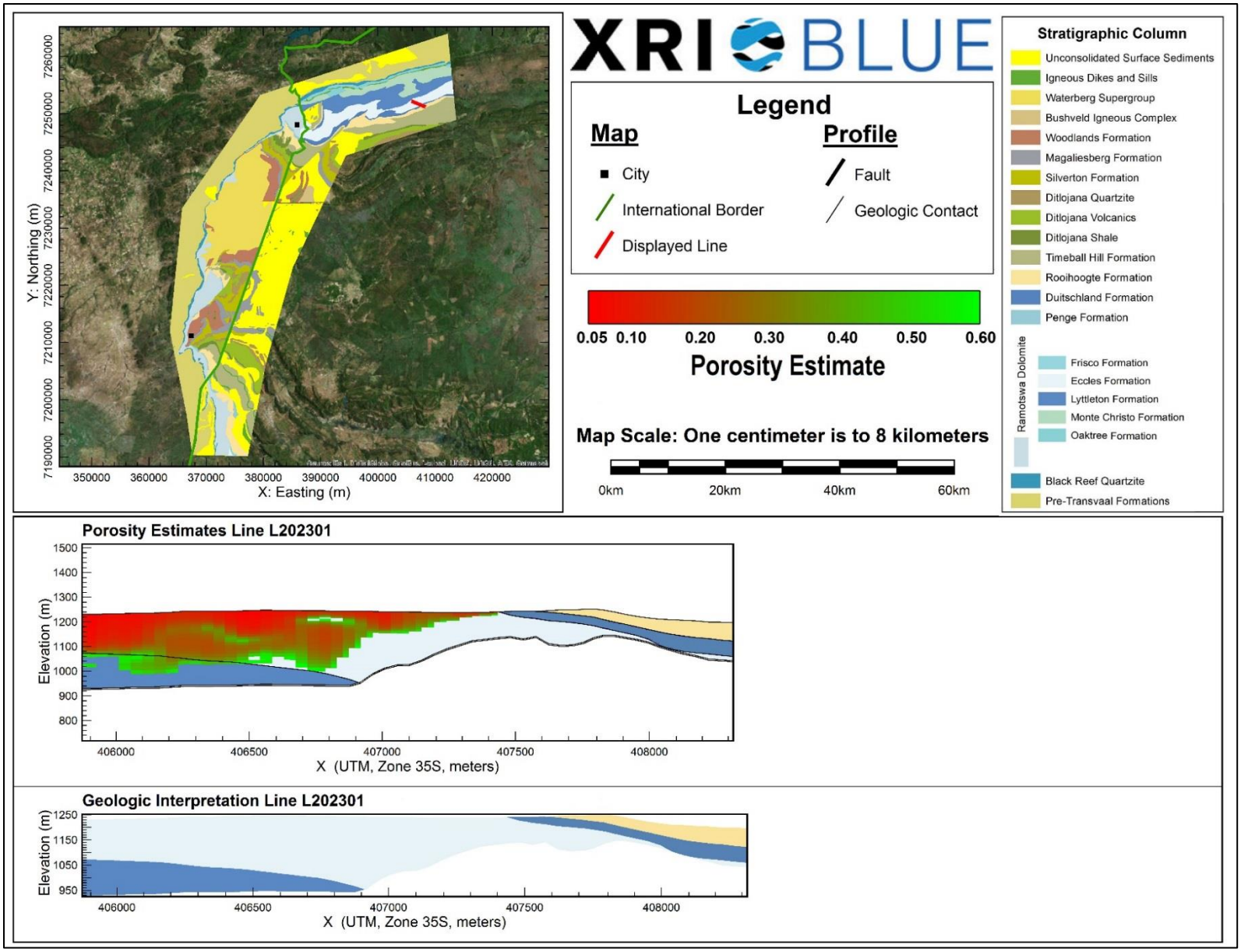

Porosity Estimates and Interpreted Geology Profile for L202301.

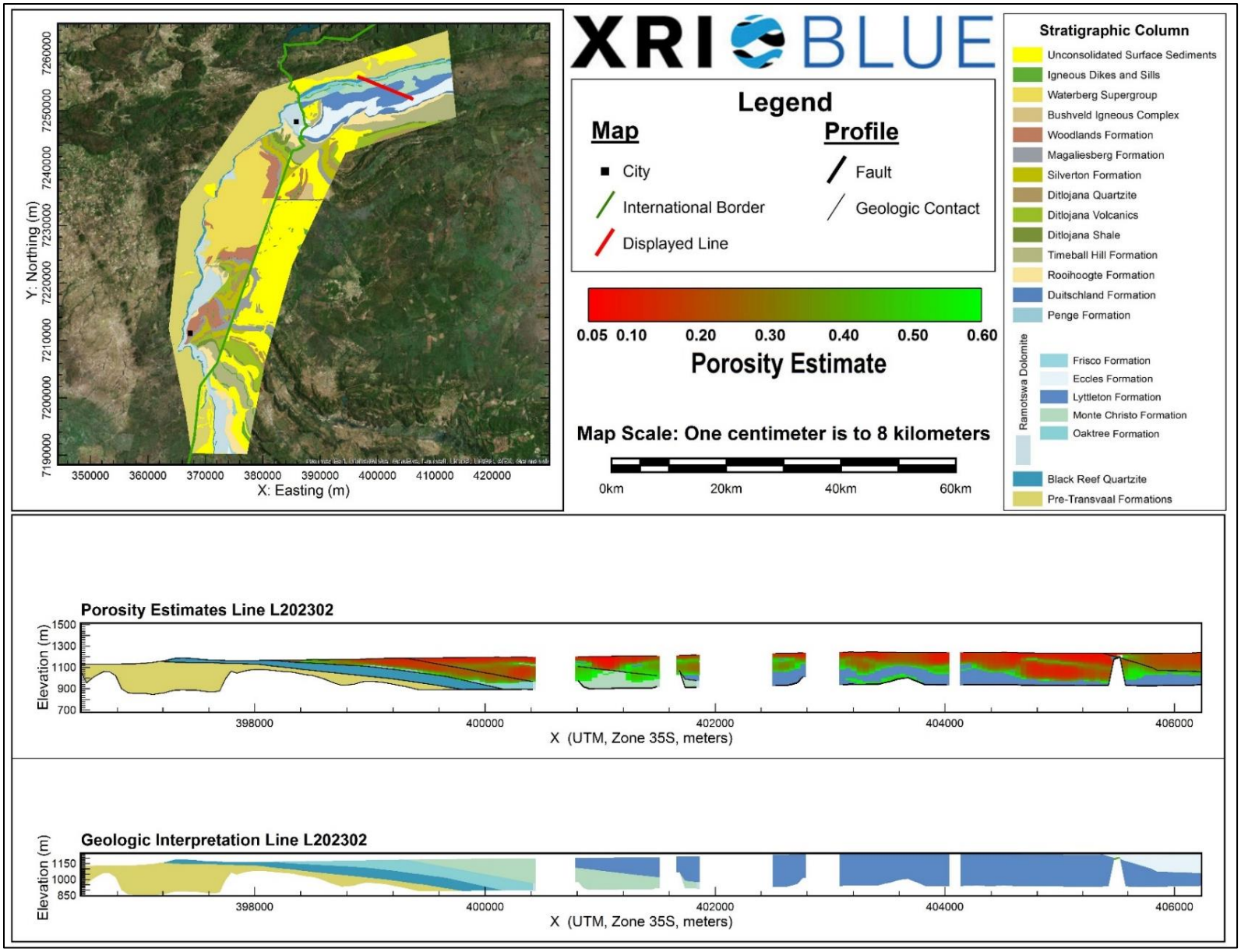

Porosity Estimates and Interpreted Geology Profile for L202302.

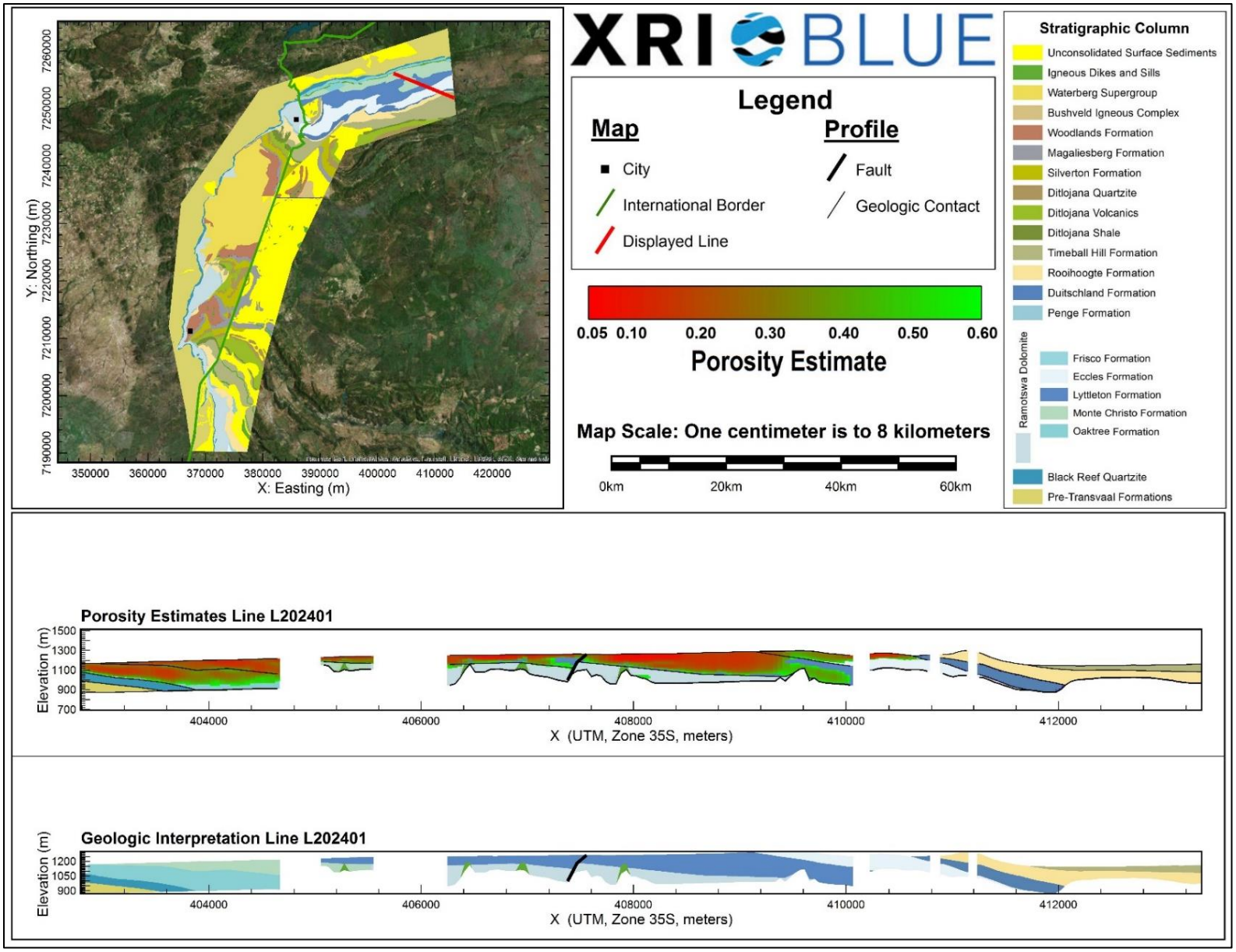

Porosity Estimates and Interpreted Geology Profile for L202401.

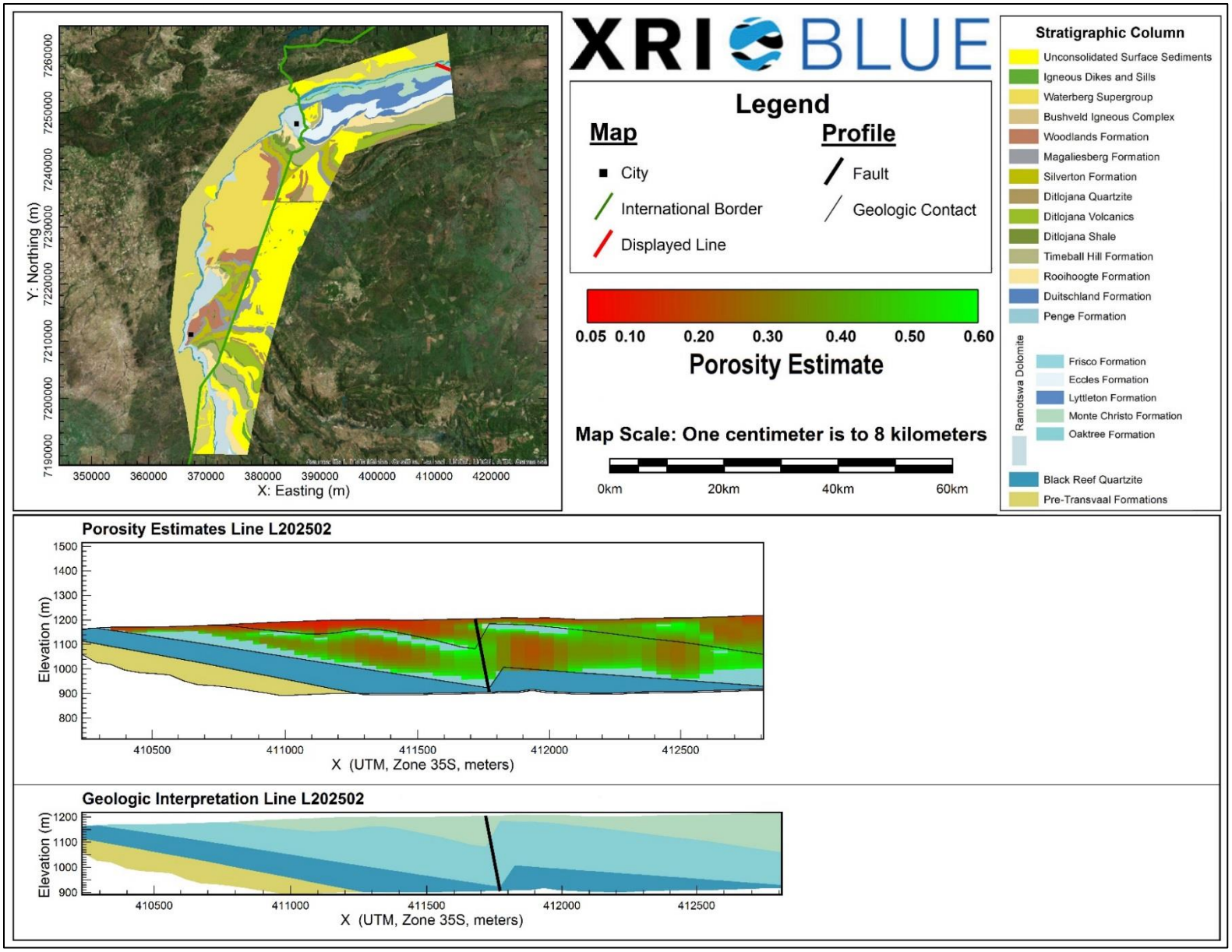

Porosity Estimates and Interpreted Geology Profile for L202502.

Appendix D: Estimated Hydraulic Conductivity Profiles

Table 3 provides the details of the interpreted geology .xyz file for the Ramotswa Project Area. Specifically the first column in Table 1 is the Header or name for each unique column in the .xyz file, the second column in Table 1 is the type of data that is presented, and the third column in Table 1 is a brief description of the data that is provided for each specific column (with units).

To view this .xyz file in Microsoft Excel, the user should open the file, which will cause a "Text Import Wizard" Popup Box to be displayed. For Step 1, make sure that the box for "Delimited" is checked, and that the "Start import at row" is set to "6", then click the "Next" button. For Step 2, the "Tab" and "Comma" Delimiters boxes should be checked, then click the "Next" button. For the Step 3, all the defaults can be left alone, and the "Finish" button can be clicked. Following these steps should allow the file to be correctly imported into Microsoft Excel with all the correct headers.

XRI used both Geosoft's Oasis Montaj (http://www.geosoft.com/products/oasis-montaj/overview) and Encom's PA (https://www.pitneybowes.com/pbencom/products/geophysics/encom-pa.html) software packages to view and interpret data for this project. An alternative software option for 3D viewing of this data that is Golden Software's Voxler (http://www.goldensoftware.com/products/voxler).

This .xyz file is the basis of the Estimated Hydraulic Conductivity Profiles included in Appendix D. The only resistivity data included in the .xyz file is resistivity that is greater than the resistivity threshold of 40 Ω-m. The hydraulic conductivity estimates included in the .xyz file are hydraulic conductivity estimates that are within the interpreted extent of the Dolomite. Any hydraulic conductivity estimates that are beneath the DOI Upper or Lower values should be interpreted with a degree of skepticism. Within the .xyz file if the symbol "*" is observed that indicates that the hydraulic conductivity estimate has not been calculated at that specific location and depth due to the fact that either the Dolomite is not interpreted to be present at that location, or the resistivity of the Dolomite is below the resistivity threshold of 40 Ω-m. The remainder of Appendix D is used to display all the unique Estimated Hydraulic Conductivity Profiles for the Ramotswa Project Area. The Estimated Hydraulic Conductivity Profiles are displayed with a 1:1 horizontal and vertical ratio, each profile is uniquely scaled so that the information for an entire flight line is displayed in one figure. While the specifics of each profile may be difficult to view in the figure, the Ramotswa_Dolomite_Hydraulic_Conductivity_Estimates.xyz file provided along with this report give all of the necessary data to understand the estimated hydraulic conductivity of the Dolomite aquifer in the Ramotswa Project Area.

Table 3: Explanation of the Estimated Hydraulic Conductivity .xyz file of the Ramotswa Project Area.

Database Header	Data Type	Description
LINE	Point	Line Number
X	Point	X Coordinate of Data Point (WGS84 UTM Zone 35S meters)
Y	Point	Y Coordinate of Data Point (WGS84 UTM Zone 35S meters)
Z	Point	Surface elevation based on USGS SRTM Digital Elevation Model (meters)
RHO_I_clip0	Point	Clipped Resistivity for data point of model layer 1 (ohm-meters)
RHO_I_clip 1	Point	Clipped Resistivity for data point of model layer 2 (ohm-meters)
RHO_I_clip 2	Point	Clipped Resistivity for data point of model layer 3 (ohm-meters)
RHO_I_clip 3	Point	Clipped Resistivity for data point of model layer 4 (ohm-meters)
RHO_I_clip 4	Point	Clipped Resistivity for data point of model layer 5 (ohm-meters)
RHO_I_clip 5	Point	Clipped Resistivity for data point of model layer 6 (ohm-meters)

RHO_I_clip 6	Point	Clipped Resistivity for data point of model layer 7 (ohm-meters)
RHO_I_clip 7	Point	Clipped Resistivity for data point of model layer 8 (ohm-meters)
RHO_I_clip 8	Point	Clipped Resistivity for data point of model layer 9 (ohm-meters)
RHO_I_clip 9	Point	Clipped Resistivity for data point of model layer 10 (ohm-meters)
RHO_I_clip 10	Point	Clipped Resistivity for data point of model layer 11 (ohm-meters)
RHO_I_clip 11	Point	Clipped Resistivity for data point of model layer 12 (ohm-meters)
RHO_I_clip 12	Point	Clipped Resistivity for data point of model layer 13 (ohm-meters)
RHO_I_clip 13	Point	Clipped Resistivity for data point of model layer 14 (ohm-meters)
RHO_I_clip 14	Point	Clipped Resistivity for data point of model layer 15 (ohm-meters)
RHO_I_clip 15	Point	Clipped Resistivity for data point of model layer 16 (ohm-meters)
RHO_I_clip 16	Point	Clipped Resistivity for data point of model layer 17 (ohm-meters)
RHO_I_clip 17	Point	Clipped Resistivity for data point of model layer 18 (ohm-meters)
RHO_I_clip 18	Point	Clipped Resistivity for data point of model layer 19 (ohm-meters)
RHO_I_clip 19	Point	Clipped Resistivity for data point of model layer 20 (ohm-meters)
RHO_I_clip 20	Point	Clipped Resistivity for data point of model layer 21 (ohm-meters)
RHO_I_clip 21	Point	Clipped Resistivity for data point of model layer 22 (ohm-meters)
RHO_I_clip 22	Point	Clipped Resistivity for data point of model layer 23 (ohm-meters)
RHO_I_clip 23	Point	Clipped Resistivity for data point of model layer 24 (ohm-meters)
RHO_I_clip 24	Point	Clipped Resistivity for data point of model layer 25 (ohm-meters)
RHO_I_clip 25	Point	Clipped Resistivity for data point of model layer 26 (ohm-meters)
RHO_I_clip 26	Point	Clipped Resistivity for data point of model layer 27 (ohm-meters)
RHO_I_clip 27	Point	Clipped Resistivity for data point of model layer 28 (ohm-meters)
RHO_I_clip 28	Point	Clipped Resistivity for data point of model layer 29 (ohm-meters)
RHO_I_clip 29	Point	Clipped Resistivity for data point of model layer 30 (ohm-meters)
DEP_BOT0	Point	Depth to the bottom of model layer 1 in the AEM model (meters)
DEP_BOT1	Point	Depth to the bottom of model layer 2 in the AEM model (meters)
DEP_BOT2	Point	Depth to the bottom of model layer 3 in the AEM model (meters)
DEP_BOT3	Point	Depth to the bottom of model layer 4 in the AEM model (meters)
DEP_BOT4	Point	Depth to the bottom of model layer 5 in the AEM model (meters)
DEP_BOT5	Point	Depth to the bottom of model layer 6 in the AEM model (meters)
DEP_BOT6	Point	Depth to the bottom of model layer 7 in the AEM model (meters)
DEP_BOT7	Point	Depth to the bottom of model layer 8 in the AEM model (meters)
DEP_BOT8	Point	Depth to the bottom of model layer 9 in the AEM model (meters)
DEP_BOT9	Point	Depth to the bottom of model layer 10 in the AEM model (meters)
DEP_BOT10	Point	Depth to the bottom of model layer 11 in the AEM model (meters)
DEP_BOT11	Point	Depth to the bottom of model layer 12 in the AEM model (meters)
DEP_BOT12	Point	Depth to the bottom of model layer 13 in the AEM model (meters)
DEP_BOT13	Point	Depth to the bottom of model layer 14 in the AEM model (meters)
DEP_BOT14	Point	Depth to the bottom of model layer 15 in the AEM model (meters)
DEP_BOT15	Point	Depth to the bottom of model layer 16 in the AEM model (meters)
DEP_BOT16	Point	Depth to the bottom of model layer 17 in the AEM model (meters)
DEP_BOT17	Point	Depth to the bottom of model layer 18 in the AEM model (meters)
DEP_BOT18	Point	Depth to the bottom of model layer 19 in the AEM model (meters)

DEP_BOT19	Point	Depth to the bottom of model layer 20 in the AEM model (meters)
DEP_BOT20	Point	Depth to the bottom of model layer 21 in the AEM model (meters)
DEP_BOT21	Point	Depth to the bottom of model layer 22 in the AEM model (meters)
DEP_BOT22	Point	Depth to the bottom of model layer 23 in the AEM model (meters)
DEP_BOT23	Point	Depth to the bottom of model layer 24 in the AEM model (meters)
DEP_BOT24	Point	Depth to the bottom of model layer 25 in the AEM model (meters)
DEP_BOT25	Point	Depth to the bottom of model layer 26 in the AEM model (meters)
DEP_BOT26	Point	Depth to the bottom of model layer 27 in the AEM model (meters)
DEP_BOT27	Point	Depth to the bottom of model layer 28 in the AEM model (meters)
DEP_BOT28	Point	Depth to the bottom of model layer 29 in the AEM model (meters)
DOI_UPPER	Point	Shallow DOI estimate for data point (meters)
DOI_LOWER	Point	Deep DOI estimate for data point (meters)
RD_Top	Point	Interpreted top of the Ramotswa Dolomite (meters)
RD_Base	Point	Interpreted base of the Ramotswa Dolomite (meters)
Conductivity_Estimate0	Point	Estimated hydraulic conductivity of model layer 1 in the AEM model (meters per day)
Conductivity_Estimate1	Point	Estimated hydraulic conductivity of model layer 2 in the AEM model (meters per day)
Conductivity_Estimate2	Point	Estimated hydraulic conductivity of model layer 3 in the AEM model (meters per day)
Conductivity_Estimate3	Point	Estimated hydraulic conductivity of model layer 4 in the AEM model (meters per day)
Conductivity_Estimate4	Point	Estimated hydraulic conductivity of model layer 5 in the AEM model (meters per day)
Conductivity_Estimate5	Point	Estimated hydraulic conductivity of model layer 6 in the AEM model (meters per day)
Conductivity_Estimate6	Point	Estimated hydraulic conductivity of model layer 7 in the AEM model (meters per day)
Conductivity_Estimate7	Point	Estimated hydraulic conductivity of model layer 8 in the AEM model (meters per day)
Conductivity_Estimate8	Point	Estimated hydraulic conductivity of model layer 9 in the AEM model (meters per day)
Conductivity_Estimate9	Point	Estimated hydraulic conductivity of model layer 10 in the AEM model (meters per day)
Conductivity_Estimate10	Point	Estimated hydraulic conductivity of model layer 11 in the AEM model (meters per day)
Conductivity_Estimate11	Point	Estimated hydraulic conductivity of model layer 12 in the AEM model (meters per day)
Conductivity_Estimate12	Point	Estimated hydraulic conductivity of model layer 13 in the AEM model (meters per day)
Conductivity_Estimate13	Point	Estimated hydraulic conductivity of model layer 14 in the AEM model (meters per day)
Conductivity_Estimate14	Point	Estimated hydraulic conductivity of model layer 15 in the AEM model (meters per day)
Conductivity_Estimate15	Point	Estimated hydraulic conductivity of model layer 16 in the AEM model (meters per day)

Conductivity_Estimate16	Point	Estimated hydraulic conductivity of model layer 17 in the AEM model (meters per day)
Conductivity_Estimate17	Point	Estimated hydraulic conductivity of model layer 18 in the AEM model (meters per day)
Conductivity_Estimate18	Point	Estimated hydraulic conductivity of model layer 19 in the AEM model (meters per day)
Conductivity_Estimate19	Point	Estimated hydraulic conductivity of model layer 20 in the AEM model (meters per day)
Conductivity_Estimate20	Point	Estimated hydraulic conductivity of model layer 21 in the AEM model (meters per day)
Conductivity_Estimate21	Point	Estimated hydraulic conductivity of model layer 22 in the AEM model (meters per day)
Conductivity_Estimate22	Point	Estimated hydraulic conductivity of model layer 23 in the AEM model (meters per day)
Conductivity _Estimate23	Point	Estimated hydraulic conductivity of model layer 24 in the AEM model (meters per day)
Conductivity_Estimate24	Point	Estimated hydraulic conductivity of model layer 25 in the AEM model (meters per day)
Conductivity_Estimate25	Point	Estimated hydraulic conductivity of model layer 26 in the AEM model (meters per day)
Conductivity_Estimate26	Point	Estimated hydraulic conductivity of model layer 27 in the AEM model (meters per day)
Conductivity_Estimate27	Point	Estimated hydraulic conductivity of model layer 28 in the AEM model (meters per day)
Conductivity_Estimate28	Point	Estimated hydraulic conductivity of model layer 29 in the AEM model (meters per day)
Conductivity_Estimate29	Point	Estimated hydraulic conductivity of model layer 30 in the AEM model (meters per day)

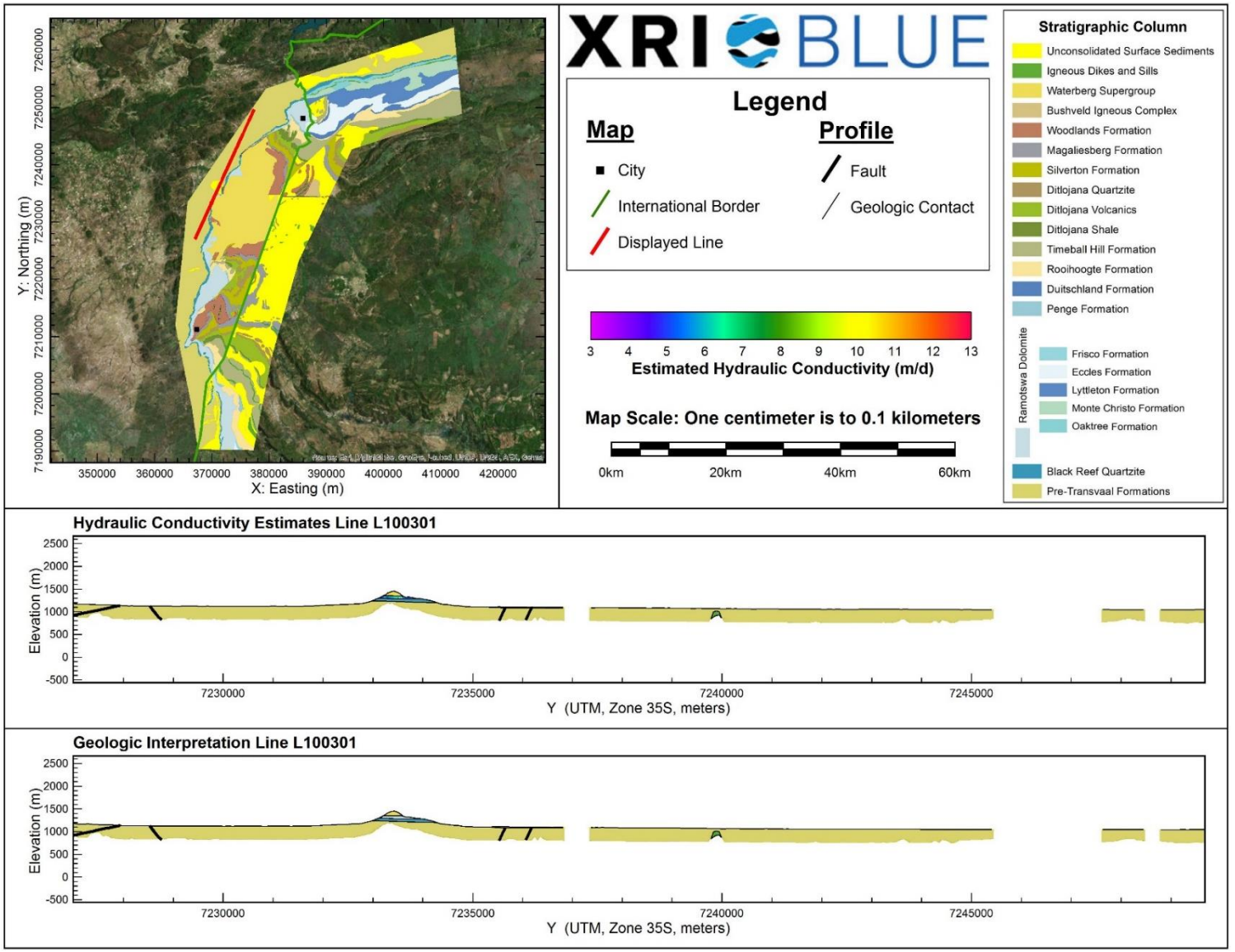

Hydraulic Conductivity Estimates and Interpreted Geology Profile for L100301.

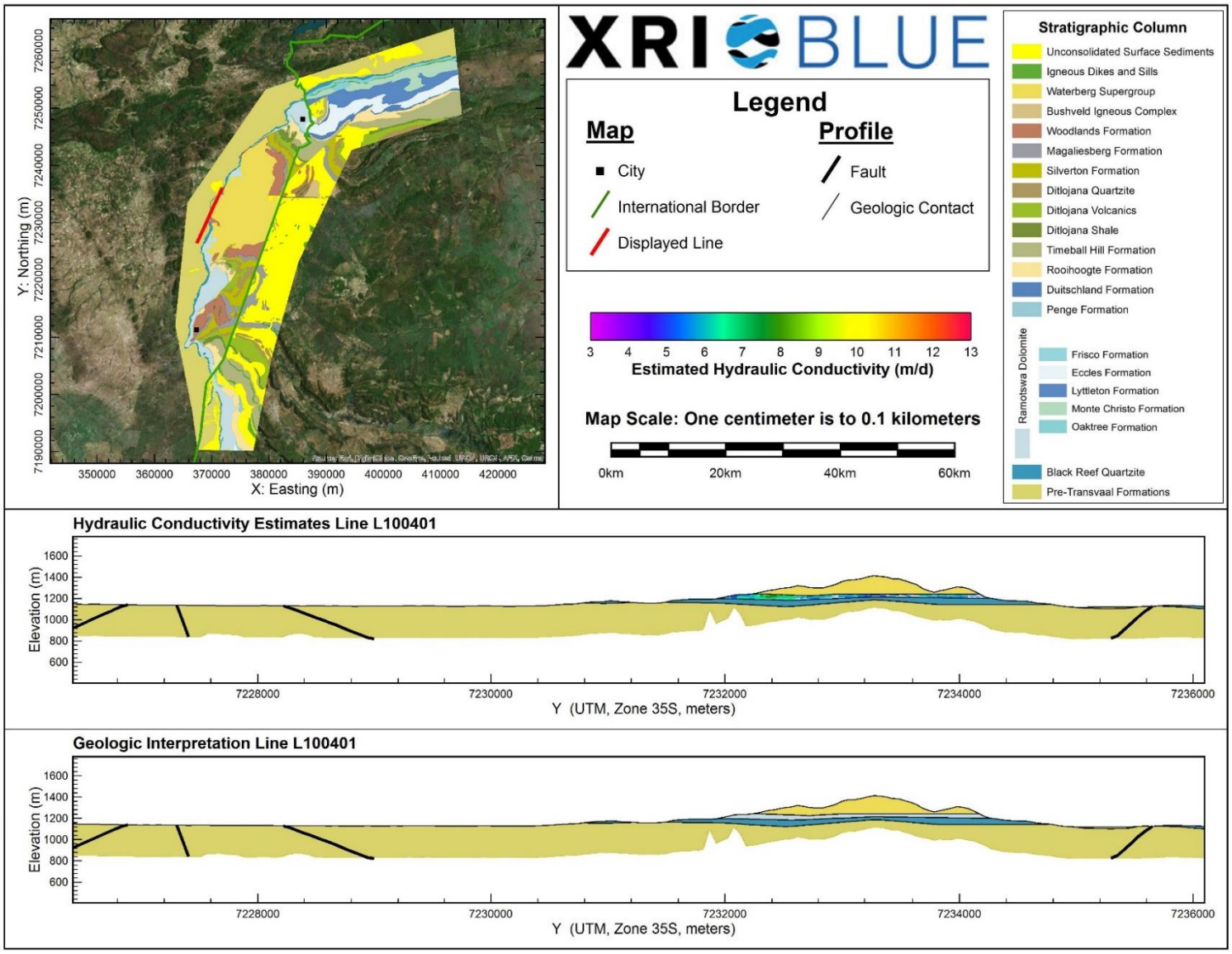

Hydraulic Conductivity Estimates and Interpreted Geology Profile for L100401.

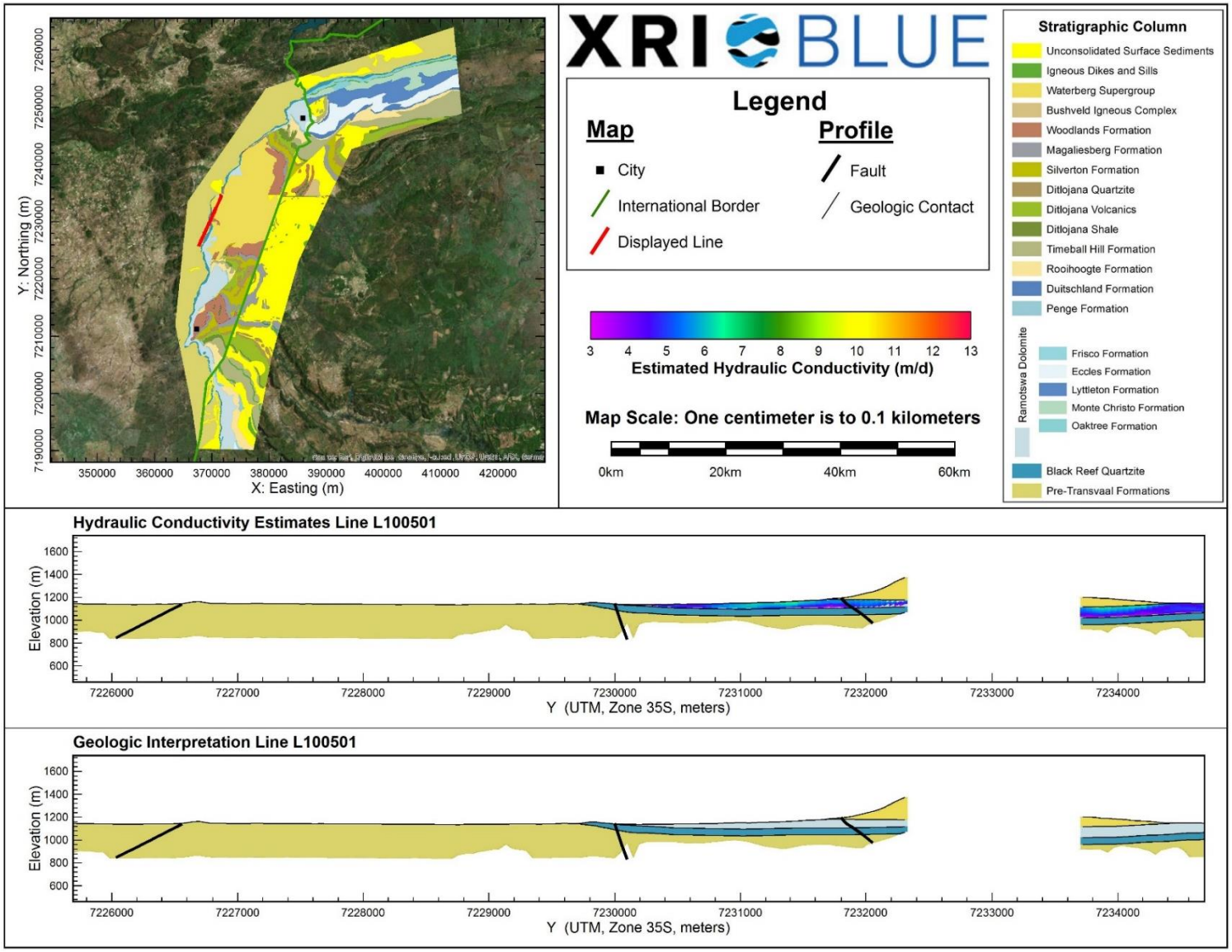

Hydraulic Conductivity Estimates and Interpreted Geology Profile for L100501.

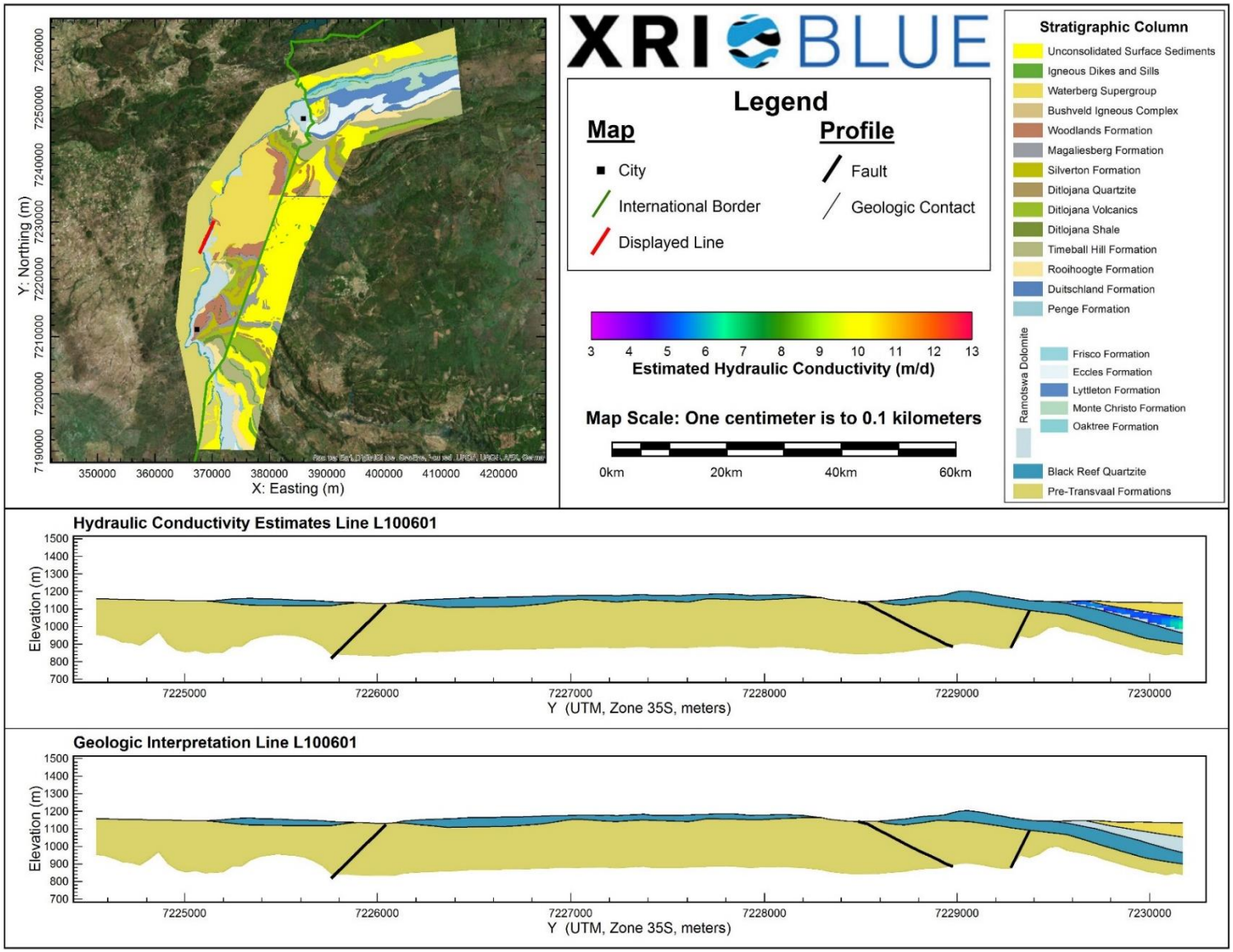

Hydraulic Conductivity Estimates and Interpreted Geology Profile for L100601.

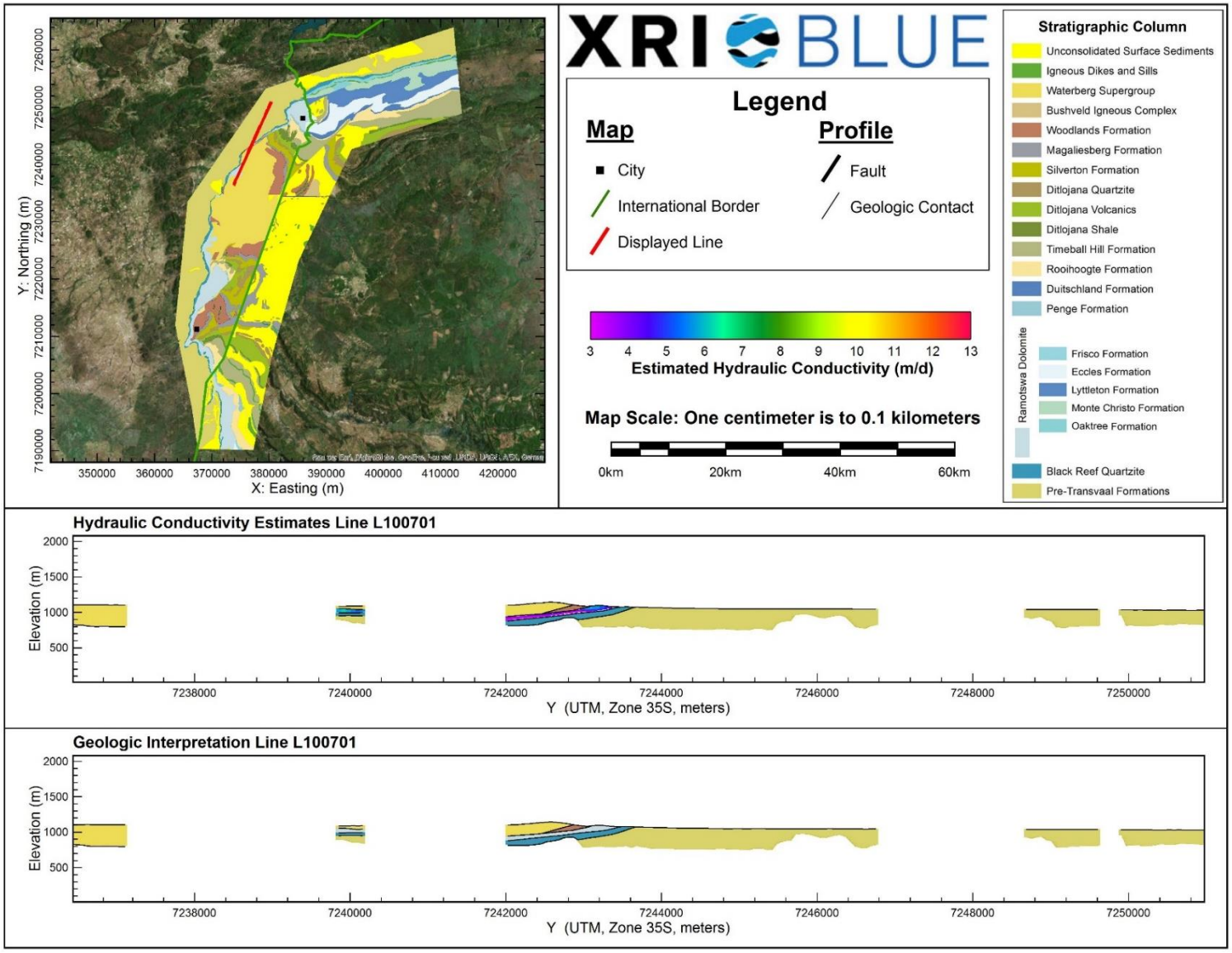

Hydraulic Conductivity Estimates and Interpreted Geology Profile for L100701.

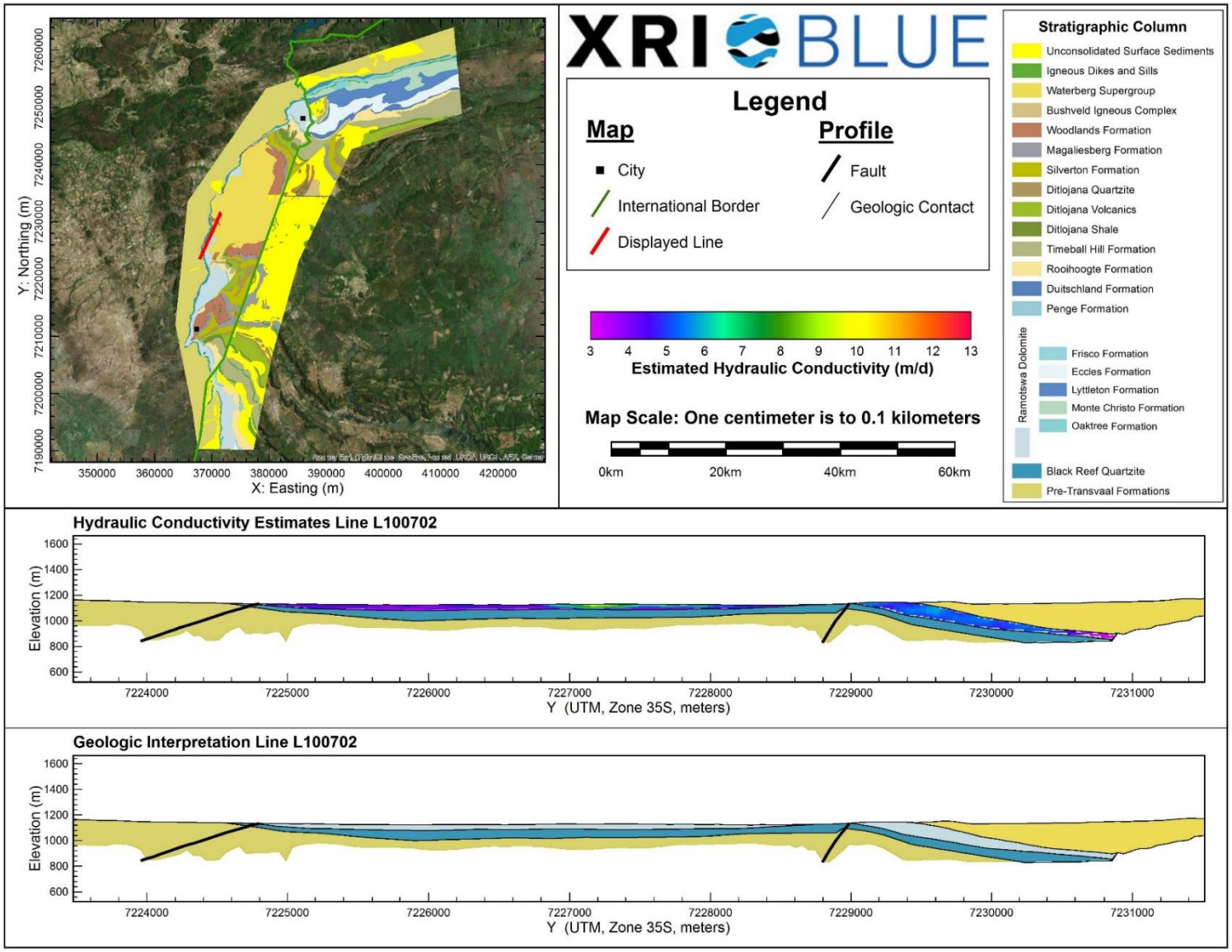

Hydraulic Conductivity Estimates and Interpreted Geology Profile for L100702.

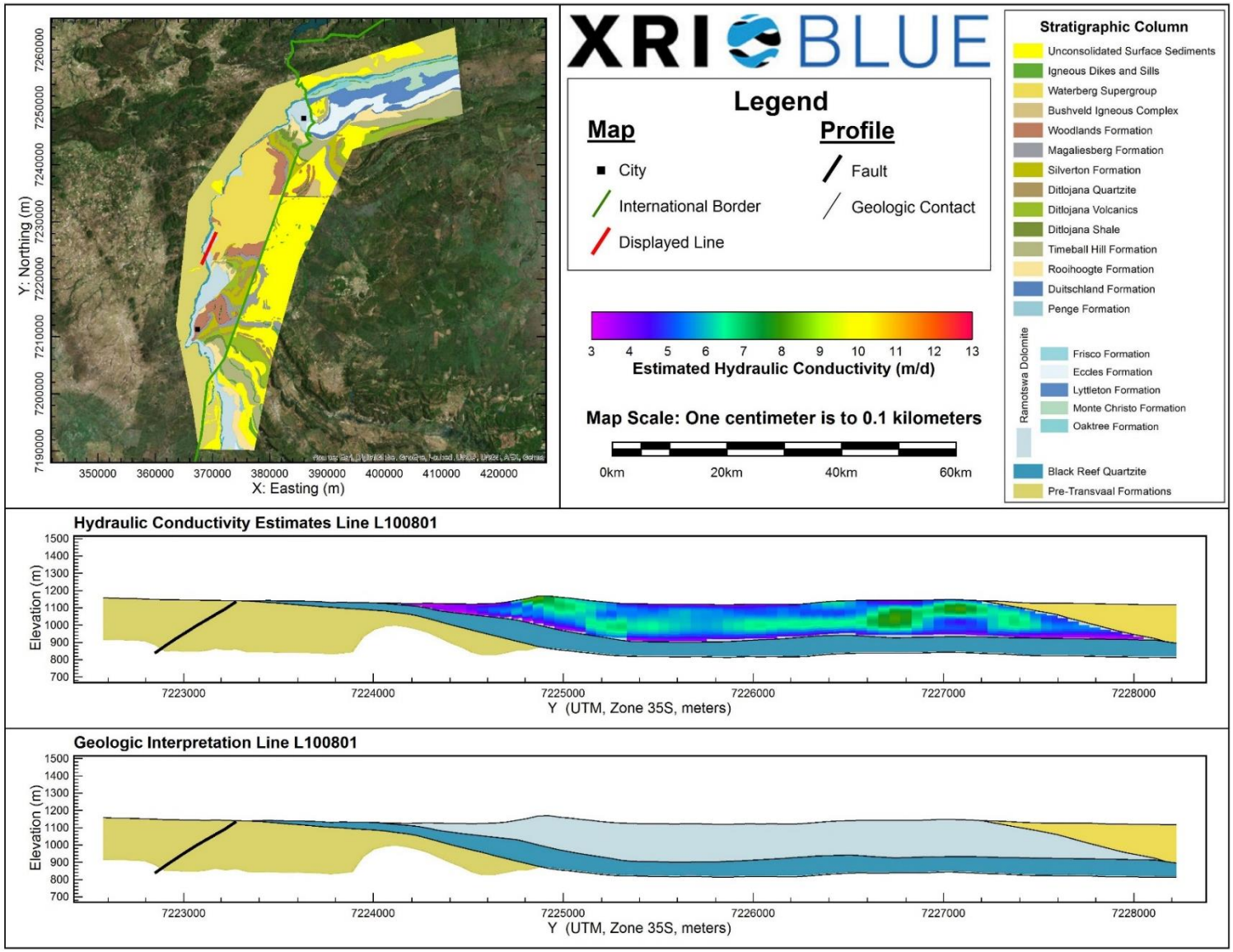

Hydraulic Conductivity Estimates and Interpreted Geology Profile for L100801.

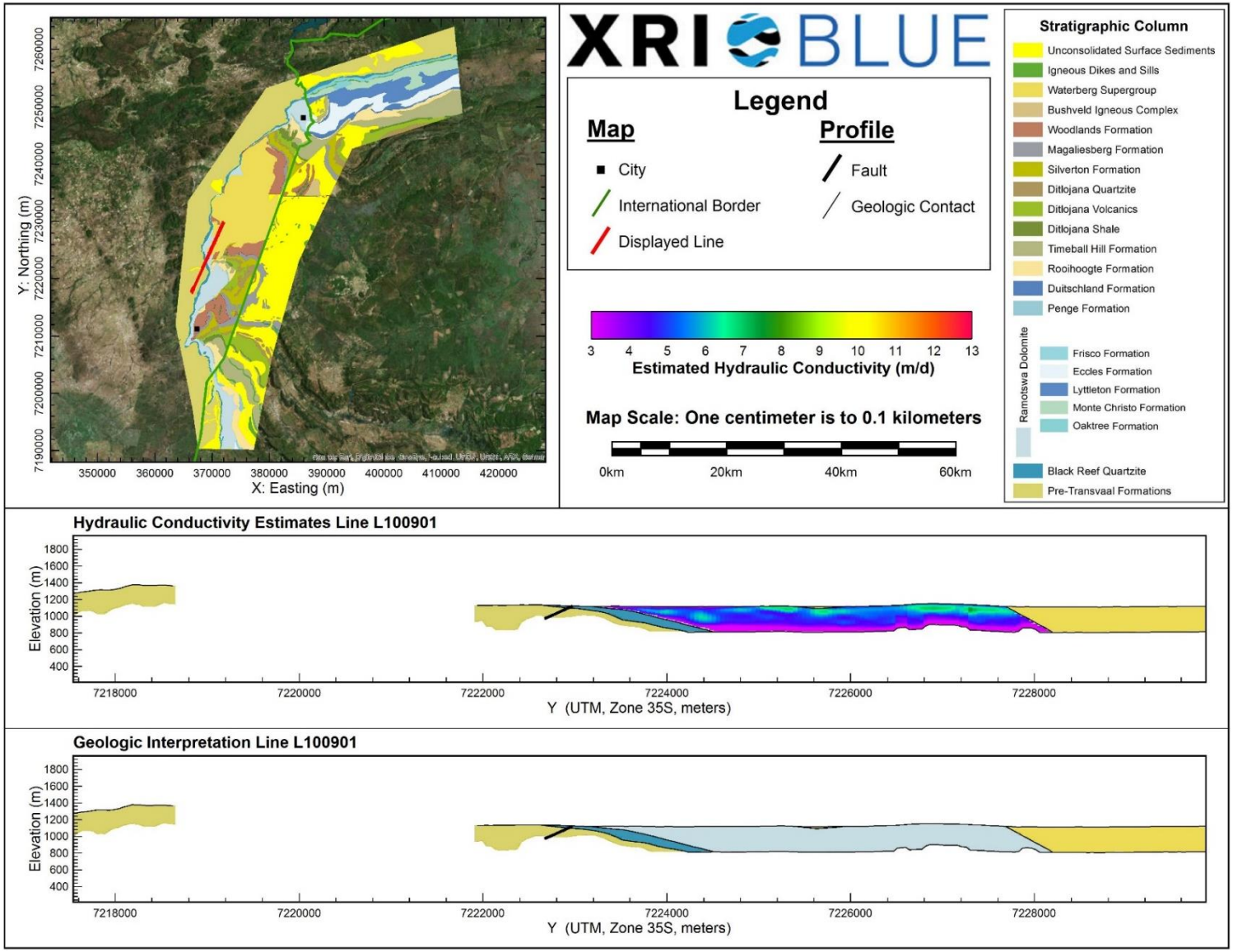

Hydraulic Conductivity Estimates and Interpreted Geology Profile for L100901.

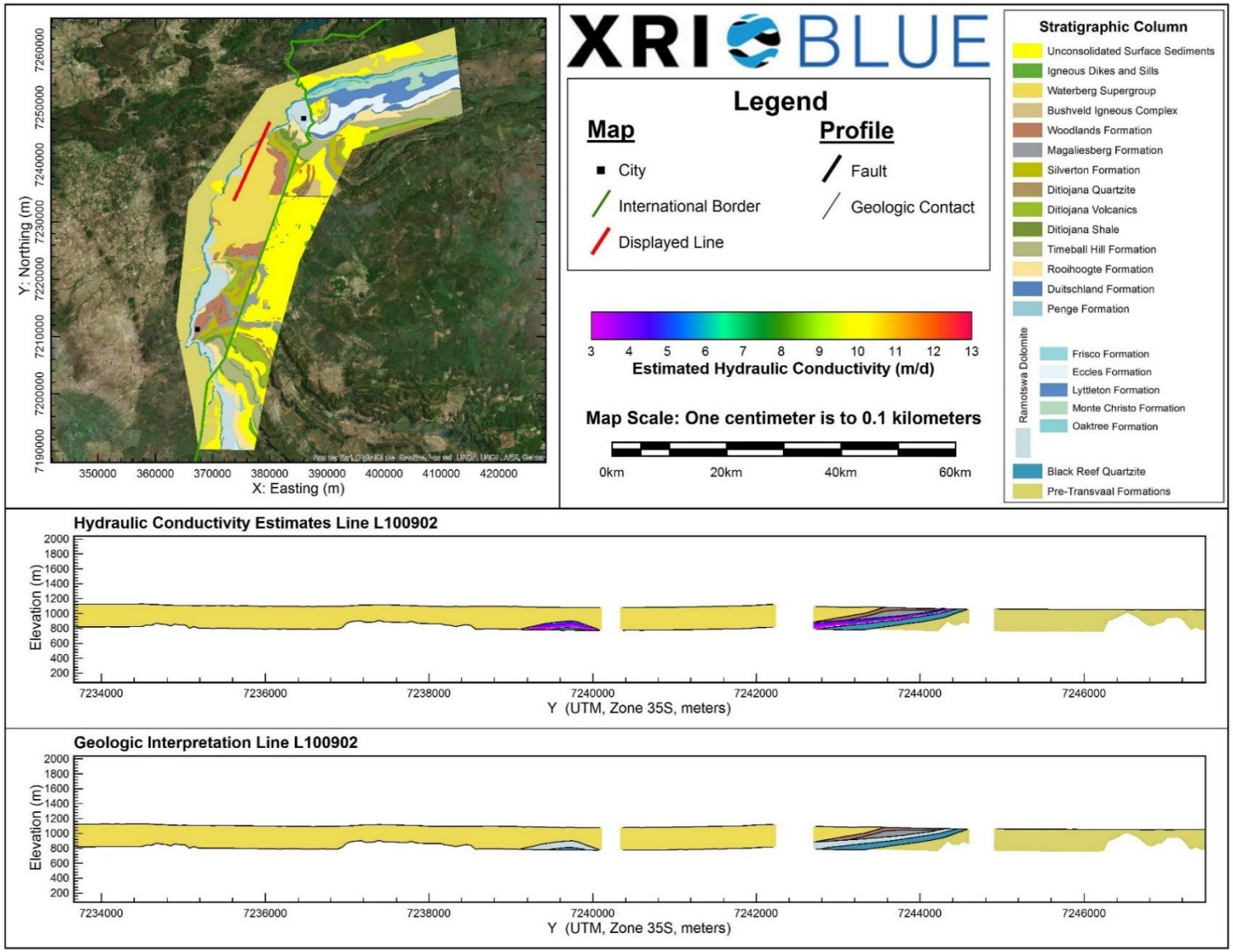

Hydraulic Conductivity Estimates and Interpreted Geology Profile for L100902.

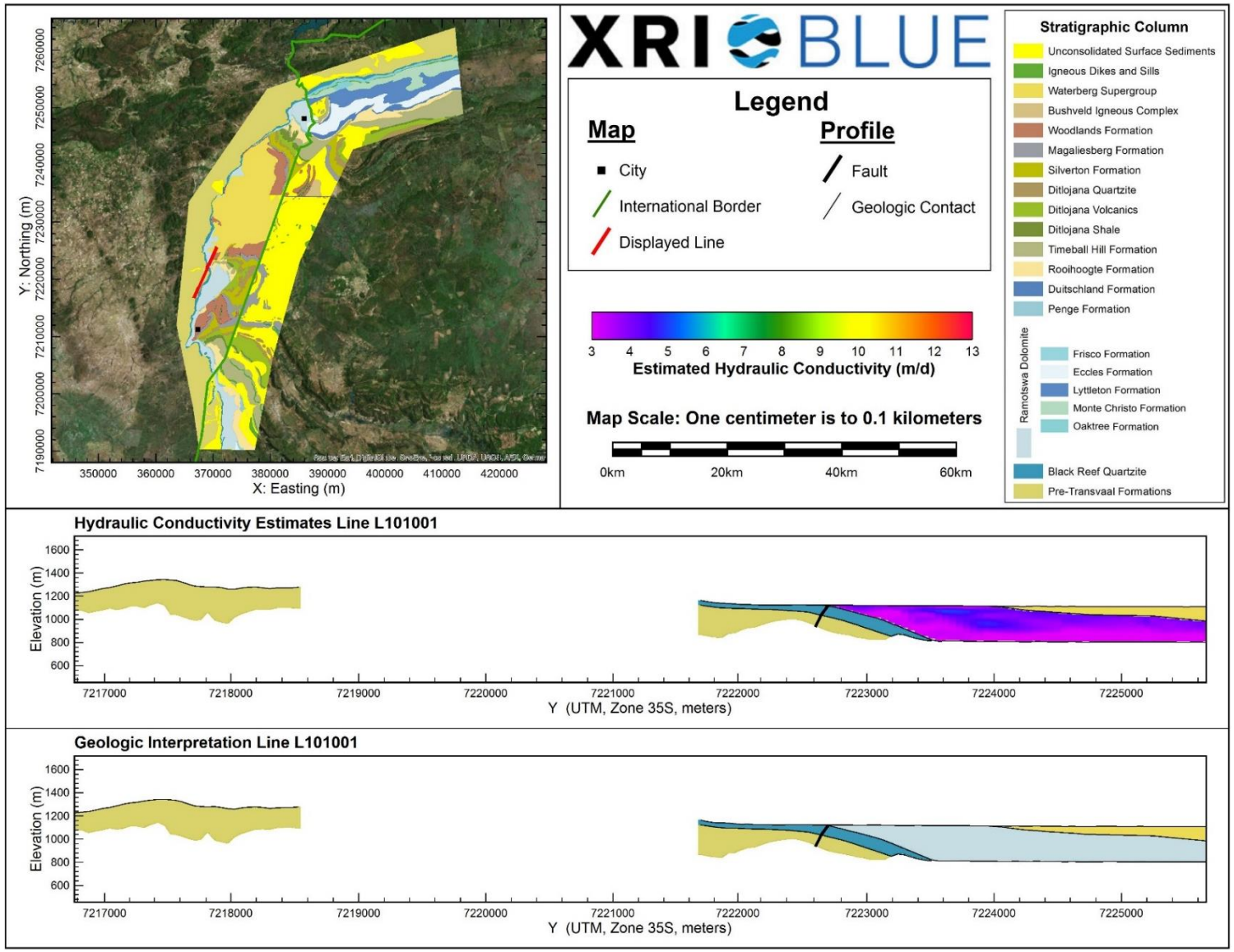

Hydraulic Conductivity Estimates and Interpreted Geology Profile for L101001.

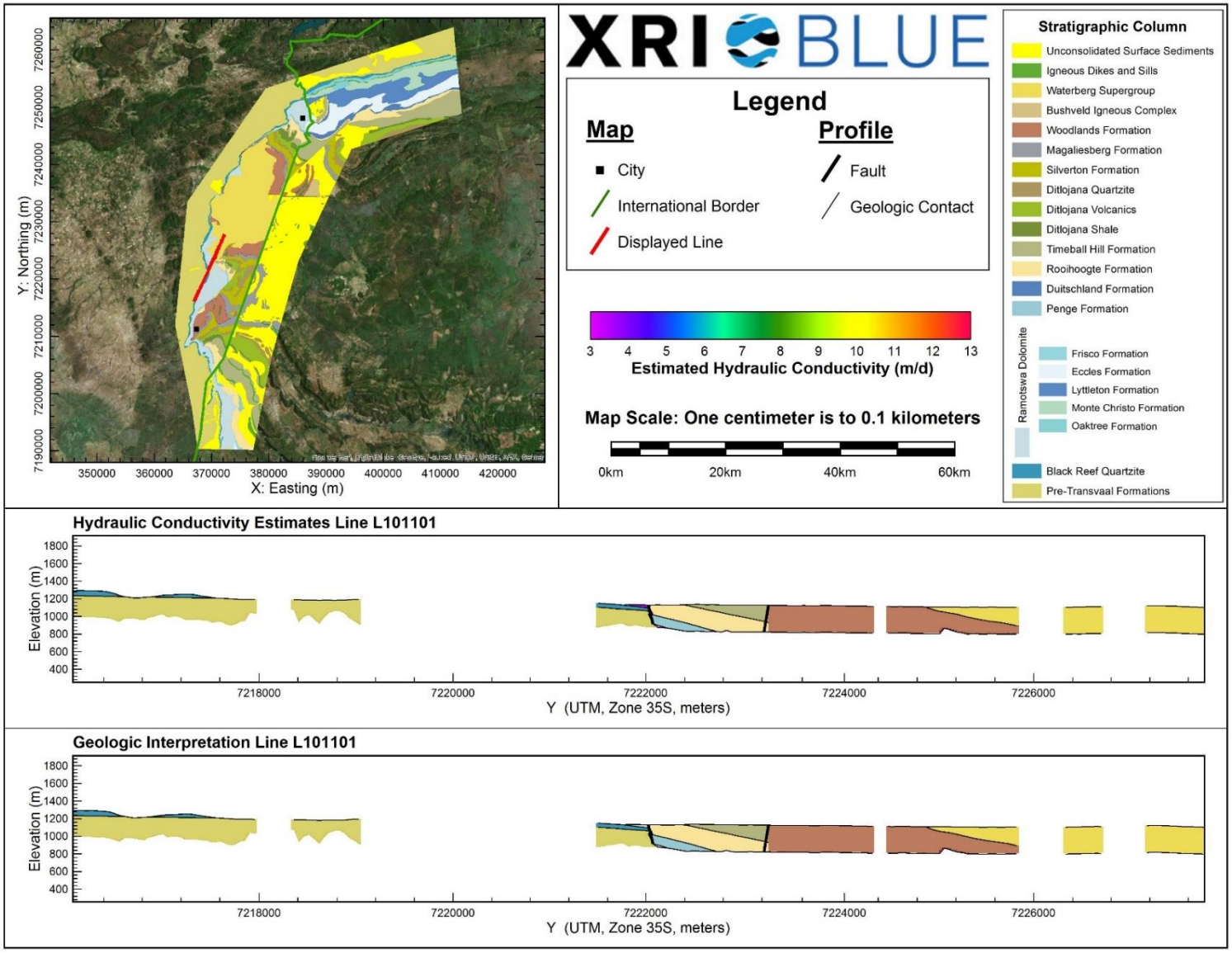

Hydraulic Conductivity Estimates and Interpreted Geology Profile for L101101.

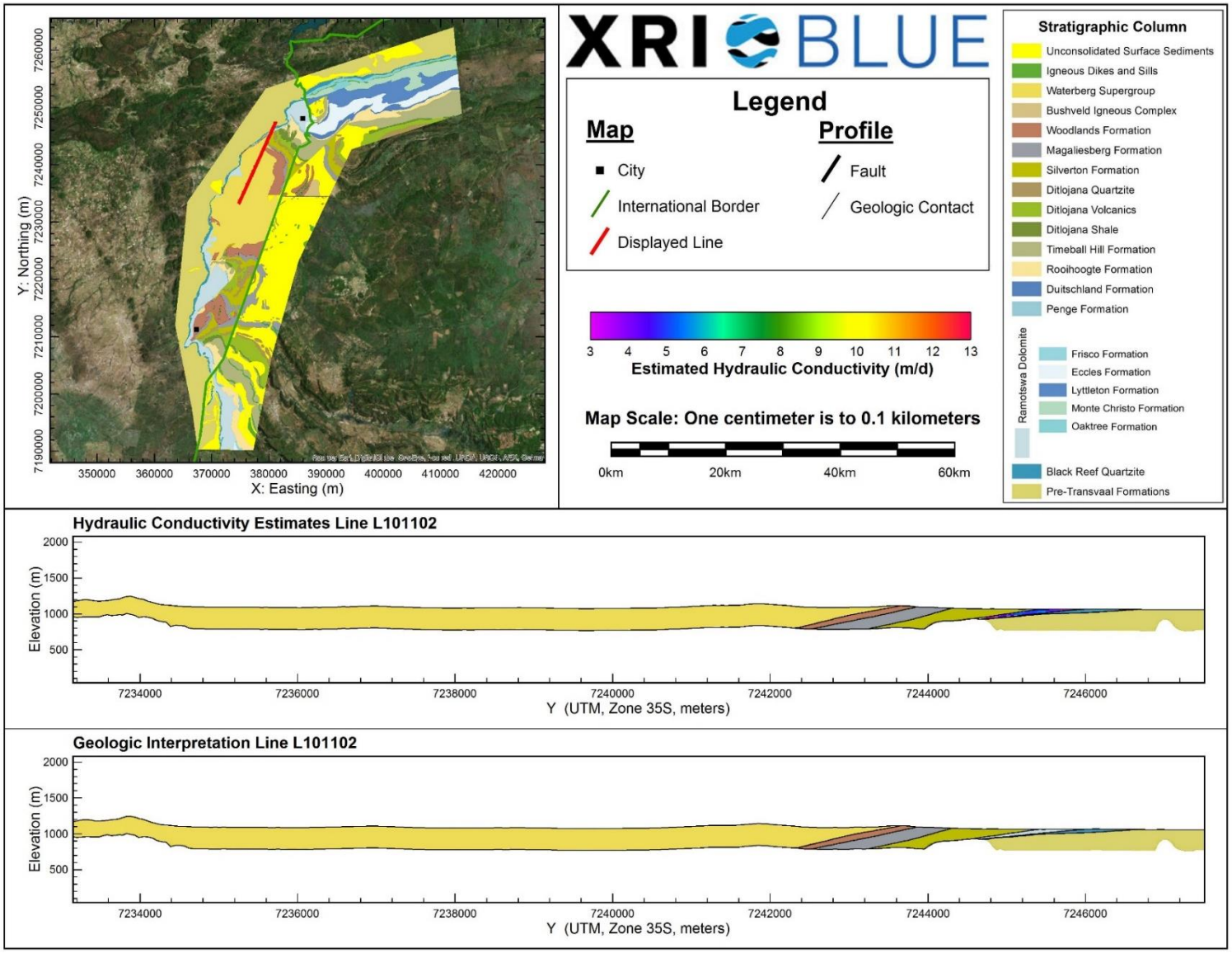

Hydraulic Conductivity Estimates and Interpreted Geology Profile for L101102.

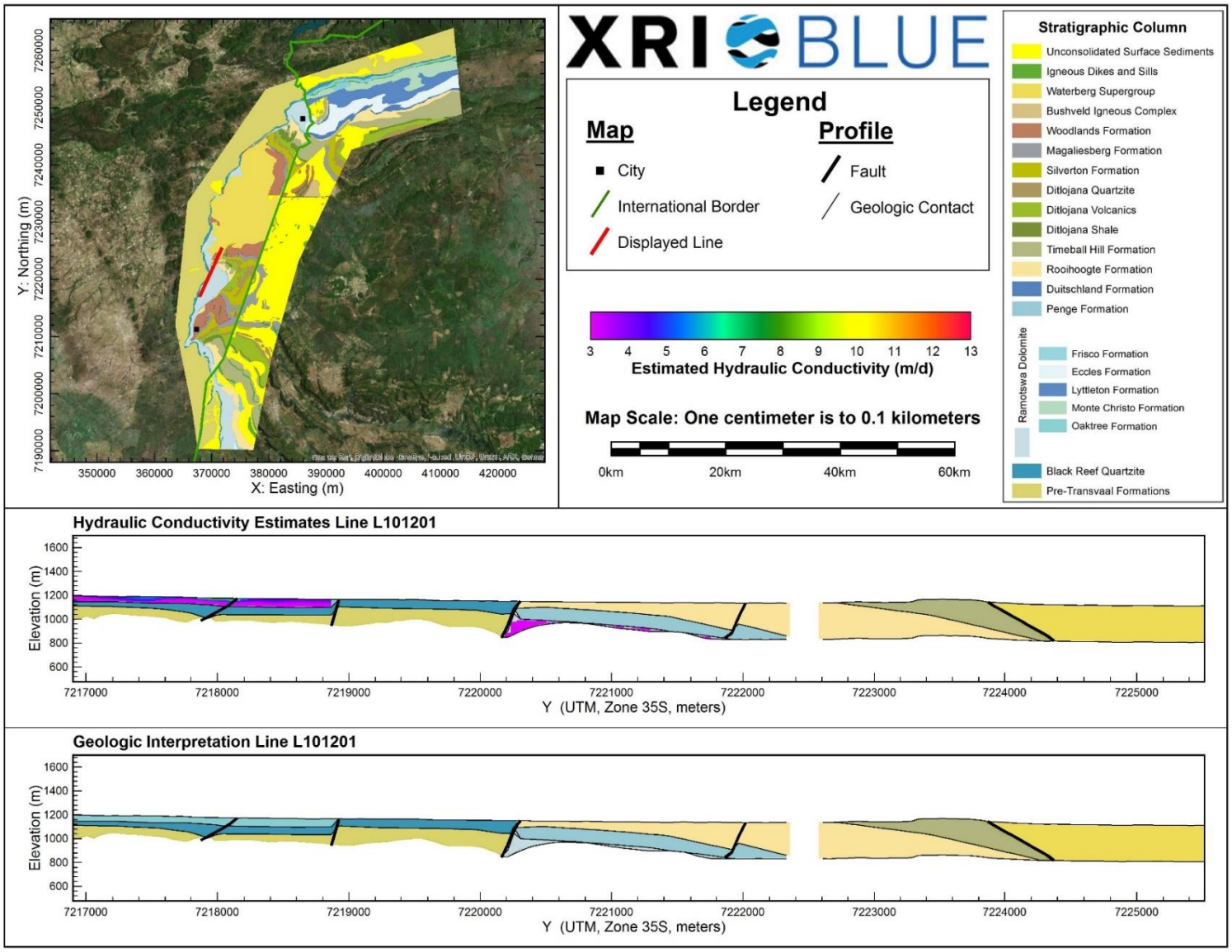

Hydraulic Conductivity Estimates and Interpreted Geology Profile for L101201.

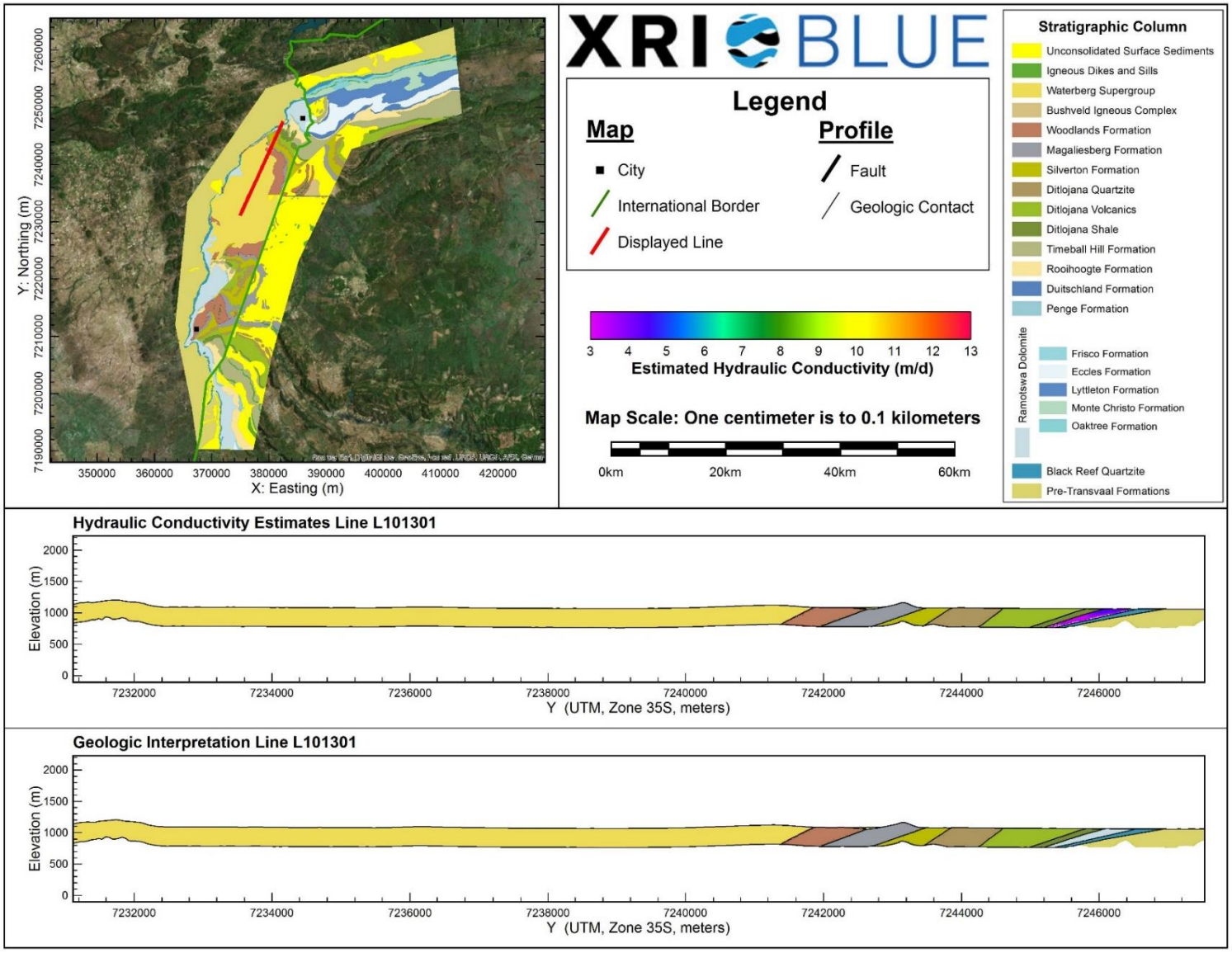

Hydraulic Conductivity Estimates and Interpreted Geology Profile for L101301.

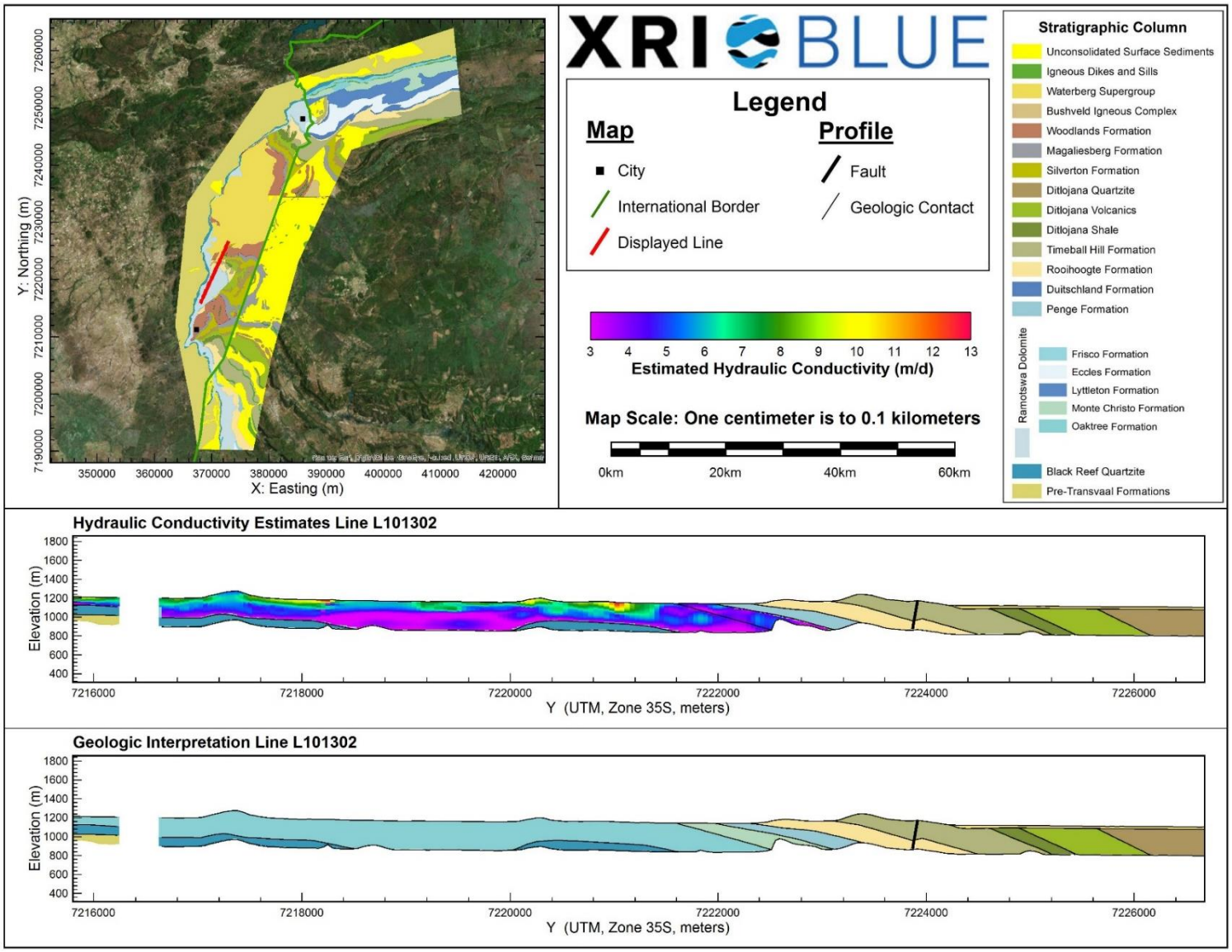

Hydraulic Conductivity Estimates and Interpreted Geology Profile for L101302.

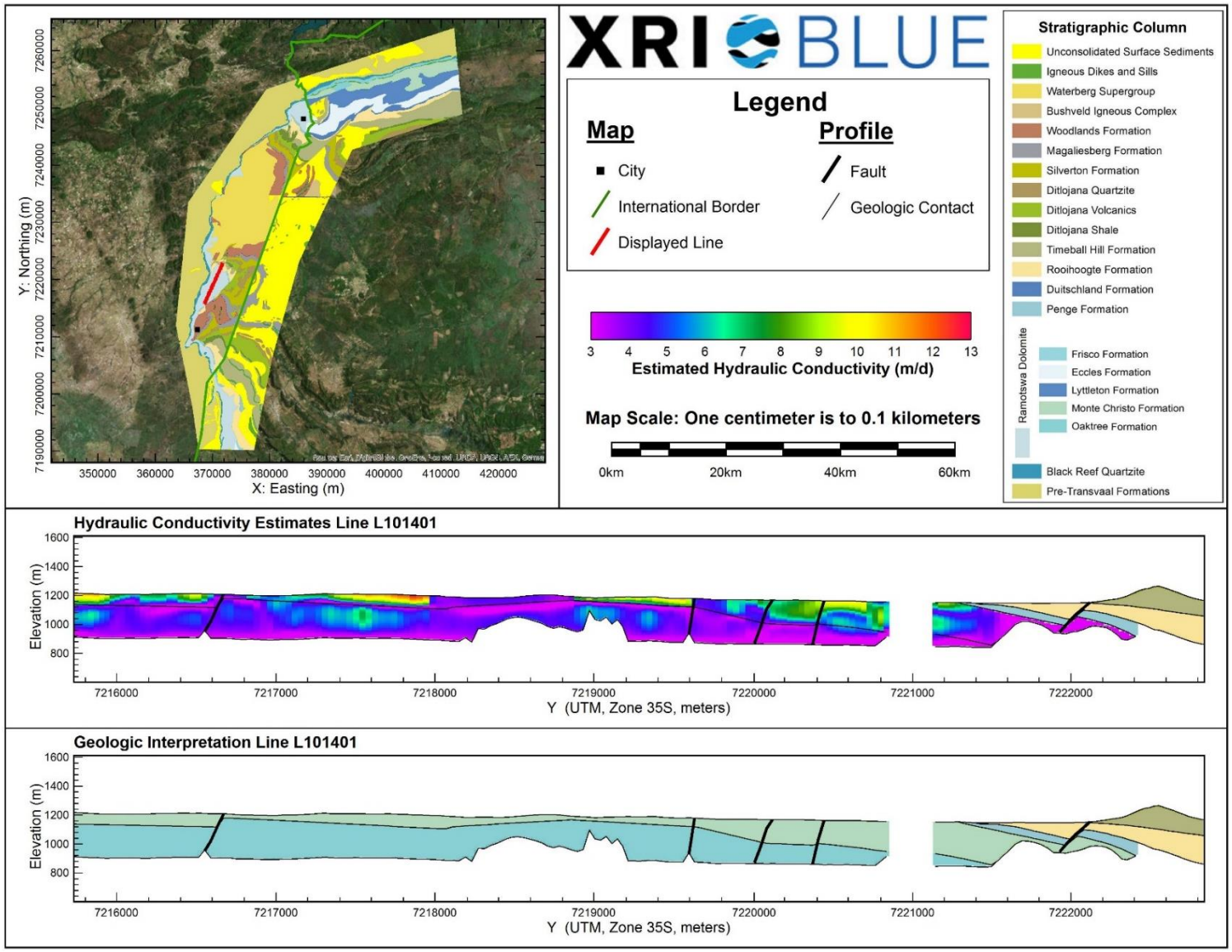

Hydraulic Conductivity Estimates and Interpreted Geology Profile for L101401.

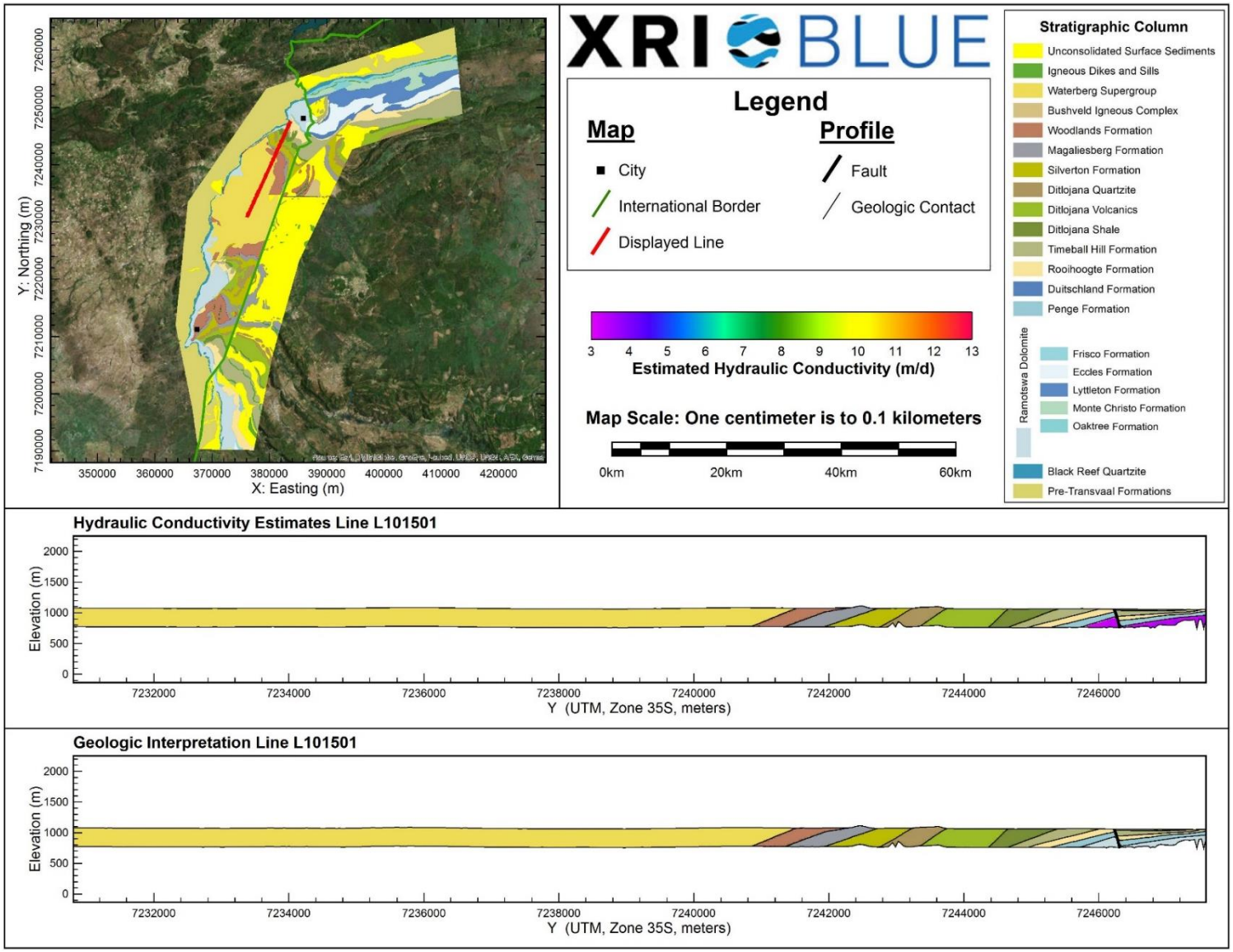

Hydraulic Conductivity Estimates and Interpreted Geology Profile for L101501.

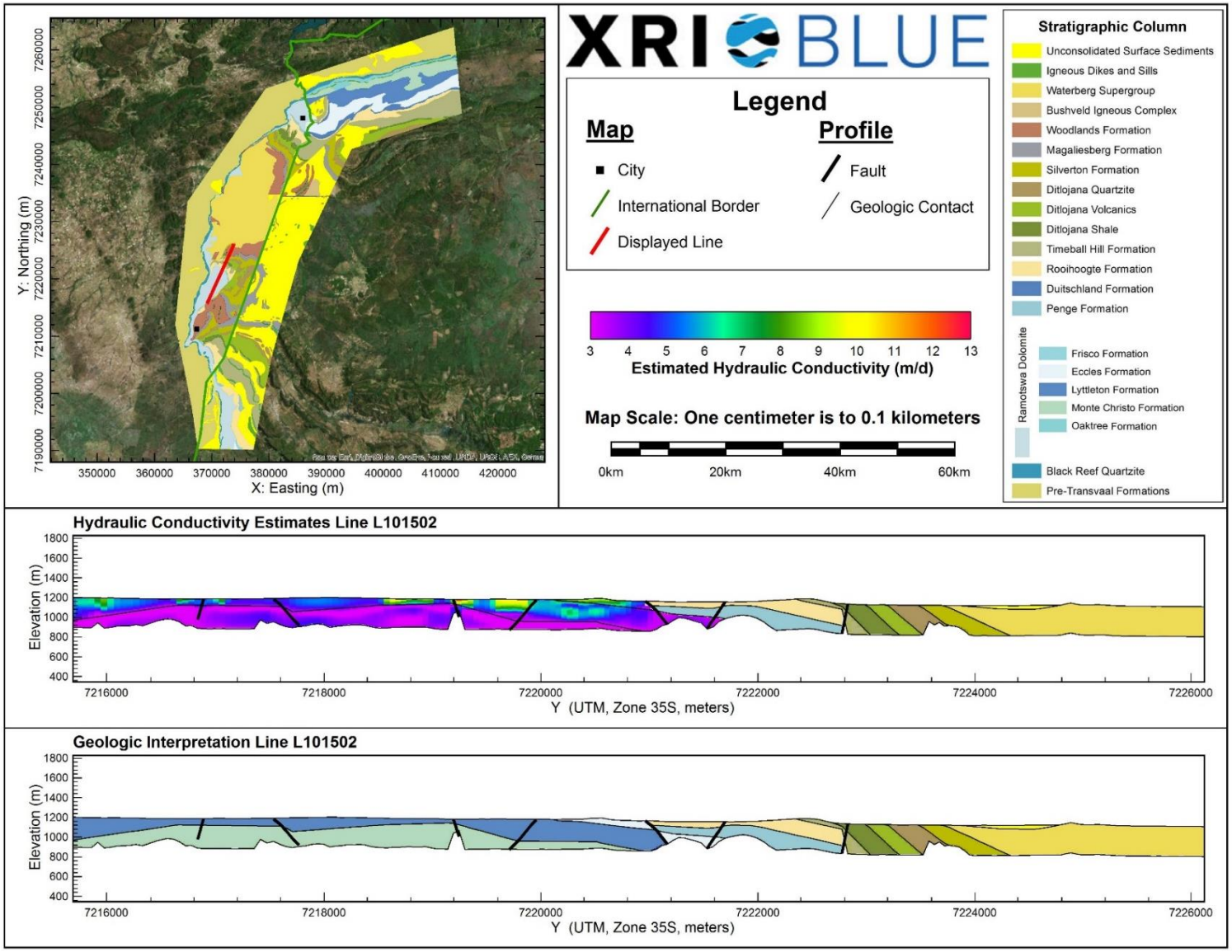

Hydraulic Conductivity Estimates and Interpreted Geology Profile for L101502.

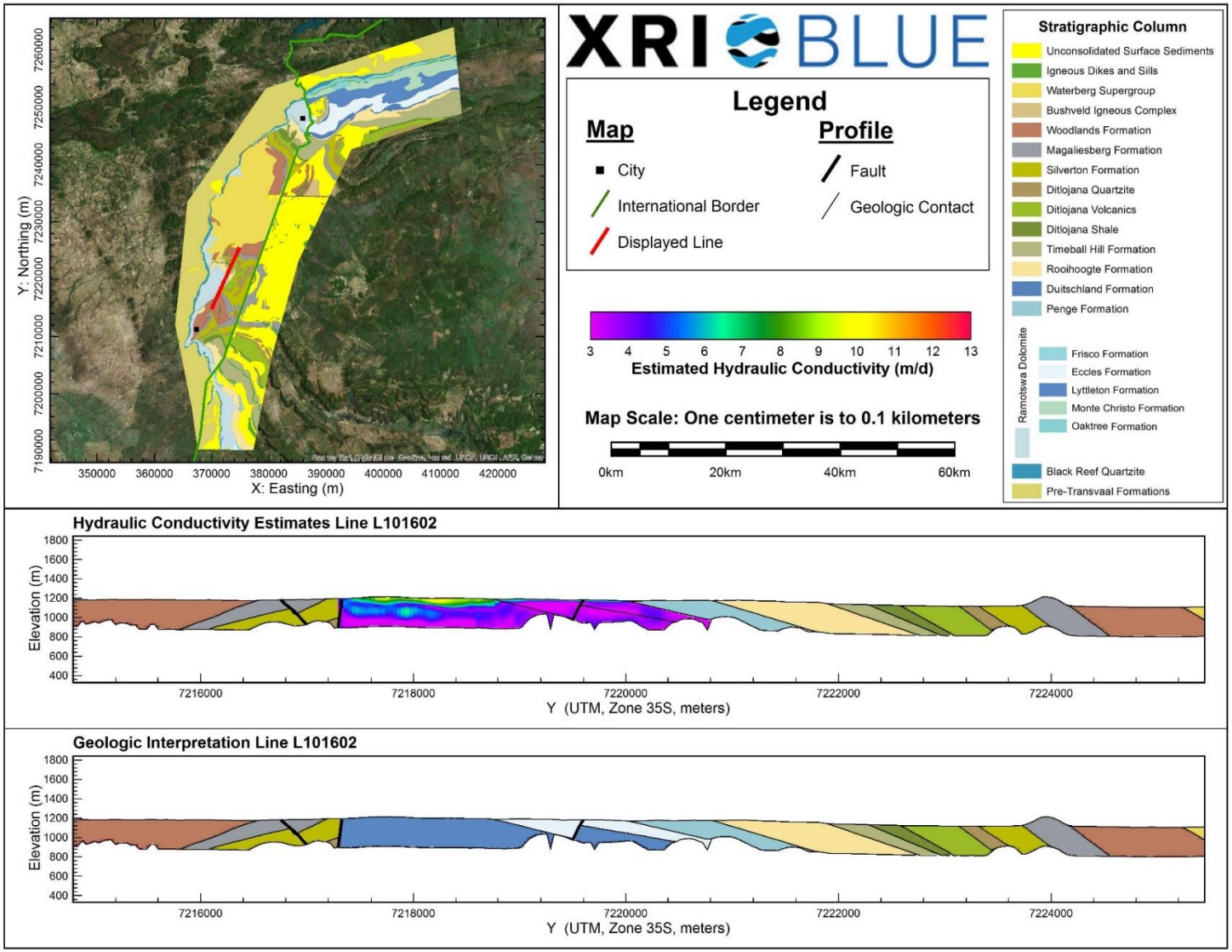

Hydraulic Conductivity Estimates and Interpreted Geology Profile for L101602.

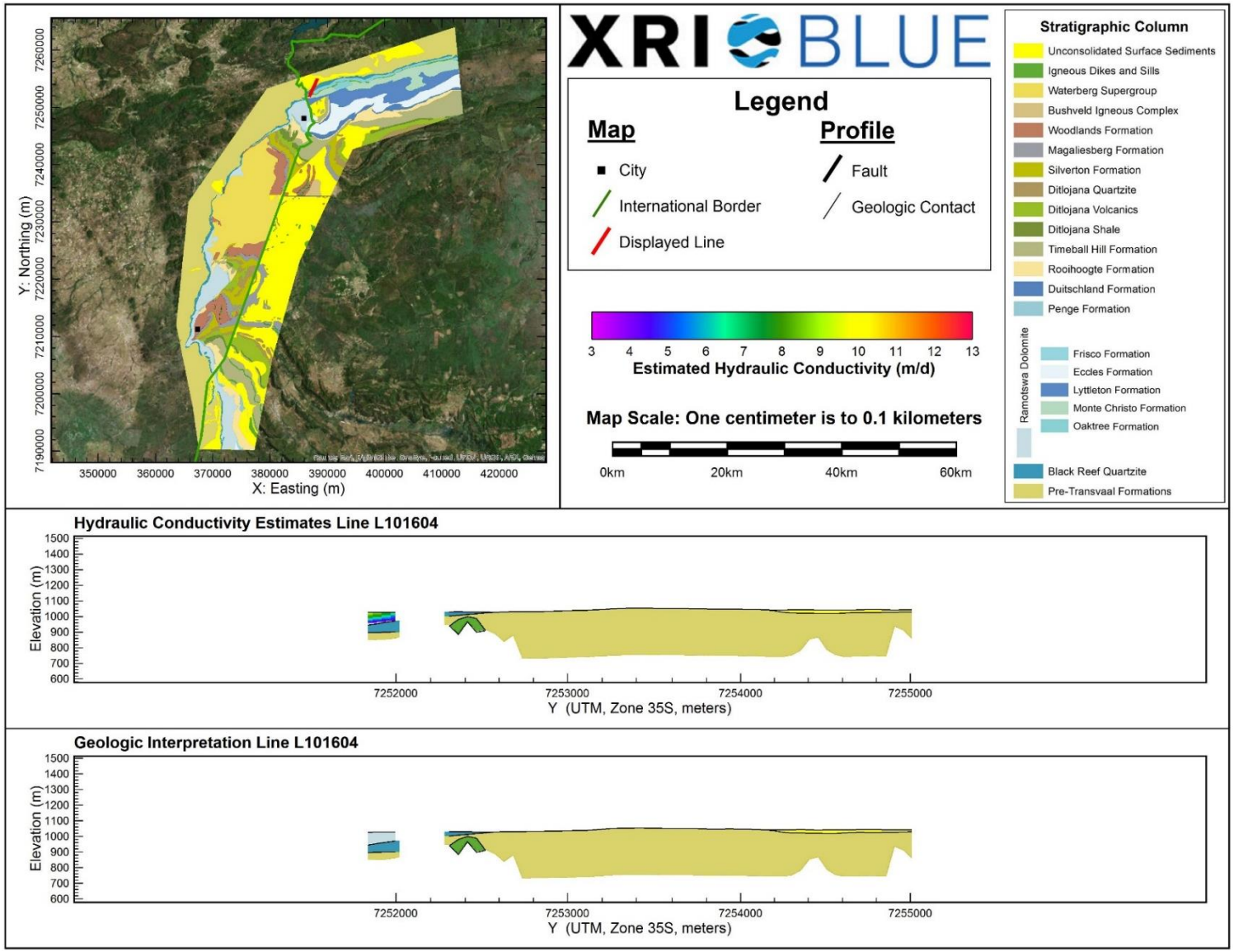

Hydraulic Conductivity Estimates and Interpreted Geology Profile for L101604.

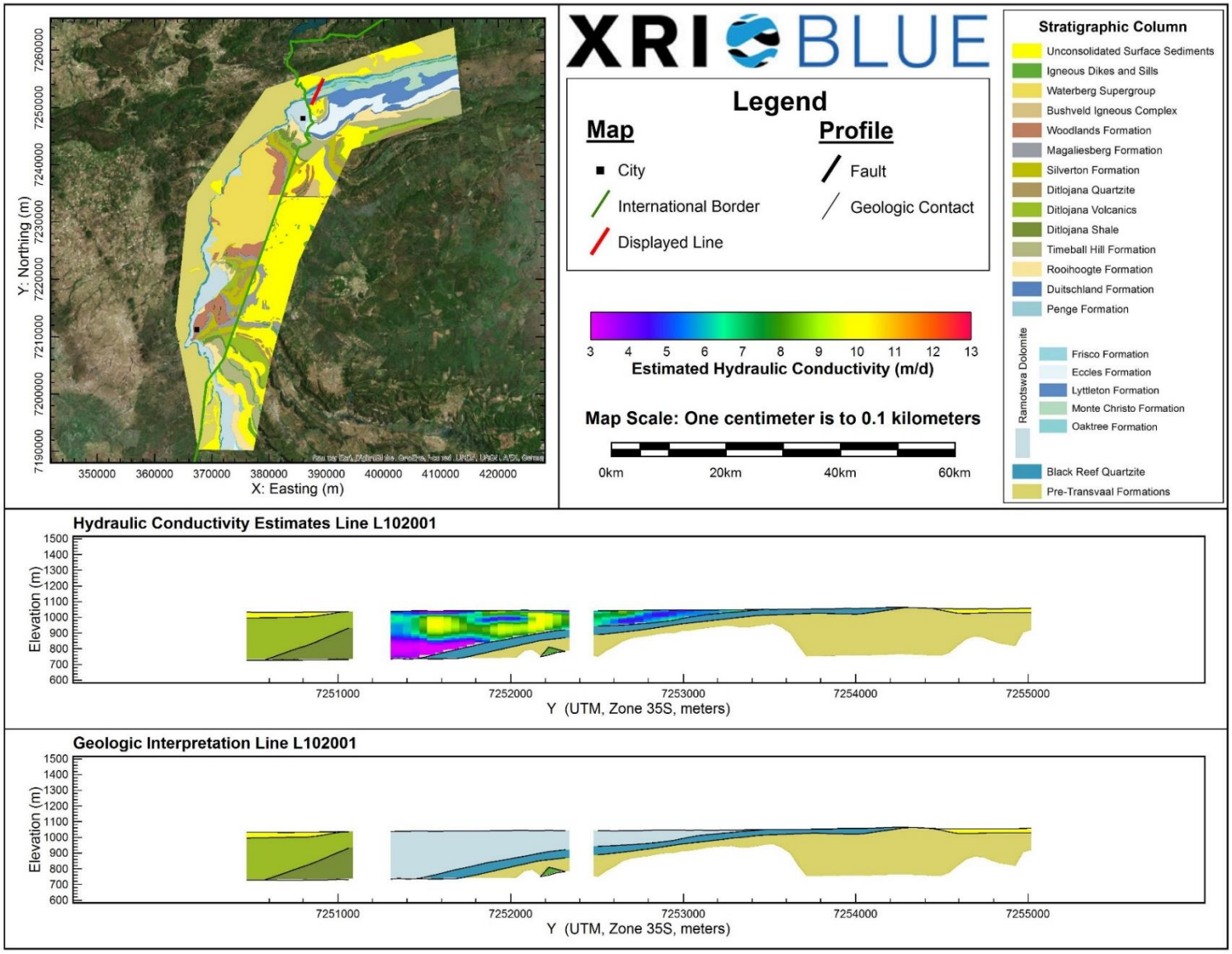

Hydraulic Conductivity Estimates and Interpreted Geology Profile for L102001.

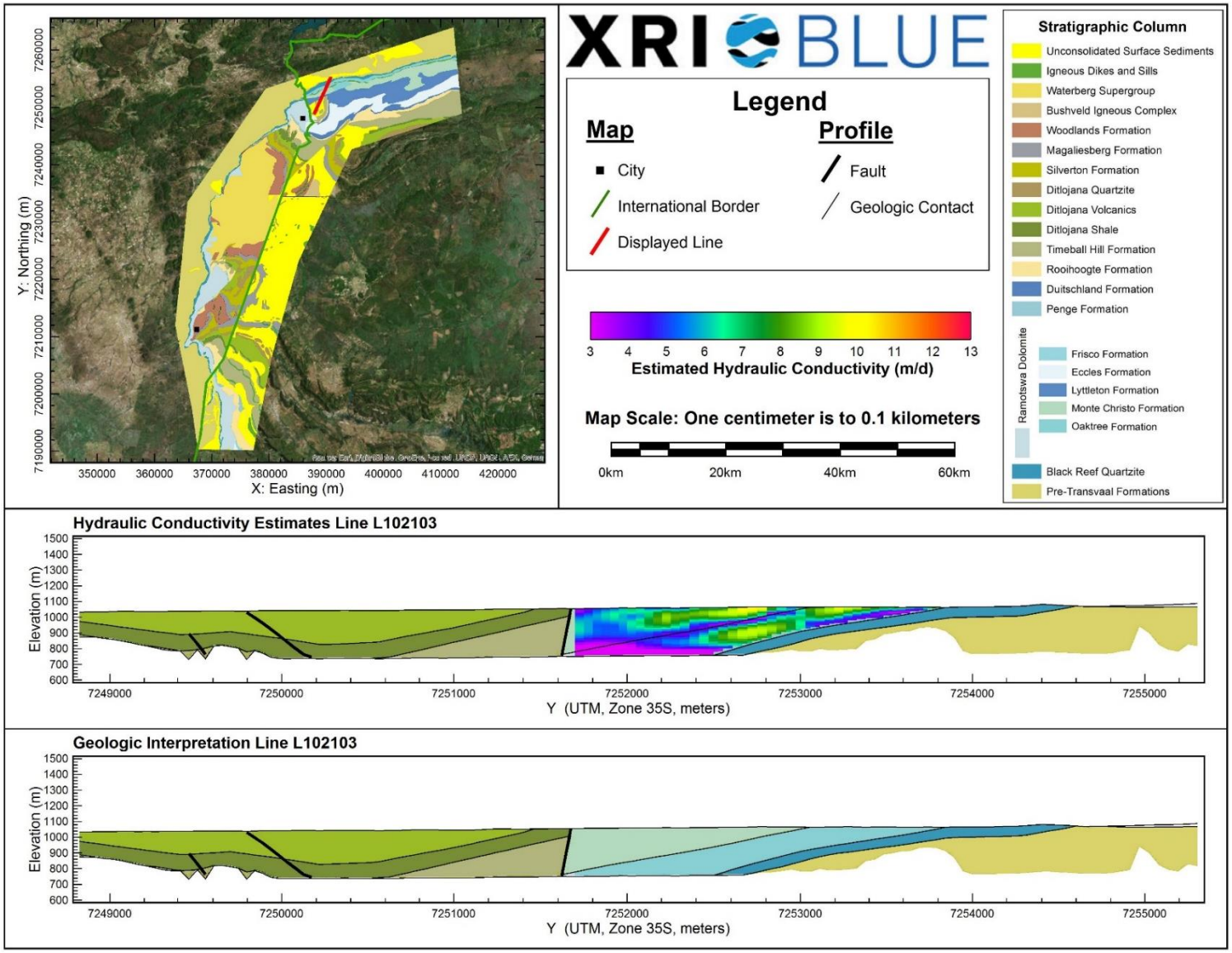

Hydraulic Conductivity Estimates and Interpreted Geology Profile for L102103.

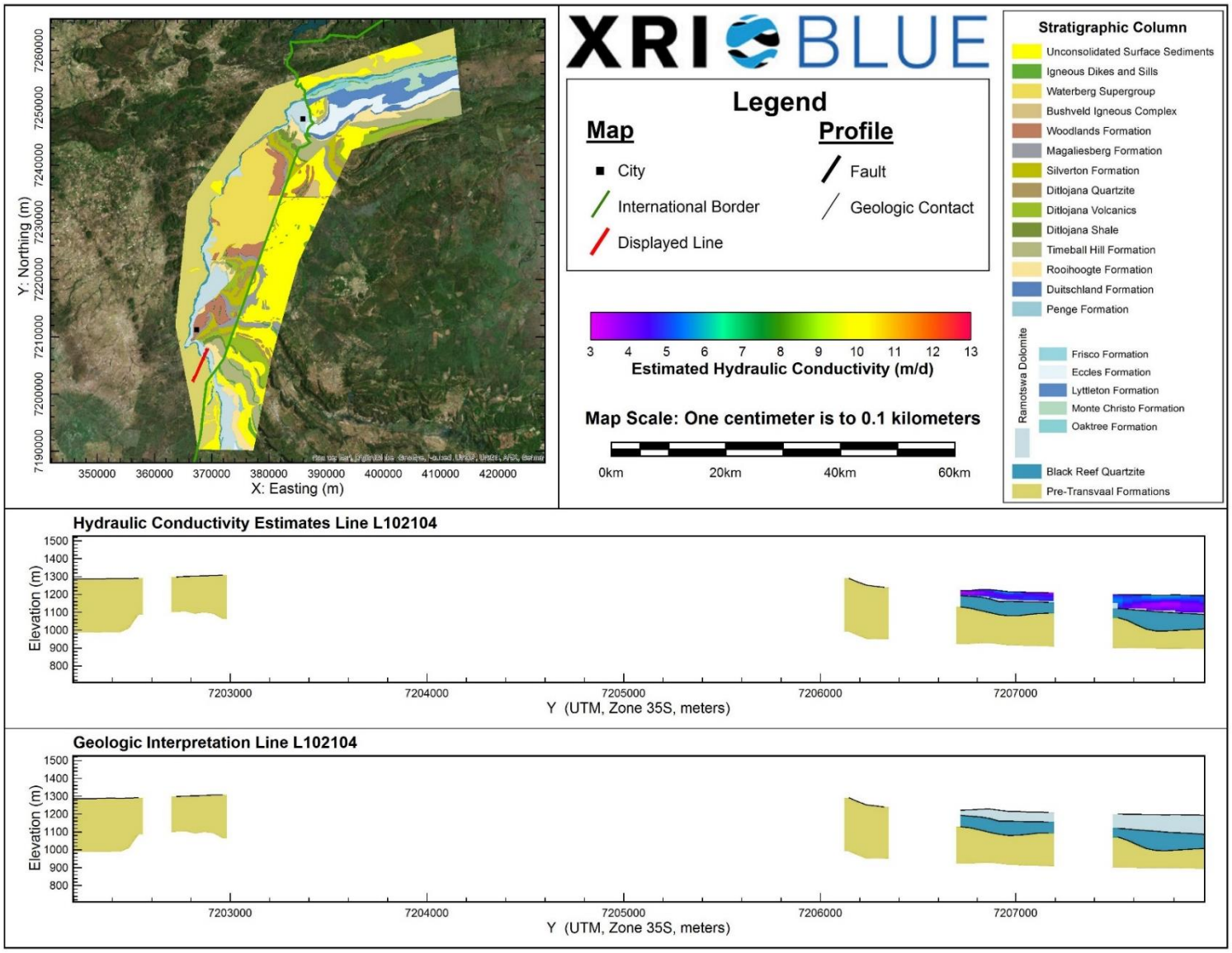

Hydraulic Conductivity Estimates and Interpreted Geology Profile for L102104.

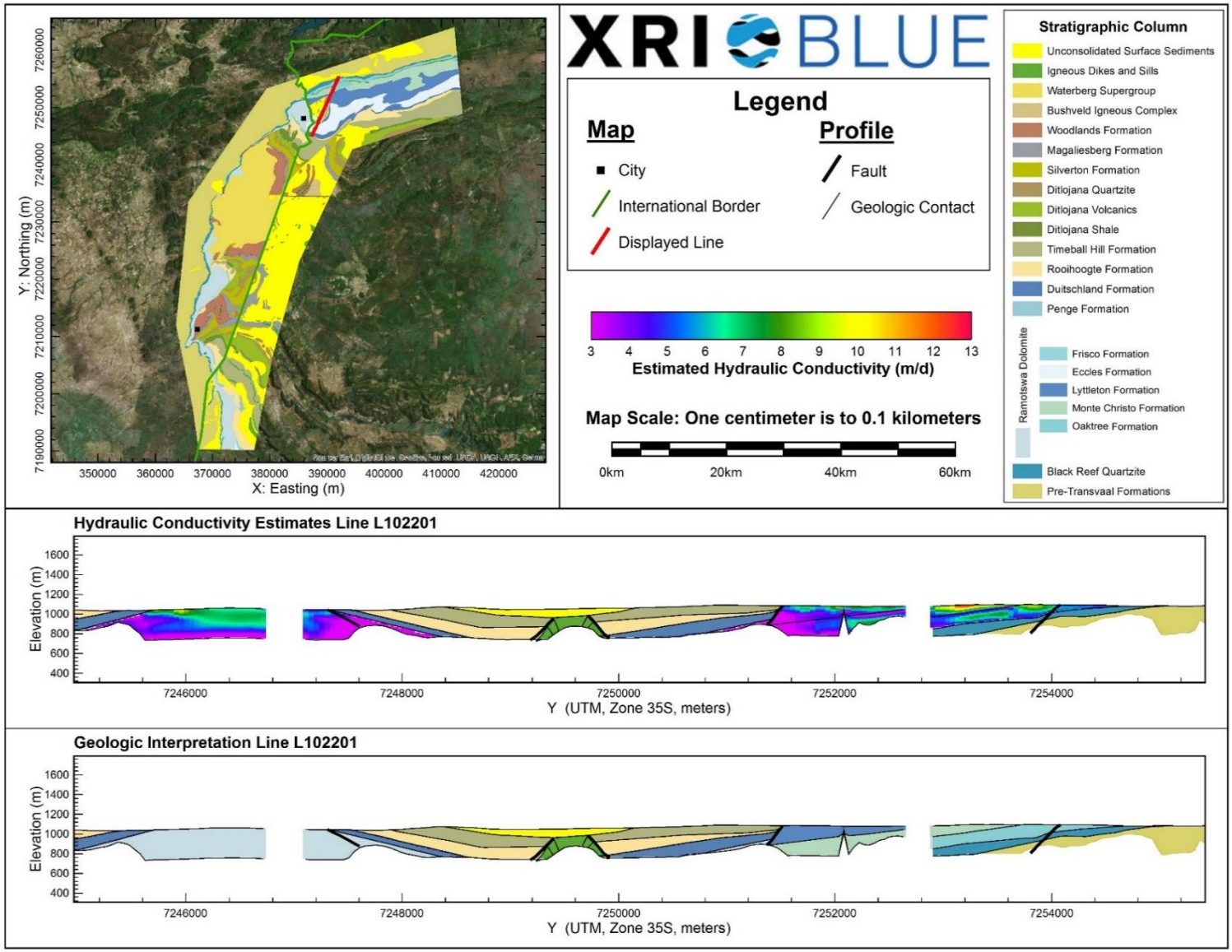

Hydraulic Conductivity Estimates and Interpreted Geology Profile for L102201.

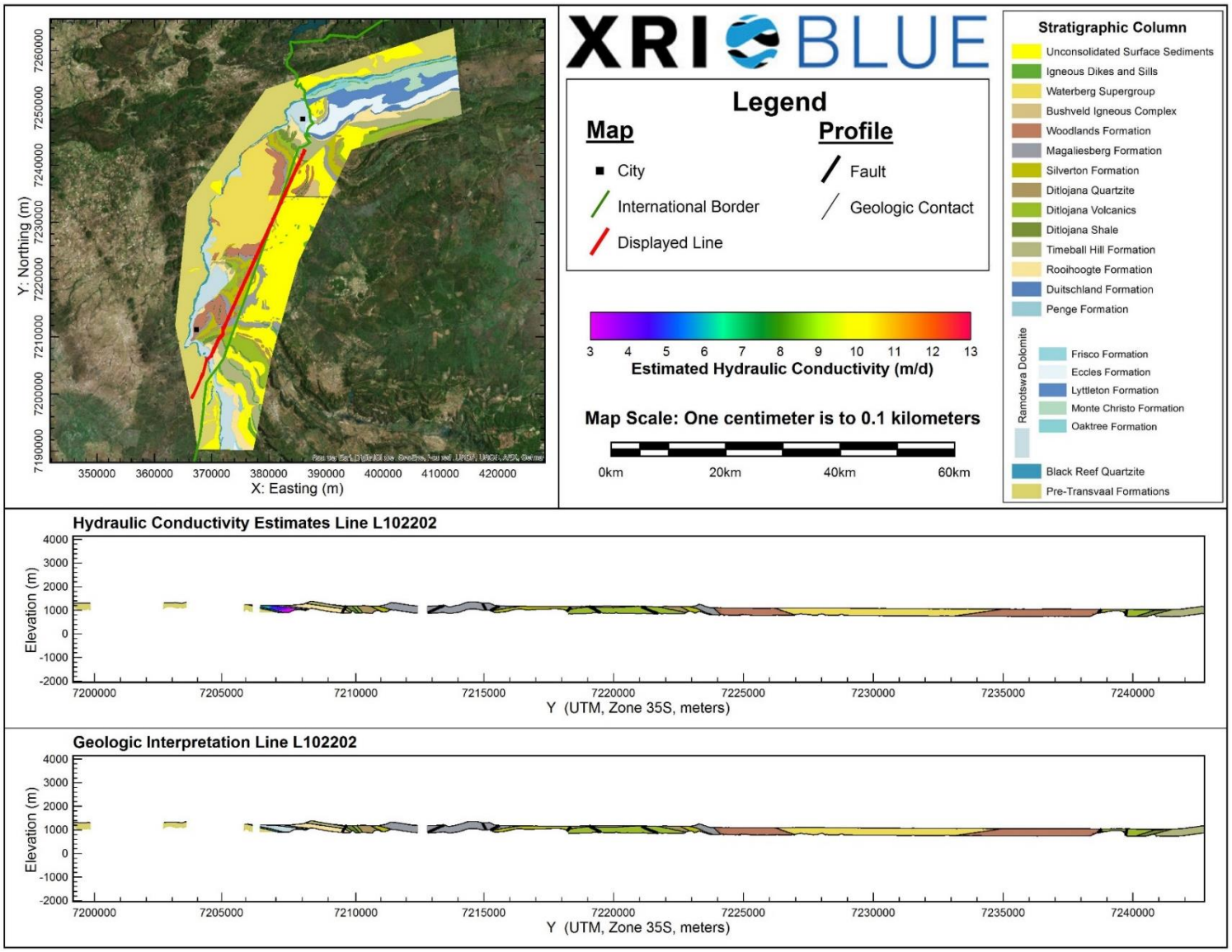

Hydraulic Conductivity Estimates and Interpreted Geology Profile for L102202.

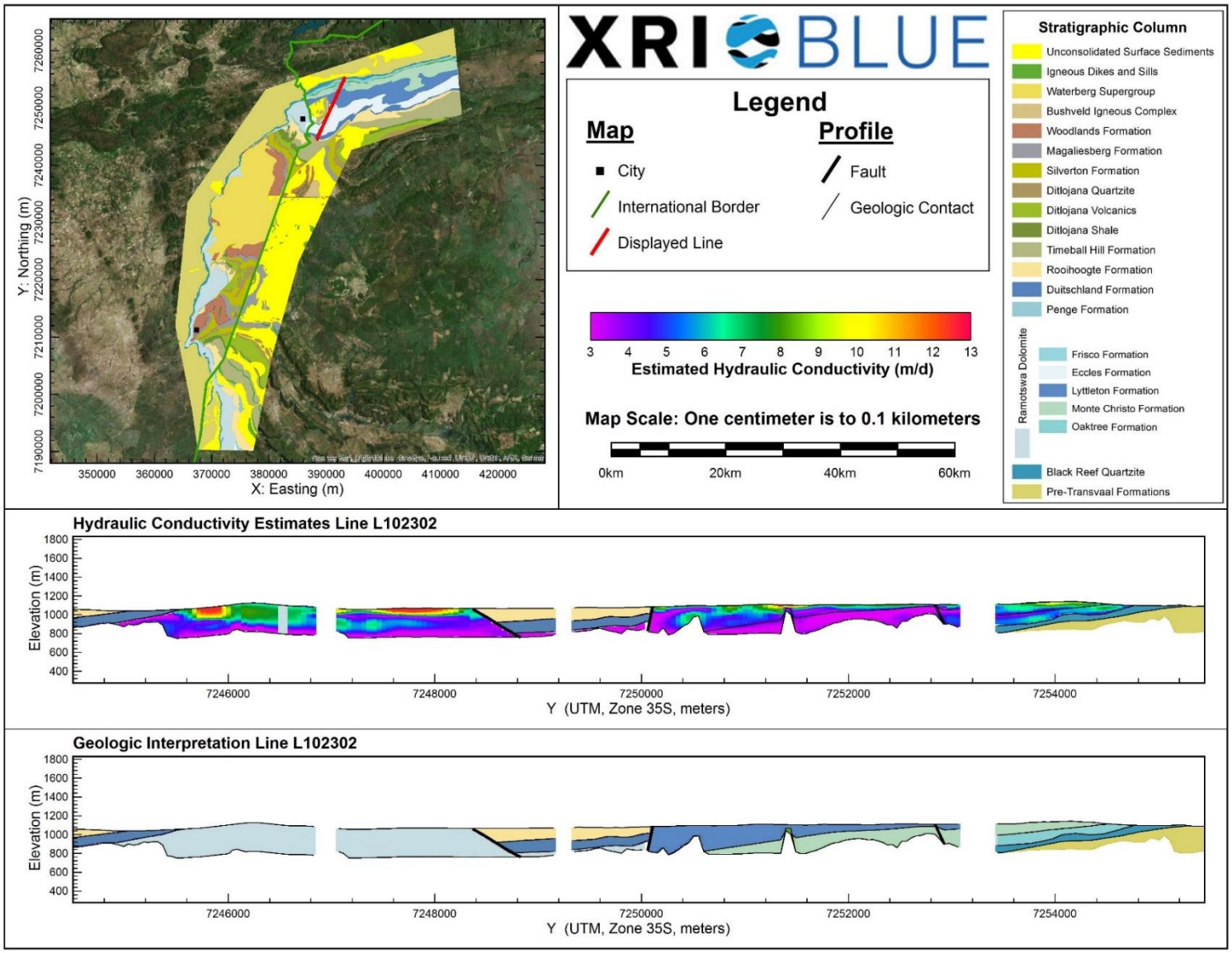

Hydraulic Conductivity Estimates and Interpreted Geology Profile for L102302.

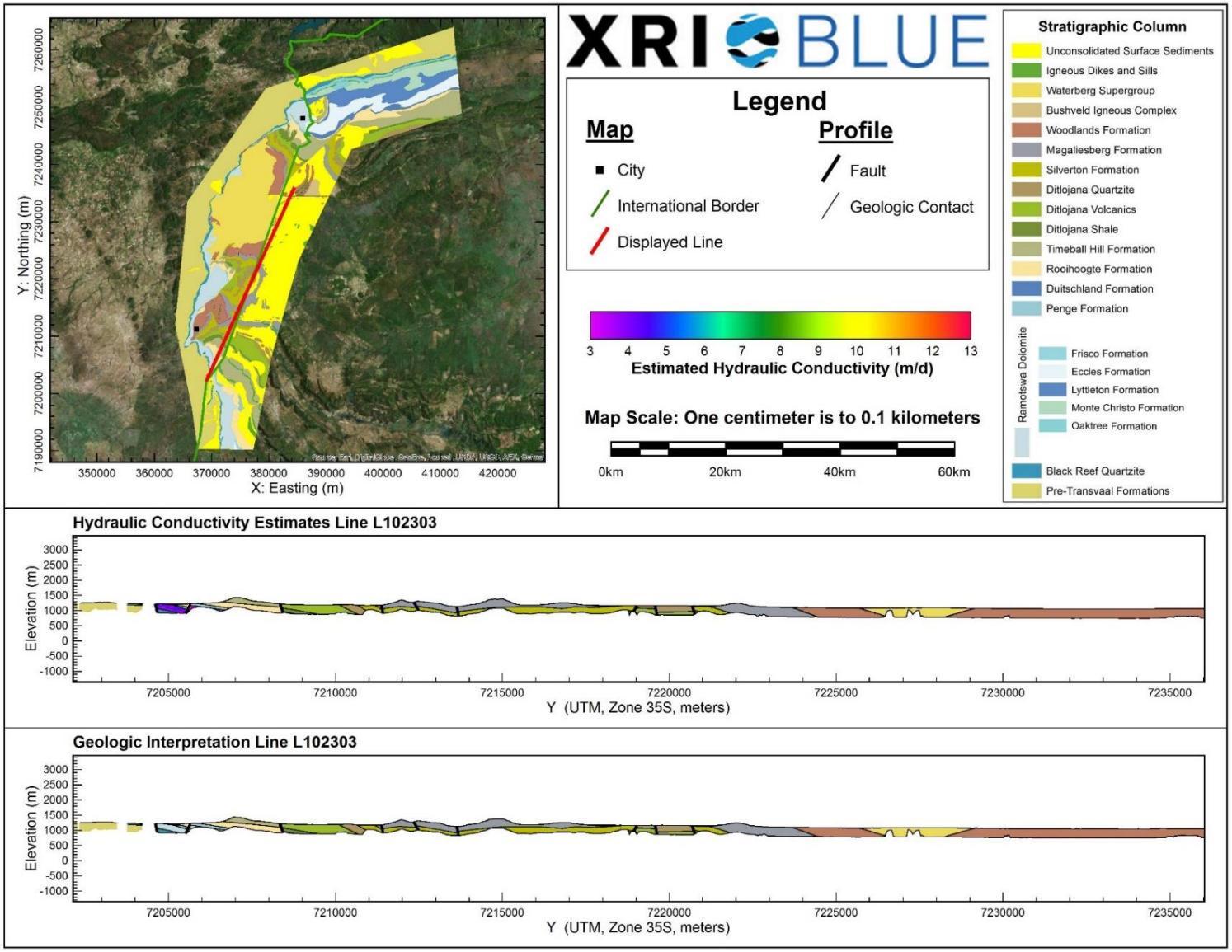

Hydraulic Conductivity Estimates and Interpreted Geology Profile for L102303.

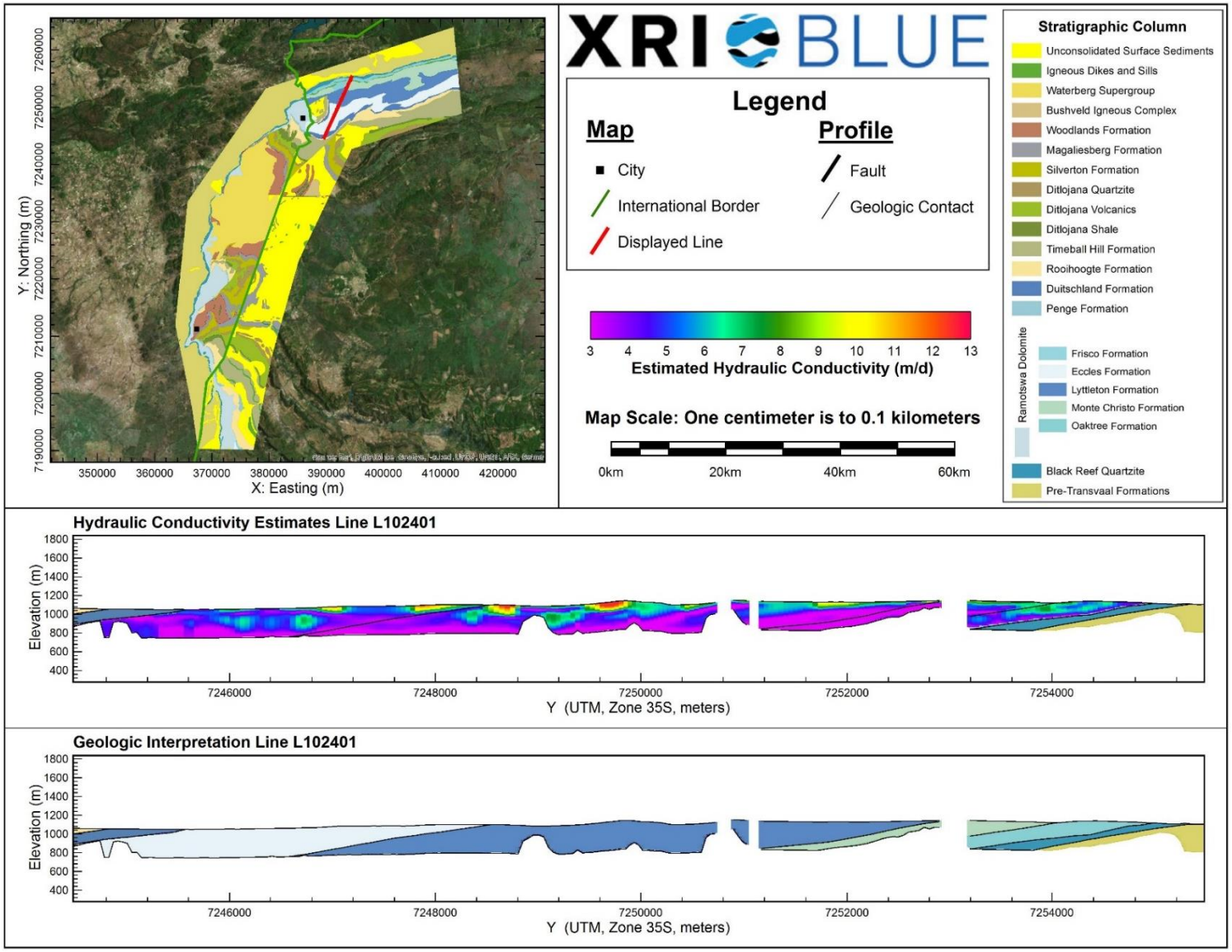

Hydraulic Conductivity Estimates and Interpreted Geology Profile for L102401.

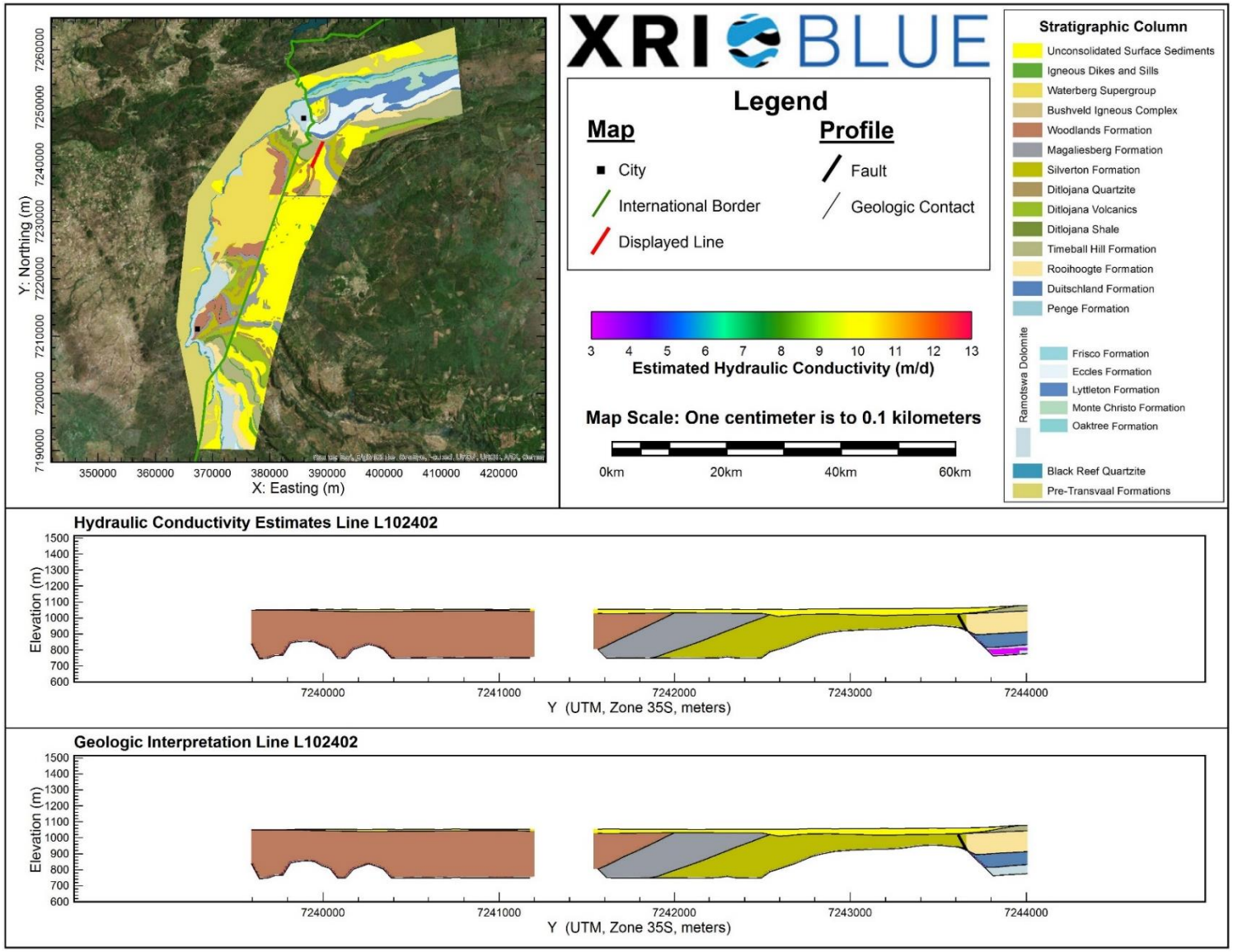

Hydraulic Conductivity Estimates and Interpreted Geology Profile for L102402.

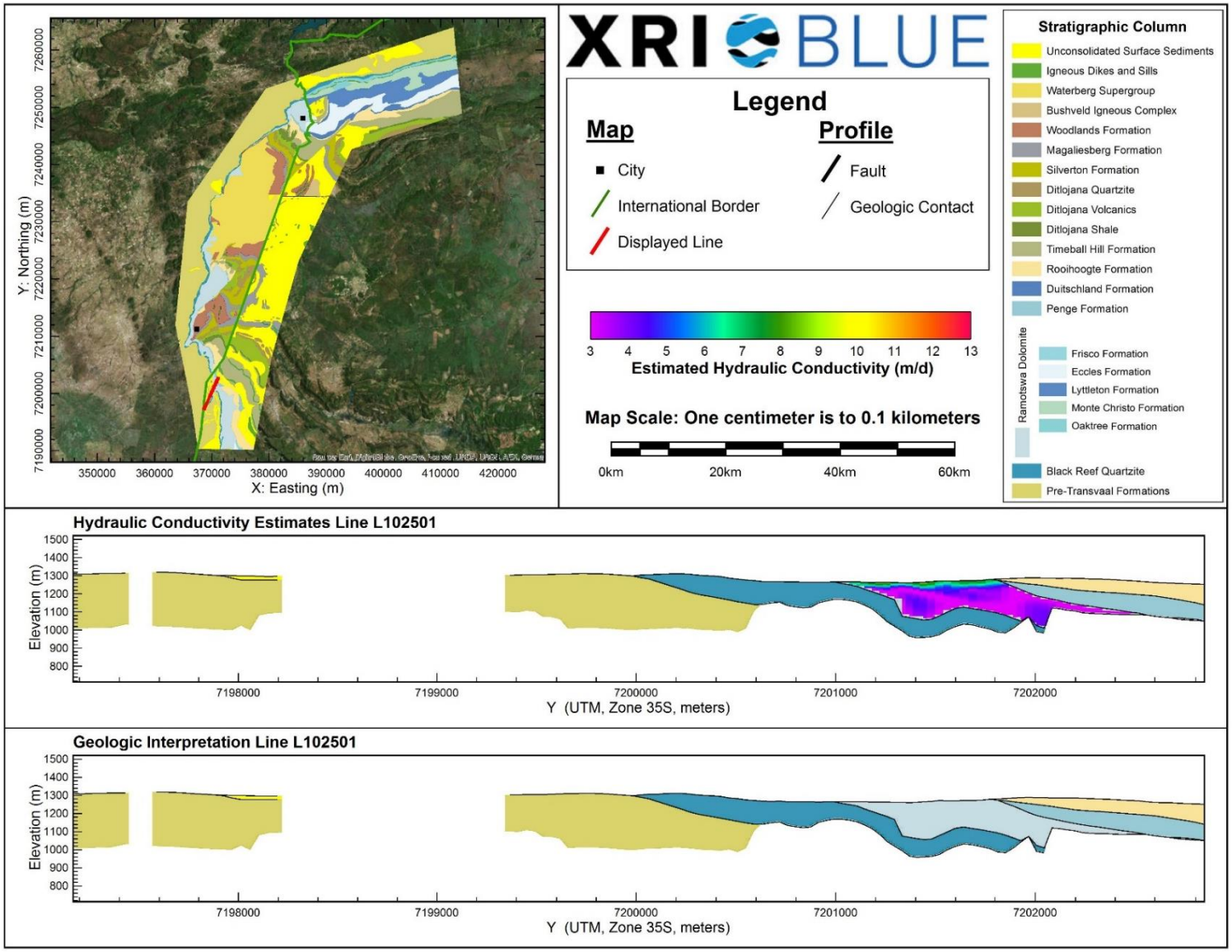

Hydraulic Conductivity Estimates and Interpreted Geology Profile for L102501.

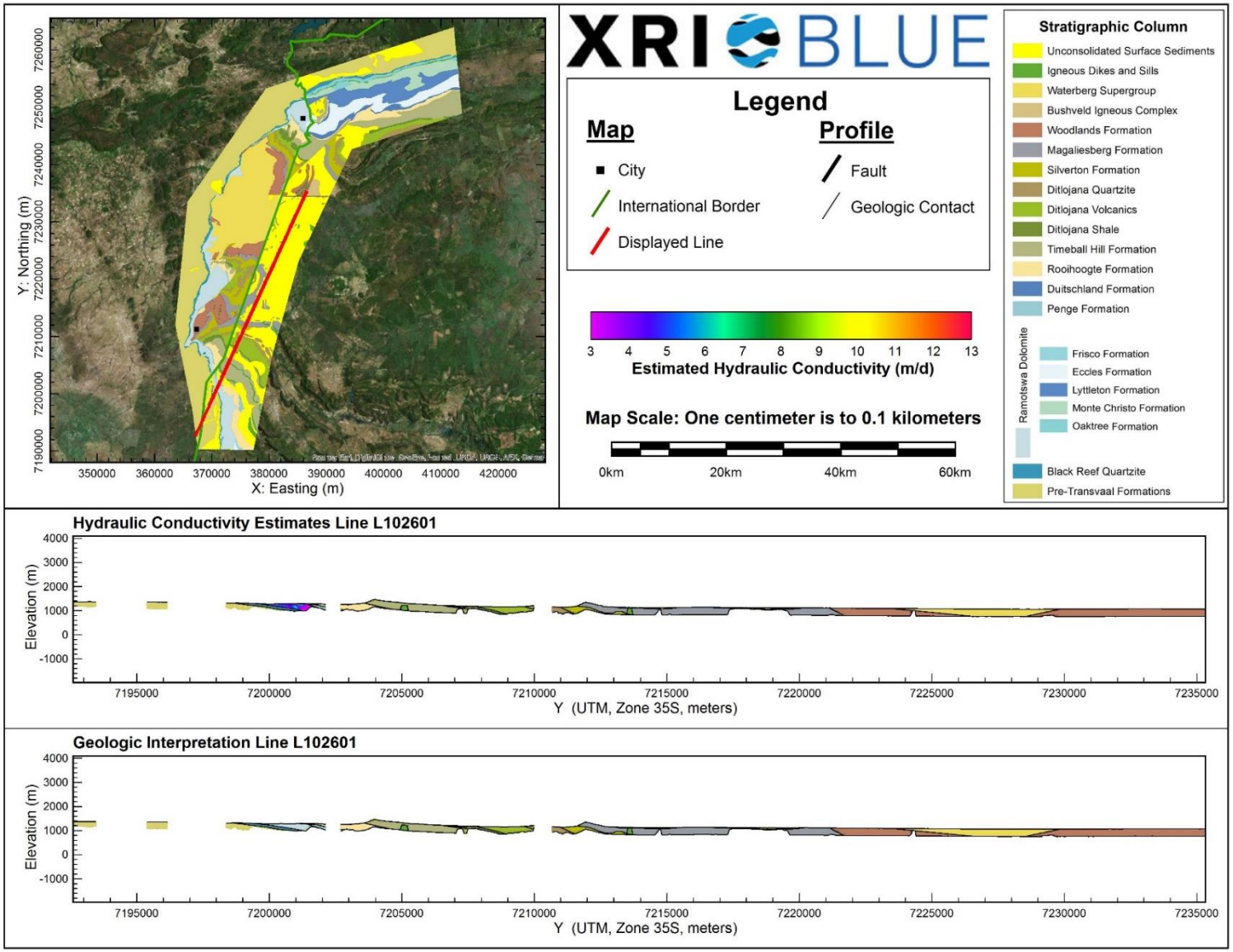

Hydraulic Conductivity Estimates and Interpreted Geology Profile for L102601.

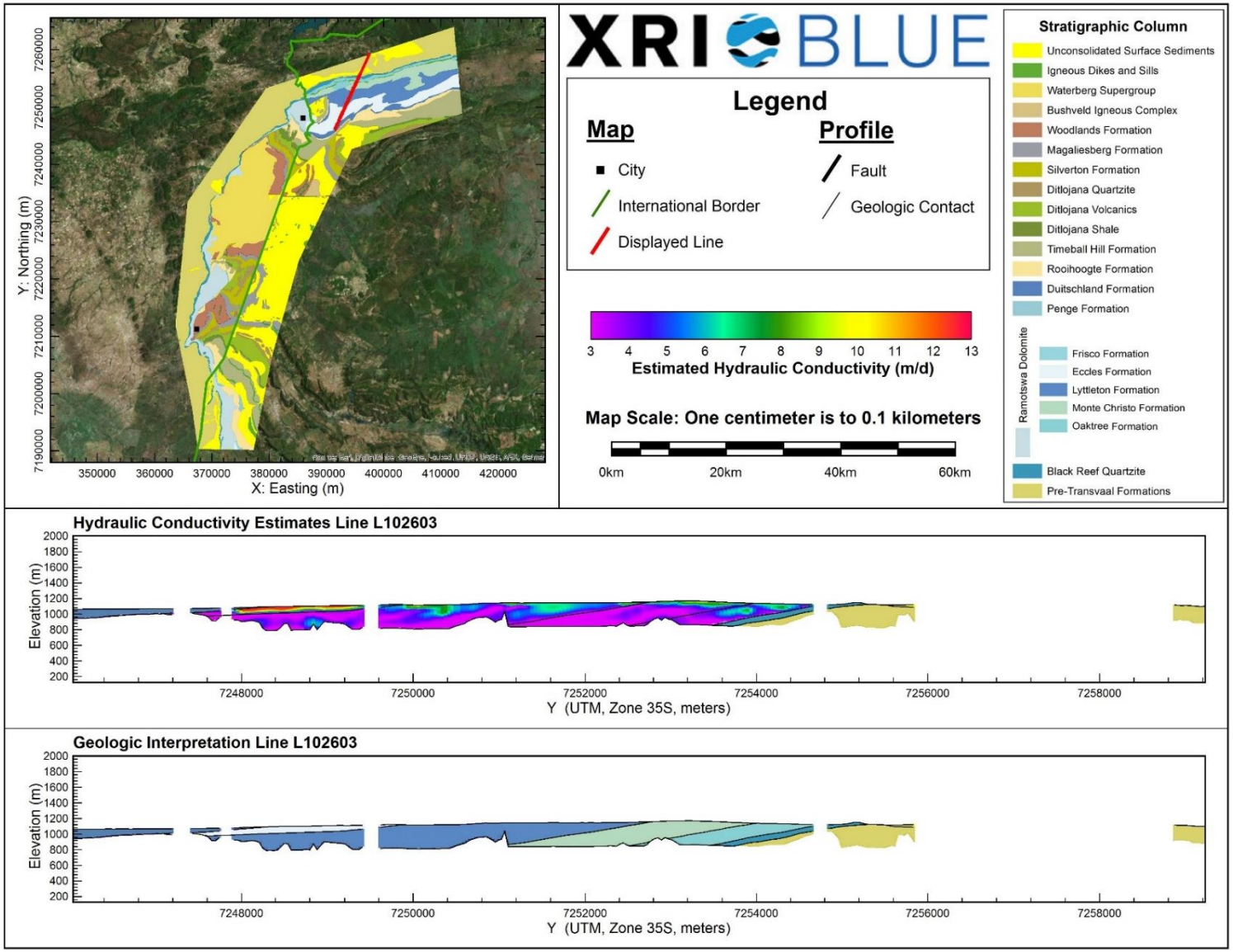

Hydraulic Conductivity Estimates and Interpreted Geology Profile for L102603.

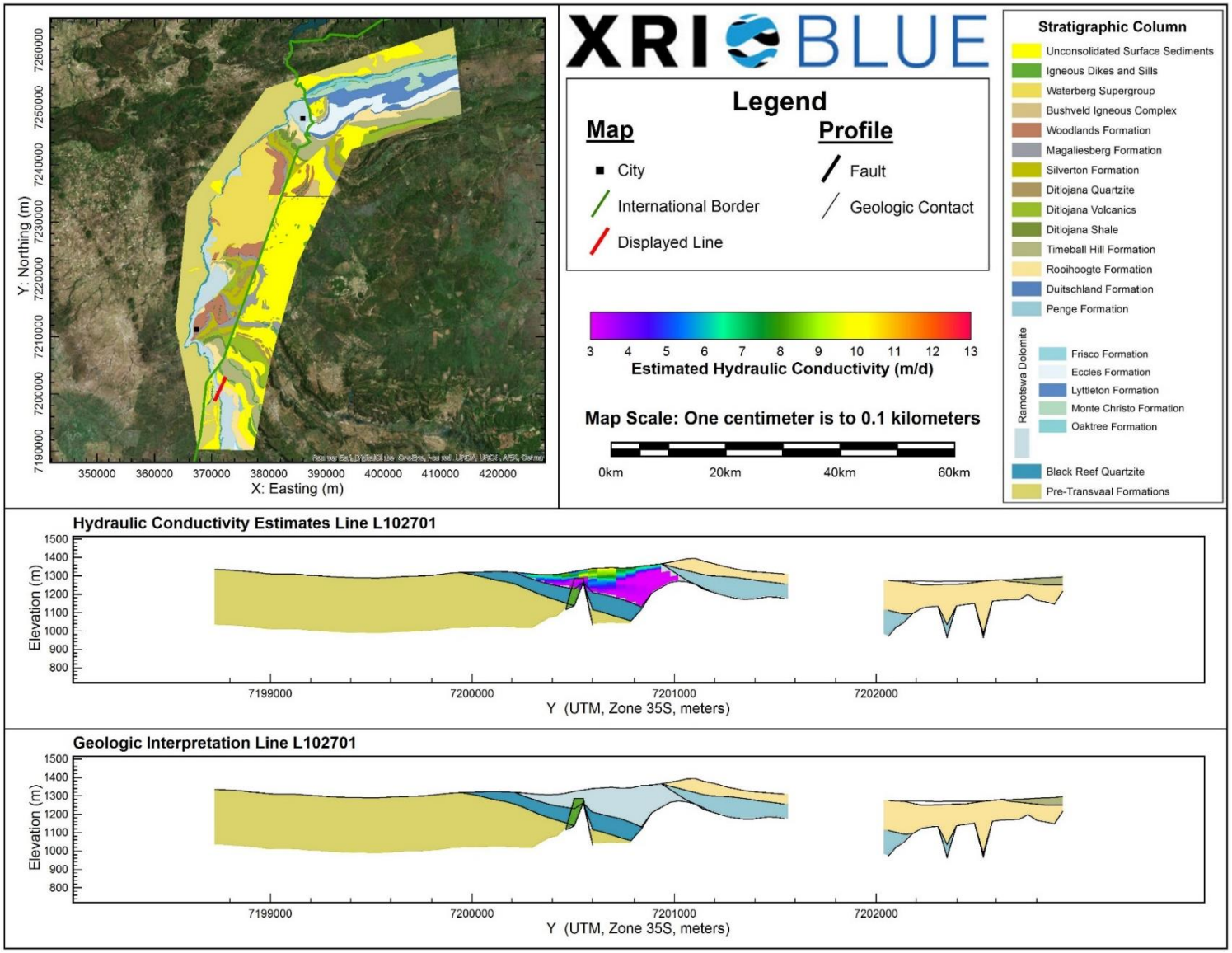

Hydraulic Conductivity Estimates and Interpreted Geology Profile for L102701.

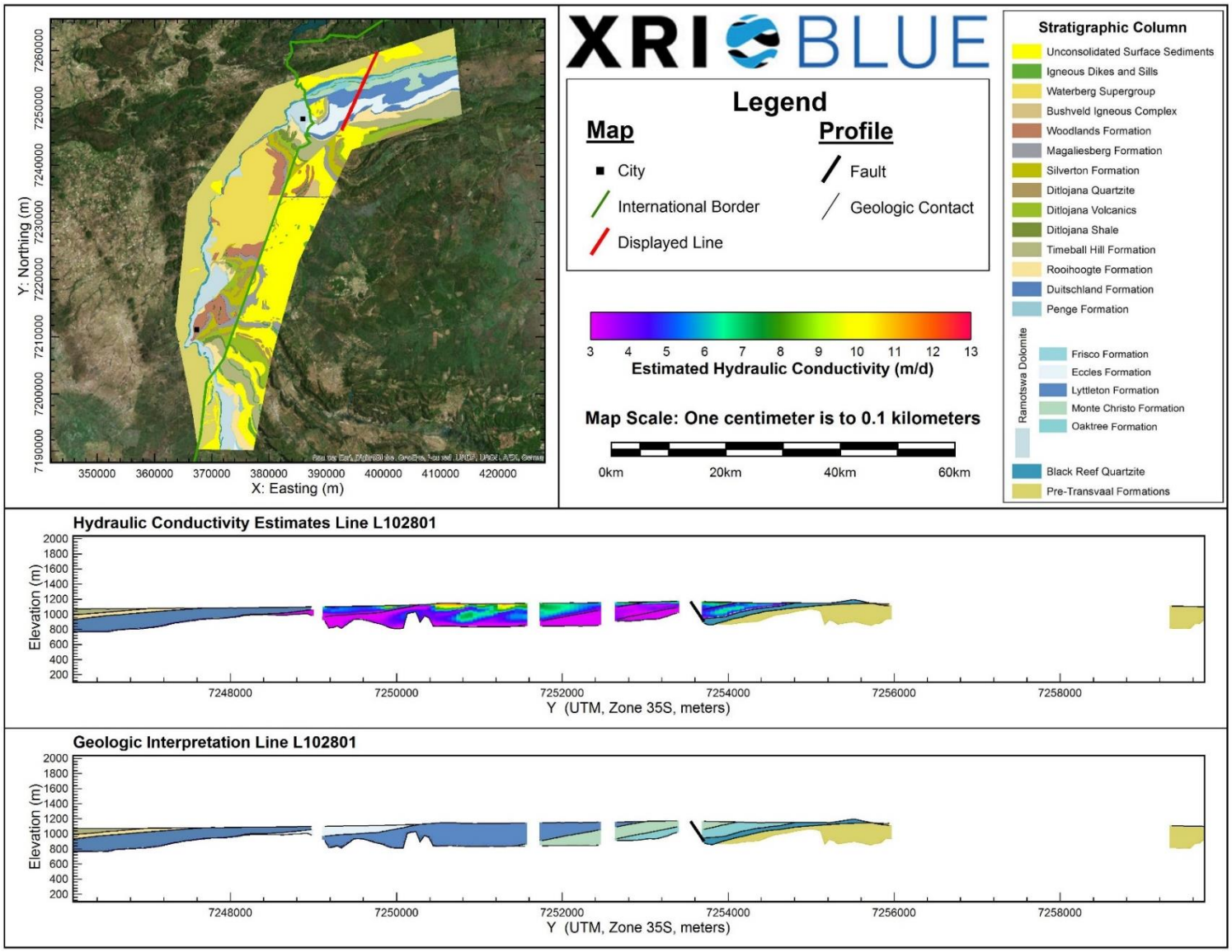

Hydraulic Conductivity Estimates and Interpreted Geology Profile for L102801.

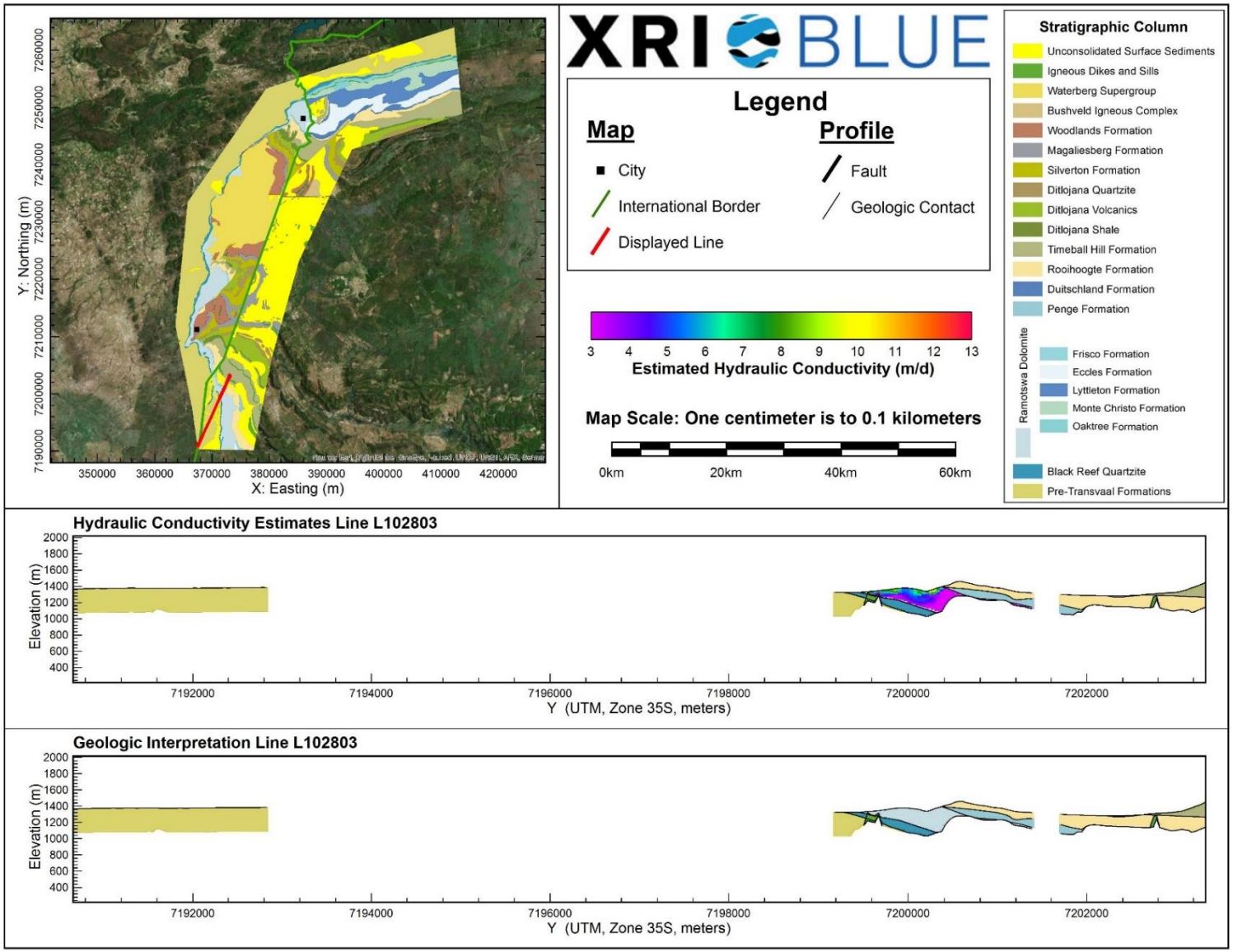

Hydraulic Conductivity Estimates and Interpreted Geology Profile for L102803.

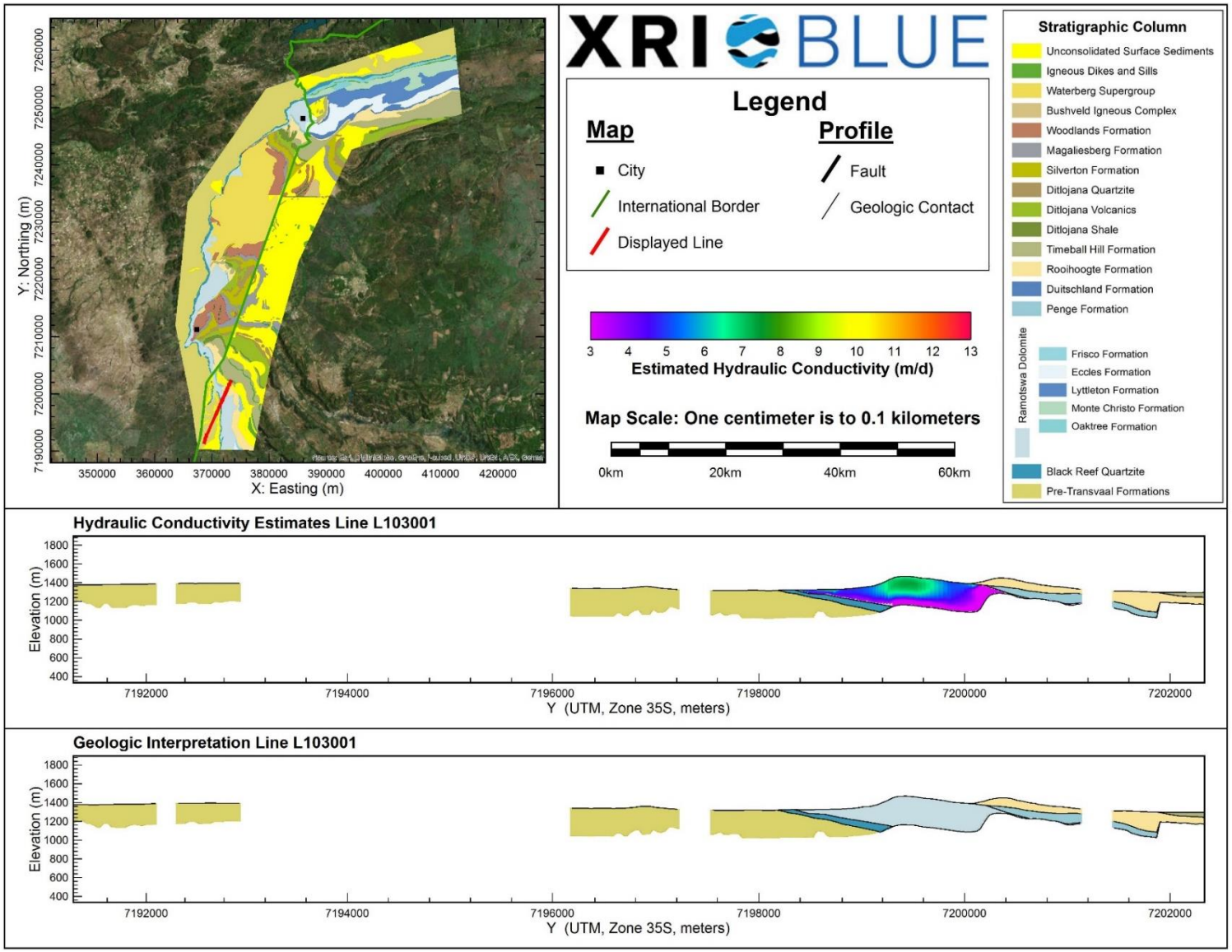

Hydraulic Conductivity Estimates and Interpreted Geology Profile for L103001.

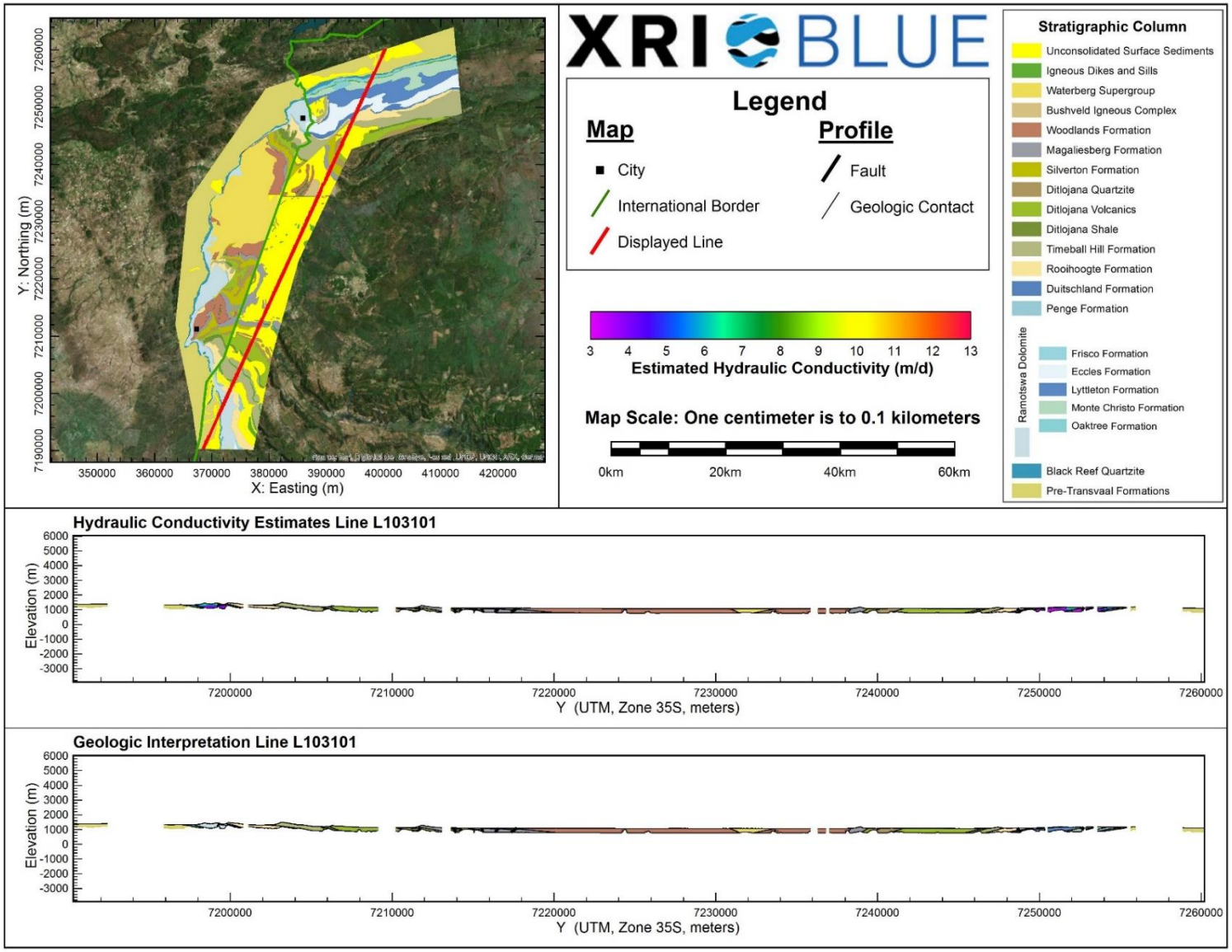

Hydraulic Conductivity Estimates and Interpreted Geology Profile for L103101.

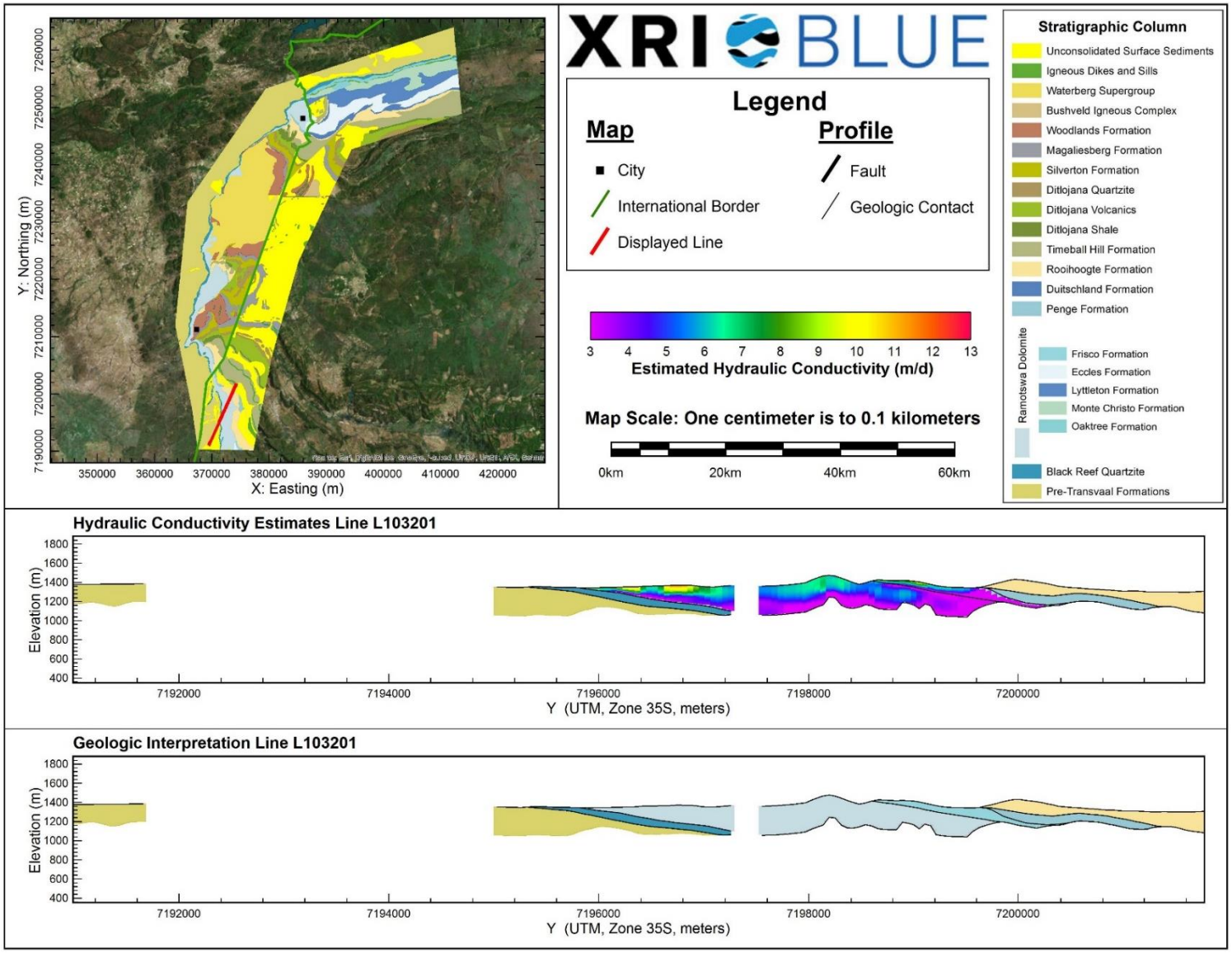

Hydraulic Conductivity Estimates and Interpreted Geology Profile for L103201.

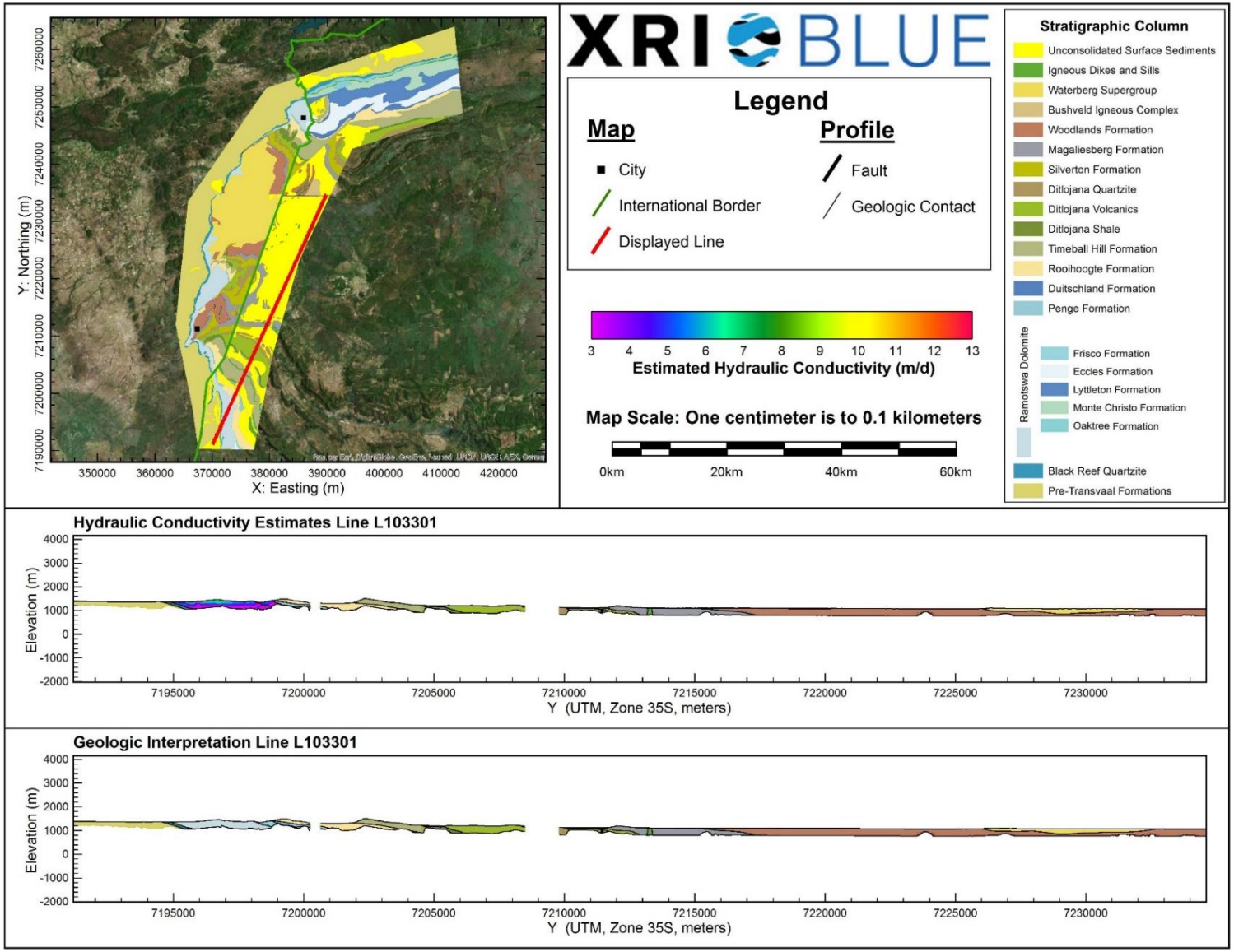

Hydraulic Conductivity Estimates and Interpreted Geology Profile for L103301.

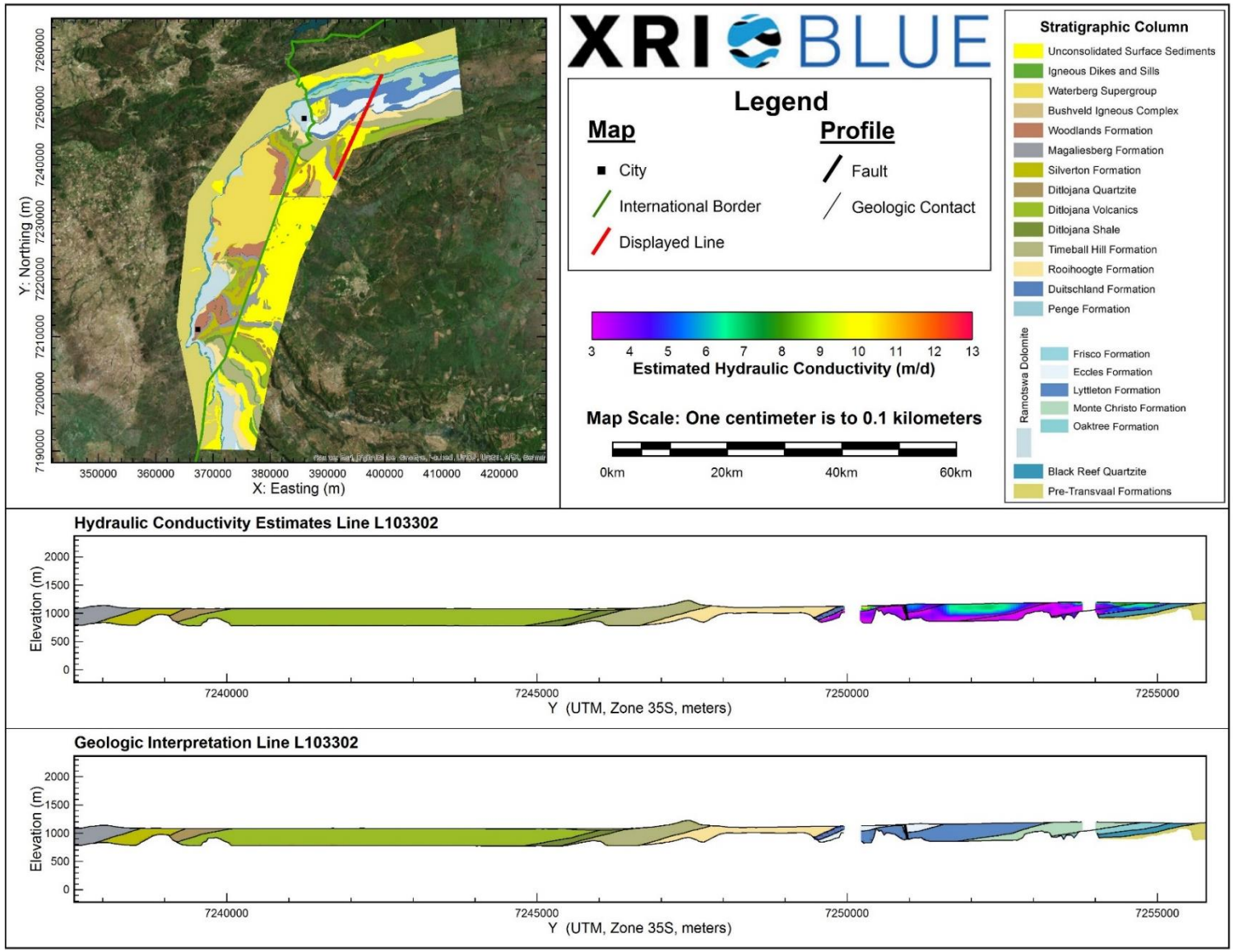

Hydraulic Conductivity Estimates and Interpreted Geology Profile for L103302.

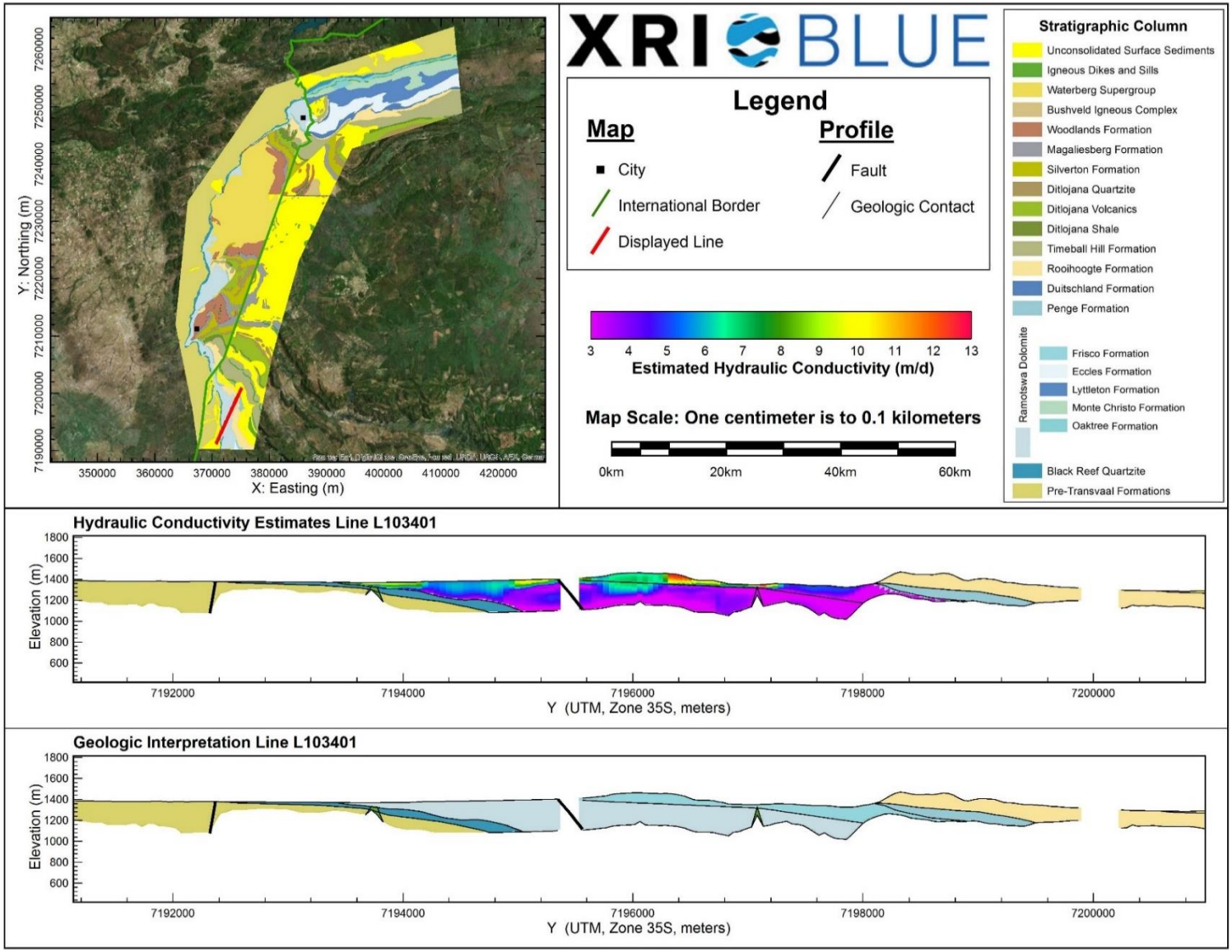

Hydraulic Conductivity Estimates and Interpreted Geology Profile for L103401.

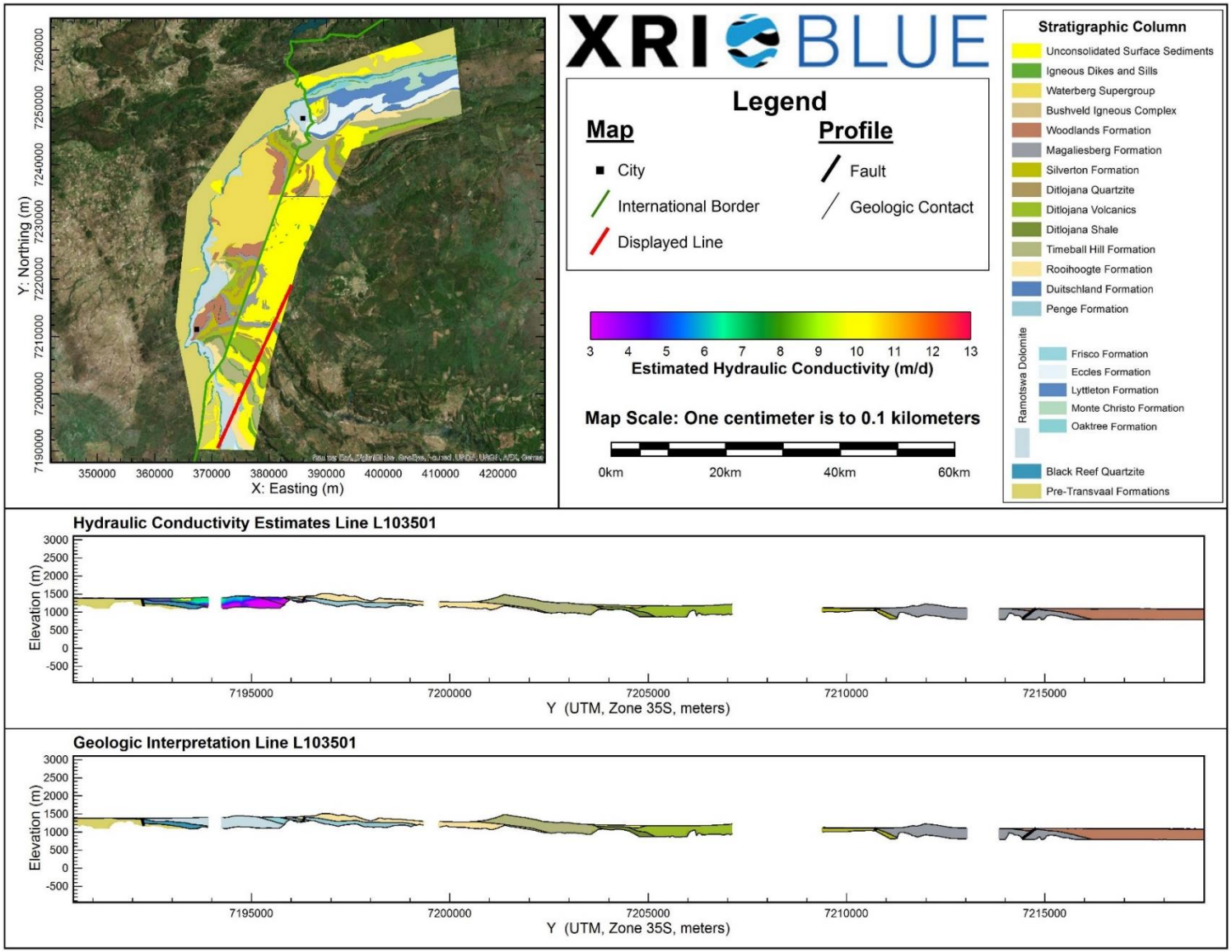

Hydraulic Conductivity Estimates and Interpreted Geology Profile for L103501.

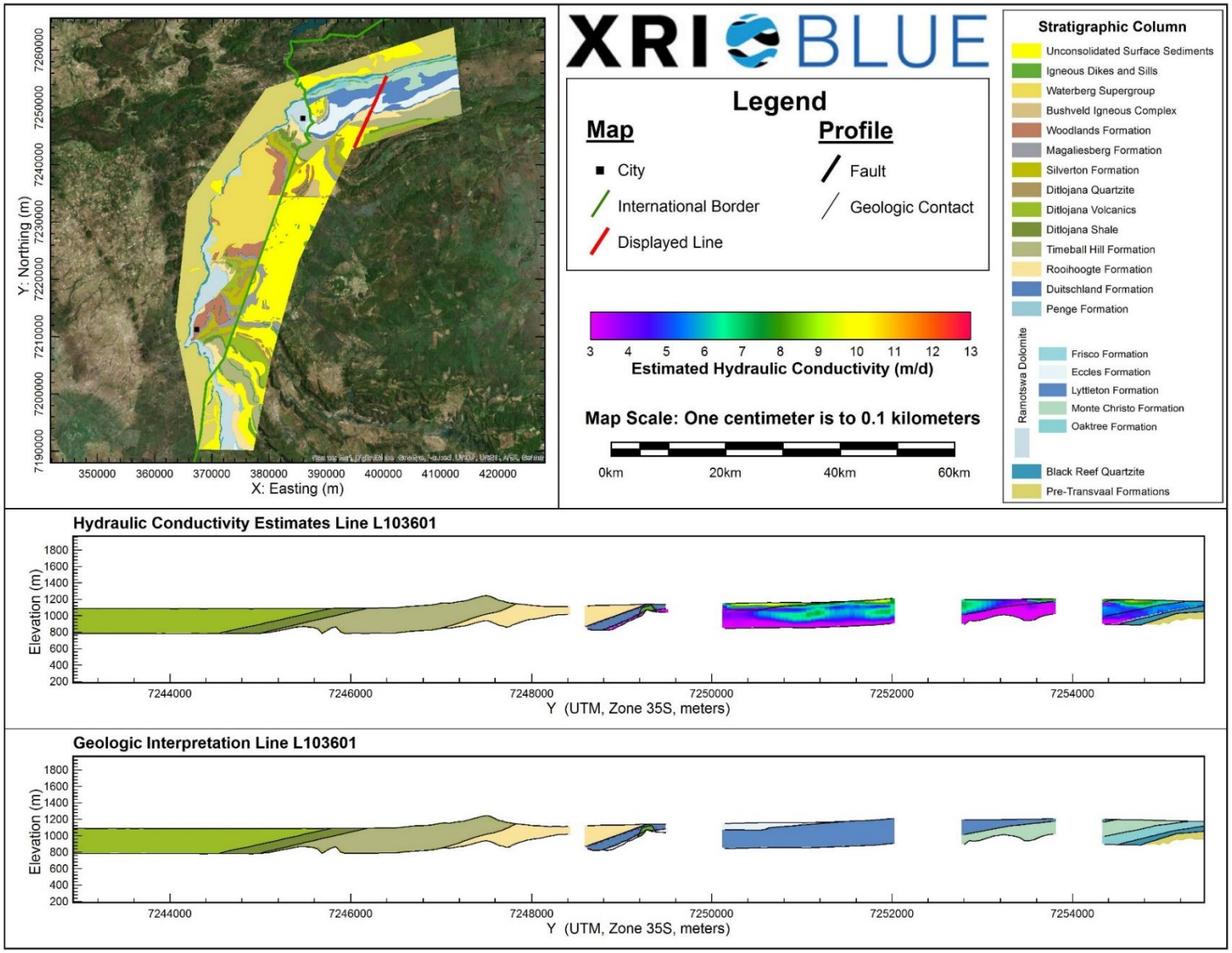

Hydraulic Conductivity Estimates and Interpreted Geology Profile for L103601.

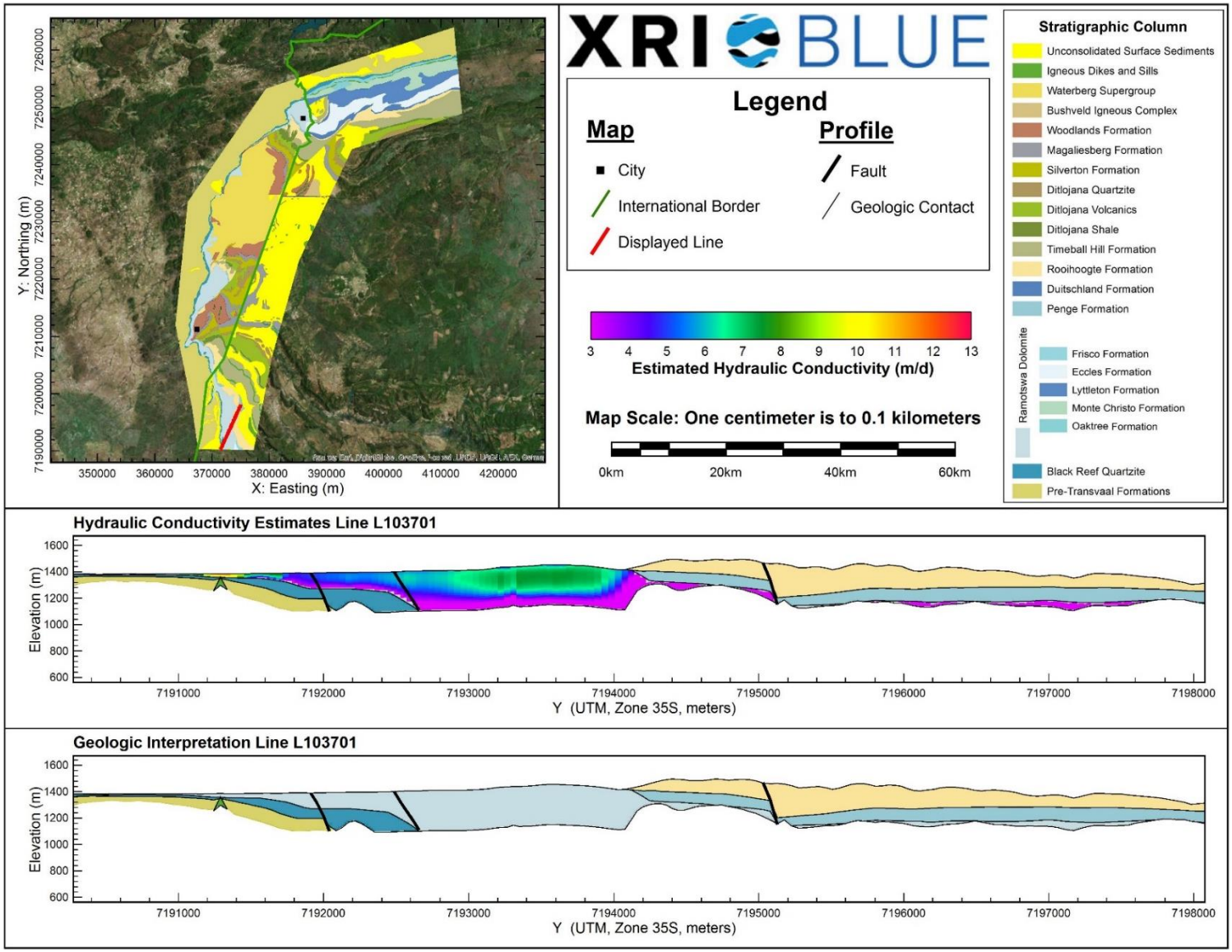

Hydraulic Conductivity Estimates and Interpreted Geology Profile for L103701.

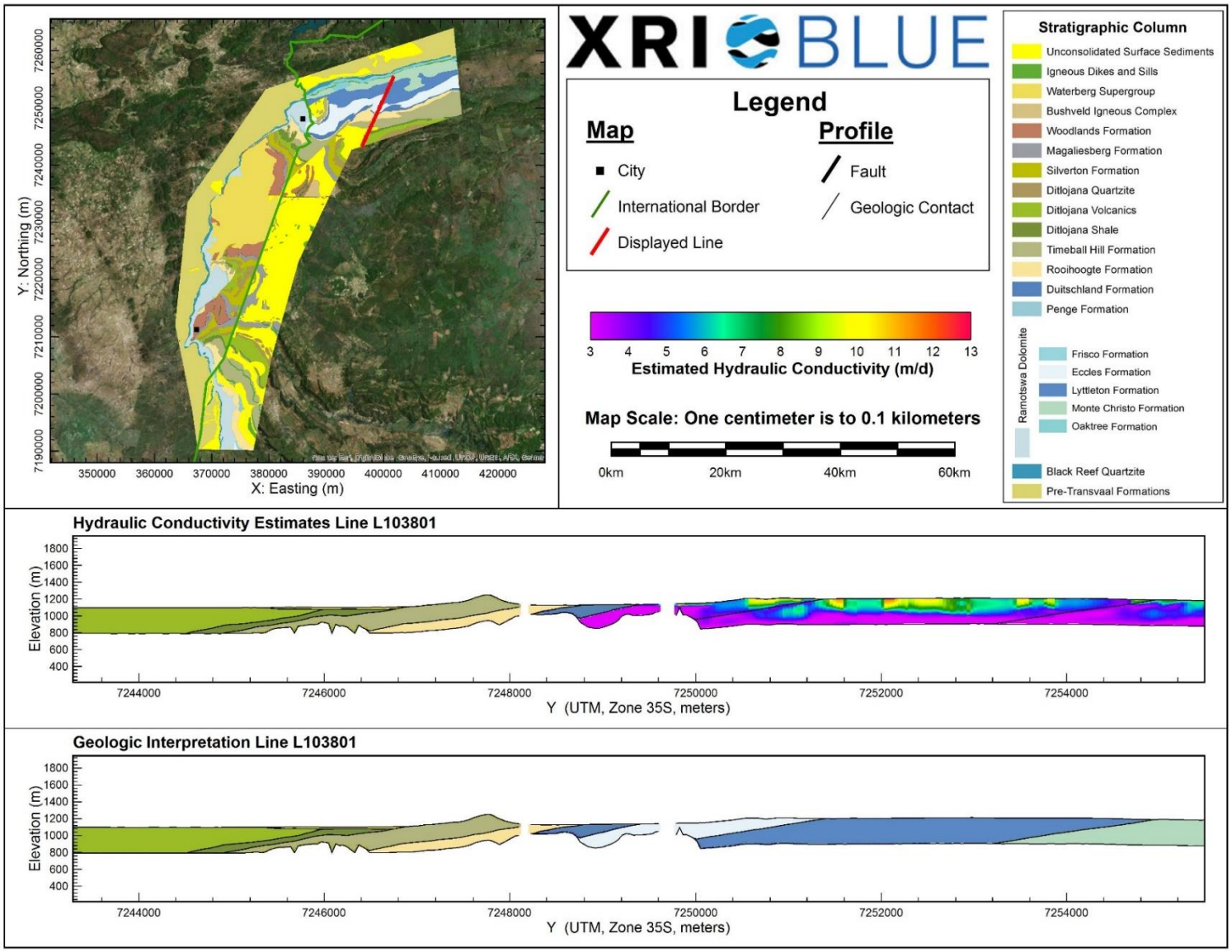

Hydraulic Conductivity Estimates and Interpreted Geology Profile for L103801.

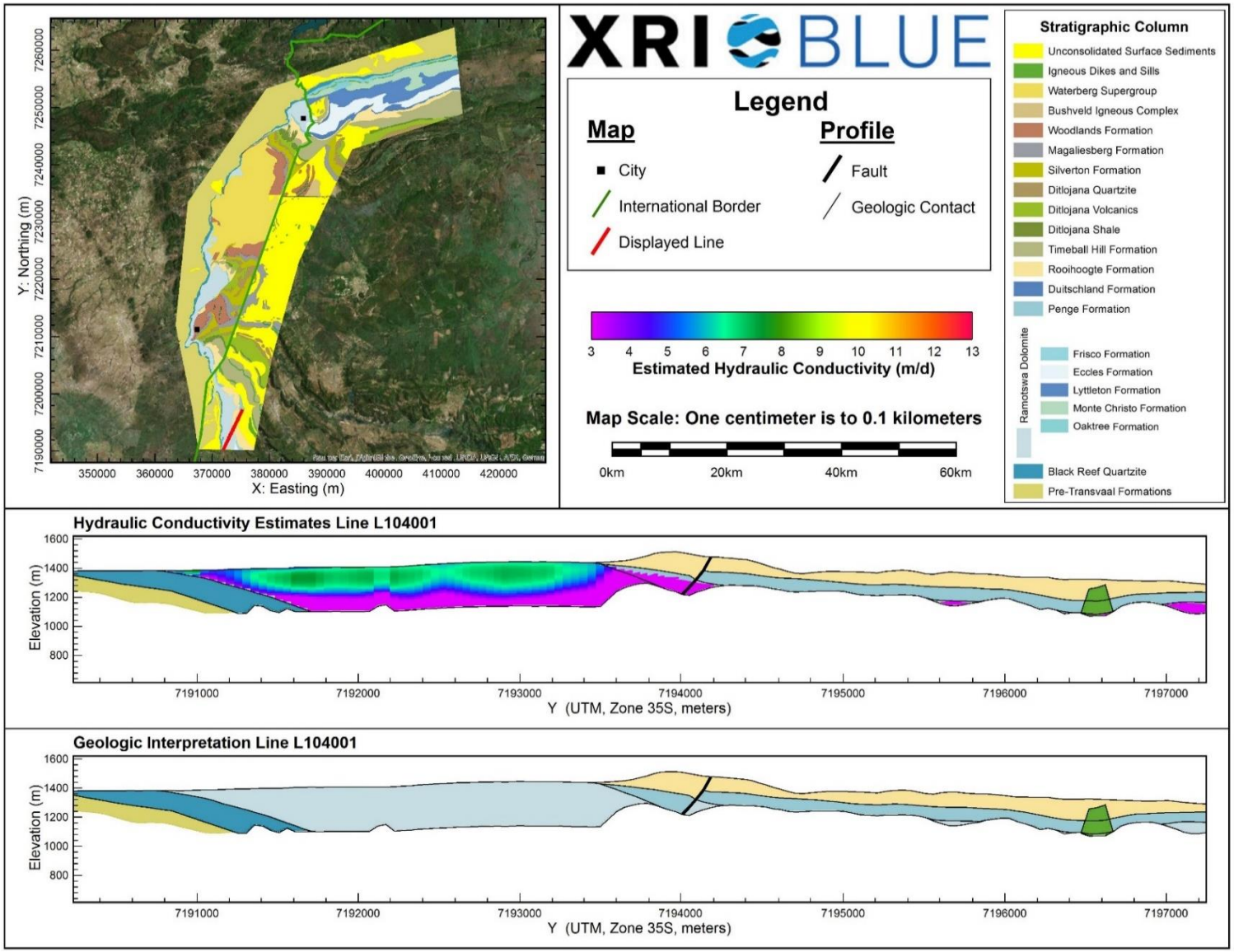

Hydraulic Conductivity Estimates and Interpreted Geology Profile for L104001.

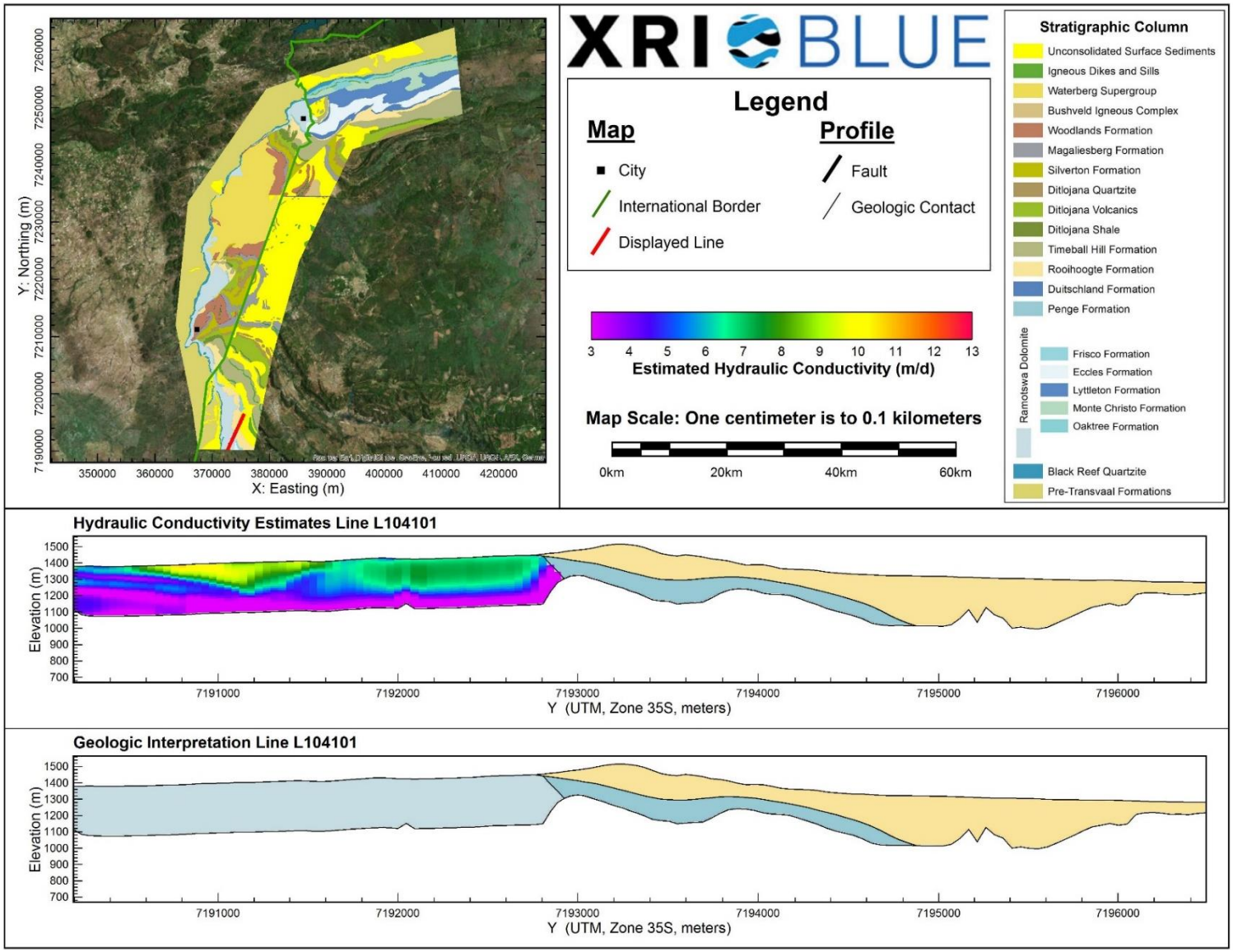

Hydraulic Conductivity Estimates and Interpreted Geology Profile for L104101.

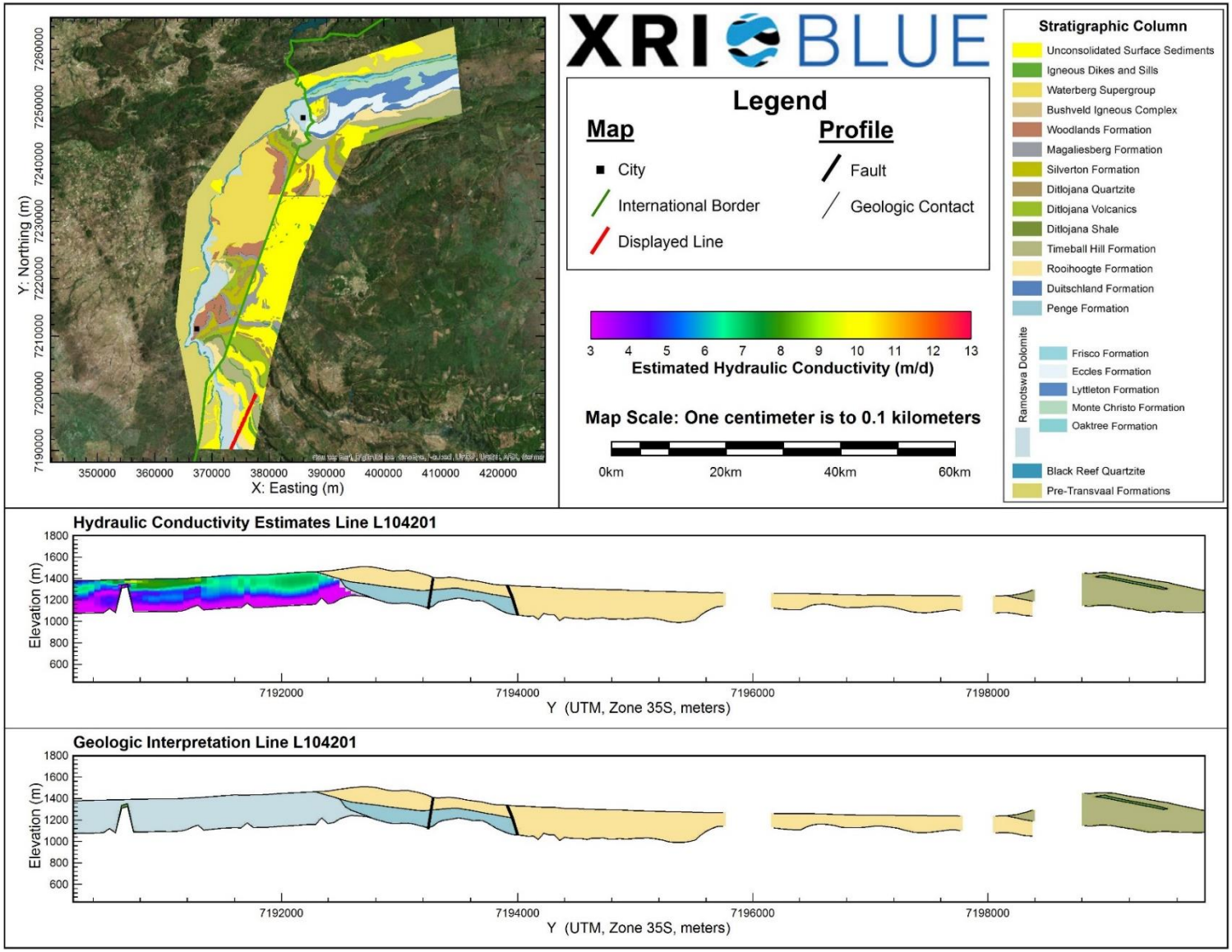

Hydraulic Conductivity Estimates and Interpreted Geology Profile for L104201.

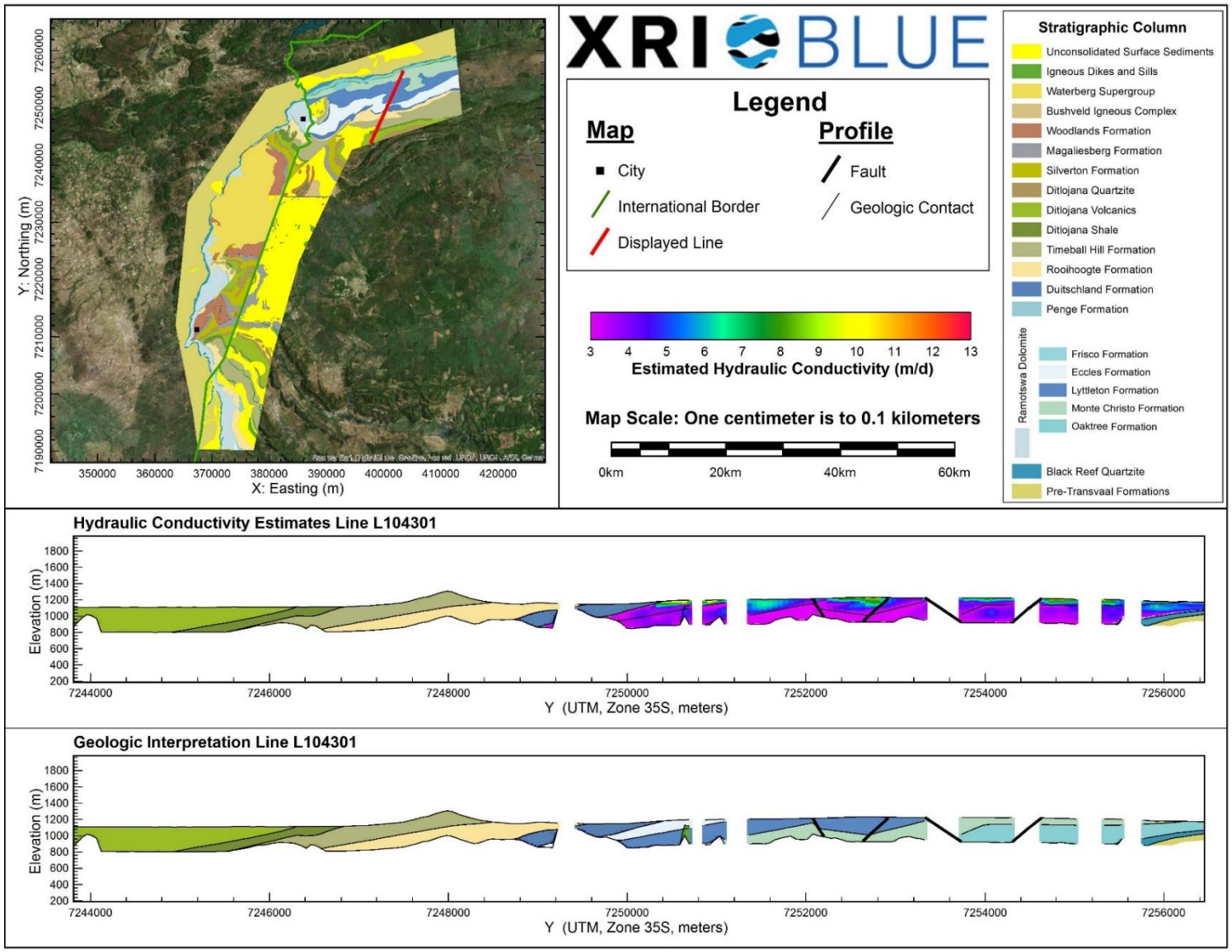

Hydraulic Conductivity Estimates and Interpreted Geology Profile for L104301.

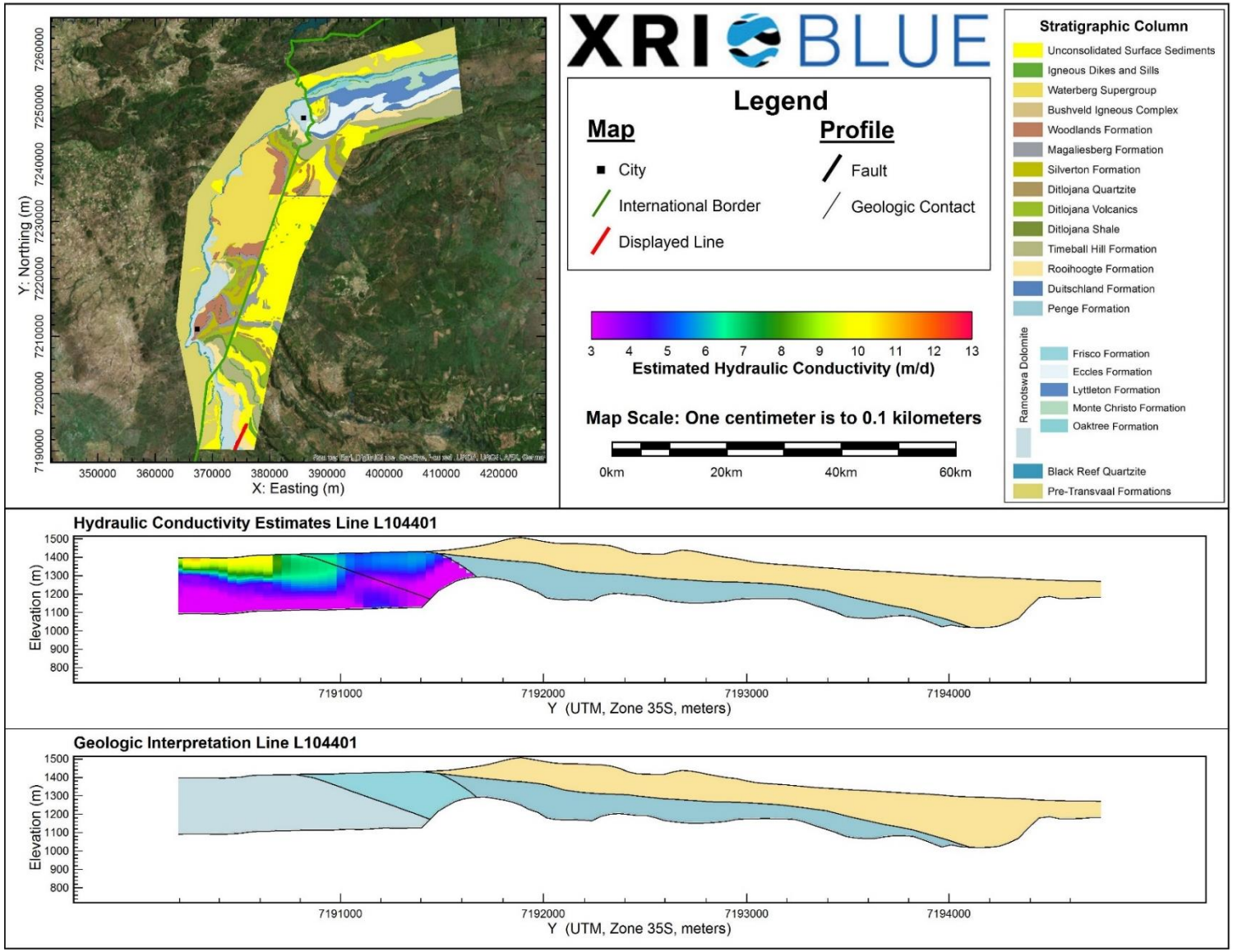

Hydraulic Conductivity Estimates and Interpreted Geology Profile for L104401.

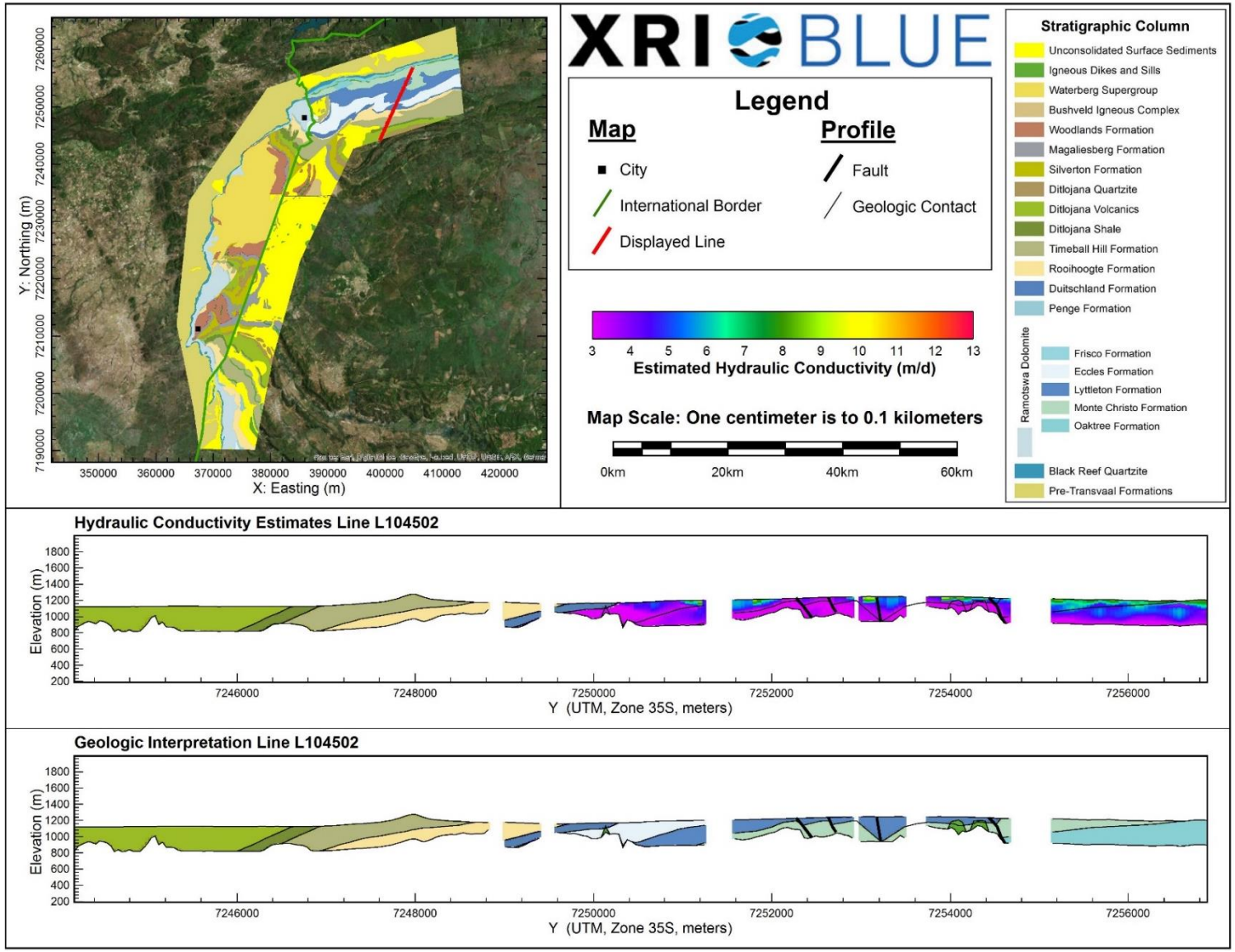

Hydraulic Conductivity Estimates and Interpreted Geology Profile for L104502.

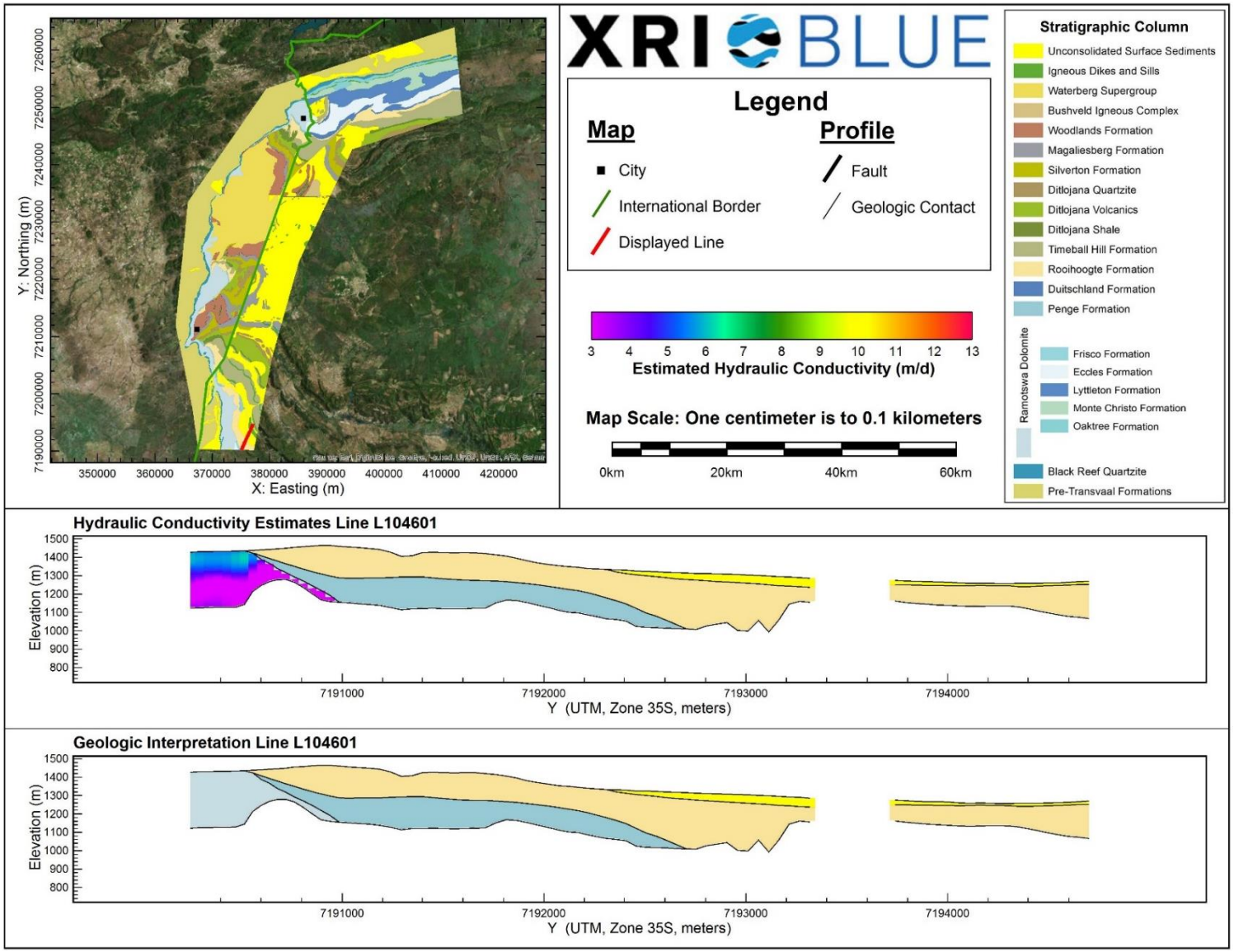

Hydraulic Conductivity Estimates and Interpreted Geology Profile for L104601.

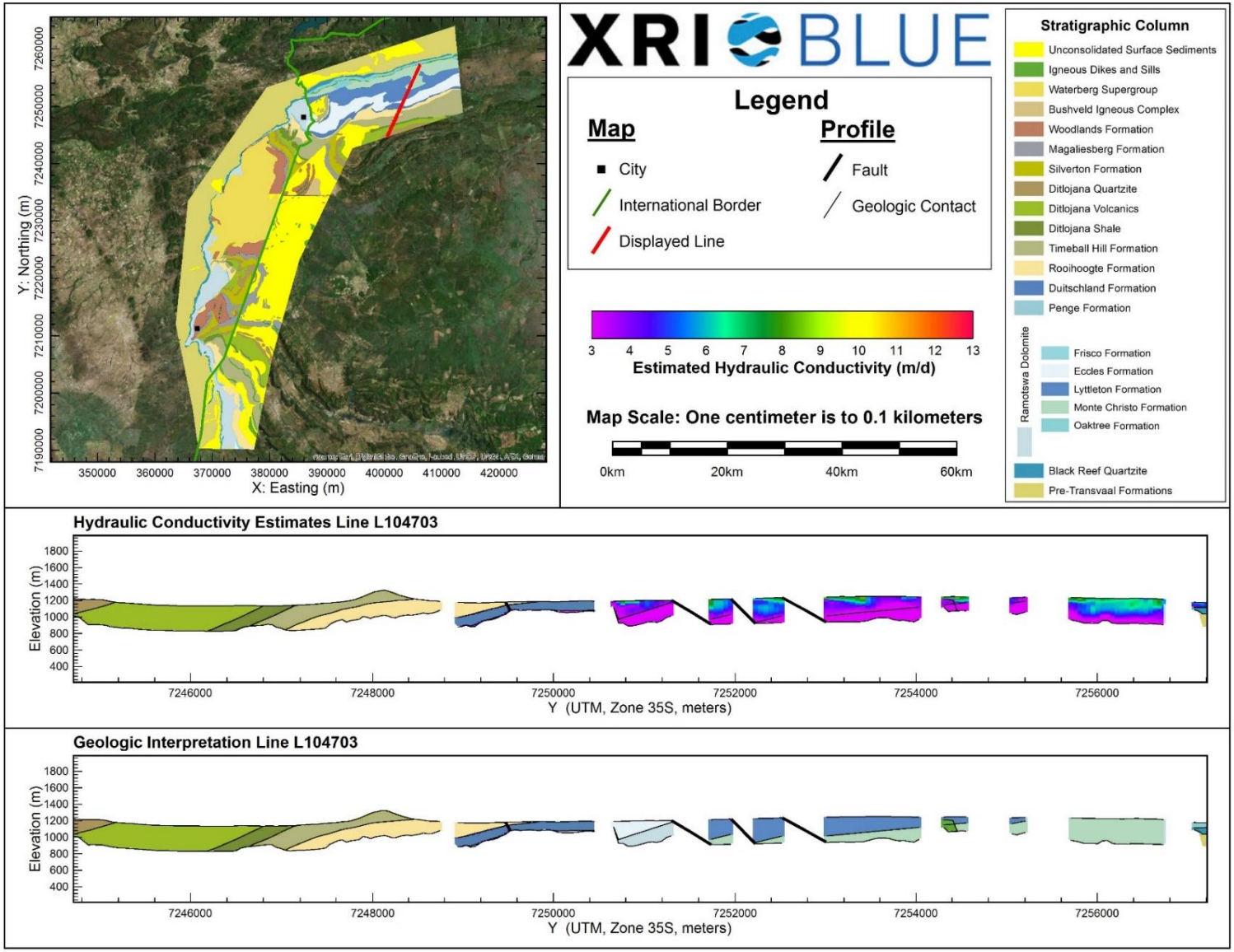

Hydraulic Conductivity Estimates and Interpreted Geology Profile for L104703.

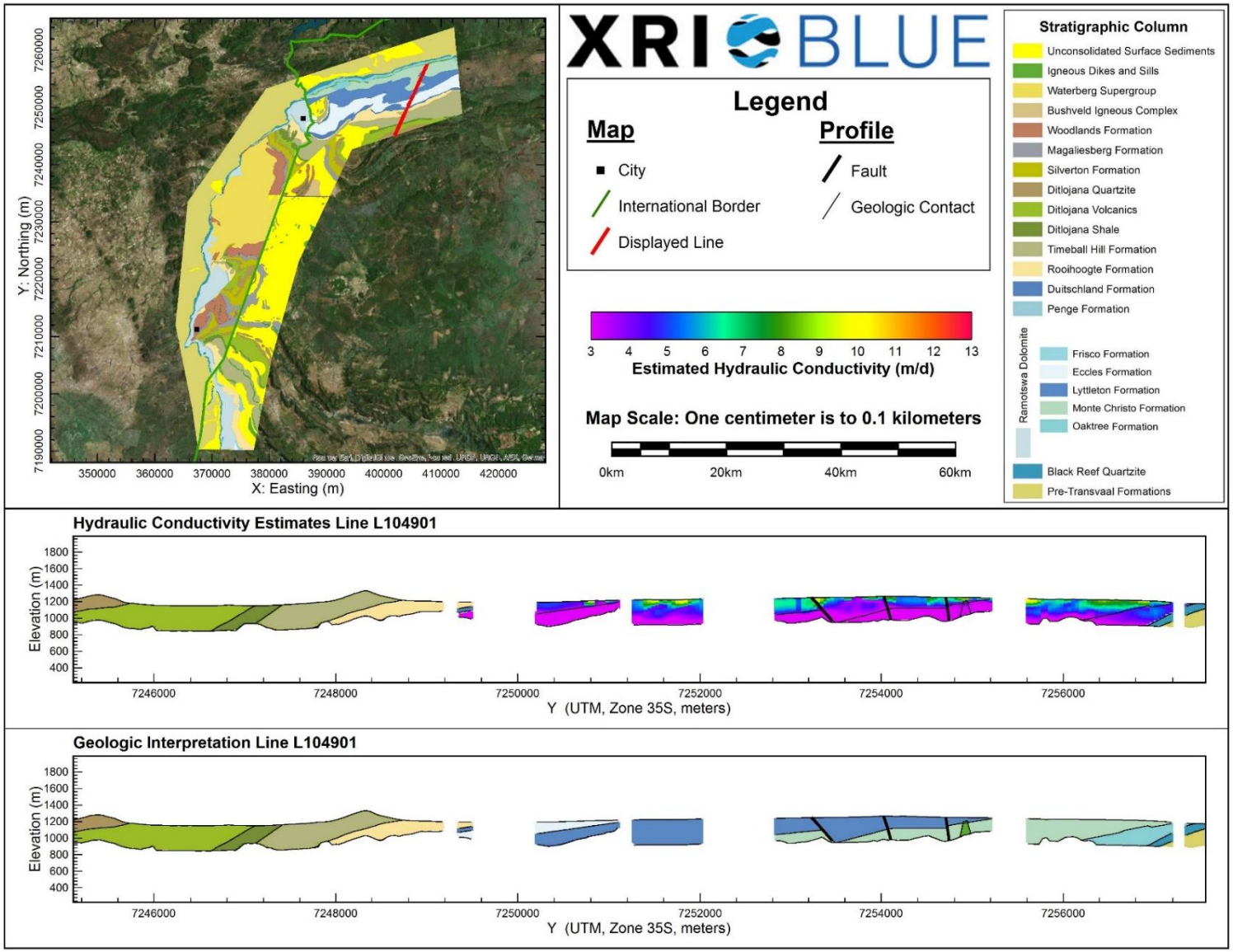

Hydraulic Conductivity Estimates and Interpreted Geology Profile for L104901.

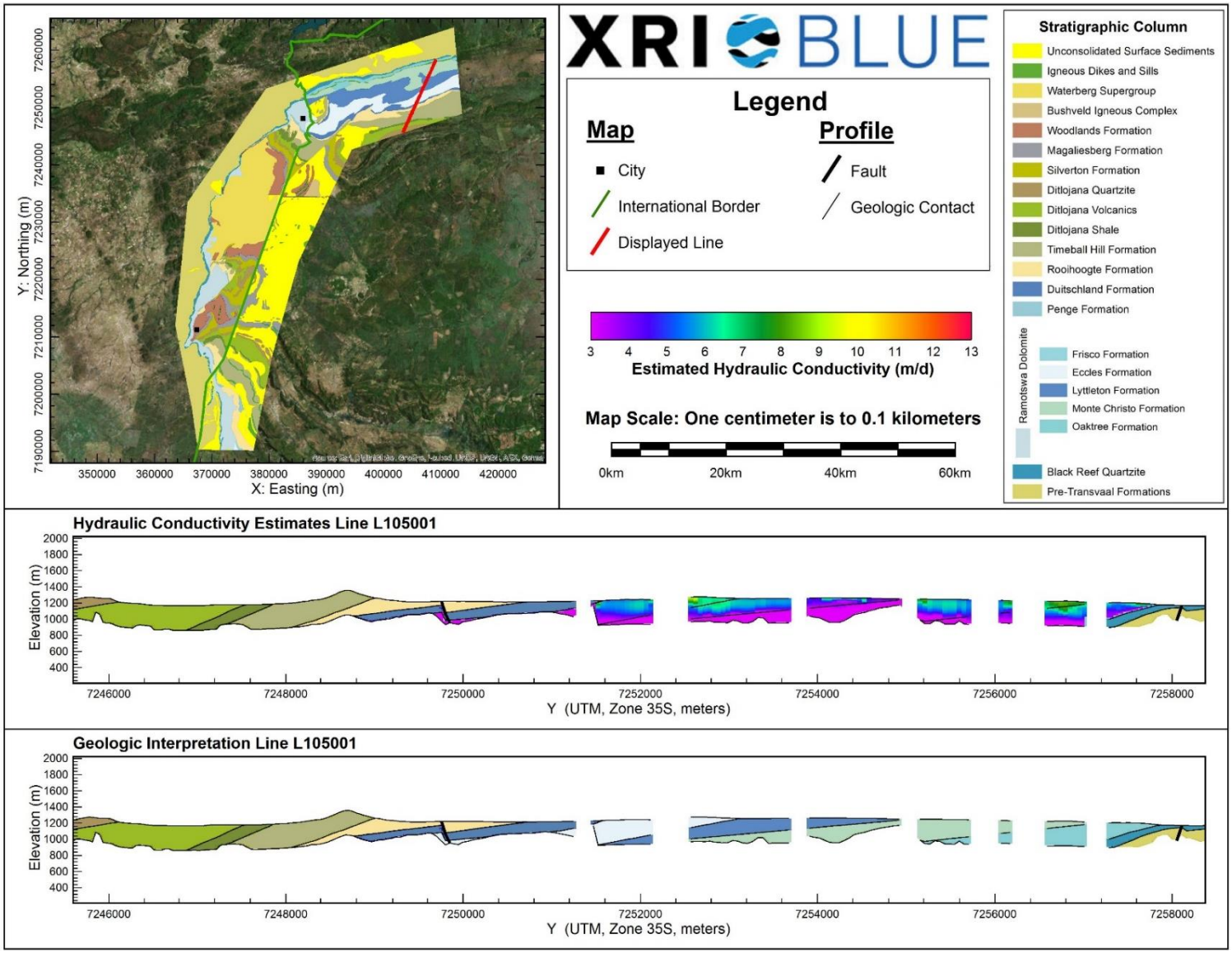

Hydraulic Conductivity Estimates and Interpreted Geology Profile for L105001.

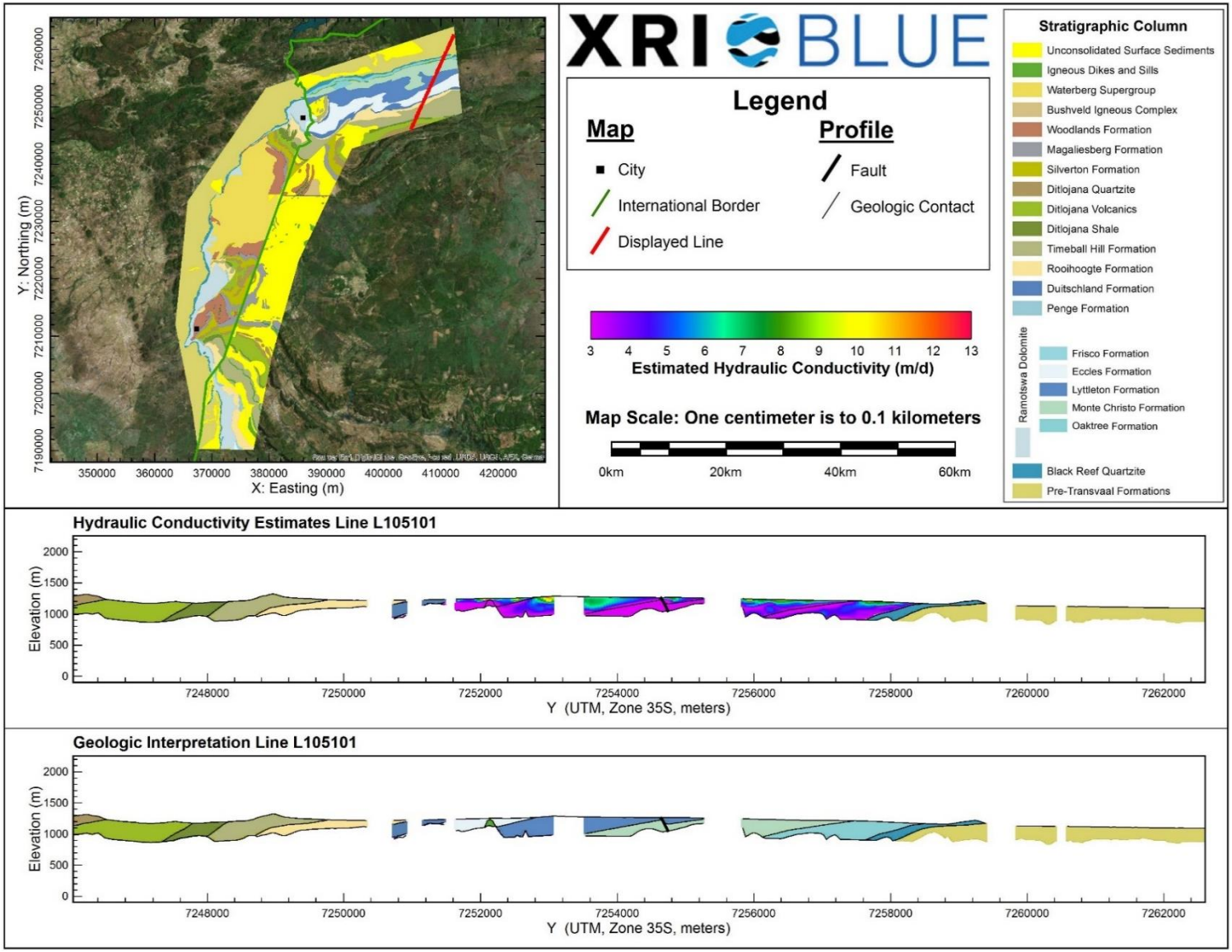

Hydraulic Conductivity Estimates and Interpreted Geology Profile for L105101.

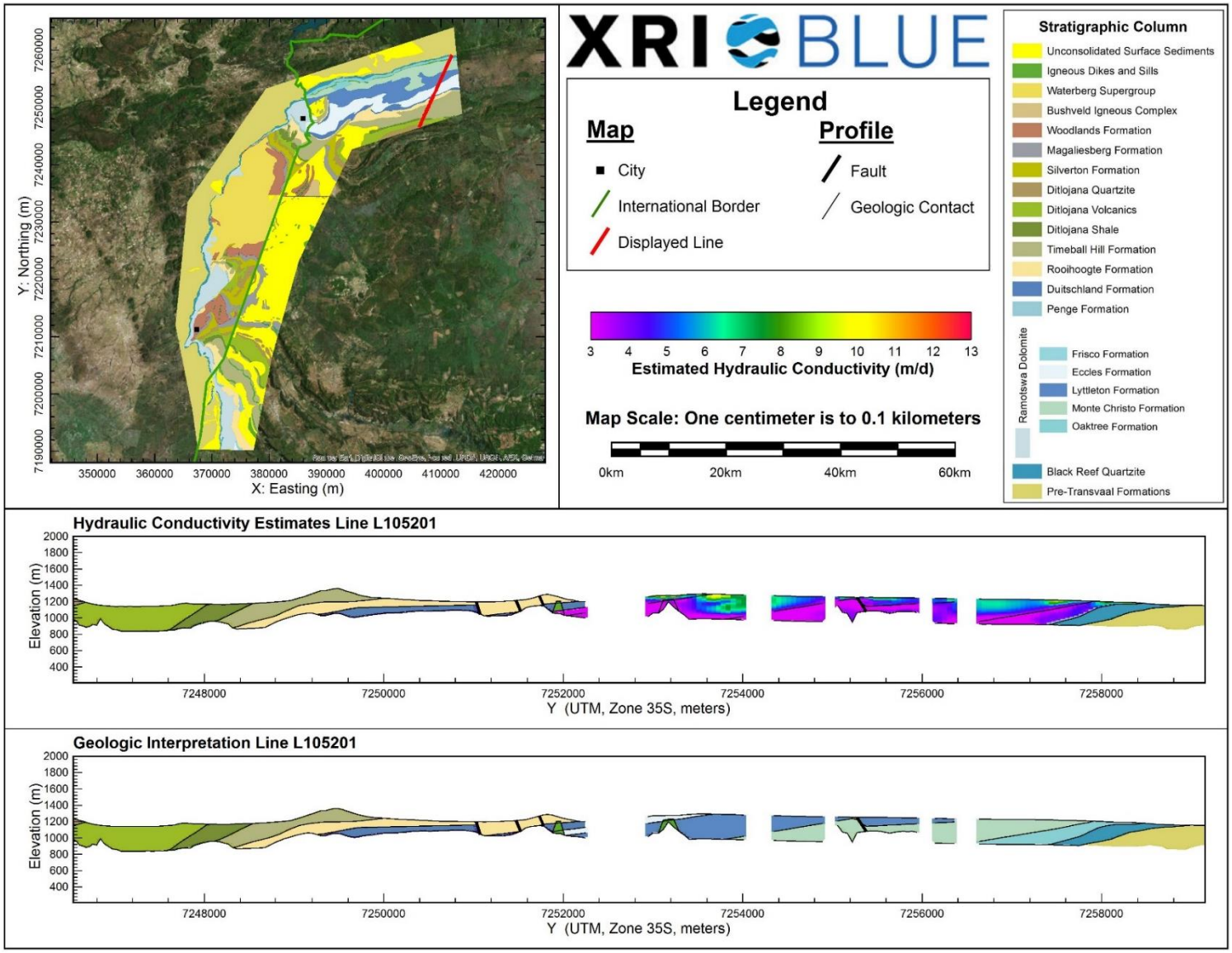

Hydraulic Conductivity Estimates and Interpreted Geology Profile for L105201.

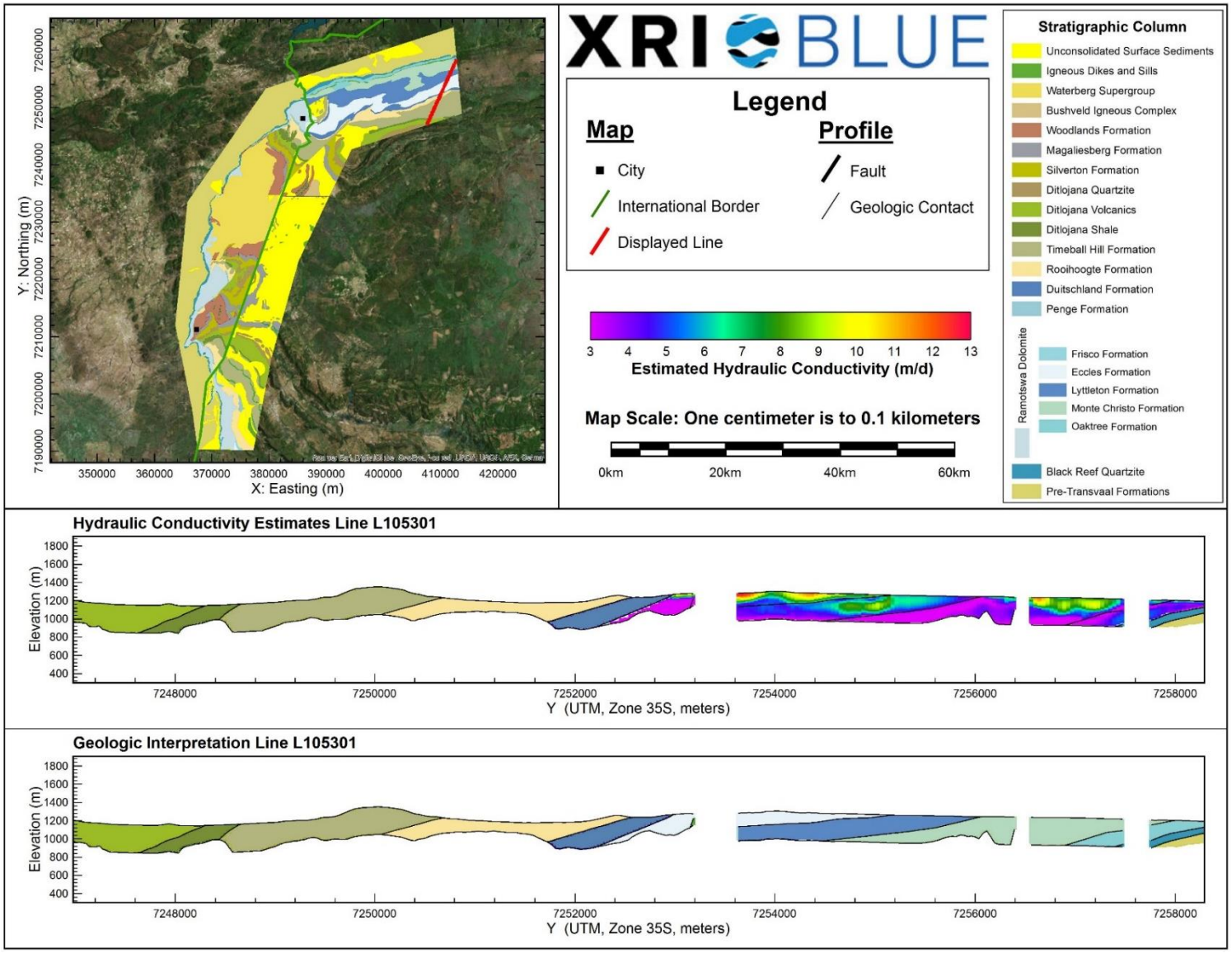

Hydraulic Conductivity Estimates and Interpreted Geology Profile for L105301.

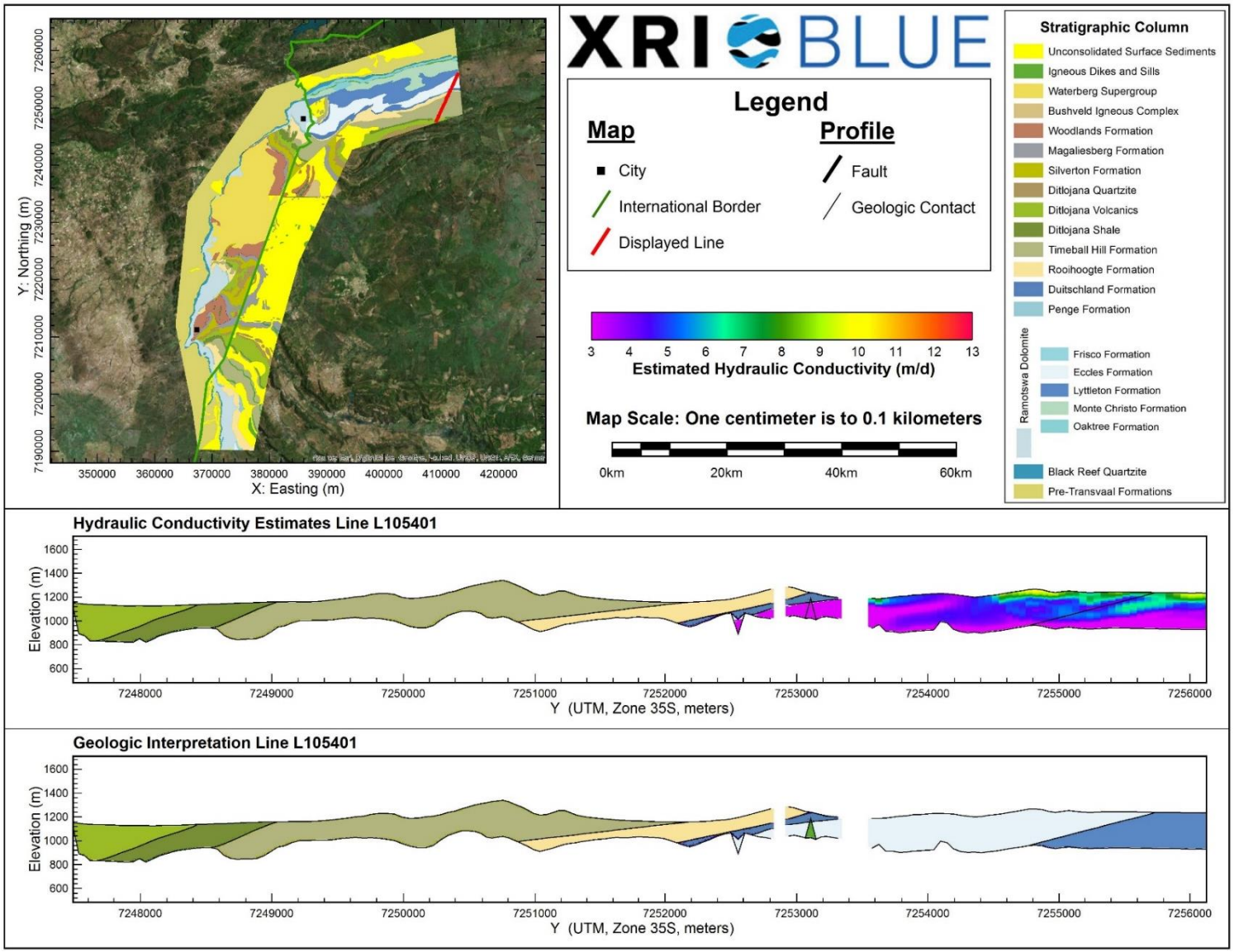

Hydraulic Conductivity Estimates and Interpreted Geology Profile for L105401.

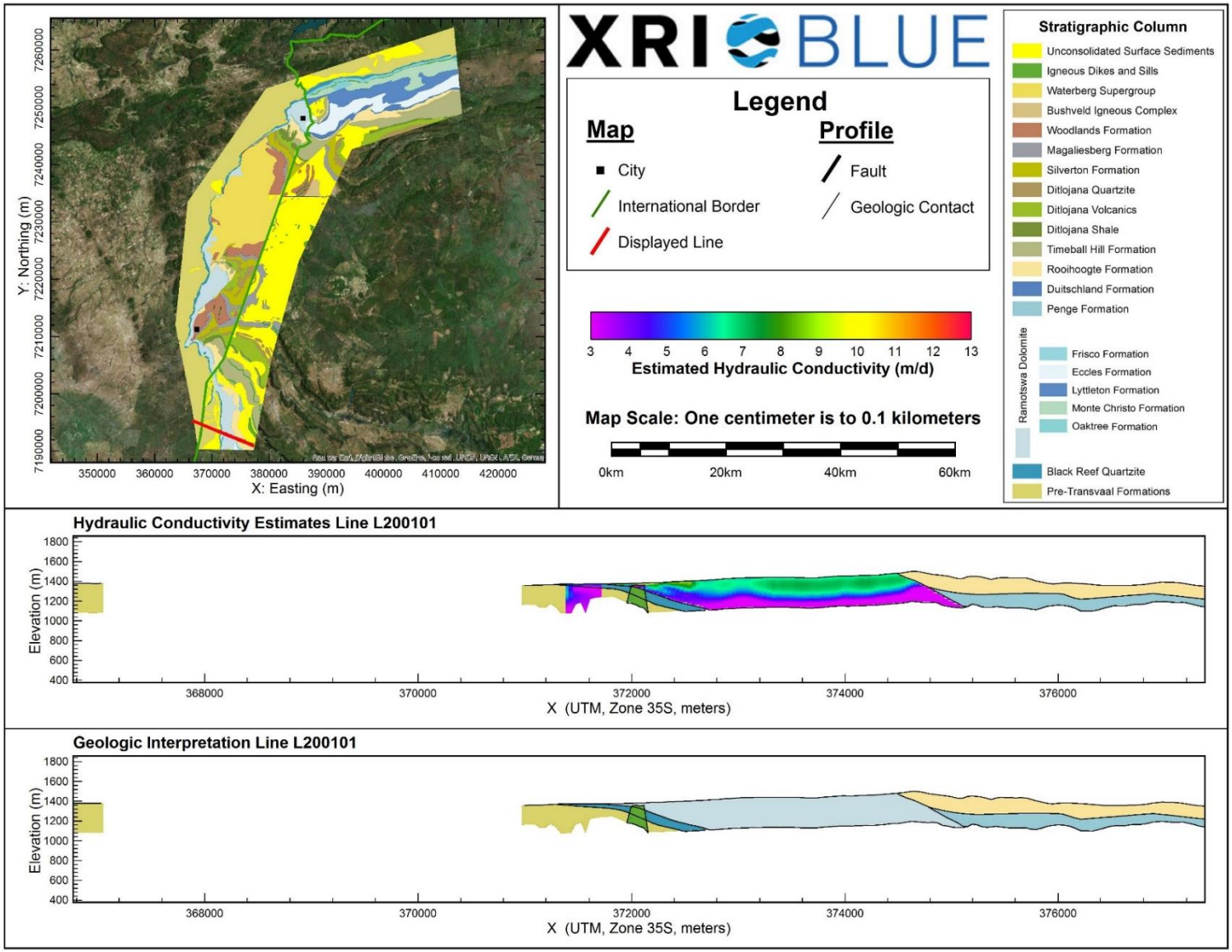

Hydraulic Conductivity Estimates and Interpreted Geology Profile for L200101.

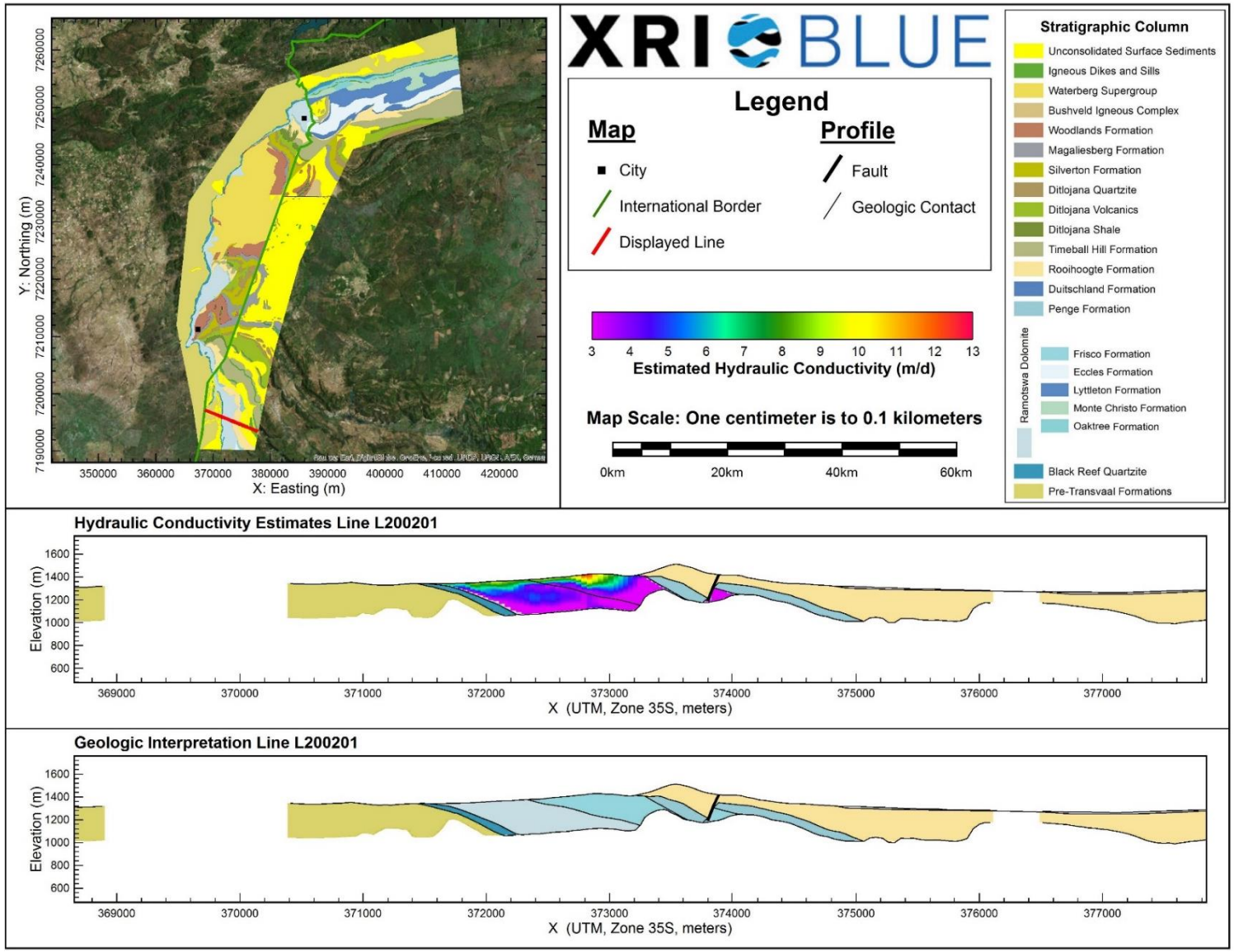

Hydraulic Conductivity Estimates and Interpreted Geology Profile for L200201.

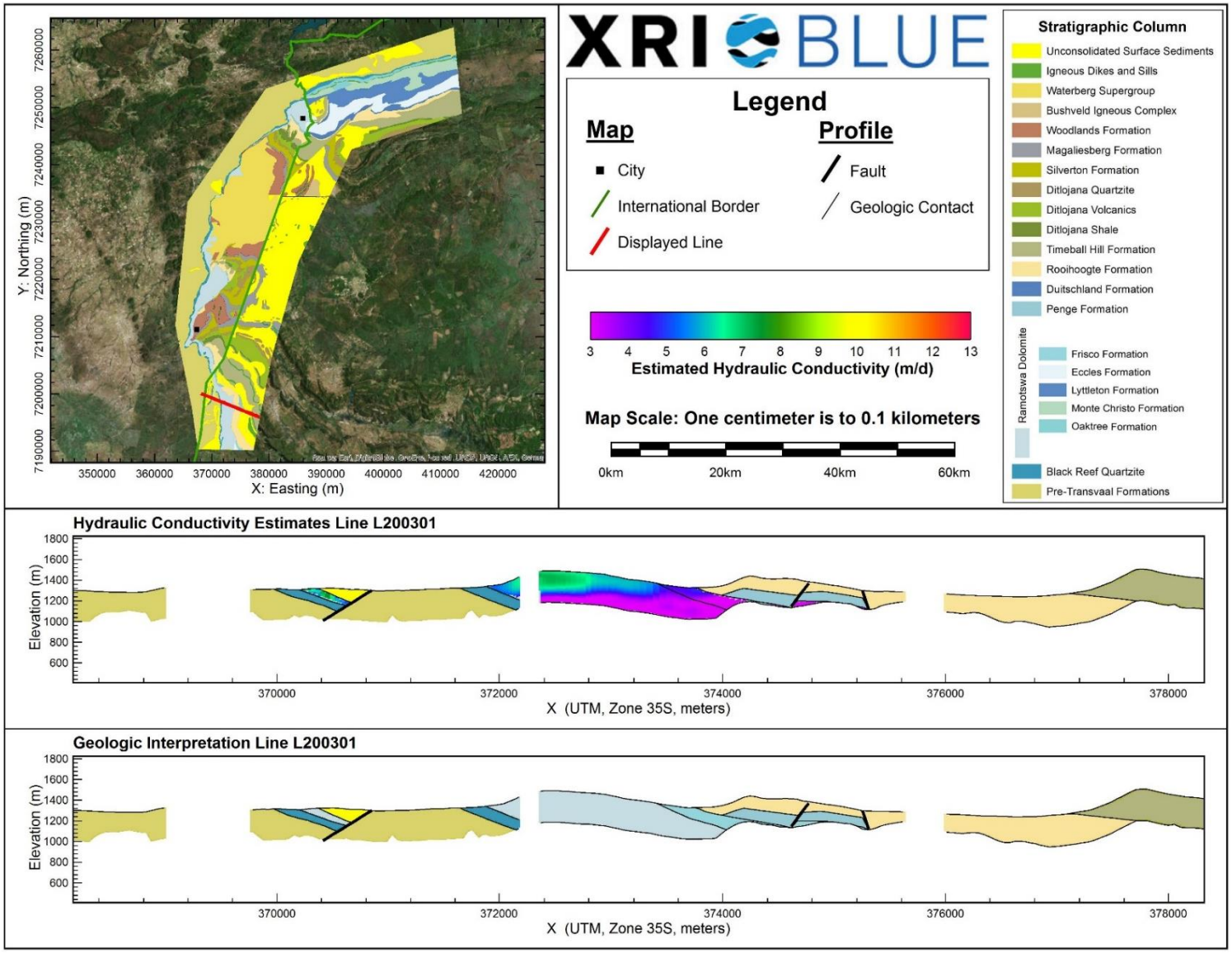

Hydraulic Conductivity Estimates and Interpreted Geology Profile for L200301.

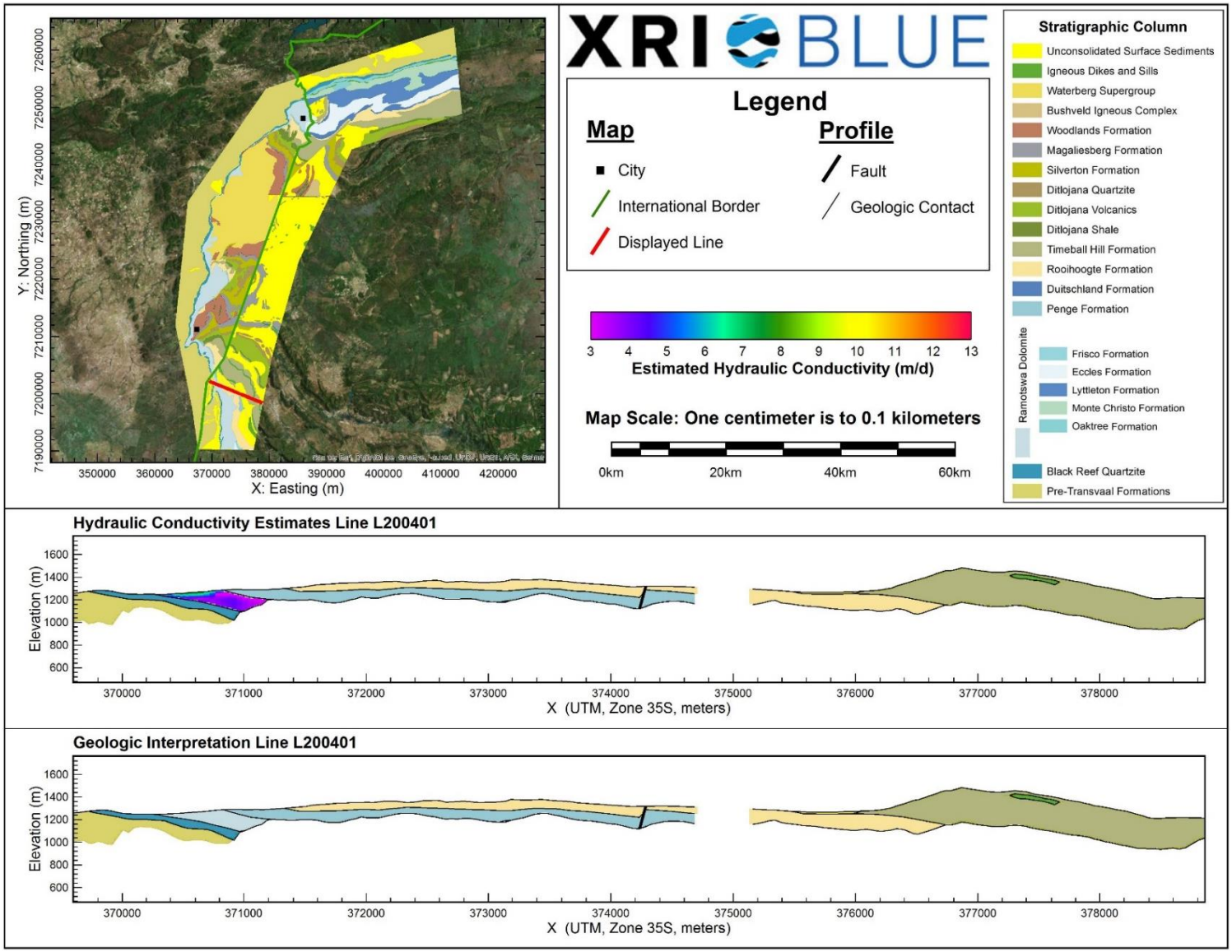

Hydraulic Conductivity Estimates and Interpreted Geology Profile for 200401.

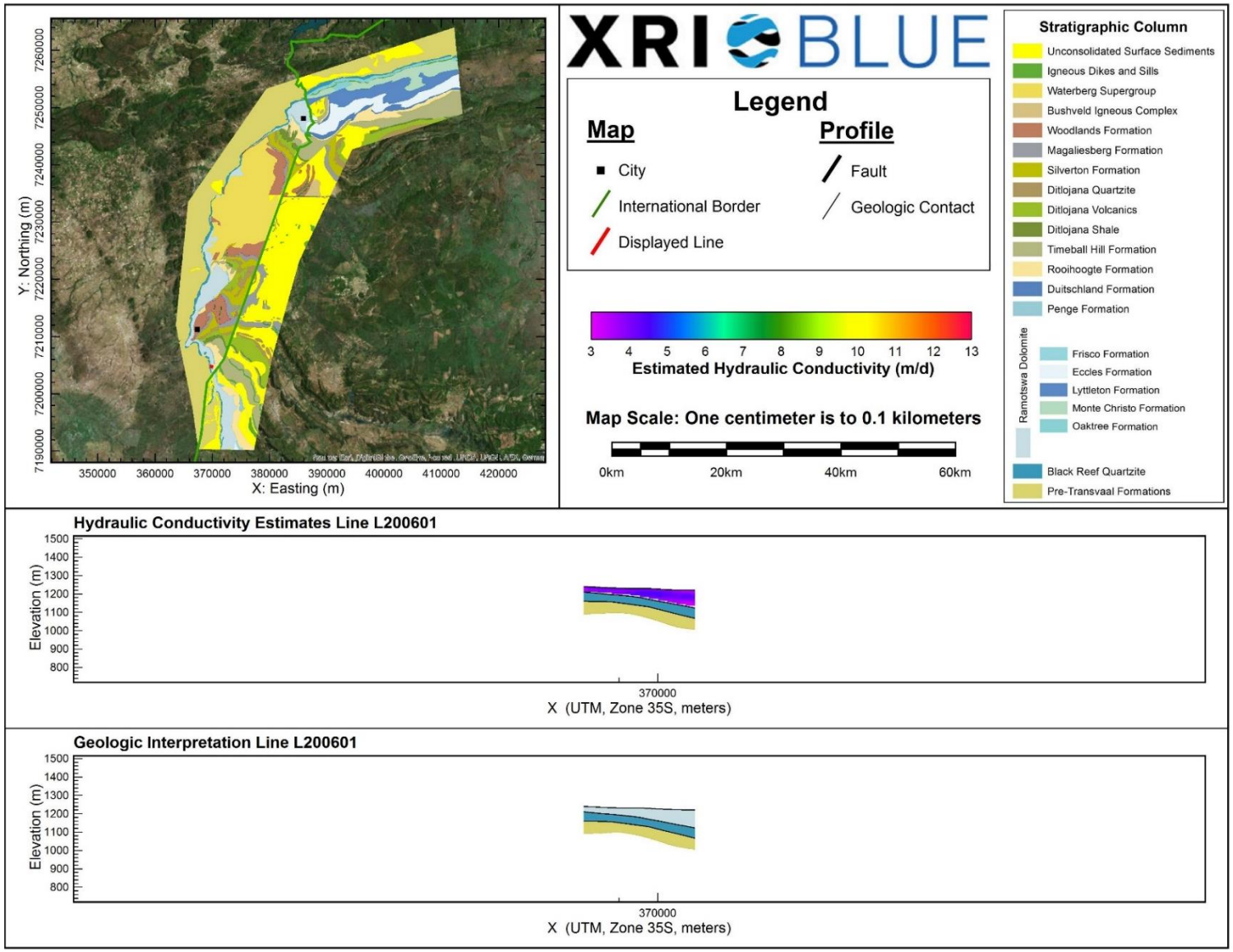

Hydraulic Conductivity Estimates and Interpreted Geology Profile for L200601.

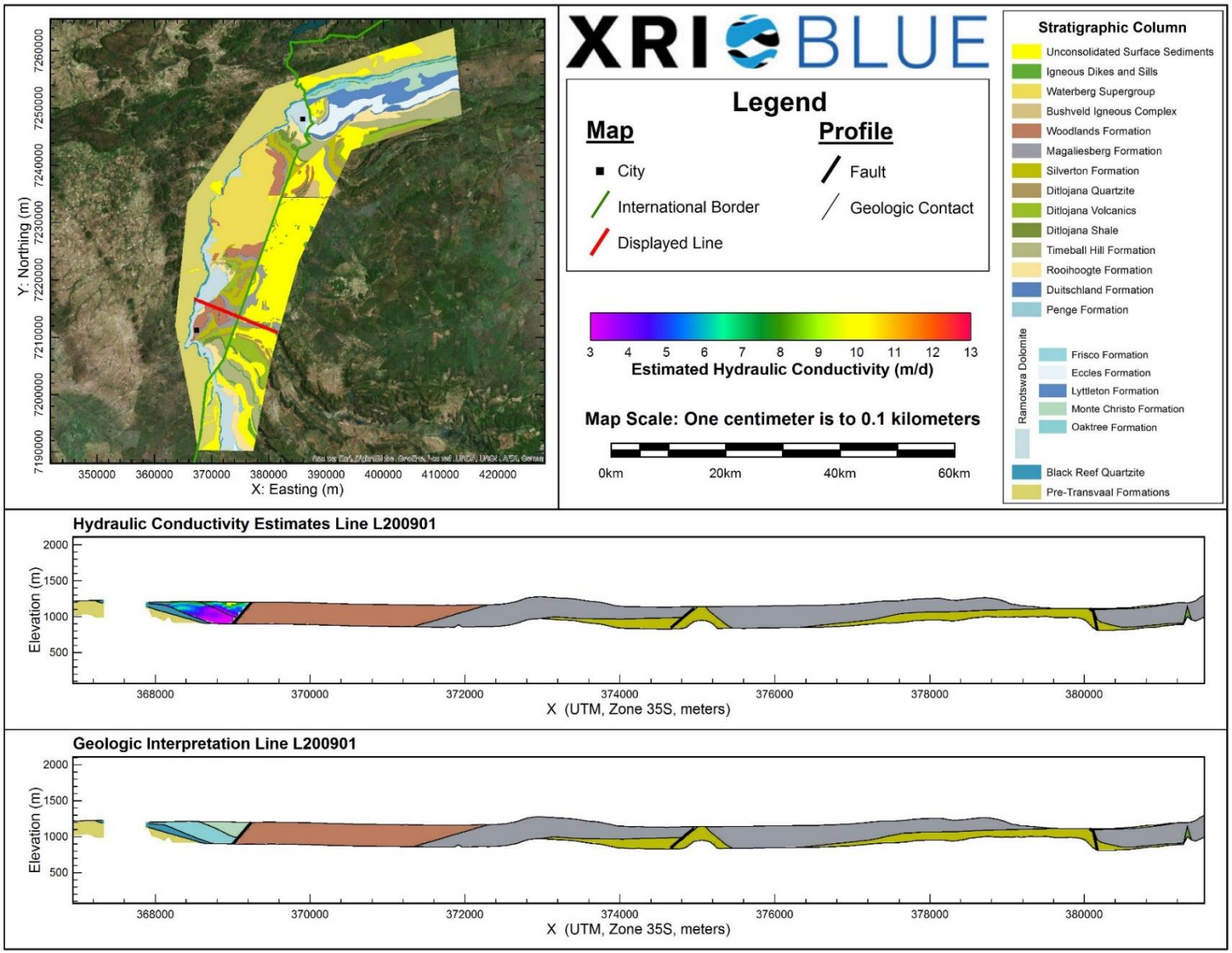

Hydraulic Conductivity Estimates and Interpreted Geology Profile for L200901.

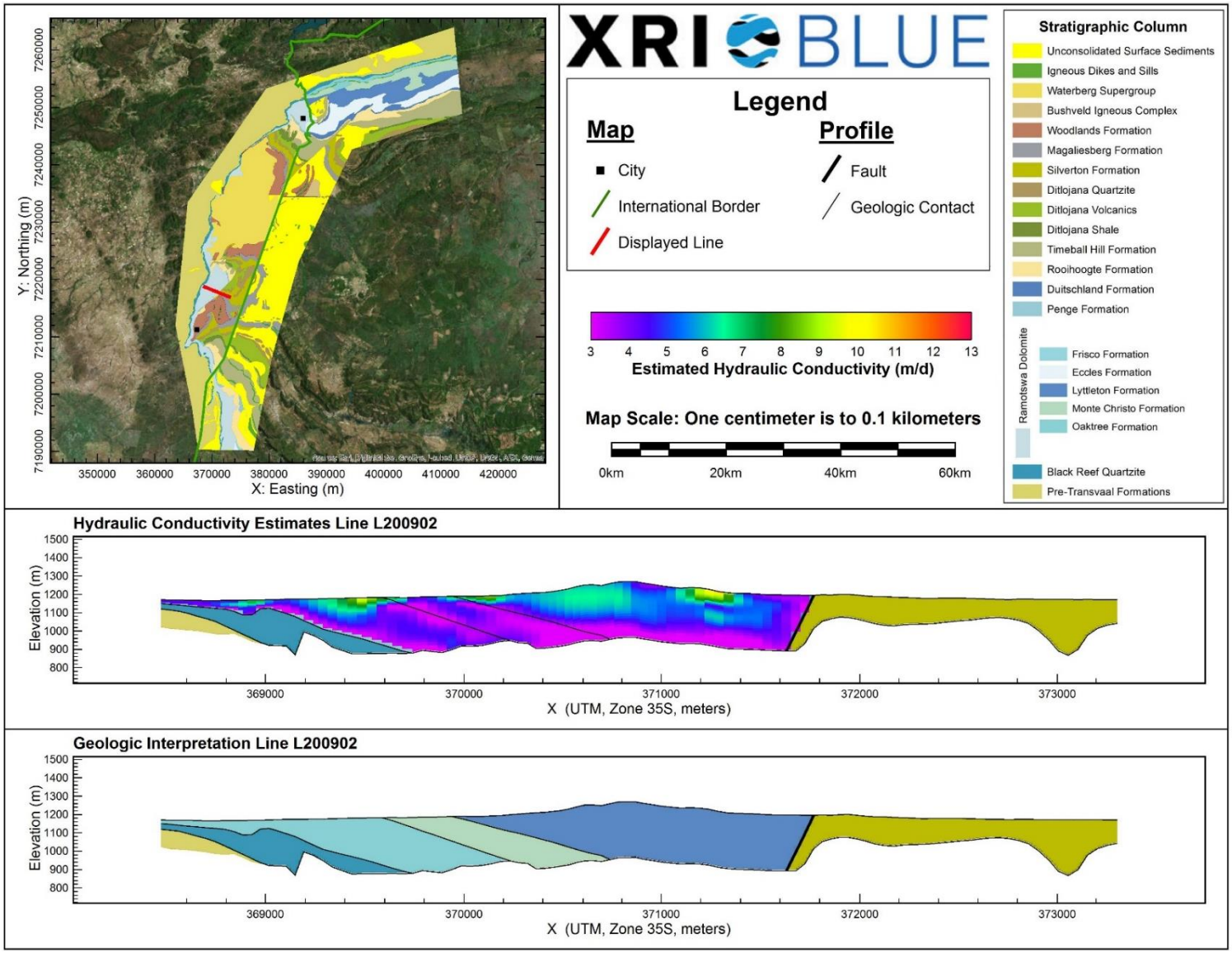

Hydraulic Conductivity Estimates and Interpreted Geology Profile for L200902.

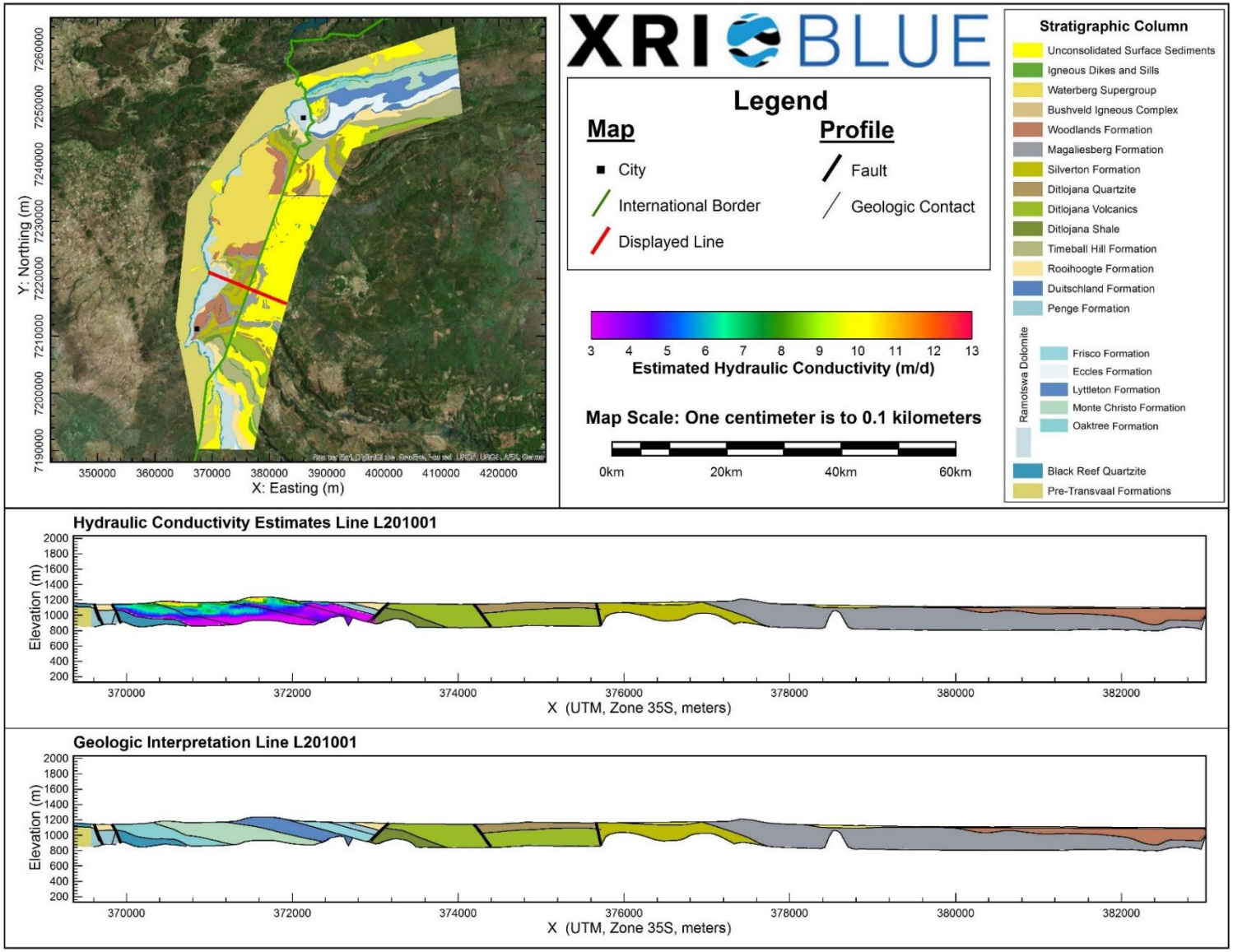

Hydraulic Conductivity Estimates and Interpreted Geology Profile for L201001.

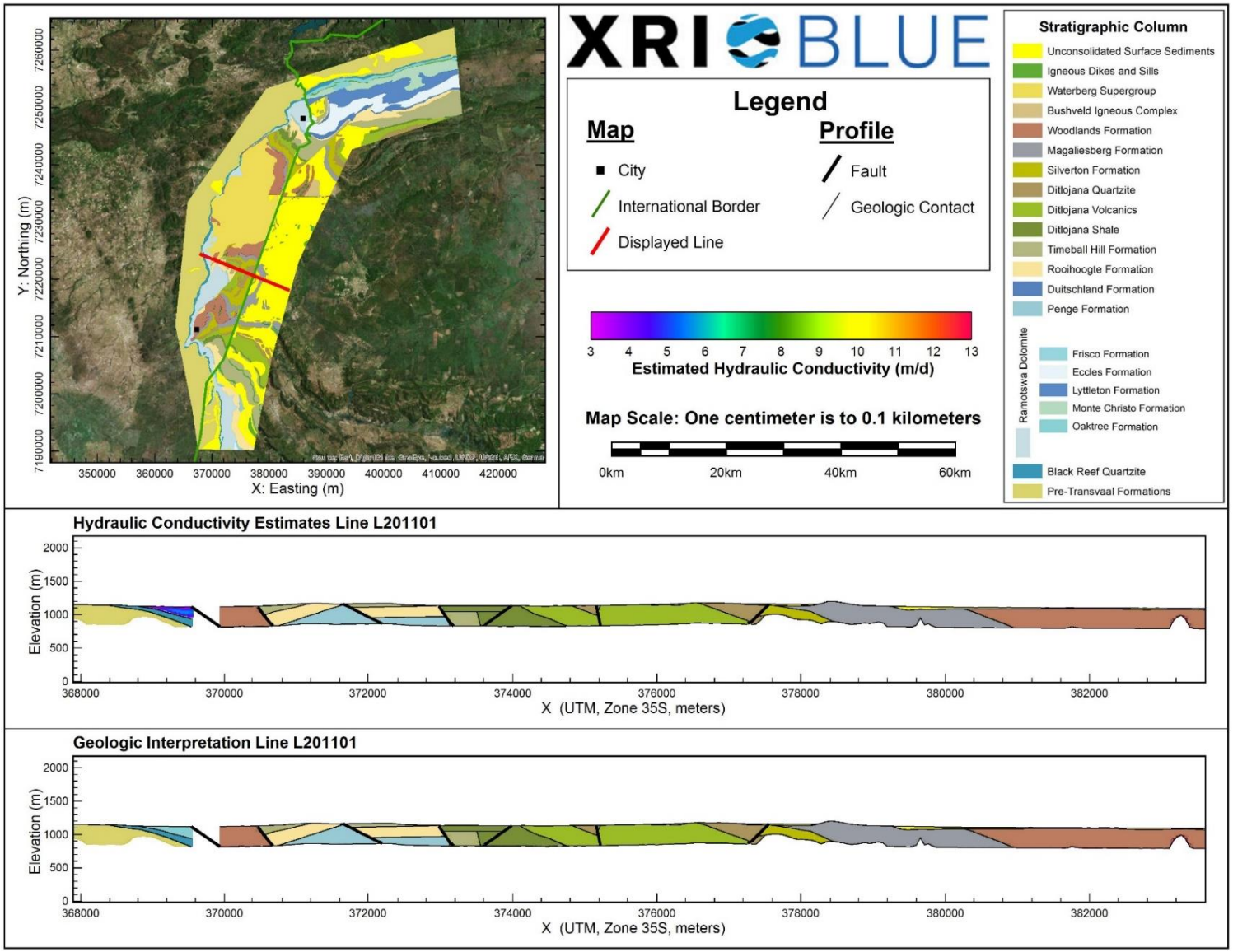

Hydraulic Conductivity Estimates and Interpreted Geology Profile for L201101.

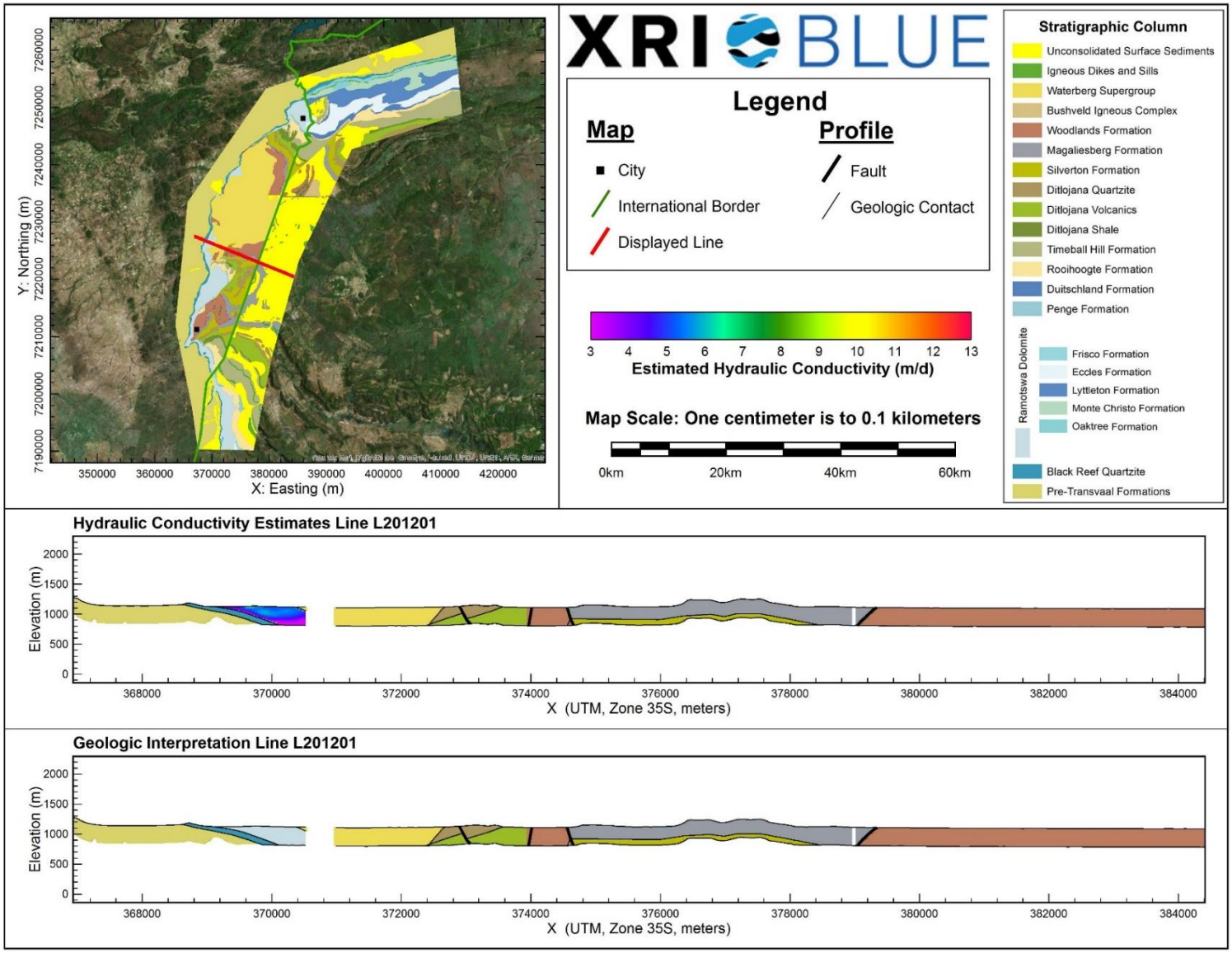

Hydraulic Conductivity Estimates and Interpreted Geology Profile for L201201.

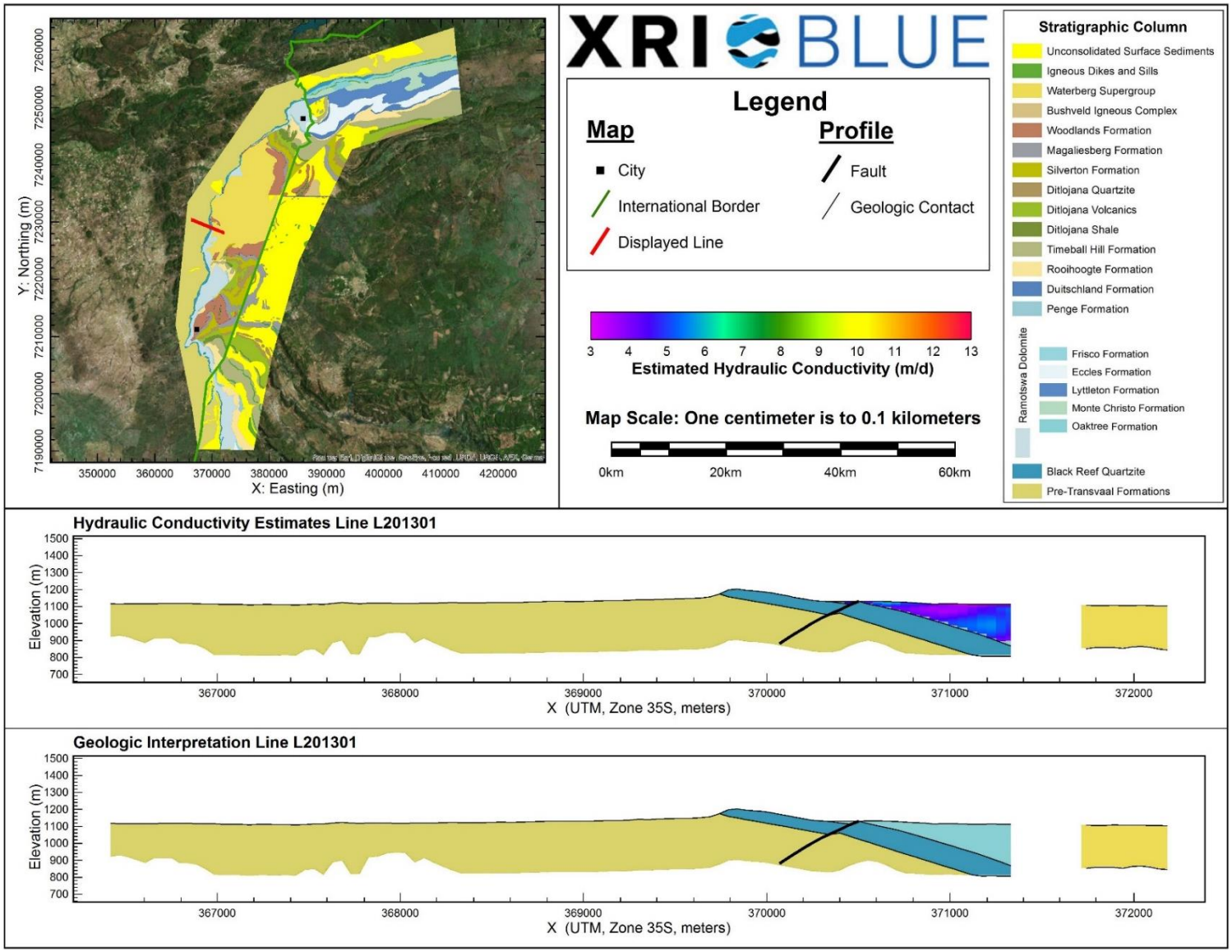

Hydraulic Conductivity Estimates and Interpreted Geology Profile for L201301.

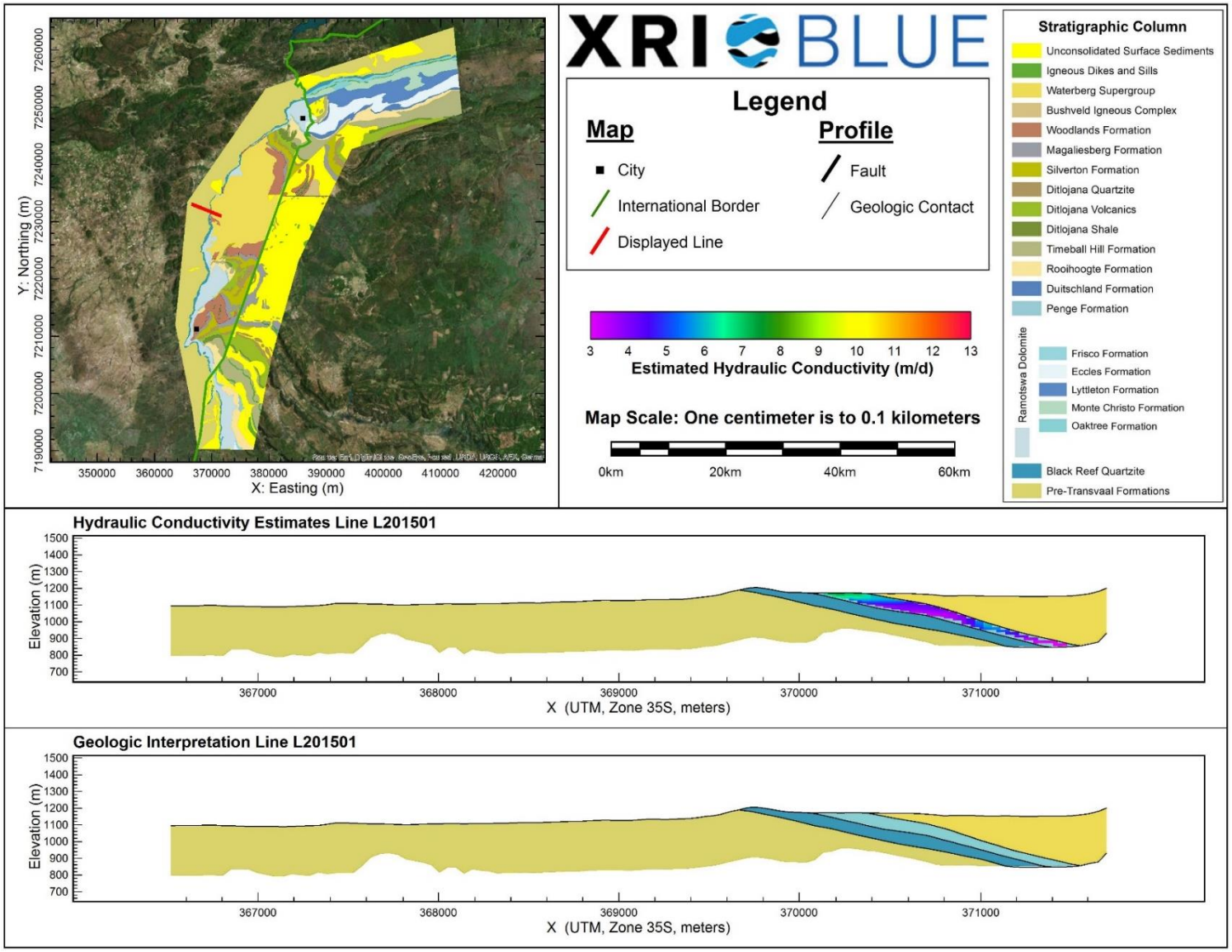

Hydraulic Conductivity Estimates and Interpreted Geology Profile for L201501.

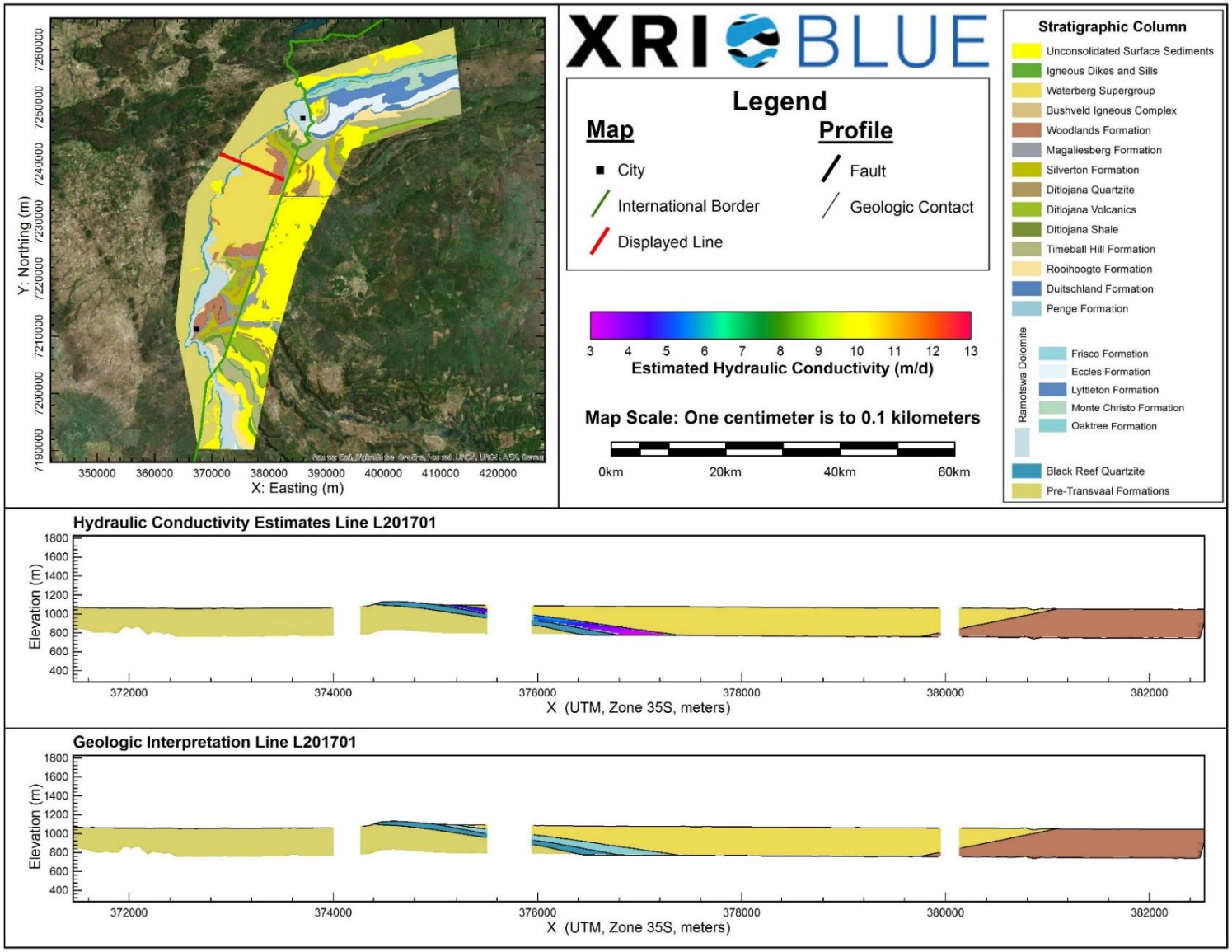

Hydraulic Conductivity Estimates and Interpreted Geology Profile for L201701.

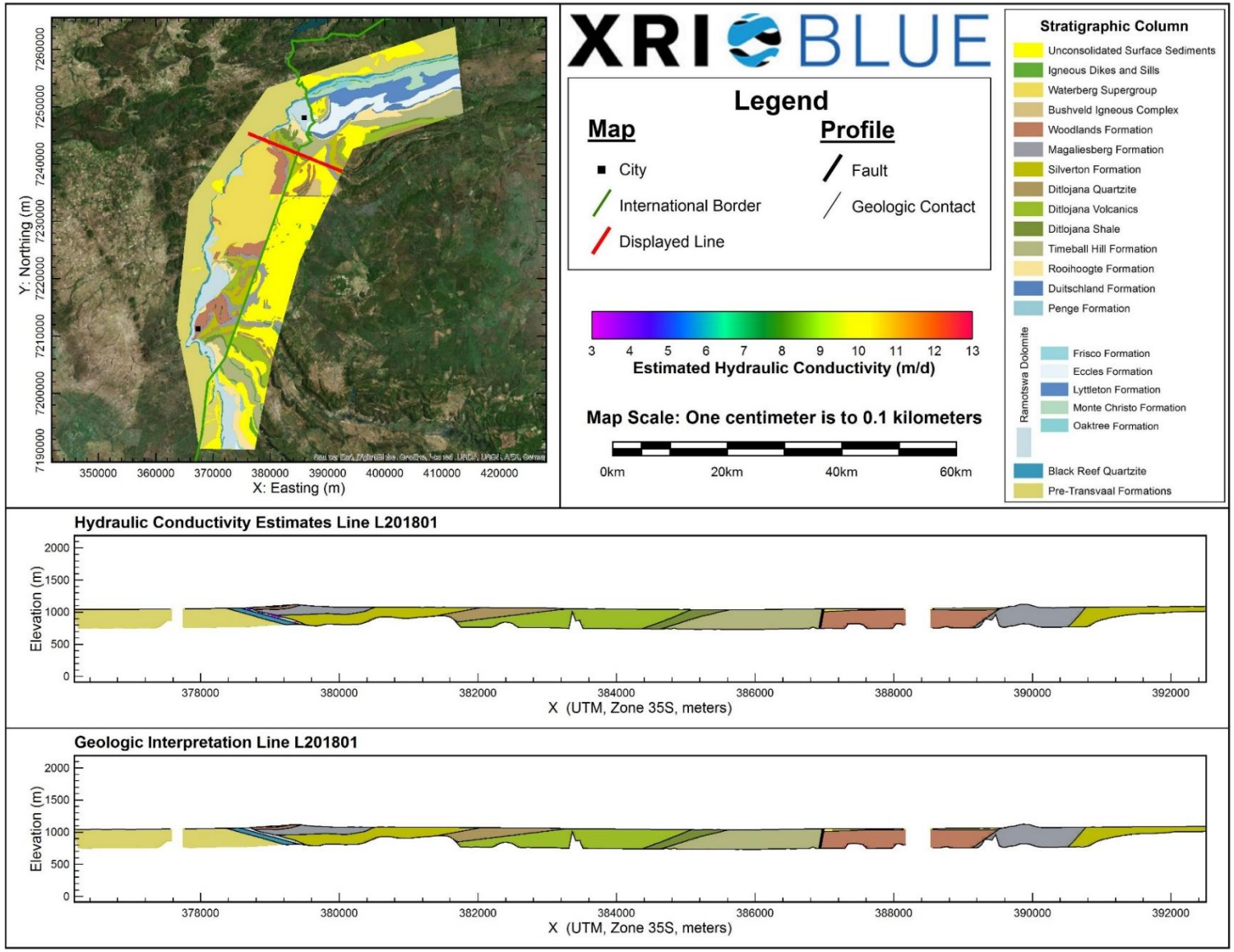

Hydraulic Conductivity Estimates and Interpreted Geology Profile for L201801.

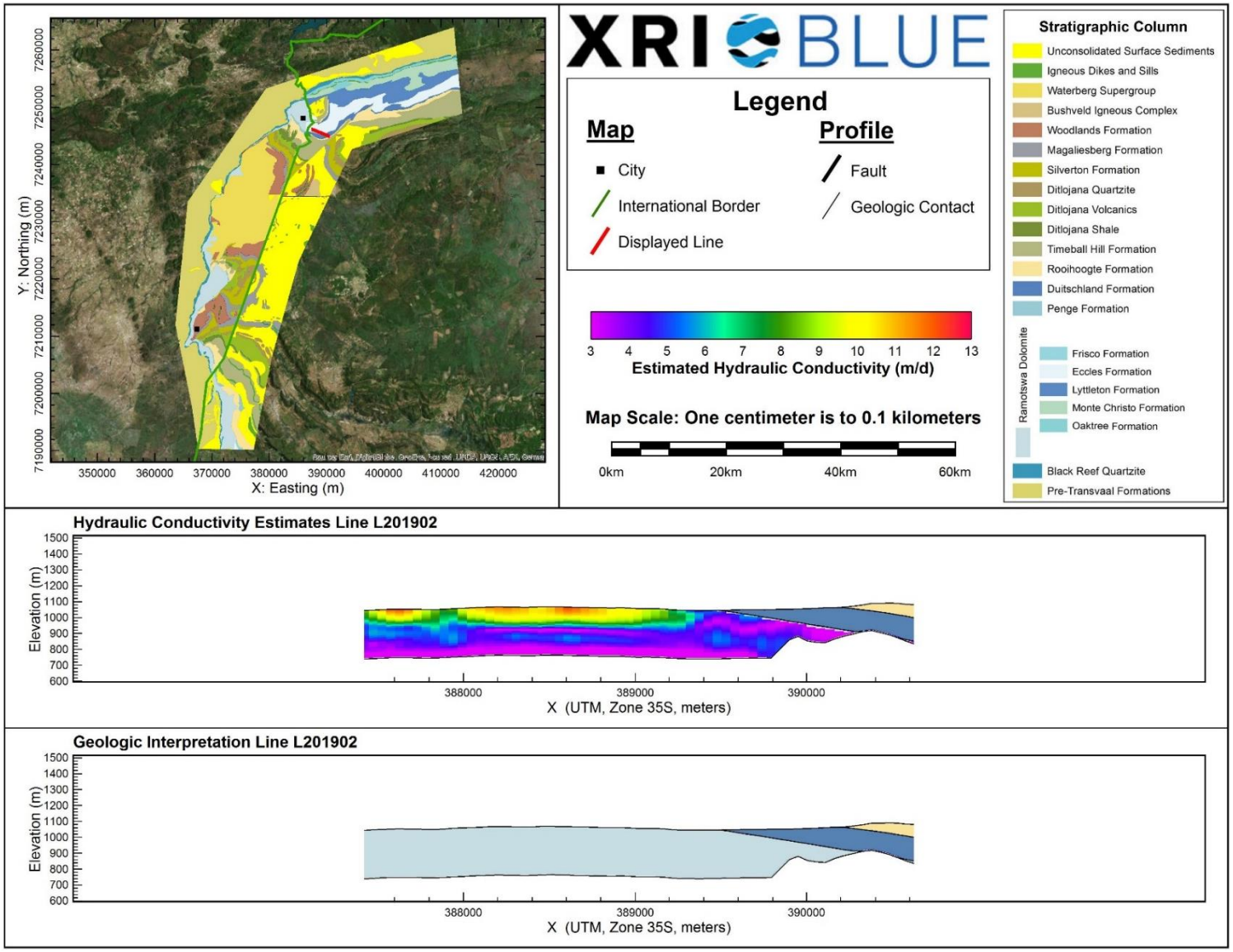

Hydraulic Conductivity Estimates and Interpreted Geology Profile for L201902.

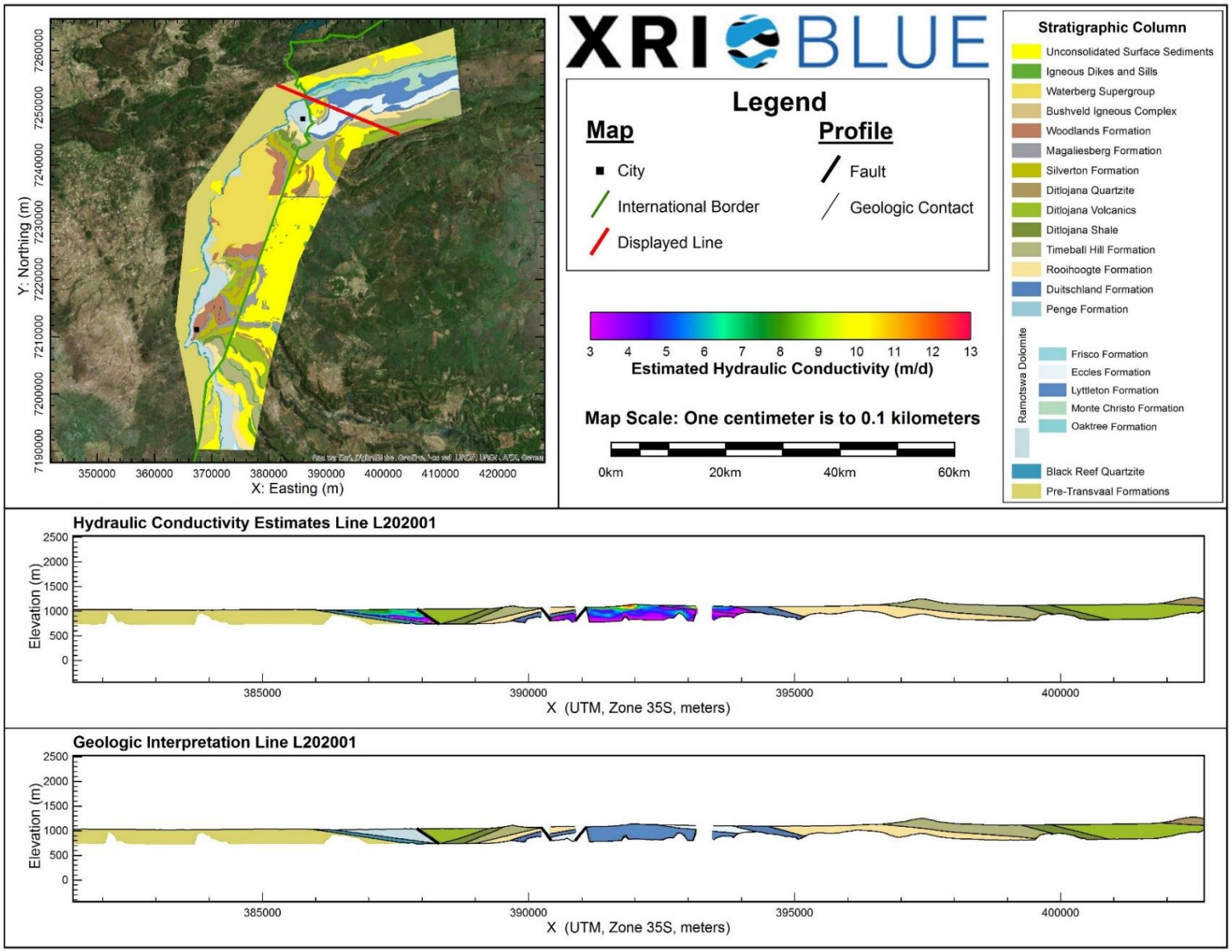

Hydraulic Conductivity Estimates and Interpreted Geology Profile for L202001.

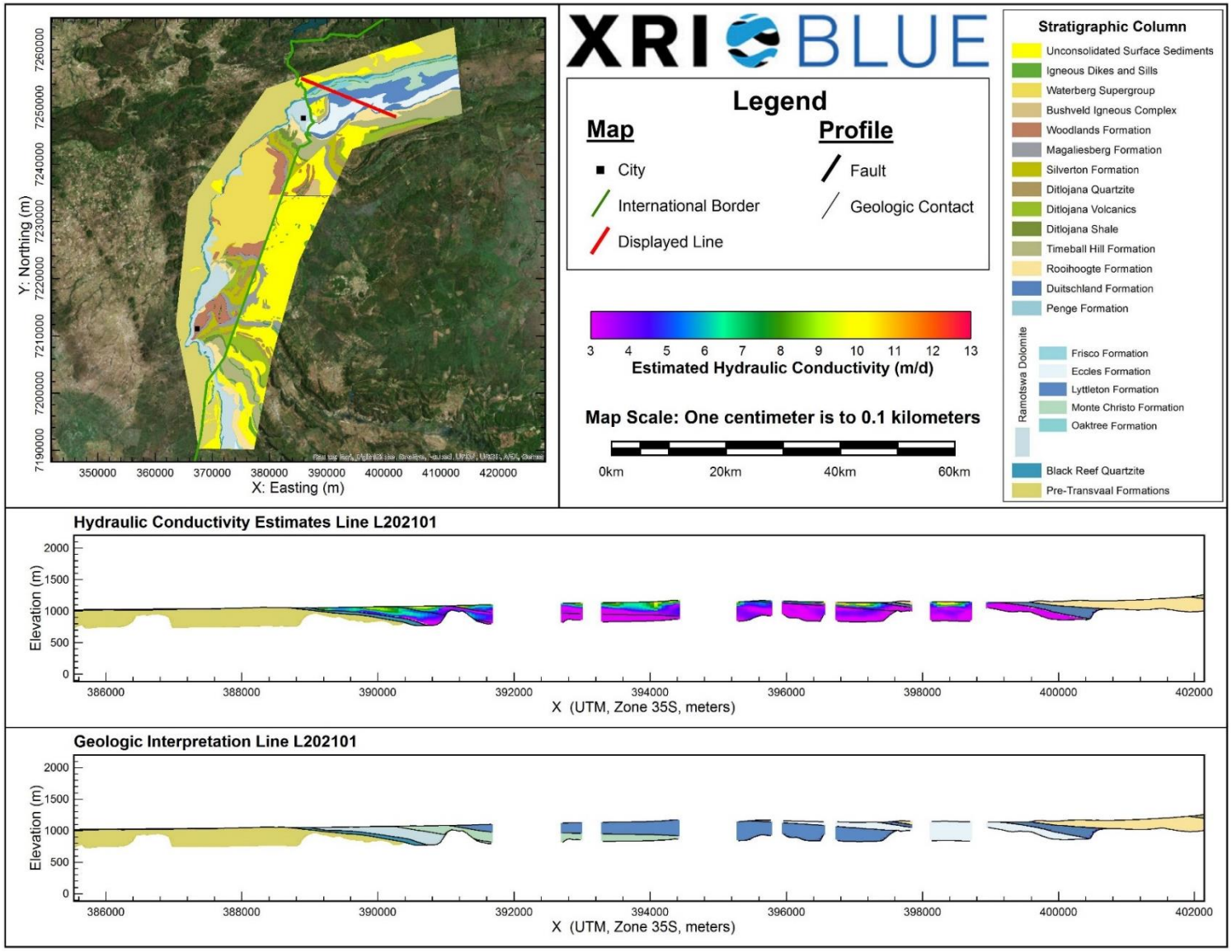

Hydraulic Conductivity Estimates and Interpreted Geology Profile for L202101.

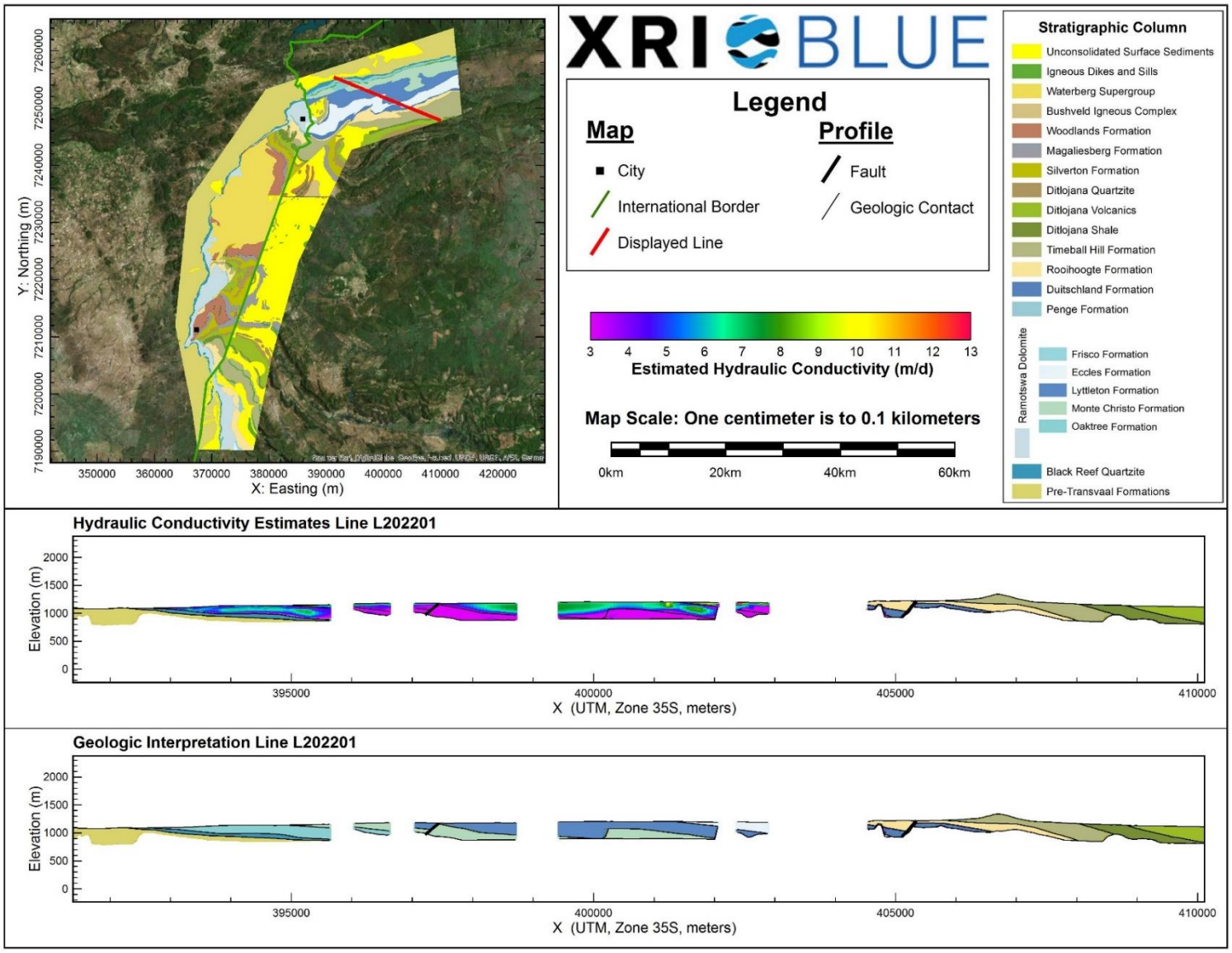

Hydraulic Conductivity Estimates and Interpreted Geology Profile for L202201.

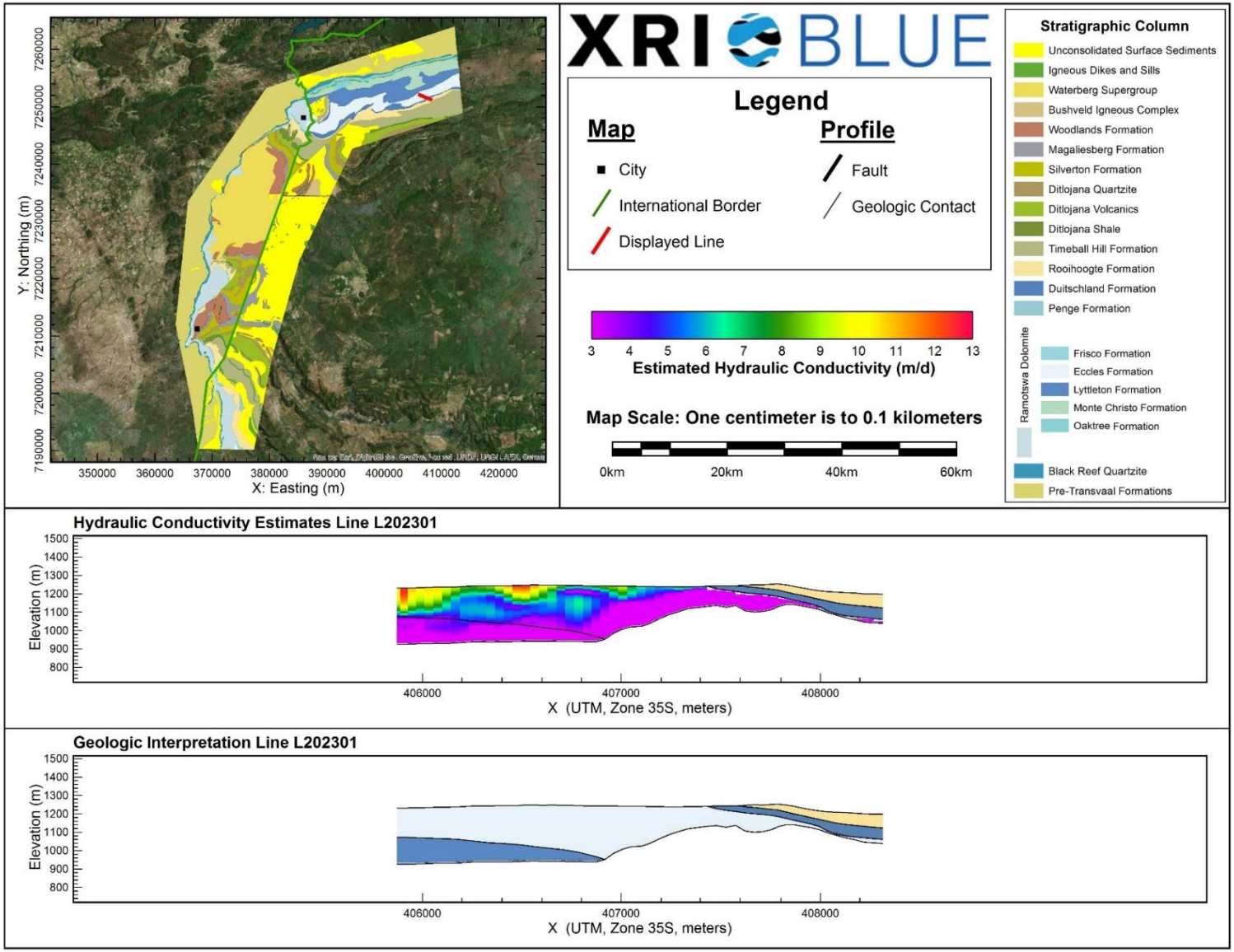

Hydraulic Conductivity Estimates and Interpreted Geology Profile for L202301.

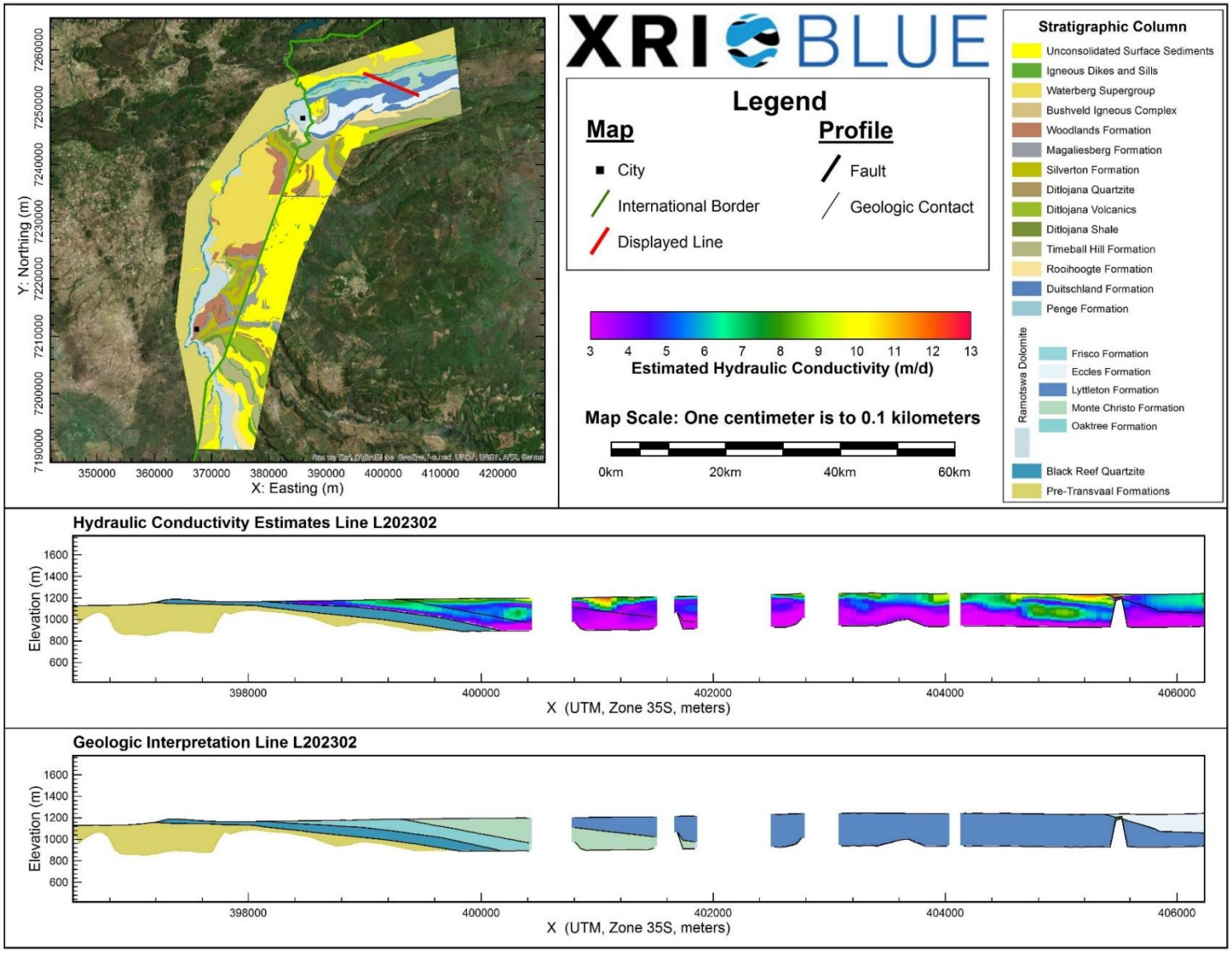

Hydraulic Conductivity Estimates and Interpreted Geology Profile for L202302.

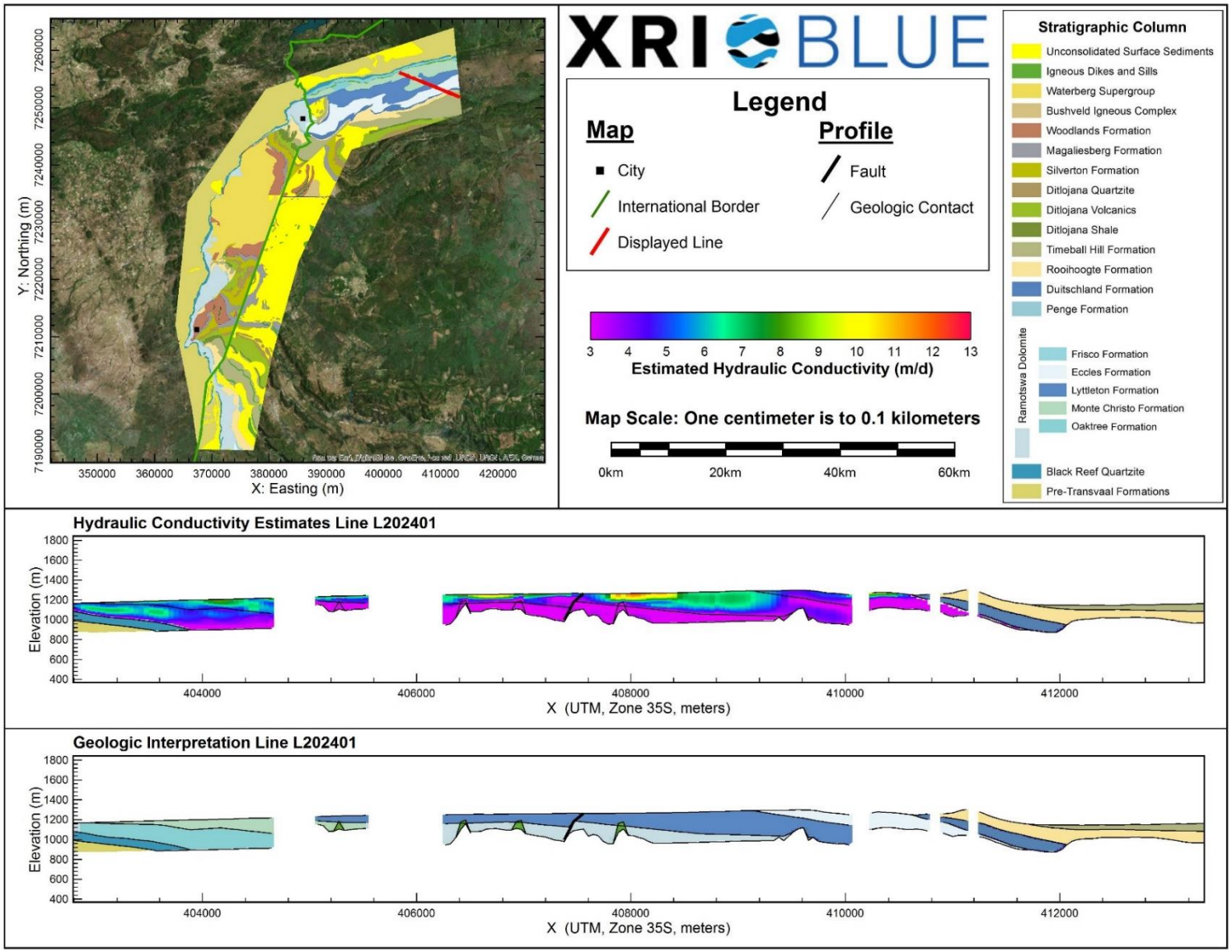

Hydraulic Conductivity Estimates and Interpreted Geology Profile for L202401.

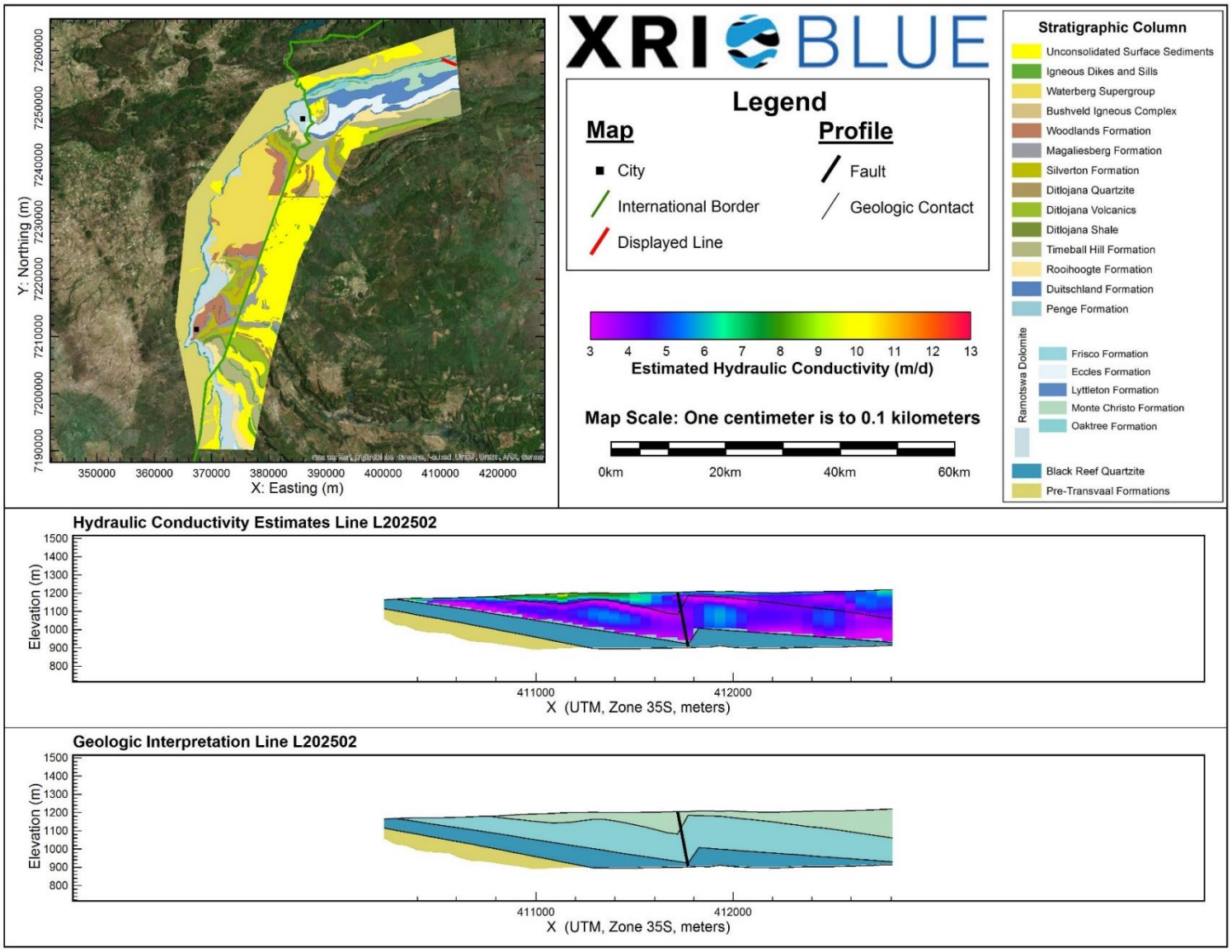

Hydraulic Conductivity Estimates and Interpreted Geology Profile for L202502.

Appendix E: 3D Model Grids of Interpreted Geology in Small Areas

There are two unique areas in the Ramotswa Project Area, where realistic and geologically valid grids of the interpreted formations could be created. Area 1 is in South Africa near the town of Radikhudu, and Area 2 is in Botswana between the towns of Lobatse and Otse. Only the geologic units that have been interpreted to be present within the two areas have been gridded. The .grd (grid) files that can be opened and viewed in Golden Software's Surfer (http://www.goldensoftware.com/products/surfer) and similar programs. Table 4 provides the details of the file name of each geologic grid (.grd) file provided, area of grid, and a description of the geologic data provided in each grid. The .grd files uses the WGS84 UTM Zone 35 South coordinate system with an X (Easting), Y (Northing), and Z (Formation specifics) unit of meters.

In addition, profiles of the interpreted geology grids through Areas 1 and 2 are included in Appendix E. The Interpreted Geology Profiles are displayed with a 1:1 horizontal and vertical ratio, each profile is uniquely scaled so that the information for an entire flight line is displayed in one figure. While the specifics of each profile may be difficult to view in the figure, the various .grd and .xyz files of interpreted geology provided along with this report give all of the necessary data to understand the geologic interpretations in the Ramotswa Project Area.

Table 4: Explanation of the Geologic Grid .grd files of the Ramotswa Project Area.

.grd file name	Area	Description of geologic data
A1_BlackReef_top	Area 1 (South Africa)	Interpreted top of the Black Reef Formation (meters)
A1_DOI	Area 1 (South Africa)	Calculated Depth of Investigation (Lower) of the model (meters)
A1_Frisco_base	Area 1 (South Africa)	Interpreted base of the Frisco Formation (meters)
A1_Penge top	Area 1 (South Africa)	Interpreted top of the Penge Formation (meters)
A1_PreTransvaal_top	Area 1 (South Africa)	Interpreted top of the pre Transvaal Formations (meters)
A1_Ramotswa_Dolomite_top	Area 1 (South Africa)	Interpreted top of the Ramotswa Dolomite (meters)
A1_Rooihoogte_top	Area 1 (South Africa)	Interpreted top of the Rooihoogte Formation (meters)
A2_BlackReef_top	Area 2 (Botswana)	Interpreted top of the Black Reef Formation (meters)
A2_DOI	Area 2 (Botswana)	Calculated Depth of Investigation (Lower) of the model (meters)
A2_Lyttleton_top	Area 2 (Botswana)	Interpreted top of the Lyttleton Formation (meters)
A2_MonteChristo_top	Area 2 (Botswana)	Interpreted top of the Monte Christo Formation (meters)
A2_OakTree_top	Area 2 (Botswana)	Interpreted top of the Oaktree Formation (meters)
A2_Penge_top	Area 2 (Botswana)	Interpreted top of the Penge Formation (meters)
A2_PreTransvaal_top	Area 2 (Botswana)	Interpreted top of the pre Transvaal Formations (meters)
A2_RamotswaDolomite_top	Area 2 (Botswana)	Interpreted top of the Ramotswa Dolomite (meters)
A2_Rooihoogte_top	Area 2 (Botswana)	Interpreted top of the Rooihoogte Formation (meters)
A2_TimeballHill_top	Area 2 (Botswana)	Interpreted top of the Timeball Hill Formation (meters)
A2_Woodlands_top	Area 2 (Botswana)	Interpreted top of the Woodlands Formation (meters)

Appendix F: List of attached files provided with the Report

The following files listed below have been included along with the Report:

1.) "Ramotswa_Inverted_Flight_Names.kmz" – a .kmz file to be viewed in Google Earth™ that shows the location of the unique AEM flight lines, and will display the associated flight line name when a unique flight line is clicked on.
2.) "Ramotswa_Interpreted_Collapse_Features.kmz" – a .kmz file to be viewed in Google Earth™ that shows unique collapse features interpreted from the AEM data within the Ramotswa Project Area.
3.) "Ramotswa_Linear_Magnetic_Anomalies.kmz" – a .kmz file to be viewed in Google Earth™ that shows unique linear mag anomalies interpreted to be dikes within the Ramotswa Project Area.
4.) "Ramotswa_Interpreted_Dikes.kmz" - a .kmz file to be viewed in Google Earth™ that shows unique dikes interpreted from the AEM data within the Ramotswa Project Area.
5.) Ramotswa_Interpreted_Faults.kmz"– a .kmz file to be viewed in Google Earth™ that shows unique faults interpreted from the AEM data within the Ramotswa Project Area.
6.) "Ramotswa_Interpreted_Dolomite_Compartments.kmz" - a .kmz file to be viewed in Google Earth™ that shows unique dolomite compartments interpreted from the airborne magnetic data within the Ramotswa Project Area.
7.) "Ramotswa_Geologic_Interpretations.xyz" – a .xyz file of the interpreted tops and bottoms of the geologic formations within the Ramotswa Project Area
8.) "Ramotswa_Dolomite_Porosity_Estimates.xyz" – a .xyz file of the porosity estimates of the Ramotswa Dolomite within the Ramotswa Project area.
9.) "Ramotswa_Dolomite_Hydraulic_Conductivity_Estimates.xyz" – a .xyz file of the hydraulic conductivity estimates of the Ramotswa Dolomite within the Ramotswa Project area.
10.)"A1_BlackReef_top.grd" – a .grd file of the gridded interpreted top of the Black Reef Formation in Area 1 (South Africa) within the Ramotswa Project Area.
11.) "A1_DOI.grd" – a .grd file of the gridded calculated Depth of Investigation in Area 1 (South Africa) within the Ramotswa Project Area.
12.)"A1_Frisco_base.grd" – a .grd file of the gridded interpreted base of the Frisco Formation in Area 1 (South Africa) within the Ramotswa Project Area.
13.)"A1_Penge_top.grd" – a .grd file of the gridded interpreted top of the Penge Formation in Area 1 (South Africa) within the Ramotswa Project Area.
14.)"A1_PreTransvaal_top.grd" – a .grd file of the gridded interpreted top of the pre Transvaal Formations in Area 1 (South Africa) within the Ramotswa Project Area.
15.)"A1_RamotswaDolomite_top.grd" – a .grd file of the gridded interpreted top of the Ramotswa Dolomite in Area 1 (South Africa) within the Ramotswa Project Area.
16.)"A1_Rooihoogte_top.grd" – a .grd file of the gridded interpreted top of the Rooihoogte Dolomite in Area 1 (South Africa) within the Ramotswa Project Area.
17.)"A2_BlackReef_top.grd" – a .grd file of the gridded interpreted top of the Black Reef Formation in Area 2 (Botswana) within the Ramotswa Project Area.
18.) "A2_DOI.grd" – a .grd file of the gridded calculated Depth of Investigation in Area 2 (Botswana) within the Ramotswa Project Area.
19.)"A2_Lyttleton_top.grd" – a .grd file of the gridded interpreted top of the Lyttleton Formation in Area 2 (Botswana) within the Ramotswa Project Area.
20.)"A2_MonteChristo_top.grd" – a .grd file of the gridded interpreted top of the Monte Christo Formation in Area 2 (Botswana) within the Ramotswa Project Area.
21.)"A2_OakTree_top.grd" – a .grd file of the gridded interpreted top of the Oaktree Formation in Area 2 (Botswana) within the Ramotswa Project Area.

22.)“A2_Penge_top.grd” – a .grd file of the gridded interpreted top of the Penge Formation in Area 2 (Botswana) within the Ramotswa Project Area.
23.)“A2_PreTransvaal_top.grd” – a .grd file of the gridded interpreted top of the pre Transvaal Formations in Area 2 (Botswana) within the Ramotswa Project Area.
24.)“A2_RamotswaDolomite_top.grd” – a .grd file of the gridded interpreted top of the Ramotswa Dolomite in Area 2 (Botswana) within the Ramotswa Project Area.
25.)“A2_Rooihoogte_top.grd” – a .grd file of the gridded interpreted top of the Rooihoogte Dolomite in Area 2 (Botswana) within the Ramotswa Project Area.
26.)A2_TimeballHill_top.grd” – a .grd file of the gridded interpreted top of the Timeball Hill Formation in Area 2 (Botswana) within the Ramotswa Project Area.
27.)“A2_Woodlands_top.grd” – a .grd file of the gridded interpreted top of the Woodlands Formation in Area 2 (Botswana) within the Ramotswa Project Area.